Catalogue of Flat-Band Stoichiometric Materials

Nicolas Regnault,[1, 2, *] Yuanfeng Xu,[3, †] Ming-Rui Li,[4, ‡] Da-Shuai Ma,[5, ‡] Milena Jovanovic,[6]
Ali Yazdani,[1] Stuart S. P. Parkin,[3] Claudia Felser,[7] Leslie M. Schoop,[6] N. Phuan
Ong,[1] Robert J. Cava,[6] Luis Elcoro,[8, ‡] Zhi-Da Song,[1, ‡] and B. Andrei Bernevig[1, 9, 10, §]

[1] *Department of Physics, Princeton University, Princeton, New Jersey 08544, USA*
[2] *Laboratoire de Physique de l'Ecole normale supérieure,*
ENS, Université PSL, CNRS, Sorbonne Université,
Université Paris-Diderot, Sorbonne Paris Cité, 75005 Paris, France
[3] *Max Planck Institute of Microstructure Physics, 06120 Halle, Germany*
[4] *Department of Physics, Tsinghua University, Beijing, 100084, China*
[5] *Beijing Key Laboratory of Nanophotonics and Ultrafine Optoelectronic Systems,*
School of Physics, Beijing Institute of Technology, Beijing 100081, China
[6] *Department of Chemistry, Princeton University, Princeton, New Jersey 08544, USA*
[7] *Max Planck Institute for Chemical Physics of Solids, 01187 Dresden, Germany*
[8] *Department of Condensed Matter Physics, University of the Basque Country UPV/EHU, Apartado 644, 48080 Bilbao, Spain*
[9] *Donostia International Physics Center, P. Manuel de Lardizabal 4, 20018 Donostia-San Sebastian, Spain*
[10] *IKERBASQUE, Basque Foundation for Science, Bilbao, Spain*

(Dated: April 5, 2022)

Topological electronic flatten bands near or at the Fermi level are a promising avenue towards unconventional superconductivity and correlated insulating states. However, the related experiments are mostly limited to the engineered materials, such as moiré systems[1–3]. Here we present a catalogue of all the three-dimensional stoichiometric materials with flat bands around the Fermi level that exist in nature. We consider 55,206 materials from the Inorganic Crystal Structure Database catalogued using the Topological Quantum Chemistry website[4,5], which provides their structural parameters, space group, band structure, density of states and topological characterization. We combine several direct signatures and properties of band flatness to a high-throughput analysis of all crystal structures. In particular, we identify materials hosting line-graph or bipartite sublattices - either in two or three dimensions - likely leading to flat bands. From this trove of information, we create the Materials Flatband Database website, a powerful search engine for future theoretical and experimental studies. We use it to extract a curated list of 2,379 materials, with among them 345 promising candidates, potentially hosting flat bands whose charge centers are not strongly localized on the atomic sites. We showcase five representative materials: $KAg[CN]_2$, $Pb_2Sb_2O_7$, Rb_2CaH_4, Ca_2NCl and WO_3. We provide a theoretical explanation for the origin of their flat bands close to the Fermi energy using the S-matrix method introduced in a parallel work[6].

I. INTRODUCTION

Electrons whose energy dispersion is bound within a narrow window are conjectured to exhibit a wide-range of interesting physics phenomena. Such electrons form a high density of states "flat band", where many-body effects dominate over the kinetic energy and where Fermi-surface physics gives way to strongly interacting, non-Fermi liquid behavior[7]. The archetypal - and until recently the only experimentally discovered - such system is the Fractional Quantum Hall effect[8,9] where anyonic (potentially non-Abelian[10]) quasi-particle excitations can appear under a fractional filling of an electronic flat band that develops in the presence of a large magnetic field. New developments in engineered solid-state materials have now shown that flat bands can exist even in the absence of a large magnetic field. In moiré materials such as (but not limited to) twisted bilayer graphene (TBG)[1–3], flat electronic bands are obtained by creating large, many nanometer-size moiré unit cell which folds and flattens the initial band structure of the material. This flatness plays a crucial role in the physics of TBG, leading to, e.g., both the correlated insulator states and of the strong-coupling superconductivity that renders the TBG phase diagram akin to that of the high-temperature cuprates. However, as the unit cell is large, the electron density in moiré samples is necessarily low, preventing new type of physics associated with high electron density[11,12]. This renders the yet elusive prediction of flat bands in non-moiré, stoichiometric crystals of immediate importance.

In the present article and its accompanying Supplementary Information (SI), we address for the question of predicting and classifying all the flat bands in all the stoichiometric crystals currently present in nature, keeping in mind that not all flat bands are created equal. Extremely localized orbitals - or large unit cells with well-separated atoms - can easily give rise to mundane flat atomic bands (FAB), as the kinetic energy is suppressed by the vanishing overlap between atomic wave-

---

[*] regnault@princeton.edu; These authors contributed equally
[†] yfxu@mpi-halle.mpg.de; These authors contributed equally
[‡] These authors contributed equally
[§] bernevig@princeton.edu; These authors contributed equally

functions, as schematically shown in Fig. 1(a). The FAB is very common in layered and heavy fermion systems. At the opposite side of the spectrum are the flat topological bands (FTB) created by completely extended wavefunctions (such as is the case in TBG), as shown in the schematic Fig. 1(b). (See Appendix B for a more detailed discussion of the FAB and FTB.) There, the quenching of the kinetic energy arises from interference effects despite large electron orbital overlaps and hopping. The latter type of bands can host many exotic quantum phenomena, including magnetism, fractional quantum Hall effect at zero field[13–16], unconventional superconductivity[2,17,18], non-Fermi liquid behavior[7] and anomalous Landau level beyond the Onsager's rule[19]. Such topological bands can enhance the superfluid weight in twisted bilayer graphene[20,21] and could lead to high-temperature superconductivity. Ideal FTB near the Fermi level in crystalline materials has not yet been found; the only experimentally found FTBs are in the engineered TBG. A third type, the flat obstructed atomic band (FOAB) lies at the interface between the polar opposites FAB and FTB: while the electron's symmetric Wannier function can be localized in real space, the Wannier center is pinned and centered at an empty site[22,23] and hence delocalized from the atomic sites, as illustrated in Fig. 1(c).

We present and implement algorithms for the detection and classification of flat bands near the Fermi level. Using the materials in our database Topological Quantum Chemistry website (TQCDB) (which contains most ICSD stoichiomentric structures) obtained in previous works[4,5,22], we build the complementary Materials Flatband Database website (MFBDB), where different algorithms and search options for flat bands are provided to the user. First, we perform a brute-force search based on complementary "flatness" criteria such as bandwidth and density of states (DOS), to predict all the (thousands) flat-band materials in the ICSD database. We classify these bands based on their topologies. Second, using a theory that we have developed in Ref.[6] encompassing generic orbital systems with or without SOC, we perform a targeted search of flat-band materials based on the lattice geometry (such as Kagome, pyrochlore, Lieb, bipartite or split sublattices) of the compounds, whose information is present in the X-ray diffraction data on TQCDB or ICSD. We show that geometry-based theoretical models based on the S-matrix method[6] fit our ab-initio calculations of the flat bands remarkably well. Third, we also perform a manual check of thousands of materials for the best flat bands and select 2,379 materials with high-quality flat bands near the Fermi level. In the main text, we showcase our methods, theoretical understanding and predictive power for five represented flat-band materials, while in the Supplementary Material we present thousands of others. Our classification and predictions take into account the different flat band natures, including their topological character, and our database is coupled to the Materials Project and NIMS Materials Database, providing information about the magnetic and superconducting properties (including high T_c) of the candidate materials.

II. DATABASE OF FLAT BANDS MATERIALS

In this work, we have used the TQCDB[4,5] as our materials database. We summarize its main feature in the Methods section and provide its detailed overview in Appendix C 1. As we are interested in flat bands near the Fermi energy, we discard materials containing rare-earth elements (with the exception of La atom) and actinides as these elements usually lead to spurious flat bands due to f electrons in the ab-initio calculations. In total, 55,206 ICSD entries have been considered for our high-throughput search for flat bands. The automated search is based on two main, complementary, approaches: the detection of flat bands in the band structure and the DOS, and the identification of special sublattices that lead to band flattening. We will now detail each of them.

A. High-throughput search of flat-bands

For determining band flatness, we rely on calculations where the spin-orbit coupling (SOC) is neglected. While SOC plays an important role in the topological features near the Fermi level, it does not drastically alter the band structure nor the DOS around the Fermi energy E_F ±2eV region where we focus our search. For each ICSD entry, our database provides the ab-initio paramagnetic-phase electronic band structure along paths made of straight lines in the Brillouin zone connecting high symmetry points (" high symmetry lines "). Each high symmetry line is well defined in every space group (SG) and it has been discretized, irrespective of its length, into 20 equally distant k-points (*i.e.*, points in the BZ). Since we are interested in low-energy physics, we focus our investigations on the flatness of the two highest/lowest occupied/empty bands around E_F, which in turn is reached when the occupation number of bands equals half the number of valence electrons. While paramagnetic calculations would failed to capture (anti-)ferromagnetic ground states, we discuss in Appendix G four representative ferromagnetic compounds. Our ferromagnetic calculations both matches the experimental results and while preserving the flat bands obtained in the paramagnetic calculations remain near the Fermi level.

As motivated in Section I, we investigate bands that are flat in *parts* of (but not necessarily over the entire) the BZ. Thus for each ICSD entry, we search for *flat-band segments*: a series of L consecutive k-points along the high symmetry lines of the band structure (we use $L = 10, 20, 30, 40$ or 50), where the energy band width is smaller than a tunable threshold ω (ranging from 25meV to 150meV). The number of such flat segments for every band analyzed provides a convenient signature of band flatness. In Appendix C 2 a, we provide a full discussion of the definition, the algorithm and the statistics of flat-band segments around E_F.

The presence of a flat-band segment alone is not sufficient to predict the presence of interesting physics associated with it: a (quasi) one-dimensional system would equally exhibit a flat-band segment in the directions perpendicular to its dispersive direction. However, peaks (or their absence) in the DOS offer a simple and efficient way to filter out such pathological cases. Thus for each ICSD entry, we map the position and width of all DOS peaks in an energy region of ±5eV around E_F. More details about the DOS peak detection are given in Appendix C 2 b.

B. Automated identification of sublattices

Geometric frustration in (line-graph and bipartite) lattices is known to give rise to exact FTBs[24–29]. While initially predicted for s-orbitals, this property was recently generalized to a slew of other possible orbital/lattice combinations[6]. This provides a crucial starting point to understand and predict flat bands in crystalline materials: if a material hosts a line-graph or bipartite lattice as a part of its lattice structure (a "sublattice"), and if this sublattice is only weakly perturbed or deformed by the remaining atoms or orbitals, we expect to observe FTBs. To explain the origin of the flat bands found in our high-throughput search, we have automated, using the structural parameters of every ICSD entry, the detection of five types of line-graph or bipartite sublattices: the Kagome, pyrochlore, Lieb, bipartite or split sublattices as detailed in Appendix D and Appendix E.

In 3D, the Kagome, pyrochlore and Lieb lattices can be mathematically characterized by special occupied Wyckoff positions in certain SGs. Using the crystalline structures of materials, we have developed a space-group method to detect the line-graph and Lieb sublattices in the Methods section. Although the space-group method provides a fast way to find the symmetric Kagome, pyrochlore and Lieb sublattices in crystalline materials, the exact sublattice might be spoiled by the presence of other atoms of the *same element* on (or close to) this sublattice. Moreover, the space-group method discards approximate sublattices which could also exhibit quasi-flat bands. To solve these issues, we have further developed a *geometric method* which solely relies on the geometric features of these three sublattice types (discussed in Appendix D 2) and ignores the exact SG restrictions. In Appendix D 3, we have provided a detailed presentation of our algorithms implementing the geometric method for each type of sublattice. Equipped with these methods, we sort all the possible sublattices in a material in two categories: the *rigorous sublattices* which satisfy both methods and the *approximate sublattices* which only satisfy the geometric method but capture weak distortions of rigorous sublattices.

A bipartite lattice with chiral symmetry is formed by two sublattices L and $\tilde{L}$ with the kinetic hopping *only* between L and $\tilde{L}$. As proposed in Ref.[6] and briefly introduced in the Methods section and Appendix E 1, a general method, namely the S-matrix method, can be used to explain the origin of flat bands in crystalline materials whose lattice contains a bipartite or split sublattice. We have developed an algorithm (detailed in Appendix E) to search for bipartite lattices from the structural parameters of each ICSD entry with the following necessary simplifying assumptions for a high-throughput analysis. For each crystal structure in the MFBDB, we solely rely on the geometric distance between two atoms to infer the amplitude of kinetic hopping between them. By ignoring the small hopping terms based on a tunable cutoff, we identify if a crystalline material has a bipartite sublattice with a different number of atoms in its L and $\tilde{L}$ sublattices. In the algorithm, a special case of bipartite sublattice, namely the split sublattice which has been proposed to host FTBs[28], is also detected and tagged.

III. RESULTS

We now summarize the main results obtained in the present high-throughput search. First we discuss the number of geometric sublattices detected by our algorithms and the public website we have developed to search for materials with flat bands based on the criterion in Section II. We discuss a manually curated list of 2,379 materials potentially hosting FTBs, obtained using our toolset. Then, we showcase five best representative flat-band materials and explain the flat-band segments in their band structures using the S-matrix method[6].

A. Statistics and website

By applying the automated analysis of the lattice structure to the 55,206 ICSD entries of the MFBDB, we have performed a high-throughput search of the rigorous and approximate Kagome, Lieb, pyrochlore sublattices, the bipartite/split lattice with different number of atoms on their further sublattices. 6,120 ICSDs with at least one Kagome (rigorous or approximate) sublattice have been found, including 4,192 ICSDs with a Kagome sublattice labeled as rigorous, 1,666 ICSDs with a pyrochlore sublattice (rigorous or approximate) and 1,541 ICSDs with a rigorous pyrochlore sublattice. For the Lieb lattice, there are 1,590 ICSDs hosting such a sublattice, including 1,202 ICSDs with rigorous Lieb sublattices. At least one bipartite sublattice (irrespective of the cutoffs) is found among 21,175 ICSDs and split sublattices are found in 8,224 ICSDs. A breakdown of these statistics per SG is provided in Appendix C 3. The brute-force scan of the band structures along the high symmetry lines was performed for several threshold parameters. The number of ICSDs exhibiting flat-band segments varies strongly on these parameters; for a detailed statistical analysis see Appendix C 2 a.

The data generated through the automated algorithms discussed in Section II is available through our MFBDB(see Appendix C 2 for an overview of the search engine). We actually used this website to perform an extensive investigation of promising candidate materials exhibiting flat bands or large segment of flat bands close to the Fermi energy. The outcome of our search is provided as a list of *curated flat-band materials* in Appendix H 1. This list contains 6,338 ICSD entries that can be regrouped into 2,379 unique materials, *i.e.*, ICSDs sharing the same stoichiometric formula, SG and topological property at the Fermi energy (as defined in Appendix C 1). The complete set of criteria applied to select these materials is provided in Appendix H 1, and it includes the distance to the Fermi energy, the flat band width and topology, and the presence of a peak in the DOS. We have excluded cases where the flat bands were *clear* FAB from the list of curated flat-band materials, and they are listed in Appendix H 2. The statistics of detected sublattices among the curated materials are provided in Table I.

B. Flat-band material candidates

Among the 2,379 high-quality flat-band materials, we select 345 best representative flat-band materials in Appendix H 3 for further experimental investigation. Most of the 345 materials host one (or more than one) of the Kagome, pyrochlore, Lieb, bipartite and split sublattices in their crystal structures. For each of the five types of sublattice, we select one representative material, which hosts best flat-band segments on (or close to) the Fermi level, and explain its physical origin using the S-matrix method[6]. All of the five representative flat-band materials are chemically realistic, experimentally paramagnetic and not Mott insulators, which is consistent with our paramagnetic calculations.

The five typical materials are $KAg[CN]_2$ [ICSD 30275, SG 163 ($P\bar{3}1c$)] with approximate Kagome sublattice formed by Ag atoms, $Pb_2Sb_2O_7$ [ICSD 27120, SG 227 ($Fd\bar{3}m$)] with pyrochlore sublattice formed by Pb atoms, Rb_2CaH_4 [ICSD 65196, SG 139 ($I4/mmm$)] with Lieb sublattice formed by Ca and H atoms, Ca_2NCl [ICSD 62555, SG 166 ($R\bar{3}m$)] with bipartite sublattice formed by Ca and N atoms, and WO_3 [ICSD 108651, SG 221 ($Pm\bar{3}m$)] with split sublattice formed by W and O atoms. Their crystal structures are shown in Fig. 2(a)-(e) and the orbital characters of the flat bands in the five materials are shown in the orbital-projected band structures in Fig. 2(f)-(j). As detailed in Appendix F, based on the crystal structure and orbital-projected bands of these materials, we have constructed effective tight-binding Hamiltonians using the S-matrix method[6] and found that they can successfully explain the origins of flat bands. The flat bands of other materials of similar crystal structures can be found in the MFBDB. In the Methods section, we use Ca_2NCl to showcase the application of the S-matrix method in explaining the origin of flat bands.

IV. DISCUSSION

We have performed, for the first time, a high-throughput search for flat electronic bands near the Fermi level and for the detection of line-graph and bipartite sublattices from the crystal structures of stoichiometric crystalline materials. We have further classified the flat bands by their topology, DOS, length of band flatness, and the types of lattices formed by the atoms whose orbitals contribute to the flat band. By successfully applying our algorithms to 55,206 ICSD entries, we have found that 24,052 (43.57%) out of all the ICSD entries host *at least* one of the Kagome, pyrochlore, Lieb, bipartite or split sublattices in their crystal structures. This proportion is raised to 59.26% for our *manually curated list* of 6,338 ICSDs (2,379 unique materials) and 73.87% for the *best representative flat-band materials*. The appearance of flat-bands in materials can be, in large but non-exhaustive part, theoretically understood using the S-matrix method[6], as we have exemplified in five prototypical compounds. All the results obtained in this work and detailed in the supplementary Appendices can be accessed on the MFBDB. Our results pave the way for future theoretical and experimental studies on flat-band materials combining topology and interactions and leading to exotic quantum phenomena, such as magnetism, non-Fermi liquid behavior and superconductivity. Such flat-band investigations are, at present, confined to engineered twisted moire lattices in two dimensions. While the present work studies flat bands in paramagnetic band structures of 3D materials, our methods can be adapted to detect flat bands in magnetic band structures, 2D mono-layer materials, phonons and photonic crystals. Furthermore, the further classification of FOAB's will enlarge the set of flat bands whose center of charge is away from the atomic positions.

Methods

Topological Quantum Chemistry website The database used as an input the structural parameters of stoichiometric materials reported in the Inorganic Crystal Structure Database (ICSD)[30]. For each entry, ab-initio calculations were performed using Density Functional Theory (DFT)[31,32] and its implementation in the Vienna Ab-initio Simulation Package (VASP)[33,34], with and without accounting for the spin-orbit coupling (SOC). The database provides the structural parameters, the band dispersion along high symmetry lines, the DOS, and the topological characterization for each set of bands in the material's band structure for each of the 69,730 ICSD entries.

Space-group method of detecting line-graph and Lieb sublattices To detect a Kagome, pyrochlore or Lieb sublattice in crystalline materials, we have first identified the *minimal* SGs that support these three lattices and the corresponding Wyckoff positions (see details in Appendix D 1). Then, through group-subgroup relations and the split relations between the sets of Wyckoff positions on the *Bilbao Crystallographic Server* (BCS)[35,36], we have obtained all the SGs which host these lattices. The results are tabulated in the Table V and Table VI of Appendix D. We dub the detection of sublattices using this tabulated information as the *space-group method*.

A brief introduction of the S-matrix method. Denoting $|L|$ and $|\tilde{L}|$ the number of atoms or orbitals in the L and $\tilde{L}$ further sublattices of the bipartite or split sublattice of a material (assuming $|L| \geq |\tilde{L}|$), the Bloch Hamiltonian associated to a bipartite sublattice of a material reads

$$H(\boldsymbol{k}) = \begin{pmatrix} 0 & S^{\dagger}(\boldsymbol{k}) \\ S(\boldsymbol{k}) & 0 \end{pmatrix}. \tag{1}$$

Here $S(\boldsymbol{k})$ is a matrix with dimension $|L| \times |\tilde{L}|$ and $\boldsymbol{k}$ is the momentum in the Brillouin zone. A bipartite lattice with $|L| \neq |\tilde{L}|$ hosts flat bands in its band structure. For example, the Hamiltonian of Eq. 1 has at least $|L|+|\tilde{L}|-2\times rank(S(\boldsymbol{k}))$ zero-energy states, *i.e.*, the band structure has at least $|L|+|\tilde{L}|-2\times rank(S(\boldsymbol{k}))$ exact flat bands. It is also very likely that these bands exhibit non-trivial topology[6]. While the other $2\times rank(S(\boldsymbol{k}))$ bands are dispersive, they are related by chiral symmetry. Although in real crystalline materials the chiral symmetry is generally broken by the intra-sublattice hopping, we find in Ref.[6] that this S-matrix method goes beyond the chiral symmetry. For a generalized bipartite lattice including the intra-sublattice coupling $A(k)(B(k))$ of sublattice $L(\tilde{L})$, if $A(k)$ has a momentum-independent eigenvalue $E = E_0$ with degeneracy n_0 and $|\tilde{L}| < n_0 \leq |L|$, then $H(k)$ also has at least $n_0 - |\tilde{L}|$ perfectly flat bands at energy $E = E_0$ irrespective of $B(k)$. Moreover, the eigenstates of these $n_0 - |\tilde{L}|$ flat bands identical to those of the system with chiral symmetry[6].

The origin of flat bands in $\mathbf{Ca_2NCl}$: application of S-matrix method. As shown in Fig. 2(d) in the main text, the 3D crystal structure of Ca_2NCl is stacked, composed alternating Ca_2N and Cl layers. In each Ca_2N layer, the Ca and N atoms occupy honeycomb (with buckling) and triangular sublattices, respectively. The Cl layer also forms a triangular lattice. As shown in Fig. 2(i), the flat band and the lower dispersive bands next to it are mainly contributed by the p orbitals of N atoms. By constructing the maximal localized Wannier functions (MLWF)[37], we extract an effective tight-binding model for these p bands and find that its hoppings - which are computed from ab-intio methods without any additional theoretical input - obey a set of fine-tuned conditions, which in turn give rise to flatness of the top p band. As an example, the amplitude of σ-bond comes out to almost exactly the -3 times of π-bond. (See Appendix F 4 for more details.) Since similar flat bands also exist in many other materials of the same structure (*e.g.* Ca_2NBr, Sr_2NCl *et al.*), and similar fine-tuned tight-binding ab-initio model, this points to a deeper reason for the fine-tuning conditions.

This deep reason is the S-matrix theory. We notice that the nearest neighbors of the N atoms are the Ca atoms and hence that Ca and N atoms form a bipartite sublattice if only the nearest neighbors hoppings are considered in a theoretical model of the bands. As analyzed in Fig. 2(i), the conduction bands around $E = 3$eV are mainly contributed by the s and d orbitals on the Ca atoms and the three valence bands in the energy window $-3 \sim 0$eV are mainly contributed by the p orbitals on N atoms and partially contributed by the hybridized orbitals consisting of s and d_{z^2} orbitals on Ca. Since the s and d_{z^2} orbitals form the same representation (A_1) of the point group symmetry C_{3v} isomorphic to the site-symmetry group of Ca sites, they hybridize with each other to form two hybridized orbitals. It is a reasonable simplification to only take into account the hybridized orbital with the lowest energy, which we refer to as the s orbital in the following. A tight-binding model including both the N and Ca atoms is naturally an S-matrix theory of a bipartite lattice, where the L sublattice of the bipartite (sub)-lattice consists of p orbitals at the triangular lattice formed by N and the $\tilde{L}$ sublattice consists of (hybridized) s orbitals at the honeycomb lattice (with buckling) formed by Ca. The onsite energy of s orbitals (Δ_s) is about 3eV. Following the argument below Eq. 1, there must be $|L|+|\tilde{L}|-2\times rank(S(\mathbf{k})) = 3+2-4 = 1$ flat band at $E = 0$. (See Appendix F 4 for the explicit form of $S(\mathbf{k})$.) As detailed in Appendix F 4, the S-matrix band structure matches the first-principles band structure very well. Furthermore, the S-matrix theory also explains the fine-tuning conditions in the extracted tight-binding Hamiltonian from the MLWFs: the perturbative effective Hamiltonian for the p bands, $-S(\mathbf{k})S^{\dagger}(\mathbf{k})/\Delta_s$, perfectly reproduces the fine-tuning conditions of the ab-initio model. Therefore, the S-matrix theory is a faithful explanation for the flat band in Ca_2NCl.

ACKNOWLEDGMENTS

We are grateful to Xi Dai, Dumitru Calugaru, Aaron Chew, Maia Vergniory and Christie Chiu for helpful discussions. We thank the referees for their suggestions that helped improving our manuscript. We acknowledge the computational resources Cobra/Draco in the Max Planck Computing and Data Facility (MPCDF) and Atlas in the Donostia International Physics Center (DIPC). This research also used the resources of the National Energy Research Scientific Computing Center (NERSC), a U.S. Department of Energy Office of Science User Facility operated under Contract No. DE-AC02-05CH11231. This work is part of a project that has received funding from the European Research Council (ERC) under the European Union's Horizon 2020 research and innovation programme (grant agreement no. 101020833). B.A.B. and N.R. were also supported by the U.S. Department of Energy (Grant No. DE-SC0016239), and were partially supported by the National Science Foundation (EAGER Grant No. DMR 1643312), a Simons Investigator grant (No. 404513), the Office of Naval Research (ONR Grant No. N00014-20-1-2303), the Packard Foundation, the Schmidt Fund for Innovative Research, the BSF Israel US foundation (Grant No. 2018226), the Gordon and Betty Moore Foundation through Grant No. GBMF8685 towards the Princeton theory program, and a Guggenheim Fellowship from the John Simon Guggenheim Memorial Foundation. A.Y., N.P.O., R.J.C., L.M.S., B.A.B. and N.R. were supported by the NSF-MRSEC (Grant No. DMR-2011750). A.Y. was supported by NSF-DMR-1904442. B.A.B., L.M.S. and N.R. gratefully acknowledge financial support from the Schmidt DataX Fund at Princeton University made possible through a major gift from the Schmidt Futures Foundation. L.M.S. acknowledges financial support from the Packard and Sloan Foundation. B.A.B. received additional support from the Max Planck Society. L.E. was supported by the Government of the Basque Country (Project IT1301-19) and the Spanish Ministry of Science and Innovation (PID2019-106644GB-I00). C.F. was supported by the European Research Council (ERC) Advanced Grant No. 742068 “TOP-MAT”, Deutsche Forschungsgemeinschaft (DFG) through SFB 1143, and the Würzburg-Dresden Cluster of Excellence on Complexity and Topology in Quantum Matter-ct.qmat (EXC 2147, Project No. 390858490). S.S.P.P. acknowledges funding by the Deutsche Forschungsgemeinschaft (DFG, German Research Foundation) – Project number 314790414.

Author contribution

B.A.B. and N.R. conceived this work; N.R. and M.R.L. performed the high-throughput calculations with the help from L.E. and Y.X.; Y.X., D.S.M., Z.D.S, M.R.L., L.E. and N.R. worked out the theoretical explanations for the flat-band materials detailed in Appendix F; The material lists in Appendix H were manually selected by Y.X., M.R.L., Z.D.S, M.J. and N.R.; N.R. built the flat-band material database; D.S.M. performed the ab-initio ferromagnetic calculations advised by Y.X.; M.J., L.S., C.F. helped curate the list of materials to find the most experimentally relevant. All authors discussed the results and wrote the main text and the Methods; Y.X., Z.D.S, M.R.L, D.S.M, M.J., L.E. and N.R. wrote the supplementary materials.

Competing interests

The authors declare no competing interests.

Corresponding authors

Correspondence and requests for materials should be addressed to B. Andrei Bernevig or Nicolas Regnault or Yuanfeng Xu.

Data availability All data is available in the Supplementary Information and through our public website Materials Flatband Database website(https://www.topologicalquantumchemistry.fr/flatbands).

---

[1] R. Bistritzer and A. H. MacDonald, Moiré bands in twisted double-layer graphene, Proceedings of the National Academy of Sciences **108**, 12233 (2011).

[2] Y. Cao, V. Fatemi, S. Fang, K. Watanabe, T. Taniguchi, E. Kaxiras, and P. Jarillo-Herrero, Unconventional superconductivity in magic-angle graphene superlattices, Nature **556**, 43 (2018).

[3] Y. Cao, V. Fatemi, A. Demir, S. Fang, S. L. Tomarken, J. Y. Luo, J. D. Sanchez-Yamagishi, K. Watanabe, T. Taniguchi, E. Kaxiras, *et al.*, Correlated insulator behaviour at half-filling in magic-angle graphene superlattices, Nature **556**, 80 (2018).

[4] M. G. Vergniory, L. Elcoro, C. Felser, N. Regnault, B. A. Bernevig, and Z. Wang, A complete catalogue of high-quality topological materials, Nature **566**, 480 (2019).

[5] M. G. Vergniory, B. J. Wieder, L. Elcoro, S. S. P. Parkin, C. Felser, B. A. Bernevig, and N. Regnault, All Topological Bands of All Stoichiometric Materials, arXiv e-prints , arXiv:2105.09954 (2021).

[6] D. Călugăru, A. Chew, L. Elcoro, Y. Xu, N. Regnault, Z.-D. Song, and B. A. Bernevig, General construction and topological classification of crystalline flat bands, Nature Physics **18**, 185 (2022).

[7] P. Kumar, S. Peotta, Y. Takasu, Y. Takahashi, and P. Törmä, Flat-band-induced non-fermi-liquid behavior of multicomponent fermions, Physical Review A **103**, L031301 (2021).

[8] D. C. Tsui, H. L. Stormer, and A. C. Gossard, Two-dimensional magnetotransport in the extreme quantum limit, Phys. Rev. Lett. **48**, 1559 (1982).

[9] R. B. Laughlin, Anomalous quantum Hall effect: an incompressible quantum fluid with fractionally charged excitations, Phys. Rev. Lett. **50**, 1395 (1983).

[10] G. Moore and N. Read, Nonabelions in the fractional quantum Hall effect, Nuclear Physics B **360**, 362 (1991).

[11] A. Drozdov, M. Eremets, I. Troyan, V. Ksenofontov, and S. I. Shylin, Conventional superconductivity at 203 kelvin at high pressures in the sulfur hydride system, Nature **525**, 73 (2015).

[12] A. Drozdov, P. Kong, V. Minkov, S. Besedin, M. Kuzovnikov, S. Mozaffari, L. Balicas, F. Balakirev, D. Graf, V. Prakapenka, *et al.*, Superconductivity at 250 k in lanthanum hydride under high pressures, Nature **569**, 528 (2019).

[13] E. Tang, J.-W. Mei, and X.-G. Wen, High-temperature fractional quantum hall states, Physical review letters **106**, 236802 (2011).

[14] T. Neupert, L. Santos, C. Chamon, and C. Mudry, Fractional quantum hall states at zero magnetic field, Physical review letters **106**, 236804 (2011).

[15] D. Sheng, Z.-C. Gu, K. Sun, and L. Sheng, Fractional quantum hall effect in the absence of landau levels, Nature communications **2**, 1 (2011).

[16] N. Regnault and B. A. Bernevig, Fractional chern insulator, Physical Review X **1**, 021014 (2011).

[17] L. Balents, C. R. Dean, D. K. Efetov, and A. F. Young, Superconductivity and strong correlations in moiré flat bands, Nature Physics **16**, 725 (2020).

[18] V. Peri, Z.-D. Song, B. A. Bernevig, and S. D. Huber, Fragile topology and flat-band superconductivity in the strong-coupling regime, Physical review letters **126**, 027002 (2021).

[19] J.-W. Rhim, K. Kim, and B.-J. Yang, Quantum distance and anomalous landau levels of flat bands, Nature **584**, 59 (2020).

[20] F. Xie, Z. Song, B. Lian, and B. A. Bernevig, Topology-bounded superfluid weight in twisted bilayer graphene, Physical review letters **124**, 167002 (2020).

[21] S. Peotta and P. Törmä, Superfluidity in topologically nontrivial flat bands, Nature communications **6**, 1 (2015).

[22] B. Bradlyn, L. Elcoro, J. Cano, M. G. Vergniory, Z. Wang, C. Felser, M. I. Aroyo, and B. A. Bernevig, Topological quantum chemistry, Nature **547**, 298 (2017).

[23] Y. Xu, L. Elcoro, Z.-D. Song, M. Vergniory, C. Felser, S. S. Parkin, N. Regnault, J. L. Mañes, and B. A. Bernevig, Filling-enforced obstructed atomic insulators, arXiv preprint arXiv:2106.10276 (2021).

[24] A. Mielke, Exact ground states for the hubbard model on the kagome lattice, Journal of Physics A: Mathematical and General **25**, 4335 (1992).

[25] H. Tasaki, From Nagaoka's Ferromagnetism to Flat-Band Ferromagnetism and Beyond: An Introduction to Ferromagnetism in the Hubbard Model, Progress of Theoretical Physics **99**, 489 (1998).

[26] D. L. Bergman, C. Wu, and L. Balents, Band touching from real-space topology in frustrated hopping models, Phys. Rev. B **78**, 125104 (2008).

[27] Z. Liu, F. Liu, and Y.-S. Wu, Exotic electronic states in the world of flat bands: From theory to material, Chinese Physics B **23**, 077308 (2014).

[28] D.-S. Ma, Y. Xu, C. S. Chiu, N. Regnault, A. A. Houck, Z. Song, and B. A. Bernevig, Spin-orbit-induced topological flat bands in line and split graphs of bipartite lattices, Phys. Rev. Lett. **125**, 266403 (2020).

[29] C. S. Chiu, D.-S. Ma, Z.-D. Song, B. A. Bernevig, and A. A. Houck, Fragile topology in line-graph lattices with two, three, or four gapped flat bands, Phys. Rev. Research **2**, 043414 (2020).

[30] Inorganic Crystal Structure Database (ICSD), (Fachinformationszentrum Karlsruhe, Karlsruhe, Germany, 2015).

[31] P. Hohenberg and W. Kohn, Inhomogeneous electron gas, Phys. Rev. **136**, B864 (1964).

[32] W. Kohn and L. J. Sham, Self-consistent equations including exchange and correlation effects, Phys. Rev. **140**, A1133 (1965).

[33] G. Kresse and J. Hafner, *Ab initio* molecular dynamics for open-shell transition metals, Phys. Rev. B **48**, 13115 (1993).

[34] G. Kresse and J. Furthmüller, Efficiency of ab-initio total energy calculations for metals and semiconductors using a plane-wave basis set, Computational Materials Science **6**, 15 (1996).

[35] S. Ivantchev, E. Kroumova, G. Madariaga, J. M. Pérez-Mato, and M. I. Aroyo, *SUBGROUPGRAPH*: a computer program for analysis of group–subgroup relations between space groups, Journal of Applied Crystallography **33**, 1190 (2000).

[36] S. Ivantchev, E. Kroumova, M. I. Aroyo, J. M. Perez-Mato, J. M. Igartua, G. Madariaga, and H. Won-

dratschek, *SUPERGROUPS* – a computer program for the determination of the supergroups of the space groups, Journal of Applied Crystallography **35**, 511 (2002).

[37] I. Souza, N. Marzari, and D. Vanderbilt, Maximally localized wannier functions for entangled energy bands, Phys. Rev. B **65**, 035109 (2001).

[38] H. C. Po, A. Vishwanath, and H. Watanabe, Symmetry-based indicators of band topology in the 230 space groups, Nature Communications **8**, 50 (2017).

[39] J. Kruthoff, J. de Boer, J. van Wezel, C. L. Kane, and R.-J. Slager, Topological Classification of Crystalline Insulators through Band Structure Combinatorics, Physical Review X **7**, 041069 (2017).

[40] A. M. Turner, Y. Zhang, and A. Vishwanath, Entanglement and inversion symmetry in topological insulators, Phys. Rev. B **82**, 241102 (2010).

[41] T. L. Hughes, E. Prodan, and B. A. Bernevig, Inversion-symmetric topological insulators, Phys. Rev. B **83**, 245132 (2011).

[42] C. Fang, M. J. Gilbert, and B. A. Bernevig, Bulk topological invariants in noninteracting point group symmetric insulators, Phys. Rev. B **86**, 115112 (2012).

[43] H. C. Po, H. Watanabe, and A. Vishwanath, Fragile topology and wannier obstructions, Phys. Rev. Lett. **121**, 126402 (2018).

[44] J. Cano, B. Bradlyn, Z. Wang, L. Elcoro, M. G. Vergniory, C. Felser, M. I. Aroyo, and B. A. Bernevig, Topology of disconnected elementary band representations, Phys. Rev. Lett. **120**, 266401 (2018).

[45] A. Bouhon, A. M. Black-Schaffer, and R.-J. Slager, Wilson loop approach to fragile topology of split elementary band representations and topological crystalline insulators with time-reversal symmetry, Phys. Rev. B **100**, 195135 (2019).

[46] B. Bradlyn, Z. Wang, J. Cano, and B. A. Bernevig, Disconnected elementary band representations, fragile topology, and Wilson loops as topological indices: An example on the triangular lattice, Physical Review B **99**, 045140 (2019).

[47] Z.-D. Song, L. Elcoro, Y.-F. Xu, N. Regnault, and B. A. Bernevig, Fragile Phases as Affine Monoids: Classification and Material Examples, Physical Review X **10**, 031001 (2020), publisher: American Physical Society.

[48] Y. Hwang, J. Ahn, and B.-J. Yang, Fragile topology protected by inversion symmetry: Diagnosis, bulk-boundary correspondence, and wilson loop, Phys. Rev. B **100**, 205126 (2019).

[49] A. Alexandradinata, J. Höller, C. Wang, H. Cheng, and L. Lu, Crystallographic splitting theorem for band representations and fragile topological photonic crystals, Physical Review B **102**, 115117 (2020).

[50] Z. Song, T. Zhang, Z. Fang, and C. Fang, Quantitative mappings between symmetry and topology in solids, Nature Communications **9**, 3530 (2018).

[51] Z. Song, T. Zhang, and C. Fang, Diagnosis for Nonmagnetic Topological Semimetals in the Absence of Spin-Orbital Coupling, Physical Review X **8**, 031069 (2018).

[52] E. Khalaf, H. C. Po, A. Vishwanath, and H. Watanabe, Symmetry indicators and anomalous surface states of topological crystalline insulators, Phys. Rev. X **8**, 031070 (2018).

[53] J.-W. Rhim and B.-J. Yang, Classification of flat bands according to the band-crossing singularity of bloch wave functions, Phys. Rev. B **99**, 045107 (2019).

[54] H. C. Po, L. Zou, T. Senthil, and A. Vishwanath, Faithful tight-binding models and fragile topology of magic-angle bilayer graphene, Phys. Rev. B **99**, 195455 (2019).

[55] D. Leykam, A. Andreanov, and S. Flach, Artificial flat band systems: from lattice models to experiments, Advances in Physics: X **3**, 1473052 (2018).

[56] Z.-D. Song, L. Elcoro, Y.-F. Xu, N. Regnault, and B. A. Bernevig, Fragile phases as affine monoids: Classification and material examples, Phys. Rev. X **10**, 031001 (2020).

[57] N. Claussen, B. A. Bernevig, and N. Regnault, Detection of topological materials with machine learning, Phys. Rev. B **101**, 245117 (2020).

[58] G. Kresse and D. Joubert, From ultrasoft pseudopotentials to the projector augmented-wave method, Phys. Rev. B **59**, 1758 (1999).

[59] J. P. Perdew, K. Burke, and M. Ernzerhof, Generalized gradient approximation made simple, Phys. Rev. Lett. **77**, 3865 (1996).

[60] D. Hobbs, G. Kresse, and J. Hafner, Fully unconstrained noncollinear magnetism within the projector augmented-wave method, Phys. Rev. B **62**, 11556 (2000).

[61] M. G. Vergniory, L. Elcoro, Z. Wang, J. Cano, C. Felser, M. I. Aroyo, B. A. Bernevig, and B. Bradlyn, Graph theory data for topological quantum chemistry, Phys. Rev. E **96**, 023310 (2017).

[62] S. Kirklin, J. E. Saal, B. Meredig, A. Thompson, J. W. Doak, M. Aykol, S. Rühl, and C. Wolverton, The open quantum materials database (oqmd): assessing the accuracy of dft formation energies, npj Computational Materials **1**, 1 (2015).

[63] S. P. Ong, W. D. Richards, A. Jain, G. Hautier, M. Kocher, S. Cholia, D. Gunter, V. L. Chevrier, K. A. Persson, and G. Ceder, Python materials genomics (pymatgen): A robust, open-source python library for materials analysis, Computational Materials Science **68**, 314 (2013).

[64] A. Togo and I. Tanaka, `Spglib`: a software library for crystal symmetry search (2018), arXiv:1808.01590 [cond-mat.mtrl-sci].

[65] S. Piskunov, E. Kotomin, E. Heifets, J. Maier, R. Eglitis, and G. Borstel, Hybrid dft calculations of the atomic and electronic structure for abo3 perovskite (0 0 1) surfaces, Surface Science **575**, 75 (2005).

[66] T. Jia, Z. Zeng, H. Lin, Y. Duan, and P. Ohodnicki, First-principles study on the electronic, optical and thermodynamic properties of abo 3 (a= la, sr, b= fe, co) perovskites, Rsc Advances **7**, 38798 (2017).

[67] R. I. Eglitis and A. I. Popov, Systematic trends in (0 0 1) surface ab initio calculations of abo3 perovskites, Journal of Saudi Chemical Society **22**, 459 (2018).

[68] N. P. Quirk, L. T. Nguyen, J. H. ant R. J. Cava, and N. P. Ong, *In preparation*.

[69] C. Barreteau, F. Ducastelle, and T. Mallah, A bird's eye view on the flat and conic band world of the honeycomb and kagome lattices: towards an understanding of 2d metal-organic frameworks electronic structure, Journal of Physics: Condensed Matter **29**, 465302 (2017).

[70] C. Fang and L. Fu, New classes of topological crystalline insulators having surface rotation anomaly, Science advances **5**, eaat2374 (2019).

[71] S. L. Dudarev, G. A. Botton, S. Y. Savrasov, C. J.

Humphreys, and A. P. Sutton, Electron-energy-loss spectra and the structural stability of nickel oxide: An lsda+u study, Phys. Rev. B **57**, 1505 (1998).

[72] J. Longo, P. Raccah, and J. Goodenough, Magnetic properties of srruo3 and caruo3, Journal of Applied Physics **39**, 1327 (1968).

[73] S. Bushmeleva, V. Y. Pomjakushin, E. Pomjakushina, D. Sheptyakov, and A. Balagurov, Evidence for the band ferromagnetism in srruo3 from neutron diffraction, Journal of magnetism and magnetic materials **305**, 491 (2006).

[74] G. Cao, S. McCall, M. Shepard, J. Crow, and R. Guertin, Thermal, magnetic, and transport properties of single-crystal sr 1- x ca x ruo 3 (0¡˜ x¡˜ 1. 0), Physical Review B **56**, 321 (1997).

[75] R. A. Lalancette, N. Elliott, and I. Bernal, Crystal structures and magnetic properties of a 2 mncl 6 salts (a= nh 4+, k+ and rb+), Journal of Crystal and Molecular Structure **2**, 143 (1972).

[76] M. Faizan, S. Khan, G. Murtaza, A. Khan, and A. Laref, Electronic and magnetic properties of alkali metal chlorides a2mcl6 (a= k, rb, cs; m= mn, mo): A density functional theory study, International Journal of Modern Physics B **33**, 1950072 (2019).

[77] C. Khattak, D. Cox, and F. Wang, Magnetic ordering in ba2mnreo6, Journal of Solid State Chemistry **13**, 77 (1975).

[78] M. Otto, R. Van Woerden, P. Van der Valk, J. Wijngaard, C. Van Bruggen, C. Haas, and K. Buschow, Half-metallic ferromagnets. i. structure and magnetic properties of nimnsb and related inter-metallic compounds, Journal of Physics: Condensed Matter **1**, 2341 (1989).

[79] A. Jain, S. P. Ong, G. Hautier, W. Chen, W. D. Richards, S. Dacek, S. Cholia, D. Gunter, D. Skinner, G. Ceder, and K. a. Persson, The Materials Project: A materials genome approach to accelerating materials innovation, APL Materials **1**, 011002 (2013).

[80] M. Tanifuji, A. Matsuda, and H. Yoshikawa, Materials data platform - a fair system for data-driven materials science, in *2019 8th International Congress on Advanced Applied Informatics (IIAI-AAI)* (2019) pp. 1021–1022.

[81] V. Jovic, R. J. Koch, S. K. Panda, H. Berger, P. Bugnon, A. Magrez, R. Thomale, K. E. Smith, S. Biermann, C. Jozwiak, A. Bostwick, E. Rotenberg, D. D. Sante, and S. Moser, The dirac nodal line network in non-symmorphic rutile semimetal ruo$_2$ (2019), arXiv:1908.02621 [cond-mat.mes-hall].

[82] J.-C. Crivello and V. Paul-Boncour, Relation between the weak itinerant magnetism in a2ni7 compounds (a=y, la) and their stacked crystal structures, Journal of Physics: Condensed Matter **32**, 145802 (2020).

[83] Z. Liu, S. Yang, H. Su, L. Zhou, X. Lu, Z. Liu, J. Gao, Y. Huang, D. Shen, Y. Guo, H. Weng, and S. Wang, Non-fermi-liquid behavior and saddlelike flat band in the layered ferromagnet alfe$_2$b$_2$, Phys. Rev. B **101**, 245129 (2020).

[84] H. Liu, Y. Cao, Y. Xu, D. J. Gawryluk, E. Pomjakushina, S.-Y. Gao, P. Dudin, M. Shi, L. Yan, Y.-f. Yang, and H. Ding, Observation of flat bands due to band hybridization in the 3*d*-electron heavy-fermion compound CaCu$_3$Ru$_4$o$_{12}$, Phys. Rev. B **102**, 035111 (2020).

[85] J.-X. Yin, S. S. Zhang, G. Chang, Q. Wang, S. S. Tsirkin, Z. Guguchia, B. Lian, H. Zhou, K. Jiang, I. Belopolski, *et al.*, Negative flat band magnetism in a spin–orbit-coupled correlated kagome magnet, Nature Physics **15**, 443 (2019).

[86] Y. Xu, J. Zhao, C. Yi, Q. Wang, Q. Yin, Y. Wang, X. Hu, L. Wang, E. Liu, G. Xu, and et al., Electronic correlations and flattened band in magnetic weyl semimetal candidate co3sn2s2, Nature Communications **11**, 10.1038/s41467-020-17234-0 (2020).

[87] M. Kang, S. Fang, L. Ye, H. C. Po, J. Denlinger, C. Jozwiak, A. Bostwick, E. Rotenberg, E. Kaxiras, J. G. Checkelsky, and et al., Topological flat bands in frustrated kagome lattice cosn, Nature Communications **11**, 10.1038/s41467-020-17465-1 (2020).

[88] Z. Liu, M. Li, Q. Wang, G. Wang, C. Wen, K. Jiang, X. Lu, S. Yan, Y. Huang, D. Shen, J.-X. Yin, Z. Wang, Z. Yin, H. Lei, and S. Wang, Orbital-selective dirac fermions and extremely flat bands in frustrated kagome-lattice metal cosn, Nature Communications **11**, 4002 (2020).

[89] B. C. Sales, W. R. Meier, A. F. May, J. Xing, J.-Q. Yan, S. Gao, Y. H. Liu, M. B. Stone, A. D. Christianson, Q. Zhang, and M. A. McGuire, Tuning the flat bands of the kagome metal cosn with fe, in, or ni doping, Phys. Rev. Materials **5**, 044202 (2021).

[90] J. G. Azadani, W. Jiang, J.-P. Wang, and T. Low, Ferromagnetic phase of the spinel compound mgv$_2$o4 and its spintronics properties, Phys. Rev. B **102**, 155144 (2020).

[91] S. Park, S. Kang, H. Kim, K. H. Lee, P. Kim, S. Sim, N. Lee, B. Karuppannan, J. Kim, J. Kim, K. I. Sim, M. J. Coak, Y. Noda, C.-H. Park, J. H. Kim, and J.-G. Park, Kagome van-der-waals pd3p2s8 with flat band (2020), arXiv:2011.09357 [cond-mat.mtrl-sci].

[92] K.-H. Ahn, W. E. Pickett, and K.-W. Lee, Coexistence of triple nodal points, nodal links, and unusual flat bands in intermetallic aPd$_3$ (a = Pb, sn), Phys. Rev. B **98**, 035130 (2018).

[93] M. A. Khan, P.-H. Chang, N. Ghimire, T. M. Bretz-Sullivan, A. Bhattacharya, J. S. Jiang, J. Singleton, and J. F. Mitchell, Fermi surface topology and nontrivial berry phase in the flat-band semimetal pd$_3$Pb, Phys. Rev. B **101**, 245113 (2020).

[94] M. G. Yamada and G. Jackeli, Magnetic and electronic properties of spin-orbit coupled dirac electrons on a (001) thin film of double-perovskite sr2femoo6, Physical Review Materials **4**, 10.1103/physrevmaterials.4.074007 (2020).

[95] T. Y. Yang, Q. Wan, Y. H. Wang, M. Song, J. Tang, Z. W. Wang, H. Z. Lv, N. C. Plumb, M. Radovic, G. W. Wang, G. Y. Wang, Z. Sun, R. Yu, M. Shi, Y. M. Xiong, and N. Xu, Evidence of orbit-selective electronic kagome lattice with planar flat-band in correlated paramagnetic ycr6ge6 (2019), arXiv:1906.07140 [cond-mat.mtrl-sci].

[96] Q. Wang, Y. Xu, R. Lou, Z. Liu, M. Li, Y. Huang, D. Shen, H. Weng, S. Wang, and H. Lei, Large intrinsic anomalous hall effect in half-metallic ferromagnet co 3 sn 2 s 2 with magnetic weyl fermions, Nature communications **9**, 1 (2018).

[97] E. Liu, Y. Sun, N. Kumar, L. Muechler, A. Sun, L. Jiao, S.-Y. Yang, D. Liu, A. Liang, Q. Xu, *et al.*, Giant anomalous hall effect in a ferromagnetic kagome-lattice semimetal, Nature physics **14**, 1125 (2018).

[98] T. Graf, C. Felser, and S. S. Parkin, Simple rules for the understanding of heusler compounds, Progress in solid state chemistry **39**, 1 (2011).

[99] Y. Kurosaki, S. Yabuuchi, A. Nishide, N. Fukatani, and J. Hayakawa, Crystal growth and flat-band effects on thermoelectric properties of fe2tial-based full-heusler thin films, AIP Advances **10**, 115313 (2020).

[100] T. Klimczuk, C. Wang, K. Gofryk, F. Ronning, J. Winterlik, G. H. Fecher, J.-C. Griveau, E. Colineau, C. Felser, J. D. Thompson, *et al.*, Superconductivity in the heusler family of intermetallics, Physical Review B **85**, 174505 (2012).

[101] J. Winterlik, G. H. Fecher, C. Felser, M. Jourdan, K. Grube, F. Hardy, H. Von Löhneysen, K. Holman, and R. Cava, Ni-based superconductor: Heusler compound zrni 2 ga, Physical Review B **78**, 184506 (2008).

[102] J. Winterlik, G. H. Fecher, and C. Felser, Electronic and structural properties of palladium-based heusler superconductors, Solid state communications **145**, 475 (2008).

[103] C. Felser, Metal–metal distances, electron counts, and superconducting tc's in am2b2c, Journal of Solid State Chemistry **160**, 93 (2001).

[104] C. Timm, A. Schnyder, D. Agterberg, and P. Brydon, Inflated nodes and surface states in superconducting half-heusler compounds, Physical Review B **96**, 094526 (2017).

[105] Y. Nakajima, R. Hu, K. Kirshenbaum, A. Hughes, P. Syers, X. Wang, K. Wang, R. Wang, S. R. Saha, D. Pratt, *et al.*, Topological rpdbi half-heusler semimetals: A new family of noncentrosymmetric magnetic superconductors, Science advances **1**, e1500242 (2015).

[106] O. Pavlosiuk, D. Kaczorowski, X. Fabreges, A. Gukasov, and P. Wiśniewski, Antiferromagnetism and superconductivity in the half-heusler semimetal hopdbi, Scientific reports **6**, 1 (2016).

[107] C. Fu, S. Bai, Y. Liu, Y. Tang, L. Chen, X. Zhao, and T. Zhu, Realizing high figure of merit in heavy-band p-type half-heusler thermoelectric materials, Nature communications **6**, 1 (2015).

[108] W. G. Zeier, J. Schmitt, G. Hautier, U. Aydemir, Z. M. Gibbs, C. Felser, and G. J. Snyder, Engineering half-heusler thermoelectric materials using zintl chemistry, Nature Reviews Materials **1**, 1 (2016).

[109] M. Pena and J. Fierro, Chemical structures and performance of perovskite oxides, Chemical reviews **101**, 1981 (2001).

[110] H. W. Eng, P. W. Barnes, B. M. Auer, and P. M. Woodward, Investigations of the electronic structure of d0 transition metal oxides belonging to the perovskite family, Journal of Solid State Chemistry **175**, 94 (2003).

[111] T. Atou, H. Chiba, K. Ohoyama, Y. Yamaguchi, and Y. Syono, Structure determination of ferromagnetic perovskite bimno3, Journal of Solid State Chemistry **145**, 639 (1999).

[112] D. Meng, H. Guo, Z. Cui, C. Ma, J. Zhao, J. Lu, H. Xu, Z. Wang, X. Hu, Z. Fu, *et al.*, Strain-induced high-temperature perovskite ferromagnetic insulator, Proceedings of the National Academy of Sciences **115**, 2873 (2018).

[113] T. Goto, Y. Yamasaki, H. Watanabe, T. Kimura, and Y. Tokura, Anticorrelation between ferromagnetism and ferroelectricity in perovskite manganites, Physical Review B **72**, 220403 (2005).

[114] H. Liu and X. Yang, A brief review on perovskite multiferroics, Ferroelectrics **507**, 69 (2017).

[115] A. Filippetti and N. A. Hill, Coexistence of magnetism and ferroelectricity in perovskites, Physical Review B **65**, 195120 (2002).

[116] J. G. Bednorz and K. A. Müller, Possible high t c superconductivity in the ba- la- cu- o system, Zeitschrift für Physik B Condensed Matter **64**, 189 (1986).

[117] T. He, Q. Huang, A. Ramirez, Y. Wang, K. Regan, N. Rogado, M. Hayward, M. Haas, J. Slusky, K. Inumara, *et al.*, Superconductivity in the non-oxide perovskite mgcni 3, Nature **411**, 54 (2001).

[118] R. Cava, B. Batlogg, J. Krajewski, R. Farrow, L. J. Rupp, A. White, K. Short, W. Peck, and T. Kometani, Superconductivity near 30 k without copper: the ba 0.6 k 0.4 bio 3 perovskite, Nature **332**, 814 (1988).

[119] A. E. Maughan, A. M. Ganose, D. O. Scanlon, and J. R. Neilson, Perspectives and design principles of vacancy-ordered double perovskite halide semiconductors, Chemistry of Materials **31**, 1184 (2019).

[120] N. R. Wolf, B. A. Connor, A. H. Slavney, and H. I. Karunadasa, Doubling the stakes: The promise of halide double perovskites, Angewandte Chemie International Edition (2021).

[121] L. M. Schoop, L. Müchler, C. Felser, and R. Cava, Lone pair effect, structural distortions, and potential for superconductivity in tl perovskites, Inorganic chemistry **52**, 5479 (2013).

[122] A. K. Eriksson, S.-G. Eriksson, S. Ivanov, C. S. Knee, J. Eriksen, H. Rundlöf, and M. Tseggai, High temperature phase transition of the magnetoelectric double perovskite sr2nimoo6 by neutron diffraction, Materials research bulletin **41**, 144 (2006).

[123] M. J. Martínez-Lope, J. A. Alonso, and M. T. Casais, Synthesis, crystal and magnetic structure of the double perovskites a2nimoo6 (a= sr, ba): A neutron diffraction study, European Journal of Inorganic Chemistry **2003**, 2839 (2003).

[124] L. Jiao, Q. Xu, Y. Cheon, Y. Sun, C. Felser, E. Liu, and S. Wirth, Signatures for half-metallicity and nontrivial surface states in the kagome lattice weyl semimetal co 3 sn 2 s 2, Physical Review B **99**, 245158 (2019).

[125] W. M. Skinner, G. Qian, and A. N. Buckley, Electronic environments in ni3pb2s2 (shandite) and its initial oxidation in air, Journal of Solid State Chemistry **206**, 32 (2013).

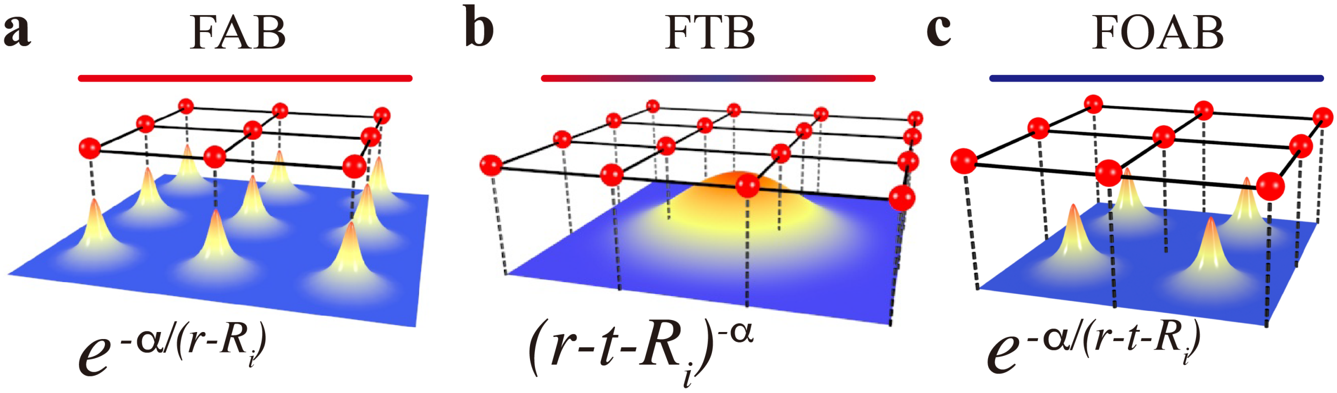

Figure 1. An illustration of the three possible types of flat bands. (a) Flat atomic band (FAB): the Wannier functions associated to the flat bands are exponentially localized on the atoms' sites. (b) Flat topological band (FTB): the Bloch states are extended (with potentially a power law decay) in at least one direction of the lattice. (c) Flat obstructed atomic band (FOAB): as opposed to FAB, the corresponding Wannier functions are exponentially localized but on an empty site. In the figures, the atom sites of the 2D lattices are represented with red spheres. Below the lattices are the Bloch wave functions of the flat bands associated with their decay law, where R_i is the position of atom i, t is a fractional lattice vector and α is a positive coefficient.

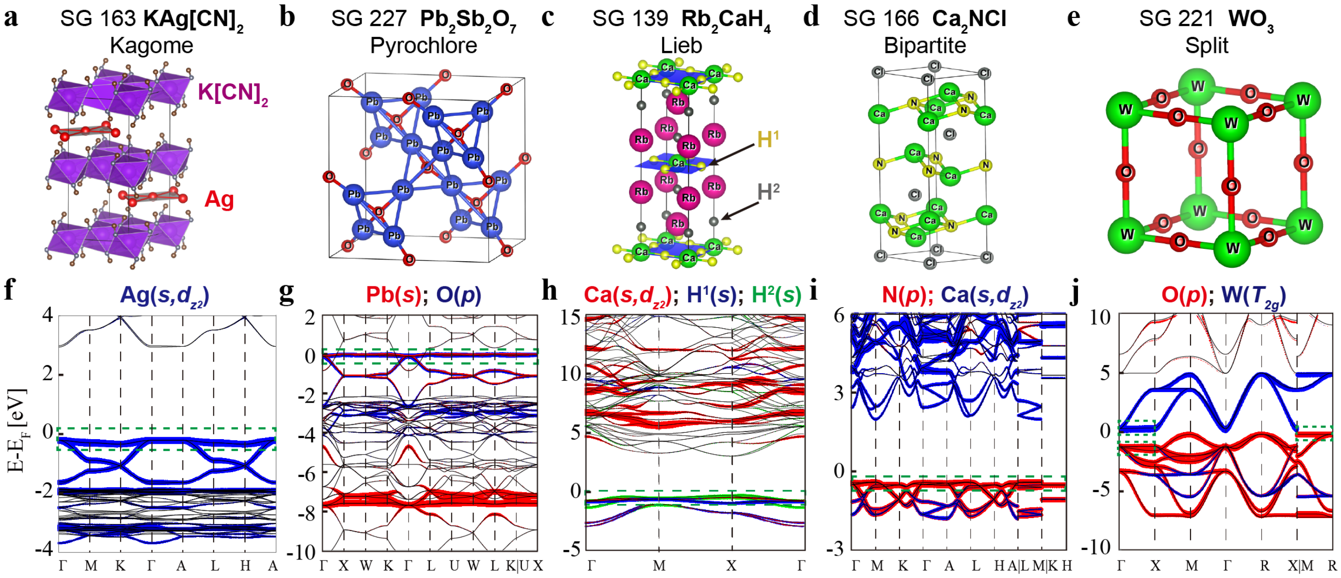

Figure 2. Crystal and band structures of the representative flat-band materials. The crystal structures of (a) KAg[CN]$_2$ which hosts an approximate Kagome sublattice formed by the Ag atoms (in red color), (b) Pb$_2$Sb$_2$O$_7$ with Pb atoms at the Wyckoff position 16d forming a pyrochlore sublattice, (c) Rb$_2$CaH$_4$ with the H atoms at 4c (*i.e.*, the H^1 atoms in yellow color) and the Ca atoms at 2a position forming a Lieb sublattice, (d) Ca$_2$NCl which is stacked by alternating the Ca$_2$N and Cl layers, where the Ca$_2$N layer is identified as a bipartite sublattice in our algorithm, (e) WO$_3$ with the W and O atoms forming a split lattice. For each material, its band structure and the orbital characterization of the flat bands is plotted and analyzed below its crystal structure. Based on the band structure analysis, the flat bands close to the Fermi level are explained by the S-matrix method in Appendix F. In the crystal structure plots, SG, chemical formula and the type of sublattice host in the material are provided on the top of each panel. In the band structure plots, the flat-band segments close to the Fermi level are indicated by the dashed green lines. Orbital characters of the colored bands are provided on the top of each panel.

	All ICSDs	Curated	Best
# ICSDs	55,206	6,338	949
# Materials	28,169	2,379	345
Kagome	6,120 (11.09%)	1,699 (26.81%)	516 (54.37%)
Pyrochlore	1,666 (3.02%)	296 (4.67%)	77 (8.11%)
Lieb	1,590 (2.88%)	721 (11.38%)	151 (15.91%)
Bipartite	21,175 (38.36%)	3,138 (49.51%)	432 (45.52%)
Split	8,224 (14.90%)	1,920 (30.29%)	354 (37.30%)
None	31,154 (56.43%)	2,582 (40.74%)	248 (26.13%)

Table I. Statistics of the ICSD entries in the database hosting at least one sublattice for each lattice type. In the first row, we give the number of ICSDs entries for the database (first column), for the list of curated flat-band materials (second column) and for the best representative flat-band materials (third column). The second line provides the number of unique materials for the database, the list of curated flat-band materials and the best representative flat-band materials. The third, fourth, fifth, sixth and seventh rows are the statistics for the Kagome, pyrochlore, Lieb, bipartite with different number of atoms on sublattices and split lattices. An ICSD entry is considered as hosting a given type of lattice if the algorithms discussed in Section II B have found at least one such a lattice irrespective of the cutoffs or being a rigorous or approximate sublattice. Note that an ICSD entry might host more than one type of sublattices. The eighth row provides the statistics for the ICSDs where no sublattices have been detected. For each column, the percentages are computed with respect to the number of ICSDs provided in the first row.

Supplementary Information for "Catalogue of Flat-Band Stoichiometric Materials"

CONTENTS

LIST OF TABLES

Appendix A: Introduction to the Supplementary Information

In this work, we have presented a catalogue of stoichiometric materials hosting flat bands near the Fermi energy. In addition to the main text, we provide below Supplementary Appendices giving an in-depth discussion of our methodology and several lists of curated materials. Appendix B is devoted to the detailed definition of two types of flat bands: flat atomic bands and flat topological bands. In Appendix C, we give an overview of the Topological Quantum Chemistry website on which we rely on for our catalogue of flat-band materials. We present the Materials Flatband Database website and the theory and algorithms for the detection of flat-band segments and density of states peaks. We also provide detailed statistics about the materials hosting the five types of sublattices leading to flat bands (namely the Kagome, pyrochlore, generic bipartite, split and Lieb lattices). We then present Appendices about these five types of sublattices. Appendix D focuses on Kagome, pryochlore and Lieb sublattices. We cover both the crystal symmetries of these lattices, the three dimensional space groups compatible with them and their geometrical features. We also detail the algorithms we have designed for a high throughput search in our database of materials. In Appendix E, we give a short overview of the bipartite and split lattices and most specifically of our new theoretical method for finding flat bands, the S-matrix method, detailed in[6]. We present all the technical details of the algorithms we build in order to automatically look for bipartite and split sublattices in our material database. In Appendix F, we provide the theoretical explanations for the presence of flat bands in seven prototypical materials: WO_3 [ICSD 108651, SG 221 ($Pm\bar{3}m$)], $Pb_2Sb_2O_7$ [ICSD 27120, SG 227 ($Fd\bar{3}m$)], $CaNi_5$ [ICSD 54474, SG 191 ($P6/mmm$)], Ca_2NCl [ICSD 62555, SG 166 ($R\bar{3}m$)], Rb_2CaH_4 [ICSD 65196, SG 139 ($I4/mmm$)], $KAg[CN]_2$ [ICSD 30275, SG 163 ($P\bar{3}1c$)] and $RbMo_3S_3$ [ICSD 644175, SG 176 ($P6_3/m$)]. To test the validity of our high-throughput search based on paramagnetic calculations for potentially magnetic materials, we study in Appendix G four materials using ab-initio calculation with on-site Hubbard interaction for d and f electrons, namely $SrRuO_3$[ICSD 69360, SG 221 ($Pm\bar{3}m$)], Rb_2MnCl_6[ICSD 9347 SG 225 ($Fm\bar{3}m$)], Ba_2MnReO_6[ICSD 4169 SG 225 ($Fm\bar{3}m$)] and NiMnSb [ICSD 54255, SG 216 ($F\bar{4}3m$). With magnetizations close to their experimental values, the flat band features are barely affected. Finally in Appendix H, we give a list of 2,379 manually curated materials with flat bands near the Fermi energy. For convenience, materials with flat atomic bands are separated from the ones with flat bands occur from wave function interference. Moreover we have selected 345 compounds hosting the most remarkable flat bands and we provide their band structure and density of states.

Appendix B: Flat bands with different topologies

In real materials, electronic bands can be flat in the entire Brillouin zone (BZ) or only be flatten along some specific high-symmetry paths. In this appendix, we provide a detailed description of the two types of flat bands, namely the flat atomic bands and the flat topological bands, and provide several mechanisms that could give rise to them.

1. Flat atomic bands

In crystalline materials, a set of bands that are flat in all directions or some particular directions is referred to as flat atomic bands if they form a band representation (BR) that can be induced from local orbitals. The flat atomic bands are induced from local orbitals and hence by definition have a *trivial* topology[22,38,39]. However, in practice, it is difficult to fully determine whether a set of bands is a BR: the full determination requires the Bloch wave functions over the whole Brillouin zone. Instead, we use the symmetry eigenvalues (the representations formed by the Bloch bands) to diagnose whether a set of bands is *consistent* with a BR. When the symmetry eigenvalues of a set of flat bands are consistent with a BR induced from local orbitals, we *label* the set of bands as flat atomic bands. With this approach, it is possible that some bands labeled as flat atomic bands are nevertheless topological with some topology not diagnosed by symmetry eigenvalues. A simple example is a 2D Chern insulator with inversion symmetry. When the Chern number is odd, the inversion eigenvalues are not consistent with any BR[40–42]. However, when the Chern number is even, the inversion eigenvalues can be the same as the eigenvalues of some BRs.

When the flat atomic bands are flat in *all* the directions, the flat atomic bands are in the atomic limit, where the hopping between some orbitals of neighboring atoms is infinitesimal, as illustrated in Fig. 1(a) of the main text. In Appendix H 2, we provide a list of manually selected materials hosting flat atomic bands.

As an example of flat atomic bands, we consider the compound $Al_{12}Ca_8O_{24}S_2$ [ICSD 67589, SG 217 ($I\bar{4}3m$)] shown in Fig. 3. It has several flat bands below the Fermi level (with band index $-6 \sim -1$). The BR of these bands are induced from the orbitals $\bar{E}_2 \oplus \bar{F}$ at $2a$ position, which are occupied by S atoms. In Fig. 3, we plot the atom-projected band structure and density of states of the compound $Al_{12}Ca_8O_{24}S_2$. We find that the flat bands arise from the S atom orbitals, as indicated by the green lines. The flatness of the p bands of S atoms is due to two reasons: on one

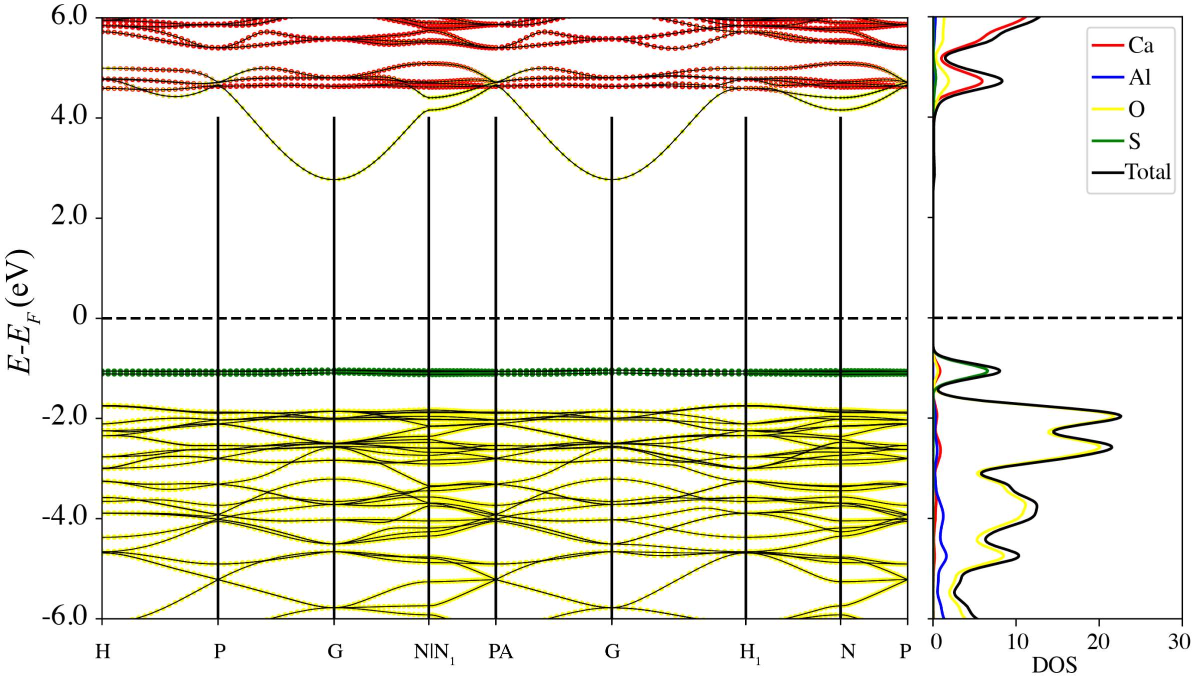

Figure 3. Atom-projected band structure along the high-symmetry path (left panel) and density of states (right panel) for $Al_{12}Ca_8O_{24}S_2$ [ICSD 67589, SG 217 ($I\bar{4}3m$)]. The weight of orbitals on Ca, Al, O and S atoms are represented by the red, blue, yellow and green points and lines, respectively.

hand, there is a big enough difference of the onsite energy between the p orbitals on S and the orbitals on other atoms; on the other hand, the distance between two neighboring S atoms (about 8Å) is so large that the kinetic energy between the S p orbitals is small. Hence, the flat bands contributed by the p orbitals of S are flat atomic bands.

The flat atomic bands that are flat only in one or two directions can be understood as layered systems, where the inter-layer kinetic energy is weak. In this case, all bands are flat along the inter-layer direction(s). When the bands are flat in one (two) direction(s), each "layer" is a 2D plane (1D chain).

Note that heavy fermion systems may host another class of flat bands in the atomic limit. These bands are formed by localized $4f$ or $5f$ orbitals and are extremely flat. As the mean field approximation adopted in the first principle calculations fails to characterize the strong correlation of f electron, we ignore the heavy fermion systems in this work as we will discuss in Appendix C.

2. Flat topological bands

Apart from the flat atomic bands defined in Appendix B 1, the flat bands might be topologically nontrivial: when a set of bands that are flat in all or some particular directions do not form any BR, *i.e.*, cannot be induced from local orbitals, the set of bands forms a set of flat topological bands. Since by the definition the topological bands are not equivalent to any local orbitals, the Wannier functions of the topological bands that preserve the symmetry of the system must be extended, *i.e.*, not exponentially localized, as shown in Fig. 1(b) of the main text. In this work and as explained in the last subsection, we only make use of symmetry eigenvalues to diagnose the topology. Hence a set of flat topological bands might potentially be misdiagnosed as flat atomic bands. However, all the diagnosed flat topological bands must be topological.

There are two types of flat topological bands: the stable topological bands and the fragile topological bands[43–49]. The former is realized as a non-integer linear combination (NLC) of elementary BR (EBR) or split elementary BR (SEBR)[22,38,39,50–52], and the later can be realized as a difference (but not a sum) of EBRs. Since we only rely on symmetry eigenvalues, a flat stable topological band could be labeled as fragile in this work if its symmetry eigenvalues are consistent with a difference of EBRs. On the contrary, all bands labeled as stable topological must be stable topological because by definition their symmetry eigenvalues are not consistent with any BR or difference of BRs. Exact flat fragile bands have been found in several lattice models[29,53,54]. The S-matrix method introduced in Appendix E and in Ref.[6] is a general mechanism to generate exact flat fragile bands. On the other hand, no examples of rigorously flat (*i.e.*, dispersionless) stable topological bands have yet been found with compact support hopping. Nevertheless, quasi-flat stable topological bands were recently found in line-graph and split-line-graph lattice models with spin-orbit coupling[28,55].

Appendix C: Database of materials with flat bands selected from TQC database

In this Appendix, we will introduce the database of materials that we are relying on for this high-throughput search of flat-band materials. We will also present the Materials Flatband Database website and the different algorithms and search options that are provided to the user. The tools that we publicly provide through this website have been used to obtain the curated list of flat-band materials that we will present in Appendix H.

1. An overview of the Topological material database

For our high-throughput search of materials with flat bands, we have relied on the data and database of the Topological Quantum Chemistry website. It was originally built for Ref.[4] and upgraded both in terms of materials and features in Ref.[5]. Beyond the two original publications related to this database, this database was also used to look for the best candidate materials with fragile bands[56] and to develop machine learning approach to topological feature predictions[57]. We review here some important properties of this database.

The ab-initio calculations of the database were performed using Density Functional Theory (DFT)[31,32] and its implementation in the Vienna Ab-initio Simulation Package (VASP)[33,34]. For each material calculation, we used as input the structural parameters reported on the Inorganic Crystal Structure Database (ICSD)[30]. We treated the interaction between the ion cores and the valence electrons using the projector augmented-wave method[58]. For the exchange-correlation potential, we used the generalized gradient approximation (GGA) with the Perdew-Burke-Ernzerhof parameterization for solids[59]. Effects of spin-orbit coupling were accounted by using the second variation method[60]. For the plane-wave expansion, we employed a Γ-centered $\boldsymbol{k}$-point grid of size (11×11×11) for reciprocal space integration and a 550 eV energy cutoff. The density of states (DOS) was evaluated on a Γ-centered $\boldsymbol{k}$-point grid of size (11×11×11) and using the Methfessel-Paxton algorithm of order 1. We emphasize that all of the first-principle calculations are paramagnetic, *i.e.*, without the onsite spin polarization. The magnetic properties at low temperature reported on Topological Quantum Chemistry website are extracted from the Materials Project.

The Topological Quantum Chemistry website is built upon the systematic ab-initio calculation of 85,700 ICSD entries of stoichiometric materials. Among these entries, the calculation with spin-orbit coupling was performed successfully for 73,234 materials. All of them are available through the website. Calculations without spin-orbit coupling are also available although a small fraction (4.78% of the successfully processed ICSD entries with spin-orbit coupling) did not converge. 19,798 of the available materials (*i.e.*, 27.03%) contain rare-earth elements (La, Ce, Pr, Nd, Pm, Sm, Eu, Gd, Tb, Dy, Ho, Er, Tm, and Yb) and actinides (Ac, Th, Pa, U, Np, Pu, Am, Cm, Bk, Cf, Es, Fm, Md, No and Lr) which may exhibit strong correlation effects and usually lead to spurious flat bands in the DFT calculations. For these reasons, we have discarded these materials from our flat-bandsurvey with one exception, compounds containing La as rare-earth elements. Indeed for the ab-initio calculation, La is always a cation in such compounds and the bands originated from these f orbits are usually away from the Fermi energy. In our database, there are 2,689 ICSD entries (*i.e.*, 3.67%) corresponding to this situation. There, the f bands originated from the La atoms are located at least 1eV above E_f (typically around 2eV). We have highlighted some of these materials in Appendix H 3.

Many ICSD entries correspond to the same stoichiometric formula and the same space group (SG), leading most of the time (but not always) to, e.g., the same topological properties at the Fermi level. For this reason the Topological Quantum Chemistry website defines the notion of *unique materials*, including all the ICSD entries having the same stoichiometric formula, SG and topological classification at the Fermi level. This database contains 38,298 such unique materials. While in some cases, all ICSD entries within a given unique materials have band structures and densities of states barely distinguishable by eye, they might in general exhibit some subtle differences for these two quantities. Automated search of flat-band features from the band structure or the density of states should thus be performed on every ICSD belonging to all unique materials.

2. The flat-band material database

The website Materials Flatband Database website relies on the database provided in Topological Quantum Chemistry website. It offers a dedicated search interface to look for materials with flat-band features close to the Fermi energy. As discussed above, we have filtered out those that contain any rare-earth elements except La. Moreover, to search for flat bands or flat bands along some high symmetry lines, we only focus on the DFT calculations performed without spin-orbit coupling: the band structures and density of states are usually similar with or without spin-orbit coupling, thus only considering the later simplifies the automated search without introducing any bias. Overall, the user has access to 55,206 ICSD entries (28,169 unique materials). The three main tools that we provide to search for flat bands are based on flat segments in the electronic band structure or peaks in the density of states or sublattices. We will now detail these two former, the later will be discussed in Appendix C 3.

a. *Band structure and flat-band segments*

For each ICSD entry, we have access to the electronic band structure computed along high symmetry lines and without spin-orbit coupling. These band structures include all bands up to two times of the number of valence electrons, thus an equal number of bands above and below the last filled one. The notions of filled and empty are defined with respect to the number of electrons and the band index. Each band is evaluated along a path specific to each point group. This path is made of straight lines in the Brillouin zone (BZ) connecting two high symmetry points. The choice of these straight lines is designed to cover all cases required by band connectivity[22,61] while staying connected with the related works and databases. Each straight line is discretized into 20 equally spaced $\boldsymbol{k}$ points in the BZ, including the two end high symmetry points. Note that the distance between two consecutive discretized $\boldsymbol{k}$ points might differ from one straight line to another: we use a regular mesh with the same number (20) of points for the discretization of each line but the actual distances between two pairs of high symmetry points of the BZ do not have to be equal.

To automatically search for flat segments in a given band structure of an ICSD, we apply the following procedure:

- We only consider at most the last 2 filled bands and 2 empty bands to focus on features near the Fermi level. We require that at least one k point with an energy E in the energy window parameterized by Δ_E such that $|E - E_F| < \Delta_E$. E_F is the Fermi energy as computed from the VASP self consistent calculation[5]. If any of the last 2 filled bands and 2 empty bands does not satisfy this constraint, it is discarded.

- We define a flat segment as a series of L consecutive k points along the path in the BZ, whose bandwidth, *i.e.*, the difference between the highest energy and the lowest energy associated to these L points, is lower than some chosen value ω.

- For each band, we test the presence of flat segments starting from every possible discretized k points that define the path in the BZ. Notice that segments can overlap (see the purple and green boxes of Fig. 4). Denoting N_{BZ} the total number of discretized k points that define the path in the BZ, the number of flat segments N_{fl} is at most $N_{\mathrm{BZ}} - L + 1$. A score is then defined as the ratio

  $$\mathrm{score} = \frac{N_{\mathrm{fl}}}{N_{\mathrm{BZ}} - L + 1}. \tag{C1}$$

  For example, a perfectly flat band would have a score of 1.

- In addition, we also evaluate N_{w} the number of bands that overlap with the energy window defined by $|E - E_F| < \Delta_E$. It is used as a proxy to quantify how dense is the band structure in this energy window.

We have applied this procedure to all ICSDs using several discrete values of L (10, 20, 30, 40 and 50), Δ_E (0.5eV, 1.0eV, 1.5eV and 2.0eV), and ω (25meV, 50meV, 75meV, 100meV, 125meV and 150meV). We exemplify the search procedure in Fig. 4 for ICSD 62555. In Table II, we provide the number of ICSDs hosting flat-band segments for all values of L and ω that we have considered. Statistics is split into different minimum threshold for the best score (as defined in Eq. (C1) for an ICSD. A score greater than 0 means there is at least one flat-band segment. A score of 1, *i.e.*, the maximum score means that an ICSD has one band out of the (at most) last 2 filled bands and 2 empty bands, where every sequence of L consecutive k points along the path in the BZ with a bandwidth smaller than ω. We stress that such a score does not imply that the band has a global bandwidth smaller ω.

All the above-mentioned parameters can be selected as search criteria on the Materials Flatband Database website. In addition, a cap on N_{w}, the number of bands in the energy window, can be set to look for well separated flat-band segments from other bands. Moreover, the user can require the flat band with the highest score to be topological, either as part of a topological single set of bands or all the bands up to (and including) the best flat band being topological (see Ref.[5] for more details about the difference between these two definitions). The best score as defined

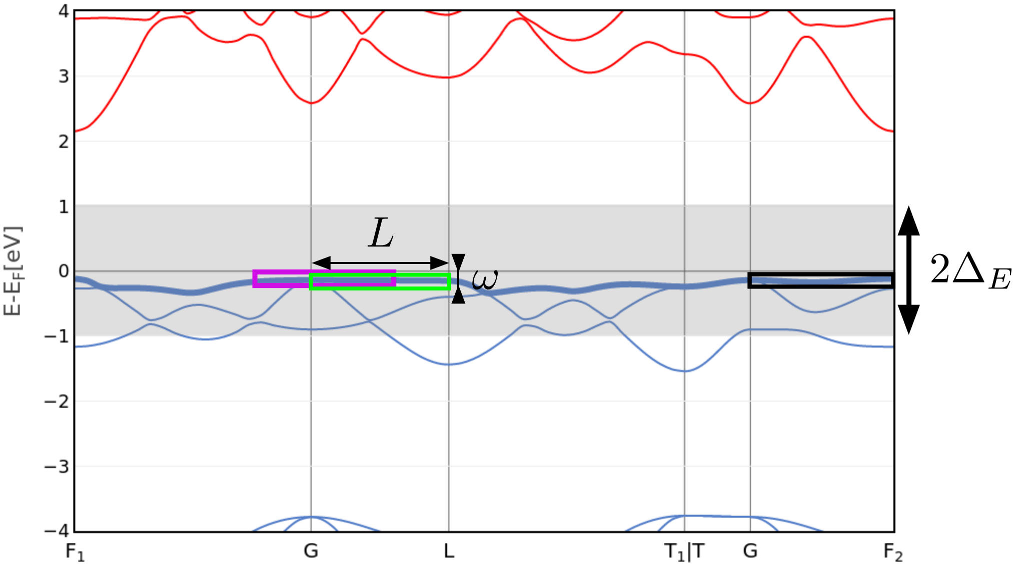

Figure 4. Example of flat-band segments found in the band structure of Ca_2NCl [ICSD 62555, SG 166 ($R\bar{3}m$)] in the space group 166 ($R\bar{3}m$), one of the best flat bands given in Appendix H 3. We have set the parameters $L = 20$, $\omega = 150$meV and $\Delta_E = 1$eV. The best flat band closest to the Fermi level is highlighted in bold blue and has a score of 0.642. The purple, green and black boxes show three segments satisfying the constraints of the algorithm discussed in Appendix C 2 a.

in Eq. (C1) is used both as a search criterion and to sort the search results. When selecting a given result, the band having the flat segment closest to the Fermi energy is displayed in bold for convenience (see Fig. 4).

Table II: Statistics about the flat-band segments of all the ICSD entries. Note that we used the energy window $\Delta_E = 0.5$eV but the numbers provided here almost never depend on this parameters. The first column is the minimal best score (as defined in Eq. (C1)) and the second column is the minimum segment length L. The other columns are the different values for the maximum bandwidth ω. We provide both the number of ICSDs hosting such a flat-band segment and the percentage with respect to the total number of ICSDs that we have considered, namely 55,206.

Min. score	L	$\omega = 25$meV	$\omega = 50$meV	$\omega = 75$meV	$\omega = 100$meV	$\omega = 125$meV	$\omega = 150$meV
0.01	10	48312 (87.5%)	52693 (95.5%)	54160 (98.1%)	54534 (98.8%)	54752 (99.2%)	54876 (99.4%)
0.01	20	29987 (54.3%)	38914 (70.5%)	43327 (78.5%)	46033 (83.4%)	47939 (86.8%)	49490 (89.7%)
0.01	30	13610 (24.6%)	22700 (41.1%)	29037 (52.6%)	33354 (60.4%)	36537 (66.2%)	38936 (70.5%)
0.01	40	7622 (13.8%)	14472 (26.2%)	19818 (35.9%)	24146 (43.7%)	27701 (50.2%)	30491 (55.2%)
0.01	50	4712 (8.5%)	10179 (18.4%)	14787 (26.8%)	18583 (33.7%)	21508 (39.0%)	24372 (44.1%)
0.25	10	18685 (33.9%)	29936 (54.2%)	36000 (65.2%)	40178 (72.8%)	43345 (78.5%)	45577 (82.6%)
0.25	20	7223 (13.1%)	14525 (26.3%)	20081 (36.4%)	24794 (44.9%)	28636 (51.9%)	31452 (57.0%)
0.25	30	3787 (6.9%)	9079 (16.4%)	13775 (24.9%)	17612 (31.9%)	20739 (37.6%)	23681 (42.9%)
0.25	40	2222 (4.0%)	6160 (11.2%)	9980 (18.1%)	13432 (24.3%)	16390 (29.7%)	18866 (34.2%)
0.25	50	1577 (2.9%)	4815 (8.7%)	8058 (14.6%)	11175 (20.2%)	13989 (25.3%)	16335 (29.6%)
0.50	10	8416 (15.2%)	16617 (30.1%)	22871 (41.4%)	27745 (50.3%)	31376 (56.8%)	34172 (61.9%)
0.50	20	2889 (5.2%)	7691 (13.9%)	12151 (22.0%)	15940 (28.9%)	19095 (34.6%)	22113 (40.1%)
0.50	30	1569 (2.8%)	4866 (8.8%)	8175 (14.8%)	11433 (20.7%)	14286 (25.9%)	16781 (30.4%)
0.50	40	1099 (2.0%)	3686 (6.7%)	6418 (11.6%)	9195 (16.7%)	11768 (21.3%)	14187 (25.7%)
0.50	50	882 (1.6%)	2989 (5.4%)	5467 (9.9%)	7952 (14.4%)	10324 (18.7%)	12541 (22.7%)
0.75	10	3415 (6.2%)	8637 (15.7%)	13323 (24.1%)	17409 (31.5%)	20847 (37.8%)	23861 (43.2%)
0.75	20	1288 (2.3%)	4275 (7.7%)	7345 (13.3%)	10408 (18.9%)	13066 (23.7%)	15519 (28.1%)
0.75	30	868 (1.6%)	2980 (5.4%)	5434 (9.8%)	8006 (14.5%)	10370 (18.8%)	12612 (22.9%)
0.75	40	733 (1.3%)	2490 (4.5%)	4734 (8.6%)	6965 (12.6%)	9202 (16.7%)	11378 (20.6%)
0.75	50	657 (1.2%)	2250 (4.1%)	4330 (7.8%)	6398 (11.6%)	8548 (15.5%)	10634 (19.3%)
1.00	10	895 (1.6%)	3073 (5.6%)	5526 (10.0%)	8005 (14.5%)	10344 (18.7%)	12638 (22.9%)
1.00	20	627 (1.1%)	2162 (3.9%)	4176 (7.6%)	6234 (11.3%)	8342 (15.1%)	10337 (18.7%)

1.00	30	587 (1.1%)	1994 (3.6%)	3922 (7.1%)	5817 (10.5%)	7907 (14.3%)	9873 (17.9%)
1.00	40	552 (1.0%)	1872 (3.4%)	3752 (6.8%)	5568 (10.1%)	7642 (13.8%)	9560 (17.3%)
1.00	50	541 (1.0%)	1813 (3.3%)	3676 (6.7%)	5463 (9.9%)	7508 (13.6%)	9436 (17.1%)

Looking for flat-band segments along the high symmetry lines does not fully take into consideration the 3D structure of a material, whose bands could be dispersive away from high-symmetry paths (as already mentioned in Appendix B 1). A typical example would be a (quasi-)one dimensional system. Any high symmetry line in the BZ perpendicular to the dispersive momentum direction of the one dimensional system would appear flat. For that reason, we also rely on a second indicator: peaks in the density of states.

b. *Peaks in the density of states*

The density of states (DOS) calculation is part of the processing applied to each ICSD entry displayed in the Topological Quantum Chemistry website (see Ref.[5] for in-depth discussion). Similarly with the search for the band structure flat-band segments, we focus on the DOS computed without spin orbit coupling. Note that we do not search for peaks in the DOS directly from the PROCAR output of VASP. Rather, we rely on the output of the python script pydos/pyband which processes the PROCAR files to generate, e.g., the DOS plots on the Topological Quantum Chemistry website.

To look for peaks in the DOS, we consider the energy range $[-5\text{eV}, 5\text{eV}]$. We compute the average DOS over this range; this value sets the minimum value to define a peak. We discretize the DOS with a step of 0.02eV to avoid spurious peaks from fast variations. We then apply the following algorithm:

1. We look for the largest value among the discretized DOS. It should be larger than the average DOS. The energy E_{peak} associated to this largest value sets the DOS peak position.

2. We compute W_{peak} the peak width as its Gaussian width, *i.e.*, the full width at half maximum of the peak.

3. All points of the discretized DOS within the peak width are discarded.

4. All points around the peak width where the DOS continues to decrease away from the maximum are also discarded (to avoid considering the tails of the peak as other peaks).

5. The procedure is then repeated from the first step until all discretized DOS values have been discarded or are lower than the average DOS.

This crude algorithm offers a reliable and simple way to find DOS peaks. In Fig. 5, we provide an example of DOS peak processed information by this procedure.

All ICSD DOSes available on Materials Flatband Database website have been processed with this algorithm. While not directly accessible, the DOS peak information is used by the search engine when activating "Require a DOS peak near Ef". Two search parameters can be tuned: the peak maximum distance to the Fermi level, *i.e.*, the maximal value for $|E_{\text{peak}} - E_F|$ where E_{peak} is the peak position and the maximal Gaussian width W_{peak} for the peak closest to Fermi level. These search parameters can be used as the unique criteria or combined with other criteria such as the sublattice features or the existence of flat-band segments along the high symmetry lines.

3. **Sublattices and database**

For all the ICSDs provided in Materials Flatband Database website, we have performed an automated search for five types of sublattices, namely Kagome, pyrochlore, generic bipartite (with a different number of atoms in the two subsets), split and Lieb sublattices. This automated search will be detailed in Appendices D and E. The full list of sublattices for each ICSD are given on their respective webpage on Materials Flatband Database website. Moreover, the presence of sublattices can be used as a search criterion when looking for flat-band materials.

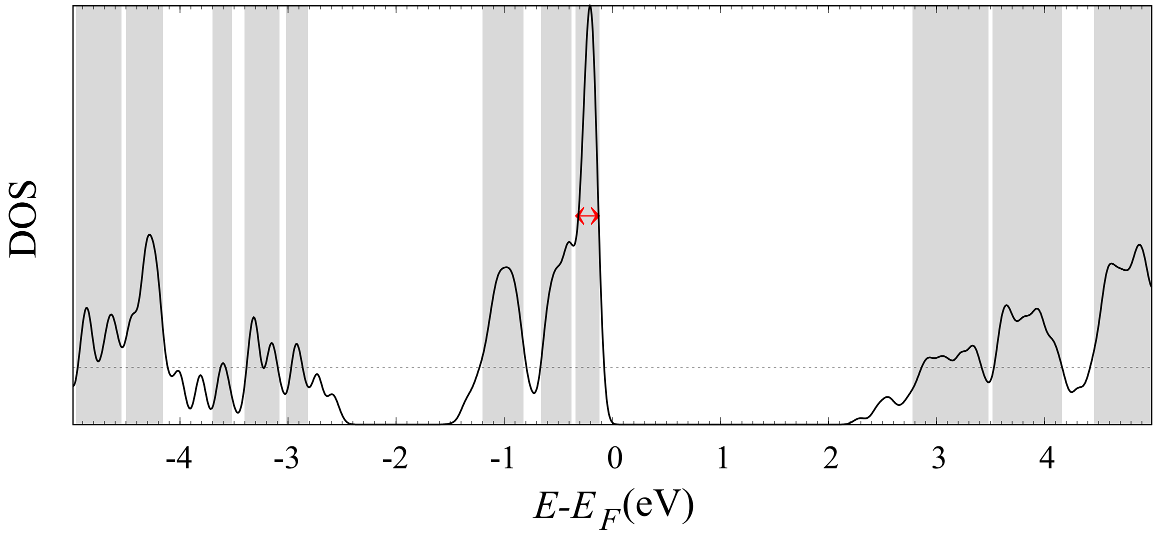

Figure 5. Example of DOS peak information based on the DFT calculations for Ca_2NBr [ICSD 153105, SG 166 ($R\bar{3}m$)] in the space group 166 ($R\bar{3}m$), one of the best flat bands given in Appendix H 3. The most prominent peak is located at $E_{\text{peak}} - E_F \simeq -0.22\text{eV}$. The red double arrows indicates the Gaussian width $W_{\text{peak}} \simeq 0.22\text{eV}$ of this peak. The dotted line is the average density of states over the energy range $[-5\text{eV}, 5\text{eV}]$. The gray areas indicate the extension of each peak.

Table III: *Upper part*: Statistics of the ICSD entries in the database hosting at least one Kagome or Pyrochlore sublattice and an additional sublattice: Lieb, bipartite or split. In the first row, we give the number of ICSDs entries for the database (first column), for the list of curated flat-band materials (second column) and for the best representative flat-band materials (third column). The second and third rows provide the number of ICSD entries with a Kagome (second row) or pyrochlore (third row) for each category (all ICSDs, curated flat-band materials and best representative flat-band materials). The fourth, fifth, and sixth rows are the statistics for ICSD with a Kagome sublattice and either a Lieb, bipartite with different number of atoms on sublattices and split lattices. An ICSD entry is considered as hosting a given type of lattice if the algorithms discussed in Section "Automated identification of line-graph and bipartite sublattices"of the main text have found at least one such a lattice irrespective of the cutoffs or being a rigorous or approximate sublattice. The seventh, eighth, and ninth rows are similar to the fourth, fifth, and sixth rows but for pyrochlore rather than Kagome sublattices. *Lower part*: Statistics of the ICSD entries in the database hosting one type of sublattice. The tenth, eleventh, twelfth and thirteenth rows give the number of ICSDs hosting only a Kagome, pryrochlore, Lieb or bipartite sublattice respectively. All percentage are expressed with respect to the numbers in the second row.

	All ICSDs	Curated	Best
# ICSDs	55,206	6,338	949
Kagome	6,120 (11.09%)	1,699 (26.81%)	516 (54.37%)
Pyrochlore	1,666 (3.02%)	296 (4.67%)	77 (8.11%)
Kagome and Lieb	916 (1.66%)	537 (8.47%)	135 (14.23%)
Kagome and Bipartite	3,244 (5.88%)	1,081 (17.06%)	247 (26.03%)
Kagome and Split	1,974 (3.58%)	904 (14.26%)	228 (24.03%)

Pyrochlore and Lieb	0 (0.00%)	0 (0.00%)	0 (0.00%)
Pyrochlore and Bipartite	968 (1.75%)	172 (2.71%)	16 (1.69%)
Pyrochlore and Split	338 (0.61%)	66 (1.04%)	10 (1.05%)
Only Kagome	2,178 (3.95%)	494 (7.79%)	208 (21.92%)
Only Pyrochlore	698 (1.26%)	124 (1.96%)	61 (6.43%)
Only Lieb	1 (0.00%)	0 (0.00%)	0 (0.00%)
Only Bipartite	17,258 (31.26%)	1,873 (29.55%)	169 (17.81%)

For sake of completeness, we now discuss the frequency of appearance for the sublattice types among the 55,206 ICSD entries in our database. Note that our figures here are based on ICSDs rather than unique materials. Indeed, tiny differences in the atom positions from one ICSD to another one associated to the same unique material might lead to threshold effect: a sublattice close to the maximum error bar of the automated search algorithm for one ICSD might be slightly beyond the error bar for another ICSD. From our survey, we have found that 24,052 ICSDs (43.57%) have at least one sublattice. A large fraction of the ICSDs, 38.36% (*i.e.*, 21,175 ICSDs), have at least one bipartite sublattice. For the Kagome sublattices, 6,120 ICSDs (11.09%), the majority are rigorous Kagome sublattices (4,192 ICSDs, 7.59%) as defined in Appendix D. The approximate Kagome sublattices are found in 2,100 ICSDs (3.80%). Note that an ICSD can have both a rigorous and an approximate Kagome distinct sublattice. A similar analysis can be performed for the Lieb sublattices: there are 1,590 ICSDs (2.88%) with Lieb sublattices, including 1,202 ICSDs (2.18%) with rigorous Lieb sublattices and 438 ICSDs (0.79%) with approximate Lieb sublattices, as defined in Appendix D. Pyrochlore sublattices have been found in 1,666 ICSDs (3.02%), including 1,541 ICSDs hosting (2.79%) rigorous sublattices and 125 ICSDs hosting (0.23%). Finally, split sublattices were detected in 8,224 ICSDs (14.90%). As mentioned in the caption of Table I in the main text, an ICSD entry might host more than one type of sublattices. A trivial example is a pyrochlore sublattice that implies the existence of Kagome sublattices. More interestingly, we provide in Table III the number of ICSDs hosting either a Kagome or a pyrochlore sublattice and any of the three other types of sublattices we have considered: Lieb, bipartite and split sublattices. We also provide in this table, the number of ICSDSs hosting a single type of sublattice. Note that the flat bands in a compound hosting solely a bipartite lattice may only be understood in the S-matrix formalism.[6] Additionally, a breakdown of the number of ICSDs per space group that have a given sublattice type among the 5 types we have searched for is available in Table IV.

Table IV: Statistics about ICSD entries with either Kagome, pyrochlore, bipartite, split or Lieb sublattices. The first column is the space group number, the second column is the number of ICSDs that have been processed per SG. The third (seventh) column provides the number of ICSDs per SG having at least one rigorous or approximate Kagome (Lieb) sublattice. The fourth, fifth and sixth columns give the number of ICSDs per SG with at least one pyrochlore, bipartite and split sublattice respectively. Note that we count an ICSD entry as having a bipartite or split sublattice, if it hosts such a sublattice irrespective of the cutoffs defined in Appendix E. Note that not all the 2D Lieb-sublattice materials are labeled as a 3D bipartite/split sublattice in the results of our algorithm and further discussion can be referred to Appendix E 2.

SG	# ICSDs	# ICSDs with Kagome	# ICSDs with pyrochlore	# ICSDs with bipartite	# ICSDs with split	# ICSDs with Lieb
1	221	2 (0.9%)	—	104 (47.1%)	59 (26.7%)	—
2	1677	8 (0.5%)	—	701 (41.8%)	218 (13.0%)	—
3	14	—	—	7 (50.0%)	3 (21.4%)	—
4	275	—	—	122 (44.4%)	43 (15.6%)	—
5	182	1 (0.6%)	—	91 (50.0%)	37 (20.3%)	—
6	38	2 (5.3%)	—	13 (34.2%)	6 (15.8%)	—
7	141	—	—	77 (54.6%)	45 (31.9%)	—
8	164	8 (4.9%)	—	73 (44.5%)	22 (13.4%)	1 (0.6%)
9	272	3 (1.1%)	1 (0.4%)	145 (53.3%)	44 (16.2%)	—
10	38	2 (5.3%)	—	13 (34.2%)	4 (10.5%)	—

11	677	1 (0.1%)	—	260 (38.4%)	51 (7.5%)	—
12	1528	24 (1.6%)	—	656 (42.9%)	165 (10.8%)	1 (0.1%)
13	246	1 (0.4%)	—	164 (66.7%)	54 (21.9%)	—
14	3370	2 (0.1%)	—	1494 (44.3%)	473 (14.0%)	—
15	2270	5 (0.2%)	—	1303 (57.4%)	449 (19.8%)	—
16	2	—	—	2 (100%)	1 (50.0%)	—
17	8	—	—	3 (37.5%)	3 (37.5%)	1 (12.5%)
18	41	—	—	20 (48.8%)	12 (29.3%)	—
19	327	—	—	116 (35.5%)	25 (7.7%)	—
20	72	1 (1.4%)	—	43 (59.7%)	33 (45.8%)	—
21	10	—	—	4 (40.0%)	4 (40.0%)	—
22	7	—	—	3 (42.9%)	1 (14.3%)	—
23	15	—	—	8 (53.3%)	3 (20.0%)	—
24	3	2 (66.7%)	—	3 (100%)	3 (100%)	—
25	56	—	—	27 (48.2%)	18 (32.1%)	—
26	74	1 (1.4%)	—	41 (55.4%)	18 (24.3%)	1 (1.4%)
27	1	—	—	1 (100%)	1 (100%)	—
28	17	—	—	1 (5.9%)	—	—
29	85	—	—	27 (31.8%)	9 (10.6%)	—
30	6	—	—	5 (83.3%)	1 (16.7%)	1 (16.7%)
31	240	8 (3.3%)	—	89 (37.1%)	13 (5.4%)	—
32	12	—	—	9 (75.0%)	2 (16.7%)	—
33	379	2 (0.5%)	—	200 (52.8%)	70 (18.5%)	—
34	28	2 (7.1%)	—	12 (42.9%)	10 (35.7%)	—
35	8	—	—	6 (75.0%)	3 (37.5%)	—
36	372	1 (0.3%)	—	227 (61.0%)	94 (25.3%)	—
37	7	—	—	7 (100%)	2 (28.6%)	—
38	81	10 (12.3%)	—	33 (40.7%)	19 (23.5%)	13 (16.1%)
39	13	—	—	6 (46.1%)	1 (7.7%)	1 (7.7%)
40	60	—	—	24 (40.0%)	8 (13.3%)	—
41	43	—	—	23 (53.5%)	20 (46.5%)	—
42	4	—	—	—	—	—
43	121	—	—	52 (43.0%)	29 (24.0%)	—
44	80	4 (5.0%)	2 (2.5%)	21 (26.2%)	5 (6.2%)	—
45	11	—	—	8 (72.7%)	5 (45.5%)	2 (18.2%)
46	81	5 (6.2%)	2 (2.5%)	52 (64.2%)	42 (51.9%)	20 (24.7%)
47	62	1 (1.6%)	—	52 (83.9%)	50 (80.7%)	3 (4.8%)
48	2	—	—	1 (50.0%)	1 (50.0%)	—
50	7	—	—	2 (28.6%)	2 (28.6%)	1 (14.3%)
51	115	—	—	46 (40.0%)	16 (13.9%)	2 (1.7%)
52	46	1 (2.2%)	—	37 (80.4%)	15 (32.6%)	—
53	26	—	—	3 (11.5%)	—	—
54	22	—	—	3 (13.6%)	3 (13.6%)	—
55	337	—	—	164 (48.7%)	35 (10.4%)	—
56	29	—	—	21 (72.4%)	14 (48.3%)	—
57	143	1 (0.7%)	—	54 (37.8%)	27 (18.9%)	—
58	461	—	—	162 (35.1%)	27 (5.9%)	—
59	278	—	—	98 (35.2%)	28 (10.1%)	—
60	222	—	—	150 (67.6%)	22 (9.9%)	—
61	211	—	—	84 (39.8%)	25 (11.8%)	—
62	4313	15 (0.3%)	—	1956 (45.4%)	503 (11.7%)	8 (0.2%)
63	1307	9 (0.7%)	—	417 (31.9%)	132 (10.1%)	2 (0.1%)
64	395	8 (2.0%)	—	149 (37.7%)	95 (24.1%)	57 (14.4%)
65	192	4 (2.1%)	—	92 (47.9%)	52 (27.1%)	4 (2.1%)
66	37	—	—	30 (81.1%)	27 (73.0%)	1 (2.7%)
67	40	—	—	5 (12.5%)	3 (7.5%)	—
68	19	—	—	9 (47.4%)	6 (31.6%)	—
69	59	11 (18.6%)	—	26 (44.1%)	8 (13.6%)	—
70	174	5 (2.9%)	5 (2.9%)	81 (46.5%)	38 (21.8%)	—
71	355	5 (1.4%)	—	76 (21.4%)	45 (12.7%)	1 (0.3%)
72	183	—	—	100 (54.6%)	63 (34.4%)	—
73	18	—	—	5 (27.8%)	—	—
74	221	33 (14.9%)	4 (1.8%)	115 (52.0%)	58 (26.2%)	4 (1.8%)
75	5	—	—	4 (80.0%)	4 (80.0%)	—

76	11	—	—	4 (36.4%)	2 (18.2%)	—
77	2	—	—	—	—	—
78	1	—	—	—	—	—
79	13	—	—	3 (23.1%)	1 (7.7%)	—
80	3	—	—	3 (100%)	2 (66.7%)	—
81	18	—	—	5 (27.8%)	1 (5.6%)	—
82	261	—	—	174 (66.7%)	50 (19.2%)	—
83	6	—	—	1 (16.7%)	1 (16.7%)	—
84	30	—	—	9 (30.0%)	4 (13.3%)	—
85	49	—	—	27 (55.1%)	3 (6.1%)	—
86	43	—	—	5 (11.6%)	2 (4.7%)	—
87	256	8 (3.1%)	—	140 (54.7%)	115 (44.9%)	—
88	275	—	—	187 (68.0%)	16 (5.8%)	—
90	5	—	—	5 (100%)	2 (40.0%)	—
91	8	—	—	8 (100%)	2 (25.0%)	—
92	131	—	—	83 (63.4%)	71 (54.2%)	—
94	1	—	—	1 (100%)	—	—
95	3	—	—	3 (100%)	1 (33.3%)	—
96	37	1 (2.7%)	1 (2.7%)	11 (29.7%)	6 (16.2%)	—
97	1	—	—	—	—	—
98	7	—	—	3 (42.9%)	2 (28.6%)	—
99	182	48 (26.4%)	—	158 (86.8%)	152 (83.5%)	45 (24.7%)
100	37	—	—	32 (86.5%)	17 (46.0%)	—
102	12	—	—	5 (41.7%)	1 (8.3%)	—
103	9	—	—	—	—	—
104	4	—	—	2 (50.0%)	1 (25.0%)	—
105	4	—	—	—	—	—
106	1	—	—	1 (100%)	—	—
107	84	—	—	13 (15.5%)	9 (10.7%)	—
108	14	—	—	8 (57.1%)	4 (28.6%)	—
109	33	—	—	6 (18.2%)	—	—
110	36	—	—	33 (91.7%)	25 (69.4%)	—
111	24	5 (20.8%)	—	19 (79.2%)	—	—
112	4	—	—	3 (75.0%)	3 (75.0%)	—
113	143	—	—	97 (67.8%)	77 (53.9%)	—
114	41	—	—	19 (46.3%)	11 (26.8%)	—
115	23	2 (8.7%)	—	6 (26.1%)	2 (8.7%)	—
116	25	—	—	9 (36.0%)	4 (16.0%)	—
117	9	—	—	5 (55.6%)	3 (33.3%)	—
118	11	—	—	3 (27.3%)	2 (18.2%)	—
119	49	1 (2.0%)	—	24 (49.0%)	10 (20.4%)	—
120	22	—	—	8 (36.4%)	6 (27.3%)	—
121	193	—	—	50 (25.9%)	17 (8.8%)	—
122	502	—	—	78 (15.5%)	53 (10.6%)	—
123	521	51 (9.8%)	—	177 (34.0%)	146 (28.0%)	119 (22.8%)
124	33	—	—	6 (18.2%)	—	—
125	36	—	—	15 (41.7%)	6 (16.7%)	—
126	9	—	—	5 (55.6%)	4 (44.4%)	—
127	271	—	—	72 (26.6%)	47 (17.3%)	8 (3.0%)
128	56	—	—	9 (16.1%)	6 (10.7%)	—
129	889	3 (0.3%)	—	108 (12.2%)	68 (7.7%)	3 (0.3%)
130	55	—	—	32 (58.2%)	19 (34.5%)	—
131	36	—	—	7 (19.4%)	—	—
132	10	1 (10.0%)	—	5 (50.0%)	1 (10.0%)	—
133	5	—	—	1 (20.0%)	1 (20.0%)	—
134	9	2 (22.2%)	—	2 (22.2%)	2 (22.2%)	—
135	76	—	—	66 (86.8%)	2 (2.6%)	—
136	710	—	—	552 (77.8%)	14 (2.0%)	2 (0.3%)
137	126	—	—	104 (82.5%)	34 (27.0%)	—
138	17	—	—	9 (52.9%)	7 (41.2%)	—
139	1772	21 (1.2%)	—	502 (28.3%)	406 (22.9%)	338 (19.1%)
140	777	—	—	228 (29.3%)	145 (18.7%)	40 (5.2%)
141	403	25 (6.2%)	20 (5.0%)	200 (49.6%)	15 (3.7%)	2 (0.5%)
142	73	—	—	26 (35.6%)	16 (21.9%)	—

143	18	2 (11.1%)	—	13 (72.2%)	3 (16.7%)	—
144	31	—	—	13 (41.9%)	12 (38.7%)	—
145	5	—	—	2 (40.0%)	2 (40.0%)	—
146	105	3 (2.9%)	—	59 (56.2%)	10 (9.5%)	—
147	74	1 (1.4%)	—	43 (58.1%)	11 (14.9%)	—
148	740	10 (1.4%)	—	434 (58.6%)	122 (16.5%)	—
149	15	9 (60.0%)	—	15 (100%)	6 (40.0%)	—
150	73	3 (4.1%)	—	57 (78.1%)	27 (37.0%)	—
151	4	—	—	3 (75.0%)	—	—
152	269	—	—	194 (72.1%)	179 (66.5%)	—
153	1	—	—	—	—	—
154	138	—	—	109 (79.0%)	108 (78.3%)	—
155	57	2 (3.5%)	—	25 (43.9%)	7 (12.3%)	—
156	221	5 (2.3%)	—	116 (52.5%)	1 (0.5%)	—
157	26	4 (15.4%)	—	21 (80.8%)	18 (69.2%)	—
158	3	—	—	3 (100%)	1 (33.3%)	—
159	57	7 (12.3%)	—	45 (79.0%)	6 (10.5%)	—
160	291	51 (17.5%)	—	143 (49.1%)	21 (7.2%)	11 (3.8%)
161	246	4 (1.6%)	—	200 (81.3%)	32 (13.0%)	—
162	65	12 (18.5%)	—	60 (92.3%)	27 (41.5%)	—
163	73	6 (8.2%)	—	45 (61.6%)	25 (34.2%)	—
164	789	127 (16.1%)	—	390 (49.4%)	70 (8.9%)	—
165	56	—	—	17 (30.4%)	9 (16.1%)	—
166	1173	292 (24.9%)	2 (0.2%)	392 (33.4%)	125 (10.7%)	—
167	845	7 (0.8%)	—	664 (78.6%)	263 (31.1%)	53 (6.3%)
169	1	—	—	1 (100%)	—	—
173	163	7 (4.3%)	—	115 (70.5%)	46 (28.2%)	—
174	46	—	—	17 (37.0%)	—	—
175	2	—	—	1 (50.0%)	1 (50.0%)	—
176	312	8 (2.6%)	—	145 (46.5%)	15 (4.8%)	—
177	3	—	—	3 (100%)	3 (100%)	—
180	92	—	—	24 (26.1%)	20 (21.7%)	—
181	15	—	—	6 (40.0%)	6 (40.0%)	—
182	48	1 (2.1%)	—	44 (91.7%)	25 (52.1%)	—
183	3	—	—	—	—	—
185	73	1 (1.4%)	—	41 (56.2%)	9 (12.3%)	—
186	716	89 (12.4%)	—	191 (26.7%)	18 (2.5%)	—
187	227	10 (4.4%)	—	22 (9.7%)	1 (0.4%)	—
188	27	—	—	24 (88.9%)	11 (40.7%)	—
189	383	1 (0.3%)	—	80 (20.9%)	14 (3.7%)	—
190	63	—	—	16 (25.4%)	7 (11.1%)	—
191	662	374 (56.5%)	—	59 (8.9%)	25 (3.8%)	—
192	14	13 (92.9%)	—	13 (92.9%)	6 (42.9%)	—
193	362	3 (0.8%)	—	46 (12.7%)	15 (4.1%)	—
194	2643	681 (25.8%)	—	544 (20.6%)	172 (6.5%)	—
195	1	—	—	1 (100%)	1 (100%)	—
196	1	—	—	—	—	—
197	36	—	—	35 (97.2%)	9 (25.0%)	—
198	315	—	—	64 (20.3%)	17 (5.4%)	—
199	37	—	—	27 (73.0%)	12 (32.4%)	—
200	25	6 (24.0%)	—	3 (12.0%)	3 (12.0%)	—
201	6	2 (33.3%)	—	6 (100%)	3 (50.0%)	—
202	26	—	—	—	—	—
203	8	8 (100%)	6 (75.0%)	6 (75.0%)	—	—
204	235	98 (41.7%)	—	126 (53.6%)	26 (11.1%)	8 (3.4%)
205	357	—	—	62 (17.4%)	3 (0.8%)	—
206	154	—	—	131 (85.1%)	1 (0.7%)	—
208	2	—	—	—	—	—
210	1	—	—	1 (100%)	1 (100%)	—
211	1	—	—	1 (100%)	1 (100%)	—
212	29	6 (20.7%)	—	21 (72.4%)	7 (24.1%)	—
213	41	1 (2.4%)	—	22 (53.7%)	21 (51.2%)	—
214	17	—	—	11 (64.7%)	—	—
215	93	54 (58.1%)	—	12 (12.9%)	1 (1.1%)	—

216	1561	108 (6.9%)	79 (5.1%)	58 (3.7%)	7 (0.5%)	—
217	150	37 (24.7%)	—	51 (34.0%)	18 (12.0%)	—
218	98	—	—	85 (86.7%)	81 (82.7%)	—
219	13	12 (92.3%)	—	12 (92.3%)	1 (7.7%)	—
220	117	—	—	38 (32.5%)	1 (0.8%)	—
221	2271	1344 (59.2%)	—	841 (37.0%)	831 (36.6%)	828 (36.5%)
223	451	—	—	13 (2.9%)	—	—
224	41	5 (12.2%)	—	36 (87.8%)	35 (85.4%)	—
225	4221	647 (15.3%)	9 (0.2%)	320 (7.6%)	245 (5.8%)	8 (0.2%)
226	57	1 (1.8%)	—	1 (1.8%)	—	—
227	1971	1688 (85.6%)	1535 (77.9%)	1101 (55.9%)	369 (18.7%)	—
229	471	14 (3.0%)	—	19 (4.0%)	6 (1.3%)	1 (0.2%)
230	6	—	—	1 (16.7%)	1 (16.7%)	—
Total	55206	6120 (11.1%)	1666 (3.0%)	21175 (38.4%)	8224 (14.9%)	1590 (2.9%)

Appendix D: Automated search for materials with Kagome, pyrochlore or Lieb sublattice

In Appendix C, we have provided statistics about the crystal sublattices found in the materials of Topological Quantum Chemistry website. These sublattices fall into five classes, namely the Kagome, pyrochlore, bipartite, split or Lieb sublattices. The two line-graph lattices, Kagome and pyrochlore lattices, and Lieb lattice exhibit flat bands in their respective band structure *only* when the related tight-binding Hamiltonian satisfies the following strict condition: the hopping amplitudes between any two nearest-neighbor sites are non-zero and equal. In real crystalline materials, equality between two hopping amplitudes can be guaranteed only when they are related by symmetries. Otherwise such a fine tuning is never achieved exactly. For these reasons, in real crystalline materials, only the Kagome and pyrochlore lattices among the line-graph lattices can be physically realized. For bipartite and split lattices, the condition is: the hopping amplitude is zero between any two unconnected sites.

In this appendix, we first analyze the crystal symmetries and the geometrical features of Kagome, pyrochlore and Lieb lattices. Then, by using their geometrical features, we have designed an algorithm to systematically search for the rigorous and approximate Kagome, pyrochlore or Lieb sublattices in real materials.

1. Crystal symmetries of Kagome, pyrochlore and Lieb lattices

As shown in Fig. 6(a), the Kagome lattice in 2D consists of the $3c$ Wyckoff position of the wallpaper group $p6mm$. Among the 3D space groups, there are three different minimal space groups rigorously compatible with the symmetry of the Kagome lattice: $P\bar{3}$ (SG 147), $P6$ (SG 168) and $I23$ (SG 197), of which the Wyckoff positions $3e$ or $3f$, $3c$ and $6b$ form a Kagome sublattice, respectively.

Using the group-subgroup relations on the *Bilbao Crystallographic Server* (BCS)[35,36], we have obtained all the space groups that are super-groups of the three minimal space groups for Kagome lattices. We analyzed the subduction of the Wyckoff positions from super-groups to the minimal groups. The Wyckoff positions that form a Kagome sublattice in the super-groups have been obtained and are tabulated in Table V. There, we show all the crystal lattices of the 40 3D space groups that have Kagome sublattices once their corresponding Wyckoff positions provided in this table are occupied by atoms. Note that in the above subduction of Wyckoff positions, if a Wyckoff position of a super-group splits into a Wyckoff position that forms a Kagome sublattice and some other types of Wyckoff positions coplanar to this Kagome sublattice, then the redundant Wyckoff positions spoil the Kagome lattice. Such situation happens, e.g., with the Wyckoff position $12c$ of $Im\bar{3}m$(SG 229). Thus, we have discarded such cases in Table V.

We now turn to the pyrochlore lattice. As shown in Fig. 6(b), a pyrochlore lattice is a 3D lattice. The minimal space groups hosting a pyrochlore lattice are $Fd\bar{3}$ (SG 203) and $F4_132$ (SG 210), of which the Wyckoff positions $16c$ or $16d$ with site-symmetry group isomorphic to point group symmetry $\bar{3}m$ form the pyrochlore lattice. Using the same method as of the Kagome lattice, we have obtained all the space groups that are super-groups of the two minimal space groups of the pyrochlore lattice. They are tabulated in Table V, including the corresponding Wyckoff positions that should be occupied to get a pyrochlore lattice. Note that since pyrochlore lattice is a 3D lattice, only the Wyckoff positions tabulated in Table V can be occupied. Any other Wyckoff position occupied by the same element will spoil the exact pyrochlore lattice.

Finally, the Lieb lattice shown in Fig. 6(c), is a 2D lattice associated to the wallpaper group $p4mm$. It is made of two different Wyckoff positions, $1a$ and $2c$. In 3D, the minimal space groups hosting Lieb lattices are $P4/m$ (SG 83), $P4_2/m$ (SG 84) and $P4/n$ (SG 85). In Table VI, we tabulate these three minimal space groups and their related

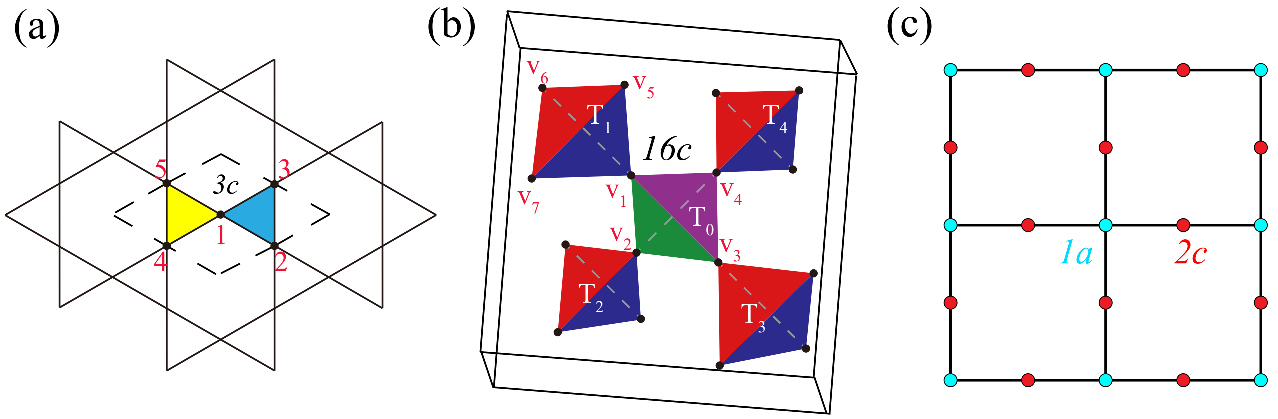

Figure 6. Crystal structures of Kagome, pyrochlore and Lieb lattices. (a) The Wyckoff position $3c$ of the wallpaper group $p6mm$ form a Kagome Lattice in 2D. The two equilateral triangles formed by the respective set of sites {1,2,3} and {1,4,5} are related by a vertical two-fold rotational symmetry centered at the site 1. (b) The Wyckoff position $16c$ in space group $Fd\bar{3}m$ form a pyrochlore lattice in 3D. The pyrochlore lattice is formed by the regular tetrahedrons which share vertices with each others. For example, the two regular tetrahedrons T_0 and T_1 that formed by the sets of vertices $\{v_1, v_2, v_3, v_4\}$ and $\{v_1, v_5, v_6, v_7\}$, respectively, share the vertex v_1. Moreover, each site of the pyrochlore sublattice is also shared by three Kagome planes. For example, the triangle formed by the vertices $\{v_1, v_2, v_3\}$ in T_0 is co-planar with the triangle formed by the vertices $\{v_1, v_5, v_6\}$ in T_1. There are four equivalent Kagome sublattices related by the point group symmetry ($\bar{3}m$) of the pyrochlore lattice. (c) The Wyckoff positions $1a$ and $2c$ of the wallpaper group $p4mm$ form a Lieb lattice in 2D. The 2c sites (red) are at the middle point of their two NN 1a sites (blue). The 1a sites have four C_4 symmetry related 2c sites NNs.

super-groups having Lieb sublattice, providing the related Wyckoff positions. We have also discarded the Wyckoff positions of any super-group that split into a Wyckoff position that forms a Lieb sublattice and some other types of Wyckoff positions coplanar to this Lieb sublattice, just like what we have done for the Kagome lattice.

Table V: The Wyckoff positions (WPs) of 3D space groups forming Kagome or pyrochlore sublattice on special Miller plane. For each case of each SG, the column 'WP' provides the WP which form a Kagome or pyrochlore sublattice when it's occupied. The column '$\overline{WP}$' provides all the Wyckoff positions which are defined on the same plane with the Kagome lattice formed by 'WP'. When one (or more than one) of the Wyckoff positions in '$\overline{WP}$' is occupied by the atoms of the same element with 'WP', the Kagome lattice formed by the Wyckoff position in 'WP' will be spoiled. For each case, the column 'Plane' provides the Miller indices of the Kagome sublattice formed by 'WP'. Miller indices are given in the basis of the lattice vector of the conventional unit-cell (using the standard convention of the *Bilbao Crystallographic Server*). The column 'Lattice' indicates the type of sublattice formed by the corresponding Wyckoff positions. 'K' and 'P' stand for the Kagome and pyrochlore sublattice, respectively.

SG	WP	$\overline{WP}$	Plane	Lattice	SG	WP	$\overline{WP}$	Plane	Lattice
147 $P\bar{3}$	3e	1a	[0 0 1]	K	147 $P\bar{3}$	3f	1b	[0 0 1]	K
148 $R\bar{3}$	9d	3b	[0 0 1]	K	148 $R\bar{3}$	9e	3a	[0 0 1]	K
162 $P\bar{3}1m$	3f	1a, 2c, 6i	[0 0 1]	K	162 $P\bar{3}1m$	3g	1b, 2d, 6j	[0 0 1]	K
163 $P\bar{3}1c$	6g	2b	[0 0 1]	K	164 $P\bar{3}m1$	3e	1a, 6g	[0 0 1]	K
164 $P\bar{3}m1$	3f	1b, 6h	[0 0 1]	K	165 $P\bar{3}c1$	6e	2b	[0 0 1]	K
166 $R\bar{3}m$	9d	3b, 18g	[0 0 1]	K	166 $R\bar{3}m$	9e	3a, 18f	[0 0 1]	K
167 $R\bar{3}c$	18d	6b	[0 0 1]	K	168 $P6$	3c	1a, 2b, 6d	[0 0 1]	K
175 $P6/m$	3f	1a, 2c, 6j	[0 0 1]	K	175 $P6/m$	3g	1b, 2d, 6k	[0 0 1]	K
175 $P6/m$	6i	2e, 4h, 12l	[0 0 1]	K	176 $P6_3/m$	6g	2b	[0 0 1]	K
177 $P622$	3f	1a, 2c, 6j, 6l	[0 0 1]	K	177 $P622$	3g	1b, 2d, 6k, 6m	[0 0 1]	K
177 $P622$	6i	2e, 4h, 12n	[0 0 1]	K	183 $P6mm$	3c	1a, 2b, 6d, 6e, 12f	[0 0 1]	K
184 $P6cc$	6c	2a, 4b, 12d	[0 0 1]	K	191 $P6/mmm$	3f	1a, 2c, 6j, 6l, 12p	[0 0 1]	K
191 $P6/mmm$	3g	1b, 2d, 6k, 6m, 12q	[0 0 1]	K	191 $P6/mmm$	6i	2e, 4h, 12n, 12o, 24r	[0 0 1]	K
192 $P6/mcc$	6f	2a, 4c, 12j, 12k	[0 0 1]	K	192 $P6/mcc$	6g	2b, 4d, 12l	[0 0 1]	K
192 $P6/mcc$	12i	4e, 8h, 24m	[0 0 1]	K	193 $P6_3/mcm$	6f	2b, 4d, 12i	[0 0 1]	K
194 $P6_3/mmc$	6g	2a, 12i	[0 0 1]	K	195 $P23$	3c	1a	[1 1 1]	K
195 $P23$	3d	1b	[1 1 1]	K	197 $I23$	6b	2a	[1 1 1]	K

200 $Pm\bar{3}$	3c	1a	[1 1 1]	K	200 $Pm\bar{3}$	3d	1b	[1 1 1]	K
201 $Pn\bar{3}$	6d	2a	[1 1 1]	K	202 $Fm\bar{3}$	24d	4b	[1 1 1]	K
202 $Fm\bar{3}$	24d	4a	[1 1 1]	K	203 $Fd\bar{3}$	16c	16d	[1 1 1]	K
203 $Fd\bar{3}$	16d	16c	[1 1 1]	K	204 $Im\bar{3}$	6b	2a	[1 1 1]	K
207 $P432$	3c	1a, 12i	[1 1 1]	K	207 $P432$	3d	1b, 12j	[1 1 1]	K
208 $P4_232$	6d	2a	[1 1 1]	K	209 $F432$	24d	4b, 48h	[1 1 1]	K
209 $F432$	24d	4a, 48g	[1 1 1]	K	210 $F4_132$	16c	16d, 48g	[1 1 1]	K
210 $F4_132$	16d	16c, 48g	[1 1 1]	K	211 $I432$	6b	2a, 24h	[1 1 1]	K
215 $P\bar{4}3m$	3c	1a	[1 1 1]	K	215 $P\bar{4}3m$	3d	1b	[1 1 1]	K
217 $I\bar{4}3m$	6b	2a	[1 1 1]	K	218 $P\bar{4}3n$	6b	2a	[1 1 1]	K
219 $F\bar{4}3c$	24c	8a	[1 1 1]	K	219 $F\bar{4}3c$	24d	8b	[1 1 1]	K
221 $Pm\bar{3}m$	3c	1a, 12i	[1 1 1]	K	221 $Pm\bar{3}m$	3d	1b, 12j	[1 1 1]	K
222 $Pn\bar{3}n$	6b	2a, 24h	[1 1 1]	K	223 $Pm\bar{3}n$	6b	2a	[1 1 1]	K
224 $Pn\bar{3}m$	6d	2a	[1 1 1]	K	225 $Fm\bar{3}m$	24d	4b, 48i	[1 1 1]	K
225 $Fm\bar{3}m$	24d	4a, 48h	[1 1 1]	K	226 $Fm\bar{3}c$	24c	8a, 96h	[1 1 1]	K
226 $Fm\bar{3}c$	24d	8b	[1 1 1]	K	227 $Fd\bar{3}m$	16c	16d, 96h	[1 1 1]	K
227 $Fd\bar{3}m$	16d	16c, 96h	[1 1 1]	K	228 $Fd\bar{3}c$	48d	16a	[1 1 1]	K
229 $Im\bar{3}m$	6b	2a, 24h	[1 1 1]	K	203 $Fd\bar{3}$	16c	-	-	P
203 $Fd\bar{3}$	16d	-	-	P	210 $F4_132$	16c	-	-	P
210 $F4_132$	16d	-	-	P	227 $Fd\bar{3}m$	16c	-	-	P
227 $Fd\bar{3}m$	16d	-	-	P					

Table VI: The Wyckoff positions (WP) of 3D space groups forming Lieb sublattice on special Miller plane. For each case of each SG, the column 'WP(1a)' is the WP which forms the '1a' site of the Lieb lattice in Figure 6(c). The column 'WP(2c)' provides the list of WPs which form the 2c sites of the Lieb lattice in Figure 6(c). The column 'WP(empty)' provides all the WPs that are defined on the same plane with the WPs in 'WP(1a)' and 'WP(2c)'. If one (or more than one) of the WP in 'WP(empty)' is occupied by any atoms, the Lieb lattice will be spoiled. For each case, the Miller indices are always [0 0 1], given in the basis of the lattice vector of the conventional unit-cell (using the standard convention of the *Bilbao Crystallographic Server*).

SG	WP(1a)	WP(2c)	WP(empty)	SG	WP(1a)	WP(2c)	WP(empty)
83 $P4/m$	1c	2e	1a, 4j	83 $P4/m$	1a	2e	1c, 4j
83 $P4/m$	1d	2f	1b, 4k	83 $P4/m$	1b	2f	1d, 4k
84 $P4_2/m$	2d	2a, 2b	2c, 4j	84 $P4_2/m$	2c	2a, 2b	2d, 4j
84 $P4_2/m$	2b	2c, 2d	2a, 4j	84 $P4_2/m$	2a	2c, 2d	2b, 4j
85 $P4/n$	2a	4d		85 $P4/n$	2b	4e	
87 $I4/m$	2b	4c	2a, 8h	87 $I4/m$	2a	4c	2b, 8h
87 $I4/m$	4d	8f		89 $P422$	1c	2e	1a, 4j, 4l, 4o
89 $P422$	1a	2e	1c, 4j, 4l, 4o	89 $P422$	1d	2f	1b, 4k, 4m, 4n
89 $P422$	1b	2f	1d, 4k, 4m, 4n	93 $P4_222$	2d	2a, 2b	2c, 4j, 4k, 4l, 4m
93 $P4_222$	2c	2a, 2b	2d, 4j, 4k, 4l, 4m	93 $P4_222$	2b	2c, 2d	2a, 4j, 4k, 4l, 4m
93 $P4_222$	2a	2c, 2d	2b, 4j, 4k, 4l, 4m	97 $I422$	2b	4c	2a, 8g, 8h, 8i
97 $I422$	2a	4c	2b, 8g, 8h, 8i	111 $P\bar{4}2m$	1d	2e	1a, 4i, 4l
111 $P\bar{4}2m$	1a	2e	1d, 4i, 4l	111 $P\bar{4}2m$	1c	2f	1b, 4j, 4k
111 $P\bar{4}2m$	1b	2f	1c, 4j, 4k	112 $P\bar{4}2c$	2d	2a, 2c	2b, 4g, 4h, 4i, 4j
112 $P\bar{4}2c$	2c	2b, 2d	2a, 4g, 4h, 4i, 4j	112 $P\bar{4}2c$	2b	2a, 2c	2d, 4g, 4h, 4i, 4j
112 $P\bar{4}2c$	2a	2b, 2d	2c, 4g, 4h, 4i, 4j	121 $I\bar{4}2m$	2b	4c	2a, 8f, 8g
121 $I\bar{4}2m$	2a	4c	2b, 8f, 8g	123 $P4/mmm$	1c	2f	1a, 4j, 4l, 4n, 8p
123 $P4/mmm$	1a	2f	1c, 4j, 4l, 4n, 8p	123 $P4/mmm$	1d	2e	1b, 4k, 4m, 4o, 8q
123 $P4/mmm$	1b	2e	1d, 4k, 4m, 4o, 8q	124 $P4/mcc$	2d	4e	2b, 8m
124 $P4/mcc$	2b	4e	2d, 8m	124 $P4/mcc$	2c	4f	2a, 8j, 8k, 8l
124 $P4/mcc$	2a	4f	2c, 8j, 8k, 8l	125 $P4/nbm$	2c	4e	2a, 8i, 8k

125 $P4/nbm$	2a	4e	2c, 8i, 8k	125 $P4/nbm$	2d	4f	2b, 8j, 8l
125 $P4/nbm$	2b	4f	2d, 8j, 8l	126 $P4/nnc$	2b	4c	2a, 8h, 8i, 8j
126 $P4/nnc$	2a	4c	2b, 8h, 8i, 8j	126 $P4/nnc$	4d	8f	
128 $P4/mnc$	2b	4c	2a, 8h	128 $P4/mnc$	2a	4c	2b, 8h
129 $P4/nmm$	2a	4d	8g	129 $P4/nmm$	2b	4e	8h
130 $P4/ncc$	4b	8d		131 $P4_2/mmc$	2d	2a, 2b	2c, 4j, 4k, 4l, 4m, 8q
131 $P4_2/mmc$	2c	2a, 2b	2d, 4j, 4k, 4l, 4m, 8q	131 $P4_2/mmc$	2b	2c, 2d	2a, 4j, 4k, 4l, 4m, 8q
131 $P4_2/mmc$	2a	2c, 2d	2b, 4j, 4k, 4l, 4m, 8q	132 $P4_2/mcm$	2c	4f	2a, 4i, 4j, 8n
132 $P4_2/mcm$	2a	4f	2c, 4i, 4j, 8n	132 $P4_2/mcm$	2d	4e	2b, 8l, 8m
132 $P4_2/mcm$	2b	4e	2d, 8l, 8m	133 $P4_2/nbc$	4b	8e	4a, 8h, 8i
133 $P4_2/nbc$	4a	8e	4b, 8h, 8i	134 $P4_2/nnm$	2b	4c	2a, 8i, 8j
134 $P4_2/nnm$	2a	4c	2b, 8i, 8j	134 $P4_2/nnm$	4d	4e, 4f	8k, 8l
136 $P4_2/mnm$	2b	4c	2a, 4f, 4g, 8i	136 $P4_2/mnm$	2a	4c	2b, 4f, 4g, 8i
138 $P4_2/ncm$	4a	4c, 4d	8g, 8h	139 $I4/mmm$	2b	4c	2a, 8h, 8i, 8j, 16l
139 $I4/mmm$	2a	4c	2b, 8h, 8i, 8j, 16l	139 $I4/mmm$	4d	8f	16k
140 $I4/mcm$	4b	8e	4a, 16i, 16j	140 $I4/mcm$	4a	8e	4b, 16i, 16j
195 $P23$	3c	3d	1a, 6f, 6g, 6h	195 $P23$	3d	3c	1a, 6f, 6g, 6h
195 $P23$	1a	3d	3c, 6f, 6g, 6h	195 $P23$	3c	3d	1b, 6g, 6h, 6i
195 $P23$	3d	3c	1b, 6g, 6h, 6i	195 $P23$	1b	3c	3d, 6g, 6h, 6i
197 $I23$	6b	6b	2a, 12d, 12e	200 $Pm\bar{3}$	3c	3d	1a, 6e, 6f, 6g, 12j
200 $Pm\bar{3}$	3d	3c	1a, 6e, 6f, 6g, 12j	200 $Pm\bar{3}$	1a	3d	3c, 6e, 6f, 6g, 12j
200 $Pm\bar{3}$	3c	3d	1b, 6f, 6g, 6h, 12k	200 $Pm\bar{3}$	3d	3c	1b, 6f, 6g, 6h, 12k
200 $Pm\bar{3}$	1b	3c	3d, 6f, 6g, 6h, 12k	201 $Pn\bar{3}$	6d	6d	2a, 12f, 12g
202 $Fm\bar{3}$	4b	24d	4a, 24e, 48h	202 $Fm\bar{3}$	4a	24d	4b, 24e, 48h
202 $Fm\bar{3}$	8c	24d	48g	204 $Im\bar{3}$	6b	6b	2a, 12d, 12e, 24g
207 $P432$	3c	3d	1a, 6e, 12h, 12i	207 $P432$	3d	3c	1a, 6e, 12h, 12i
207 $P432$	1a	3d	3c, 6e, 12h, 12i	207 $P432$	3c	3d	1b, 6f, 12h, 12j
207 $P432$	3d	3c	1b, 6f, 12h, 12j	207 $P432$	1b	3c	3d, 6f, 12h, 12j
208 $P4_232$	6d	6d	2a, 6e, 6f, 12h, 12i, 12j	208 $P4_232$	6e	4b, 4c	12k, 12l
209 $F432$	4b	24d	4a, 24e, 48g, 48h	209 $F432$	4a	24d	4b, 24e, 48g, 48h
209 $F432$	8c	24d	48i	211 $I432$	6b	6b	2a, 12d, 12e, 24g, 24h
211 $I432$	12d	8c	24i	215 $P\bar{4}3m$	3c	3d	1a, 6f, 12h
215 $P\bar{4}3m$	3d	3c	1a, 6f, 12h	215 $P\bar{4}3m$	1a	3d	3c, 6f, 12h
215 $P\bar{4}3m$	3c	3d	1b, 6g, 12h	215 $P\bar{4}3m$	3d	3c	1b, 6g, 12h
215 $P\bar{4}3m$	1b	3c	3d, 6g, 12h	217 $I\bar{4}3m$	6b	6b	2a, 12d, 12e, 24f
218 $P\bar{4}3n$	6b	6b	2a, 6c, 6d, 12f, 12g, 12h	219 $F\bar{4}3c$	24c	24d	8a, 48f
219 $F\bar{4}3c$	24d	24c	8a, 48f	219 $F\bar{4}3c$	8a	24d	24c, 48f
219 $F\bar{4}3c$	24c	24d	8b, 48g	219 $F\bar{4}3c$	24d	24c	8b, 48g
219 $F\bar{4}3c$	8b	24c	24d, 48g	221 $Pm\bar{3}m$	3c	3d	1a, 6e, 12h, 12i, 24k
221 $Pm\bar{3}m$	3d	3c	1a, 6e, 12h, 12i, 24k	221 $Pm\bar{3}m$	1a	3d	3c, 6e, 12h, 12i, 24k
221 $Pm\bar{3}m$	3c	3d	1b, 6f, 12h, 12j, 24l	221 $Pm\bar{3}m$	3d	3c	1b, 6f, 12h, 12j, 24l
221 $Pm\bar{3}m$	1b	3c	3d, 6f, 12h, 12j, 24l	222 $Pn\bar{3}n$	6b	6b	2a, 12d, 12e, 24g, 24h
222 $Pn\bar{3}n$	12d	8c		223 $Pm\bar{3}n$	6b	6b	2a, 6c, 6d, 12f, 12g, 12h, 24k
223 $Pm\bar{3}n$	6c	6d, 8e	24j	224 $Pn\bar{3}m$	6d	6d	2a, 12f, 12g, 24h
224 $Pn\bar{3}m$	12f	4b, 4c	24i, 24j	225 $Fm\bar{3}m$	4b	24d	4a, 24e, 48h, 48i, 96j
225 $Fm\bar{3}m$	4a	24d	4b, 24e, 48h, 48i, 96j	225 $Fm\bar{3}m$	8c	24d	48g
226 $Fm\bar{3}c$	24c	24d	8b, 48e, 96i	226 $Fm\bar{3}c$	24d	24c	8b, 48e, 96i
226 $Fm\bar{3}c$	8b	24c	24d, 48e, 96i	226 $Fm\bar{3}c$	24c	24d	8a, 48f, 96h
226 $Fm\bar{3}c$	24d	24c	8a, 48f, 96h	226 $Fm\bar{3}c$	8a	24d	24c, 48f, 96h
228 $Fd\bar{3}c$	48d	48d	16a, 96f	229 $Im\bar{3}m$	6b	6b	2a, 12d, 12e, 24g, 24h, 48j
229 $Im\bar{3}m$	12d	8c	48i				

2. Geometrical features of standard Kagome, pyrochlore and Lieb lattices

Using the above symmetry analysis, it is straightforward to systematically filter out the crystalline materials exhibiting *rigorous* Kagome, pyrochlore or Lieb sublattices by checking the occupied Wyckoff positions. However, in many of the 3D crystalline materials, there are no rigorous line-graph or Lieb sublattices, only approximate ones. These *approximate* Kagome, pyrochlore or Lieb sublattices are not part of Tables V or VI. Still, they can be obtained from these rigorous sublattices by weak lattice distortion. When this distortion is weak enough, the lattice might still hosts (almost) flat bands. As the *approximate* Kagome, pyrochlore and Lieb sublattices do not satisfy the minimal symmetry groups of the rigorous ones, the only efficient method to identify them is comparing their geometrical structures with those of the rigorous sublattices. In this subsection, we will analyze the key geometrical features of the rigorous Kagome, pyrochlore and Lieb lattices, which are schematically shown in Fig. 6. In the next subsection, we will rely on these features to design numerical algorithms for searching approximate line-graph and Lieb sublattices in real crystalline materials.

Kagome Lattice The rigorous Kagome lattice in 2D, as shown in Fig. 6(a), is made of three equivalent sites corresponding to the Wyckoff position $3c$ in one unit cell with wallpaper group $p6mm$. For convenience, we label the five sites of $3c$ as 1, 2, 3, 4 and 5, where the sites 4 and 5 differ from sites 3 and 2, respectively, by a lattice translation. The 2D point group of $3c$ is $2mm$, which includes a vertical two-fold rotational symmetry and two vertical mirror symmetries. So the two regular triangles formed by sites $\{1, 2, 3\}$ and sites $\{1, 4, 5\}$, respectively, are related by the two-fold rotational symmetry.

Thus, there are two key geometrical features for the rigorous Kagome lattice in Fig. 6(a):

1. For each site on the 2D lattice, it has only four co-planar nearest neighbor (NN) sites on the same plane.
2. Each site and its four NN sites form two equilateral triangles, which are related by a vertical C_2 symmetry.

If a 2D sublattice occupied by the same chemical element of a given material can be characterized by the above two geometrical features within a certain threshold (as will be discussed in the next subsection), then we label it as an approximate Kagome sublattice.

Pyrochlore Lattice As shown in Fig. 6(b), the rigorous pyrochlore lattice is a 3D line-graph lattice. Its geometry has the two following features:

1. The unit cell of the 3D lattice is constructed by five regular tetrahedrons, each two of which share one vertex. For example, in Fig. 6(b), the regular tetrahedron T_0 formed by the vertices $\{v_1, v_2, v_3, v_4\}$ and another regular tetrahedron T_1 formed by the vertices $\{v_1, v_5, v_6, v_7\}$ share the vertex v_1.
2. Each of the four triangle surfaces in one tetrahedron is always co-planar with one triangle surface of its NN tetrahedron and the two co-planar triangles form a Kagome sublattice. For example, the triangle formed by the vertices $\{v_1, v_2, v_3\}$ in T_0 is co-planar with the triangle formed by the vertices $\{v_1, v_5, v_6\}$ in T_1 and these vertices form a Kagome sublattice. There are four equivalent Kagome sublattices which are related by the point group symmetry of the pyrochlore lattice ($\bar{3}m$).

Thus, for a 3D sublattice which is formed by the same chemical element of a given material, if it can be characterized by the above two geometrical features within a certain threshold, we consider it as an approximate pyrochlore sublattice.

Lieb lattice The rigorous Lieb lattice is a 2D lattice formed by two non-equivalent atom sites, the blue and red sites as indicated in Fig. 6(c). The blue sites form a square lattice and the red sites are on the middle of the bonds between two adjacent blue sites.

Lieb lattice has the following three key geometrical features:

1. It has two non-equivalent atom sites, $\{A_1\}$ and $\{A_2\}$, which are co-planar. Each atom in $\{A_1\}$ always has two NN sites, which belong to $\{A_2\}$. Each atom site in $\{A_2\}$ always has four NN sites, which belong to $\{A_1\}$.
2. Each of the atom sites in $\{A_1\}$ is in the middle of its two NN sites.
3. The four bonds which connect the atom in $\{A_2\}$ and its four NN sites are related by a four-fold rotational symmetry.

A 2D sublattice occupied by one or two different chemical elements of a given material and satisfying the two above geometrical features within a certain threshold, is labelled as an approximate Lieb sublattice.

3. Algorithms to search for Kagome, pyrochlore and Lieb sublattices

The symmetry properties and the key geometrical features of rigorous Kagome, pyrochlore and Lieb lattices enable the high-throughput search for both rigorous and approximate line-graph sublattices in real materials. Using the key geometrical features as discussed in Appendix D 2, we have designed numerical algorithms to search for Kagome, pyrochlore and Lieb sublattices from the crystal lattice of real materials. Whether or not the line-graph and Lieb sublattices also satisfy the symmetry analysis of Appendix D 1, we classify them into rigorous or approximate.

a. Kagome and pyrochlore sublattices

There are four steps to identify a Kagome or pyrochlore sublattice from the crystal lattice of a material.

Step 1 For each material, its crystal structure is parsed from the *POSCAR* file, which was used in the first-principle calculations[5]. The crystal symmetry and the list of occupied Wyckoff letters of the non-equivalent atom sites are analyzed by the *Pymatgen* package.

Step 2 By grouping together the atom sites of the same chemical element in one unit cell, the crystal lattice is divided into several sets. For convenience, a set will be denoted by $\{A_i\}$ where A_i denotes a single atom. The two following steps are applied to each set until we exhaust all possible sublattices.

Step 3 For each atom site in a certain set $\{A_i\}$, we check if it satisfies the following four criteria sequentially:

- C1 The atom site has and only has four co-planar nearest neighbor (NN) or next nearest neighbor (NNN) sites, which also belong to $\{A_i\}$, *on certain Miller planes*. If true, we refer this atom site as a representative site and obtain the corresponding Miller indices $[hkl]$.
- C2 By calculating the length of the bonds between the representative atom site and its four NN/NNN sites and the angles between the four bonds, we check whether the five sites form two regular triangles related by a vertical C_2 symmetry, which is centered at the representative atom site.
- C3 Each of the four NN/NNN atom sites also satisfies the first two criteria.
- C4 Each atom site in the set $\{A_i\}$ satisfies the criteria C1,C2 and C3 on three different Miller planes.

Step 4 If a set (or part of a set) satisfies the criteria C1, C2 and C3, it is classified as a Kagome sublattice. If it moreover satisfies C4, it is also tagged as a pyrochlore sublattice.

The flow chart of this algorithm is shown in Fig. 7. Based on this algorithm, we have developed a *Python*-based code to identify if the crystal lattice of a material has any Kagome or pyrochlore sublattice. In this code, we rely on several functions of the *Pymatgen* package[62]. The function *Pymatgen.core.structure.get_neighbors* is used to get the neighboring sites of an atom and the function *pymatgen.core.structure.get_angle* is used to calculate the angle between two bonds. The Miller indices are obtained using the function *pymatgen.core.lattice.get_miller_index_from_coords*. Our algorithm requires a set of threshold parameters to distinguish a regular triangle. More precisely, the threshold is set to ±20% of the NN/NNN bonds' length when identifying two equivalent bonds. A threshold of ±2° is applied to discriminate two identical angles.

b. Lieb sublattice

We apply a five-step process to identify a Lieb sublattice from a 3D crystal lattice of material.

Step 1 For each material, its crystal structure is parsed from the *POSCAR* file, which was used in the first-principle calculations[5]. The crystal symmetry and the list of Wyckoff letters of the non-equivalent atom sites are analyzed by the *Pymatgen* package.

Step 2 We obtain all the NN sites for each atom site in the lattice.

Step 3 We select all the atom sites that have only two NN sites of identical element and are at the equal distance of its NN sites. Such atom sites are referred as 'middle sites' and labeled as A_1. The NN sites of A_1 are labeled as A_2.

Step 4 For each of the 'middle sites' obtained in Step 3, we check sequentially the following four criteria:

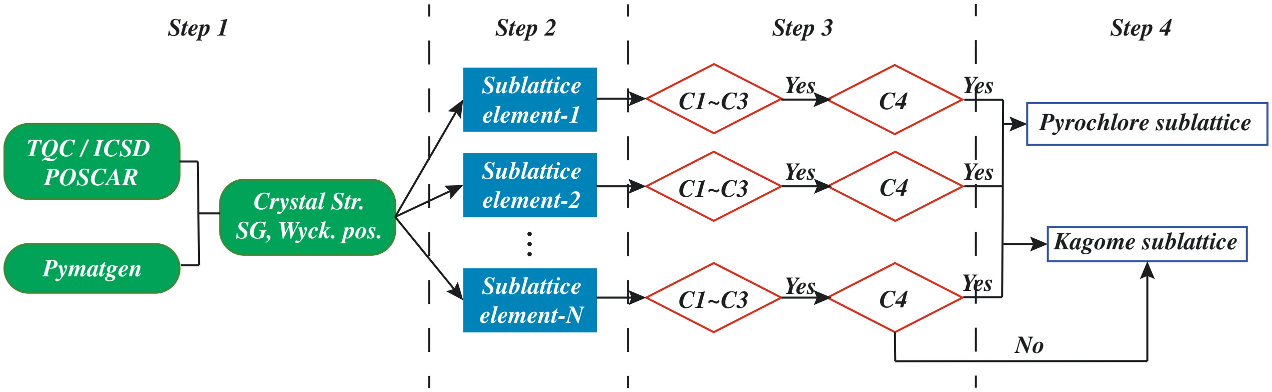

Figure 7. The flow chart of the Kagome or pyrochlore sublattice identification from a 3D crystal lattice. Starting from the crystal structure of material provided as a *POSCAR* file, the crystal symmetry and the Wyckoff positions of each distinct element are analyzed by the *Pymatgen* package. For each sublattice, the criteria C1, C2 and C3 are applied to identify if the sublattice is a Kagome plane. If at this stage, a 2D Kagome sublattice has been identified, the criterion C4 is applied to test if the crystal structure also hosts a 3D pyrochlore sublattice.

C1 For a given 'middle site' A_1, each of its two NN sites A_2 has and only has four NN sites, which are *co-planar on certain Miller planes* and are also labeled as A_1 in Step 3.

C2 The four NNs of A_2 are of identical element. And the four bonds connecting A_2 and its four NN sites are of equal length and the angles between any two neighbor bonds equals to 90°.

C3 Both of the two NN sites A_2 of a 'middle site' A_1 satisfy the criterion C2 on the same plane.

C4 All the 'middle sites' on the same plane satisfy simultaneously criteria C1, C2 and C3.

Step 5 If there is a 2D sublattice, of which the atom sites satisfy the criteria C1 to C4 in step 4, it is classified as a Lieb lattice and the Miller indices of the Lieb sublattice are recorded.

The algorithm flow chart is provided in Fig. 8. We have implemented this algorithm in a *Python*-based code. It detects if the crystal lattice of a material has a Lieb sublattice. Our code uses a set of threshold parameters to identify whether two bonds are equal or an angle matches the expected value: a threshold is set to ±20% of the NN bonds' length to identify two equivalent bonds and a threshold of ±10° is applied to discriminate two identical angles. In real crystalline materials in the Materials Flatband Database website, Lieb sublattices tend to be spoiled by lattice distortion. In this section, a larger threshold is used to identify an approximate Lieb lattice.

c. *Rigorous and approximate sublattices*

As discussed in Appendix D 1, rigorous sublattices can be identified from the space group and the corresponding occupied Wyckoff positions in the Table V or VI. Although these two features are analyzed for each crystal structure in the database using *Pymatgen* package[63,64], they are not enough to confirm that a given material hosts a rigorous sublattice. Indeed, the sublattice might be spoiled by the presence of other in-plane atoms of the *same element* on (or close to) this sublattice. For example, in SG 147 ($P\bar{3}$), the Kagome sublattice formed by the Wyckoff position $3e$ with atom A occupied will be spoiled by the Wyckoff position $1a$ if $1a$ is also occupied by the identical atom. Note that the site of $1a$ is exactly on the Kagome plane formed by $3e$. The two algorithms described in Appendix D 3(a), were designed to detect such situations. Indeed in the geometric method algorithm described above, such cases are discarded when applying criterion C1. Note that if the sublattice has as a nearest neighbor other atoms of *different type*, the flat bands emerging from the sublattice are usually preserved. For example, $Co_3Sn_2S_2$ [ICSD 5435, SG 166 ($R\bar{3}m$)], the Sn atoms sit at the center of the Co Kagome sublattice hexagons. Still flat bands are observed in the band structure (shown in Fig. 9a). Conversely, Pt_2HgSe_3 [ICSD 185808, SG 164 ($P\bar{3}m1$)] has a Kagome lattice made of Pt atoms at Wyckoff positions $3e$. But the Pt atoms at Wyckoff positions $1a$ spoils the Kagome sublattice and the band structure (shown in Fig. 9b) does not exhibit any flat band. Rather than discarding cases where atoms of a different type are nearest neighbors, we have added on the Materials Flatband Database website for each sublattice

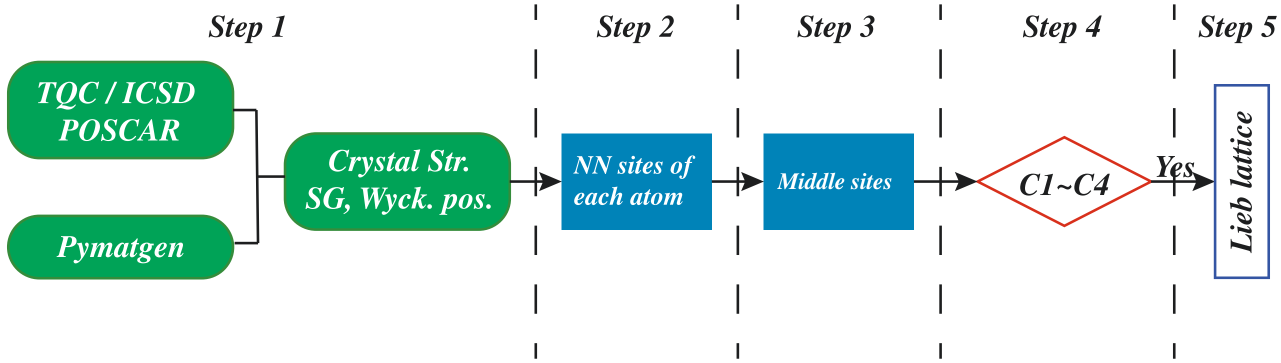

Figure 8. The flow chart of the Lieb sublattice identification from a 3D crystal lattice. Starting from the crystal structure of materials provided as a *POSCAR* file, the crystal symmetry and the Wyckoff positions of each distinct element are analyzed by the *Pymatgen* package. The second step identifies the nearest neighbor(NN) sites of each atom. If an atom is at the middle of its two NN sites, it is referred to as the 'middle-site' (Step 3). Then at Step 4, the criteria from C1 to C4 are applied to check if the *middle sites* and their NN sites form a Lieb sublattice.

description, the location and type of any additional nearest neighbor atoms, (see for example the Kagome sublattice description for $Co_3Sn_2S_2$).

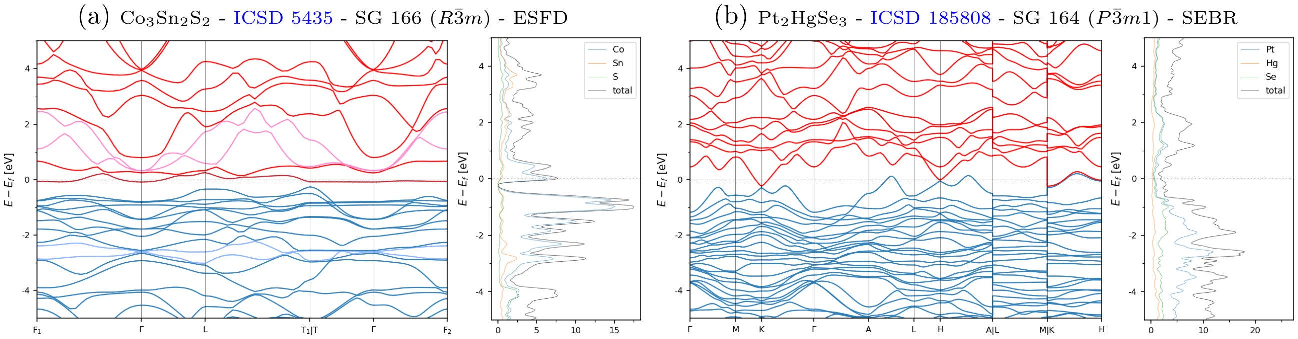
(a) $Co_3Sn_2S_2$ - ICSD 5435 - SG 166 ($R\bar{3}m$) - ESFD

(b) Pt_2HgSe_3 - ICSD 185808 - SG 164 ($P\bar{3}m1$) - SEBR

Figure 9. (a) Band structure of $Co_3Sn_2S_2$ [ICSD 5435, SG 166 ($R\bar{3}m$)]. (b) Band structure of Pt_2HgSe_3 [ICSD 185808, SG 164 ($P\bar{3}m1$)].

For that reason, a material is tagged as having a *rigorous* Kagome, pyrochlore or Lieb sublattice if, within its space group, its occupied Wyckoff positions belong to the corresponding set of Wyckoff positions in the Table V or VI *and* if the material successfully passes the corresponding test set by our algorithms. If a material does not satisfy the symmetry features of Appendix D 1 but still successfully passes the corresponding test set by our algorithms, then the material is tagged as having an *approximate* Kagome, pyrochlore or Lieb sublattice.

Among the 55,206 ISCD entries that we have considered, 4,192 ICSDs (7.59%) host at least one rigorous Kagome sublattice, while 2,100 ICSDs (3.80%) host at least one approximate Kagome sublattice. Similarly, we found 1,541 ICSDs (2.79%) with at least one rigorous pyrochlore sublattice, 125 ICSDs (0.23%) with at least one approximate pyrochlore sublattice, 1,202 ICSDs (2.18%) with at least one rigorous Lieb sublattice, 438 ICSDs (0.79%) with at least one approximate Lieb sublattice. Note that an entry might have both a rigorous and an approximate sublattices.

Appendix E: Automated search for materials with bipartite or split sublattices

Beyond the line-graph lattices, *i.e.*, Kagome and pyrochlore lattices, and the Lieb lattice that were introduced in Appendix D, split and bipartite lattices could also host exactly flat bands[6]. Recently, these two types of lattices were shown to host topologically non-trivial bands[28], which indicates that the the Wannier states cannot be localized.

A bipartite lattice is a lattice such that all its sites can be divided into two sublattices, L and $\tilde{L}$. Hopping bonds *only* exist in between sites in L and sites in $\tilde{L}$, but do not exist within sites of the same sublattice. Considering the translational symmetry of crystalline materials in 3D, the graph formed by the sites in L and $\tilde{L}$ and the bonds connecting them can be either mathematically connected in *at least* one dimension or disconnected in all the dimensions. If the graph of a bipartite sublattice is disconnected, we refer to it as a *disconnected bipartite sublattice*. For example, the three green atoms in Figure 13(a) is typically a group of isolated atoms in the crystal lattice and hence they form a disconnected bipartite sublattice. Otherwise, when the graph of a bipartite sublattice is connected in *at least* one dimension, we refer it to as the *connected bipartite sublattice*. For example, a collection of the one dimensional bipartite chains is considered as a connected bipartite sublattice. In this work, we mainly focus on the bipartite lattice with connected graph and refer the bipartite lattice with disconnected graph as a molecular lattice. A molecular lattice also hosts flat bands but they are in the atomic limit and is thus disregarded as discussed in Appendix B 1. A split lattice is a special case of bipartite lattice: each site i in sublattice $\tilde{L}$ has the same hopping term to its two (and exactly two) connected sites in sublattice L. For example, the Lieb lattice shown in Fig. 6(c) is a two dimensional case of both a bipartite lattice and a split lattice. The red sites correspond to the sublattice $\tilde{L}$ and the sublattice L is made of the blue sites. In the Lieb lattice, bonds only connect the blue sites in $\tilde{L}$ to the red sites in L, and each site in L is at the center of its two connected neighbors.

The flat bands that exist in bipartite or split lattice can be explained with the S-matrix method[6]. In this appendix, we provide a brief introduction to the S-matrix method that we will use in Appendix F. More details about this method can be found in Ref.[6]. We then detail a numerical algorithm based on geometrical features that allows for a systematic search for crystal structures with bipartite or split sublattices among the stoichiometric materials in Topological Quantum Chemistry website.

1. S-matrix method

Given a bipartite lattice with its two sublattices labeled as L and $\tilde{L}$, we assume the number of orbitals per unit cell in L (denoted $|L|$) is always larger than that in $\tilde{L}$ (denoted $|\tilde{L}|$) , *i.e.*, $|L|>|\tilde{L}|$. Since hopping terms only occur between sites of L and $\tilde{L}$, the tight binding Hamiltonian can be expressed in momentum space using the S-matrix as

$$H(\boldsymbol{k}) = \begin{pmatrix} 0 & S^\dagger(\boldsymbol{k}) \\ S(\boldsymbol{k}) & 0 \end{pmatrix}, \tag{E1}$$

where $S(\boldsymbol{k})$ is a matrix with dimension $|L| \times |\tilde{L}|$ and $\boldsymbol{k}$ is the momentum in the Brillouin zone. Thus, the square of the eigenvalues of $H(\boldsymbol{k})$ are given by the eigenvalues of $(H(\boldsymbol{k}))^2 = \begin{pmatrix} \tilde{T}(\boldsymbol{k}) & 0 \\ 0 & T(\boldsymbol{k}) \end{pmatrix}$, where $\tilde{T}(\boldsymbol{k}) = S^\dagger(\boldsymbol{k})S(\boldsymbol{k})$, $T(\boldsymbol{k}) = S(\boldsymbol{k})S^\dagger(\boldsymbol{k})$. Both the matrices $T(\boldsymbol{k})$ and $\tilde{T}(\boldsymbol{k})$ are positive semidefinite. As shown in the example in the end of this subsection, T and $\tilde{T}$ serve as the effective Hamiltonians of L and $\tilde{L}$ (after a rescale of energy), respectively, if L and $\tilde{L}$ have different on-site energies.

We first prove that $T(\boldsymbol{k})$ and $\tilde{T}(\boldsymbol{k})$ have the same positive eigenvalues with identical multiplicities. For any eigenstate of $\tilde{T}(\boldsymbol{k})$, $\tilde{\phi} = \tilde{\phi}(\boldsymbol{k})$, that satisfies $\tilde{T}(\boldsymbol{k})\tilde{\phi} = E\tilde{\phi}$ and $E > 0$, we can construct $\phi = S(\boldsymbol{k})\tilde{\phi}$. Then we have $T(\boldsymbol{k})\phi = S(\boldsymbol{k})S^\dagger(\boldsymbol{k})S(\boldsymbol{k})\tilde{\phi} = S(\boldsymbol{k})E\tilde{\phi} = ES(\boldsymbol{k})\tilde{\phi} = E\phi$, meaning ϕ is an eigenstate of $T(\boldsymbol{k})$ with the same eigenvalue E. Considering two eigenstates of $\tilde{T}$ satisfying $\tilde{T}(\boldsymbol{k})\tilde{\phi_i} = E_i\tilde{\phi_i}$ and $\tilde{T}(\boldsymbol{k})\tilde{\phi_j} = E_j\tilde{\phi_j}$, we have $< \tilde{\phi_i}|\tilde{\phi_j} >=< \phi_i|S^\dagger(\boldsymbol{k})S(\boldsymbol{k})|\phi_j >=< \phi_i|\tilde{T}(\boldsymbol{k})|\phi_j >= E_j < \phi_i|\phi_j >\propto \delta_{i,j}$. Thus $T(\boldsymbol{k})$ and $\tilde{T}(\boldsymbol{k})$ have identical positive eigenvalues, including their multiplicities. From this property, we deduce that $T(\boldsymbol{k})$ and $\tilde{T}(\boldsymbol{k})$ lead to the same dispersive bands in the spectrum of $H(\boldsymbol{k})$. Moreover it results in a set of perfectly flat bands at $E = 0$ with degeneracy $D = |L| + \left|\tilde{L}\right| - 2 \times \operatorname{rank}\left(S(\boldsymbol{k})\right)$. (As a special case, if $S(\boldsymbol{k})S^\dagger(\boldsymbol{k})$ has full rank, there are $|L| - \left|\tilde{L}\right|$ flat bands in the spectrum of both $H(\boldsymbol{k})$ and $T(\boldsymbol{k})$.)

As an example, we consider a two dimensional bipartite lattice formed by s orbitals at the Kagome sublattice and the honeycomb sublattice, as shown in Fig. 10(a). We refer to the honeycomb sublattice as $\tilde{L}$ and the Kagome sublattice as L. Only hopping terms between nearest neighbors are taken into account and all of them are assumed to have the same amplitude. The lattice vectors $\boldsymbol{a}_i (i = 1, 2)$ are shown in Fig. 10(a). In this basis and focusing on the unit cell, the atoms in $\tilde{L}$ are located at $(\frac{1}{3}, \frac{2}{3})$, $(\frac{2}{3}, \frac{1}{3})$ and the atoms in L are at $(\frac{1}{2}, 0)$, $(\frac{1}{2}, \frac{1}{2})$, $(0, \frac{1}{2})$. We can write

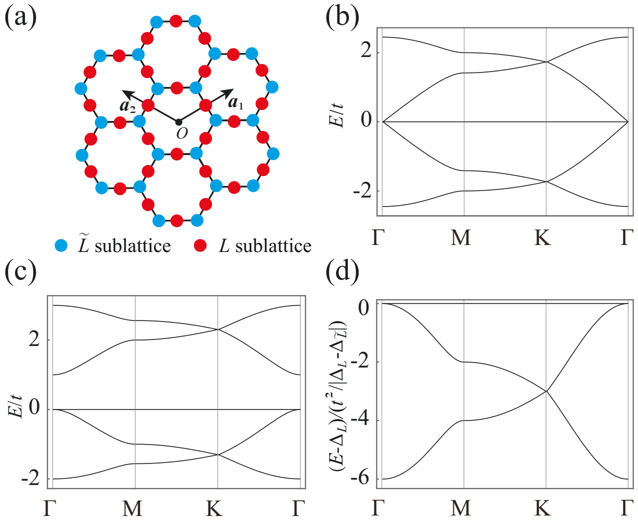

Figure 10. (a) An example of bipartite lattice consists of honeycomb lattice ($\tilde{L}$ sublattice in blue) and Kagome lattice (L sublattice in red). (b) Band structure of Hamiltonian $H_{L\oplus\tilde{L}}$ in Eq. (E3) without any on-site energy, *i.e.*, $\Delta_L = \Delta_{\tilde{L}} = 0$. (c) Band structure of Hamiltonian $H_{L\oplus\tilde{L}}$ in Eq. (E3) and $\Delta_L = 0$, $\Delta_{\tilde{L}} = |t|$. (d) The band structure of the effective Hamiltonian H_L in Eq. (E7) and $\Delta_L = 0$, $\Delta_{\tilde{L}} = |t|$.

the explicit form of the S matrix as

$$S^\dagger(\boldsymbol{k}) = t\begin{pmatrix} 1 & 1 & e^{ik_1} \\ e^{ik_2} & 1 & 1 \end{pmatrix}, \tag{E2}$$

with t being the strength of the nearest neighbor coupling. In the absence of on-site energy, this model is just the split graph lattice of the honeycomb lattice. The Hamiltonian can then be built using Eq. (E1) and the corresponding band structure is shown in Fig. 10(b).

As shown in, *e.g.* Ref.[6], flat bands in line-graph lattices might also be understood within the S-matrix formalism. For pedagogical purposes, we solely focus on the Kagome lattice which is the line-graph lattice of the honeycomb lattice. Starting from the previous example, we further add the on-site energies $\Delta_{\tilde{L}}$ and Δ_L on the sublattices $\tilde{L}$ and L. Then the total Hamiltonian of the bipartite lattice $L \oplus \tilde{L}$ reads

$$H_{L\oplus\tilde{L}}(\boldsymbol{k}) = \begin{pmatrix} \Delta_{\tilde{L}} \cdot \mathbb{I}_{2\times 2} & S^\dagger(\boldsymbol{k}) \\ S(\boldsymbol{k}) & \Delta_L \cdot \mathbb{I}_{3\times 3} \end{pmatrix}. \tag{E3}$$

A typical example of band structure associated to this Hamiltonian is shown in Fig. 10(c). Moreover, one has

$$\left(H_{L\oplus\tilde{L}}(\boldsymbol{k}) - \Delta_{\tilde{L}} \cdot \mathbb{I}_{5\times 5}\right)\left(H_{L\oplus\tilde{L}}(\boldsymbol{k}) - \Delta_L \cdot \mathbb{I}_{5\times 5}\right) = \begin{pmatrix} S^\dagger(\boldsymbol{k})S(\boldsymbol{k}) & 0 \\ 0 & S(\boldsymbol{k})S^\dagger(\boldsymbol{k}) \end{pmatrix}. \tag{E4}$$

We assume the eigenvalues of $S^\dagger S$ are $\lambda_i (i = 1, 2)$. Then, the eigenvalues of $H_{L\oplus\tilde{L}}$ are given by $\varepsilon^2 - (\Delta_L + \Delta_{\tilde{L}})\,\varepsilon + \Delta_L\Delta_{\tilde{L}} - \lambda_i = 0$,

$$\varepsilon = \frac{(\Delta_L + \Delta_{\tilde{L}}) \pm \sqrt{(\Delta_L - \Delta_{\tilde{L}})^2 + 4\lambda_i}}{2}. \tag{E5}$$

Based on Eq. (E5), when $\Delta_L \neq \Delta_{\tilde{L}}$, we can derive the individual effective Hamiltonian for either $\tilde{L}$ or L by applying the second-order perturbation theory as

$$H_{\tilde{L}}(\boldsymbol{k}) \approx \Delta_{\tilde{L}} - S^\dagger(\boldsymbol{k})S(\boldsymbol{k})/(\Delta_L - \Delta_{\tilde{L}}), \tag{E6}$$

and

$$H_L(\boldsymbol{k}) \approx \Delta_L + S(\boldsymbol{k})S^\dagger(\boldsymbol{k})/(\Delta_L - \Delta_{\tilde{L}}), \tag{E7}$$

respectively. Hence, the band structures of H_L and $H_{\tilde{L}}$ are given by the spectra of $T(\boldsymbol{k})$ and $\tilde{T}(\boldsymbol{k})$ (after a rescaling of energy), respectively. As shown in Fig. 10(d), there is one flat band of degeneracy $D = |L| - \text{rank}(S(\boldsymbol{k})) = 1$ at Δ_L in the band structure of H_L. The effective Hamiltonian for the sublattice L of Eq. (E7) is nothing else than the Kagome tight binding Hamiltonian, with the nearest coupling $t^2/(\Delta_L - \Delta_{\tilde{L}})$ and on-site energy Δ_L. Thus we have explained the flat band in the Kagome lattice through the S-matrix formalism.

2. Algorithms to search for bipartite and split sublattices in crystalline materials

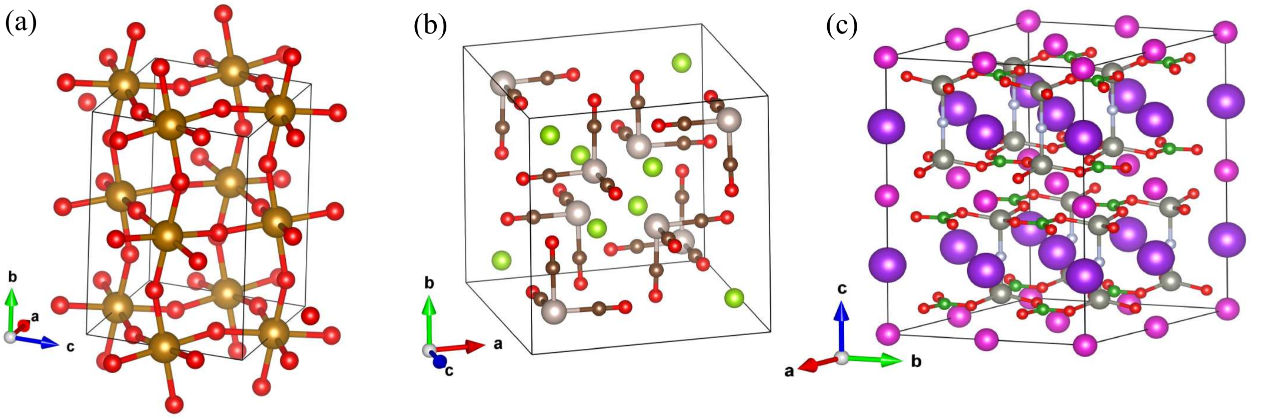

Figure 11. (a) The crystal structure of $CaFeO_3$ [ICSD 92330, SG 62 ($Pnma$)], where Fe, O are represented by the yellow, red balls and the Ca atoms are ignored. In this material, O and Fe form the sublattices L and $\tilde{L}$ respectively, of a bipartite lattice and the number of O and Fe atoms are different: $|L| = 3$ and $|\tilde{L}| = 1$. (b)The crystal structure of $C_{12}O_3Ru_4Se_4$ [ICSD 92913, SG 217 ($I\bar{4}3m$)], where the Ru, Se, C and O atoms are represented by the grey, green, brown and red balls, respectively. In this material, Ru, C and O form a molecular-cluster which results in the flat atomic bands. The molecular lattices like this one are excluded by the algorithm we have developed. (c)The crystal structure of a $2 \times 2 \times 1$ supercell of $CdZn_2KB_2O_6F$ [ICSD 248025, SG 163 ($P\bar{3}1c$)], where Cd, Zn, K, F, B and O are represented by the purple, grey, blue, white, green and red balls, respectively. In this material, there are two connected subsets along the z direction. Each connected subset is a bipartite lattice with different number of atoms in its two sublattices. F and O atoms form the L sublattice and B and Zn atoms form the $\tilde{L}$ sublattice ($|L| = 7$ and $|\tilde{L}| = 4$).

In most cases, bipartite sublattices in a crystalline material are not exact if all of the possible hopping terms are considered. There usually exist hoppings between sites of the same sublattice. Nevertheless, a bipartite sublattice dressed by some additional small enough hopping terms could give rise to almost flat bands. For a systematic search of bipartite and split lattices, we solely rely on the geometric distance between two atoms to infer the hopping term amplitude between them. We can then ignore hopping terms which are likely to be small, and identify compounds that have connected bipartite sublattices.

Our algorithm requires a cutoff for the hopping distance above which we assume two atoms are not connected by a hopping term. We base this cutoff on the shortest bond in a crystal structure we want to analyze. Thus for a crystalline material, the first step is to set the cutoff of the hopping distance. In practice, we set the cutoff of the hopping distance τ using the following formula:

$$\tau = \lambda \max(d, x), \tag{E8}$$

where d is the length of the shortest bond in the lattice. To avoid the cases where d would be too small and thus excluding some non-negligible hopping terms, we also set the lower bound of d as x. λ (≥ 1) is a multiplicative coefficient to define the cutoff based on the distance $\max(d, x)$. For this article and on the Materials Flatband

Database website, we have considered the values $\lambda = 1.2, 1.5$ and 1.7 and $x = 1.5, 1.8, 2.1, 2.4$ and 2.7Å.

For example in the material $\mathrm{CaFeO_3}$[ICSD 92330, SG 62 ($Pnma$)] shown in Fig. 11(a), by setting the parameters $\lambda = 1.2$ and $x = 1.5$Å, the shortest bond is the $\mathrm{Fe-O}$ bond and $d = 1.91$Å. The hopping distance between Ca and Fe or O are larger than the cutoff $\tau = 1.2d = 2.29$Å. Hence, Ca atoms are ignored. The bonds lower than τ are assumed to be always connected, thus Fe and O form a bipartite sublattice. Indeed, the Fe atoms form the sublattice L and the O atoms form the sublattice $\tilde{L}$. The difference of the atom number between L and $\tilde{L}$ is 2.

We now describe the algorithm (see its flow chart in Fig. 14) that we have designed to identify a bipartite sublattice from a crystalline material:

Step 1 We find the shortest bond in the 3D crystal lattice and refer its length as d. Then, the cutoff of the hopping distance is set as $\tau = \lambda \max(d, x)$ using the two external parameters x and λ.

Step 2 For each pair of atoms, if the distance between them is smaller than the cutoff τ, we assume the hopping between them is nonzero and we label one as the neighbor of the other one. Otherwise, we consider there is no hopping between them.

Step 3 An atom that has less than two neighbors is considered as a part of a molecular-like cluster, which could contribute to trivial flat atomic bands. We discard such atoms. By repeating this procedure and as shown in Fig. 13, in the end a molecular-like cluster is either deleted (if it was fully disconnected from any other atom) or reduced to a single atom (if the molecular-like cluster was attached to a set of connected atoms via a single atom).

C1 After Step 3, if all the atoms are deleted in the unit cell, there is no bipartite sublattice. Otherwise, the following steps are applied to the remaining atoms.

Step 4 For the set of atoms that are not deleted in Step 3, they can always be divided into several connected subsets, where the hopping term is non-zero between two neighbors within the same subset and is zero between any two atoms in different subsets.Using the results we obtained in Step 2, we can get all the connected subsets. For each connected subset, we apply the following steps.

Step 5 To check if a connected subset $\mathcal{B}$ is a bipartite sublattice or not, we first define two temporary sets, L and $\tilde{L}$, and a *source set* S. Then, we choose randomly an atom from $\mathcal{B}$ and distribute it to S. We iterate over the following Step 6 and Step 7 to populate L and $\tilde{L}$ with the atoms in $\mathcal{B}$.

Step 6 From the connected subset $\mathcal{B}$, we take all the atoms, which are not in L or $\tilde{L}$ but are neighbors of the atoms in S, as the (new) *target set* T. We distribute all the atoms in S to L and all the atoms in T to $\tilde{L}$. Then we check if L and $\tilde{L}$ satisfy the following two criteria:

C2 Any atom in L (or $\tilde{L}$) is not the neighbor of any other atoms in the same sublattice; Otherwise, the connected subset $\mathcal{B}$ is not a bipartite lattice and we go back to Step 5, moving to the next connected subset.

C3 If all the atoms in the connected subset $\mathcal{B}$ have been distributed into either L or $\tilde{L}$ then we go to C4; otherwise, we go to Step 7.

Step 7 We take all the atoms, which are not in L or $\tilde{L}$ but are the neighbors of the atoms in T, as the new *source set* S. Then we empty the *target set* T and repeat Step 6.

C4 If the numbers of atoms in L and $\tilde{L}$ are nonzero and different, the connected subset $\mathcal{B}$ is tagged as a bipartite lattice with different numbers of atoms in its two sublattices and we go to C5.

C5 For the bipartite lattice with two sublattices L and $\tilde{L}$ (up to a relabelling, we can always assume $L > \tilde{L}$), we further check if it is a split lattice. If any atom in L has exactly two neighbors in $\tilde{L}$, and is at equal distance to its two neighbors, the bipartite lattice is also a split lattice. For this step, our algorithm uses a threshold corresponding to ±20% of the length of the shorter bond to test if two distances are identical.

To illustrate how our algorithm works for the bipartite lattice with different number of atoms on sublattices, we apply it to an example of the material $\mathrm{CdZn_2KB_2O_6F}$ [ICSD 248025, SG 163 ($P\bar{3}1c$)] whose crystal structure is shown in both Fig. 11(c) and Fig. 12(a).

Step 1 In the first step, we identify that the bond between O (red atoms in Figure 12(a)) and B (green atoms in Figure 12(a)) is the shortest bond in $\mathrm{CdZn_2KB_2O_6F}$. As the length of this shortest bond is 1.38Å and less than 1.5Å, we set the cutoff of the hopping distance as $\tau = 1.5 \times 1.5 = 2.25$Å.

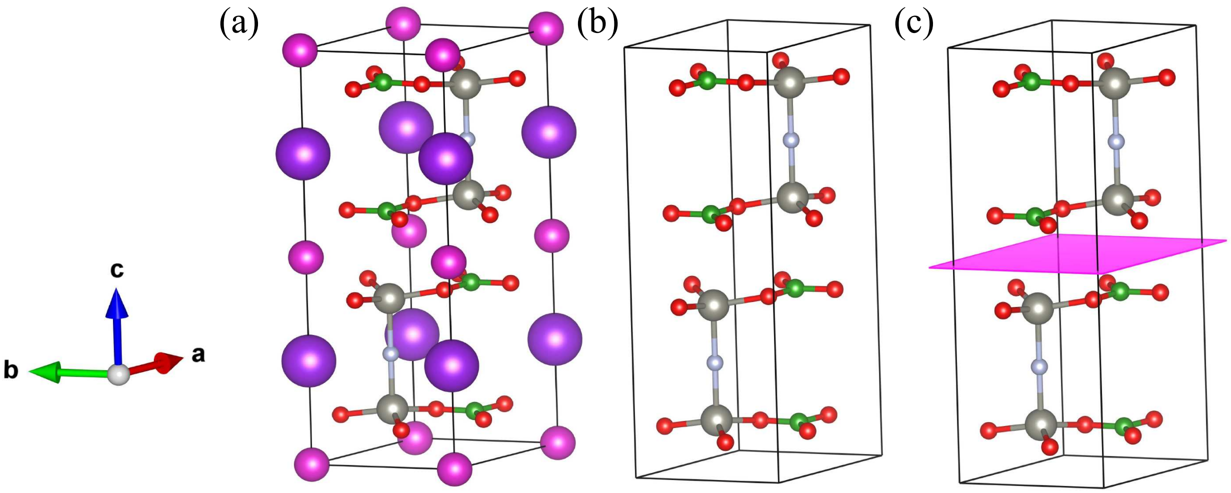

Figure 12. (a)The crystal structure of a unit cell of $CdZn_2KB_2O_6F$ [ICSD 248025, SG 163 ($P\bar{3}1c$)], where Cd, Zn, K, F, B and O are represented by the purple, grey, blue, white, green and red balls, respectively. Only the bonds whose lengths are smaller than the cutoff $\tau = 2.25\mathring{A}$ that is considered in Step 2 are shown. (b) The lattice structure after Step 3, all the Cd and K atoms are deleted and all the Zn atoms, B atoms, O atoms and F atoms are left. (c) In Step 3, we identify two connected subsets which are separated by the purple plane. In the explanation of our algorithm for this material we consider the subset above the purple plane first.

Step 2 Then, we discard the bonds of length larger than τ and only assume the bonds of length smaller than τ to have nonzero hopping amplitude. For example, by ignoring the bonds with zero hopping amplitude, the crystal structure of $CdZn_2KB_2O_6F$ is plotted in Fig. 12(a), where the length of each plotted bond is less than the cutoff $\tau = 2.25$Å.

Step 3 If an atom has no, or only one, bond left, we delete it from the lattice. In the case of $CdZn_2KB_2O_6F$, all of the Cd atoms (the purple atoms in Figure 12(a)) and K atoms (the blue atoms in Figure 12(a)) have no bond left. Thus, they are removed from the lattice. And the lattice structure after this step is shown in Figure 12(b).

C1 As shown in Figure 12(b), following Step 3, all the Zn atoms (the grey atoms in Figure 12(a)), B atoms, O atoms and F atoms (the white atom in Figure 12(a)) are left in the unit cell, so continue to Step 4.

Step 4 Using the results obtained in Step 2, (*i.e.*, which hoppings considered in Figure 12(b)), we find two *connected* subsets, which are separated by the [0 0 1] Miller plane at $z = 0.5c$ (where c is the lattice constant along z direction) in the lattice, as shown in Figure 12(c).

Step 5 For both of the connected subsets in Figure 12(c), we check whether they are bipartite sublattice separately. Now, we take the one above the purple plane in Figure 12(c) as an example. For convenience, we name this connected subset as $\mathcal{B}$. Considering the double counting problem of the O atoms at the unit cell's boundary, there are six O atoms, one F atom, two Zn atoms and two B atoms in $\mathcal{B}$. We first define two temporary sets, L and $\tilde{L}$, and a *source set* S. Then, we choose randomly an atom from $\mathcal{B}$ and distribute it to S. Here, we choose one F atom from $\mathcal{B}$.

Step 6 From the connected subset $\mathcal{B}$, we take the two Zn atoms, which are neighbors of the F atom in S, as the *target set* T. We distribute all the atoms in S (*i.e.*, one F atom) to L and all the atoms in T (*i.e.*, two Zn atoms) to $\tilde{L}$. Then we check if L and $\tilde{L}$ satisfy the C2 and C3.

C2 As obtained in Step 2, the two Zn atoms in $\tilde{L}$ are not neighbors to each other and there is only one F atom in L. Thus C2 is satisfied.

C3 In the connected subset $\mathcal{B}$, there still are six O and two B atoms left to be distributed, so C3 is not satisfied and we proceed to Step 7.

Step 7 We take the neighbors of the two Zn atoms in T, *i.e.*, the six O atoms, as the new *source set* S. Then we empty the *target set* T and repeat Step 6.

Step 6 From the connected subset $\mathcal{B}$, we take the neighbors of the six O atoms of S, *i.e.*, the two B atoms which are not in L or $\tilde{L}$, as the new *target set* T. We distribute all the atoms in S (*i.e.*, the six O atoms) to L and all the atoms in T (*i.e.*, two B atoms) to $\tilde{L}$. Then we check if L and $\tilde{L}$ satisfy C2 and C3.

C2 As obtained in Step 2, the two Zn and the two B atoms in $\tilde{L}$ are not neighbors to each other. The six O and the F atom in L are not neighbors to each other. So C2 is satisfied.

C3 All the atoms in $\mathcal{B}$ have been distributed to either L or $\tilde{L}$. So C3 is satisfied and we move to C4.

C4 The number of atoms in L is 7 which includes six O atoms and one F atom, while the number of atoms in $\tilde{L}$ is 4 which includes two Zn atoms and two B atoms. So C4 is satisfied and the connected subset $\mathcal{B}$ is a bipartite lattice with different numbers of atoms in its two sublattices. Then, we check the criteria in C5.

C5 We further check if this subset is a split lattice. Since none of the atoms in L are at equal distance to their two neighbors in $\tilde{L}$ up to our threshold, the bipartite lattice is not a split lattice.

Step5 All the above steps are repeated for the lower connected subset as obtained in Step 4.

Within the above algorithm, we found that the subset $\mathcal{B}$ is a bipartite lattice with sublattice L and $\tilde{L}$. L includes six O atoms and one F atom while $\tilde{L}$ includes two Zn atoms and two B atoms.

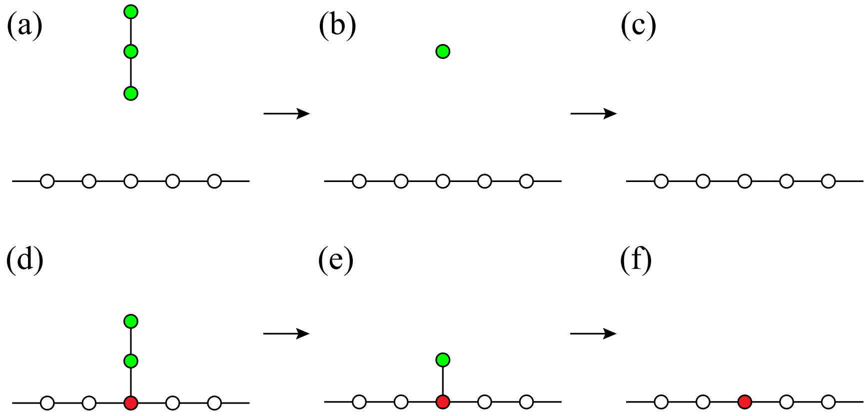

Figure 13. Two of the possible cases when removing a molecular cluster. (a)-(c) The molecular cluster is made of the three green sites and is completely detached from the the fully connected sites (white circles). Acting with Step 3 once, we remove two out of the three green sites. Applying Step 3 a second time, we completely get rid of the molecular cluster. (d)-(f) The molecular cluster is made of the two green sites and one red site belonging to fully connected sites. Repetitively acting on the molecular cluster using Step 3, we end up with a single site of the molecular cluster (in red).

To illustrate how the molecular lattices are excluded, we consider the example $C_{12}O_3Ru_4Se_4$[ICSD 92913, SG 217 ($I\bar{4}3m$)], whose crystal structure is shown in Fig. 11(b). Applying our algorithm to this material leads to the following sequence:

Step 1 In the first step, we identify that the bond between C atoms (brown atoms in Figure 11(b)) and O atoms (red atoms in Figure 11(b)) is the shortest bond in $C_{12}O_3Ru_4Se_4$. As the length of this shortest bond is smaller than 1.5Å, we set the cutoff of the hopping distance as $\tau = \lambda 1.5$Å.

Step 2 Then, we discard the bonds of length larger than τ and only the bonds of length smaller than τ are assumed to have nonzero hopping. For example, by ignoring the bonds with zero hopping, the crystal structure of $C_{12}O_3Ru_4Se_4$ is plotted in Fig. 11(b) for $\tau = 1.5 \times 1.5 = 2.25$Å, where the length of each plotted bond is less than the cutoff $\tau = 2.25$Å.

Step 3 If an atom has no or only one bond left, we delete it from the lattice. In the case of $C_{12}O_3Ru_4Se_4$, all of the Se atoms (green atoms in Figure 11(b)) have no bond left and every O atom has only one bond. Thus, both of them are removed from the lattice. Then, each of the left C atoms (brown atoms in Figure 11(b)) only has one bond and should be removed. After that, the Ru atoms (grey atoms in Figure 11(b)) get isolated and hence are also removed. Finally, all the atoms are removed from the lattice and this material does not belong to a *connected* bipartite lattice.

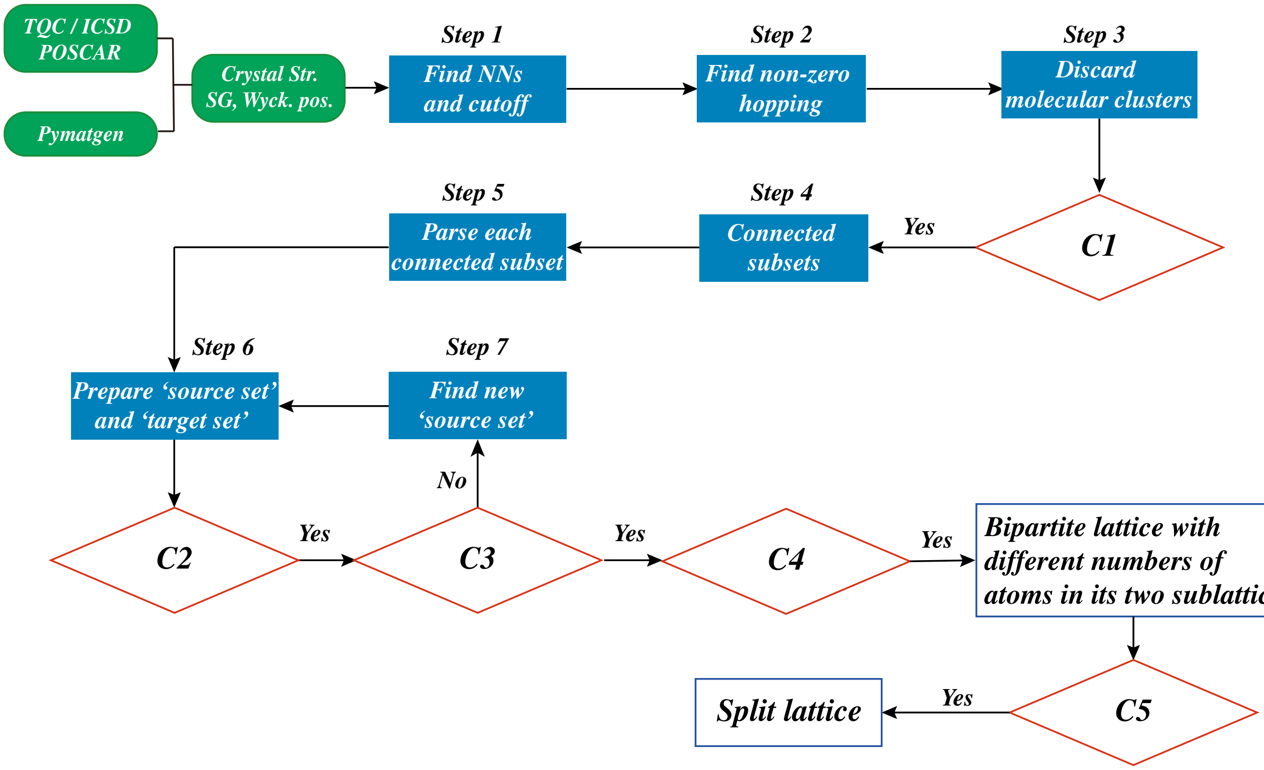

Figure 14. The flow chart of the algorithm identifying bipartite sublattices from a 3D crystal lattice. Starting from the crystal structure of a material given by its *POSCAR* file, we use the *Pymatgen* package to analyze the crystal symmetry and the Wyckoff positions of each distinct element. Step 1 is applied to identify the nearest neighbor(NN) sites of each atom and set the cutoff of the hopping distance. In Step 2, if the hopping distance is within the cutoff, the hopping amplitude is set to non-zero; otherwise, the hopping amplitude is set to zero; In Step 3, the molecular-like clusters are removed and we exit the algorithm through C1 if there has no atom left. In Step 4, for the set of atoms that are not removed in Step 3, they are divided into several connected subsets, where the hopping amplitude is non-zero between two neighbors within the same subset and is zero between any two atoms in different connected subsets. The Steps 5, 6 and 7 and the criteria C2 and C3 are applied to each connected subset to identify the bipartite sublattice based on the neighbors of each atom as extracted in Step 2. The criteria C4 is applied to check whether the numbers of the atoms in the two sublattices L and $\tilde{L}$ are different. If a bipartite lattice is detected, an additional test based on the criteria C5 is performed to check if the bipartite lattice is also a split lattice.

In this work, we applied our algorithm using different values for the cutoff parameters λ and x in Eq. (E8). As we mentioned above, we adopted the values of λ to be 1.2, 1.5 and 1.7 and the values of x to be 1.5, 1.8, 2.1, 2.4 and 2.7Å. We have scanned the materials available in the database of Appendix C to search for bipartite sublattices potentially leading to flat bands, *i.e.*, $|L| \neq |\tilde{L}|$ and split sublattices. The individual results are available on the Materials Flatband Database website. The bipartite sublattice statistics for each setting are provided in Table VII.

Table VII: Statistics for the ICSD entries with either bipartite or split sublattices with respect to the lower bound of d and the multiplicative factor λ that define the distance cutoff in Eq. (E8). The first and second columns are the values of x and λ. The third column is the number of ICSD entries hosting at least one bipartite sublattice and the fourth column is the number of ICSD entries hosting at least one split sublattice among the bipartite sublattices. All percentages are computed with respect to the total number of ICSD entries that have been considered (55,206 ICSDs).

x	d	# ICSDs with bipartite	# ICSDs with split
$x = 1.5$Å	$\lambda = 1.2$	15662 (28.4%)	7811 (14.2%)
$x = 1.5$Å	$\lambda = 1.5$	6011 (10.9%)	1235 (2.2%)
$x = 1.5$Å	$\lambda = 1.7$	217 (0.4%)	31 (0.1%)
$x = 1.8$Å	$\lambda = 1.2$	18459 (33.4%)	7282 (13.2%)
$x = 1.8$Å	$\lambda = 1.5$	1879 (3.4%)	296 (0.5%)
$x = 1.8$Å	$\lambda = 1.7$	64 (0.1%)	6 (0.0%)

$x = 2.1$Å	$\lambda = 1.2$	14895 (27.0%)	4721 (8.6%)
$x = 2.1$Å	$\lambda = 1.5$	697 (1.3%)	102 (0.2%)
$x = 2.1$Å	$\lambda = 1.7$	6 (0.0%)	1 (0.0%)
$x = 2.4$Å	$\lambda = 1.2$	4704 (8.5%)	1339 (2.4%)
$x = 2.4$Å	$\lambda = 1.5$	245 (0.4%)	22 (0.0%)
$x = 2.4$Å	$\lambda = 1.7$	—	—
$x = 2.7$Å	$\lambda = 1.2$	2863 (5.2%)	617 (1.1%)
$x = 2.7$Å	$\lambda = 1.5$	37 (0.1%)	4 (0.0%)
$x = 2.7$Å	$\lambda = 1.7$	—	—

Discussion At the end of this section, we comment on the relation between Lieb, bipartite and split sublattices in crystalline materials. As we defined before, the split sublattice is a special case of bipartite sublattice and each of the split sublattices we obtained in our results *has to* be a bipartite sublattice. Mathematically, the Lieb lattice is a special case of both bipartite and split sublattices in 2D. However, in 3D crystalline materials, the conditions in our method to identify a 2D Lieb sublattice is not stringent enough to identify if the 2D Lieb sublattice is also a bipartite or split sublattice in 3D. In our geometric algorithm for Lieb sublattice, we only consider the NN bonds and the atoms on (or close to) a 2D plane. In the algorithm for bipartite sublattice, we set a cutoff τ for the hopping distance and consider all the hoppings of distance less than the cutoff τ. Hence more hoppings and atoms are involved and it could make a Lieb-sublattice material not a bipartite-sublattice material. Actually we have only found one such case when a Lieb lattice is not a bipartite lattice in our database, *i.e.*, H_3F_3GaN [ICSD 89503, SG 39 ($Aem2$)].

Appendix F: Theoretical explanations for flat bands in representative materials

In this appendix, we discuss seven typical materials among the 345 materials that will be presented in Appendix H 3 which host clear flat bands at or near the Fermi level. Here we explain the origins of these flat bands. The seven materials are WO_3 [ICSD 108651, SG 221 ($Pm\bar{3}m$)], $Pb_2Sb_2O_7$ [ICSD 27120, SG 227 ($Fd\bar{3}m$)], $CaNi_5$ [ICSD 54474, SG 191 ($P6/mmm$)], Ca_2NCl [ICSD 62555, SG 166 ($R\bar{3}m$)], Rb_2CaH_4 [ICSD 65196, SG 139 ($I4/mmm$)], KAg[CN]$_2$ [ICSD 30275, SG 163 ($P\bar{3}1c$)], and $RbMo_3S_3$ [ICSD 644175, SG 176 ($P6_3/m$)]. The first six materials have a bipartite sublattice in the crystal lattice and the flat bands can be explained using the S-matrix method, as introduced in Appendix E and in Ref.[6]. For the last example, $RbMo_3S_3$, the flat bands are due to the quasi-1D character and the weak inter-chain couplings of this material.

1. WO_3

The crystal structure of WO_3 [ICSD 108651, SG 221 ($Pm\bar{3}m$)] is shown in Fig. 15(a). W and O occupy the $1a$ and $3c$ Wyckoff positions, respectively. From its band structure without SOC considered, as plotted in Fig. 15(c), there are three connected bands at (and above) the Fermi level. Along the high-symmetry paths $\Gamma \to$ X, X $\to$ M and M $\to$ R, there is always one out of the three bands that is extremely flat (but not necessarily at the Fermi level). By analyzing the orbital-projected band structure obtained from the first-principles calculation, the three bands come from the d_{xy}, d_{yz} and d_{xz} orbitals of W, which form the 3 dimensional single-valued irrep T_{2g} of the site-symmetry-group O_h of the $1a$ position. Below the T_{2g} bands of W, there is another set of valence bands coming from p orbitals of O, as indicated by the red lines in Fig. 15(c), of which the highest bands are also flat. Similar structures of flat bands also exist in the perovskites with the chemical formulae ABO_3 or BO_3 in SG 211 ($Pm\bar{3}m$)[65–67], where B is a transition element with $3d$ electrons in the outer shell sitting at the $1a$ (or $1b$) Wyckoff position and O sits at the $3c$ (or $3d$) Wyckoff position.

Both the flat conduction bands (along some paths) and the flat valence bands can be explained using the S-matrix method, as introduced in Appendix E. For the case in WO_3, we refer to the sublattices of W and O as two sublattices $\tilde{L}$ and L. Then, the lattice of $L \oplus \tilde{L}$ is a bipartite lattice if only the bonds connecting W and its NN O atoms are taken into account. As explained in the above tight-binding method, the bands near the Fermi level come from d_{yz}, d_{xz}, and d_{xy} orbitals on W and the p orbitals on O. We introduce the Bloch basis as

$$|\phi_\alpha(\boldsymbol{k})\rangle = \sum_{\mathbf{R}} e^{i\mathbf{R}\cdot\boldsymbol{k}} |\alpha, \mathbf{R}\rangle , \qquad |\phi_a(\boldsymbol{k})\rangle = \sum_{\mathbf{R}} e^{i\mathbf{R}\cdot\boldsymbol{k}} |a, \mathbf{R}\rangle , \tag{F1}$$

where α indexes the three d orbitals, a indexes the nine p orbitals on the three O atoms, and $\mathbf{R}$ indexes the lattice

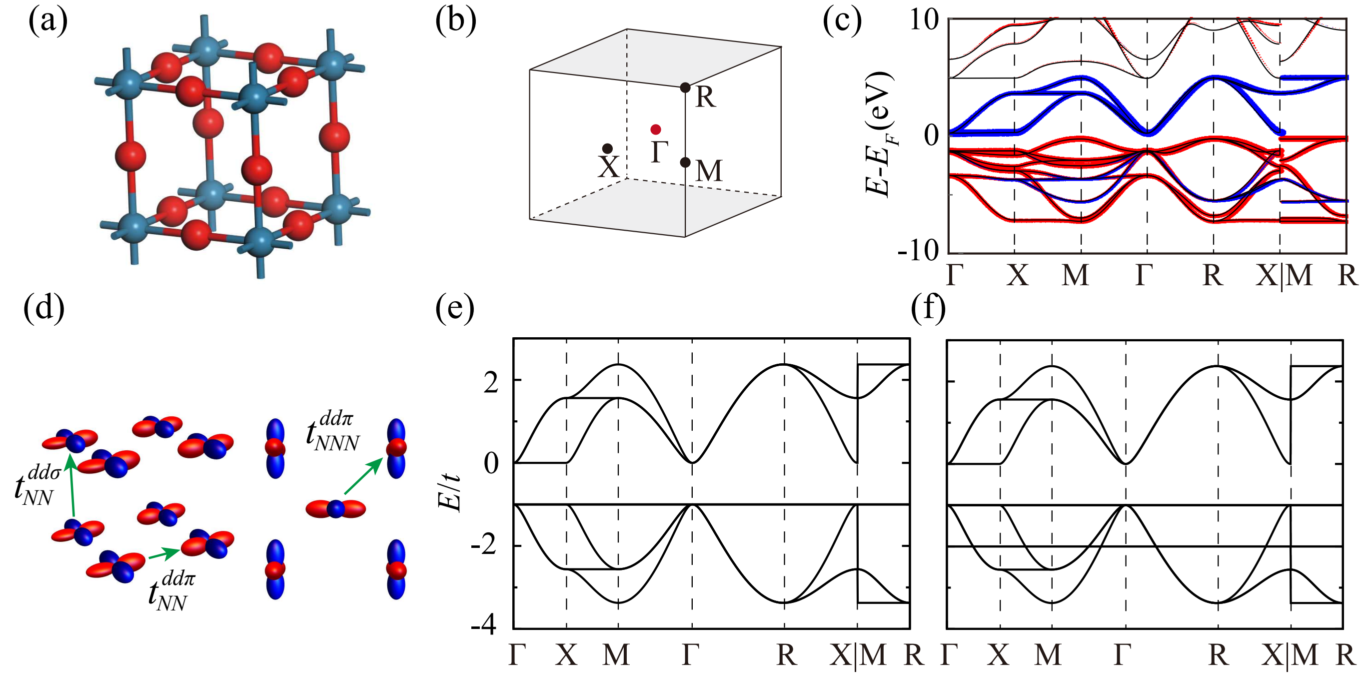

Figure 15. (a) The crystal structure of $\mathrm{WO_3}$. W and O are represented by the blue and red balls, respectively. (b) The bulk BZ of $\mathrm{WO_3}$. (c) Orbital-projected band structure of $\mathrm{WO_3}$ without spin-orbit coupling. The weights of d_{xy},d_{yz} and d_{zx} orbitals on W are highlighted in blue, and the weights of the p orbits on O are highlighted in red. (d) The schematic of the three different hopping terms that are considered in Eq. (F7). (e) The band structure of the bipartite lattice $L \oplus \tilde{L}$ constructed from the S matrix in Eq. (F2). We have chosen $\Delta = -|t|$ for our calculation. (f) The band structure of the bipartite lattice $L \oplus \tilde{L}$ with an additional onsite term δ that splits the A_{2u} and E_u orbitals at the O atoms.

vectors, respectively. $\alpha = 1, 2, 3$ correspond to the d_{xy}, d_{yz}, and d_{xz} orbitals, respectively, $a = i + 3(j-1)$ correspond to the p_x $(i = 1)$, p_y $(i = 2)$, p_z $(i = 3)$ orbitals at the jth site of the $3c$ Wyckoff position, respectively. Here $j = 1, 2, 3$ correspond to the sites $(\frac{1}{2}, 0, 0)$, $(0, \frac{1}{2}, 0)$ and $(0, 0, \frac{1}{2})$, respectively. Notice that we have chosen a periodic gauge for the basis in Eq. (F1), *i.e.*, the basis is invariant if we change $\boldsymbol{k}$ to $\boldsymbol{k} + \mathbf{G}$ with $\mathbf{G}$ being a vector of the reciprocal lattice. We will use this periodic gauge throughout this section. The S matrix of this bipartite lattice is given by $S^\dagger_{\alpha a}(\boldsymbol{k}) = \langle \phi_\alpha(\boldsymbol{k})| \hat{H} |\phi_a(\boldsymbol{k})\rangle$. This 3×9-dimensional $S^\dagger(\boldsymbol{k})$ matrix is

$$S^\dagger(\boldsymbol{k}) = t \begin{pmatrix} 0 & 0 & 0 & 0 & 0 & 1-e^{-ik_z} & 0 & 1-e^{-ik_y} & 0 \\ 0 & 0 & 1-e^{-ik_z} & 0 & 0 & 0 & 1-e^{-ik_x} & 0 & 0 \\ 0 & 1-e^{-ik_y} & 0 & 1-e^{-ik_x} & 0 & 0 & 0 & 0 & 0 \end{pmatrix}. \tag{F2}$$

Here t is the hopping between the d_{xy} orbital at $(0, 0, 0)$ and p_x orbital at $(\frac{1}{2}, 0, 0)$ which can be obtained from the maximally localized Wannier function (MLWF) calculations[37] and is -1.654 eV. Here, we build the MLWF by the p orbitals and the T_{2g} orbitals of W atom. The inter-sublattice couplings *e.g.* the coupling between p_z orbitals at $(0, 0, \frac{1}{2})$ and $(0, \frac{1}{2}, 0)$ (0.179 eV), and the coupling between d_{xy} orbitals at $(0, 0, 0)$ and $(1, 0, 0)$ (-0.222 eV) are ignored. Since these couplings are much smaller than those we consider, neglecting these couplings is reasonable. Other NN hoppings between T_{2g} and p orbitals are equivalent to this hopping due to the symmetries. We further assume the onsite energy of p orbitals as Δ (< 0), then the total Hamiltonian reads

$$H_{L\oplus\tilde{L}}(\boldsymbol{k}) = \begin{pmatrix} 0_{3\times 3} & S^\dagger(\boldsymbol{k}) \\ S(\boldsymbol{k}) & \Delta \cdot \mathbb{I}_{9\times 9} \end{pmatrix}. \tag{F3}$$

To discover the flat valence bands (over the whole Brillouin zone), we consider the SVD decomposition of the $S(\boldsymbol{k})$ matrix as $S(\boldsymbol{k}) = U(\boldsymbol{k})\Sigma(\boldsymbol{k})V^\dagger(\boldsymbol{k})$, where $U(\boldsymbol{k})$ is a nine-by-nine unitary matrix, $V(\boldsymbol{k})$ is a three-by-three unitary matrix, and $\Sigma(\boldsymbol{k})$ is a nine-by-three rectangular diagonal matrix with real non-negative diagonal elements. We apply the unitary transformation to the Hamiltonian

$$\begin{pmatrix} V^\dagger(\boldsymbol{k}) & 0_{3\times 9} \\ 0_{9\times 3} & U^\dagger(\boldsymbol{k}) \end{pmatrix} \cdot H_{L\oplus\tilde{L}}(\boldsymbol{k}) \cdot \begin{pmatrix} V(\boldsymbol{k}) & 0_{3\times 9} \\ 0_{9\times 3} & U(\boldsymbol{k}) \end{pmatrix} = \begin{pmatrix} 0_{3\times 3} & \Sigma^T(\boldsymbol{k}) \\ \Sigma(\boldsymbol{k}) & \Delta\cdot\mathbb{I}_{9\times 9} \end{pmatrix}. \tag{F4}$$

Suppose that the diagonal elements of $\Sigma(\boldsymbol{k})$ are $\xi_n(\boldsymbol{k})$ with $n = 1, 2, 3$, then the system has six branches of dispersive bands $\frac{\Delta}{2} \pm \sqrt{\xi_n^2(\boldsymbol{k}) + \Delta^2/4}$ and six flat bands at Δ. If one branch of $\xi_n(\boldsymbol{k})$ is a constant ξ_c over the whole Brillouin zone, we would have one more flat band at $\frac{\Delta}{2} \pm \sqrt{\xi_c^2 + \Delta^2/4}$ and an additional flat band at 0. For a generic Hamiltonian in form of Eq. (F3), there are $|L| - \mathrm{rank}(S(\boldsymbol{k}))$ states at Δ and $|\tilde{L}| - \mathrm{rank}(S(\boldsymbol{k}))$ states at 0. The other $2 \times \mathrm{rank}(S(\boldsymbol{k}))$ states must have energies either below (above) Δ or above (below) 0 for negative (positive) Δ. The particular $S(\boldsymbol{k})$ matrix defined in Eq. (F2) has rank three at generic momenta, hence there are 6 flat bands at the energy Δ, as shown in Fig. 15(e).

Since the T_{2g}-bands and p-bands are well separated in energy, we can derive the individual effective Hamiltonians for them by applying the second-order perturbation theory, already exemplified in Appendix E 1, as

$$H_{\tilde{L}}(\boldsymbol{k}) \approx -S^\dagger(\boldsymbol{k})S(\boldsymbol{k})/\Delta, \tag{F5}$$

and

$$H_L(\boldsymbol{k}) \approx \Delta + S(\boldsymbol{k})S^\dagger(\boldsymbol{k})/\Delta, \tag{F6}$$

respectively (The exact expressions are provided in Appendix E 1). The effective Hamiltonian of T_{2g}-bands is a diagonal matrix

$$H_{\tilde{L}}(\boldsymbol{k}) = -2t^2/\Delta \begin{pmatrix} 2-\cos k_y - \cos k_z & 0 & 0 \\ 0 & 2-\cos k_x - \cos k_z & 0 \\ 0 & 0 & 2-\cos k_x - \cos k_y \end{pmatrix}. \tag{F7}$$

With parameters given by $t_{NN}^{dd\pi} = -t^2/|\Delta|$, $t_{NN}^{dd\delta} = t_{NNN}^{dd\pi} = 0$, $\Delta_d = -\frac{4t^2}{\Delta} = \frac{4t^2}{|\Delta|}$. Δ_d is the onsite energy of T_{2g} orbitals, $t_{NN}^{dd\pi}$ ($t_{NNN}^{dd\pi}$) is the amplitude of the NN (NNN) in-plane hopping while $t_{NN}^{dd\delta}$ is the amplitude of NN out-of-plane hopping, as schematically shown in Fig. 15(d). Taking the T_{2g} orbitals as basis, we built the MLWF. The values of Δ_d, $t_{NN}^{dd\pi}$, $t_{NNN}^{dd\pi}$ and $t_{NN}^{dd\delta}$ are 2.45eV, -0.62eV, 0.01eV and -0.006eV, respectively. Then, the Hamiltonian in Eq. (F7) is a diagonal matrix with elements $2t_{NN}^{dd\pi}\left\{\cos k_y + \cos k_z,\ \cos k_x + \cos k_z,\ \cos k_x + \cos k_y\right\}$ (up to the constant shift Δ_d). We can prove that there is always a flat band along a path parallel to the direction of the k_i ($i = x, y, z$) axis, and the energy of the flat band is $E = 2t_{NN}^{dd\pi}(\cos k_j + \cos k_k)$, where $i \neq j \neq k$.

- Along the high-symmetry path Γ → X, with $k_y = k_z = 0$, the Hamiltonian in Eq. (F7) becomes a diagonal matrix with three diagonal elements, $2t_{NN}^{dd\pi}\left\{2,\ 1+\cos k_x,\ 1+\cos k_x\right\} + \{\Delta_d, \Delta_d, \Delta_d\}$, resulting in one flat band at $E = 4t_{NN}^{dd\pi} + \Delta_d$=-0.03eV. This flat band has a touching point at the Γ point with a double-degenerate dispersive band.
- Along the high-symmetry path X → M, with $k_x = \pi$ and $k_z = 0$, the Hamiltonian in Eq. (F7) becomes a diagonal matrix with three diagonal elements, $2t_{NN}^{dd\pi}\left\{1+\cos k_y,\ 0, -1+\cos k_y\right\} + \{\Delta_d, \Delta_d, \Delta_d\}$, resulting in one flat band at $E = \Delta_d$=2.45eV. This flat band has touching points at X and M points with two dispersive bands, respectively.
- Along the high-symmetry path R → M, with $k_x = k_y = \pi$, the Hamiltonian in Eq. (F7) becomes a diagonal matrix with three diagonal elements, $2t_{NN}^{dd\pi}\left\{-1+\cos k_z,\ -1+\cos k_z, -2\right\} + \{\Delta_d, \Delta_d, \Delta_d\}$, resulting in a flat bands at $E = -4t_{NN}^{dd\pi} + \Delta_d$=4.93eV. This flat band has a touching point at R point with a double-degenerate dispersive band.

The dispersion of the valence bands from the first-principle calculations is more complicated than the dispersion of the valence bands in the S-matrix model, as can be seen by comparing Fig. 15(c) and Fig. 15(e). Indeed, we have omitted several symmetry-allowed terms in the S-matrix model. For example, the site-symmetry-groups of the O atoms are all D_{4h}. The p_x, p_y, p_z orbitals form a two-dimensional irrep E_u and a one-dimensional irrep A_{2u} of the point group D_{4h}. The two irreps in principle should have different onsite energies due to the crystal field splitting.

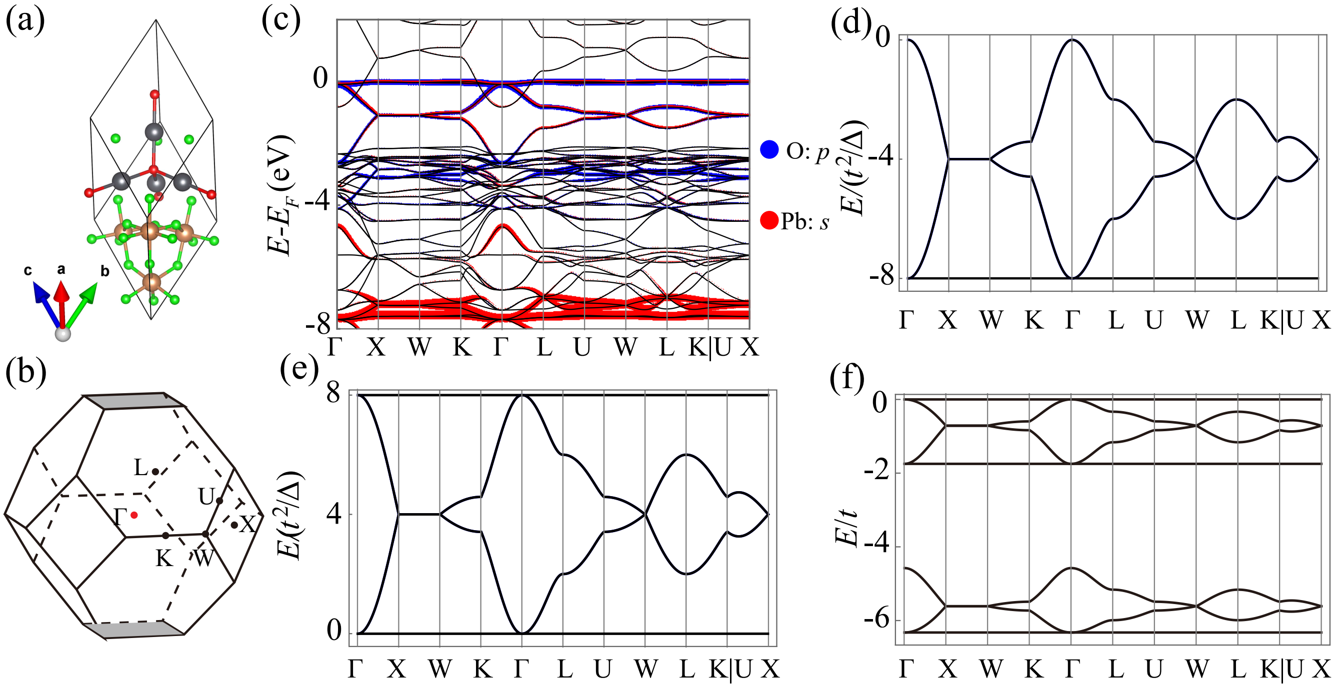

Figure 16. (a) The crystal structure of $Pb_2Sb_2O_7$. The Pb and Sb atoms are in gray and brown, respectively. The O atoms at $8b$ and $48f$ are in red and green, respectively. (b) The bulk BZ of $Pb_2Sb_2O_7$. (c) Band structure calculated by GGA-PBE of $Pb_2Sb_2O_7$ without spin-orbit coupling. The weights of the s orbital on Pb and the p orbitals on O atoms that are located at $8b$ are highlighted in red and blue, respectively. (d) The band structure of Hamiltonian $H_{\tilde{L}}$ in Eq. (F10). (e) The band structure of Hamiltonian H_L in Eq. (F10). (f) The band structure of Hamiltonian $H_{L\oplus\tilde{L}}$ in Eq. (F9).

In the S-matrix construction we have set both onsite energies as Δ for simplicity. Now we consider splitting the A_{2u} and E_u orbitals by adding an additional onsite energy δ on the A_{2u} orbitals. Notice that the A_{2u} irreps at $(\frac{1}{2},0,0)$, $(0,\frac{1}{2},0)$, $(0,0,\frac{1}{2})$ are formed by p_x, p_y, and p_z orbitals, respectively. From the S-matrix in Eq. (F2), one can see that these A_{2u} orbitals are decoupled from the other orbitals. Hence, for $\delta = 0$, the A_{2u} orbitals contribute to three of the six flat bands at Δ. A nonzero δ just shifts the energy of these three flat bands to $\Delta+\delta$, as shown in Fig. 15(f), where δ is set to $-|t|$ (note that δ does not have to be equal to Δ). The band structure with nonzero δ still has perfect flat-band segments in the valence bands. These flat bands will have finite band widths if the (smaller) hopping terms between p orbitals at different O atoms are taken into account. We leave this discussion for future studies.

The above analysis using the S-matrix method could be adapted to explain the flat bands of the other perovskites, such as ReO_3 [ICSD 16810, SG 221 ($Pm\bar{3}m$)][68], NbF_3 [ICSD 25596, SG 221 ($Pm\bar{3}m$)], $BaTiO_3$ [ICSD 27971, SG 221 ($Pm\bar{3}m$)], $CaTiO_3$ [ICSD 162924, SG 221 ($Pm\bar{3}m$)], $SrTiO_3$ [ICSD 80874, SG 221 ($Pm\bar{3}m$)], $NaNbO_3$ [ICSD 28588, SG 221 ($Pm\bar{3}m$)], $NaTaO_3$ [ICSD 88378, SG 221 ($Pm\bar{3}m$)], $CrLaO_3$ [ICSD 28930, SG 221 ($Pm\bar{3}m$)], $CrSrO_3$ [ICSD 108903, SG 221 ($Pm\bar{3}m$)], $BaFeO_3$ [ICSD 29096, SG 221 ($Pm\bar{3}m$)], $SrFeO_3$ [ICSD 91062, SG 221 ($Pm\bar{3}m$)], $LaFeO_3$ [ICSD 29118, SG 221 ($Pm\bar{3}m$)], $LaMnO_3$ [ICSD 674501, SG 221 ($Pm\bar{3}m$)], $SrRuO_3$ [ICSD 82983, SG 221 ($Pm\bar{3}m$)], $BaRuO_3$ [ICSD 673893, SG 221 ($Pm\bar{3}m$)], $SrCoO_3$ [ICSD 77142, SG 221 ($Pm\bar{3}m$)], $SrVO_3$ [ICSD 88982, SG 221 ($Pm\bar{3}m$)], $CaTcO_3$ [ICSD 671082, SG 221 ($Pm\bar{3}m$)], $SrTcO_3$ [ICSD 109076, SG 221 ($Pm\bar{3}m$)], $CaTcO_3$ [ICSD 671086, SG 221 ($Pm\bar{3}m$)], $TiPbO_3$ [ICSD 187295, SG 221 ($Pm\bar{3}m$)], $CrPbO_3$ [ICSD 160196, SG 221 ($Pm\bar{3}m$)], $CaMnO_3$ [ICSD 168902, SG 221 ($Pm\bar{3}m$)], $SrMnO_3$ [ICSD 188415, SG 221 ($Pm\bar{3}m$)], $VPbO_3$ [ICSD 187637, SG 221 ($Pm\bar{3}m$)], $KNbO_3$ [ICSD 190920, SG 221 ($Pm\bar{3}m$)], and $VBaO_3$ [ICSD 191203, SG 221 ($Pm\bar{3}m$)]. Note that all of these materials are listed in Appendix H 1.

2. $Pb_2Sb_2O_7$

The crystal structure of $Pb_2Sb_2O_7$ [ICSD 27120, SG 227 ($Fd\bar{3}m$)(origin choice 1 as defined on the *Bilbao Crystallographic Server*)] is shown in Fig. 16(a). The $16d$ and $16c$ Wyckoff positions are occupied by the Pb and Sb atoms, respectively. O atoms occupy two different Wyckoff positions, $8b$ and $48f$. As tabulated in Table V, each of the sublattices formed by Pb and Sb is a pyrochlore lattice, which is a 3D line-graph lattice that could host flat bands[26]. As shown in the orbital-projected band structure of $Pb_2Sb_2O_7$ in Fig. 16(c), around the Fermi level, there are two flat bands mainly composed by the p orbitals of the O located at the $8b$ position. As indicated in the orbital-projected band structure, the p orbitals of O are hybridized with the s orbitals of Pb. The other bands between -8eV and -2eV are mainly contributed by the O atoms at the $48f$ Wyckoff position. The hybridization between the s orbitals of O at $8b$ and these bands is tiny because the distances from the O atoms at $8b$ to the Sb atoms and O atoms at $48f$ are larger than those to the Pb atoms. In fact, in Materials Flatband Database website and Appendix H 1, the crystal structure of $Pb_2Sb_2O_7$ is identified to have a bipartite lattice formed by Pb and the O at $8b$. As shown below, the flat bands come from the S-matrix of this bipartite lattice.

We refer to the two sublattices formed by O (at $8b$) and Pb (at $16d$) as L and $\tilde{L}$, respectively. Then, the lattice of $L \oplus \tilde{L}$ is a bipartite lattice if only the bonds connecting Pb and its NN O atoms are taken into account. We construct the S matrix by putting three p orbitals at each of the $8b$ positions $\left(\frac{1}{2},\frac{1}{2},\frac{1}{2}\right)$, $\left(\frac{3}{4},\frac{3}{4},\frac{3}{4}\right)$ and an s orbital at each of the $16d$ positions $\left(\frac{5}{8},\frac{5}{8},\frac{5}{8}\right)$,$\left(\frac{5}{8},\frac{5}{8},\frac{1}{8}\right)$,$\left(\frac{5}{8},\frac{1}{8},\frac{5}{8}\right)$ and $\left(\frac{1}{8},\frac{5}{8},\frac{5}{8}\right)$, with coordinates given in the primitive unit cell spanned by $\boldsymbol{a}_1 = a(0,1/2,1/2)$, $\boldsymbol{a}_2 = a(1/2,0,1/2)$, $\boldsymbol{a}_3 = a(1/2,1/2,0)$, with a being the lattice parameter. We use α and a to label the orbitals in the sublattices $\tilde{L}$ and L, respectively. The index $\alpha = 1,2,3,4$ corresponds to the four s orbitals at the four sites in $\tilde{L}$. The index $a = i + 2(j-1)$ corresponds to the p_x $(j=1)$, p_y $(j=2)$, p_z $(j=3)$ orbitals at the i'th site $(i=1,2)$ in L. Then the S matrix can be written as

$$S^\dagger(\boldsymbol{k}) = t \begin{pmatrix} 1 & -1 & 1 & -1 & 1 & -1 \\ -1 & e^{-ik_3} & -1 & e^{-ik_3} & 1 & -e^{-ik_3} \\ -1 & e^{-ik_2} & 1 & -e^{-ik_2} & -1 & e^{-ik_2} \\ 1 & -e^{-ik_1} & -1 & e^{-ik_1} & -1 & e^{-ik_1} \end{pmatrix}. \tag{F8}$$

Here, t is the strength of the coupling between s orbital at $\left(\frac{5}{8},\frac{5}{8},\frac{5}{8}\right)$ and p_x orbital at $\left(\frac{1}{2},\frac{1}{2},\frac{1}{2}\right)$, and (k_1,k_2,k_3) is the coordinate of the momentum $\boldsymbol{k} = \sum_{i=1}^{3} k_i \boldsymbol{b}_i$, where $\boldsymbol{b}_i$ is the reciprocal lattice basis corresponding to the $\boldsymbol{a}_i$ given above. We assume the onsite energies of the p and s orbitals to be Δ_s and Δ_p, respectively, and they satisfy $\Delta_s < \Delta_p < 0$. Although Δ_s and Δ_p are free parameters, to simplify the expression of the following Hamiltonian and the associated eigenvalues of flat bands, we choose a set of particular values $\Delta_p = \left(\sqrt{2}-\sqrt{10}\right)|t|$, $\Delta_s = -\left(\sqrt{2}+\sqrt{10}\right)|t|$. The total Hamiltonian is given by

$$H_{L\oplus\tilde{L}}(\boldsymbol{k}) = \begin{pmatrix} \Delta_s \mathbb{I}_{4\times4} & S^\dagger(\boldsymbol{k}) \\ S(\boldsymbol{k}) & \Delta_p \mathbb{I}_{6\times6} \end{pmatrix}. \tag{F9}$$

Following the same analysis below Eq. (F3), one can find that there will be $|L| - \mathrm{rank}(S(\boldsymbol{k}))$ states at the energy Δ_p and $|\tilde{L}| - \mathrm{rank}(S(\boldsymbol{k}))$ states at the energy Δ_s. While the other $2 \times \mathrm{rank}(S(\boldsymbol{k}))$ states have the energies $\frac{\Delta_s+\Delta_p}{2} \pm \sqrt{\xi_n^2(\boldsymbol{k}) + (\Delta_s-\Delta_p)^2/4}$, with $\xi_n(\boldsymbol{k})$ being the nonzero singular values of $S(\boldsymbol{k})$. Since $\mathrm{rank}(S(\boldsymbol{k})) = |\tilde{L}| = 4$ at generic momenta, there are two flat bands at $E = \Delta_p \approx -1.75|t|$, as shown in Fig. 16(e). The effective Hamiltonian for L (p-bands) and $\tilde{L}$ (s-bands) can be derived through the second order perturbation theory as

$$H_L(\boldsymbol{k}) \approx \Delta_p + \frac{S(\boldsymbol{k})S^\dagger(\boldsymbol{k})}{\Delta_p - \Delta_s}, \quad H_{\tilde{L}}(\boldsymbol{k}) \approx \Delta_s - \frac{S^\dagger(\boldsymbol{k})S(\boldsymbol{k})}{\Delta_p - \Delta_s}, \tag{F10}$$

respectively. The energy spectra of $H_{\tilde{L}}$ and H_L are given in Fig. 16(d) and (e), respectively, which qualitatively reproduce the band structures of $H_{\tilde{L}\oplus L}(\boldsymbol{k})$.

One may notice that in addition to the flat bands at Δ_p, there are two other sets of flat bands at the top and the bottom of the band structure of $H_{L\oplus\tilde{L}}$ which are both double-degenerate. They come from the double-degenerate singular value $2\sqrt{2}t$ of $S(\boldsymbol{k})$ at arbitrary $\boldsymbol{k}$. Indeed from the above analysis, this singular value leads to flat bands at $\frac{\Delta_s+\Delta_p}{2} \pm \sqrt{8t^2 + (\Delta_s-\Delta_p)^2/4}$, *i.e.*, 0 and $-2\sqrt{10}|t|$, respectively. The flat band at zero energy corresponds to the first-principles flat band at the Fermi level (Fig. 16(c)). Hence, the bipartite lattice in this example give rise to the flat bands at $E = \Delta_p$, which come from the rank of $S(\boldsymbol{k})$, as well as to the two degenerate extra flat bands which come from the particular singular values of $S(\boldsymbol{k})$.

The band structure features obtained from S-matrix method is consistent with the first-principle calculations of $Pb_2Sb_2O_7$. Such an analysis applies to some other materials with the pyrochlore structure, such as $Sn_2Nb_2O_7$ [ICSD 163817, SG 227 ($Fd\bar{3}m$)], $Ca_2Nb_2O_7$ [ICSD 22411, SG 227 ($Fd\bar{3}m$)], $Bi_2Pt_2O_7$ [ICSD 202346, SG 227 ($Fd\bar{3}m$)], $Bi_2Ir_2O_7$ [ICSD 161103, SG 227 ($Fd\bar{3}m$)], $Bi_2Rh_2O_7$ [ICSD 161099, SG 227 ($Fd\bar{3}m$)], $Ge_2In_2O_7$ [ICSD 239593, SG 227 ($Fd\bar{3}m$)], and $Sn_2Ta_2O_7$ [ICSD 27119, SG 227 ($Fd\bar{3}m$)]. Note that all of these materials are part of the curated

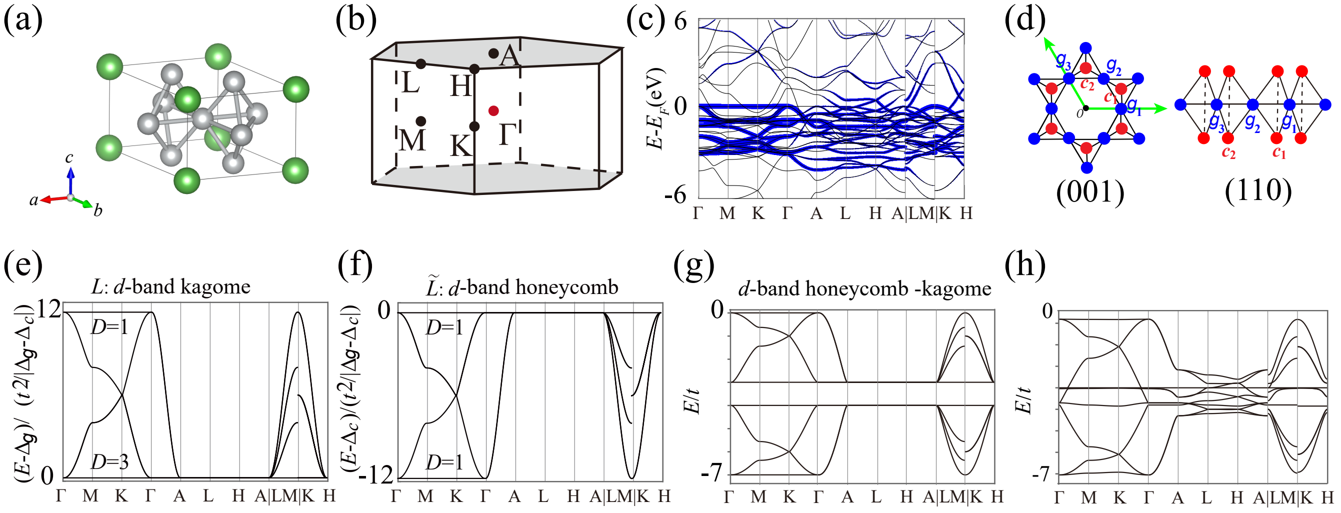

Figure 17. (a) The crystal structure of CaNi$_5$. The Ca and Ni atoms are represented by the green and gray balls, respectively. (b) The bulk BZ of CaNi$_5$. (c) Band structure of CaNi$_5$ without spin-orbit coupling, where the weights of d_{xz} and d_{yz} orbitals on Ni are highlighted in blue. (d) The schematic pictures of the top- and side-view (*i.e.*, along the respective (001) and (110) directions) of the bipartite lattice in CaNi$_5$. (e) and (f) The band structures of the effective Hamiltonians of d_{xz}, d_{yz} orbitals on Kagome (L) and honeycomb ($\tilde{L}$) lattices, where the effective Hamiltonians are obtained from the S-matrix method through second order perturbation theory. The degeneracy D of each segment of flat bands is indicated in the plots. (g) The band structure of d_{xz}, d_{yz} orbitals on the bipartite lattice $\tilde{L} \oplus L$. (h) The band structure of $\tilde{L} \oplus L$ with intra-sublattice couplings.

list in Appendix H 1.

3. CaNi$_5$

The crystal structure of CaNi$_5$ [ICSD 54474, SG 191 ($P6/mmm$)] is shown in Fig. 17(a). The $1a$ Wyckoff position is occupied by Ca and both the $3g$ and $2c$ Wyckoff positions are occupied by Ni. The band structure of CaNi$_5$ is plotted in Fig. 17(c), which has an extremely flat band at the Fermi level in the $k_z = 0$ plane. By analyzing the orbital-projected band structure, we find that the flat bands mainly arise from the d_{xz} and d_{yz} orbitals on Ni.

In CaNi$_5$, Ni form two sublattices: Ni atoms at $2c$ form a honeycomb sublattice, and Ni atoms at $3g$ form a Kagome sublattice. In the following, to understand the origin of this flat band, we first only consider couplings between two sublattices. We will consider couplings within each sublattice at the end of this subsection. We refer to the sublattices formed by Ni atoms at $2c$ and $3g$ as $\tilde{L}$ and L, respectively. We label the $3g$ and $2c$ positions as g_i $(i = 1,2,3)$ and c_i $(i = 1,2)$, respectively, as shown in Fig. 17 (d). They form a bipartite lattice since we ignore the hoppings within each of them. We introduce the S matrix formed by the d_{xz} and d_{yz} orbitals in $\tilde{L}$ and L as $S^\dagger_{\alpha a} = \langle \phi_\alpha(\boldsymbol{k})| H |\phi_a(\boldsymbol{k})\rangle$. $\alpha = i + 2(j-1)$ corresponds to the d_{yz} $(j = 1)$, d_{xz} $(j = 2)$ orbitals at the ith site $(i = 1,2)$ in $\tilde{L}$. $a = i + 3(j-1)$ corresponds to the d_{yz} $(j = 1)$, d_{xz} $(j = 2)$ orbitals at the ith site $(i = 1,2,3)$ in L. Based on the MLWF, we consider the coupling between d_{xz} orbital at c_2 and d_{yz} orbital at g_3 and set its strength to t. The S-matrix reads

$$S^\dagger(\boldsymbol{k}) = \frac{t}{4}\left(1+e^{ik_3}\right)\begin{pmatrix} 4 & 1 & e^{ik_1} & 0 & -\sqrt{3} & \sqrt{3}e^{ik_1} \\ 4e^{ik_2} & 1 & 1 & 0 & -\sqrt{3} & \sqrt{3} \\ 0 & -\sqrt{3} & \sqrt{3}e^{ik_1} & 0 & 3 & 3e^{ik_1} \\ 0 & -\sqrt{3} & \sqrt{3} & 0 & 3 & 3 \end{pmatrix}, \tag{F11}$$

where (k_1, k_2, k_3) are the coordinates of the momentum $\boldsymbol{k} = \sum_{i=1}^{3} k_i \boldsymbol{b}_i$, where $\boldsymbol{b}_i$ is the reciprocal lattice basis corresponding to the primitive unit cell spanned by $\boldsymbol{a}_1 = b(1,0,0)$, $\boldsymbol{a}_2 = b(-1/2, \sqrt{3}/2, 0)$, $\boldsymbol{a}_3 = c(0,0,1)$, with b and c being the lattice parameters. Note that the values of the hopping amplitudes appearing in $S^\dagger_{i,j}(\boldsymbol{k})$ are constrained by the space group symmetries.

The Hamiltonians of the bipartite lattice $L \oplus \tilde{L}$ and the $\tilde{L}$ and L are given by Eqs. (F9) and (F10) except that

$\{\Delta_s, \Delta_p\}$ should be replaced by $\{\Delta_c, \Delta_g\}$. Here Δ_c is the onsite energy of d orbitals on the honeycomb lattice and Δ_g is the onsite energy of d orbitals on the Kagome lattice. In the following we choose $\Delta_c = -4|t|$ and $\Delta_g = -3|t|$. The $S(\boldsymbol{k})$ matrix has rank three at generic momentum. Following the same analysis below Eq. (F3), one can find that in the band structure of $H_{L\oplus\tilde{L}}$ there will be $|L| - \mathrm{rank}(S(\boldsymbol{k})) = 3$ states at the energy Δ_g and $|\tilde{L}| - \mathrm{rank}(S(\boldsymbol{k})) = 1$ states at the energy Δ_c, as shown in Fig. 17(g). In addition, since S has a constant singular value $2\sqrt{3}t|\cos\frac{k_3}{2}|$ in a horizontal plane with fixed k_3, due to the discussion below Eq. (F3), there is a set of 2D flat bands at $\frac{\Delta_g+\Delta_c}{2} \pm \sqrt{12t^2\cos^2\frac{k_3}{2} + (\Delta_g - \Delta_c)^2/4}$. For $k_3 = 0$, the two additional flat bands at $E = 0$ and $E = -7t$, respectively.

The effective Hamiltonian $H_{\tilde{L}} \approx \Delta_c - S^\dagger(\boldsymbol{k})S(\boldsymbol{k})/(\Delta_g - \Delta_c)$ describes a 3D system consisting of honeycomb lattice layers. It has single particle dimension four. Since $S(\boldsymbol{k})$ has rank three over the whole Brillouin zone (or smaller ranks at high symmetry momenta) and has a constant singular value $2\sqrt{3}t|\cos\frac{k_3}{2}|$ in a horizontal plane with fixed k_3, the band structure of $H_{\tilde{L}}$ has a 3D flat band at $E = \Delta_c$ and a 2D flat band $E = \Delta_c - \frac{12t^2}{\Delta_g-\Delta_c}\cos^2\frac{k_3}{2}$ in any fixed-k_3 plane (Fig. 17(f))[69]. Similarly, the effective Hamiltonian of the Kagome lattice ($H_L \approx \Delta_g - S(\boldsymbol{k})S^\dagger(\boldsymbol{k})/(\Delta_c - \Delta_g)$), which has dimension six, has a three-fold degenerate 3D flat band at $E = \Delta_g$ and a 2D flat band at $E = \Delta_g - \frac{12t^2}{\Delta_c-\Delta_g}\cos^2\frac{k_3}{2}$ in any fixed-k_3 plane (Fig. 17(e)).

Comparing with the band structure from first-principle calculations in Fig. 17(c), we identify the flat band of $L \oplus \tilde{L}$ at $E = 0$ as the flat band near the Fermi level in $\mathrm{CaNi_5}$. To further check the robustness of the flat bands in Fig. 17(g), we consider the couplings within each sublattice. We set the hopping between d_{yz} orbital at c_1 and d_{xz} orbital at c_2 (d_{yz} orbital at g_1 and d_{yz} orbital at g_2), as well as the equivalent hopping terms due to symmetries, to $0.1t$ ($0.2t$) (Fig. 17(d)). The resulting band structure is shown in Fig. 17(h). One can see that these intra-sublattice hopping terms barely have any effect on the flat band at $E = 0$ and $E = -7t$ in the $k_3 = 0$ plane.

The above explanations of the extremely flat band in $\mathrm{CaNi_5}$ can also be applied to some other materials with $\mathrm{AB_5}$-type structure in SG 191 ($P6/mmm$), such as $\mathrm{LaNi_5}$ [ICSD 242027,SG 191 ($P6/mmm$)], $\mathrm{ScNi_5}$ [ICSD 646468, SG 191 ($P6/mmm$)], $\mathrm{CaPd_5}$ [ICSD 106357, SG 191 ($P6/mmm$)], $\mathrm{SrPd_5}$ [ICSD 105707, SG 191 ($P6/mmm$)], $\mathrm{BaPd_5}$ [ICSD 616030, SG 191 ($P6/mmm$)], $\mathrm{YNi_5}$ [ICSD 647075, SG 191 ($P6/mmm$)] and $\mathrm{YFe_5}$ [ICSD 103699, SG 191 ($P6/mmm$)]. Note that all of these materials are listed in Appendix H 1.

4. $\mathrm{Ca_2NCl}$

The crystal structure and BZ of $\mathrm{Ca_2NCl}$ [ICSD 62555, SG 166 ($R\bar{3}m$)] are shown in Figs. 18(a) and (b), respectively. Since it is a layered material, we have chosen to use the conventional unit cell rather than the primitive unit cell for the band structure calculation. The $3a$, $3b$ and $6c$ Wyckoff positions are occupied by the Cl, N and Ca atoms, respectively. The lattice parameters of the conventional cell are $a = b = 3.67$Å and $c = 19.89$Å. As shown in the band structure in Fig. 18(c), the highest valence band is flat along all the high-symmetry paths. From the orbital-projected band structure, we see that the dominant contribution to the flat band comes from the p orbitals of N. Since the distance between two neighboring N layers is large ($c/3 = 6.63$Å), in the following we will omit the inter-layer couplings. This is a reasonable approximation because, as shown in Fig. 18(c), the band dispersion of the non-flat bands in the k_z direction, *e.g.* paths ΓA, LM, KH, is weak compared to the in-plane dispersion.

To explain the flat bands in Fig. 18(c), we first build a 2D tight-binding model consisting of p_x, p_y and p_z orbitals on the N atoms in a single N layer. The N atoms in a single layer form a simple triangular lattice. The tight-binding Hamiltonian on the p_x, p_y, p_z orbitals is given by

$$H\left(\boldsymbol{k}\right) = 2\begin{pmatrix} H_{12}\left(\boldsymbol{k}\right) & H_3\left(\boldsymbol{k}\right) \\ H_3^\dagger\left(\boldsymbol{k}\right) & \Delta + t_z^{pp\pi}\left[\cos k_1 + \cos k_2 + \cos\left(k_1+k_2\right)\right] \end{pmatrix}, \tag{F12}$$

with the terms

$$H_{12}\left(\boldsymbol{k}\right) = \begin{pmatrix} t^{pp\sigma}\cos k_1 + \frac{t^{pp\sigma}+3t^{pp\pi}}{4}\left[\cos k_2 + \cos\left(k_1+k_2\right)\right] & \frac{\sqrt{3}(t^{pp\pi}-t^{pp\sigma})}{4}\left[\cos k_2 - \cos\left(k_1+k_2\right)\right] \\ \frac{\sqrt{3}(t^{pp\pi}-t^{pp\sigma})}{4}\left[\cos k_2 - \cos\left(k_1+k_2\right)\right] & t^{pp\pi}\cos k_1 + \frac{3t^{pp\sigma}+t^{pp\pi}}{4}\left[\cos k_2 + \cos\left(k_1+k_2\right)\right] \end{pmatrix}. \tag{F13}$$

and

$$H_3^\dagger\left(\boldsymbol{k}\right) = \begin{pmatrix} \frac{\sqrt{3}t^p}{8}\left[\cos k_2 - \cos\left(k_1+k_2\right)\right] & \frac{t^p}{8}\left[-2\cos k_1 + \cos k_2 + \cos\left(k_1+k_2\right)\right] \end{pmatrix} \tag{F14}$$

Here $t^{pp\pi}$ and $t^{pp\sigma}$ are the π-bond and σ-bond strengths between p_x and p_y orbitals, $t_z^{pp\pi}$ is the π-bond strength

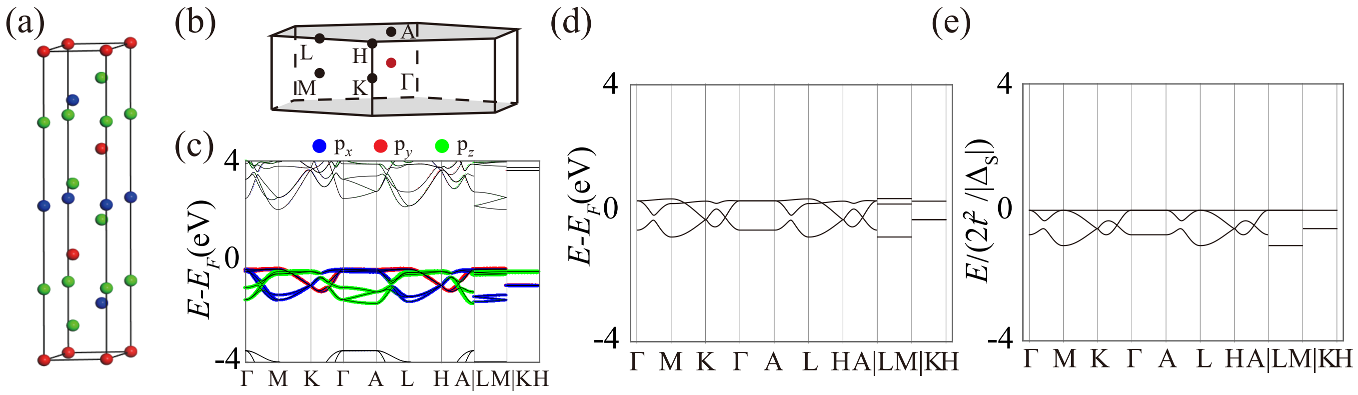

Figure 18. (a) The crystal structure of Ca$_2$NCl, where the N atoms are represented by the blue balls. (b) The bulk BZ of Ca$_2$NCl. (c) Band structure of Ca$_2$NCl without spin-orbit coupling. The weights of the p orbits N on the highest set of valence bands are highlighted in blue for the p_x orbitals, red for the p_y orbitals and green for the p_z orbitals. (d) Band structure of the three band Hamiltonian in Eq. (F12) with the parameters extracted from the MLWF calculation. (e) Band structure given by the S-matrix method given in Eq. (F18).

between p_z orbitals, and $t^p/8$ is the strength of coupling between a p_y orbital at $(0,0,0)$ and a p_z orbital at $(0,1,0)$. As mentioned in Appendix F 3, the hopping amplitudes appearing in Eq. (F12) are constrained by the space group symmetries. (k_1,k_2) is the coordinate of the momentum $\boldsymbol{k}=\sum_{i=1}^{2}k_i\boldsymbol{b}_i$, where $\boldsymbol{b}_i$ is the reciprocal lattice basis corresponding to the unit cell spanned by $\boldsymbol{a}_1=a(1,0)$, $\boldsymbol{a}_2=a(-\frac{1}{2},\frac{\sqrt{3}}{2})$. We set the difference of the onsite energy of p_z and $p_{x,y}$ orbitals as Δ. From the MLWF we extract the parameters $\Delta=0.04$eV, $t^{pp\sigma}=0.21$eV, $t_z^{pp\pi}=-0.10$eV, $t^{pp\pi}=-0.08$eV, and $t^p=0.16$eV. The tight-binding band structure is shown in Fig. 18(d). It correctly reproduces the flat band from the first-principles calculation. We find that the flatness comes from a set of conditions for the hopping terms that are approximately satisfied in the MLWF model. As an example, we take the path ΓM ($k_1=0$) to show one such conditions. In this path, the Hamiltonian is simplified to

$$H(0,k_2)=2\begin{pmatrix} t^{pp\sigma}+\frac{t^{pp\sigma}+3t^{pp\pi}}{2}\cos k_2 & 0 & 0 \\ 0 & t^{pp\sigma}+\frac{3t^{pp\sigma}+t^{pp\pi}}{2}\cos k_2 & -\frac{t^p}{4}+\frac{t^p}{4}\cos k_2 \\ 0 & -\frac{t^p}{4}+\frac{t^p}{4}\cos k_2 & \Delta+t_z^{pp\pi}(1+2\cos k_2) \end{pmatrix} \tag{F15}$$

There would be an *exact* flat band at $E=2t^{pp\sigma}$ along this path if $t^{pp\sigma}+3t^{pp\pi}=0$. This condition is approximately satisfied by the actual values extracted from MLWFs ($t^{pp\sigma}+3t^{pp\pi}=-0.03$eV). As shown in Fig. 18(d), if the condition $t^{pp\sigma}+3t^{pp\pi}=0$ is not strictly satisfied well, the band near $E=2t^{pp\sigma}$ becomes weakly dispersive but is still relatively flat. This follows from the first-principles calculations.

The bands around 3eV in Fig. 18(c) are mostly due to the Ca atoms. We notice that the nearest neighbors of N atoms are the Ca atoms. Hence the strongest hopping terms in this system are those between N and Ca atoms. In the following, we construct a S-matrix between the N and Ca atoms and derive Eq. (F12) as an effective Hamiltonian from the second-order perturbation of this S-matrix model. The set of conditions that guarantee the flat band are automatically implied by the S-matrix. We refer to the sublattices formed by Ca atoms and N atoms as $\tilde{L}$ and L, respectively. We introduce the S matrix formed by the s or d_z^2 orbital in $\tilde{L}$ and p orbitals in L as $S_{\alpha a}^{\dagger}=\langle\phi_\alpha(\boldsymbol{k})|\,H\,|\phi_a(\boldsymbol{k})\rangle$. The index $\alpha=(1,2)$ corresponds to the s orbitals at $(\frac{1}{3},\frac{2}{3},x)$ and $(\frac{1}{3},\frac{2}{3},1-x)$ in $\tilde{L}$. $\alpha=(1,2,3)$ corresponds to the p_x, p_y and p_z orbitals at $(0,0,1/2)$ in L. The S-matrix reads

$$S^{\dagger}(\boldsymbol{k})=\frac{t}{4}\begin{pmatrix} -\sqrt{3}\left(-1+e^{ik_1}\right)e^{ik_2} & -e^{i(k_1+k_2)}-e^{ik_2}+2 & 2\lambda\left(1+e^{ik_2}+e^{i(k_1+k_2)}\right) \\ -\sqrt{3}\left(-1+e^{ik_1}\right) & -2e^{i(k_1+k_2)}+e^{ik_1}+1 & -2\lambda\left(1+e^{ik_1}+e^{i(k_1+k_2)}\right) \end{pmatrix}, \tag{F16}$$

Here, t is the strength of coupling between the s or d_z^2 orbital at $(\frac{1}{3},\frac{2}{3},x)$ and the p_y orbital at $(0,0,0)$, λt is the strength of coupling between the s orbital at $(\frac{1}{3},\frac{2}{3},x)$ and the p_z orbital at $(0,0,0)$. The Hamiltonians of the bipartite lattice $L\oplus\tilde{L}$ and the $\tilde{L}$ and L are given by Eq. (F9) and Eq. (F10), where $\Delta_p=0$ is the onsite energy of L and

$\Delta_s > 0$ is the onsite energy of $\tilde{L}$. The effective Hamiltonian of L (p-bands) is given by

$$H_L(\boldsymbol{k}) \approx -\frac{S(\boldsymbol{k})S^\dagger(\boldsymbol{k})}{\Delta_s}, \tag{F17}$$

The explicit form of H_L is given by

$$\begin{aligned} H_L(\boldsymbol{k}) &\approx -\frac{S(\boldsymbol{k})S^\dagger(\boldsymbol{k})}{\Delta_s} \\ &= \frac{-t^2}{4\Delta_s}\begin{pmatrix} 3-3\mathrm{cos}k_1 & \sqrt{3}\left[\mathrm{cos}k_2-\cos\left(k_1+k_2\right)\right] & \sqrt{3}\lambda\left[\mathrm{cos}k_2-\cos\left(k_1+k_2\right)\right] \\ \sqrt{3}\left[\mathrm{cos}k_2-\cos\left(k_1+k_2\right)\right] & 3+\mathrm{cos}k_1-2\left[\mathrm{cos}k_2+\cos\left(k_1+k_2\right)\right] & \lambda\left[-2\mathrm{cos}k_1+\mathrm{cos}k_2+\cos\left(k_1+k_2\right)\right] \\ \sqrt{3}\lambda\left[\mathrm{cos}k_2-\cos\left(k_1+k_2\right)\right] & \lambda\left[-2\mathrm{cos}k_1+\mathrm{cos}k_2+\cos\left(k_1+k_2\right)\right] & 4\lambda^2\left[\frac{3}{2}+\mathrm{cos}k_1+\mathrm{cos}k_2+\cos\left(k_1+k_2\right)\right] \end{pmatrix}. \end{aligned} \tag{F18}$$

From the MLWF we know that the strength of coupling between the s orbital at $(\frac{1}{3},\frac{2}{3},x)$ and the p_y orbital at $(0,0,0)$ is bigger than that of coupling between the s orbital at $(\frac{1}{3},\frac{2}{3},x)$ and the p_z orbital at $(0,0,0)$. Meanwhile, they have opposite sign. Thus, we set $\lambda \simeq -0.71$ in the calculation. The band structure of the L sublattice is shown in Fig. 18(e). Since the rank of $S(\boldsymbol{k})$ is two at generic momentum, there is a single flat band at $E=0$. H_L has the same form as Eq. (F12) with the five parameters given by $t^{pp\sigma} = 3t^2/(8\Delta_s)$, $t^{pp\pi} = -t^2/(8\Delta_s)$, $t_z^{pp\pi} = -\lambda^2 t^2/(2\Delta_s)$, $t^p = -\lambda t^2/\Delta_s$, and $\Delta = -3t^2/(8\Delta_s)(2\lambda^2-1)$. Since the S-matrix only has two free parameters, the yielded five parameters will satisfy three conditions which are $t_p^2 = 16t^{pp\pi}t_z^{pp\pi}$, $3t_p^2 = 32(\Delta + 2t^{pp\pi})t^{pp\pi}$, and $t^{pp\sigma} + 3t^{pp\pi} = 0$. Note that the last condition $t^{pp\sigma} + 3t^{pp\pi} = 0$, which is responsible for the flat band in the path ΓM was also derived in Eq. (F15) from the MLWF model.

The bands obtained from first-principle calculations are more complicated than the S-matrix band. For example, the p_z-band has a non-negligible bandwidth along the k_3 direction, implying that the hopping terms between p_z orbitals in different layers are not negligible. Thus, a more realistic model can be obtained by adding these hopping terms to the S-matrix model.

The explanations that we have developed above can be applied to some other compounds, such as Ca_2NBr [ICSD 62556, SG 166 ($R\bar{3}m$)], Sr_2NCl [ICSD 172595, SG 166 ($R\bar{3}m$)], Sr_2NBr [ICSD 172601, SG 166 ($R\bar{3}m$)], Ca_2N [ICSD 90632, SG 166 ($R\bar{3}m$)]. Note that all of these materials are part of the curated list provided in Appendix H 1.

5. Rb_2CaH_4

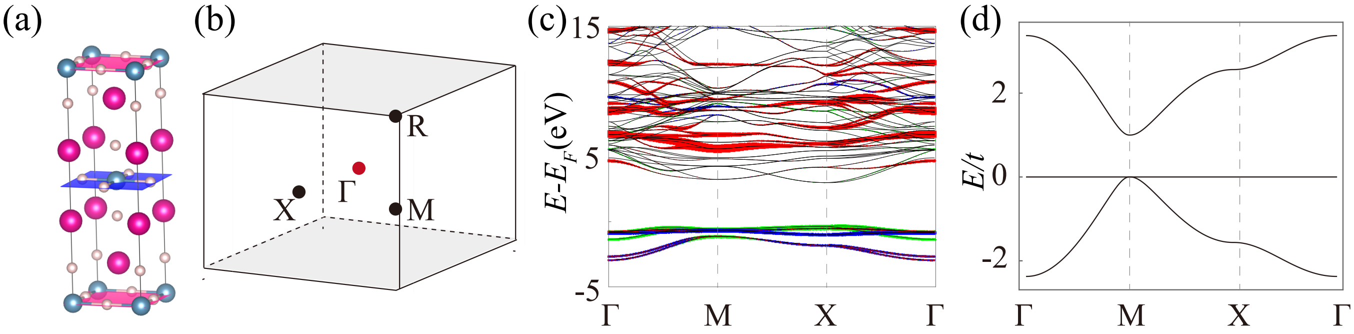

Figure 19. (a) The crystal structure of the unit cell of Rb_2CaH_4, where the Ca, H, and Rb atoms are represented by the cyan, pink, and purple balls, respectively. The Ca and H atoms form two Lieb lattices on the (001) Miller plane, as indicated by the pink and blue planes at $z=0$ and $z=0.5c$ (where c is the lattice constant along the (001) direction of the unit cell).(b) The 3D bulk BZ of Rb_2CaH_4. (c) Orbital-projected band structure along the in-plane high-symmetry k-paths of Rb_2CaH_4 in the absence of spin-orbit coupling. The weight of s orbitals on H atoms sitting at $4c$ and $4e$ are highlighted in blue and green, respectively, and the weight of s and d_z^2orbitals on Ca atoms at $2e$ is highlighted in red. (d) The band structure along the in-plane high-symmetry k-paths of the Lieb lattice given by the S-matrix method with $\delta = t$.

The crystal structure of Rb_2CaH_4 [ICSD 65196, SG 139 ($I4/mmm$)] is shown in Fig. 19(a). The $4e$ and $2a$ Wyckoff positions are occupied by the Rb and Ca atoms, respectively. H atoms occupy two non-equivalent Wyckoff positions, $4c$ and $4e$. Ca atoms and the H atoms at $4e$ form two Lieb sublattices in one unit cell, which could host flat topological bands[28], as shown in Fig. 19(a).

From the band structures calculations (without SOC) in the Materials Flatband Database website, there are a set of flat bands near the Fermi level. As plotted in Fig. 19(c), we have analyzed the orbital-projected band structure of Rb_2CaH_4 and found the flat bands are mainly composed by the s orbitals on H atoms sitting at the $4c$ and $4e$ positions. We also find that all the four bands contributed by the s orbitals on H atoms at $4e$ are flat in the whole BZ and they are flat atomic bands, which can be explained by the weak hybridization between H atoms at $4e$ and the other atoms. While for the four bands which are contributed by the s orbitals on H atoms sitting at $4c$, only two of them are flat and the other two bands are dispersive, implying a larger kinetic energy of the s electron at $4c$. In the following, we discard the flat atomic bands contributed by the H atoms at $4e$ and explain the origin of the other flat bands contributed by the H atoms at $4c$ using S-matrix method.

In the crystal structure of Rb_2CaH_4, the distance between two neighboring Lieb sublattices is so large (7.42Å) that the coupling between them is weak. Thus, we can simplify the 3D crystal lattice in Rb_2CaH_4 with a 2D Lieb lattice, which is indicated by the pink plane in Fig. 19(a). For the 2D lieb lattice, we refer to the two sublattices formed by putting s orbitals at H sublattice *i.e.*, $\{(\frac{1}{2},0),\ (0,\frac{1}{2})\}$ and putting s or d_z^2 orbitals at Ca sublattice *i.e.*, $(0,0)$ as L and $\tilde{L}$, respectively. Then the S matrix can be written as

$$S^\dagger(\boldsymbol{k}) = t\left(\begin{array}{cc} 1+e^{-ik_1} & 1+e^{-ik_2} \end{array}\right) \tag{F19}$$

where t is the strength of the coupling between the s orbital at $(\frac{1}{2},0)$ and the s or d_z^2 orbital at $(0,0)$, ;(k_1,k_2) are the coordinates of the momentum $\boldsymbol{k}=\sum_{i=1}^{2}k_i\boldsymbol{b}_i$, where $\boldsymbol{b}_i$ is the reciprocal lattice vector that corresponds to the in-plane lattice vectors $\boldsymbol{a}_1=a(1,0)$ and $\boldsymbol{a}_2=a(0,1)$ (where a is the in-plane lattice constant). We assume the on-site energy of s orbital on H is 0 and that of the Ca atom is Δ. Then the total Hamiltonian of the bipartite lattice reads

$$H_{L\oplus\tilde{L}}(\boldsymbol{k}) = \left(\begin{array}{cc} \Delta & S^\dagger(\boldsymbol{k}) \\ S(\boldsymbol{k}) & 0_{2\times 2} \end{array}\right). \tag{F20}$$

As the band structure of this Lieb lattice plotted in Fig. 19(d), there is a flat band at 0, which corresponds to the flat bands contributed by the s orbitals of H at $4c$ in the first-principles calculations. Note that the weak band splitting of the dispersive bands of energy range from -5eV to -1eV comes from the weak coupling between the two Lieb lattices in the (001) direction. The explanations that we have developed above can be applied to some other compounds, such as Cs_2MgH_4 [ICSD 162261, SG 139 ($I4/mmm$)], and K_2MgH_4 [ICSD 68358, SG 139 ($I4/mmm$)].

6. $KAg[CN]_2$

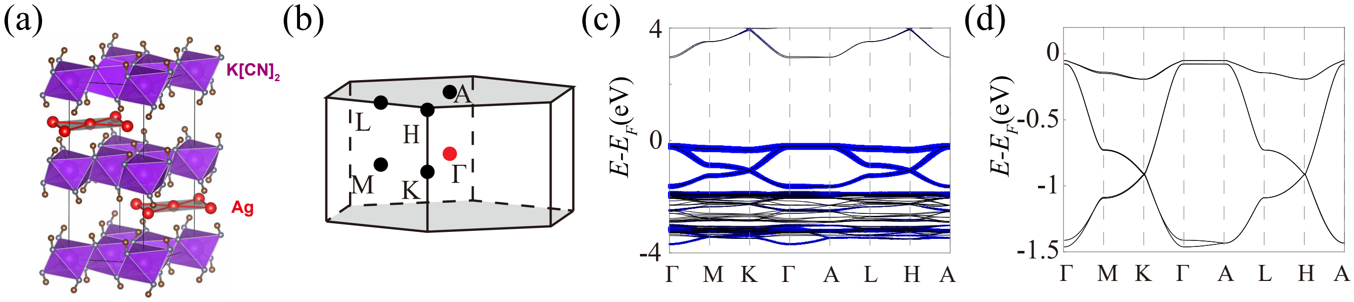

Figure 20. (a) The crystal structure of $KAg[CN]_2$ which is a stacking of alternating molecular layer of $K[CN]_2$ and Kagome layer of Ag atoms (in red color). (b) The bulk BZ of $KAg[CN]_2$ with its high-symmetry k points. (c) The orbital-projected band structure of $KAg[CN]_2$ along the high-symmetry lines from the first-principle calculation without SOC. The bands contributed by the s and d_{z^2} orbitals on Ag atoms are highlighted in blue. (d) The band structure of $KAg[CN]_2$ from the first-principle calculation with SOC (zoomed over the energy range -1.5eV and 0.5eV), where the minimal direct band gap between the flat bands and the dispersive bands is about 25 meV.

As shown in the Fig. 20(a), the crystal structure of $KAg[CN]_2$ [ICSD 30275, SG 163 ($P\bar{3}1c$)] is a layered structure of alternating molecular layers of $K[CN]_2$ and approximate Kagome layers of Ag atoms. The Ag atoms sitting at $6h$ Wyckoff position form two layers of *approximate* Kagome sublattices per unit cell on the (001) plane as indicated by the red spheres in Fig. 20(a). We emphasize that generic $6h$ positions do not form a Kagome lattice guaranteed by symmetries. However, the actual positions of the Ag atoms form an approximate Kagome lattice.

As shown in the band structure without SOC in Fig. 20(c) and on the Materials Flatband Database website, there are two spinless flat bands near the Fermi level and the flat bands are mainly contributed by the hybridized orbital of the s and d_{z^2} orbitals on Ag atoms. The distance between two neighboring Kagome sublattices is so large (8.90Å) that the coupling between them is weak and hence all the bands along the ΓA path are flat. Thus, we can simplify the 3D crystal lattice in KAg[CN]$_2$ to a 2D Kagome lattice. Since the s and d_{z^2} orbitals form the same single-value irrep A of the point group symmetry C_2 at the Wyckoff position $6h$, they in general hybridize with each other and form two hybridized orbitals. We model the six bands in the energy range $-1.5 \sim 0$eV in Fig. 20(c) by a single hybridized orbital - the one with lower energy - at every Ag atom. In the following we refer to this hybridized orbital as s orbital because it transforms under the symmetries as an s orbital. The flat bands of s-orbital Kagome lattice have been fully studied in several previous works[24,26–28,69]. In Appendix E 1, we have also constructed the effective Hamiltonian of the s-orbital Kagome model and explained the origin of its flat bands using an alternative S-matrix method.

In the presence of SOC[28], the flat bands of the s-orbital Kagome lattice in 2D are gapped from the dispersive bands in the whole BZ and have a strong topology[22], *i.e.*, the $\mathbb{Z}_2$ topological insulator phase protected by time-reversal symmetry. For the 3D material KAg[CN]$_2$, as shown in Fig. 20(d), the SOC also fully gaps the flat bands from the dispersive bands. A representation analysis shows that the SOC-gapped flat bands host at least a fragile topology: The irreps of the flat bands at the high-symmetry k points, $\{\bar{A}_4\bar{A}_4, \bar{\Gamma}_4\bar{\Gamma}_5+\bar{\Gamma}_6\bar{\Gamma}_7, \bar{H}_4\bar{H}_5+\bar{H}_6, \bar{K}_4\bar{K}_5+\bar{K}_6, \bar{L}_2\bar{L}_2, \bar{M}_3\bar{M}_4+\bar{M}_5\bar{M}_6\}$, can only be written as a difference of two BRs, *e.g.* $\bar{E}_1@c\oplus{}^1\bar{E}^2\bar{E}@d\ominus\bar{E}_1@a$, but not a sum of BRs. The fragile topology has also been identified in Ref.[47]. However, here we argue that the topology of the SOC-gapped flat bands might be a *stable higher-order topology with hinge states* rather than a fragile topology. According to Ref.[28], the single-layer Kagome lattice with SOC is a 2D $\mathbb{Z}_2$ topological insulator. Then there will be two layers of 2D topological insulators per unit cell occupying the $6h$ positions. Because the $6h$ positions include all the C_{2x}-axes (and equivalent axes due to C_{3z} and inversion symmetries), all the C_{2x}-axes are occupied by the 2D topological insulators. This state is nothing but a layer construction of the C_2 and time-reversal protected higher-order topological insulator[50,70].

7. RbMo$_3$S$_3$

RbMo$_3$S$_3$ [ICSD 644175, SG 176 ($P6_3/m$)] possesses flat bands at the Fermi level. The crystal structure of RbMo$_3$S$_3$ is shown in Fig. 21(a), where Mo and S atoms form a quasi-1D atomic chain along the z direction. The band structure of RbMo$_3$S$_3$ is shown in Fig. 21(c). There are flat bands on the $k_z = 0$ and $k_z = \pi$ planes located at the Fermi level. These flat bands are mainly composed of the E_{1g} orbitals of Mo atoms. By constructing the MLWF, we find that the maximal hopping strength between the E_{1g} orbitals of two neighboring chains is about 0.01eV, which is much smaller than the maximal intra-chain hopping (0.76eV). Hence, the flatness of bands at the Fermi level is due to the weak inter-chain coupling of the quasi-1D crystal structure.

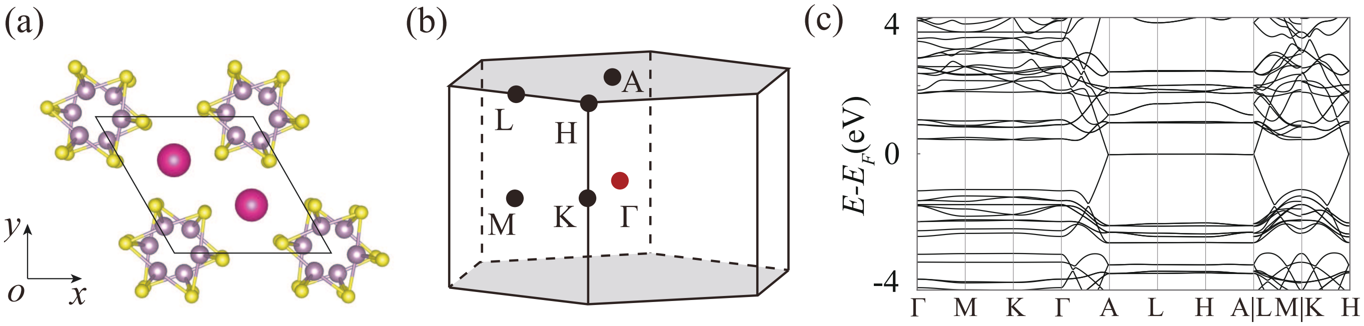

Figure 21. (a) The crystal structure of RbMo$_3$S$_3$. The Mo (in purple) and S atoms (in yellow) form a 1D atomic chain along the z direction. (b) The bulk BZ of RbMo$_3$S$_3$. (c) Band structure of RbMo$_3$S$_3$ from first-principle calculations where spin-orbit coupling is ignored.

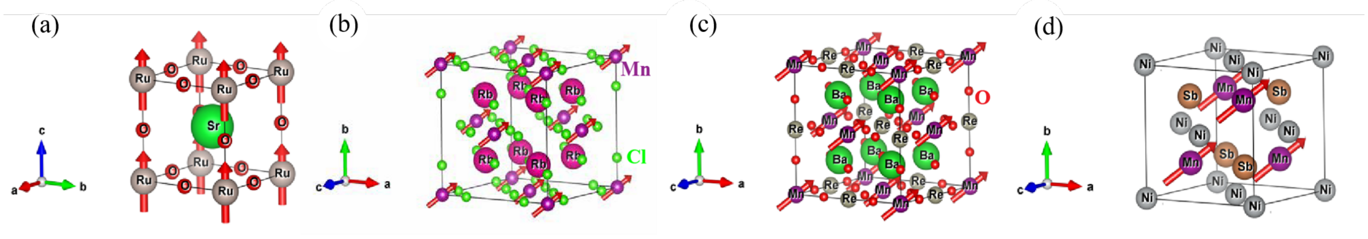

Figure 22. The experimental crystal and magnetic structures of the flat-band materials (a) $SrRuO_3$[ICSD 69360, SG 221 ($Pm\bar{3}m$)], (b) Rb_2MnCl_6[ICSD 9347 SG 225 ($Fm\bar{3}m$)], (c) Ba_2MnReO_6[ICSD 4169 SG 225 ($Fm\bar{3}m$)] and (d) NiMnSb [ICSD 54255, SG 216 ($F\bar{4}3m$).

Appendix G: Examples of magnetic flat-band materials

In the present work, flat-band materials are obtained from the Topological Quantum Chemistry website by analyzing their crystal and band structures. As discussed in Appendix C, all the first-principles calculations performed on the Topological Quantum Chemistry website are forced to be paramagnetic, *i.e.*, without the on-site spin polarization. However, the paramagnetic phase might not be the ground state for all flat-band materials. In Appendix H, we have tagged the materials whose ground states are likely to be magnetic, reporting their magnetic properties found on the Materials Project. To theoretically predict the magnetic properties of materials, we need to compare the total energy of different magnetic configurations in the ab-initio calculations.

In this appendix, we showcase four flat-band materials with experimentally known ferromagnetic ground states and compare the total energies of the paramagnetic and ferromagnetic states obtained from the first-principles calculations. The four materials are $SrRuO_3$[ICSD 69360, SG 221 ($Pm\bar{3}m$)], Rb_2MnCl_6[ICSD 9347 SG 225 ($Fm\bar{3}m$)], Ba_2MnReO_6[ICSD 4169 SG 225 ($Fm\bar{3}m$)] and NiMnSb [ICSD 54255, SG 216 ($F\bar{4}3m$). Their experimental crystal and magnetic structures are shown in Fig. 22.

For the ferromagnetic calculations we adopt the GGA+U method (LDAUTYPE=2, *i.e.*, the simplified (rotationally invariant) approach to the LSDA+U method[71]), which considers the on-site Hubbard U value of d or f electron in the mean-field approximation. By comparing the total energy of the non-magnetic and ferromagnetic phases for different U values (varying from 0 to 5eV) with and without SOC, as provided in the Tables XI-X, we find that the ferromagnetic phases always have a lower energy and hence the paramagnetic phase is not the ground state of these materials. The theoretically obtained magnetic moments of these four materials are in *good agreement with the experimental results*. Therefore, their magnetic ground states could be captured by the GGA+U method. Here we take $U = 3$ eV for Ru and $U = 4$ eV for Mn atom to meet the experimental results of magnetic structure. As shown in Figs. 23-26, with the on-site Hubbard U value of d or f electron in the mean field approximation is considered, the flat bands of the selected materials in the paramagnetic calculations are preserved and remain near the Fermi level. For example, in the ferromagnetic calculations of $SrRuO_3$[ICSD 69360, SG 221 ($Pm\bar{3}m$)] shown in Fig. 23 (for two different values of U and providing both the paramagnetic and the ferromagnetic band structures), the flat bands along high symmetry lines ΓX and MR at Fermi level are not settling at $E = 0$ anymore but split into two sets of flat bands near the Fermi level. Similar conclusions hold for the three other ferromagnetic materials that we have considered in this Appendix. While a high-throughput ferromagnetic calculation is out of reach, these examples provide compelling evidence that the flat bands found in the paramagnetic calculations discussed in the results section of the manuscript, will remain in the ferromagnetic calculations.

Table VIII. The total energy comparison for paramagnetic and ferromagnetic states of $SrRuO_3$[ICSD 69360, SG 221 ($Pm\bar{3}m$)]. In the FM case the magnetization points along the [001] direction of the conventional unit cell. Here, we only provide the z-component of the magnetic moment m_z in the last column. The ground atste of this material is reported to be ferromagnetic with moment 2.8 $\mu B/Ru$[72–74]. Our calculations show that the ferromagnetic (FM) state is more stable than the nonmagnetic (NM) state.

			U=0	**U=1**	**U=2**	**U=3**	**U=4**	**U=5**
Non-SOC	NM	Total energy (eV)	0	1.046	2.074	3.088	4.091	5.06
	FM	Total energy (eV)	-0.079	0.839	1.730	2.608	3.464	4.271
		Mag-mom (μB)	1.594	2.250	2.254	2.262	2.629	2.733
SOC	NM	Total energy (eV)	0.000	1.032	2.030	2.980	3.828	4.585
	FM	Total energy (eV)	-0.078	0.841	1.731	2.602	3.451	4.265
		$m_z(\mu\text{B})$	1.6077	2.118	2.231	2.244	2.259	2.808

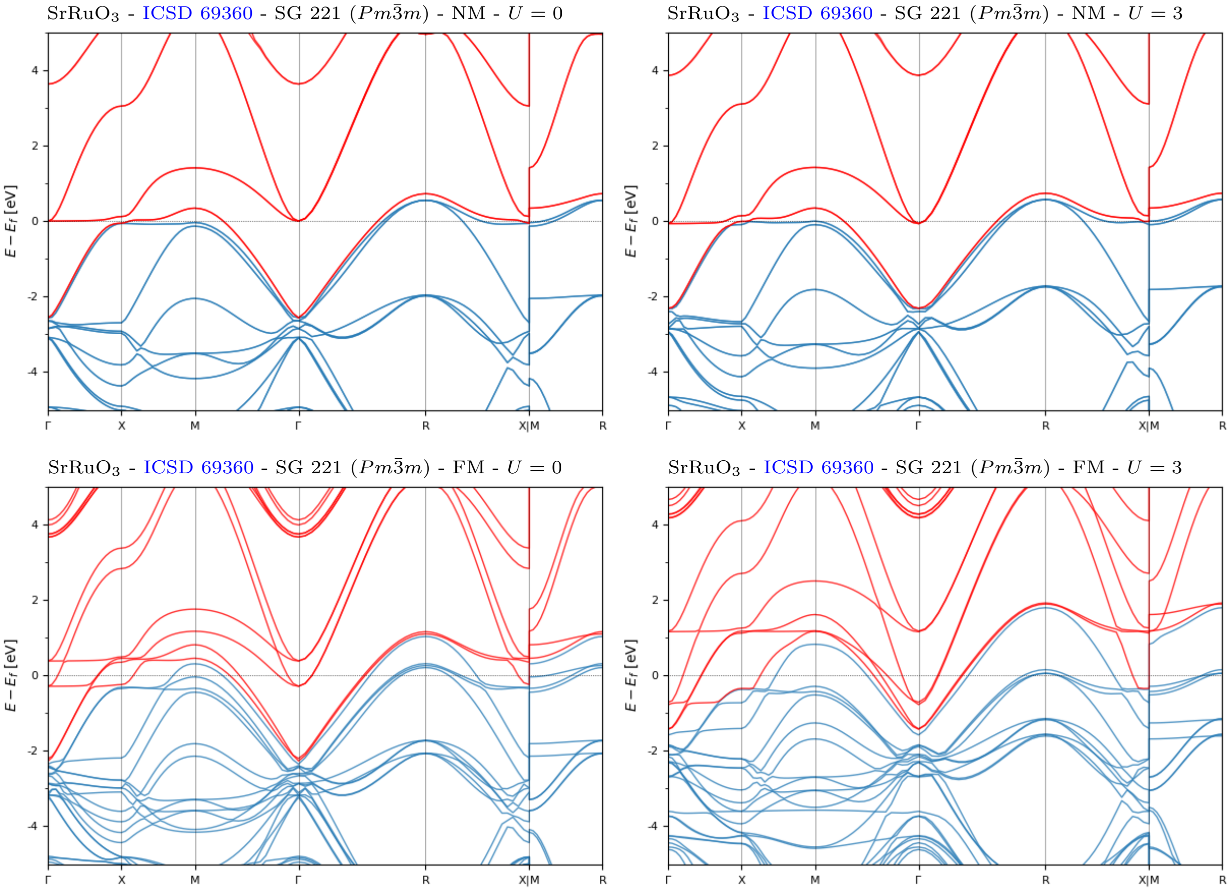
$SrRuO_3$ - ICSD 69360 - SG 221 ($Pm\bar{3}m$) - NM - $U = 0$

$SrRuO_3$ - ICSD 69360 - SG 221 ($Pm\bar{3}m$) - NM - $U = 3$

$SrRuO_3$ - ICSD 69360 - SG 221 ($Pm\bar{3}m$) - FM - $U = 0$

$SrRuO_3$ - ICSD 69360 - SG 221 ($Pm\bar{3}m$) - FM - $U = 3$

Figure 23. Band structure for $SrRuO_3$[ICSD 69360, SG 221 ($Pm\bar{3}m$)] obtained with an on-site Hubbard U value for d or f electron in the mean-field approximation and including the spin-orbit coupling. Plots in the upper panel are for paramagnetic calculations (NM) while those of the lower panel are for ferromagnetic calculations (FM). Here we have considered both $U = 0$ (left panel) and $U = 3$ (right panel).

Table IX. The total energy comparison for paramagnetic and ferromagnetic states of Rb_2MnCl_6[ICSD 9347, SG 225 ($Fm\bar{3}m$)]. In the FM case the magnetization points along the [1,1,$\bar{1}$] direction of the conventional unit cell. Here, we only provide the x-component of the magnetic moment m_x in the last column. The lattice victors of the primary unit cell are $\boldsymbol{a_1} = a\left(\begin{array}{ccc} 0 & 1/2 & 1/2 \end{array}\right)$, $\boldsymbol{a_2} = a\left(\begin{array}{ccc} 1/2 & 0 & 1/2 \end{array}\right)$ and $\boldsymbol{a_3} = a\left(\begin{array}{ccc} 1/2 & 1/2 & 0 \end{array}\right)$ with a is the lattice parameter. The total magnetic moment is 3 $\mu B/Mn$ which is in good agreement with the experimental 3.9 $\mu B/Mn$[75,76]. The results show that the ferromagnetic (FM) state is more stable than the nonmagnetic (NM) state.

			U=0	**U=1**	**U=2**	**U=3**	**U=4**	**U=5**
Non-SOC	NM	Total energy (eV)	0.000	1.219	2.433	3.641	4.841	6.031
	FM	Total energy (eV)	-1.793	-1.092	-0.419	0.224	0.833	1.407
		Mag-mom (μB)	3.000	3.000	3.000	2.999	3.000	3.000
SOC	NM	Total energy (eV)	0.000	1.051	2.040	2.983	3.845	4.519
	FM	Total energy (eV)	-1.807	-1.102	-0.425	0.222	0.837	1.417
		m_x(μB)	1.732	1.732	1.732	1.732	1.732	1.732

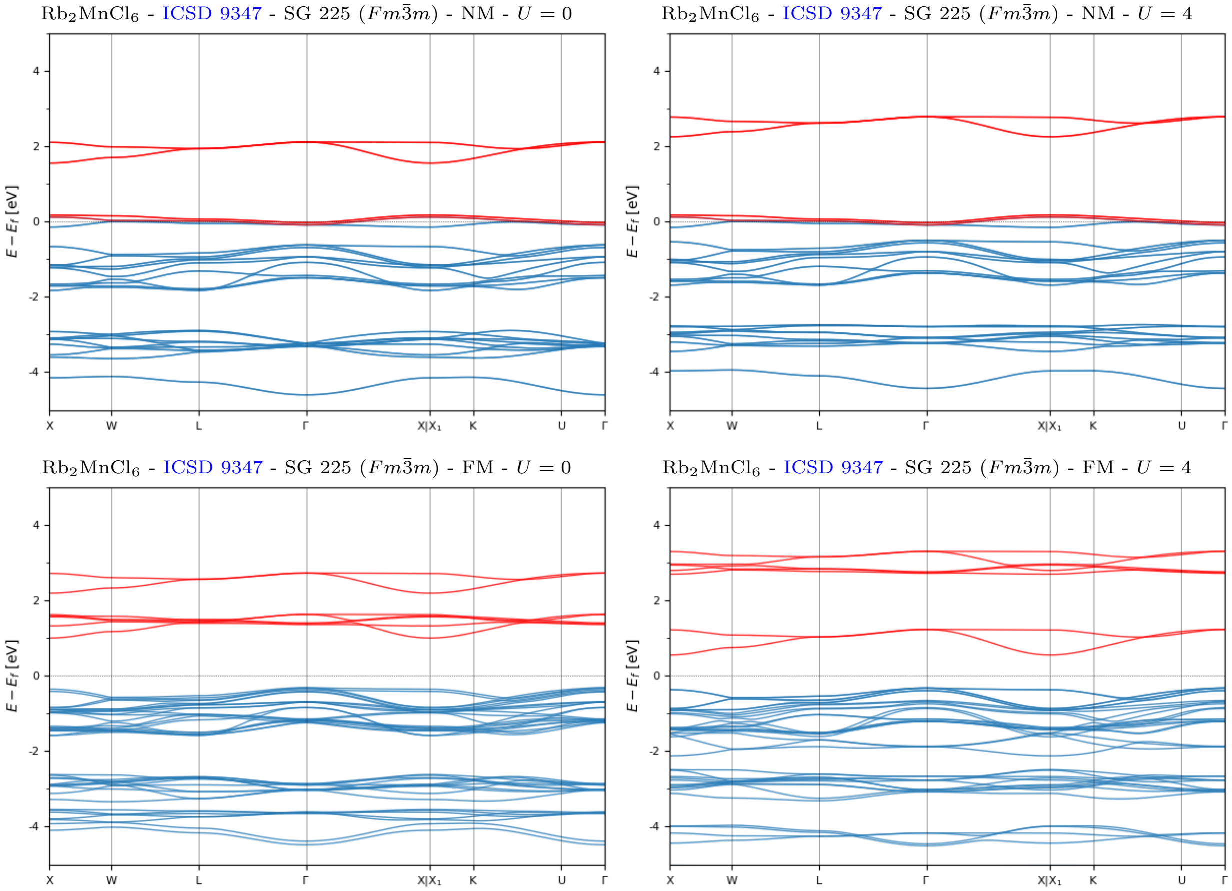

Rb_2MnCl_6 - ICSD 9347 - SG 225 ($Fm\bar{3}m$) - NM - $U = 0$

Rb_2MnCl_6 - ICSD 9347 - SG 225 ($Fm\bar{3}m$) - NM - $U = 4$

Rb_2MnCl_6 - ICSD 9347 - SG 225 ($Fm\bar{3}m$) - FM - $U = 0$

Rb_2MnCl_6 - ICSD 9347 - SG 225 ($Fm\bar{3}m$) - FM - $U = 4$

Figure 24. Band structure for Rb_2MnCl_6[ICSD 9347, SG 225 ($Fm\bar{3}m$)] obtained with an on-site Hubbard U value for d or f electron in the mean-field approximation and including the spin-orbit coupling. Plots in the upper panel are for paramagnetic calculations (NM) while those of the lower panel are for ferromagnetic calculations (FM). Here we have considered both $U = 0$ (left panel) and $U = 4$ (right panel).

Table X. The total energy comparison for paramagnetic and ferromagnetic states of Ba_2MnReO_6[ICSD 4169, SG 225 ($Fm\bar{3}m$)]. In the FM case the magnetization points along the $[1,1,\bar{1}]$ direction of the conventional cell. Here, we only give the x-component of the magnetic moment m_x in the last column. The lattice victors of the primary unit cell are $\boldsymbol{a_1} = a\begin{pmatrix} 0 & 1/2 & 1/2 \end{pmatrix}$, $\boldsymbol{a_2} = a\begin{pmatrix} 1/2 & 0 & 1/2 \end{pmatrix}$ and $\boldsymbol{a_3} = a\begin{pmatrix} 1/2 & 1/2 & 0 \end{pmatrix}$ with a is the lattice parameter. The theoretical magnetic moment is 4 $\mu B/Mn$ which is in good agreement with the experimental 3.9 $\mu B/Mn$[77]. It shows that the ferromagnetic (FM) state is more stable than the nonmagnetic (NM) state.

			U=0	**U=1**	**U=2**	**U=3**	**U=4**	**U=5**
Non-SOC	NM	Total energy (eV)	0.000	0.902	1.760	2.572	3.337	4.056
	FM	Total energy (eV)	-1.331	-0.869	-0.502	-0.201	0.053	0.278
		Mag-mom (μB)	3.124	3.506	3.8272	3.999	4.000	4.000
SOC	NM	Total energy (eV)	0.000	0.903	1.762	2.571	3.331	4.044
	FM	Total energy (eV)	-1.269	-0.804	-0.431	-0.126	0.131	0.357
		$m_x(\mu$B)	1.828	2.044	2.207	2.321	2.332	2.335

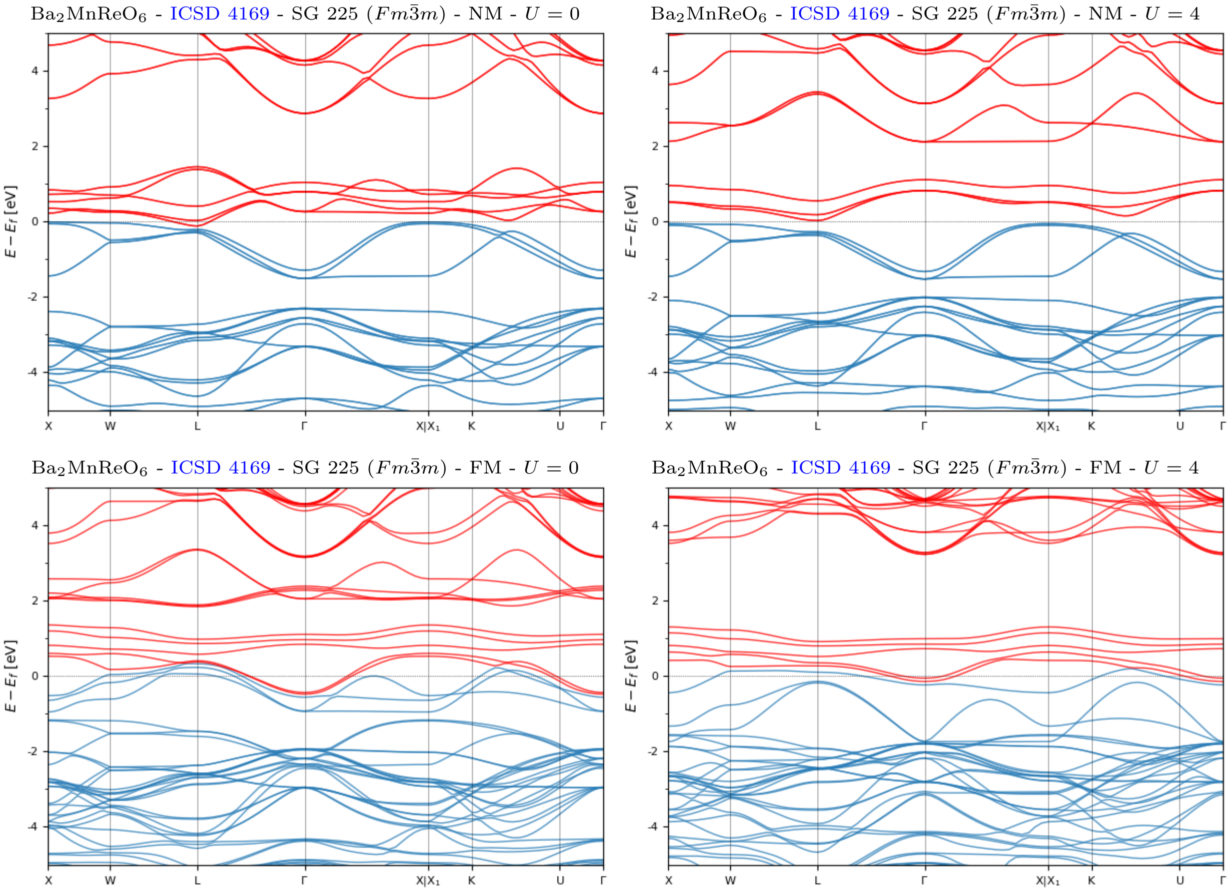

Figure 25. Band structure for Ba_2MnReO_6[ICSD 4169, SG 225 ($Fm\bar{3}m$)] obtained with an on-site Hubbard U value for d or f electron in the mean-field approximation and including the spin-orbit coupling. Plots in the upper panel are for paramagnetic calculations (NM) while those of the lower panel are for ferromagnetic calculations (FM). Here we have considered both $U = 0$ (left panel) and $U = 4$ (right panel).

Table XI. The total energy comparison for paramagnetic and ferromagnetic states of NiMnSb[ICSD 54255, SG 216 ($F\bar{4}3m$))]. In the FM case the magnetization points along the [1,1,$\bar{1}$] direction of the conventional cell. Here, we only provide the x-component of the magnetic moment m_x in the last column. The lattice victors of the primary unit cell are $\boldsymbol{a_1} = a\begin{pmatrix} 0 & 1/2 & 1/2 \end{pmatrix}$, $\boldsymbol{a_2} = a\begin{pmatrix} 1/2 & 0 & 1/2 \end{pmatrix}$ and $\boldsymbol{a_3} = a\begin{pmatrix} 1/2 & 1/2 & 0 \end{pmatrix}$ with a is the lattice parameter. The total magnetic moment is 4 $\mu B/Mn$ and is in good agreement with the experiments (4.2 $\mu B/Mn$)[78]. The results show that the ferromagnetic (FM) state is more stable than the nonmagnetic or paramagnetic (NM) state.

			U=0	**U=1**	**U=2**	**U=3**	**U=4**	**U=5**
Non-SOC	NM	Total energy (eV)	0	1.246	2.488	3.658	5.003	6.247
	FM	Total energy (eV)	-1.445	-0.842	-0.301	0.176	0.59	0.954
		Mag-mom (μB)	4.000	4.000	4.040	4.150	4.225	4.289
SOC	NM	Total energy (eV)	0	1.236	2.399	3.405	4.300	5.115
	FM	Total energy (eV)	-1.434	-0.833	-0.292	0.185	0.598	0.965
		m_x(μB)	2.309	2.310	2.335	2.396	2.441	2.481

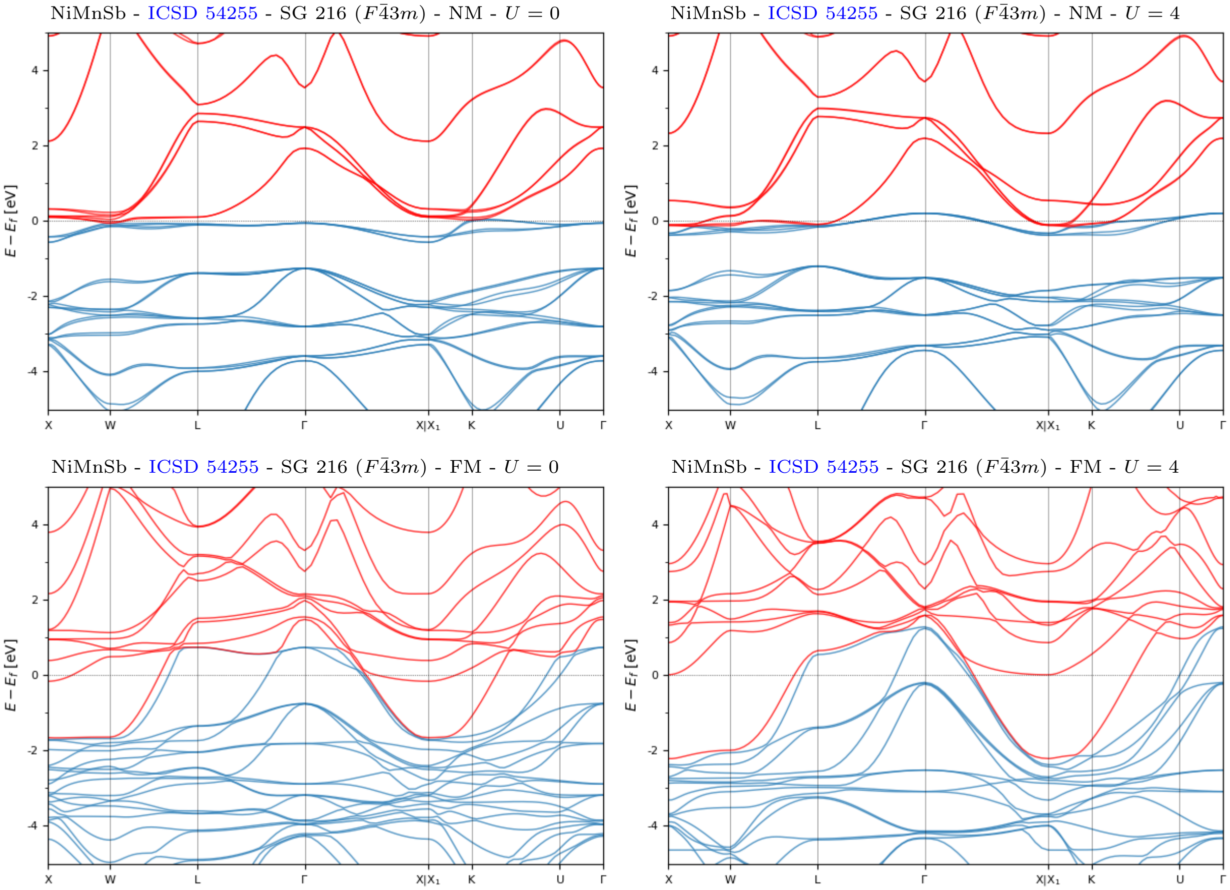
NiMnSb - ICSD 54255 - SG 216 ($F\bar{4}3m$) - NM - $U = 0$

NiMnSb - ICSD 54255 - SG 216 ($F\bar{4}3m$) - NM - $U = 4$

NiMnSb - ICSD 54255 - SG 216 ($F\bar{4}3m$) - FM - $U = 0$

NiMnSb - ICSD 54255 - SG 216 ($F\bar{4}3m$) - FM - $U = 4$

Figure 26. Band structure for NiMnSb[ICSD 54255, SG 216 ($F\bar{4}3m$)] obtained with an on-site Hubbard U value for d or f electron in the mean-field approximation and including the spin-orbit coupling. Plots in the upper panel are for paramagnetic calculations (NM) while those of the lower panel are for ferromagnetic calculations (FM). Here we have considered both $U = 0$ (left panel) and $U = 4$ (right panel).

Appendix H: Disconnected flat bands manually selected from flat-band database

In this appendix, we provide a list of curated materials with flat bands. The analysis was manually performed on the database presented in Appendix C 1. For convenience, materials with flat atomic bands are handled separately. We highlight 345 compounds hosting the most interesting flat-band features by providing their band structure and DOS.

1. List of curated materials with flat bands

We start with the list of 2,379 curated unique materials (as defined in Appendix C 1), corresponding to 6,338 ICSD entries. This list is available in Table XII. It was obtained by performing a manual search in our database, using the tools available on Materials Flatband Database website. We have applied several criteria to obtain this list:

- We required that the region of $\Delta_E = 0.5\text{eV}$ around the Fermi level (as defined in Appendix C 2 a) to host only a few bands along the high symmetry lines so that the flat bands can be easily distinguished from the dispersing bands.
- Materials with trivial flat atomic bands, of which the BRs are classified as topologically trivial (*i.e.*, LCEBR), have been excluded at this stage. The methodology to detect these materials will be detailed in Appendix H 2, including a complete list of candidates.
- We fixed the band width of the flat-band segment to be less than $\omega = 0.1\text{eV}$ (see Appendix C 2 a).
- We requested to have at least one DOS peak in the region $[-1\text{eV}, 1\text{eV}]$ around Fermi level with a Gaussian width W_{peak} smaller than 1eV (see Appendix C 2 b).

Note that for a given unique compound, we might have one ICSD fulfilling all these criteria and another ICSD not satisfying one of them. Indeed, we use sharp cutoffs and different ICSD entries of a unique compound might have slightly different band structure or DOS (as explained in Appendix C). One such example is $K_2O_7Zn_6$ [ICSD 1120, SG 102 ($P4_2nm$)] and [ICSD 2496, SG 102 ($P4_2nm$)]. The former fulfills our conditions, the latter does not. Since the differences are barely noticeable, we include all the ICSD entries of a unique compound as soon as one of them satisfies all the criteria defined above.

For each entry in Table XII, we provide the chemical formula, space group, all related ICSD numbers and possible sublattices that we have found using the procedures described in Appendices D and E. We also provide three additional attributes. First, we rely on the Materials Project[79] to give the magnetic properties (when available). Similarly, we indicate if a material is know to be superconductor based on the information from the NIMS Materials Database[80]. Finally, we tag some materials as "high quality". These materials have a structure determination including refinement (in case of powder data including Rietveld refinement), temperature factors, pressure in the range of $0.09 - 0.11\text{MPa}$, temperature within the range of $285 - 300\text{K}$ and standard deviation given for cell parameters. These are basically compounds whose crystallographic structure has been well-determined and are easy to synthesize.

Among the 2,379 curated unique materials, some of them have already been theoretically analyzed or experimentally probed in the context of flat-band materials. While we cannot pretend to be exhaustive, we list below 11 such materials, their related references and the main features of their studies.

- RuO_2 [ICSD 172178, SG 136 ($P4_2/mnm$)] was studied by angle-resolved photoemission spectroscopy (ARPES) experiments in Ref.[81] and was reported to host topologically trivial flat-band surface state.
- The electronic structure properties of Y_2Ni_7 [ICSD 647060, SG 166 ($R\bar{3}m$)] have been theoretically studied in Ref.[82], pointing toward the presence the flat bands to explain the magnetic properties of these materials.
- $AlFe_2B_2$ [ICSD 241907, SG 65 ($Cmmm$)] is a layered ferromagnet studied by ARPES in Ref.[83] and have been shown to host flat bands near the Fermi energy.
- Flat bands near the Fermi level have been observed in ARPES for $CaCu_3Ru_4O_{12}$ [ICSD 95715, SG 204 ($Im\bar{3}$)] in Ref.[84].
- In Ref.[85], a scanning tunneling microscopy (STM) experiment was performed on the ferromagnetic $Co_3Sn_2S_2$ [ICSD 624867, SG 166 ($R\bar{3}m$)]. A pronounced conductance peak near the Fermi level was observed and identified as arising from the flat bands. In Ref.[86], the flat bands of ferromagnetic $Co_3Sn_2S_2$ were also associated to a sharp peak in the optical conductivity measurement.

- Topological flat bands in the vicinity of the Fermi level in CoSn [ICSD 161118, SG 191 ($P6/mmm$)] were studied theoretically and observed in the ARPES experiments in Ref.[87,88]. The tuning of the flat bands in doped CoSn was also reported experimentally in Ref.[89].
- The material MgV_2O_4 [ICSD 674693, SG 216 ($F\bar{4}3m$)] in its ferromagnetic phase was predicted by first-principles calculations in Ref.[90] to host a three-dimensional flat band near the Fermi energy.
- $Pd_3P_2S_8$ [ICSD 16296, SG 164 ($P\bar{3}m1$)] with a Kagome van-der-Waals structure was experimentally studied in Ref.[91] where the magnetic measurements were explained by the flat bands predicted in the first-principles calculations.
- Pd_3Pb [ICSD 42600, SG 221 ($Pm\bar{3}m$)] was studied theoretically in Ref.[92] and experimentally by Shubnikov–de Haas oscillations in Ref.[93], pointing toward a flat-band semimetal.
- A minimal microscopic model within a large-S expansion based was built for Sr_2FeMoO_6 [ICSD 181752, SG 225 ($Fm\bar{3}m$)] in Ref.[94], leading to the spin-polarized flat bands and four massive or massless Dirac dispersions.
- YCr_6Ge_6 [ICSD 658018, SG 191 ($P6/mmm$)] has been probed by ARPES in Ref.[95] to unveil planar flat bands associated to the Kagome sublattice.

Table XII: Manually curated list of materials with flat bands. We provide in this table the list of the 2,379 entries of curately chosen flat-band materials, indexed by the first column. The second column gives the chemical formula, the third column the space group symbol (and number in parentheses). The fourth column indicates the topological classification at the Fermi level: topological insulator (TI), topological semi-metal (SM) or trivial insulator (Triv.). The fifth column indicates if the material also belongs to the list of best materials given in Appendix H 3 and the figure displaying its band structure and DOS. The sixth column details the sublattices found for each material and common to every ICSD entries of this material. Here ’k’ stands for Kagome, ’p’ for pyrochlore, ’b’ for bipartite, ’s’ for split lattice and ’l’ for Lieb sublattice. A star superscript after ’k’ (’l’) indicate that only approximate Kagome (Lieb) sublattices were found (as defined in Appendix D). The seventh column gives the magnetic properties as obtained from Materials Project (NM for non-magnetic, FM for ferromagnetic, AFM for anti-ferromagnetic, FiM for ferrimagnetic, ’—’ when the information is not available). The eighth column indicates if the material is known to be superconductor according to the NIMS Materials Database. ’SC’ stands for superconductor while ’SC*’ means that alloys based on this material are superconductor. The ninth column tells which material are ”high-quality” as defined in Appendix H 1. The last column gives all the ICSD entries related to each material. If a given ICSD has additional sublattices compared to those common to all ICSD entries, a superscript label provides the list of these additional sublattices.

Num.	chem. formula	space group	Topo. at E_f	best	sublat.	magn.	super-conduct.	high quality	ICSDs
1	Al_2O_3	$P1$ (1)	Triv.	—	—	NM	—	HQ	173014
2	$AgBrO_2$	$P1$ (1)	Triv.	Fig. 28	—	—	—	—	670051
3	$LiNa_5N_2$	$P1$ (1)	Triv.	—	—	—	—	—	92316
4	$AgHO_2$	$P1$ (1)	Triv.	Fig. 28	—	—	—	—	670060
5	$CaNi_5H$	$P1$ (1)	SM	—	—	FM	—	—	189752$^{(k)}$ 189753
6	$Na_4Sn_2Ge_4O_{12}(OH)_4$	$P\bar{1}$ (2)	Triv.	—	—	NM	—	—	15017
7	$NaI(H_2O)_2$	$P\bar{1}$ (2)	Triv.	—	—	NM	—	—	23134
8	$(S_2N_3)VCl_2$	$P\bar{1}$ (2)	Triv.	—	(b)	NM	—	HQ	30742 61351
9	$Cu(SeO_4)(H_2O)$	$P\bar{1}$ (2)	TI	—	—	FM	—	HQ	39887
10	$Na_6Li_2(W_2O_{10})$	$P\bar{1}$ (2)	Triv.	—	(b)	NM	—	HQ	49027
11	$K_2Cu_3(SeO_3)_4$	$P\bar{1}$ (2)	SM	—	(b,s)	FM	—	HQ	50541
12	$Cu(F(AuF_4))$	$P\bar{1}$ (2)	SM	Fig. 28	(b,s)	FM	—	—	62544
13	$K_3Cu_2((P_2O_7)H(P_2O_7))$	$P\bar{1}$ (2)	TI	—	(b)	FM	—	HQ	62742
14	$((NO)(HF_2))(IF_5)$	$P\bar{1}$ (2)	Triv.	—	—	—	—	—	71582
15	$Cu_3Bi_4V_2O_{14}$	$P\bar{1}$ (2)	SM	Fig. 28	(b,s)	FM	—	HQ	75222
16	$Ca(SnF_3)_2$	$P\bar{1}$ (2)	Triv.	—	(b)	NM	—	HQ	92907
17	$K_2Cu(Fe(CN)_6)$	$P\bar{1}$ (2)	SM	—	—	FM	—	HQ	99499
18	$Na_2(Cu_2Si_4O_{11})(H_2O)_2$	$P\bar{1}$ (2)	Triv.	Fig. 28	(b,s)	FM	—	HQ	154123 414048
19	$(CH_3)_2SeO$	$P\bar{1}$ (2)	Triv.	—	—	NM	—	HQ	171011
20	$Cd(HCO(NH_2))_2I_2$	$P\bar{1}$ (2)	Triv.	—	—	NM	—	HQ	192774
21	$RbSbBrF_3$	$P\bar{1}$ (2)	Triv.	—	—	NM	—	—	200109
22	$Na_2Cu_2(Si_4O_{11})$	$P\bar{1}$ (2)	Triv.	—	(b,s)	FM	—	HQ	240930
23	$Ti_2P_2O_9$	$P\bar{1}$ (2)	Triv.	—	(b)	—	—	—	243672
24	$Pb_2(HgO_2)(CrO_4)$	$P\bar{1}$ (2)	Triv.	—	(b)	NM	—	HQ	280778
25	$Rb(VO_2(IO_3)_2)$	$P\bar{1}$ (2)	Triv.	—	—	NM	—	HQ	281304
26	$K_2Cu_3(Ge_5O_{14})$	$P\bar{1}$ (2)	SM	—	(b)	FM	—	HQ	410828

27	$(Hg_2)((H_4TeO_6)(H_6TeO_6))(H_2O)_2$	$P\bar{1}$ (2)	Triv.	—	—	NM	—	—	412799
28	W_2NCl_8	$P\bar{1}$ (2)	SM	—	(b,s)	FM	—	HQ	415768
29	$Na_2(SO_4)(BF_3)$	$P\bar{1}$ (2)	Triv.	—	—	NM	—	HQ	424150
30	$SrHg(As_2O_7)$	$P\bar{1}$ (2)	Triv.	—	(b)	NM	—	—	430291
31	$BaHg(As_2O_7)$	$P\bar{1}$ (2)	Triv.	—	(b)	NM	—	—	430292
32	Nb_2Se_9	$P\bar{1}$ (2)	Triv.	—	—	NM	—	—	645386 8179 62538
33	$NaAlSi_3O_8$	$P\bar{1}$ (2)	Triv.	—	(b,s)	—	—	—	670020 34870 34871 34872 68913 77421 77422 77423 77424 77425 109006 171090 171091 171092
34	$Ag(SbF_6)_2$	$P\bar{1}$ (2)	SM	—	(b,s)	FM	—	—	65186
35	$Al(OH)_3$	$P\bar{1}$ (2)	Triv.	—	—	NM	—	—	164050 164049
36	$BaCu(P_2O_7)$	$P\bar{1}$ (2)	TI	—	(b)	FM	—	HQ	66534
37	$BaCu(P_2O_7)$	$P\bar{1}$ (2)	TI	—	(b)	—	—	HQ	192060
38	$Bi_2Pb_2V_2O_{10}$	$P\bar{1}$ (2)	Triv.	—	(b)	NM	—	HQ	56791
39	$PbBiO(VO_4)$	$P\bar{1}$ (2)	Triv.	—	(b)	NM	—	—	419126 419121
40	$CaCl_2(H_2O)_4$	$P\bar{1}$ (2)	Triv.	—	—	NM	—	—	8061
41	$Ca(Ge_2O_5)$	$P\bar{1}$ (2)	Triv.	—	(b,s)	NM	—	—	14005 151568 151569 151570 151571 151572 151573 151574 151575 151576 151577 151586
42	$(Zn(H_2O)_6)(SnF_3)_2$	$P\bar{1}$ (2)	Triv.	—	—	—	—	HQ	166589
43	$Mg_2B_2O_5$	$P\bar{1}$ (2)	Triv.	—	(b)	NM	—	—	24789 79721
44	$Cs_2(Sn_2S_4(S_2))$	$P\bar{1}$ (2)	Triv.	—	—	NM	—	HQ	73008
45	$V_2Te_2O_7F_2$	$P\bar{1}$ (2)	Triv.	—	(b)	FM	—	HQ	173748
46	$Na_2Pd(SeO_4)_2$	$P\bar{1}$ (2)	Triv.	—	(b)	NM	—	HQ	249506
47	$Ag(PdF_6)$	$P\bar{1}$ (2)	TI	—	(b,s)	FM	—	HQ	51507
48	$K_2Co(SeO_4)_2(H_2O)_2$	$P\bar{1}$ (2)	SM	—	—	AFM	—	HQ	98686
49	$Na(BSi_3O_8)$	$P\bar{1}$ (2)	Triv.	—	(b,s)	NM	—	—	16907
50	$PbBiO(PO_4)$	$P\bar{1}$ (2)	Triv.	—	—	NM	—	HQ	419125
51	$LiFe(SO_4)F$	$P\bar{1}$ (2)	Triv.	—	(b)	AFM	—	—	180389 182944 194597
52	$InAsO_4(H_2O)$	$P\bar{1}$ (2)	Triv.	—	—	NM	—	HQ	170760
53	$Al_{11}Mn_4$	$P\bar{1}$ (2)	SM	—	—	FM	—	—	10509 57975
54	$Na_2Cu(C_2O_4)_2(H_2O)_2$	$P\bar{1}$ (2)	SM	—	—	FM	—	HQ	40090
55	$Sc(PS_4)$	$P\bar{1}$ (2)	Triv.	—	(b)	NM	—	HQ	67559
56	Au_4Cl_8	$P\bar{1}$ (2)	Triv.	—	—	NM	—	HQ	201436
57	$NaYP_2S_6$	$P\bar{1}$ (2)	Triv.	—	—	—	—	—	431533
58	$NaZnP_2O_6OH$	$P\bar{1}$ (2)	Triv.	—	—	NM	—	HQ	39491
59	$PbPt_2O_4$	$P\bar{1}$ (2)	TI	—	(k*,b)	NM	—	HQ	59657 82204
60	Sr_2MgMoO_6	$P\bar{1}$ (2)	Triv.	—	(b,s)	—	—	HQ	173119
61	$Sr(OH)Cl(H_2O)_4$	$P\bar{1}$ (2)	Triv.	—	—	NM	—	—	71446
62	$YBr(MoO_4)$	$P\bar{1}$ (2)	Triv.	—	(b)	—	—	—	242056
63	$YBr(WO_4)$	$P\bar{1}$ (2)	Triv.	—	(b)	NM	—	HQ	428802
64	As_2O_3	$P2$ (3)	Triv.	—	—	—	—	HQ	238656 238657 238658 238659 238660 238661
65	$Na_2(ZnSi_3O_8)$	$P2_1$ (4)	Triv.	—	(b,s)	NM	—	HQ	924 20114 200440
66	$CaCuO_2$	$P2_1$ (4)	Triv.	—	(b,s)	NM	—	—	84868
67	$BaCu_2Cl_2(Te_2O_6)$	$P2_1$ (4)	Triv.	—	(b)	FM	—	HQ	85786
68	$PbCu_2(TeO_3)_2Cl_2$	$P2_1$ (4)	Triv.	—	(b)	FM	—	HQ	189155
69	$SrCu_2(TeO_3)_2Cl_2$	$P2_1$ (4)	Triv.	—	(b)	FM	—	HQ	416653
70	$Cu(IO_3)_2$	$P2_1$ (4)	SM	—	(b,s)	FM	—	HQ	4327
71	$LiIn(P_2O_7)$	$P2_1$ (4)	Triv.	—	(b)	NM	—	HQ	60935
72	$LiSc(P_2O_7)$	$P2_1$ (4)	Triv.	—	(b)	NM	—	HQ	91496
73	$Na(BSi_2O_5)(OH)_2$	$P2_1$ (4)	Triv.	—	—	NM	—	HQ	12134
74	Te_2O_5	$P2_1$ (4)	Triv.	—	(b,s)	NM	—	—	2523 191342
75	$NbOI_2$	$C2$ (5)	Triv.	Fig. 28	(b,s)	NM	—	HQ	36255
76	$NbOBr_2$	$C2$ (5)	Triv.	Fig. 28	(b,s)	NM	—	HQ	416669
77	$Pb_3(VO_4)_2$	$C2$ (5)	Triv.	—	—	NM	—	HQ	29359 67604$^{(b)}$ 67605$^{(b)}$ 69800$^{(b)}$
78	$Sr_4Zn_3F_{14}$	Cm (8)	Triv.	—	(k*,b)	—	—	HQ	72991
79	Ca_2CoO_3	Cm (8)	SM	—	—	FM	—	HQ	95439
80	$SbTaON_2$	Cm (8)	Triv.	—	(b,s)	—	—	—	674163
81	$SbNbN_2O$	Cm (8)	Triv.	—	(b,s)	—	—	—	674153
82	$TeGeN_2O$	Cm (8)	Triv.	—	(b,s)	—	—	—	674160
83	$Cd_2O(OH)_2(H_2O)$	Cm (8)	Triv.	—	—	NM	—	HQ	40185 40186

84	$Na_4(CO_4)$	Cm (8)	Triv.	—	—	NM	—	—	245413 245414 245410$^{(b)}$
85	$K_4(CO_4)$	Cm (8)	Triv.	—	—	NM	—	—	245424 245426 245421
86	SiO_2	Cc (9)	Triv.	—	(b,s)	NM	—	—	75662 81381 413210
87	$Ba_2WO_3F_4$	Cc (9)	Triv.	—	—	NM	—	HQ	201653 33271 673319
88	$KSbB_2O_6$	Cc (9)	Triv.	—	(b)	NM	—	HQ	238073
89	$Cs_2CuP_2O_7$	Cc (9)	SM	—	(b)	FM	—	—	430123
90	$LiVO_3$	Cc (9)	Triv.	—	—	—	—	HQ	23477
91	$TiZrSe_4$	$P2/m$ (10)	TI	—	(b)	NM	—	—	104188
92	$CrAuTe_4$	$P2/m$ (10)	SM	Fig. 29	—	FM	—	HQ	150279
93	$Cu(IO_3)_2$	$P2_1/m$ (11)	SM	—	(b)	FM	—	HQ	2232
94	Ca_3VN_3	$P2_1/m$ (11)	Triv.	—	(b)	NM	—	—	41060
95	$CuWO_3F_2$	$P2_1/m$ (11)	SM	—	(b,s)	FM	—	HQ	60759
96	$K(VO)H(SeO_3)_2$	$P2_1/m$ (11)	SM	—	(b)	FM	—	HQ	82535
97	$(NH_4)(H(VO)(SeO_3)_2)$	$P2_1/m$ (11)	SM	—	—	FM	—	—	97400
98	$PbPdSi(P_2O_7)_2$	$P2_1/m$ (11)	Triv.	—	(b,s)	NM	—	—	195306 420535
99	$Na_3Ni(PO_4)(CO_3)$	$P2_1/m$ (11)	Triv.	—	(b)	AFM	—	HQ	237798
100	$K_3(Ru(P_2Se_6)(P_3Se_4))$	$P2_1/m$ (11)	Triv.	—	—	NM	—	—	406200
101	$(NO)Cu(NO_3)_3$	$P2_1/m$ (11)	SM	—	—	—	—	HQ	422033
102	$Cu_3GeP_2O_{10}$	$P2_1/m$ (11)	SM	—	(b)	FM	—	—	426627
103	As_4S_5	$P2_1/m$ (11)	Triv.	—	—	NM	—	HQ	16107 98901
104	$Ba_2(Zn_2F_7Cl)$	$P2_1/m$ (11)	Triv.	—	(b,s)	NM	—	HQ	79478
105	$Ba_2(Co_2F_7Cl)$	$P2_1/m$ (11)	Triv.	Fig. 29	(b,s)	FM	—	HQ	79479
106	$Ba_2Ni_2F_7Cl$	$P2_1/m$ (11)	Triv.	Fig. 29	(b,s)	FM	—	HQ	84782
107	$CuZnCl(OH)_3$	$P2_1/m$ (11)	SM	—	(b)	FM	—	—	252429
108	$Cu_2Sc_2(Ge_4O_{13})$	$P2_1/m$ (11)	Triv.	—	(b)	FM	—	—	99599 99600 99601 99602 99603
109	$Y_3(VO_5)(OH)_3$	$P2_1/m$ (11)	SM	—	—	FM	—	HQ	262400
110	$La_3(VO_5)(OH)_3$	$P2_1/m$ (11)	SM	—	—	AFM	—	HQ	262402
111	$Na_3In(PO_4)_2$	$P2_1/m$ (11)	Triv.	—	(b)	NM	—	HQ	87833 90941
112	$PbSO_4(PbO)_2$	$P2_1/m$ (11)	Triv.	—	—	NM	—	—	30711 61427$^{(b)}$ 61428$^{(b)}$ 63639$^{(b)}$ 100681$^{(b)}$
113	$TlCu(OH)SO_4$	$P2_1/m$ (11)	SM	—	(b)	FM	—	HQ	36581
114	$La_3Os_2O_{10}$	$C2/m$ (12)	SM	—	—	FM	—	HQ	10104
115	MoV_2O_8	$C2/m$ (12)	TI	Fig. 29	(b)	NM	—	—	28471
116	LiH_2PO_2	$C2/m$ (12)	Triv.	—	—	NM	—	HQ	59823 250176
117	$Sr_7Re_4O_{19}$	$C2/m$ (12)	Triv.	—	(b,s)	FM	—	HQ	93804
118	(Sr_2CoO_3)	$C2/m$ (12)	SM	Fig. 29	—	FM	—	—	99894
119	Cr_3O_8	$C2/m$ (12)	TI	Fig. 29	(b)	FM	—	—	155847
120	Cr_3O_8	$C2/m$ (12)	Triv.	—	—	FM	—	—	155848
121	$LiH_3As_2O_7$	$C2/m$ (12)	Triv.	—	—	NM	—	HQ	172988
122	$MgBr_2(H_2O)_6$	$C2/m$ (12)	Triv.	—	—	NM	—	HQ	189844
123	Br_6Si_2	$C2/m$ (12)	Triv.	—	—	NM	—	—	239354
124	Br_4Nb	$C2/m$ (12)	Triv.	—	(b,s)	NM	—	—	239640
125	Li_2CrCl_4	$C2/m$ (12)	Triv.	—	(b)	FM	—	HQ	403035
126	$BaAu_2(SO_4)_4$	$C2/m$ (12)	Triv.	—	(b)	NM	—	HQ	427677
127	$ReSCl_3$	$C2/m$ (12)	Triv.	—	(b,s)	—	—	—	429458
128	Li_4N_1	$C2/m$ (12)	Triv.	—	—	—	—	—	675129
129	$AgPdZr_2F_{11}$	$C2/m$ (12)	Triv.	—	—	FM	—	HQ	65181
130	$NaPd(Zr_2F_{11})$	$C2/m$ (12)	Triv.	—	—	FM	—	HQ	77241
131	$NaCo(Zr_2F_{11})$	$C2/m$ (12)	SM	—	—	FM	—	HQ	81221
132	$NaNi(Zr_2F_{11})$	$C2/m$ (12)	Triv.	—	—	FM	—	HQ	81222
133	$NaZn(Zr_2F_{11})$	$C2/m$ (12)	Triv.	—	—	NM	—	HQ	81223
134	CaC_2	$C2/m$ (12)	Triv.	—	—	NM	—	HQ	54185 54188 94385 252719 252725 252728 252731 252740 252743 252746 252749 252752 252755 252758 252761 252764 252767 252770 252773 252776 290833 411190 672970
135	$Mg(CrO_4)$	$C2/m$ (12)	Triv.	—	(b)	NM	—	—	18120
136	$Ag_3In(PO_4)_2$	$C2/m$ (12)	Triv.	—	(b)	NM	—	HQ	245001
137	Ga_2O_3	$C2/m$ (12)	Triv.	—	(b)	NM	—	HQ	34243 83645 166198 184327 603563 673058
138	Al_2O_3	$C2/m$ (12)	Triv.	—	(b)	NM	—	HQ	82504 673079
139	$La_6I_5Ge_3$	$C2/m$ (12)	SM	—	(b)	—	—	HQ	414175

140	$\mathrm{YCl(MoO_4)}$	$C2/m$ (12)	Triv.	—	(b)	NM	—	HQ	249647
141	$\mathrm{K_2Na(Ag(CN)_2)_3}$	$C2/m$ (12)	Triv.	Fig. 29	(k*,b)	NM	—	HQ	59723 59724 59725 59726
142	$\mathrm{Pb_2O(SO_4)}$	$C2/m$ (12)	Triv.	—	—	NM	—	HQ	14246$^{(b,s)}$ 29268$^{(b,s)}$ 30627 35757
143	$\mathrm{Pb_2O(WO_4)}$	$C2/m$ (12)	Triv.	—	—	NM	—	—	61399
144	$\mathrm{Pb_2Co(WO_6)}$	$C2/m$ (12)	SM	—	(b,s)	AFM	—	HQ	77912
145	$\mathrm{TlFeS_2}$	$C2/m$ (12)	Triv.	—	—	NM	—	—	30011 63381
146	$\mathrm{TlFeS_2}$	$C2/m$ (12)	TI	—	—	NM	—	—	600815 659748
147	$\mathrm{Ba_3Y_2PtCu_2O_{10}}$	$C2/m$ (12)	TI	—	(b,s)	NM	—	HQ	62390
148	$\mathrm{Y_2Ba_3Cu_2PtO_{10}}$	$C2/m$ (12)	TI	—	(b,s)	NM	—	HQ	65614
149	$\mathrm{Y_5Mo_2O_{12}}$	$C2/m$ (12)	SM	Fig. 29	(b)	FM	—	HQ	60957 62215
150	$\mathrm{K(H_2PO_4)}$	$P2/c$ (13)	Triv.	Fig. 30	—	NM	—	HQ	79341
151	$\mathrm{RbLi_2Ga_2(BO_3)_3}$	$P2/c$ (13)	Triv.	—	(b)	NM	—	HQ	280205
152	$\mathrm{Na(CN)(H_2O)_2}$	$P2_1/c$ (14)	Triv.	—	—	NM	—	—	830 2244 16765
153	$\mathrm{Li(NH_4)(PO_3F)}$	$P2_1/c$ (14)	Triv.	—	—	NM	—	—	1439
154	$\mathrm{Li_2(SO_4)}$	$P2_1/c$ (14)	Triv.	—	(b)	NM	—	HQ	2512 58 23723 30276
155	$\mathrm{B_2F_4}$	$P2_1/c$ (14)	Triv.	—	—	NM	—	—	27867
156	$\mathrm{WO_3}$	$P2_1/c$ (14)	Triv.	—	(b)	NM	—	—	31823$^{(s)}$ 190632 647640$^{(s)}$ 673316$^{(s)}$ 84848$^{(s)}$ 190631$^{(s)}$ 14332$^{(s)}$ 16080 17003$^{(s)}$ 50727 80056$^{(s)}$ 80057 190630$^{(s)}$
157	$\mathrm{Cs(HSO_4)}$	$P2_1/c$ (14)	Triv.	—	—	NM	—	HQ	67108 39252 91808 291375 291374
158	$\mathrm{Mo(As_2O_7)}$	$P2_1/c$ (14)	Triv.	—	(b,s)	NM	—	—	72518
159	$\mathrm{Cu(HSeO_3)_2(H_2O)_2}$	$P2_1/c$ (14)	SM	—	—	FM	—	—	80932
160	$\mathrm{Cd(MoO_2)(PO_4)}$	$P2_1/c$ (14)	Triv.	—	(b)	FM	—	—	82090
161	$\mathrm{(HCONH_2)_2(Cu(HCOO)_2)}$	$P2_1/c$ (14)	SM	—	—	FM	—	—	109973 194113
162	$\mathrm{Pb_2Cu(BO_3)_2}$	$P2_1/c$ (14)	SM	—	(b)	FM	—	HQ	155317
163	$\mathrm{Mg(SiO_3)}$	$P2_1/c$ (14)	Triv.	—	—	NM	—	—	159550 15805$^{(b,s)}$ 24270$^{(b)}$ 30893$^{(b)}$ 30895$^{(b)}$ 34163$^{(b)}$ 92750$^{(b)}$ 159551$^{(b)}$ 159552$^{(b)}$ 159553$^{(b)}$ 180445$^{(b)}$ 196432$^{(b)}$ 201535$^{(b)}$
164	$\mathrm{Sn_2(P_2O_7)}$	$P2_1/c$ (14)	Triv.	—	—	NM	—	HQ	170847
165	$\mathrm{K_2(SeMoO_6)}$	$P2_1/c$ (14)	Triv.	—	—	NM	—	—	412999
166	$\mathrm{OsOF_4}$	$P2_1/c$ (14)	Triv.	—	—	NM	—	HQ	417246
167	$\mathrm{KAgAsS_2}$	$P2_1/c$ (14)	Triv.	Fig. 30	—	—	—	—	431760
168	$\mathrm{Na_2TeO_3}$	$P2_1/c$ (14)	Triv.	—	—	NM	—	—	100693
169	ScOF	$P2_1/c$ (14)	Triv.	—	(b)	NM	—	HQ	24112 100562 100563 100564
170	$\mathrm{Ca_2(SiO_4)}$	$P2_1/c$ (14)	Triv.	—	—	NM	—	HQ	963$^{(b)}$ 16616$^{(b)}$ 24640 79550 79551 79552 79553$^{(b)}$ 79554 79555$^{(b)}$ 81096$^{(b)}$ 196150$^{(b)}$ 245074$^{(b)}$ 245075$^{(b)}$ 245076$^{(b)}$ 245077$^{(b)}$ 245078$^{(b)}$ 245079$^{(b)}$ 245080$^{(b)}$ 421708$^{(b)}$ 280995$^{(b)}$
171	$\mathrm{Cu(HSeO_3)_2}$	$P2_1/c$ (14)	SM	—	—	FM	—	HQ	29538 51676$^{(b)}$
172	$\mathrm{Cu(OH)Cl}$	$P2_1/c$ (14)	TI	—	—	FM	—	HQ	38384
173	$\mathrm{Cu(OH)Cl}$	$P2_1/c$ (14)	TI	—	—	FM	—	HQ	91088
174	$\mathrm{Cs_2(As_2F_8O_2)}$	$P2_1/c$ (14)	Triv.	—	—	NM	—	HQ	6070
175	$\mathrm{K_2(W_2O_7)}$	$P2_1/c$ (14)	Triv.	—	(b,s)	NM	—	HQ	67284
176	$\mathrm{KCuCl_3}$	$P2_1/c$ (14)	Triv.	—	—	FM	—	HQ	15590 109325 252663
177	$\mathrm{Cu(AlAsO_5)}$	$P2_1/c$ (14)	Triv.	—	(b)	NM	—	—	91551
178	$\mathrm{VO_2}$	$P2_1/c$ (14)	Triv.	—	(b)	FM	—	—	15889 34033 74705 602360 647604 647610
179	$\mathrm{Na_2(Ni(H_2O)_2)(V_2O_4F_6)}$	$P2_1/c$ (14)	Triv.	—	—	FM	—	—	424345
180	$\mathrm{Na_2(PdF_4)}$	$P2_1/c$ (14)	Triv.	—	(b)	NM	—	HQ	33889 71101
181	$\mathrm{CuSb_2O_6}$	$P2_1/c$ (14)	SM	—	(b)	FM	—	—	30410 71762 80576 628623$^{(s)}$
182	$\mathrm{Y(NiO_3)}$	$P2_1/c$ (14)	Triv.	—	(b)	FM	—	HQ	88043 89417 92047 191790
183	$\mathrm{K_2(Pt(CN)_4I_2)}$	$P2_1/c$ (14)	Triv.	—	—	NM	—	HQ	413706
184	$\mathrm{Rb_2(Pt(CN)_4I_2)}$	$P2_1/c$ (14)	Triv.	—	—	NM	—	HQ	421673
185	$\mathrm{XeF_4}$	$P2_1/c$ (14)	Triv.	—	—	NM	—	HQ	26626 27467
186	$\mathrm{VF_4}$	$P2_1/c$ (14)	SM	—	(b,s)	FM	—	—	65785
187	$\mathrm{Ag(AuF_4)_2}$	$P2_1/c$ (14)	SM	—	(b,s)	FM	—	HQ	85416
188	$\mathrm{Na_4Sn_3F_{10}}$	$C2/c$ (15)	Triv.	—	(b)	NM	—	—	9891
189	$\mathrm{V_2O_4(H_2O)_2}$	$C2/c$ (15)	SM	—	—	FM	—	—	16727

190	$V(S_2)_2$	$C2/c$ (15)	Triv.	—	—	NM	—	—	16797 64770 428285
191	$Na_2(Nb_4O_{11})$	$C2/c$ (15)	Triv.	—	(b)	—	—	—	18305
192	$Li_2Cu(P_2O_7)$	$C2/c$ (15)	SM	—	(b)	FM	—	HQ	72485 160321
193	$((CH_3)_2NH_2)(Cu(HCOO)_3)$	$C2/c$ (15)	SM	—	—	FM	—	—	110500 151227
194	$PbPd_2O_4$	$C2/c$ (15)	Triv.	Fig. 30	(b)	NM	—	HQ	263050
195	$K(Cl_3(MoOCl_2)_2)$	$C2/c$ (15)	Triv.	—	(b)	FM	—	HQ	410954
196	Ag_4CuTeO_6	$C2/c$ (15)	SM	—	(b)	FM	—	HQ	416931
197	$(NH_4)_2(MoO_2S_2)$	$C2/c$ (15)	Triv.	—	—	NM	—	HQ	41688 423990
198	$BaCu(SeO_3)_2$	$C2/c$ (15)	SM	—	(b,s)	FM	—	HQ	202388
199	$SrCu(SeO_3)_2$	$C2/c$ (15)	SM	—	(b,s)	FM	—	HQ	202389
200	$Cs_2MoO_2S_2$	$C2/c$ (15)	Triv.	—	—	NM	—	HQ	423982 423983
201	$Rb_2MoO_2S_2$	$C2/c$ (15)	Triv.	—	—	NM	—	HQ	423992
202	$Cs(Sb_2F_7)$	$C2/c$ (15)	Triv.	—	—	NM	—	—	14119 24741
203	$Cu(H_2PO_2)_2(CO(NH_2)_2)$	$C2/c$ (15)	SM	—	—	FM	—	—	279589(b) 279590 279591
204	$Cu_2(P_4O_{12})$	$C2/c$ (15)	TI	—	(b)	FM	—	—	23756
205	$(N_2H_5)(BF_4)$	$C2/c$ (15)	Triv.	—	—	NM	—	—	9895 245055
206	$Na_2Cu(P_2O_7)$	$C2/c$ (15)	SM	—	(b)	FM	—	HQ	79868 80418
207	$CaNi(BP_2O_7(OH)_3)$	$C2/c$ (15)	Triv.	—	—	FM	—	—	409898
208	$LaCu_2O_4$	$C2/c$ (15)	SM	—	(b,s)	—	—	HQ	83486
209	YCu_2O_4	$C2/c$ (15)	SM	Fig. 30	(b,s)	—	—	HQ	83493
210	$NiZn(P_4O_{12})$	$C2/c$ (15)	Triv.	—	(b)	FM	—	—	37137
211	$La(MnO_3)$	$C2/c$ (15)	Triv.	—	(b,s)	FM	—	HQ	150258
212	$VOSb_2O_4$	$C2/c$ (15)	SM	—	(b)	FM	—	HQ	2292 27800
213	Sr_3CuPtO_6	$C2/c$ (15)	SM	—	(b,s)	FM	—	HQ	66347 72721
214	$(VO)(PO_3)_2$	$C2/c$ (15)	SM	—	(b)	FM	—	HQ	39762 160942 160943 160944
215	Sc_4OsCl_4	$C2/c$ (15)	Triv.	—	—	NM	—	HQ	421532
216	$MgTeMoO_6$	$P2_12_12$ (18)	Triv.	—	(b)	NM	—	HQ	184714
217	$Zn(TeMoO_6)$	$P2_12_12$ (18)	Triv.	—	(b,s)	NM	—	HQ	250523 163981
218	As_2O_5	$P2_12_12_1$ (19)	Triv.	—	(b,s)	NM	—	HQ	987 654040
219	$AsPO_5$	$P2_12_12_1$ (19)	Triv.	—	(b)	NM	—	HQ	36649
220	$SbAsO_5$	$P2_12_12_1$ (19)	Triv.	—	(b)	NM	—	HQ	36650
221	$NaCu(PO_4)$	$P2_12_12_1$ (19)	SM	—	(b)	FM	—	HQ	35451
222	$BaVS_3$	$C222_1$ (20)	SM	—	(b,s)	FM	—	HQ	63230
223	GeTiONF	$Pmm2$ (25)	Triv.	—	—	—	—	—	674260
224	$KCu(CO_3)F$	$Pmc2_1$ (26)	SM	—	(b)	FM	—	HQ	75401
225	$CsBi(Nb_2O_7)$	$Pmc2_1$ (26)	Triv.	—	(b,s)	NM	—	HQ	96510 162981 162982 162983 162984
226	$Bi_2(MoO_6)$	$Pca2_1$ (29)	Triv.	—	—	NM	—	—	14266 47139(b) 201685(b)
227	$InO(OH)$	$Pmn2_1$ (31)	Triv.	—	—	NM	—	HQ	15082 166253
228	LiV_2O_5	$Pmn2_1$ (31)	SM	—	(b)	FM	—	HQ	88640
229	$Cu(NH_4)(PO_4)(H_2O)$	$Pmn2_1$ (31)	SM	—	—	FM	—	HQ	250189
230	$(NH_4)(Co(PO_4)(H_2O))$	$Pmn2_1$ (31)	SM	—	—	AFM	—	HQ	280044
231	$(NH_4)(NiPO_4)(H_2O)$	$Pmn2_1$ (31)	Triv.	—	—	FM	—	HQ	424553
232	V_2O_5	$Pmn2_1$ (31)	Triv.	—	(b)	NM	—	—	15984(s) 29140 41030 82151(s) 157988(s)
233	$SrGaH_5$	$Pna2_1$ (33)	Triv.	—	—	NM	—	—	240697
234	FeP	$Pna2_1$ (33)	SM	—	—	—	—	HQ	15057
235	$Rb(AlSiO_4)$	$Pna2_1$ (33)	Triv.	—	(b,s)	NM	—	—	4335 160823
236	$Cs(AlSiO_4)$	$Pna2_1$ (33)	Triv.	—	(b,s)	NM	—	HQ	160822(k) 186607(k) 186608 186609 186610
237	$TlTeVO_5$	$Pna2_1$ (33)	Triv.	—	(b)	NM	—	—	173863 173864
238	FeS_2	$Pnn2$ (34)	Triv.	—	—	NM	—	HQ	42726
239	$FeTe_2$	$Pnn2$ (34)	Triv.	—	—	—	—	HQ	42727 633870
240	$Ba_2Ge_2TiO_8$	$Cmm2$ (35)	Triv.	—	(b,s)	—	—	HQ	39133
241	$BaZnF_4$	$Cmc2_1$ (36)	Triv.	Fig. 30	(b,s)	—	—	—	672719 16925 182604 182605 182606 182607 182609 402925 402926
242	$Al_5(BO_3)O_6$	$Cmc2_1$ (36)	Triv.	—	(b)	NM	—	HQ	20172 167307 167308(s) 167309 167310 167311 167312 167313 167314 167315 167316 190085
243	$BaNiF_4$	$Cmc2_1$ (36)	Triv.	—	(b,s)	FM	—	—	23141 261190 410708
244	$BaCoF_4$	$Cmc2_1$ (36)	SM	—	(b,s)	FM	—	HQ	26067 261189
245	$BaVS_3$	$Cmc2_1$ (36)	SM	—	(b,s)	FM	—	HQ	52692 63229 154182 616099
246	$Rb_2(PbO_3)$	$Cmc2_1$ (36)	Triv.	—	(b,s)	NM	—	—	1413

247	$Na_3(VOS_3)$	$Cmc2_1$ (36)	Triv.	—	—	NM	—	HQ	281593$^{(b)}$ 415217
248	$Sr_2(Ta_2O_7)$	$Cmc2_1$ (36)	Triv.	—	(b,s)	NM	—	HQ	16388
249	$Na_2(W_2O_7)$	$Cmc2_1$ (36)	Triv.	—	(b,s)	NM	—	HQ	65780
250	$CaGa(BO_3)O$	$Ccc2$ (37)	Triv.	—	(b)	NM	—	HQ	93390
251	$Ba(TiO_3)$	$Amm2$ (38)	Triv.	—	(b)	NM	—	HQ	154346 161341 31155$^{(k,s,l)}$ 73637$^{(k,s,l)}$ 73638$^{(k,s,l)}$ 73639$^{(k,s,l)}$ 73640$^{(k,s,l)}$ 73641$^{(k,s,l)}$ 161419$^{(k,s)}$ 186460$^{(s,l)}$ 237106$^{(s,l)}$ 237109$^{(s,l)}$
252	$Rb_4(CO_4)$	$Amm2$ (38)	Triv.	—	—	NM	—	—	245441
253	$K(NbO_3)$	$Amm2$ (38)	Triv.	—	(b,s,l*)	NM	—	—	9533$^{(k)}$ 14363 190922$^{(k)}$
254	$Pb(ZrO_3)$	$Amm2$ (38)	Triv.	—	(b,s,l*)	NM	—	HQ	39607
255	$Ag_2(TeO_2(OH)_4)$	$Fdd2$ (43)	Triv.	—	(b)	NM	—	HQ	240968
256	$Rb_2((Al_2Si_3)O_{10})$	$Fdd2$ (43)	Triv.	—	(b,s)	NM	—	—	180324
257	IrF_4	$Fdd2$ (43)	SM	—	(b,s)	FM	—	—	23483
258	$Bi_2(CO_3)O_2$	$Imm2$ (44)	Triv.	Fig. 30	—	NM	—	HQ	94740 252588
259	$Fe(Ti_3O_7)$	$Imm2$ (44)	Triv.	—	—	FM	—	—	190042
260	W_6PCl_{17}	$Imm2$ (44)	Triv.	—	—	AFM	—	HQ	422270
261	$Ba_4In_6O_{13}$	$Iba2$ (45)	Triv.	Fig. 30	(b)	NM	—	—	72887
262	$Ag(C(CN)_3)$	$Ima2$ (46)	Triv.	—	—	NM	—	HQ	43823 428560
263	$Sr(TiO_3)$	$Ima2$ (46)	Triv.	—	(b,s)	NM	—	—	182248
264	$Pb(TiO_3)$	$Pmmm$ (47)	Triv.	—	(b,s,l*)	—	—	—	27949
265	$YBaCo_2O_5$	$Pmmm$ (47)	SM	—	(b,s)	FM	—	—	171433 247220
266	$LaBa_2Cu_3O_7$	$Pmmm$ (47)	TI	Fig. 31	(b,s)	NM	—	—	81167
267	$YBa(Fe_2O_5)$	$Pmmm$ (47)	SM	—	(b,s)	FM	—	—	164176 281205 281206
268	SiO_2	$Pnnn$ (48)	Triv.	—	(b,s)	NM	—	—	170533
269	SiO_2	$Pban$ (50)	Triv.	—	(b,s)	NM	—	—	170535
270	$La_2(NiO_4)$	$Pban$ (50)	Triv.	—	(b,s,l*)	FM	—	HQ	201940
271	$Cu(H_2PO_2)_2$	$Pmma$ (51)	SM	—	—	FM	—	HQ	280921
272	$CuCo_2Ge_2$	$Pmma$ (51)	SM	—	—	FM	—	HQ	62856
273	$Cu(GeO_3)$	$Pmma$ (51)	SM	—	(b)	FM	—	HQ	25754 50329 50331 56606 56607 56699 56701 78475 85325 85326 89400 89401 89402 89403 89404 89405 89406 89407 246664 411018 411019
274	$Cu(SiO_3)$	$Pmma$ (51)	SM	—	(b)	FM	—	HQ	89669
275	$LaCoAl_4$	$Pmma$ (51)	TI	—	—	NM	—	HQ	9986
276	$Ga(GaCl_4)$	$Pnna$ (52)	Triv.	—	(b)	NM	—	HQ	14218 62664 66548
277	$In(InBr_4)$	$Pnna$ (52)	Triv.	—	(b)	NM	—	HQ	60851 62240
278	$CuPtO_2$	$Pmna$ (53)	SM	—	—	—	—	—	670125
279	$Na_3Cu_4S_4$	$Pbam$ (55)	SM	—	—	NM	—	HQ	10004
280	$Na_2(TiCl_4)$	$Pbam$ (55)	Triv.	—	(b)	FM	—	HQ	400264
281	$Bi_2Al_4O_9$	$Pbam$ (55)	Triv.	—	(b)	NM	—	—	20069 26807 88775 200051 236561 251938
282	$Rb(VOF_3)$	$Pbam$ (55)	TI	—	(b,s)	FM	—	HQ	249403 426620
283	$YCrB_4$	$Pbam$ (55)	Triv.	—	—	NM	—	—	16171
284	YVB_4	$Pbam$ (55)	TI	—	—	NM	—	—	615679
285	$Na_2(MnCl_4)$	$Pbam$ (55)	SM	—	(b)	FM	—	HQ	9136
286	Sc_2CrB_6	$Pbam$ (55)	TI	—	—	FM	—	—	99646
287	Sc_4Cl_6B	$Pbam$ (55)	SM	—	(b)	NM	—	HQ	201977
288	Sc_4Cl_6N	$Pbam$ (55)	SM	—	(b)	NM	—	HQ	201979
289	Bi_3NF_6	$Pbcm$ (57)	Triv.	—	(b)	NM	—	—	79395
290	Fe_2C	$Pbcm$ (57)	TI	—	(b)	—	—	—	670573
291	$Ca_2(AsO_4)Cl$	$Pbcm$ (57)	Triv.	—	(b)	NM	—	—	26234
292	$ScFe_2Si_2$	$Pbcm$ (57)	SM	—	—	FM	—	HQ	402545 633456
293	$(NH_4)(VO_3)$	$Pbcm$ (57)	Triv.	—	—	NM	—	—	1487
294	NaO_2	$Pnnm$ (58)	SM	—	—	FM	—	—	26583 87179 87180 87181 180562 673259
295	$Li_4Ca(BO_3)_2$	$Pnnm$ (58)	Triv.	—	—	NM	—	HQ	99503 239000
296	MnB_4	$Pnnm$ (58)	SM	—	(b)	FM	—	HQ	194807
297	FeB_4	$Pnnm$ (58)	Triv.	—	—	NM	—	—	196424 425311 670854
298	$Ba_2CoCl_2(SeO_3)_2$	$Pnnm$ (58)	SM	—	(b)	AFM	—	HQ	280965

299	$Al_2(SiO_4)O$	*Pnnm* (58)	Triv.	—	—	NM	—	—	$24275^{(b)}$ $26688^{(b)}$ $30677^{(b)}$ $30678^{(b)}$ $30679^{(b)}$ $30680^{(b)}$ $76936^{(b)}$ $84613^{(b)}$ $84614^{(b)}$ $85743^{(b)}$ 86340 $92634^{(b)}$ $92635^{(b)}$ $100395^{(b)}$ $100396^{(b)}$ $100397^{(b)}$ $100398^{(b)}$ $100399^{(b)}$ $169412^{(b)}$ $172725^{(b)}$ $172726^{(b)}$ $172727^{(b)}$ $172728^{(b)}$ $172729^{(b)}$ $172730^{(b)}$ $172731^{(b)}$ $172732^{(b)}$
300	$CuZn(AsO_4)(OH)$	*Pnnm* (58)	Triv.	—	(b)	FM	—	—	160894
301	CrO_2	*Pnnm* (58)	Triv.	—	(b)	FM	—	—	155832 185886 290478 290479 290480
302	$FeSe_2$	*Pnnm* (58)	Triv.	—	—	NM	—	—	25680 42041 42115 44751 633469 633479
303	FeS_2	*Pnnm* (58)	Triv.	—	—	NM	—	—	26756 42415 42416 109374 633255 633275 633304
304	$CoAs_2$	*Pnnm* (58)	SM	—	—	NM	SC	—	610034
305	MnS_2	*Pnnm* (58)	SM	Fig. 31	—	FM	—	—	643441
306	$Fe(NCNH)_2$	*Pnnm* (58)	Triv.	—	—	NM	—	HQ	419222 422725
307	$CaBi(CO_3)OF$	*Pmmn* (59)	Triv.	—	—	NM	—	HQ	87759
308	$Na_2(TiO)(GeO_4)$	*Pmmn* (59)	Triv.	—	(b,s)	NM	—	HQ	160149
309	$CoCu_2O_3$	*Pmmn* (59)	SM	Fig. 31	—	FM	—	HQ	33996
310	$Na(V_2O_5)$	*Pmmn* (59)	SM	—	(b)	FM	—	HQ	$59345^{(s)}$ $88354^{(s)}$ 88861 88862 $88863^{(s)}$ 88864 $89411^{(s)}$ 89412 89413 $92954^{(s)}$ 251182 $409210^{(s)}$
311	LiV_2O_5	*Pmmn* (59)	SM	—	(b,s)	—	—	HQ	88639
312	$CsMgH_3$	*Pmmn* (59)	Triv.	—	(b)	NM	—	—	159177
313	$CrOCl$	*Pmmn* (59)	SM	—	(b)	FM	—	HQ	4086 28318
314	$FeOCl$	*Pmmn* (59)	SM	—	(b)	AFM	—	HQ	16013 27136 40963 167393
315	$RuCl_3$	*Pmmn* (59)	Triv.	—	—	FM	—	HQ	414041
316	$Sr(V_3O_7)$	*Pmmn* (59)	SM	—	(b)	AFM	—	HQ	241176 241177 241178 241179 241180 241181 241182 241183 241184 241185 241186 241187
317	$FeNb_2O_6$	*Pbcn* (60)	Triv.	—	(b)	FM	—	—	15855 31943 151720
318	$Fe(Nb_2O_6)$	*Pbcn* (60)	TI	—	(b)	FM	—	—	24216
319	$CuNb_2O_6$	*Pbcn* (60)	SM	—	(b)	FM	—	—	71606 74424 79455 $80316^{(s)}$
320	$CoNb_2O_6$	*Pbcn* (60)	SM	—	(b)	FM	—	—	182710 182711
321	$Na_2(Si_2O_5)$	*Pbcn* (60)	Triv.	—	(b,s)	NM	—	—	34669
322	$O(CN)_2$	*Pbca* (61)	Triv.	—	—	—	—	—	670397
323	$Te(CN)_2$	*Pbca* (61)	Triv.	—	—	—	—	—	670400
324	$Cu(SeO_3)$	*Pbca* (61)	Triv.	—	(b)	NM	—	—	29506 61342
325	WO_3	*Pnma* (62)	Triv.	—	(b,s)	NM	—	—	836
326	$Mg_3(SiO_4)F_2$	*Pnma* (62)	Triv.	—	(b)	NM	—	—	15203 252073
327	K_2ClO_3N	*Pnma* (62)	Triv.	—	—	NM	—	HQ	28211
328	$Li(CN)$	*Pnma* (62)	Triv.	—	—	NM	—	—	77321
329	$AgHg_2O_2(NO_3)$	*Pnma* (62)	Triv.	—	—	NM	—	—	89685
330	$K_2Pd(P_2S_6)$	*Pnma* (62)	Triv.	—	—	NM	—	—	165316
331	$PbPd(P_2O_7)$	*Pnma* (62)	Triv.	—	(b)	NM	—	—	195305 420534
332	$WO_3(H_2O)$	*Pnma* (62)	Triv.	—	—	NM	—	HQ	201806
333	MoO_2	*Pnma* (62)	Triv.	—	(b)	—	—	—	243549
334	$KYTe_2O_6$	*Pnma* (62)	Triv.	—	(b)	NM	—	—	291295
335	$LiSr(BS_3)$	*Pnma* (62)	Triv.	—	(b)	NM	—	HQ	380105
336	$(AgF)(AuF_6)$	*Pnma* (62)	SM	—	(b)	NM	—	—	422686
337	$(NH_4)(Co(PO_4))(H_2O)$	*Pnma* (62)	SM	—	—	FM	—	—	424548
338	Al_2FeC	*Pnma* (62)	TI	—	(b,s)	—	—	—	670820
339	Li_2C_2	*Pnma* (62)	Triv.	—	—	—	—	—	671756 671757 671758 671759 671760 671761 671762 671763 671764 671765 671766 671767 671768 671769 671770 671771
340	$Al_2(SiO_4)O$	*Pnma* (62)	Triv.	—	(b)	NM	—	—	25711 31115 85200 85201 85202 85203 85204 85744 86342 $92632^{(s)}$ 92633 96722 100450 100451 100452 100453 100454 172720 172721 172722 172723 172724 92636 92637
341	$Li(VO)(AsO_4)$	*Pnma* (62)	SM	Fig. 31	(b)	FM	—	—	90991
342	$FeOOH$	*Pnma* (62)	SM	—	—	AFM	—	—	239321 239322 239323 239324 245057

343	$PbCO_3$	$Pnma$ (62)	Triv.	—	—	NM	—	HQ	6178 36164 36554 56101 166089 190074 247490 247491 247492 247493
344	$Cd_2(OH)_3Cl$	$Pnma$ (62)	Triv.	—	(b)	NM	—	—	39285 83524
345	$SnSO_4$	$Pnma$ (62)	Triv.	—	—	NM	—	—	2748 25838 245904
346	$Ca(B_2Si_2O_8)$	$Pnma$ (62)	Triv.	—	(b,s)	NM	—	—	6254 20590 26491 29545 29546 29547 29548 29549 29550 30296
347	PbF_2	$Pnma$ (62)	Triv.	—	—	NM	—	—	36275 14324 154994 154995 154996 154997 154998 161080 161391 161392 161393 161394 673364
348	Tl_2BeF_4	$Pnma$ (62)	Triv.	—	—	NM	—	HQ	171178 171179 171180 171181 171182 171183
349	Cs_2CuCl_4	$Pnma$ (62)	SM	—	—	FM	—	HQ	9468 15699 91186 91187 91188 169176
350	Cs_2CuBr_4	$Pnma$ (62)	SM	—	—	FM	—	HQ	10185 26024 169179
351	$Rb_5(SiAs_3)$	$Pnma$ (62)	Triv.	—	—	NM	—	—	300191
352	$Cu(IO_3)(OH)$	$Pnma$ (62)	SM	—	(b)	FM	—	HQ	41804
353	$In(PO_4)$	$Pnma$ (62)	Triv.	—	(b)	NM	—	HQ	85579
354	$K_2(S_3O_6)$	$Pnma$ (62)	Triv.	—	—	NM	—	—	8200
355	$Tl_2(SeO_4)$	$Pnma$ (62)	Triv.	—	—	NM	—	HQ	73411 99382 99383 419775 419776 419777
356	$K_2(VO_2F_3)$	$Pnma$ (62)	Triv.	—	—	NM	—	—	9122 60621
357	$K(P_4N_7)$	$Pnma$ (62)	Triv.	—	(b,s)	NM	—	—	410630
358	$Cs(P_4N_7)$	$Pnma$ (62)	Triv.	—	(b)	NM	—	—	410632
359	$CuInO(PO_4)$	$Pnma$ (62)	SM	—	(b)	FM	—	—	89606
360	$Cu(SeO_3)$	$Pnma$ (62)	SM	—	(b)	FM	—	HQ	498 51847 97747
361	CrP	$Pnma$ (62)	SM	—	—	FM	—	—	5418 42079 42080 42081 42082 43247 53200 53201 76028 626498 626502 626514
362	$MnAs$	$Pnma$ (62)	TI	—	—	FM	—	—	9496 16543 41759 250011 610846
363	MnP	$Pnma$ (62)	TI	—	—	FM	—	—	30412 43246 43399 60880 61136 76089 76090 76091 643200 643213 643217 643220
364	$FeAs$	$Pnma$ (62)	SM	—	—	FM	—	—	30413 34036 42447 42448 42449 42450 42451 48031 48033 48034 48035 48036 610452 610474
365	FeP	$Pnma$ (62)	SM	—	—	FM	SC	HQ	43248 43400 62607 633046 633050
366	Na_2NiInF_7	$Pnma$ (62)	Triv.	—	(b,s)	FM	—	—	72110
367	$Na_2Ni(HPO_3)_2$	$Pnma$ (62)	Triv.	Fig. 31	(b)	FM	—	—	247564
368	$LiCu_2O_2$	$Pnma$ (62)	SM	—	(b)	FM	—	HQ	71221 71683 188111
369	$Li(Sb_2F_7)$	$Pnma$ (62)	Triv.	—	(b,s)	NM	—	—	428176
370	$FeMg(SiO_4)$	$Pnma$ (62)	Triv.	—	(b)	FM	—	—	164171 164172
371	$AgCu(VO_4)$	$Pnma$ (62)	SM	—	(b)	FM	—	HQ	419201 419202
372	P_2O_5	$Pnma$ (62)	Triv.	—	(b,s)	NM	—	—	16611 29045 79698
373	$NaZn(MoO_4)(OH)$	$Pnma$ (62)	Triv.	—	(b)	NM	—	—	9783
374	$Pb(V_2O_6)$	$Pnma$ (62)	Triv.	—	—	NM	—	—	6109
375	$NaTaO_3$	$Pnma$ (62)	Triv.	—	—	NM	—	—	$980^{(b,s)}$ 23319 $88375^{(b,s)}$ $150430^{(b,s)}$ $173757^{(b,s)}$ $239690^{(b,s)}$ $241443^{(b,s)}$
376	$YTiO_3$	$Pnma$ (62)	SM	—	(b)	FM	SC*	HQ	8150 84608 84609 84610 174118
377	$Na(NiF_3)$	$Pnma$ (62)	Triv.	Fig. 31	(b)	FM	—	—	9008 25533 72319 192140 192142 192144 200062
378	$La(GaO_3)$	$Pnma$ (62)	Triv.	—	—	NM	—	—	41280 $50388^{(b,s)}$ $51285^{(b,s)}$ $73759^{(b,s)}$ $73760^{(b,s)}$ $73761^{(b,s)}$ $79662^{(b,s,l)}$ $88146^{(b,s)}$ $88259^{(b,s)}$ $88349^{(b,s)}$ $91786^{(b,s)}$ $94299^{(b,s)}$ $98168^{(b,s)}$ $98410^{(b,s)}$ $153307^{(b,s)}$ $160233^{(b,s)}$ $160234^{(b,s)}$ $160235^{(b,s)}$ $161782^{(b,s)}$
379	$La(VO_3)$	$Pnma$ (62)	Triv.	—	(b,s)	AFM	—	—	63520 73898 73899 185831
380	$Na(ZnF_3)$	$Pnma$ (62)	Triv.	—	(b)	NM	—	HQ	69349 72320
381	$La(MnO_3)$	$Pnma$ (62)	Triv.	—	(b)	FM	—	—	$82226^{(s)}$ $82228^{(s)}$ $88388^{(s)}$ 90424 $161928^{(s)}$ $161929^{(s)}$ $180180^{(s)}$ 185279 252946
382	$Y(CoO_3)$	$Pnma$ (62)	Triv.	—	(b)	FM	—	HQ	155834 155835 155836 155837 155838
383	$Ca(SiO_3)$	$Pnma$ (62)	Triv.	—	(b,s)	NM	—	—	240462 240463 240464 240465 240466 240467 240468 240469
384	$Rb(Li(NH_2)_2)$	$Pnma$ (62)	Triv.	—	—	NM	—	—	95786
385	$Sr(VO_3)Cl$	$Pnma$ (62)	Triv.	—	(b,s)	NM	—	HQ	50787

386	$BaCs(VS_4)$	$Pnma$ (62)	Triv.	—	(b)	NM	—	HQ	430160
387	MnO_2	$Pnma$ (62)	SM	—	(b)	AFM	—	—	20228 24034 78331 171866
388	Ca_5Sb_3	$Pnma$ (62)	SM	—	—	NM	—	—	2065 619564
389	Ca_5Bi_3	$Pnma$ (62)	SM	—	—	NM	—	—	2140 616533
390	$Y_4Ti(SiO_4)_2OF_6$	$Cmcm$ (63)	Triv.	—	(b)	NM	—	—	20003
391	$K(FeF_4)$	$Cmcm$ (63)	SM	—	(b,s)	FM	—	—	23588 60615
392	$(PbF_2)_7(PbI_2)$	$Cmcm$ (63)	Triv.	—	—	NM	—	HQ	$36337^{(b,s)}$ 431846
393	$(CuO_2)_4$	$Cmcm$ (63)	SM	—	(b,s)	FM	—	HQ	54129
394	$BaVS_3$	$Cmcm$ (63)	SM	Fig. 31	(k*)	—	—	HQ	63228
395	$Tl_2(AlF_5)$	$Cmcm$ (63)	Triv.	—	—	NM	—	—	109365
396	CuO_2	$Cmcm$ (63)	SM	—	(b,s)	FM	—	HQ	150913
397	$Mg(Al_2O_4)$	$Cmcm$ (63)	Triv.	—	(b)	NM	—	—	161057
398	$LiFeP$	$Cmcm$ (63)	TI	—	—	NM	—	—	187134
399	$BaCu_2(Ge_3O_9)(H_2O)$	$Cmcm$ (63)	TI	—	—	FM	—	—	424818
400	AlF_3	$Cmcm$ (63)	Triv.	—	(k*,b,s)	NM	—	HQ	202681
401	KFe_2S_3	$Cmcm$ (63)	SM	—	(b)	FM	—	—	632396 99507
402	$Ca_3(VN_3)$	$Cmcm$ (63)	Triv.	—	(b)	NM	—	—	72118
403	$NiSO_4$	$Cmcm$ (63)	Triv.	Fig. 31	(b)	AFM	—	—	16691 16741 33737
404	$Ni(SeO_4)$	$Cmcm$ (63)	Triv.	Fig. 32	(b)	FM	—	—	25700
405	$TiPO_4$	$Cmcm$ (63)	SM	—	(b)	FM	—	HQ	36520 431885
406	$Rb(Fe_2Se_3)$	$Cmcm$ (63)	SM	—	—	FM	—	HQ	81547
407	$Cs(Fe_2Se_3)$	$Cmcm$ (63)	SM	—	—	FM	—	HQ	81549 187535
408	$Cs(Fe_2S_3)$	$Cmcm$ (63)	SM	—	(b)	FM	—	HQ	99504
409	$Tl(Fe_2S_3)$	$Cmcm$ (63)	SM	—	(b)	NM	—	HQ	166049
410	$BaFe_2Se_3$	$Cmcm$ (63)	TI	—	—	FM	SC	HQ	290594 290596
411	KFe_2Se_3	$Cmcm$ (63)	SM	—	—	FM	—	HQ	424671 424672
412	$TiCu_2$	$Cmcm$ (63)	TI	—	—	NM	—	—	629379 629386 629405
413	$K_2(NiP_2)$	$Cmcm$ (63)	Triv.	—	—	NM	—	HQ	300119
414	$K_2(NiAs_2)$	$Cmcm$ (63)	Triv.	—	—	NM	—	HQ	300120
415	Cs_2NiP_2	$Cmcm$ (63)	Triv.	—	—	—	—	—	656056
416	Cs_2PtSb_2	$Cmcm$ (63)	Triv.	—	—	NM	—	—	658700
417	Cs_2PdSb_2	$Cmcm$ (63)	Triv.	—	—	NM	—	—	658702
418	Cs_2NiBi_2	$Cmcm$ (63)	Triv.	—	—	—	—	—	658704
419	$K_3Pt_2O_4$	$Cmcm$ (63)	SM	—	(b,s)	FM	—	—	14158
420	$KCuZrF_7$	$Cmcm$ (63)	Triv.	—	(b,s)	FM	—	—	92469
421	$KCuHfF_7$	$Cmcm$ (63)	Triv.	—	(b,s)	FM	—	—	92470
422	$Mg(V_2O_5)$	$Cmcm$ (63)	TI	—	(b)	FM	—	HQ	50979 50981
423	$Li(V_2O_5)$	$Cmcm$ (63)	SM	—	(b,s)	FM	—	HQ	50980 50982 201974
424	$LiFe(PO_4)$	$Cmcm$ (63)	Triv.	—	(b)	AFM	—	HQ	97766
425	$LiNi(PO_4)$	$Cmcm$ (63)	Triv.	—	(b)	AFM	—	HQ	97767
426	$CuMgVO_4$	$Cmcm$ (63)	Triv.	—	(b)	NM	—	—	239746
427	Al_2La_2Ge	$Cmcm$ (63)	TI	—	—	NM	—	HQ	423614
428	$Na(NbO_3)$	$Cmcm$ (63)	Triv.	—	(b,s)	NM	—	—	$22065^{(l)}$ 23323 192404 192405 280098
429	$Na(TaO_3)$	$Cmcm$ (63)	Triv.	—	(b,s)	NM	—	HQ	23320 $23321^{(l)}$ 88376 239691 241444 241445 280099
430	$FeTi_2O_5$	$Cmcm$ (63)	TI	—	(b)	FM	—	—	37231
431	$SrCuO_2$	$Cmcm$ (63)	SM	—	—	NM	SC	—	16217 77291 83051 93653 202992 670129
432	$CuBaO_2$	$Cmcm$ (63)	SM	—	—	—	SC	—	670104
433	$La_2(CuO_4)$	$Cmce$ (64)	SM	—	(b)	NM	—	—	$1076^{(s,l)}$ 41499 $50265^{(s,l)}$ $67837^{(s,l)}$ $69311^{(s,l)}$ $69312^{(s,l)}$ $72237^{(s,l)}$ $73906^{(s,l)}$ $73907^{(s,l)}$ $73908^{(s,l)}$ $73909^{(s,l)}$ $73910^{(s,l)}$ $74145^{(s,l)}$ $74150^{(s,l)}$ $75891^{(s,l)}$ $78194^{(s,l)}$ $78237^{(s,l)}$ $78287^{(s,l)}$ $78288^{(s,l)}$ $78289^{(s,l)}$ $78290^{(s,l)}$ $78291^{(s,l)}$ $78292^{(s,l)}$ $78293^{(s,l)}$ $78294^{(s,l)}$ $78295^{(s,l)}$ $78296^{(s,l)}$ $78297^{(s,l)}$ $78298^{(s,l)}$ $78299^{(s,l)}$ $78300^{(s,l)}$ $87969^{(s,l)}$ $89173^{(s,l)}$ $173891^{(s,l)}$ $173893^{(s,l)}$ $173895^{(s,l)}$ $186588^{(s,l)}$ $261661^{(s,l)}$
434	$La_2(NiO_4)$	$Cmce$ (64)	Triv.	—	(b,s)	AFM	—	HQ	$50244^{(l)}$ $56318^{(l)}$ $63398^{(l)}$ $67838^{(l)}$ 69752 $69754^{(l)}$ $69755^{(l)}$
435	Rb_2CuCl_4	$Cmce$ (64)	SM	—	(b,s)	FM	—	HQ	$15145^{(l)}$ 55013

436	$Rb_2CuCl_2Br_2$	*Cmce* (64)	SM	—	(b)	FM	—	HQ	15147
437	K_2CuF_4	*Cmce* (64)	SM	—	(b,s,l*)	FM	—	HQ	38426 174116
438	Cs_2AgF_4	*Cmce* (64)	SM	—	(b,s,l*)	FM	—	—	155817 155818
439	Ba_5Sb_4	*Cmce* (64)	Triv.	—	—	NM	—	HQ	280022
440	$Na(IO_3)$	*Cmmm* (65)	TI	Fig. 32	(k*,b,s,l*)	NM	—	—	33664
441	$Ca(TiO_3)$	*Cmmm* (65)	Triv.	—	(k*,b,s,l*)	NM	—	—	187294
442	Na_3B_{20}	*Cmmm* (65)	SM	—	—	NM	—	HQ	407159 410247
443	$AuMgO_2$	*Cmmm* (65)	Triv.	—	—	—	—	—	670092
444	Mo_2CuGa_5	*Cmmm* (65)	TI	—	—	—	—	—	670139
445	$AlFe_2B_2$	*Cmmm* (65)	SM	—	—	FM	—	—	20322 23205 239296 241907 241908 241909 251811
446	YNi_4Si	*Cmmm* (65)	SM	—	—	NM	—	—	290731
447	$LaNi_4Si$	*Cmmm* (65)	SM	—	—	NM	—	—	290732
448	Al_3Ni_5	*Cmmm* (65)	SM	—	—	NM	—	—	58041 191113 608803
449	Ga_3Ni_5	*Cmmm* (65)	SM	—	—	NM	—	—	103861 634860 634865
450	KSc_2F_7	*Cmmm* (65)	Triv.	—	—	NM	—	HQ	47227
451	$Li_2(MnBr_4)$	*Cmmm* (65)	SM	—	(b)	FM	—	HQ	33865
452	$MnPt_3O_6$	*Cmmm* (65)	SM	—	(b)	FM	—	HQ	35337
453	$ZnPt_3O_6$	*Cmmm* (65)	Triv.	—	(b)	NM	—	HQ	35339
454	$CdPt_3O_6$	*Cmmm* (65)	Triv.	—	(b)	NM	—	HQ	35407
455	$K_2Na(FeO_3)$	*Cmme* (67)	SM	—	(b)	AFM	—	—	36380
456	FeSe	*Cmme* (67)	Triv.	—	—	FM	—	—	182545 169283
457	Pb_2OFCl	*Cmme* (67)	Triv.	—	—	NM	—	HQ	200211 200212 200213
458	LiFeAs	*Cmme* (67)	TI	—	—	FM	—	—	168206
459	FeSe	*Cmme* (67)	TI	—	—	NM	—	HQ	166441 169295 169299 169303 169306 169309 169311 169313 169315
460	FeSe	*Cmme* (67)	TI	—	—	NM	—	HQ	169285
461	SiO_2	*Ccce* (68)	Triv.	—	(b,s)	NM	—	—	170527
462	$Cs_2Pd_3Se_4$	*Fmmm* (69)	Triv.	—	(k*,b)	NM	—	HQ	33892
463	$Cs_2Ni_3S_4$	*Fmmm* (69)	Triv.	—	(k*,b)	NM	—	—	627055
464	$Rb_2Pb(Cu(NO_2)_6)$	*Fmmm* (69)	SM	—	—	FM	—	HQ	372
465	$PbK_2(Cu(NO_2)_6)$	*Fmmm* (69)	SM	—	—	FM	—	HQ	1274
466	$K_2Ba(Cu(NO_2)_6)$	*Fmmm* (69)	SM	—	—	FM	—	HQ	1830
467	$K_2Ca(Cu(NO_2)_6)$	*Fmmm* (69)	SM	—	—	FM	—	HQ	6183
468	$Cs_2PbCu(NO_2)_6$	*Fmmm* (69)	SM	—	—	—	—	HQ	8284 8285 56252 56253
469	Cu_2Cl_2O	*Fddd* (70)	TI	—	(b)	FM	—	—	1055 96610
470	K_4P_6	*Fddd* (70)	Triv.	—	—	NM	—	HQ	33260
471	$Cu_{16}O_8Cl_{16}$	*Fddd* (70)	TI	—	(b)	—	—	—	430861
472	$RbVSe_2$	*Fddd* (70)	Triv.	—	(b,s)	NM	—	HQ	415479
473	$CaBi_2(CO_3)_2O_2$	*Immm* (71)	TI	—	—	NM	—	HQ	94741
474	K_3Ir	*Immm* (71)	TI	—	—	—	—	—	674660
475	Sr_2FeO_3	*Immm* (71)	Triv.	—	—	AFM	—	HQ	251018 251019 251020
476	$Sr_3(Fe_2O_5)$	*Immm* (71)	Triv.	—	(b,s)	FM	—	HQ	420234
477	$Cs(FeS_2)$	*Immm* (71)	TI	—	(b,s)	FM	—	—	25697 53234 201112
478	$RbFeS_2$	*Immm* (71)	TI	—	(b,s)	FM	—	—	633207
479	Li_2NiO_2	*Immm* (71)	Triv.	—	(b)	FM	—	—	25000
480	$Li_2(CuO_2)$	*Immm* (71)	SM	—	(b)	FM	—	—	25001 67204 67205 202996 238945 47106 67150 67151 291072
481	Na_2PtO_2	*Immm* (71)	Triv.	—	(b)	NM	—	—	25018
482	$VOCl_2$	*Immm* (71)	SM	—	(b,s)	FM	—	—	24380
483	$VOBr_2$	*Immm* (71)	SM	—	(b,s)	FM	—	—	24381
484	$PtSO_4$	*Ibam* (72)	Triv.	—	(b)	—	—	—	671488
485	$K_2(MnS_2)$	*Ibam* (72)	SM	Fig. 32	(b,s)	FM	—	HQ	65453
486	$Rb_2(MnS_2)$	*Ibam* (72)	SM	Fig. 32	(b,s)	AFM	—	HQ	65454
487	$Cs_2(MnS_2)$	*Ibam* (72)	SM	Fig. 32	(b,s)	FM	—	HQ	65455
488	$K_2(MnSe_2)$	*Ibam* (72)	SM	Fig. 32	(b,s)	FM	—	HQ	65456
489	$Rb_2(MnSe_2)$	*Ibam* (72)	SM	Fig. 32	(b,s)	FM	—	HQ	65457
490	$Cs_2(MnSe_2)$	*Ibam* (72)	SM	Fig. 33	(b,s)	FM	—	HQ	65458
491	$Rb_2(MnTe_2)$	*Ibam* (72)	SM	Fig. 33	(b,s)	FM	—	HQ	65460
492	$Cs_2(MnTe_2)$	*Ibam* (72)	SM	Fig. 33	(b,s)	FM	—	HQ	65461
493	K_2CoS_2	*Ibam* (72)	SM	—	(b,s)	FM	—	HQ	67387 623958 623960

494	Rb_2CoS_2	*Ibam* (72)	SM	—	(b,s)	FM	—	HQ	67388
495	Cs_2CoS_2	*Ibam* (72)	SM	—	(b,s)	FM	—	HQ	67389
496	K_2CoSe_2	*Ibam* (72)	SM	—	(b,s)	FM	—	HQ	67390
497	Rb_2CoSe_2	*Ibam* (72)	SM	—	(b,s)	FM	—	HQ	67391
498	Cs_2CoSe_2	*Ibam* (72)	SM	—	(b,s)	FM	—	HQ	67392
499	Na_2CoSe_2	*Ibam* (72)	SM	—	(b,s)	FM	—	—	624264
500	$Na_3(AlAs_2)$	*Ibam* (72)	Triv.	—	(b)	NM	—	HQ	63149
501	$Na_3(AlP_2)$	*Ibam* (72)	Triv.	—	(b)	NM	—	HQ	73278 402081
502	$K_3(InP_2)$	*Ibam* (72)	Triv.	—	(b,s)	NM	—	HQ	73281 300141
503	$KAg(CO_3)$	*Ibca* (73)	Triv.	—	—	NM	—	HQ	26632 31021 242236 242239 409484
504	$CsMoO_2F_3$	*Imma* (74)	Triv.	—	—	NM	—	HQ	9710
505	$Na_4Ni(P_2O_7)F_2$	*Imma* (74)	Triv.	—	(b)	AFM	—	—	251665 251666
506	$MgAlBO_4$	*Imma* (74)	Triv.	—	(b)	—	—	—	670206
507	Na_2NiGaF_7	*Imma* (74)	Triv.	—	(k*,b,s)	FM	—	HQ	408111
508	$Cs(Pd_2F_5)$	*Imma* (74)	Triv.	—	(b,s)	FM	—	—	35284
509	$RbPd_2F_5$	*Imma* (74)	Triv.	—	(b,s)	FM	—	HQ	72299
510	$Zn(AlF_5)(H_2O)_2$	*Imma* (74)	Triv.	—	—	NM	—	HQ	245171
511	$LiCuVO_4$	*Imma* (74)	SM	—	—	FM	—	HQ	15836$^{(b)}$ 26992$^{(b)}$ 65677$^{(b)}$ 72846$^{(b)}$ 261517$^{(b)}$ 290738 290739 291437$^{(b)}$ 291440$^{(b)}$ 291441$^{(b)}$
512	$Mg_2(SiO_4)$	*Imma* (74)	Triv.	—	—	NM	—	HQ	6311$^{(b)}$ 23597$^{(b)}$ 27530$^{(b)}$ 83784 83785 83786 83787 63178$^{(b)}$ 66490$^{(b)}$ 100725$^{(b)}$ 159955$^{(b)}$ 171064$^{(b)}$ 171065$^{(b)}$ 171066$^{(b)}$ 290205$^{(b)}$ 290206$^{(b)}$ 290207$^{(b)}$ 290208$^{(b)}$ 670570$^{(b)}$
513	$Ca(SiO_3)$	*Imma* (74)	Triv.	—	(b,s)	NM	—	—	240422 240423 240424 240425 240426 240427 240428 240429
514	$K_4(CuV_5O_{15}Cl)$	*P4* (75)	SM	—	(b,s)	FM	—	HQ	401042
515	$WOCl_4$	*I4* (79)	Triv.	—	—	NM	—	HQ	25519 426524
516	$(NH_4)(WAgS_4)$	$I\bar{4}$ (82)	Triv.	—	—	NM	—	HQ	84370
517	$Cs(As_4F_{13})$	$I\bar{4}$ (82)	Triv.	—	—	NM	—	HQ	281641
518	$RbLa(Si(CN_2)_4)$	$I\bar{4}$ (82)	Triv.	—	—	NM	—	HQ	419337
519	ZrF_4	$P4_2/m$ (84)	Triv.	—	—	NM	—	—	35100
520	$Cs_2(V_4O_9)$	$P4_2/m$ (84)	Triv.	—	(b)	FM	—	HQ	79408
521	$CuCl(B(OH)_4)$	$P4/n$ (85)	SM	—	—	FM	—	HQ	56963
522	$(AgF)(BF_4)$	$P4/n$ (85)	SM	—	—	NM	—	HQ	80645 80646
523	$(VO)(PO_4)$	$P4/n$ (85)	Triv.	—	(b)	NM	—	HQ	425536 77598 108983
524	$Ca(V_4O_9)$	$P4/n$ (85)	TI	—	(b)	FM	—	HQ	2556 90927
525	$Sr(V_4O_9)$	$P4/n$ (85)	TI	—	(b)	FM	—	HQ	90926
526	$(VO)MoO_4$	$P4/n$ (85)	SM	—	(b,s)	AFM	—	HQ	27315
527	As_2O_3	$P4_2/n$ (86)	Triv.	—	(b,s)	NM	—	—	183096
528	$N_4P_4Br_8$	$P4_2/n$ (86)	Triv.	—	—	NM	—	—	2716
529	$BaFe_2S_4$	$I4/m$ (87)	SM	—	—	FM	—	HQ	23081
530	$Rb_2(TeBr_6)$	$I4/m$ (87)	Triv.	—	—	NM	—	HQ	49520
531	Bi_4RuI_2	$I4/m$ (87)	Triv.	—	—	NM	—	HQ	406949
532	$(NH_3)_4Pd(N_3)_4Pd$	$I4/m$ (87)	Triv.	—	—	—	—	HQ	410384
533	VAu_4	$I4/m$ (87)	SM	—	—	FM	—	—	612460
534	$Ni(VO(PO_4))_2(H_2O)_4$	$I4/m$ (87)	TI	—	—	FM	—	HQ	85597
535	$(Co(H_2O)_4)(VO(PO_4))_2$	$I4/m$ (87)	SM	—	—	FM	—	HQ	281336
536	$Sr_2Cu(WO_6)$	$I4/m$ (87)	SM	—	(b,s)	FM	—	—	33571 72812 88701 99303 186027 190594 193614 291133 291134 291135
537	Sr_2CuTeO_6	$I4/m$ (87)	SM	—	(b,s)	FM	—	—	33573 88702
538	$Ba_2Cu(WO_6)$	$I4/m$ (87)	SM	—	(b,s)	FM	—	HQ	72813
539	$Sr_2Fe(WO_6)$	$I4/m$ (87)	Triv.	—	(k*,b,s)	AFM	—	—	78677
540	$Ba_2Cu(TeO_6)$	$I4/m$ (87)	SM	—	(b,s)	FM	—	—	88703
541	$Sr_2Ni(WO_6)$	$I4/m$ (87)	Triv.	Fig. 34	(b,s)	AFM	—	HQ	91791 153327 190591
542	$Ba_2(FeWO_6)$	$I4/m$ (87)	Triv.	Fig. 34	(k*,b,s)	AFM	—	HQ	95518 95520 95521 95522 95523
543	Sr_2NiMoO_6	$I4/m$ (87)	Triv.	—	(b,s)	AFM	—	HQ	98191 155273 155274 155732 157020 157021 157022 157023 157025

544	$Sr_2(FeMoO_6)$	$I4/m$ (87)	Triv.	Fig. 34	(b,s)	FM	—	HQ	150701 153426 155482 157600 157601 157602 166816 172212 193690 247539 248460$^{(k)}$ 248461 248462 248463 248464
545	$Sr_2(FeReO_6)$	$I4/m$ (87)	SM	Fig. 33	(b,s)	FM	—	HQ	150702
546	$Sr_2Mg(WO_6)$	$I4/m$ (87)	Triv.	Fig. 34	(b,s)	NM	—	HQ	151703 152574 155306 155307 155308 155309 155310 168463
547	$Sr_2(NiOsO_6)$	$I4/m$ (87)	Triv.	—	(b,s)	FM	—	HQ	152440 152441 152442 152443
548	$Sr_2(CoMoO_6)$	$I4/m$ (87)	SM	Fig. 33	(b,s)	FM	—	HQ	153544 153545 153546
549	$Sr_2(NiMoO_6)$	$I4/m$ (87)	TI	—	(b,s)	AFM	—	HQ	157024 157026
550	Sr_2GaTaO_6	$I4/m$ (87)	Triv.	—	(b,s)	NM	—	HQ	172330
551	Sr_2NiReO_6	$I4/m$ (87)	SM	—	(b,s)	FM	—	HQ	173487 173490
552	Sr_2CoReO_6	$I4/m$ (87)	TI	Fig. 33	(b,s)	AFM	—	HQ	173488
553	$Sr_2Cu(MoO_6)$	$I4/m$ (87)	SM	—	(b,s)	FM	—	HQ	186038
554	Sr_2MgMoO_6	$I4/m$ (87)	Triv.	Fig. 34	(b,s)	NM	—	HQ	187662
555	Sr_2MnMoO_6	$I4/m$ (87)	SM	Fig. 33	(b,s)	FM	—	HQ	187669
556	Sr_2CoWO_6	$I4/m$ (87)	SM	Fig. 33	(b,s)	AFM	—	—	190593 245470
557	Sr_2CoNbO_6	$I4/m$ (87)	Triv.	Fig. 34	(b,s)	—	—	—	192327
558	Sr_2CoOsO_6	$I4/m$ (87)	SM	—	(b,s)	FM	—	HQ	236435 236436
559	$Sr_2Li(ReO_6)$	$I4/m$ (87)	Triv.	—	(b,s)	NM	—	—	246730 418991$^{(k)}$
560	$InK(C_2O_4)_2(H_2O)_4$	$I4_1/a$ (88)	Triv.	—	—	NM	—	—	99956
561	$Y(Pd_2O_4)$	$I4_1/a$ (88)	SM	—	(b)	NM	—	HQ	78846
562	$PbPd_2O_4$	$I4_1/a$ (88)	Triv.	Fig. 34	(b)	NM	—	HQ	263049
563	$TlTlCl_4$	$I4_1/a$ (88)	Triv.	—	(b)	NM	—	HQ	4031
564	$Ca(WO_4)$	$I4_1/a$ (88)	Triv.	—	—	NM	—	HQ	15586$^{(b)}$ 15869$^{(b)}$ 18135$^{(b)}$ 60547$^{(b)}$ 60548$^{(b)}$ 60549$^{(b)}$ 60550$^{(b)}$ 60551$^{(b)}$ 77335 155423$^{(b)}$ 155791$^{(b)}$ 157428$^{(b)}$ 193047$^{(b)}$ 193491$^{(b)}$ 291535$^{(b)}$ 671942$^{(b)}$
565	$Ca(MoO_4)$	$I4_1/a$ (88)	Triv.	—	—	NM	—	—	22351$^{(b)}$ 23699$^{(b)}$ 60552$^{(b)}$ 60553$^{(b)}$ 60554$^{(b)}$ 60555$^{(b)}$ 60556$^{(b)}$ 60557$^{(b)}$ 60558$^{(b)}$ 62219$^{(b)}$ 77334 183446 183447$^{(b)}$ 193793$^{(b)}$ 194078$^{(b)}$ 194079$^{(b)}$ 417513$^{(b)}$
566	$Zr(GeO_4)$	$I4_1/a$ (88)	Triv.	—	(b)	NM	—	HQ	29262
567	$Hf(GeO_4)$	$I4_1/a$ (88)	Triv.	—	(b,s)	NM	—	HQ	202080
568	$YNbO_4$	$I4_1/a$ (88)	Triv.	—	—	NM	—	—	239208 239209 430917 430918 430919 430920 430921 430922
569	Bi_2ZnTiO_6	$P4mm$ (99)	Triv.	—	(b,s)	NM	—	—	162766 162767 162768 186801
570	$BiFeO_3$	$P4mm$ (99)	SM	—	(b,s)	AFM	—	—	188467 188466
571	$LaCoO_3$	$P4mm$ (99)	SM	—	(b,s)	—	—	—	673191
572	$La_1Fe_1O_3$	$P4mm$ (99)	SM	—	(b,s)	—	—	—	673196
573	$BaSiO_3$	$P4mm$ (99)	Triv.	—	(b,s)	—	—	—	674089
574	$BiAlO_3$	$P4mm$ (99)	Triv.	—	(b,s)	—	—	—	674105 673462
575	$RbWNO_2$	$P4mm$ (99)	Triv.	—	(b,s)	—	—	—	674128
576	Sb_2N_2O	$P4mm$ (99)	Triv.	—	—	—	—	—	674157
577	$YTlO_2S$	$P4mm$ (99)	Triv.	—	—	—	—	—	674170
578	$CaSnO_2S$	$P4mm$ (99)	Triv.	—	—	—	—	—	674175
579	$HfMgO_2S$	$P4mm$ (99)	Triv.	—	—	—	—	—	674184
580	$YAlO_2S$	$P4mm$ (99)	Triv.	—	(b,s)	—	—	—	674195
581	$GeAlO_2F$	$P4mm$ (99)	Triv.	—	(b,s)	—	—	—	674205
582	$KSiO_2F$	$P4mm$ (99)	Triv.	—	(b,s)	—	—	—	674212
583	$GeGaO_2F$	$P4mm$ (99)	Triv.	—	—	—	—	—	674223
584	$RbSiO_2F$	$P4mm$ (99)	Triv.	—	(b,s)	—	—	—	674238
585	$SrZrO_3$	$P4mm$ (99)	Triv.	—	(b,s)	—	—	—	674926 188449
586	$YBaCuFeO_5$	$P4mm$ (99)	SM	—	(b,s)	FM	—	—	67978$^{(l)}$ 71355 87466 241398$^{(l)}$
587	$Pb(TiO_3)$	$P4mm$ (99)	Triv.	—	(b,s)	NM	—	—	1610 1611 1612 16621 31152 51838$^{(k)}$ 51839$^{(k,l)}$ 51840 51841$^{(k,l)}$ 55054 55055 55056 55057 55058 55059 55060 55061 60188 61168 61169$^{(k)}$ 90693 93553 161709 162044$^{(k)}$ 162045 162046$^{(k)}$ 162048 165498$^{(k)}$ 186727 236933
588	$K(NbO_3)$	$P4mm$ (99)	Triv.	—	(k*,b,s,l*)	NM	—	—	9532 9535 190921

589	Ba(TiO_3)	$P4mm$ (99)	Triv.	—	(b,s)	NM	—	—	$15453^{(l)}$ $23758^{(k,l)}$ $23759^{(k,l)}$ $30617^{(k,l)}$ $31153^{(k,l)}$ $34637^{(k,l)}$ $67520^{(k,l)}$ $73642^{(k)}$ $73643^{(k)}$ $73644^{(k)}$ $73645^{(k,l)}$ $73646^{(k,l)}$ 95436 99737 $100799^{(k,l)}$ $100800^{(k,l)}$ $100801^{(k,l)}$ $100802^{(k,l)}$ $100803^{(k,l)}$ $100804^{(k,l)}$ $130020^{(k)}$ $154343^{(k,l)}$ $154345^{(k,l)}$ $157806^{(k,l)}$ $161340^{(l)}$ $161418^{(l)}$ 168763 $183932^{(k,l)}$ $185407^{(k,l)}$ $186457^{(k,l)}$ 186458 186459 188644 189381 190835 $192889^{(l)}$ $237105^{(k)}$ $237107^{(k)}$ $237108^{(k)}$ $245944^{(k,l)}$ $245945^{(k,l)}$ $245946^{(k,l)}$ 248395 $252558^{(l)}$ $253030^{(k,l)}$ $253245^{(k,l)}$ $290023^{(k,l)}$ $671606^{(k,l)}$ $673334^{(k)}$
590	Sr(HfO_3)	$P4mm$ (99)	Triv.	—	(b,s,l*)	NM	—	—	161594
591	$La_1Mn_1O_3$	$P4mm$ (99)	Triv.	Fig. 34	(k*,b,s,l*)	—	—	—	673198
592	$CaHfO_3$	$P4mm$ (99)	Triv.	—	(b,s)	—	—	—	674068
593	$CaTiO_3$	$P4mm$ (99)	Triv.	—	(b,s)	—	—	—	674096
594	$KWNO_2$	$P4mm$ (99)	Triv.	—	(b,s)	—	—	—	674127
595	$ZnAlO_2F$	$P4mm$ (99)	Triv.	—	(b)	—	—	—	674207
596	$KSnO_2F$	$P4mm$ (99)	Triv.	—	(b,s)	—	—	—	674215
597	$(VO)_3(AsO_3)_2$	$P4bm$ (100)	SM	Fig. 35	(b)	FM	—	HQ	424067
598	$Ba_2(TiO)(Si_2O_7)$	$P4bm$ (100)	Triv.	—	(b)	NM	—	—	4451 15715 34453 $66628^{(s)}$ $66629^{(s)}$ 155316 201844 201845 672977
599	$Ba_2(VO)(Si_2O_7)$	$P4bm$ (100)	SM	—	(b)	FM	—	HQ	51479 98722
600	$K_2(Zn_6O_7)$	$P4_2nm$ (102)	Triv.	—	(b)	NM	—	—	1120 2496
601	$LiSr_4Si_4N_8F$	$P4nc$ (104)	Triv.	—	(b,s)	—	—	—	432269
602	$Cu(Sb_2O_4)$	$P4_2bc$ (106)	SM	—	(b)	FM	—	HQ	190731
603	Sr_2SbMnO_6	$I4mm$ (107)	Triv.	—	(b,s)	—	—	HQ	39351 190647
604	$SrCu_2(BO_3)_2$	$I4cm$ (108)	Triv.	—	(b)	FM	—	HQ	247206
605	Ca_5Ge_3	$I4cm$ (108)	SM	—	—	NM	—	—	181076
606	Li_8SeN_2	$I4_1md$ (109)	Triv.	—	—	NM	—	HQ	247255 247256 421252
607	$ZnGa_2S_4$	$P\bar{4}2m$ (111)	Triv.	—	(b)	NM	—	—	635300
608	$CdTeMoO_6$	$P\bar{4}2_1m$ (113)	Triv.	—	(b)	NM	—	HQ	93794 188038
609	Ca(FeO_2)	$P\bar{4}2_1m$ (113)	Triv.	—	—	FM	—	HQ	246244 674880
610	Ca(FeO_2)	$P\bar{4}2_1m$ (113)	TI	—	(b,s)	AFM	—	HQ	246245
611	$Ca_2Zn(Si_2O_7)$	$P\bar{4}2_1m$ (113)	Triv.	—	(b)	NM	—	HQ	18114 $30262^{(s)}$ $186944^{(s)}$
612	$Ca_2Be(Si_2O_7)$	$P\bar{4}2_1m$ (113)	Triv.	—	(b,s)	NM	—	HQ	31234 94063
613	$Sr_2Zn(Ge_2O_7)$	$P\bar{4}2_1m$ (113)	Triv.	—	(b,s)	NM	—	HQ	39159 251824 420521 670006
614	$Ba_2Cu(Ge_2O_7)$	$P\bar{4}2_1m$ (113)	SM	—	(b,s)	FM	—	—	77132
615	$Sr_2Mn(Ge_2O_7)$	$P\bar{4}2_1m$ (113)	SM	—	(b,s)	AFM	—	HQ	84033
616	$Ca_2Co(Si_2O_7)$	$P\bar{4}2_1m$ (113)	SM	—	(b)	AFM	—	HQ	94132 $94135^{(s)}$ $94137^{(s)}$ 94139
617	$Ba_2Cu(Si_2O_7)$	$P\bar{4}2_1m$ (113)	SM	—	(b,s)	FM	—	HQ	97762
618	$K_2Fe(P_2O_7)$	$P\bar{4}2_1m$ (113)	Triv.	—	—	—	—	HQ	191281
619	$K_2Cu(P_2O_7)$	$P\bar{4}2_1m$ (113)	SM	—	(b)	FM	—	HQ	191282
620	$Sr_2Co(Ge_2O_7)$	$P\bar{4}2_1m$ (113)	SM	—	(b,s)	AFM	—	HQ	262398 262399
621	$Ba_2Co(Si_2O_7)$	$P\bar{4}2_1m$ (113)	SM	—	(b,s)	AFM	—	HQ	281293
622	$Ba_2Co(Ge_2O_7)$	$P\bar{4}2_1m$ (113)	SM	—	(b,s)	AFM	—	HQ	290483 290484 423350 423351
623	$Ba_2Zn(Ge_2O_7)$	$P\bar{4}2_1m$ (113)	Triv.	—	(b,s)	NM	—	HQ	420550
624	$YBa_2CuCu_2O_6$	$P\bar{4}m2$ (115)	TI	—	(b,s)	—	—	—	63423
625	Pb_2OF_2	$P\bar{4}m2$ (115)	Triv.	—	(b)	NM	—	—	76964
626	Mo_2CuGa_5	$P\bar{4}m2$ (115)	Triv.	—	—	—	—	—	670138
627	SiO_2	$P\bar{4}c2$ (116)	Triv.	—	(b,s)	NM	—	—	170532
628	K(NbF_6)	$P\bar{4}c2$ (116)	Triv.	—	(b,s)	NM	—	—	16729
629	K(BiF_6)	$P\bar{4}c2$ (116)	Triv.	—	(b,s)	NM	—	—	25025
630	SiO_2	$P\bar{4}n2$ (118)	Triv.	—	(b,s)	NM	—	—	170511
631	$RbMnSe_2$	$I\bar{4}m2$ (119)	Triv.	—	(b,s)	FM	—	HQ	50819
632	$BaCu(Si_2O_6)$	$I\bar{4}m2$ (119)	Triv.	—	(b)	—	—	HQ	74633
633	$KMnS_2$	$I\bar{4}m2$ (119)	Triv.	—	(b,s)	—	—	—	672264
634	$KMnSe_2$	$I\bar{4}m2$ (119)	Triv.	—	(b,s)	—	—	—	672265
635	$KMnTe_2$	$I\bar{4}m2$ (119)	Triv.	—	(b,s)	—	—	—	672266 87983
636	$RbMnTe_2$	$I\bar{4}m2$ (119)	Triv.	—	(b,s)	FM	—	HQ	87984

637	KAgO	$I\bar{4}m2$ (119)	Triv.	—	(b)	—	—	HQ	24818 37324 188525
638	KCuO	$I\bar{4}m2$ (119)	Triv.	—	—	NM	—	HQ	37325 188522
639	NaAgO	$I\bar{4}m2$ (119)	Triv.	—	(b)	NM	—	HQ	49752 188524
640	NaCuO	$I\bar{4}m2$ (119)	Triv.	—	(b)	NM	—	HQ	49756 188521
641	$SrCu_2(BO_3)_2$	$I\bar{4}c2$ (120)	Triv.	—	(b)	—	—	HQ	247205
642	$(Ag(XeF_2)_2)(PF_6)$	$I\bar{4}c2$ (120)	Triv.	—	(b,s)	—	—	HQ	412662
643	$SrCu_2(BO_3)_2$	$I\bar{4}2m$ (121)	Triv.	—	(b)	FM	—	HQ	247061 247200 247201 247202 247204
644	$AgFe_2GaTe_4$	$I\bar{4}2m$ (121)	Triv.	—	—	FM	—	HQ	192470
645	$K(H_2PO_4)$	$I\bar{4}2d$ (122)	Triv.	—	(b)	NM	—	HQ	66079 30257 76195 87895
646	$Cs_2(V_4O_9)$	$I\bar{4}2d$ (122)	Triv.	—	(b)	AFM	—	HQ	79409
647	CO_2	$I\bar{4}2d$ (122)	Triv.	—	(b,s)	NM	—	—	188890 290503 674668
648	$AgAlS_2$	$I\bar{4}2d$ (122)	Triv.	—	—	NM	—	—	28744 604692 604694 604698
649	$KCoO_2$	$I\bar{4}2d$ (122)	SM	—	(b,s)	FM	—	—	4199
650	SiS_2	$I\bar{4}2d$ (122)	Triv.	—	(b,s)	NM	—	HQ	16952 291214 291215 291216 291217
651	CaF_2	$P4/mmm$ (123)	Triv.	—	—	NM	—	—	51237
652	$CsLaNb_2O_7$	$P4/mmm$ (123)	Triv.	—	(b,s)	NM	—	HQ	82378
653	$Ba(TiO_3)$	$P4/mmm$ (123)	SM	—	(b)	NM	—	—	109327
654	MgNiH	$P4/mmm$ (123)	SM	—	(b)	NM	—	—	187257
655	CsV_2OS_2	$P4/mmm$ (123)	SM	—	(b,s,l)	FM	—	—	430299
656	$CaFeO_2$	$P4/mmm$ (123)	SM	—	(b,s,l)	—	—	—	674881 173438
657	AlMn	$P4/mmm$ (123)	SM	—	—	FM	—	—	57969 608456
658	CdPt	$P4/mmm$ (123)	SM	—	—	NM	—	—	102052 102053 620293 620295 620296
659	HgPt	$P4/mmm$ (123)	SM	—	—	NM	—	—	104337
660	$HgBa_2CuO_4$	$P4/mmm$ (123)	SM	—	(b,s,l)	NM	SC	—	75720 75721 75722 75723 75724
661	Bi_2YO_4Cl	$P4/mmm$ (123)	Triv.	—	(b)	NM	—	HQ	92405
662	Bi_2YO_4Br	$P4/mmm$ (123)	Triv.	—	(b)	NM	—	HQ	92418
663	$LaCr_2Si_2C$	$P4/mmm$ (123)	SM	—	(b,s,l)	FM	—	—	160691
664	$BaPd_2As_2$	$P4/mmm$ (123)	SM	—	—	NM	—	—	36376 190705
665	$Cs_2(MnF_5)$	$P4/mmm$ (123)	Triv.	—	—	FM	—	HQ	69675
666	$K_2(AlF_5)$	$P4/mmm$ (123)	Triv.	—	—	NM	—	—	81864
667	$Rb_2(MnF_5)$	$P4/mmm$ (123)	Triv.	—	—	FM	—	HQ	82218
668	KCu_4S_3	$P4/mmm$ (123)	SM	—	—	NM	SC	HQ	23336 602356 602358$^{(b,s)}$
669	$(CuCl)LaTa_2O_7$	$P4/mmm$ (123)	SM	—	(b,s)	FM	—	HQ	51261
670	$InPd_3$	$P4/mmm$ (123)	SM	—	—	NM	—	—	59476
671	$MnRh_2Sb$	$P4/mmm$ (123)	SM	Fig. 35	—	FM	—	—	76202
672	Cu_2NiZn	$P4/mmm$ (123)	TI	—	—	NM	—	—	103079
673	$AlNi_3$	$P4/mmm$ (123)	SM	—	—	—	—	—	107862
674	Pd_3Tl	$P4/mmm$ (123)	SM	—	—	—	—	—	108675
675	Pd_3V	$P4/mmm$ (123)	SM	—	(k*)	FM	—	—	108677
676	Pt_3Al	$P4/mmm$ (123)	SM	—	(k*)	NM	—	—	109235 191186
677	Pt_3In	$P4/mmm$ (123)	SM	—	(k*)	NM	—	—	109236
678	FeNiN	$P4/mmm$ (123)	SM	—	(b)	FM	—	—	53505
679	PdO	$P4/mmm$ (123)	TI	—	—	NM	—	—	28837
680	FeSe	$P4/mmm$ (123)	SM	—	—	FM	—	—	53543 633467
681	$FeSi_2$	$P4/mmm$ (123)	TI	—	—	FM	—	HQ	5257 24360 633533 633544 633550
682	$FeSi_2$	$P4/mmm$ (123)	TI	—	—	FM	—	—	5258
683	Hg_2Rh	$P4/mmm$ (123)	SM	—	—	NM	—	—	106786
684	HgMn	$P4/mmm$ (123)	SM	—	—	FM	—	—	104323
685	HgNi	$P4/mmm$ (123)	SM	—	—	NM	—	—	104332 639119
686	NbRu	$P4/mmm$ (123)	SM	—	—	NM	—	—	105222 645296
687	NiZn	$P4/mmm$ (123)	SM	—	—	NM	—	—	105469 647134 647137
688	RuTa	$P4/mmm$ (123)	SM	—	—	NM	—	—	105995 105996 650691 650692
689	AuMn	$P4/mmm$ (123)	SM	—	—	FM	—	—	109349
690	SrSi	$P4/mmm$ (123)	SM	—	—	—	—	—	160108
691	MgNi	$P4/mmm$ (123)	TI	—	—	NM	—	—	187255
692	$K_2(PdBr_4)$	$P4/mmm$ (123)	Triv.	—	—	NM	—	HQ	1982
693	K_2PtCl_4	$P4/mmm$ (123)	Triv.	—	—	NM	—	HQ	2722$^{(b)}$ 23998$^{(b)}$ 37014$^{(b)}$ 37015$^{(b)}$ 60110 68767$^{(b)}$ 68768$^{(b)}$

694	K_2PdCl_4	$P4/mmm$ (123)	Triv.	—	—	NM	—	HQ	2723 23997 27522$^{(b)}$ 39852 65034$^{(b)}$ 65035$^{(b)}$ 65036 68769 73505 73506
695	K_2PtBr_4	$P4/mmm$ (123)	Triv.	—	—	NM	—	HQ	6063
696	$Cs_2(PdCl_4)$	$P4/mmm$ (123)	Triv.	—	—	NM	—	HQ	95813
697	$NaAlF_4$	$P4/mmm$ (123)	Triv.	—	(b,s,l)	NM	—	—	20572
698	$Rb(FeF_4)$	$P4/mmm$ (123)	SM	—	(b,s,l)	FM	—	—	21072
699	$Tl(AlF_4)$	$P4/mmm$ (123)	Triv.	—	(b,s,l)	NM	—	—	25615 200637 202453 202454
700	$LaNiO_2$	$P4/mmm$ (123)	SM	—	(b,s,l)	FM	—	—	47123 153058
701	$SrFeO_2$	$P4/mmm$ (123)	SM	—	(b,s,l)	AFM	—	HQ	173434 418603 418605 418606
702	$KCuF_3$	$P4/mmm$ (123)	SM	—	(k*,b,s,l)	—	—	—	27689
703	$K(CrF_3)$	$P4/mmm$ (123)	Triv.	—	(b,s,l)	FM	—	—	27690
704	$Ba(TiO_3)$	$P4/mmm$ (123)	Triv.	—	(k*,b,s,l)	NM	—	—	27965 27966 27967 27968 27969 27974 28620 29146 29148 29280 31884 31885 31886 31887 31888 31889 31890 67519 187292 674386
705	$Na(NbO_3)$	$P4/mmm$ (123)	Triv.	—	(k*,b,s,l)	NM	—	—	28584 28585 28586 28587
706	$Pb(TiO_3)$	$P4/mmm$ (123)	Triv.	—	(b,s,l)	—	—	—	28624 29117$^{(k)}$
707	$Tl(CuF_3)$	$P4/mmm$ (123)	SM	—	(b,s,l)	—	—	—	43457
708	$Rb(CuF_3)$	$P4/mmm$ (123)	SM	—	(b,s,l)	—	—	—	109293
709	$CsAuCl_3$	$P4/mmm$ (123)	SM	—	(k*,b,s,l)	NM	—	HQ	417373
710	$SrGaO_2F$	$P4/mmm$ (123)	Triv.	—	(b,s)	—	—	—	674208
711	$BaAlO_2F$	$P4/mmm$ (123)	Triv.	—	(b,s)	—	—	—	674211
712	$RbHfO_2F$	$P4/mmm$ (123)	Triv.	—	(b,s)	—	—	—	674219
713	$YBaMn_2O_5$	$P4/mmm$ (123)	SM	—	(b,s)	AFM	—	HQ	83690
714	$LaBaMn_2O_6$	$P4/mmm$ (123)	SM	—	(k*,b,s,l*)	FM	—	HQ	150703
715	$LaRu_2Al_2B$	$P4/mmm$ (123)	TI	—	(b,s,l)	NM	—	HQ	174342
716	$CsCa_2(Ta_3O_{10})$	$P4/mmm$ (123)	Triv.	—	(b,s,l)	NM	—	HQ	89011
717	$RbSr_2(Nb_3O_{10})$	$P4/mmm$ (123)	Triv.	—	(b,s,l)	NM	SC*	HQ	93674
718	$CsSr_2(Nb_3O_{10})$	$P4/mmm$ (123)	Triv.	—	(b,s,l)	NM	SC	HQ	93675
719	$CsBa_2(Nb_3O_{10})$	$P4/mmm$ (123)	Triv.	—	(b,s,l)	NM	SC*	HQ	93676 671284
720	$CsSr_2(Ta_3O_{10})$	$P4/mmm$ (123)	Triv.	—	(b,s,l)	NM	—	HQ	93677
721	$RbCa_2(Nb_3O_{10})$	$P4/mmm$ (123)	Triv.	—	(b,s,l)	NM	SC*	HQ	260289
722	$CsBa_2Ta_3O_{10}$	$P4/mmm$ (123)	Triv.	—	(b,s,l)	—	—	—	671285
723	$RbLa(Ta_2O_7)$	$P4/mmm$ (123)	Triv.	—	(b,s)	NM	—	HQ	81870
724	$TlYBa_2Cu_2O_7$	$P4/mmm$ (123)	TI	—	(b,s,l*)	NM	SC*	HQ	74163
725	$Ba_2YCu_3O_6$	$P4/mmm$ (123)	TI	—	(b,s)	NM	SC*	HQ	63269 63424 66903 67016 68008 68046 68290 72254 84739 203116
726	$HgBa_2CaCu_2O_6$	$P4/mmm$ (123)	TI	—	(b,s,l*)	NM	SC	—	75725 75726 75727 75728 75729 83087
727	SiO_2	$P4/nbm$ (125)	SM	—	—	NM	—	—	170502
728	SiO_2	$P4/nbm$ (125)	TI	Fig. 35	(b,s)	NM	—	—	170538
729	$RbAg_5Se_3$	$P4/nbm$ (125)	SM	—	—	NM	—	HQ	50738
730	$K_8(Tl_{10}Zn)$	$P4/nnc$ (126)	SM	—	—	NM	—	—	165614
731	SiO_2	$P4/nnc$ (126)	SM	—	—	NM	—	—	170503
732	SiO_2	$P4/nnc$ (126)	Triv.	—	—	NM	—	—	170537
733	Rb_2IN_3	$P4/mbm$ (127)	Triv.	—	—	NM	—	HQ	202077
734	$Cs_2V_3O_8$	$P4/mbm$ (127)	SM	—	(b,s)	—	—	—	239713
735	Mn_2Hg_5	$P4/mbm$ (127)	SM	—	—	—	SC	—	670164 104324
736	NaO_2	$P4/mbm$ (127)	SM	—	—	—	—	—	673261
737	$Ti_3Co_5B_2$	$P4/mbm$ (127)	SM	—	—	NM	—	—	20140
738	Mn_2Ga_5	$P4/mbm$ (127)	SM	—	—	FM	SC*	HQ	249632 634613 634639
739	$Cs_3(GeF_7)$	$P4/mbm$ (127)	Triv.	Fig. 35	—	NM	—	HQ	202917
740	$K(AlF_4)$	$P4/mbm$ (127)	Triv.	—	(b,s)	NM	—	HQ	16413 60524 201947 201948 201949
741	$Rb(AlF_4)$	$P4/mbm$ (127)	Triv.	—	(b,s)	NM	—	HQ	54120 54121 200638$^{(l)}$
742	$Rb(FeF_4)$	$P4/mbm$ (127)	SM	—	(b,s)	FM	—	HQ	85499
743	$(PbCl_2)(Pb(CO_3))$	$P4/mbm$ (127)	TI	—	—	—	—	—	38358
744	$KCuF_3$	$P4/mbm$ (127)	SM	—	(b)	FM	—	HQ	21110$^{(s,l)}$ 21111
745	$Na(TaO_3)$	$P4/mbm$ (127)	Triv.	—	(b,s)	NM	—	HQ	23322$^{(l)}$ 88377 239692 280101$^{(l)}$
746	$Na(NbO_3)$	$P4/mbm$ (127)	Triv.	—	(b,s)	NM	—	—	23563$^{(l)}$ 192406$^{(l)}$ 236892 280100

747	$NaMgF_3$	$P4/mbm$ (127)	Triv.	—	(b,s,l*)	NM	—	HQ	193088
748	$BaPtLa_2O_5$	$P4/mbm$ (127)	Triv.	—	(b,s)	NM	—	HQ	68794 670385
749	$FeMo_2B_2$	$P4/mbm$ (127)	SM	—	—	FM	—	—	5431 44292
750	W_2FeB_2	$P4/mbm$ (127)	SM	—	—	FM	—	—	43016
751	$InNi_2Sc_2$	$P4/mbm$ (127)	SM	—	—	NM	—	HQ	107333
752	$FeNb_2B_2$	$P4/mbm$ (127)	SM	—	—	FM	—	—	614047
753	$Li_2Sr_4N_8Si_4O$	$P4/mnc$ (128)	Triv.	—	(b,s)	NM	—	—	420677
754	Na_3ScF_6	$P4/mnc$ (128)	Triv.	—	(b,s)	—	—	—	671947
755	$K_2(TeBr_6)$	$P4/mnc$ (128)	Triv.	—	—	NM	—	—	37270 65117
756	$Tl_2(TeBr_6)$	$P4/mnc$ (128)	Triv.	—	—	NM	—	HQ	99127
757	WO_3	$P4/nmm$ (129)	Triv.	Fig. 35	(b,s)	NM	—	—	89092 27961$^{(l)}$ 27962$^{(l)}$ 88367$^{(k)}$ 673313$^{(k)}$
758	VSe	$P4/nmm$ (129)	SM	—	—	NM	—	—	162898
759	CrSe	$P4/nmm$ (129)	Triv.	—	—	FM	—	—	162899
760	WH_4	$P4/nmm$ (129)	Triv.	—	—	NM	—	—	247601 247602
761	HfCd	$P4/nmm$ (129)	Triv.	—	—	NM	—	—	619964
762	$AgLa(TiO_4)$	$P4/nmm$ (129)	Triv.	—	(b,s)	NM	—	—	78719
763	Sr_2NiO_3Cl	$P4/nmm$ (129)	SM	—	(b,s)	AFM	—	—	237581
764	$Ba_2Pb_4Br_2F_{10}$	$P4/nmm$ (129)	Triv.	—	—	NM	—	—	411087
765	$Ba_2Pb_4I_2F_{10}$	$P4/nmm$ (129)	Triv.	—	—	NM	—	—	411088
766	$BaNiS_2$	$P4/nmm$ (129)	TI	—	—	NM	—	—	15289 246945
767	$K(CoO_2)$	$P4/nmm$ (129)	TI	—	—	FM	—	—	15770
768	$CsLiBr_2$	$P4/nmm$ (129)	Triv.	—	—	NM	—	—	40479 245979
769	$BaHfN_2$	$P4/nmm$ (129)	Triv.	—	—	NM	—	—	50994 184052 184053 184054 184055 184056 184057
770	$Ba(ZrN_2)$	$P4/nmm$ (129)	Triv.	—	—	NM	—	—	74904 74905
771	$BaCoS_2$	$P4/nmm$ (129)	SM	—	—	FM	—	—	82639
772	$CsAgCl_2$	$P4/nmm$ (129)	Triv.	—	—	NM	—	—	150300
773	$CsAgBr_2$	$P4/nmm$ (129)	Triv.	—	—	NM	—	—	150302
774	$SrNiS_2$	$P4/nmm$ (129)	TI	—	—	—	—	—	673416
775	Ir_2YSi_2	$P4/nmm$ (129)	SM	—	—	NM	—	—	44668 181770 188325 641031 641036
776	$Sr_2Sb_2Se_4F_2$	$P4/nmm$ (129)	Triv.	—	—	NM	—	—	171430
777	Bi_2OS_2	$P4/nmm$ (129)	Triv.	—	—	NM	SC	—	196230
778	$Ca_2Ge_2Ni_2H_2$	$P4/nmm$ (129)	SM	—	—	NM	—	—	263028
779	$CsMnF_4$	$P4/nmm$ (129)	Triv.	—	(b,s)	FM	—	—	14104
780	Fe_2As	$P4/nmm$ (129)	SM	—	—	FM	—	—	16844 415628 610464 610470 610472
781	KNaO	$P4/nmm$ (129)	Triv.	—	—	NM	—	—	32743
782	FeLiP	$P4/nmm$ (129)	SM	—	—	NM	SC	—	42327 247089 632441 247248
783	MnAlGe	$P4/nmm$ (129)	TI	—	—	FM	—	—	42750 607972 607974 657172
784	MnVAs	$P4/nmm$ (129)	SM	—	—	FM	—	—	44009
785	NiRhAs	$P4/nmm$ (129)	SM	—	—	NM	—	—	44030 187596 601484
786	MgMnGe	$P4/nmm$ (129)	SM	—	—	FM	—	—	66948 66952$^{(b)}$ 66953 87116$^{(b)}$ 87117$^{(b)}$
787	CaMnSn	$P4/nmm$ (129)	SM	—	—	FM	—	—	66958$^{(b)}$ 66950 66959$^{(b)}$
788	MnFeAs	$P4/nmm$ (129)	TI	—	—	FM	—	—	93237 93238 610492
789	CoLiAs	$P4/nmm$ (129)	SM	—	—	NM	—	—	107932
790	LiFeAs	$P4/nmm$ (129)	SM	—	—	FM	SC	—	162056 162250 163870 166457 290700 610480 169175
791	LiFeP	$P4/nmm$ (129)	TI	—	—	NM	—	—	166456
792	CoMnSb	$P4/nmm$ (129)	SM	—	—	FM	—	—	248374 248375 248376 248377
793	MgCoGe	$P4/nmm$ (129)	SM	—	—	NM	—	—	418853
794	MnCuAs	$P4/nmm$ (129)	SM	—	—	FM	—	—	423230
795	GaMnGe	$P4/nmm$ (129)	SM	—	—	FM	—	—	634253 634255
796	$Fe(MoO_4)Cl$	$P4/nmm$ (129)	SM	—	(b,s)	AFM	—	—	49516 202186 202187 202188
797	$FeWO_4Cl$	$P4/nmm$ (129)	SM	—	(b,s)	AFM	—	—	80798
798	FeSe	$P4/nmm$ (129)	SM	—	—	NM	SC*	—	26889 162901 163559 163560 163561 163562 165958 165959 165960 169970 182544 185464 196297 196298 977901 977903
799	FeS	$P4/nmm$ (129)	Triv.	—	—	NM	SC	—	42977 43391 81087 182249 182250 238590 633302 182251
800	FeTe	$P4/nmm$ (129)	SM	—	—	FM	—	—	44753 169974

801	MnSe	$P4/nmm$ (129)	SM	—	—	FM	—	—	162900
802	CoSe	$P4/nmm$ (129)	SM	—	—	FM	—	—	162902
803	FeSe	$P4/nmm$ (129)	TI	—	—	NM	—	—	169253 169255 169257 169259 169261 169263 169265 169267 169269 169271 290701
804	FeTe	$P4/nmm$ (129)	TI	—	—	FM	SC*	—	180602 633877
805	FeSe	$P4/nmm$ (129)	Triv.	—	—	FM	—	—	633480
806	$K(MoO(PO_4)Cl)$	$P4/nmm$ (129)	SM	—	(b)	FM	—	—	50988
807	$Na_2(TiO)(GeO_4)$	$P4/nmm$ (129)	Triv.	—	(b,s)	NM	—	—	20129 91546 160148
808	$Li_2(VO)(SiO_4)$	$P4/nmm$ (129)	SM	—	(b)	AFM	—	—	59359 417276 $417277^{(s)}$ $417278^{(s)}$ 417279 $417280^{(s)}$ 417281 417282 417283 417284 417285 417286
809	$Ag_3Cl(CrO_4)$	$P4/nmm$ (129)	Triv.	—	(b)	NM	—	—	409541
810	LiMnP	$P4/nmm$ (129)	SM	—	—	FM	—	—	26458
811	LiMnAs	$P4/nmm$ (129)	SM	—	—	FM	—	—	26459 60739 60740 60741 60742 192817 192818 192819 192820 192821 192822 192823
812	LiMnSb	$P4/nmm$ (129)	SM	—	—	FM	—	—	642150
813	TiSe	$P4/nmm$ (129)	SM	—	—	NM	—	—	162897
814	SnO	$P4/nmm$ (129)	SM	—	—	NM	—	—	185350
815	BaBrF	$P4/nmm$ (129)	Triv.	—	—	NM	—	—	1129 2294 35393 155005
816	PbFCl	$P4/nmm$ (129)	Triv.	—	—	NM	—	—	5037 30287 31132 39165 82884 155010
817	PbFBr	$P4/nmm$ (129)	Triv.	—	—	NM	—	—	5038 30288 155011
818	BiOF	$P4/nmm$ (129)	Triv.	—	—	NM	—	—	24096 201620
819	BiOCl	$P4/nmm$ (129)	Triv.	—	—	NM	—	—	24608 29143 74502 195115 185970
820	CaHCl	$P4/nmm$ (129)	Triv.	—	—	NM	—	—	25601 37199
821	SrHCl	$P4/nmm$ (129)	Triv.	—	—	NM	—	—	25602 37200
822	BaHCl	$P4/nmm$ (129)	Triv.	—	—	NM	—	—	25603 37201
823	NaMnP	$P4/nmm$ (129)	SM	—	—	FM	—	—	26460 60726 60727 60728 60729 601595
824	NaMnAs	$P4/nmm$ (129)	SM	—	—	FM	—	—	26461 60730 60731 60732 610878
825	NaMnSb	$P4/nmm$ (129)	SM	—	—	FM	—	—	26462 60733 60734 60735 601596
826	BiOI	$P4/nmm$ (129)	Triv.	—	—	NM	—	—	29145 5036 24610 185972 391354
827	YOCl	$P4/nmm$ (129)	Triv.	—	—	NM	—	—	31667 60586
828	KMgSb	$P4/nmm$ (129)	Triv.	—	—	NM	—	—	41709
829	RbMnSb	$P4/nmm$ (129)	SM	—	—	FM	—	—	41868 643395 643396
830	CsMnSb	$P4/nmm$ (129)	SM	—	—	FM	—	—	41869 627027 627028
831	KMnP	$P4/nmm$ (129)	SM	—	—	FM	—	—	41882 89592 89593
832	KMnAs	$P4/nmm$ (129)	SM	—	—	FM	—	—	41883 60743 60744 60745
833	MnBaGe	$P4/nmm$ (129)	SM	—	—	FM	—	—	42370 66964 66965 615891
834	CaMnGe	$P4/nmm$ (129)	SM	—	—	FM	—	—	52758 66956 $66957^{(b)}$
835	MnSrGe	$P4/nmm$ (129)	SM	—	—	FM	—	—	53707 66960 66961
836	NaMnBi	$P4/nmm$ (129)	SM	—	—	FM	—	—	60736 60737 60738 601587 616814
837	CaMnSi	$P4/nmm$ (129)	SM	—	—	FM	—	—	66949 66954 66955
838	SrMnSn	$P4/nmm$ (129)	SM	—	—	FM	—	—	66951 66962 66963
839	LaMnSi	$P4/nmm$ (129)	SM	—	—	FM	—	—	75046 75047 85849 641449
840	MnYSi	$P4/nmm$ (129)	TI	—	—	FM	—	—	76235 643705
841	LaMnGe	$P4/nmm$ (129)	SM	—	—	FM	—	—	80007 80008 85857
842	LaFeSi	$P4/nmm$ (129)	SM	—	—	NM	—	—	85853 632432 656907
843	LaCoGe	$P4/nmm$ (129)	Triv.	—	—	FM	—	—	85860
844	KMnSb	$P4/nmm$ (129)	SM	—	—	FM	—	—	89590 89591 602269
845	RbMnP	$P4/nmm$ (129)	SM	—	—	FM	—	—	89594 89595 643229
846	RbMnAs	$P4/nmm$ (129)	SM	—	—	FM	—	—	89596 89597 610910
847	CoGeLa	$P4/nmm$ (129)	TI	—	—	FM	—	—	106471
848	PbFI	$P4/nmm$ (129)	Triv.	—	—	NM	—	—	150194 150195 56667 150193 155012 279599
849	NaFeAs	$P4/nmm$ (129)	SM	—	—	FM	SC	—	163143 163144
850	KMnBi	$P4/nmm$ (129)	SM	—	—	FM	—	—	601586
851	KMgAs	$P4/nmm$ (129)	Triv.	—	—	NM	—	—	610753
852	CsMnBi	$P4/nmm$ (129)	SM	—	—	FM	—	—	616575
853	RbMnBi	$P4/nmm$ (129)	SM	—	—	FM	—	—	616824
854	CoLaSi	$P4/nmm$ (129)	Triv.	—	—	FM	—	—	624027
855	CoPdP	$P4/nmm$ (129)	TI	—	(b)	NM	—	—	624599

856	CoLaSi	$P4/nmm$ (129)	SM	—	—	FM	—	—	658265
857	$BaSnF_4$	$P4/nmm$ (129)	Triv.	—	(b,s)	NM	—	—	166207 673273
858	CsMnAs	$P4/nmm$ (129)	SM	—	—	FM	—	—	40572 40573 610293
859	CsMnP	$P4/nmm$ (129)	SM	—	—	FM	—	—	89598 89599 627022
860	SrFI	$P4/nmm$ (129)	Triv.	—	—	NM	—	—	155009 159280
861	$(Fe_2As_2)(Sr_4Sc_2O_6)$	$P4/nmm$ (129)	Triv.	—	(b,s)	FM	SC	—	180528
862	$(Co_2As_2)(Sr_4Sc_2O_6)$	$P4/nmm$ (129)	SM	—	(b,s)	—	—	—	262356
863	$(Co_2P_2)(Sr_4Sc_2O_6)$	$P4/nmm$ (129)	SM	—	(b,s)	FM	—	—	262357
864	$NaKLaNbO_5$	$P4/nmm$ (129)	Triv.	—	(b)	NM	—	—	94743
865	$LaKNaTaO_5$	$P4/nmm$ (129)	Triv.	—	(b)	NM	—	—	419855
866	YOF	$P4/nmm$ (129)	Triv.	—	—	NM	—	—	76426
867	LaOF	$P4/nmm$ (129)	Triv.	—	—	NM	—	—	76427 430270$^{(b)}$
868	BiCuSeO	$P4/nmm$ (129)	Triv.	—	—	NM	—	—	74475 75128 189174 262598 674374
869	LaCoPO	$P4/nmm$ (129)	SM	—	—	FM	—	—	80203 161910 161911
870	$LaAgSb_2$	$P4/nmm$ (129)	TI	—	—	NM	—	—	95220 95221 95222 95223
871	SrCuFS	$P4/nmm$ (129)	Triv.	—	—	NM	—	—	157433
872	LaFePO	$P4/nmm$ (129)	Triv.	—	—	FM	—	—	162724 391428 420381
873	SrFeAsF	$P4/nmm$ (129)	Triv.	—	—	FM	SC	—	162808 163915 168775
874	LaFeAsO	$P4/nmm$ (129)	Triv.	—	—	AFM	—	—	163496 163497 163835 163868 173432 180438 180439 180440 184645 192739 421998 602489
875	SrCuFS	$P4/nmm$ (129)	TI	—	—	NM	—	—	172796
876	BaFCuS	$P4/nmm$ (129)	Triv.	—	—	NM	—	—	183712
877	SrFMnP	$P4/nmm$ (129)	SM	—	—	FM	—	—	189939
878	SrFMnAs	$P4/nmm$ (129)	SM	—	—	—	—	—	189940
879	SrFMnSb	$P4/nmm$ (129)	SM	—	—	FM	—	—	189941
880	CrLaAsO	$P4/nmm$ (129)	Triv.	—	—	AFM	—	—	237385 237387
881	CrLaAsO	$P4/nmm$ (129)	TI	—	—	AFM	—	—	237386
882	BaMnSbF	$P4/nmm$ (129)	SM	—	—	FM	—	—	248364 248366
883	BaMnAsF	$P4/nmm$ (129)	SM	—	—	—	—	—	248365
884	LaMnSbO	$P4/nmm$ (129)	SM	—	—	FM	—	—	419355
885	BaMnBiF	$P4/nmm$ (129)	SM	—	—	—	—	—	426033
886	$LaFeSb_2$	$P4/nmm$ (129)	SM	—	—	FM	—	—	657914 657985
887	$LaCoSb_2$	$P4/nmm$ (129)	SM	—	—	FM	—	—	657919 657990
888	VZrSi	$P4/nmm$ (129)	SM	—	—	NM	—	—	42337 652544
889	LaTiGe	$P4/nmm$ (129)	SM	—	—	NM	—	—	107617
890	HfVGe	$P4/nmm$ (129)	SM	—	—	NM	—	—	636594
891	HfVSi	$P4/nmm$ (129)	SM	—	—	NM	—	—	638931
892	WO_3	$P4/ncc$ (130)	Triv.	—	(b,s)	—	—	—	673314 50732 50733 88366
893	Ca_5Ge_3	$P4/ncc$ (130)	TI	—	—	NM	—	—	181075
894	$CuBi_2O_4$	$P4/ncc$ (130)	SM	—	(b)	FM	SC	HQ	15865 56390 67018$^{(s)}$ 68812$^{(s)}$ 68813$^{(s)}$ 68814$^{(s)}$ 68815$^{(s)}$ 69307$^{(s)}$ 69308$^{(s)}$ 69746 69747 71313$^{(s)}$ 202994$^{(s)}$
895	$PdBi_2O_4$	$P4/ncc$ (130)	Triv.	—	(b)	NM	—	HQ	200145
896	Na_2PdCl_4	$P4/ncc$ (130)	Triv.	—	(b)	NM	—	HQ	202971
897	$Sr_3(SiO_4)O$	$P4/ncc$ (130)	Triv.	—	—	NM	—	—	18151 28534 418933$^{(b)}$
898	CaNiN	$P4_2/mmc$ (131)	SM	—	(b)	NM	—	—	69044 656846
899	$KCuC_2$	$P4_2/mmc$ (131)	Triv.	—	—	NM	—	HQ	412037 412038
900	$RbCuC_2$	$P4_2/mmc$ (131)	Triv.	—	—	NM	—	HQ	412039 412040
901	IrN	$P4_2/mmc$ (131)	Triv.	—	—	NM	—	—	187717
902	SiO_2	$P4_2/mcm$ (132)	Triv.	—	(b,s)	NM	—	—	170500
903	Pb_3O_4	$P4_2/mbc$ (135)	Triv.	—	(b)	NM	—	—	4106 22325 36253 42484 647270
904	$Cu(As_2O_4)$	$P4_2/mbc$ (135)	SM	Fig. 35	(b)	FM	—	HQ	4287 16829
905	$FeO(Sb_2O_3)$	$P4_2/mbc$ (135)	Triv.	—	(b)	FM	—	HQ	4459 61466 61467 61468 61469 61470 61471 61472 61473 155151 182798
906	$FeSb_2O_4$	$P4_2/mbc$ (135)	SM	—	(b)	FM	—	—	30350 158916
907	Pb_3O_4	$P4_2/mbc$ (135)	SM	—	(b,s)	NM	—	—	647261
908	$LiSr_2(CoN_2)$	$P4_2/mnm$ (136)	SM	—	(b)	FM	—	HQ	72387
909	MoO_2	$P4_2/mnm$ (136)	Triv.	—	(b)	—	—	—	670200 99714 644069
910	Li_2S_2	$P4_2/mnm$ (136)	Triv.	—	—	—	—	—	671853

911	VF_2	$P4_2/mnm$ (136)	SM	—	(b)	—	—	—	673336 32552 38069 62768 62769 201245
912	CoF_2	$P4_2/mnm$ (136)	SM	—	(b)	—	—	—	674847 9167 14144 26604 53987 73460 98785 98786 280604
913	Hf_2Cu_2In	$P4_2/mnm$ (136)	SM	—	—	—	—	—	130032
914	$IrIn_3$	$P4_2/mnm$ (136)	SM	—	—	NM	—	HQ	407548 639819
915	$RhIn_3$	$P4_2/mnm$ (136)	SM	—	—	NM	SC	HQ	407549 640336
916	$RhGa_3$	$P4_2/mnm$ (136)	SM	—	—	NM	—	—	635208
917	$ZrNi_4P_2$	$P4_2/mnm$ (136)	SM	—	—	—	SC	HQ	40435 76681
918	$KPd(PS_4)$	$P4_2/mnm$ (136)	Triv.	—	(b,s)	NM	—	HQ	165315
919	$Li_3(BN_2)$	$P4_2/mnm$ (136)	Triv.	—	(b)	NM	—	—	71085
920	WOI_3	$P4_2/mnm$ (136)	Triv.	—	(b,s)	FM	—	HQ	65183
921	$WOCl_3$	$P4_2/mnm$ (136)	Triv.	—	(b,s)	FM	—	HQ	416393
922	$K_2Na_4(Be_2O_5)$	$P4_2/mnm$ (136)	Triv.	—	(b)	NM	—	HQ	33849
923	MnO_2	$P4_2/mnm$ (136)	SM	Fig. 35	(b)	AFM	—	HQ	393 20229 56006 73716 246888 643186 643187 643197 670198 670366
924	VO_2	$P4_2/mnm$ (136)	SM	—	(b)	FM	—	HQ	1504 4110 10141 24926 27482 34418 34420 34421 56003 66665 237337 647613 647637
925	ZnF_2	$P4_2/mnm$ (136)	Triv.	—	(b)	NM	—	HQ	9169 14146 26606 53981 76270 184219 280605
926	CrO_2	$P4_2/mnm$ (136)	Triv.	—	—	FM	—	HQ	9423$^{(b)}$ 28711$^{(b)}$ 35327 43461$^{(b)}$ 43739$^{(b)}$ 155831$^{(b)}$ 166021$^{(b)}$ 166022$^{(b)}$ 166023$^{(b)}$ 166024$^{(b)}$ 166025$^{(b)}$ 166026$^{(b)}$ 166027$^{(b)}$ 166028$^{(b)}$ 166485$^{(b)}$ 167237$^{(b)}$ 185885$^{(b)}$ 186836$^{(b)}$ 202835$^{(b)}$ 202836$^{(b)}$ 202837$^{(b)}$ 202838$^{(b)}$ 246898$^{(b)}$ 246899$^{(b)}$ 246900$^{(b)}$ 246901$^{(b)}$ 246902$^{(b)}$ 626487$^{(b)}$ 670197$^{(b)}$
927	RuO_2	$P4_2/mnm$ (136)	Triv.	—	(b)	NM	—	HQ	15071 23961 51159 56007 84575 84618 108861 172178 236962 236963 290496 647373 647376 647377 670201 670735 671872
928	Mg_2C	$P4_2/mnm$ (136)	TI	—	(b)	—	—	—	671332
929	$Zn(Sb_2O_6)$	$P4_2/mnm$ (136)	Triv.	—	(b)	NM	—	—	30409 96612
930	$Fe(Sb_2O_6)$	$P4_2/mnm$ (136)	SM	—	(b)	AFM	—	—	40344
931	$Ni(Ta_2O_6)$	$P4_2/mnm$ (136)	Triv.	Fig. 36	(b)	FM	—	HQ	61198 247807
932	$NiSb_2O_6$	$P4_2/mnm$ (136)	Triv.	—	(b)	AFM	—	—	80802 426852
933	$Cu(Ta_2O_6)$	$P4_2/mnm$ (136)	SM	Fig. 36	(b)	FM	—	—	83367
934	$Cu(Sb_2O_6)$	$P4_2/mnm$ (136)	SM	—	(b)	FM	—	HQ	84789
935	$Co(Ta_2O_6)$	$P4_2/mnm$ (136)	SM	—	(b)	AFM	—	—	166673 166674 203095 247812
936	Pb_2F_2O	$P4_2/nmc$ (137)	Triv.	—	(b)	NM	—	HQ	10416
937	$Pb_2(ZnF_6)$	$P4_2/ncm$ (138)	Triv.	—	(b,s)	NM	—	—	162073 162074
938	Ba_2CuWO_6	$I4/mmm$ (139)	SM	—	(b,s)	FM	—	—	33569
939	Cs_2CuO_2	$I4/mmm$ (139)	SM	—	(b,s,l)	FM	—	HQ	39535
940	$K_4Al_2Nb_{11}O_{20}F$	$I4/mmm$ (139)	Triv.	—	(b)	NM	—	—	65738
941	$Ba_2Cu_2(Si_4O_{12})$	$I4/mmm$ (139)	TI	—	(b)	FM	—	HQ	71535
942	$CsFe_2As_2$	$I4/mmm$ (139)	SM	—	—	FM	SC	—	74877
943	$CrNbF_6$	$I4/mmm$ (139)	SM	—	(b,s)	FM	—	HQ	75384
944	$Sr_2Cu_2MnO_2S_2$	$I4/mmm$ (139)	SM	—	(b,s,l)	AFM	SC	HQ	84734
945	V_4Zn_5	$I4/mmm$ (139)	SM	—	—	NM	—	—	106213 653404
946	LaF_3	$I4/mmm$ (139)	Triv.	—	—	NM	—	—	167555 155554 164056 96133 96134
947	C	$I4/mmm$ (139)	Triv.	—	—	NM	—	—	190717 190718 190719 182761 190716
948	CaO_2	$I4/mmm$ (139)	Triv.	—	—	—	—	—	671324 619462 20275
949	Cu_3Ti_2	$I4/mmm$ (139)	SM	—	—	FM	—	—	103132 629380 629398
950	Al_3Nb	$I4/mmm$ (139)	SM	—	—	NM	SC	—	58015 107857 186000 608658 608663 608670 608672 608682 608686 608690 670156 670759
951	Al_3V	$I4/mmm$ (139)	SM	Fig. 36	—	NM	SC	—	58201 151104 167811 609613 609617 670975
952	$InPd_3$	$I4/mmm$ (139)	TI	—	—	NM	—	—	247188 247189 420251
953	$TlPd_3$	$I4/mmm$ (139)	TI	—	—	NM	—	HQ	247272 649056 649063
954	$CrSi_2$	$I4/mmm$ (139)	SM	—	—	NM	—	—	71499
955	Ag_2Sc	$I4/mmm$ (139)	SM	—	—	NM	—	—	605791 605793
956	Au_2Hf	$I4/mmm$ (139)	SM	—	—	NM	—	—	611956

957	$Ba_2Cu_3O_4Br_2$	$I4/mmm$ (139)	SM	—	(b)	NM	—	—	36128 75576
958	$Ba_2(ZnF_6)$	$I4/mmm$ (139)	Triv.	—	(b,s,l)	NM	—	—	21054
959	$TlCo_2Se_2$	$I4/mmm$ (139)	SM	—	—	FM	—	—	67362 95138 95139 95140 95141 625007 674509
960	KCo_2Se_2	$I4/mmm$ (139)	SM	—	—	FM	—	—	67370 182837 182838 623961
961	$BaCu_2S_2$	$I4/mmm$ (139)	Triv.	—	—	NM	—	HQ	89575 203088 615832 615834 615837 670743
962	$TlCo_2S_2$	$I4/mmm$ (139)	SM	—	—	FM	—	HQ	100438 624879
963	KFe_2S_2	$I4/mmm$ (139)	SM	—	—	NM	SC*	—	186572
964	KNi_2Se_2	$I4/mmm$ (139)	SM	—	—	FM	SC	HQ	424686 641276
965	KNi_2S_2	$I4/mmm$ (139)	SM	—	—	—	SC	—	431754 641273
966	Co_2KS_2	$I4/mmm$ (139)	SM	Fig. 36	—	FM	—	—	623956
967	Co_2RbS_2	$I4/mmm$ (139)	SM	—	—	FM	—	—	624795
968	$Sr_2CoO_2Cl_2$	$I4/mmm$ (139)	SM	—	(b,s,l)	AFM	—	HQ	59697 151787 151788
969	$Sr_2CoO_2Br_2$	$I4/mmm$ (139)	SM	—	(b,s,l)	AFM	—	HQ	59698 151789 151790
970	$Sr_3(Co_2O_5Cl_2)$	$I4/mmm$ (139)	TI	Fig. 36	(b,s)	FM	—	HQ	90123 91749
971	KO_2	$I4/mmm$ (139)	SM	—	—	FM	—	HQ	38245 180563 196755 38138
972	CsO_2	$I4/mmm$ (139)	SM	—	—	FM	—	—	38247 627060 627062
973	BaC_2	$I4/mmm$ (139)	Triv.	—	—	NM	—	—	56160 88098 88101 168410 186575 615792 615794
974	RbO_2	$I4/mmm$ (139)	SM	—	—	FM	—	—	180564 196756 647338
975	CoO	$I4/mmm$ (139)	SM	—	—	AFM	—	—	53059 174027
976	MnN	$I4/mmm$ (139)	SM	—	—	FM	—	—	106932
977	Sr_2FeMoO_6	$I4/mmm$ (139)	Triv.	Fig. 37	(b,s)	—	—	—	94079 151617 169377$^{(k)}$ 184911
978	$Ba_2(FeReO_6)$	$I4/mmm$ (139)	SM	Fig. 36	(k*,b,s)	FM	—	HQ	155174
979	Sr_2VZrO_6	$I4/mmm$ (139)	SM	Fig. 36	(k*,b,s)	FM	—	—	191359
980	Sr_2VHfO_6	$I4/mmm$ (139)	SM	Fig. 36	(k*,b,s)	FM	—	—	191360
981	Sr_2CoHfO_6	$I4/mmm$ (139)	SM	—	(k*,b,s)	FM	—	—	191364
982	Sr_2FeZrO_6	$I4/mmm$ (139)	Triv.	—	—	—	—	—	191365
983	Sr_2FeHfO_6	$I4/mmm$ (139)	Triv.	—	(k*,b,s)	AFM	—	—	191366
984	$Ba_2Fe(MoO_6)$	$I4/mmm$ (139)	Triv.	Fig. 37	(k*,b,s)	FM	—	HQ	246541 246542 246543 246544
985	$Pb_2Co(TeO_6)$	$I4/mmm$ (139)	SM	—	(k*,b,s)	FM	—	HQ	405782
986	$BaBi_2Zn$	$I4/mmm$ (139)	Triv.	—	—	NM	—	—	58638
987	Bi_2CdSr	$I4/mmm$ (139)	Triv.	—	—	NM	—	HQ	58764
988	K_2CuF_4	$I4/mmm$ (139)	SM	—	(b,s,l)	FM	—	HQ	15372 31688
989	Cs_2AgF_4	$I4/mmm$ (139)	SM	Fig. 37	(b,s,l)	FM	—	—	16254
990	Cs_2CdCl_4	$I4/mmm$ (139)	Triv.	—	(b,s,l)	—	—	—	16576
991	$(SrO)_2TiO_2$	$I4/mmm$ (139)	Triv.	—	(b,s,l)	NM	SC*	—	20293 157402 194713 194714 194715 194716 194717 194718 194719
992	K_2MnF_4	$I4/mmm$ (139)	SM	—	(b,s,l)	FM	—	—	23183 23184 33521
993	$Sr_2(MnO_4)$	$I4/mmm$ (139)	SM	—	(b,s,l)	FM	—	—	26560 26561 50794
994	Sr_2SnO_4	$I4/mmm$ (139)	Triv.	—	(b,s,l)	NM	—	—	27114 84245 150387 150388 150389 150390
995	Sr_4P_2O	$I4/mmm$ (139)	Triv.	—	(b,s,l)	NM	—	HQ	33903
996	Rb_2CaH_4	$I4/mmm$ (139)	Triv.	Fig. 37	(b,s,l)	NM	—	—	65196
997	K_2MgH_4	$I4/mmm$ (139)	Triv.	Fig. 37	(b,s,l)	NM	—	—	68358
998	K_4OBr_2	$I4/mmm$ (139)	Triv.	—	(b,s,l)	NM	—	HQ	68505
999	$Ba_2(ZrS_4)$	$I4/mmm$ (139)	Triv.	—	(b,s,l)	NM	—	HQ	69853 80651
1000	Cs_2HgF_4	$I4/mmm$ (139)	Triv.	—	(b,s,l)	NM	—	—	72353
1001	Cs_2MgH_4	$I4/mmm$ (139)	Triv.	Fig. 37	(b,s,l)	NM	—	—	162261
1002	$Sr_2(CrO_4)$	$I4/mmm$ (139)	TI	—	(b,s,l)	FM	—	HQ	245595
1003	$Sr_2(CoO_4)$	$I4/mmm$ (139)	SM	—	(b,s,l)	AFM	—	HQ	246483
1004	Rb_4Br_2O	$I4/mmm$ (139)	Triv.	—	(b,s,l)	NM	—	HQ	411954
1005	$K_4(Ru_2Cl_{10}O)$	$I4/mmm$ (139)	Triv.	—	—	NM	—	HQ	8054
1006	ScLaSb	$I4/mmm$ (139)	TI	—	—	NM	—	HQ	427126
1007	YNi_2B_2C	$I4/mmm$ (139)	SM	—	(b)	NM	SC	—	41549 75816 79574 83231 89142
1008	$Li_2Sr(Ta_2O_7)$	$I4/mmm$ (139)	Triv.	—	(b)	NM	—	HQ	88464 154175 246278
1009	KCuO	$I4/mmm$ (139)	Triv.	—	—	NM	—	HQ	40158
1010	RbCuO	$I4/mmm$ (139)	Triv.	—	—	NM	—	HQ	40159
1011	Cs(AuO)	$I4/mmm$ (139)	Triv.	—	—	NM	—	HQ	409553
1012	Pd_3Tl	$I4/mmm$ (139)	SM	Fig. 37	—	NM	—	—	105729
1013	$InPd_3$	$I4/mmm$ (139)	SM	Fig. 37	—	NM	—	—	247194 247195 420250

1014	K_2NiO_2	$I4/mmm$ (139)	Triv.	—	(b)	FM	—	—	21069 201891
1015	$Na_2(HgO_2)$	$I4/mmm$ (139)	Triv.	—	(b)	NM	—	—	25511 27409
1016	$Rb_2(NiO_2)$	$I4/mmm$ (139)	Triv.	—	(b)	AFM	—	HQ	66277
1017	$Sr_2(ZnN_2)$	$I4/mmm$ (139)	Triv.	—	(b)	NM	—	HQ	80376 670402
1018	La_2PdO_4	$I4/mmm$ (139)	TI	—	(b,s,l)	NM	—	—	40262
1019	$Cs_2(PdCl_4)I_2$	$I4/mmm$ (139)	SM	—	—	NM	—	HQ	240484
1020	$Rb_3(TlF_6)$	$I4/mmm$ (139)	Triv.	—	—	NM	—	—	19075
1021	Cs_3TlF_6	$I4/mmm$ (139)	Triv.	—	—	NM	—	—	19076
1022	Rb_3YF_6	$I4/mmm$ (139)	Triv.	Fig. 38	—	NM	—	—	19077
1023	Cs_3YF_6	$I4/mmm$ (139)	Triv.	—	—	NM	—	—	19078
1024	$RbNa_2NiO_2$	$I4/mmm$ (139)	SM	—	(b)	FM	—	HQ	73209
1025	$CsK_2(CoO_2)$	$I4/mmm$ (139)	Triv.	—	(b)	AFM	—	HQ	74889
1026	Co	$I4/mmm$ (139)	SM	—	—	—	—	—	671035
1027	PbF_4	$I4/mmm$ (139)	Triv.	—	(b,s,l)	NM	—	—	16795 78895
1028	$(Cu_2S_2)(Sr_2NiO_2)$	$I4/mmm$ (139)	TI	—	(b,s,l)	FM	—	HQ	88424
1029	$K_3Zn_2F_7$	$I4/mmm$ (139)	Triv.	—	(b,s,l*)	NM	—	—	9925 100299
1030	$K_3Cu_2F_7$	$I4/mmm$ (139)	Triv.	—	(b,s,l*)	FM	—	HQ	15373
1031	$(SrO)_3(TiO_2)_2$	$I4/mmm$ (139)	Triv.	Fig. 38	(b,s,l*)	NM	—	—	20294 34629 63704
1032	$Sr_3V_2O_7$	$I4/mmm$ (139)	TI	—	(b,s,l*)	FM	—	HQ	71320 71451
1033	$K_2Sr(Ta_2O_7)$	$I4/mmm$ (139)	Triv.	—	(b,s)	NM	—	HQ	93492
1034	$CaCo_2Ge_2$	$I4/mmm$ (139)	TI	—	—	NM	—	—	406 81751
1035	$CaCo_2P_2$	$I4/mmm$ (139)	TI	—	—	FM	SC*	HQ	10462 85890 85891 85892 619210
1036	Co_2YB_2	$I4/mmm$ (139)	SM	—	—	NM	SC	HQ	23653 55298 602345 613409 613423
1037	$LaCo_2B_2$	$I4/mmm$ (139)	SM	Fig. 38	—	NM	—	HQ	41787 55297 181185 182572 182573 423045 613135
1038	Ir_2YSi_2	$I4/mmm$ (139)	SM	—	—	NM	SC	—	44667 181768 181769 188326 600299 641030
1039	$CaRh_2P_2$	$I4/mmm$ (139)	TI	Fig. 38	—	NM	SC	HQ	50185
1040	$SrRh_2P_2$	$I4/mmm$ (139)	TI	—	—	NM	—	HQ	50186
1041	$LaCo_2Si_2$	$I4/mmm$ (139)	SM	Fig. 38	—	NM	—	—	52999 90777
1042	Co_2YSi_2	$I4/mmm$ (139)	SM	—	—	NM	—	—	53088 427109 625128
1043	$LaRh_2Ge_2$	$I4/mmm$ (139)	SM	Fig. 38	—	NM	—	—	55926 81759 636847
1044	YCo_2Ge_2	$I4/mmm$ (139)	SM	—	—	NM	SC	HQ	81748 623662
1045	$LaCo_2Ge_2$	$I4/mmm$ (139)	SM	—	—	FM	—	HQ	81750 291377 623460
1046	$LaCo_2P_2$	$I4/mmm$ (139)	SM	—	—	FM	—	—	87581 87582 87583 624010
1047	$SrRh_2As_2$	$I4/mmm$ (139)	TI	—	—	NM	—	—	165120
1048	$CaFe_2As_2$	$I4/mmm$ (139)	TI	—	—	AFM	—	—	166016 182277 182278 182279
1049	$CaFe_2As_2$	$I4/mmm$ (139)	TI	—	—	AFM	SC	—	182276 192309 192310 192311
1050	$SrRh_2As_2$	$I4/mmm$ (139)	TI	—	—	NM	—	HQ	417002
1051	$CaCo_2Si_2$	$I4/mmm$ (139)	TI	—	—	NM	—	HQ	420974
1052	$CaFe_2Si_2$	$I4/mmm$ (139)	SM	—	—	FM	—	HQ	425467
1053	$LaRh_2Si_2$	$I4/mmm$ (139)	SM	—	—	NM	—	—	601417 601614 603880 604623 641747 641750 641752
1054	$CaCo_2As_2$	$I4/mmm$ (139)	TI	—	—	FM	—	—	609899
1055	Co_2LaAs_2	$I4/mmm$ (139)	SM	—	—	FM	—	—	610073
1056	$CsCo_2S_2$	$I4/mmm$ (139)	SM	—	—	FM	—	—	622529
1057	$CsCo_2Se_2$	$I4/mmm$ (139)	SM	—	—	FM	—	—	622533
1058	Co_2RbSe_2	$I4/mmm$ (139)	SM	—	—	FM	—	—	624798
1059	Co_2ScSi_2	$I4/mmm$ (139)	SM	—	—	NM	—	—	624957 624959
1060	Al_8Fe_4Y	$I4/mmm$ (139)	SM	Fig. 39	—	FM	—	—	57842 240140 240141 607728 607735
1061	$Be_{12}Pd$	$I4/mmm$ (139)	SM	—	—	NM	SC	—	109314
1062	$ScFe_4Al_8$	$I4/mmm$ (139)	SM	—	—	FM	—	HQ	240138 240139 607626
1063	Al_8Fe_4Hf	$I4/mmm$ (139)	TI	Fig. 38	—	FM	—	—	607535
1064	Al_8Fe_4Zr	$I4/mmm$ (139)	TI	Fig. 38	—	FM	—	—	607756
1065	$K(BrF_4)$	$I4/mcm$ (140)	Triv.	—	—	FM	—	—	16633 10326 16700
1066	$(K(HF_2))(IF_5)_2$	$I4/mcm$ (140)	Triv.	—	—	NM	—	—	71583
1067	$Li_5(VO)(PO_4)_2$	$I4/mcm$ (140)	TI	—	(b)	FM	—	—	245847
1068	Hf_2Ge	$I4/mcm$ (140)	SM	—	—	NM	—	—	636554
1069	$FeSn_2$	$I4/mcm$ (140)	SM	Fig. 39	—	FM	SC	—	24570 102800 103636 247483 409909 604017 633753 633760 633761
1070	$MnSn_2$	$I4/mcm$ (140)	SM	—	—	FM	SC	—	24571 102799 171198 247482 643736 643742

1071	Zr_2Si	$I4/mcm$ (140)	TI	—	—	NM	SC	—	24717 42522 652618
1072	$FeGe_2$	$I4/mcm$ (140)	SM	Fig. 39	—	FM	SC	—	42519 77313 195131 631984 631999 632023 632024
1073	$SiHf_2$	$I4/mcm$ (140)	TI	—	—	NM	SC	—	42523 638912
1074	Hf_2Ge	$I4/mcm$ (140)	TI	—	—	NM	SC	—	42524 636547 636548
1075	$CoSn_2$	$I4/mcm$ (140)	SM	—	—	NM	SC	—	102672 108319 247484 409910 625260 625263 625269
1076	$RuSn_2$	$I4/mcm$ (140)	SM	—	—	NM	—	—	105993
1077	$FeSb_2$	$I4/mcm$ (140)	TI	—	—	FM	—	—	186636 186638 186639 186640 186641 186642
1078	Zr_2Si	$I4/mcm$ (140)	SM	—	—	NM	—	—	652615
1079	Ca_5Ge_3	$I4/mcm$ (140)	SM	Fig. 39	—	NM	—	—	42139 93704 181074
1080	Ca_5Si_3	$I4/mcm$ (140)	SM	Fig. 39	—	NM	—	HQ	93699
1081	$Ba_3O(SiO_4)$	$I4/mcm$ (140)	Triv.	—	—	NM	—	HQ	1449
1082	Tl_3CoCl_5	$I4/mcm$ (140)	SM	—	(b,s)	FM	—	—	10137
1083	$Sr_3(AlO_4)F$	$I4/mcm$ (140)	Triv.	—	(b)	NM	—	HQ	50736 195183 195184
1084	$CsSn_2Br_5$	$I4/mcm$ (140)	Triv.	—	(b)	NM	—	HQ	93792 151987
1085	$AgTlI_2$	$I4/mcm$ (140)	Triv.	—	(b,s)	NM	—	—	26318
1086	$RbAuF_4$	$I4/mcm$ (140)	Triv.	—	—	NM	—	—	9907 33952
1087	$CaPdF_4$	$I4/mcm$ (140)	Triv.	—	(b)	NM	—	—	32674
1088	$CdCuF_4$	$I4/mcm$ (140)	SM	—	(b)	FM	—	HQ	73478
1089	$BaPdF_4$	$I4/mcm$ (140)	Triv.	—	—	NM	—	—	108991
1090	$PbPdF_4$	$I4/mcm$ (140)	Triv.	—	—	NM	—	—	108992
1091	$Sr(ZrO_3)$	$I4/mcm$ (140)	Triv.	Fig. 39	(b,s)	NM	—	HQ	1522 89356 89357 89358 89359 89360 89361 89362$^{(1)}$ 89363$^{(1)}$ 89364$^{(1)}$ 188451 290620 674924
1092	$Sr(TiO_3)$	$I4/mcm$ (140)	Triv.	—	(b,s)	NM	—	—	56718$^{(1)}$ 182247 182762$^{(1)}$ 182763$^{(1)}$ 182764$^{(1)}$ 248380$^{(1)}$ 290619$^{(1)}$ 673335
1093	$Ca(TiO_3)$	$I4/mcm$ (140)	Triv.	—	(b,s)	NM	—	HQ	153173$^{(1)}$ 162919 162920 162921 162922 162923
1094	$Sr(TcO_3)$	$I4/mcm$ (140)	SM	—	(b,s,l*)	NM	—	HQ	183452
1095	$Ca(SiO_3)$	$I4/mcm$ (140)	Triv.	—	(b,s)	NM	—	—	240414 240415 240416 240417 240418 240419 240420 240421
1096	Ca_5Sn_3H	$I4/mcm$ (140)	SM	—	—	NM	—	HQ	165190
1097	$SrCu_2(BO_3)_2$	$I4/mcm$ (140)	TI	—	(b)	FM	—	—	92953 247207 247208
1098	$PbSe_2$	$I4/mcm$ (140)	Triv.	—	—	NM	—	HQ	174577
1099	Cl_2O	$I4_1/amd$ (141)	Triv.	—	—	NM	—	HQ	407768
1100	TiO_2	$I4_1/amd$ (141)	Triv.	—	—	NM	—	HQ	9852$^{(b)}$ 9853$^{(b)}$ 9854$^{(b)}$ 9855$^{(b)}$ 24276$^{(b)}$ 31064$^{(b)}$ 44882$^{(b)}$ 63711$^{(b)}$ 76173$^{(b)}$ 92363$^{(b)}$ 93098$^{(b)}$ 94566$^{(b)}$ 96946$^{(b)}$ 154601$^{(b)}$ 154602$^{(b)}$ 154603$^{(b)}$ 154604$^{(b)}$ 154607$^{(b)}$ 154608$^{(b)}$ 154609$^{(b)}$ 154610$^{(b)}$ 156838$^{(b)}$ 159910$^{(b)}$ 161908$^{(b)}$ 172914$^{(b)}$ 172916$^{(b)}$ 183767$^{(b)}$ 184368$^{(b)}$ 189318$^{(b)}$ 190785$^{(b)}$ 193265$^{(b)}$ 193267$^{(b)}$ 193269$^{(b)}$ 193271$^{(b)}$ 200392$^{(b)}$ 202242$^{(b)}$ 202243$^{(b)}$ 237000$^{(b)}$ 242104$^{(b)}$ 242105$^{(b)}$ 242106$^{(b)}$ 671957$^{(b)}$ 673140 674666$^{(b)}$
1101	$Rb_4(SbBr_6)_2$	$I4_1/amd$ (141)	Triv.	—	—	NM	—	—	26058
1102	$Cs_2(SbCl_6)$	$I4_1/amd$ (141)	Triv.	—	—	NM	—	—	49706 49707$^{(b)}$ 49708$^{(b)}$
1103	$Fe_2(PO_4)O$	$I4_1/amd$ (141)	SM	—	(b)	FM	—	HQ	80554 80555 108812 108813
1104	$Li_3(BN_2)$	$I4_1/amd$ (141)	Triv.	Fig. 39	(b,s)	NM	—	HQ	155126 155127
1105	$YCrO_4$	$I4_1/amd$ (141)	SM	—	(b)	FM	—	—	26989 95971 157933
1106	$BaGeGe_3O_9$	$P3$ (143)	Triv.	—	(b,s)	NM	—	—	15674
1107	$Ba_3Si_6O_9N_4$	$P3$ (143)	Triv.	—	(b)	NM	—	HQ	415918
1108	$Na_3(ReO_5)$	$P3_1$ (144)	Triv.	—	—	—	—	HQ	36637
1109	$CsCd(NO_2)_3$	$R3$ (146)	Triv.	—	—	NM	—	HQ	95536
1110	$RbCd(NO_2)_3$	$R3$ (146)	Triv.	—	—	NM	—	HQ	95537
1111	$KCd(NO_2)_3$	$R3$ (146)	Triv.	—	—	NM	—	HQ	95538
1112	$TlCd(NO_2)_3$	$R3$ (146)	Triv.	—	—	NM	—	HQ	95539
1113	$K_2Pb_2Ge_2O_7$	$P\bar{3}$ (147)	Triv.	—	(b,s)	NM	—	—	30247
1114	$Zr_3O_5(SO_4)$	$P\bar{3}$ (147)	Triv.	—	(b)	NM	—	—	68335
1115	$Zr(HPO_3)_2$	$P\bar{3}$ (147)	Triv.	—	(b)	NM	—	HQ	74463

1116	$Ba(CoPO_4)_2$	$P\bar{3}$ (147)	Triv.	—	(b)	FM	—	HQ	250709
1117	$Ba(Al_2Si_2O_8)$	$P\bar{3}$ (147)	Triv.	—	—	NM	—	HQ	188056 191252$^{(b,s)}$
1118	$CsFe(MoO_4)_2$	$P\bar{3}$ (147)	SM	Fig. 40	(b,s)	FM	—	—	191592
1119	$CsFe(SO_4)_2$	$P\bar{3}$ (147)	SM	—	(b)	AFM	—	—	245667
1120	$RbAg_2Fe(VO_4)_2$	$P\bar{3}$ (147)	SM	Fig. 40	(b,s)	AFM	—	HQ	194588 194589
1121	$Na_2BaMgP_2O_8$	$P\bar{3}$ (147)	Triv.	—	(b)	NM	—	HQ	262716
1122	$Zn(ReO_4)_2$	$P\bar{3}$ (147)	Triv.	Fig. 40	(b,s)	NM	—	—	51017
1123	$Li_{14}Cr_2N_8O$	$P\bar{3}$ (147)	Triv.	—	(b)	NM	—	HQ	66098 151435
1124	$Li_{14}(PON_3)_2O$	$P\bar{3}$ (147)	Triv.	—	—	NM	—	HQ	428737
1125	$Na_2(SO_3)$	$P\bar{3}$ (147)	Triv.	—	—	—	—	—	4432 31816
1126	$Mn(TiO_3)$	$R\bar{3}$ (148)	TI	Fig. 40	(b)	AFM	—	HQ	60006 171579 184649
1127	$NiPbF_6$	$R\bar{3}$ (148)	Triv.	—	(b,s)	FM	—	—	15108
1128	$LiMgAlF_6$	$P321$ (150)	Triv.	—	(b)	NM	—	—	5007
1129	AlF_3	$P321$ (150)	Triv.	—	(k*,b,s)	NM	—	—	29131
1130	$Sr_3(NbGa_3Si_2O_{14})$	$P321$ (150)	Triv.	—	(b,s)	NM	—	—	181650
1131	$Pb_3Ga_2Ge_4O_{14}$	$P321$ (150)	Triv.	Fig. 40	(b,s)	NM	—	HQ	250123
1132	$Ba_3Ga_2Ge_4O_{14}$	$P321$ (150)	Triv.	—	(b,s)	NM	—	HQ	250124
1133	$Sr_3Zn_3TeP_2O_{14}$	$P321$ (150)	Triv.	—	(b)	NM	—	—	252309
1134	$Ba_3Zn_3TeP_2O_{14}$	$P321$ (150)	Triv.	—	(b)	NM	—	—	252310
1135	SiO_2	$P3_121$ (152)	Triv.	—	—	NM	—	HQ	27745$^{(b,s)}$ 29122$^{(b,s)}$ 31048$^{(b,s)}$ 40009$^{(b,s)}$ 67117$^{(b,s)}$ 67121$^{(b,s)}$ 67122$^{(b,s)}$ 67123$^{(b,s)}$ 67124$^{(b,s)}$ 67125$^{(b,s)}$ 67126$^{(b,s)}$ 74529$^{(b,s)}$ 79634$^{(b,s)}$ 79635$^{(b,s)}$ 79636$^{(b,s)}$ 79637$^{(b,s)}$ 89658$^{(b,s)}$ 89659$^{(b,s)}$ 89660$^{(b,s)}$ 89661$^{(b,s)}$ 90145$^{(b,s)}$ 93974$^{(b,s)}$ 153453$^{(b,s)}$ 153454$^{(b,s)}$ 154289$^{(b,s)}$ 200721$^{(b,s)}$ 200722$^{(b,s)}$ 200723$^{(b,s)}$ 200724$^{(b,s)}$ 200725$^{(b,s)}$ 200726$^{(b,s)}$ 200727$^{(b,s)}$ 200728$^{(b,s)}$ 200729$^{(b,s)}$ 201352$^{(b,s)}$ 201353$^{(b,s)}$ 201354$^{(b,s)}$ 247141$^{(b,s)}$ 670929
1136	GeO_2	$P3_121$ (152)	Triv.	—	(b,s)	NM	—	—	53869 53870 59624 59625 59626 59627 59628 59629 59630 59631 59632 59633 59634 59635 59636 59637 59639 79638 79639 79640 79641 79642 79643 79644 200730 200731 200732 200733 200734 200735 200736
1137	$Tl(NO_2)$	$P3_121$ (152)	Triv.	—	—	NM	—	—	50325 50326
1138	$KBe_2(BO_3)F_2$	$R32$ (155)	Triv.	—	—	NM	—	HQ	77277 155156
1139	$CsBe_2BO_3F_2$	$R32$ (155)	Triv.	—	—	NM	—	HQ	247622 260440
1140	$Na_2Ca_3Ta_2O_9$	$R32$ (155)	Triv.	—	(b)	NM	—	HQ	280154
1141	$YAl_3(BO_3)_4$	$R32$ (155)	Triv.	—	(b)	NM	—	HQ	20223 91962 187082 674788
1142	$NaK(BH_4)_2$	$P3m1$ (156)	Triv.	—	—	NM	—	—	163376
1143	$NiO(OH)$	$P3m1$ (156)	SM	—	(b)	FM	—	—	169980
1144	$LiInMo_3O_8$	$P3m1$ (156)	Triv.	—	(b)	NM	—	—	30579
1145	$Cs_3(As_5O_9)$	$P31m$ (157)	Triv.	—	(b,s)	NM	—	HQ	413151
1146	$K_3(V_5O_{14})$	$P31m$ (157)	Triv.	—	(b,s)	NM	—	HQ	24068 248227
1147	$Rb_3(V_5O_{14})$	$P31m$ (157)	Triv.	—	(b,s)	NM	—	HQ	248228 420851
1148	$Mg_3(Si_2O_5)(OH)_4$	$P31m$ (157)	Triv.	—	(b,s)	NM	—	HQ	17046 67332 67333 75933 75934 87436 87438$^{(k)}$ 163889 163890 202358$^{(k)}$ 245887$^{(k)}$
1149	Si_3N_4	$P31c$ (159)	Triv.	—	—	NM	—	—	16752 26191$^{(b)}$ 34096$^{(b)}$ 35560$^{(b)}$ 35561$^{(b)}$ 35562$^{(b)}$ 35563$^{(b)}$ 35564$^{(b)}$ 35565$^{(b)}$ 77811$^{(b)}$ 79797$^{(b)}$ 90146$^{(b)}$ 92156$^{(b)}$ 239369$^{(b)}$ 644683$^{(b)}$
1150	$Rb_2(TeW_3O_{12})$	$P31c$ (159)	Triv.	—	(k*,b)	NM	—	—	97507
1151	$Tl_2(MoO_3)_3(SeO_3)$	$P31c$ (159)	Triv.	—	(k*,b,s)	NM	—	—	167531
1152	$KAl(SiO_4)$	$P31c$ (159)	Triv.	—	(b,s)	NM	—	HQ	83449
1153	Si_3N_4	$P31c$ (159)	SM	—	(b)	FM	—	—	159207 187735
1154	$K_3MnO_4CrO_4$	$R3m$ (160)	Triv.	—	(k*,b)	NM	—	HQ	26803
1155	$Cd(CN_2)$	$R3m$ (160)	Triv.	—	—	—	—	HQ	95265
1156	Bi_2O_3	$R3m$ (160)	Triv.	—	(b,s)	NM	—	—	168810
1157	C_3N_4	$R3m$ (160)	Triv.	—	(k*,b)	NM	—	—	246660 673898 674277 674292
1158	$CrO(OH)$	$R3m$ (160)	SM	—	—	AFM	—	HQ	1372 64754 88574

1159	$NaVS_2$	$R3m$ (160)	Triv.	—	(b)	FM	—	—	644994
1160	$FeAl_2S_4$	$R3m$ (160)	Triv.	—	(b)	—	—	—	607619
1161	$Y(HCOO)_3$	$R3m$ (160)	Triv.	—	—	NM	—	—	109739
1162	$K_2Na(Ag(CN)_2)_3$	$P\bar{3}1m$ (162)	Triv.	Fig. 40	(k,b)	NM	—	HQ	65699
1163	SiO_2	$P\bar{3}1m$ (162)	TI	—	(k*,b,s)	NM	—	—	170552
1164	$Hg_2(As_2O_6)$	$P\bar{3}1m$ (162)	Triv.	—	(b,s)	—	—	HQ	411230
1165	$Ag_3(Co(CN)_6)$	$P\bar{3}1m$ (162)	Triv.	—	(k,b)	NM	—	—	16959 28501
1166	$Ag_3(Fe(CN)_6)$	$P\bar{3}1m$ (162)	SM	—	(k,b)	FM	—	—	173552 173553
1167	$Cd(Sb_2O_6)$	$P\bar{3}1m$ (162)	Triv.	Fig. 40	(b)	NM	—	HQ	71028
1168	$Ca(Sb_2O_6)$	$P\bar{3}1m$ (162)	Triv.	—	(b,s)	NM	—	HQ	74539
1169	$Sr(Sb_2O_6)$	$P\bar{3}1m$ (162)	Triv.	—	(b,s)	NM	—	HQ	74540
1170	$Co(AsO_3)_2$	$P\bar{3}1m$ (162)	SM	—	(b)	AFM	—	HQ	80350
1171	$SrRu_2O_6$	$P\bar{3}1m$ (162)	Triv.	—	(b,s)	AFM	—	HQ	248351
1172	$Cd(As_2O_6)$	$P\bar{3}1m$ (162)	Triv.	—	(b,s)	NM	—	HQ	280576
1173	$K(Ag(CN)_2)$	$P\bar{3}1c$ (163)	Triv.	Fig. 40	(k*,b)	NM	—	—	30275
1174	SiO_2	$P\bar{3}1c$ (163)	SM	—	—	NM	—	—	170495
1175	$CdZn_2KB_2O_6F$	$P\bar{3}1c$ (163)	Triv.	—	(b)	NM	—	HQ	248025
1176	$(Ag_3(H_2O)_3)(K(CN)_2)_3$	$P\bar{3}1c$ (163)	Triv.	—	(k*)	—	—	—	248371
1177	$Na_2Al_2(B_2O_7)$	$P\bar{3}1c$ (163)	Triv.	—	(b)	NM	—	HQ	93389$^{(s)}$ 237154 237155 237156 237157
1178	Ti_3O	$P\bar{3}1c$ (163)	SM	Fig. 41	(b,s)	—	—	—	20041 24082
1179	$Cu_3Zn(OH)_6Cl_2$	$P\bar{3}m1$ (164)	SM	—	(k,b)	—	—	HQ	162099
1180	$Ba_2(BO_3)Br$	$P\bar{3}m1$ (164)	Triv.	—	—	—	—	HQ	190941
1181	$Cu_3MgCl_2(OH)_6$	$P\bar{3}m1$ (164)	SM	—	(k,b)	—	—	HQ	240663
1182	POF_3	$P\bar{3}m1$ (164)	Triv.	Fig. 41	—	—	—	HQ	250498
1183	$Zn(B(CN)_4)_2$	$P\bar{3}m1$ (164)	Triv.	—	(b)	NM	—	HQ	415547
1184	$Ba_3MnNb_2O_9$	$P\bar{3}m1$ (164)	SM	—	(k,b,s)	AFM	—	HQ	171479 239731
1185	$Sr_3MgTa_2O_9$	$P\bar{3}m1$ (164)	Triv.	—	(k,b,s)	NM	—	—	194992
1186	$Ba_6IrNb_2O_{12}Cl_2$	$P\bar{3}m1$ (164)	SM	—	(k*,b,s)	FM	—	HQ	40693
1187	$Ba_5(Nb_4O_{15})$	$P\bar{3}m1$ (164)	Triv.	—	(k,b,s)	NM	—	HQ	95192 157477 674451
1188	$Mn(OH)_2$	$P\bar{3}m1$ (164)	SM	—	—	AFM	—	—	23591
1189	$ReTi_2$	$P\bar{3}m1$ (164)	SM	—	—	NM	—	—	168953
1190	TiS_2	$P\bar{3}m1$ (164)	Triv.	—	(b)	NM	SC*	—	26861 41663 52195 91579 174489 181500 601182 601315 603788 604416 651178 651186 651201 651203 651207 651212 651214 651217
1191	MnI_2	$P\bar{3}m1$ (164)	SM	—	(b)	FM	—	—	33673
1192	$MnBr_2$	$P\bar{3}m1$ (164)	SM	—	(b)	FM	—	—	60250
1193	NbS_2	$P\bar{3}m1$ (164)	SM	—	(b)	NM	—	—	237032 250594
1194	$CrSe_2$	$P\bar{3}m1$ (164)	TI	—	(b)	FM	—	—	626718
1195	$Cs(Cu_3O_2)$	$P\bar{3}m1$ (164)	Triv.	—	(k,b,s)	NM	—	HQ	413342
1196	Fe_2Si	$P\bar{3}m1$ (164)	TI	—	—	FM	—	—	161133
1197	$FeGa_2S_4$	$P\bar{3}m1$ (164)	Triv.	—	(b)	FM	—	HQ	100706 602041
1198	K_2RhF_6	$P\bar{3}m1$ (164)	SM	—	(k*)	FM	—	—	28779
1199	$Rb_2(RhF_6)$	$P\bar{3}m1$ (164)	SM	—	(k*)	FM	—	—	28780
1200	$Tl_2(SnF_6)$	$P\bar{3}m1$ (164)	Triv.	—	(k*)	NM	—	HQ	410801
1201	$NaTl_3(SO_3)_2$	$P\bar{3}m1$ (164)	Triv.	—	—	NM	—	HQ	1626
1202	$Tl_2(WO_4)$	$P\bar{3}m1$ (164)	Triv.	—	(k*,b)	NM	—	HQ	8212
1203	$Na_2(SO_4)$	$P\bar{3}m1$ (164)	SM	Fig. 41	—	FM	—	—	27955
1204	$KNa(SO_4)$	$P\bar{3}m1$ (164)	Triv.	—	—	NM	—	—	77343
1205	$K_3V(VO_4)_2$	$P\bar{3}m1$ (164)	Triv.	—	(k*,b,s)	AFM	—	HQ	100782
1206	$Ca_2(GeO_4)$	$P\bar{3}m1$ (164)	Triv.	Fig. 41	(k*,b)	NM	—	—	182051
1207	$Ca_2(SiO_4)$	$P\bar{3}m1$ (164)	Triv.	Fig. 41	(k*,b)	NM	—	—	182052
1208	$Tl_2(MoO_4)$	$P\bar{3}m1$ (164)	Triv.	—	—	NM	—	HQ	280056
1209	$RbIn(WO_4)_2$	$P\bar{3}m1$ (164)	Triv.	Fig. 42	(k*,b)	NM	—	—	24859
1210	$KAl(MoO_4)_2$	$P\bar{3}m1$ (164)	Triv.	—	(k*,b,s)	NM	—	HQ	28018
1211	$KSc(MoO_4)_2$	$P\bar{3}m1$ (164)	Triv.	—	(k*,b,s)	NM	—	HQ	28019
1212	$KFe(MoO_4)_2$	$P\bar{3}m1$ (164)	SM	Fig. 41	(k*,b,s)	AFM	—	HQ	153864
1213	$BaZr(PO_4)_2$	$P\bar{3}m1$ (164)	Triv.	—	(k*,b)	NM	—	HQ	173842
1214	$CsV(MoO_4)_2$	$P\bar{3}m1$ (164)	Triv.	—	(k*,b,s)	AFM	—	HQ	202907
1215	$RbFe(MoO_4)_2$	$P\bar{3}m1$ (164)	SM	Fig. 41	(k*,b,s)	FM	—	—	245665 250409
1216	$CsFe(MoO_4)_2$	$P\bar{3}m1$ (164)	SM	Fig. 41	(k*,b,s)	FM	—	HQ	260887

1217	Li_2MnO_2	$P\bar{3}m1$ (164)	SM	—	—	FM	—	HQ	37327
1218	$CaMn_2As_2$	$P\bar{3}m1$ (164)	TI	—	—	FM	—	HQ	41792 609906
1219	$CaMn_2P_2$	$P\bar{3}m1$ (164)	TI	—	—	FM	—	HQ	49017
1220	$SrMn_2P_2$	$P\bar{3}m1$ (164)	TI	—	—	FM	—	HQ	49019 77669 77670
1221	$LiCrS_2$	$P\bar{3}m1$ (164)	SM	—	—	FM	—	—	150674
1222	$LiTiS_2$	$P\bar{3}m1$ (164)	SM	—	—	FM	—	HQ	200709 642322
1223	$LiCrSe_2$	$P\bar{3}m1$ (164)	SM	—	—	—	—	—	252879
1224	Rb_2PdC_2	$P\bar{3}m1$ (164)	Triv.	—	—	NM	—	HQ	94394 421493 421494
1225	Rb_2PtC_2	$P\bar{3}m1$ (164)	Triv.	—	—	NM	—	HQ	94395
1226	Cs_2PdC_2	$P\bar{3}m1$ (164)	Triv.	—	—	NM	—	HQ	94396
1227	Cs_2PtC_2	$P\bar{3}m1$ (164)	Triv.	—	—	NM	—	HQ	94397
1228	K_2PdC_2	$P\bar{3}m1$ (164)	Triv.	—	—	NM	—	HQ	421489 421490
1229	K_2PtC_2	$P\bar{3}m1$ (164)	Triv.	—	—	NM	—	HQ	421491 421492
1230	$Pd_3(PS_4)_2$	$P\bar{3}m1$ (164)	Triv.	—	(k,b)	NM	—	—	16296 35361
1231	$Rb_2(Sb_2Al_2O_7)$	$P\bar{3}m1$ (164)	Triv.	—	(k*,b,s)	NM	—	HQ	154360
1232	$NaFe_2O_3$	$P\bar{3}m1$ (164)	SM	—	—	FM	—	—	200009 424349
1233	$Cs_2Mn(TeS_3)_2$	$P\bar{3}c1$ (165)	SM	—	(b,s)	FM	—	HQ	165378
1234	$KFe(MoO_4)_2$	$P\bar{3}c1$ (165)	SM	—	(b,s)	AFM	—	HQ	28020
1235	K_5CuSb_2	$R\bar{3}m$ (166)	Triv.	—	(b)	NM	—	HQ	32032
1236	$K_2Pt_3PtS_6$	$R\bar{3}m$ (166)	Triv.	Fig. 42	(k*,b)	NM	—	—	40062
1237	Li_4NCl	$R\bar{3}m$ (166)	Triv.	—	—	NM	—	HQ	84649
1238	Li_5NCl_2	$R\bar{3}m$ (166)	Triv.	—	—	NM	—	HQ	84763
1239	C_{60}	$R\bar{3}m$ (166)	Triv.	—	—	NM	—	—	95370
1240	KPd_2O_3	$R\bar{3}m$ (166)	Triv.	—	(b)	NM	—	HQ	248051
1241	$K_2Hf_3OF_{12}$	$R\bar{3}m$ (166)	Triv.	—	—	—	—	—	251076
1242	ScAlOC	$R\bar{3}m$ (166)	Triv.	—	(b)	NM	—	HQ	419683
1243	CLi_6	$R\bar{3}m$ (166)	Triv.	—	(b)	—	—	—	670920
1244	Li_3In_2	$R\bar{3}m$ (166)	SM	—	—	NM	—	HQ	10051 659829
1245	$(B_{12}C)C_2$	$R\bar{3}m$ (166)	Triv.	—	—	NM	—	—	612562
1246	Ba_2NiTeO_6	$R\bar{3}m$ (166)	TI	Fig. 42	(k*,b,s)	AFM	—	—	25005
1247	$K_2Li(AlF_6)$	$R\bar{3}m$ (166)	Triv.	—	(b,s)	NM	—	HQ	408552 37250$^{(k)}$
1248	$Cs_9Ni_9F_{27}$	$R\bar{3}m$ (166)	TI	Fig. 42	(k,b,s)	FM	—	HQ	410393
1249	In_2Se_3	$R\bar{3}m$ (166)	SM	—	(b)	NM	—	—	17007 640489 640492 640498 640512
1250	$MnCl_2$	$R\bar{3}m$ (166)	SM	—	(b)	FM	—	HQ	33752
1251	$MnBr_2$	$R\bar{3}m$ (166)	SM	—	(b)	FM	—	HQ	67500
1252	Ni_7Y_2	$R\bar{3}m$ (166)	SM	—	(k)	FM	—	—	108650 647051 647060 647076
1253	$Cs_2Cu_3ZrF_{12}$	$R\bar{3}m$ (166)	SM	—	(k,b,s)	FM	—	HQ	79114 182755
1254	$Cs_2SnCu_3F_{12}$	$R\bar{3}m$ (166)	SM	—	(k,b,s)	FM	—	HQ	291388 291391
1255	$Cu_3Zn(OH)_6Cl_2$	$R\bar{3}m$ (166)	SM	Fig. 42	(k,b)	FM	—	HQ	425834
1256	$LiVO_2$	$R\bar{3}m$ (166)	Triv.	—	—	AFM	—	—	24594 202540 202541
1257	$KCrS_2$	$R\bar{3}m$ (166)	SM	—	(b)	FM	—	—	25723 42406 42407
1258	$NaTiS_2$	$R\bar{3}m$ (166)	SM	—	(b)	FM	—	—	26305
1259	$Cu(CrO_2)$	$R\bar{3}m$ (166)	SM	—	—	AFM	SC*	—	26676 157800 163253 163254 163255 184467 189047 194151 194152 402290 670110
1260	Ba_2PCl	$R\bar{3}m$ (166)	Triv.	—	—	NM	—	—	28134
1261	$LiGaO_2$	$R\bar{3}m$ (166)	Triv.	—	—	NM	—	—	28388
1262	$RbScO_2$	$R\bar{3}m$ (166)	Triv.	—	(b)	NM	—	—	31959
1263	$NaTiO_2$	$R\bar{3}m$ (166)	SM	—	(b)	FM	—	—	43439
1264	$LiFeO_2$	$R\bar{3}m$ (166)	SM	—	—	FM	—	HQ	51207 51759 78712
1265	Ca_2NCl	$R\bar{3}m$ (166)	Triv.	Fig. 42	(b)	NM	—	HQ	62555 153101
1266	Ca_2NBr	$R\bar{3}m$ (166)	Triv.	Fig. 42	(b)	NM	—	HQ	62556 153105
1267	$Na(RhO_2)$	$R\bar{3}m$ (166)	Triv.	—	—	NM	—	HQ	66280
1268	$NaTaN_2$	$R\bar{3}m$ (166)	Triv.	—	—	NM	—	HQ	67346 67347 76382 190937 657406
1269	$NaNbN_2$	$R\bar{3}m$ (166)	Triv.	—	—	NM	—	HQ	72557 657407
1270	$Na(FeO_2)$	$R\bar{3}m$ (166)	SM	—	—	AFM	—	HQ	75588 167376 167377 187705
1271	$NaVSe_2$	$R\bar{3}m$ (166)	Triv.	—	—	FM	—	—	77597
1272	Sr_2NCl	$R\bar{3}m$ (166)	Triv.	—	—	NM	—	HQ	172595 172596 410769
1273	Sr_2NBr	$R\bar{3}m$ (166)	Triv.	—	(b)	NM	—	HQ	172600 172601
1274	$LiTiS_2$	$R\bar{3}m$ (166)	SM	—	—	FM	—	HQ	189825 189826
1275	Sr_2NI	$R\bar{3}m$ (166)	Triv.	—	(b)	NM	—	HQ	240899

1276	$NaYO_2$	$R\bar{3}m$ (166)	Triv.	—	—	—	—	—	291907
1277	$Na(VO_2)$	$R\bar{3}m$ (166)	Triv.	—	—	AFM	—	HQ	420137
1278	$KZrS_2$	$R\bar{3}m$ (166)	SM	—	(b)	NM	—	—	641350
1279	$NaYSe_2$	$R\bar{3}m$ (166)	Triv.	—	—	NM	—	—	645037
1280	Mg_2Ni_3Si	$R\bar{3}m$ (166)	TI	Fig. 42	(k)	NM	—	—	44926
1281	Fe_3S_4	$R\bar{3}m$ (166)	Triv.	—	—	NM	—	HQ	42537
1282	Mg_2Ni_3P	$R\bar{3}m$ (166)	SM	Fig. 43	(k)	NM	—	HQ	72409
1283	$K_2Zr(BO_3)_2$	$R\bar{3}m$ (166)	Triv.	—	(b)	—	—	HQ	67982
1284	$K_2Co(SeO_3)_2$	$R\bar{3}m$ (166)	SM	—	(k*,b)	AFM	—	HQ	71536
1285	$Ba_3Mn_2O_8$	$R\bar{3}m$ (166)	TI	—	(k*)	AFM	—	HQ	280045
1286	$K_2Pt_4Se_6$	$R\bar{3}m$ (166)	Triv.	—	(k*,b)	NM	—	HQ	69438
1287	$Rb_2Pt_3PtSe_6$	$R\bar{3}m$ (166)	Triv.	—	(k*,b)	NM	—	HQ	69439
1288	Na_4HgP_2	$R\bar{3}m$ (166)	Triv.	—	—	NM	—	HQ	67260
1289	K_4ZnP_2	$R\bar{3}m$ (166)	Triv.	Fig. 43	—	NM	—	HQ	67261
1290	K_4HgP_2	$R\bar{3}m$ (166)	Triv.	Fig. 43	(b)	NM	—	HQ	67263
1291	$K_4(BeP_2)$	$R\bar{3}m$ (166)	Triv.	Fig. 43	(b)	NM	—	HQ	300110
1292	$K_4(BeAs_2)$	$R\bar{3}m$ (166)	Triv.	Fig. 43	—	NM	—	HQ	300111
1293	$K_4(CdAs_2)$	$R\bar{3}m$ (166)	Triv.	Fig. 43	(b)	NM	—	HQ	300190
1294	$K_4(HgAs_2)$	$R\bar{3}m$ (166)	Triv.	Fig. 43	—	NM	—	HQ	402573
1295	K_4ZnAs_2	$R\bar{3}m$ (166)	Triv.	Fig. 43	—	NM	—	HQ	409919
1296	$Na_2(Ti_3Cl_8)$	$R\bar{3}m$ (166)	TI	Fig. 44	(k,b)	FM	—	HQ	401026
1297	NaN_3	$R\bar{3}m$ (166)	Triv.	—	—	NM	—	—	1144 34267 34674
1298	$Cd(CN_2)$	$R\bar{3}m$ (166)	Triv.	—	—	NM	—	HQ	95264
1299	Nb_2S_2C	$R\bar{3}m$ (166)	TI	—	(b)	NM	—	HQ	95110 95112
1300	Nb_3Br_8	$R\bar{3}m$ (166)	Triv.	Fig. 44	—	NM	—	HQ	25766 421609
1301	Nb_3I_8	$R\bar{3}m$ (166)	Triv.	Fig. 44	—	NM	—	HQ	25767
1302	$Co_3Sn_2S_2$	$R\bar{3}m$ (166)	SM	Fig. 44	(k,b,s)	FM	—	—	5435 173760 173761 173762 173763 173764 195422 196310 426752 426753 624867
1303	$Co_3In_2S_2$	$R\bar{3}m$ (166)	SM	—	(k,b,s)	FM	—	—	5436 195432 423459
1304	Co_3InSnS_2	$R\bar{3}m$ (166)	Triv.	Fig. 44	(k,b,s)	NM	—	—	5437 425136
1305	$Rh_3In_2S_2$	$R\bar{3}m$ (166)	SM	—	(k,b,s)	NM	—	—	5439 420726 640339
1306	Rh_3InPbS_2	$R\bar{3}m$ (166)	SM	Fig. 44	(k,b,s)	NM	—	—	5440 640213
1307	$Rh_3Pb_2Se_2$	$R\bar{3}m$ (166)	SM	—	(k,b,s)	NM	—	—	5441 648427
1308	$Ni_3Sn_2S_2$	$R\bar{3}m$ (166)	TI	—	(k,b,s)	NM	—	HQ	402458 674419
1309	$In_2Ni_3S_2$	$R\bar{3}m$ (166)	TI	—	(k,b,s)	NM	—	HQ	415258
1310	$Rh_3Sn_2S_2$	$R\bar{3}m$ (166)	SM	Fig. 44	(k,b,s)	NM	—	HQ	420728
1311	$Tl_2Ni_3S_2$	$R\bar{3}m$ (166)	TI	—	(k,b,s)	NM	—	HQ	422328
1312	$InSnCo_3S_2$	$R\bar{3}m$ (166)	SM	Fig. 44	(k,b,s)	—	—	HQ	425137
1313	$Ni_3In_2S_2$	$R\bar{3}m$ (166)	TI	—	(k,b,s)	NM	—	—	640134
1314	$Ni_3Sn_2S_2$	$R\bar{3}m$ (166)	TI	—	(k,b,s)	NM	—	—	646379 654948
1315	$Ni_3Tl_2S_2$	$R\bar{3}m$ (166)	TI	—	(k,b,s)	NM	—	—	646398
1316	$Rh_3Tl_2S_2$	$R\bar{3}m$ (166)	SM	—	(k,b,s)	NM	—	—	650236
1317	$B_{12}P_2$	$R\bar{3}m$ (166)	Triv.	Fig. 45	—	NM	—	HQ	62748
1318	$B_{12}As_2$	$R\bar{3}m$ (166)	Triv.	Fig. 45	—	NM	—	—	62749
1319	B_6As	$R\bar{3}m$ (166)	Triv.	Fig. 45	—	NM	—	HQ	68151 107916
1320	B_6P	$R\bar{3}m$ (166)	Triv.	Fig. 45	—	NM	—	—	615156 615157
1321	Sr_2N	$R\bar{3}m$ (166)	SM	—	(b)	NM	—	HQ	69016 410315 411612 414330 644701
1322	Ca_2N	$R\bar{3}m$ (166)	SM	—	(b)	NM	—	HQ	90630 90631 90632 280526 410312 411417 414329
1323	$Rb_2(OF_3(HfF_3)_3)$	$R\bar{3}m$ (166)	Triv.	—	—	NM	—	—	95847
1324	$Rb_2(OF_3(ZrF_3)_3)$	$R\bar{3}m$ (166)	Triv.	—	—	NM	—	—	95848
1325	$TlGaO_2$	$R\bar{3}m$ (166)	Triv.	Fig. 45	(k,b,s)	—	—	—	33579
1326	$ZrCl$	$R\bar{3}m$ (166)	TI	—	—	NM	—	HQ	869 20145
1327	YCl	$R\bar{3}m$ (166)	Triv.	—	—	FM	—	HQ	30708 61107
1328	SiO_2	$R\bar{3}c$ (167)	Triv.	—	(b,s)	NM	—	—	170492 170514 170539
1329	SiO_2	$R\bar{3}c$ (167)	SM	—	(b,s)	—	—	—	170515
1330	AlH_3	$R\bar{3}c$ (167)	Triv.	—	(b,s)	NM	—	—	15225 165294 168162 182533
1331	TiF_3	$R\bar{3}c$ (167)	SM	—	(b,s)	FM	—	—	52159 52162 52165 67148
1332	CrF_3	$R\bar{3}c$ (167)	SM	—	(b,s)	AFM	—	HQ	59966 59968 59969 59972 59973
1333	VF_3	$R\bar{3}c$ (167)	SM	—	(b,s)	FM	—	HQ	69167

1334	CoF_3	$R\bar{3}c$ (167)	Triv.	—	(b,s)	FM	—	HQ	77618
1335	$Cs_4(PbBr_6)$	$R\bar{3}c$ (167)	Triv.	—	(b,s)	NM	—	—	25124 162158
1336	$NaCa_3(IrO_6)$	$R\bar{3}c$ (167)	Triv.	—	(b,s)	—	—	HQ	50169
1337	Rb_4PbBr_6	$R\bar{3}c$ (167)	Triv.	—	(b)	NM	—	HQ	65300
1338	Sr_4IrO_6	$R\bar{3}c$ (167)	SM	—	(b,s)	FM	—	HQ	72926
1339	Sr_3ZnPtO_6	$R\bar{3}c$ (167)	Triv.	—	(b,s)	NM	—	HQ	81467 280519
1340	$Ca_4(IrO_6)$	$R\bar{3}c$ (167)	SM	—	(b)	FM	—	HQ	81902$^{(s)}$ 280873
1341	$Sr_3Zn(IrO_6)$	$R\bar{3}c$ (167)	SM	—	(b,s)	FM	—	HQ	81903 82658 82659 82660
1342	$Sr_3Cd(IrO_6)$	$R\bar{3}c$ (167)	SM	—	(b,s)	FM	—	HQ	81904
1343	$Sr_3Mg(PtO_6)$	$R\bar{3}c$ (167)	Triv.	—	(b,s)	NM	—	HQ	84736 281299
1344	$Sr_3Mg(IrO_6)$	$R\bar{3}c$ (167)	SM	—	(b,s)	FM	—	HQ	84737
1345	$Sr_3(PbNiO_6)$	$R\bar{3}c$ (167)	Triv.	Fig. 45	(b)	AFM	—	HQ	152588 152589$^{(s)}$ 152590$^{(s)}$ 152591$^{(s)}$ 152592$^{(s)}$ 152593$^{(s)}$
1346	$Sr_3Cd(PtO_6)$	$R\bar{3}c$ (167)	Triv.	—	(b,s)	NM	—	HQ	280518
1347	$NaBa_3IrO_6$	$R\bar{3}c$ (167)	Triv.	—	(b)	FM	—	HQ	405134
1348	Li_4OsH_6	$R\bar{3}c$ (167)	Triv.	—	(b,s)	NM	—	—	638269
1349	K_8Tl_{11}	$R\bar{3}c$ (167)	SM	—	—	NM	—	—	370009
1350	Rb_8Tl_{11}	$R\bar{3}c$ (167)	SM	—	—	NM	—	—	370035
1351	$K_3(B_3O_6)$	$R\bar{3}c$ (167)	Triv.	—	—	NM	—	—	16005
1352	$NaSn_2(PO_4)_3$	$R\bar{3}c$ (167)	Triv.	—	(b)	NM	—	—	72217 72218$^{(s)}$
1353	$LiZr_2(AsO_4)_3$	$R\bar{3}c$ (167)	Triv.	—	(b,s)	NM	—	—	190656
1354	Si_3N_4	$P6_3$ (173)	Triv.	—	—	NM	—	—	67241 74741$^{(b)}$ 74742$^{(b)}$ 74743$^{(b)}$ 74744$^{(b)}$ 74745$^{(b)}$ 74746$^{(b)}$ 74747$^{(b)}$ 74748$^{(b)}$ 74749$^{(b)}$ 74750$^{(b)}$ 74751$^{(b)}$ 74752$^{(b)}$ 74753$^{(b)}$ 74754$^{(b)}$ 74755$^{(b)}$ 77812
1355	$Cs_2(I_4O_{11})$	$P6_3$ (173)	Triv.	—	(b)	—	—	—	413942 420352
1356	$Ca(Al_2O_4)$	$P6_3$ (173)	Triv.	—	(b)	NM	—	—	157457
1357	$Cs_2(MoO_3)_3(SeO_3)$	$P6_3$ (173)	Triv.	—	(k*,b)	NM	—	—	75473
1358	$(Cs_2(SeO_3))(WO_3)_3$	$P6_3$ (173)	Triv.	—	(k*,b,s)	NM	—	—	80392
1359	$Rb_2(MoO_3)_3(SeO_3)$	$P6_3$ (173)	Triv.	—	(k*,b)	NM	—	—	167530
1360	$Cs_2TeW_3O_{12}$	$P6_3$ (173)	Triv.	—	(k*,b,s)	—	—	—	429738
1361	$K(VO_2)_3(SeO_3)_2$	$P6_3$ (173)	Triv.	—	(b,s)	NM	—	—	81231
1362	$Rb(Se_2V_3O_{12})$	$P6_3$ (173)	Triv.	—	(b,s)	NM	—	—	163600
1363	$Tl(Se_2V_3O_{12})$	$P6_3$ (173)	Triv.	—	(k*,b,s)	NM	—	—	163601
1364	$Cs(VO_2)_3(TeO_3)_2$	$P6_3$ (173)	Triv.	—	(k*,b,s)	NM	—	—	411111
1365	La_3AlTiS_7	$P6_3$ (173)	SM	Fig. 45	(b)	FM	—	—	608322
1366	La_3AlVS_7	$P6_3$ (173)	SM	Fig. 45	(b)	FM	—	—	608323
1367	La_3BeTiS_7	$P6_3$ (173)	SM	—	—	FM	—	—	616310
1368	$KAl(SiO_4)$	$P6_3$ (173)	Triv.	Fig. 46	(b,s)	NM	—	HQ	34350
1369	$Ga_9Tl_3O_2S_{13}$	$P\bar{6}$ (174)	Triv.	—	(b)	NM	—	HQ	61256
1370	$BaZn(BO_3)F$	$P\bar{6}$ (174)	Triv.	Fig. 46	(b)	NM	—	HQ	248042 429814
1371	$BaAl(BO_3)F_2$	$P\bar{6}$ (174)	Triv.	—	(b)	—	—	—	291434 409663
1372	$Pb_7F_{12}Br_2$	$P\bar{6}$ (174)	Triv.	—	—	NM	—	HQ	92293
1373	$Ca_7H_{12}Cl_2$	$P\bar{6}$ (174)	Triv.	—	—	NM	—	HQ	420927
1374	La_2ClB_3	$P\bar{6}$ (174)	SM	—	—	NM	—	HQ	417604
1375	$LiCd(BO_3)$	$P\bar{6}$ (174)	Triv.	—	(b)	NM	—	HQ	20191 20835
1376	$Mg_3F_3(BO_3)$	$P6_3/m$ (176)	Triv.	Fig. 46	(b)	—	—	HQ	4226
1377	BI_3	$P6_3/m$ (176)	Triv.	—	—	NM	SC	HQ	173375 28328 411463
1378	$NaCs_2(C_2N_3)_3$	$P6_3/m$ (176)	Triv.	Fig. 46	—	NM	—	—	407809
1379	$Pb_3Cd_3(BO_3)_4$	$P6_3/m$ (176)	Triv.	—	(k)	NM	—	—	422862
1380	$Cu_2Bi_2S_3(AlCl_4)_2$	$P6_3/m$ (176)	Triv.	—	(b,s)	NM	—	—	428727
1381	$LiCa(AlH_4)_3$	$P6_3/m$ (176)	Triv.	—	(b)	—	—	—	670844
1382	$Li_2RbCd(CO_3)_2F$	$P6_3/m$ (176)	Triv.	—	(b)	NM	—	HQ	710094
1383	$AgCd_3Hf_3F_{20}$	$P6_3/m$ (176)	SM	—	—	NM	—	—	78893
1384	$Sc_2(HPO_3)_3$	$P6_3/m$ (176)	Triv.	—	(b)	NM	—	—	409724
1385	$Pb_5(PO_4)_3F$	$P6_3/m$ (176)	Triv.	—	—	NM	—	—	20500
1386	$Ca_5(PO_4)_3F$	$P6_3/m$ (176)	Triv.	—	—	NM	—	—	24236$^{(b)}$ 30261$^{(b)}$ 38118$^{(b)}$ 52385$^{(b)}$ 56313 56314 84227 94081 94082 94083 99581 180314 193552 670544
1387	Sr_3MnN_3	$P6_3/m$ (176)	TI	—	(b)	FM	—	HQ	80772
1388	$Ba_3(CrN_3)$	$P6_3/m$ (176)	SM	—	(b)	NM	—	HQ	154802

1389	$Sr_3(CrN_3)$	$P6_3/m$ (176)	SM	—	(b)	NM	—	HQ	154803
1390	$Ba_4Nb_2O_9$	$P6_3/m$ (176)	TI	—	—	NM	—	HQ	251133
1391	BCl_3	$P6_3/m$ (176)	Triv.	—	—	NM	—	—	24526 27869
1392	BBr_3	$P6_3/m$ (176)	Triv.	—	—	NM	—	—	24527 173374
1393	$Fe_2(BP_3O_{12})$	$P6_3/m$ (176)	Triv.	—	(b)	FM	—	—	260895 420638
1394	KMo_3S_3	$P6_3/m$ (176)	SM	—	—	NM	—	HQ	30752 603631 641249
1395	$RbMo_3S_3$	$P6_3/m$ (176)	SM	—	—	NM	—	HQ	30753 603622 644175
1396	$CsMo_3S_3$	$P6_3/m$ (176)	SM	—	—	NM	—	HQ	30754 603614 627033
1397	$InMo_3Te_3$	$P6_3/m$ (176)	SM	—	—	NM	SC	HQ	53100 603669 604497 640025
1398	$TlMo_3Te_3$	$P6_3/m$ (176)	SM	—	—	NM	SC	HQ	90811 603670 644485
1399	$BaMo_3Se_3$	$P6_3/m$ (176)	SM	—	—	NM	—	—	603615 615982
1400	$NaMo_3Se_3$	$P6_3/m$ (176)	SM	—	—	NM	SC	—	603625 603827 604518 643974
1401	KMo_3Se_3	$P6_3/m$ (176)	SM	—	—	NM	SC	—	603628 604517 641256
1402	$RbMo_3Se_3$	$P6_3/m$ (176)	SM	—	—	NM	SC	—	603629 604516 644181
1403	$NaMo_3Te_3$	$P6_3/m$ (176)	SM	—	—	NM	—	—	603641 604501 643979
1404	$CsMo_3Se_3$	$P6_3/m$ (176)	SM	—	—	NM	SC	—	603651 603826 604515
1405	KMo_3Te_3	$P6_3/m$ (176)	SM	—	—	NM	—	—	603671 604500
1406	$RbMo_3Te_3$	$P6_3/m$ (176)	SM	—	—	NM	—	—	603672 604499
1407	$CsMo_3Te_3$	$P6_3/m$ (176)	SM	—	—	NM	—	—	603673 604498
1408	$La_3FeWS_3O_6$	$P6_3/m$ (176)	SM	—	(b,s)	AFM	—	HQ	380402
1409	$La_3NiWS_3O_6$	$P6_3/m$ (176)	SM	—	(b,s)	FM	—	HQ	380403
1410	$La_3CoWS_3O_6$	$P6_3/m$ (176)	Triv.	—	(b,s)	NM	—	HQ	380405
1411	$La_3MnWS_3O_6$	$P6_3/m$ (176)	SM	—	(b,s)	FM	—	HQ	380406
1412	V_3S_4	$P6_3/m$ (176)	SM	—	(b)	NM	SC	HQ	72920 72921 72922
1413	Ti_3Se_4	$P6_3/m$ (176)	SM	—	(b)	NM	—	HQ	79629
1414	$TlSbO_3$	$P6_322$ (182)	Triv.	Fig. 46	(b,s)	NM	—	—	10142
1415	SiO_2	$P6_322$ (182)	Triv.	Fig. 46	(b,s)	NM	—	—	29343
1416	$BaAl_2O_4$	$P6_322$ (182)	Triv.	—	(b,s)	NM	—	—	75427 16845 21080
1417	Ta_3CrS_6	$P6_322$ (182)	SM	—	(b)	FM	—	—	626633
1418	$RbSn(IO_6)$	$P6_322$ (182)	Triv.	—	(b,s)	NM	—	—	73614
1419	Ba_3CrS_5	$P6_3cm$ (185)	SM	—	(b,s)	FM	—	HQ	97539
1420	$Li_2Ba(SiO_4)$	$P6_3cm$ (185)	Triv.	—	(b)	NM	—	—	180289 260259
1421	C_3N_4	$P6_3cm$ (185)	Triv.	—	(b)	—	—	—	674271 674285
1422	Na_3N	$P6_3cm$ (185)	Triv.	—	—	NM	—	—	165992 165993
1423	$Li_8O_2(GeO_4)$	$P6_3cm$ (185)	Triv.	—	(b)	NM	—	HQ	65175
1424	$Li_8O_2(SiO_4)$	$P6_3cm$ (185)	Triv.	—	(b)	NM	—	HQ	65176
1425	$Mg_3(Si_2O_5(OH)_4)$	$P6_3cm$ (185)	Triv.	—	(b,s)	NM	—	—	87439 202359
1426	$Sn_6O_4(SiO_4)$	$P6_3mc$ (186)	Triv.	—	(k*,b,s)	NM	—	HQ	156236
1427	$Zn(OH)(N_3)$	$P6_3mc$ (186)	Triv.	—	—	—	—	—	196345
1428	$Li_2InMo_3O_8$	$P6_3mc$ (186)	SM	—	(b)	—	—	HQ	426618
1429	$(Al_2O_3)_5(H_2O)$	$P6_3mc$ (186)	Triv.	—	(k*)	NM	—	—	23651
1430	$Ba_3(NiSb_2O_9)$	$P6_3mc$ (186)	Triv.	—	(k*,b,s)	AFM	—	HQ	1177
1431	$Ba_3Cu(Sb_2O_9)$	$P6_3mc$ (186)	SM	Fig. 46	(k*,b,s)	FM	—	HQ	2279
1432	$La_4NS_3Cl_3$	$P6_3mc$ (186)	Triv.	—	(b)	NM	—	HQ	74902
1433	$CsCuCl_3$	$P6_3mc$ (186)	SM	—	(k*,b,s)	FM	—	HQ	2064
1434	$Cs(CrBr_3)$	$P6_3mc$ (186)	SM	—	(k*,b,s)	FM	—	HQ	2590
1435	$CsCrI_3$	$P6_3mc$ (186)	SM	—	(k*,b,s)	—	—	HQ	8105
1436	$CsCrCl_3$	$P6_3mc$ (186)	SM	—	(k*,b,s)	FM	—	HQ	10206
1437	$(Hg_3S)(AsS_3)Cl$	$P6_3mc$ (186)	Triv.	—	(k*,b)	—	—	HQ	280329
1438	$K_6(HgS_4)$	$P6_3mc$ (186)	Triv.	—	(b)	NM	—	HQ	266 47218
1439	$Na_6(MnS_4)$	$P6_3mc$ (186)	SM	—	(b)	FM	—	HQ	65447 95065 95066 642996
1440	$LaNi_5H_7$	$P6_3mc$ (186)	Triv.	—	(k*,b)	NM	—	—	96245 236996 236997
1441	$LiBH_4$	$P6_3mc$ (186)	Triv.	—	—	NM	—	HQ	95208$^{(k)}$ 186262 245569
1442	$Al(PO_4)$	$P6_3mc$ (186)	Triv.	—	(k*,b,s)	NM	—	HQ	279582
1443	$Li(BrO_4)(H_2O)_3$	$P6_3mc$ (186)	Triv.	—	—	NM	—	HQ	73706
1444	$Li(TcO_4)(H_2O)_3$	$P6_3mc$ (186)	Triv.	—	—	NM	—	HQ	422191
1445	$LaAuGe$	$P6_3mc$ (186)	SM	—	—	NM	—	HQ	405322 656867
1446	K_3TaF_8	$P6_3mc$ (186)	Triv.	—	(k*)	NM	—	HQ	248063
1447	$Mg_3BeAl_8O_{16}$	$P6_3mc$ (186)	Triv.	—	(k*,b)	NM	—	—	31227 31256
1448	$MnLa_4OSe_6$	$P6_3mc$ (186)	SM	—	(b,s)	AFM	—	HQ	391303

1449	$MnLa_4OS_6$	$P6_3mc$ (186)	SM	—	(b,s)	FM	—	HQ	391305
1450	$Na_2(MnO_4)$	$P6_3mc$ (186)	SM	—	—	FM	—	HQ	39504
1451	$Ca_2(SiO_4)$	$P6_3mc$ (186)	Triv.	—	(k*,b)	NM	—	—	182053 182054
1452	$Na(Be_4SbO_7)$	$P6_3mc$ (186)	Triv.	Fig. 46	(k*,b)	NM	—	—	27599
1453	$YBaZn_3GaO_7$	$P6_3mc$ (186)	Triv.	—	(k*,b)	NM	—	—	252148
1454	GaN	$P6_3mc$ (186)	Triv.	—	—	NM	SC	—	159250 25676 34476 41481 41483 41543 42000 54698 67769 87830 153887 153888 153889 153890 153891 156259 157398 157512 181358 184926 190424 191773 634715 671112 672115 672140 672569 672724 672741 673190 673464
1455	$Zn_2Mo_3O_8$	$P6_3mc$ (186)	Triv.	—	(b)	—	—	HQ	14321 36174 248083 260410 280130
1456	$ScZn(Mo_3O_8)$	$P6_3mc$ (186)	SM	—	(b)	FM	—	HQ	40534
1457	C_3N_4	$P\bar{6}m2$ (187)	Triv.	—	(k*,b)	NM	—	—	83265
1458	$Ba(CoO_3)$	$P\bar{6}m2$ (187)	SM	—	(b,s)	FM	—	—	88670
1459	Ca_3SiBr_2	$P\bar{6}m2$ (187)	TI	—	—	FM	—	—	89543
1460	La_2Ni_2I	$P\bar{6}m2$ (187)	SM	—	—	NM	—	HQ	165262
1461	$KCdCO_3F$	$P\bar{6}m2$ (187)	Triv.	—	—	—	—	—	239110
1462	$CaKF(CO_3)$	$P\bar{6}m2$ (187)	Triv.	—	—	—	—	HQ	262230 59878 154681 154682 154683 154685
1463	$LiAuC_2$	$P\bar{6}m2$ (187)	Triv.	—	—	NM	—	HQ	411253
1464	$InNbS_2$	$P\bar{6}m2$ (187)	TI	—	(b)	NM	—	—	74702
1465	IrLi	$P\bar{6}m2$ (187)	TI	—	—	NM	—	—	104487 659856
1466	LiPd	$P\bar{6}m2$ (187)	SM	—	—	NM	—	—	104770 104771 659883
1467	$TlTaGe_3O_9$	$P\bar{6}c2$ (188)	Triv.	—	(b,s)	NM	—	—	10383
1468	$LaSiO_2N$	$P\bar{6}c2$ (188)	SM	Fig. 47	(b)	NM	—	—	9752
1469	$Sr(GeO_3)$	$P\bar{6}2m$ (189)	Triv.	Fig. 47	—	NM	—	—	28603
1470	$Ag_2Te(VS_2)_3$	$P\bar{6}2m$ (189)	SM	—	—	FM	—	—	251064
1471	$Ba_3Nb_6Si_4O_{26}$	$P\bar{6}2m$ (189)	Triv.	—	(b)	NM	—	—	15934 16029
1472	$Ba_3Ta_6Si_4O_{26}$	$P\bar{6}2m$ (189)	Triv.	—	(b)	NM	—	—	15935 18317
1473	$Sr_3Ta_6Si_4O_{26}$	$P\bar{6}2m$ (189)	Triv.	—	(b)	NM	—	—	15936
1474	$Rb_6(Si_{10}O_{23})$	$P\bar{6}2m$ (189)	Triv.	—	(b,s)	NM	—	—	250379
1475	GaNiTi	$P\bar{6}2m$ (189)	SM	—	—	NM	—	—	103885
1476	$K_3Ta_3B_2O_{12}$	$P\bar{6}2m$ (189)	Triv.	—	(b)	NM	—	HQ	201143
1477	K_2Te_2	$P\bar{6}2m$ (189)	Triv.	—	—	NM	—	HQ	73178
1478	Rb_2Te_2	$P\bar{6}2m$ (189)	Triv.	—	—	NM	—	HQ	73179
1479	$Ti_3Rh_2In_3$	$P\bar{6}2m$ (189)	SM	—	—	NM	—	HQ	410967
1480	NbMnSi	$P\bar{6}2m$ (189)	SM	—	—	FM	—	—	24185
1481	NbCrGe	$P\bar{6}2m$ (189)	SM	—	—	FM	—	—	42061
1482	TiCoSi	$P\bar{6}2m$ (189)	SM	Fig. 47	—	FM	—	—	42735
1483	NbMnGe	$P\bar{6}2m$ (189)	SM	—	—	FM	—	—	42911 637001
1484	Al(ZrNi)	$P\bar{6}2m$ (189)	SM	—	—	NM	—	—	58080 152131 186404 410399 608967 608978
1485	ScRuGe	$P\bar{6}2m$ (189)	SM	—	—	NM	—	HQ	79595
1486	TiFeP	$P\bar{6}2m$ (189)	SM	—	—	FM	—	HQ	290889
1487	CrTiAs	$P\bar{6}2m$ (189)	SM	—	—	FM	—	—	610275
1488	FeTiAs	$P\bar{6}2m$ (189)	SM	—	—	FM	—	—	610530
1489	FeNbB	$P\bar{6}2m$ (189)	SM	—	—	FM	—	—	614046
1490	FeTaB	$P\bar{6}2m$ (189)	SM	—	—	NM	—	—	614205
1491	GeMnTa	$P\bar{6}2m$ (189)	SM	—	—	FM	—	—	637098
1492	MnTaSi	$P\bar{6}2m$ (189)	SM	—	—	FM	—	—	643653
1493	NbReSi	$P\bar{6}2m$ (189)	SM	—	—	NM	SC	—	645257
1494	ReSiTa	$P\bar{6}2m$ (189)	SM	—	—	NM	—	—	650119
1495	$Ba_3(Cr_2WO_9)$	$P\bar{6}2c$ (190)	TI	—	(b,s)	—	—	HQ	81072
1496	$K_3(Nb_3O_6)(Si_2O_7)$	$P\bar{6}2c$ (190)	Triv.	—	(b)	NM	—	—	79734
1497	HfCoSn	$P\bar{6}2c$ (190)	SM	—	—	NM	—	HQ	107472 408899
1498	ScPdSn	$P\bar{6}2c$ (190)	SM	—	—	NM	—	HQ	418976
1499	TaON	$P6/mmm$ (191)	SM	—	(k,b,s)	NM	—	—	20321
1500	$CaRh_3B_2$	$P6/mmm$ (191)	SM	—	(k,b)	NM	—	—	66767
1501	$LaFe_5H_{12}$	$P6/mmm$ (191)	SM	—	(k,b)	FM	—	—	160914
1502	RhN_2	$P6/mmm$ (191)	SM	—	—	—	—	—	671729

1503	$LaNi_5$	$P6/mmm$ (191)	SM	Fig. 47	(k)	FM	—	HQ	54245 104675 104676 104750 155045 155913 159117 161600 162124 182513 183383 189352 193881 196601 200240 242016 242017 242018 242019 242020 242026 242027 242028 242029 242030 600409 601621 602015 603845 641488 641507 641513 641518 641519 641520 641521 641522 641523 641524 641526 641529 641532 641535 641540 641542 641543 641545 641549 657601 658150 670633
1504	YNi_5	$P6/mmm$ (191)	SM	Fig. 48	(k)	FM	—	—	54422 105462 105463 603868 647059 647075 647084 647089 647093 647101 659941 673580
1505	$CaNi_5$	$P6/mmm$ (191)	SM	Fig. 47	(k)	FM	—	HQ	54474 58916 619438 619442 619446 619447 619449 619452
1506	$BaPd_5$	$P6/mmm$ (191)	SM	Fig. 47	(k)	NM	—	—	58672 616030
1507	Co_5Y	$P6/mmm$ (191)	SM	—	(k)	FM	—	—	102731 102732 106506 107253 196872 196875 600442 625573 625577 625579 625587 625591 625597 625603 625616 625623 625630 625634 625642 656885 659057 659669
1508	Fe_5Y	$P6/mmm$ (191)	SM	—	(k)	FM	—	—	103699 107256 184905
1509	Ni_5Sc	$P6/mmm$ (191)	SM	Fig. 48	(k)	FM	—	—	105336 646468
1510	Pd_5Sr	$P6/mmm$ (191)	TI	Fig. 47	(k)	NM	—	—	105707 648964
1511	$CaPd_5$	$P6/mmm$ (191)	TI	Fig. 47	(k)	NM	—	—	106357 673956
1512	$LaNi_3Rh_2$	$P6/mmm$ (191)	SM	—	(k)	FM	—	—	183385
1513	FeGe	$P6/mmm$ (191)	SM	—	(k)	FM	—	—	53459 631998 632006 632016 632022
1514	CoSn	$P6/mmm$ (191)	SM	—	(k)	NM	—	HQ	55564 102671 151390 161110 161113 161115 161116 161117 161118 625264 670158
1515	InNi	$P6/mmm$ (191)	SM	Fig. 48	(k)	NM	—	—	59435 161111 161114 161123 161124 161125 161126 185625 640117
1516	FeSn	$P6/mmm$ (191)	SM	—	(k)	FM	—	—	103634 103635 152339 161109 161112 161119 161120 161121 161122 633740 633747
1517	PtTl	$P6/mmm$ (191)	SM	—	(k)	NM	—	—	105819
1518	$ScCr_6Ge_6$	$P6/mmm$ (191)	SM	—	(k)	FM	—	—	626107
1519	YCr_6Ge_6	$P6/mmm$ (191)	SM	Fig. 48	(k)	NM	—	—	658018
1520	Li_2NaN	$P6/mmm$ (191)	SM	—	—	NM	—	—	92308
1521	$LiNa_2N$	$P6/mmm$ (191)	SM	—	—	NM	—	—	92310
1522	Na_3N	$P6/mmm$ (191)	SM	—	—	NM	—	—	165989
1523	Ta_2N_3O	$P6/mmm$ (191)	SM	—	(k,b)	FM	—	—	182352
1524	Ta_2N_3F	$P6/mmm$ (191)	TI	—	(k,b)	NM	—	—	182353
1525	$La_6Mn_2S_{10}$	$P6_3/mcm$ (193)	SM	—	(b)	FM	—	—	168592
1526	Ca_6FeN_5	$P6_3/mcm$ (193)	SM	—	(b,s)	FM	—	HQ	33796
1527	$Ca_6(MnN_3)N_2$	$P6_3/mcm$ (193)	SM	—	(b,s)	FM	—	HQ	80184
1528	La_5Sb_3Br	$P6_3/mcm$ (193)	SM	—	—	NM	—	HQ	50725
1529	La_5Sn_3Cl	$P6_3/mcm$ (193)	SM	—	—	NM	—	HQ	95238
1530	La_5Sn_3Br	$P6_3/mcm$ (193)	SM	—	—	NM	—	HQ	95239
1531	La_5Bi_3Br	$P6_3/mcm$ (193)	SM	—	—	NM	—	HQ	95241
1532	La_5Pb_3I	$P6_3/mcm$ (193)	SM	—	—	FM	—	HQ	409778
1533	Sc_5Si_3	$P6_3/mcm$ (193)	SM	—	—	NM	—	—	23932 602016 651814
1534	Hf_5Ge_3	$P6_3/mcm$ (193)	TI	—	—	NM	—	—	44361 636545
1535	Ta_5Ge_3	$P6_3/mcm$ (193)	SM	—	—	NM	—	—	56028 637960
1536	Ti_5Si_3	$P6_3/mcm$ (193)	TI	—	—	NM	SC	—	62591 168415 652424 671881
1537	Ta_5Si_3	$P6_3/mcm$ (193)	SM	—	—	NM	—	—	76159 652324 652335
1538	Hf_5Sn_3	$P6_3/mcm$ (193)	SM	—	—	NM	—	—	104273 183487 638947
1539	Ti_5Sn_3	$P6_3/mcm$ (193)	TI	—	—	NM	—	—	109292 169008 652783 652785 670883
1540	Ca_5Sb_3	$P6_3/mcm$ (193)	SM	—	—	NM	—	HQ	173026 619563
1541	Hf_5Ge_3	$P6_3/mcm$ (193)	SM	—	—	NM	—	—	636541
1542	Ti_5Si_3	$P6_3/mcm$ (193)	SM	—	—	NM	—	—	652420
1543	Zr_5Si_3	$P6_3/mcm$ (193)	SM	—	—	NM	SC	—	652605 652612 652616 652621 656924
1544	K_3N	$P6_3/mcm$ (193)	TI	Fig. 48	(b,s)	NM	—	—	99999
1545	NbI_3	$P6_3/mcm$ (193)	SM	Fig. 48	—	FM	—	—	109145

1546	SiO_2	$P6_3/mmc$ (194)	Triv.	—	(k,b,s)	NM	—	—	170481 170496 38126 40902 40903 44270 162623 162624 200478
1547	LiFeAs	$P6_3/mmc$ (194)	SM	—	—	FM	—	—	187133
1548	$KV_3Ge_2O_9$	$P6_3/mmc$ (194)	Triv.	—	(k,b,s)	FM	—	HQ	187490
1549	ZnO	$P6_3/mmc$ (194)	Triv.	—	—	—	—	—	670354 670355
1550	$SnNi_3$	$P6_3/mmc$ (194)	SM	—	(k)	—	—	—	670879 105357 150926 411928 646749 646751
1551	Cr_2AlC	$P6_3/mmc$ (194)	SM	—	(b)	NM	SC	—	42918 606181
1552	Sc_2AlC	$P6_3/mmc$ (194)	SM	—	(b)	NM	—	—	160378
1553	Sc_2InC	$P6_3/mmc$ (194)	SM	—	(b)	NM	—	—	160380 163503 163510 163511
1554	Ti_2SnC	$P6_3/mmc$ (194)	TI	—	(b)	NM	—	—	161063 161064 252840 618806
1555	$Ba_5IrIn_2Al_2O_{13}Cl$	$P6_3/mmc$ (194)	Triv.	—	(k*,b,s)	FM	—	—	71602
1556	$RbNiF_3$	$P6_3/mmc$ (194)	SM	—	(k*,b,s)	FM	—	—	15090 22127 91834
1557	$Rb(ZnF_3)$	$P6_3/mmc$ (194)	Triv.	—	(k*,b,s)	NM	—	—	41618 91835 91836
1558	$K_3Na(Re_2O_9)$	$P6_3/mmc$ (194)	Triv.	—	(b,s)	NM	—	—	73300
1559	$K_3La(Te_2O_9)$	$P6_3/mmc$ (194)	Triv.	—	(k*,b,s)	—	—	HQ	195647
1560	$Ba_3Sb_2NiO_9$	$P6_3/mmc$ (194)	SM	—	(k*,b,s)	AFM	—	—	200299
1561	$Rb_6Ni_6F_{18}$	$P6_3/mmc$ (194)	SM	Fig. 48	(k*,b,s)	FM	—	—	410390 410391
1562	$Ba(MnO_3)$	$P6_3/mmc$ (194)	Triv.	—	(k,b,s)	AFM	—	—	23874
1563	$BaNiO_3$	$P6_3/mmc$ (194)	Triv.	—	—	NM	—	—	$175^{(b,s)}$ $30661^{(k)}$
1564	$BaCoO_3$	$P6_3/mmc$ (194)	SM	—	—	FM	—	—	$922^{(b,s)}$ $26586^{(k)}$ $173504^{(b,s)}$
1565	$Cs(MnBr_3)$	$P6_3/mmc$ (194)	SM	—	(k*,b,s)	FM	—	—	2782 9703
1566	$BaVS_3$	$P6_3/mmc$ (194)	SM	Fig. 48	(k*)	FM	SC	—	8193 8194 15537 23194 62711 154181 616097 616098
1567	$Rb(MnBr_3)$	$P6_3/mmc$ (194)	SM	—	(k*)	FM	—	—	$9704^{(b,s)}$ 14077
1568	$CsMnI_3$	$P6_3/mmc$ (194)	SM	—	(k*)	FM	—	—	10042 15949 15950 15951 15952
1569	$BaMnO_3$	$P6_3/mmc$ (194)	SM	—	(b,s)	AFM	—	—	$10331^{(k)}$ 10332
1570	$CsScCl_3$	$P6_3/mmc$ (194)	SM	—	(k*)	NM	—	—	10474
1571	$Ba(VSe_3)$	$P6_3/mmc$ (194)	SM	Fig. 49	(k*)	FM	—	—	10486
1572	$RbNiCl_3$	$P6_3/mmc$ (194)	SM	—	(k*,b,s)	FM	—	—	15010
1573	$RbNiBr_3$	$P6_3/mmc$ (194)	SM	—	(k*,b,s)	FM	—	—	15011
1574	$CsVCl_3$	$P6_3/mmc$ (194)	SM	—	(k*,b,s)	FM	—	—	15932 201828 201832
1575	$BaTaS_3$	$P6_3/mmc$ (194)	SM	—	(k*)	NM	—	—	16083 616077 659541
1576	$CsVI_3$	$P6_3/mmc$ (194)	SM	—	(k*)	FM	—	—	26453 26454
1577	$CsCoCl_3$	$P6_3/mmc$ (194)	SM	—	(k*,b,s)	FM	—	—	27511
1578	$CsCrCl_3$	$P6_3/mmc$ (194)	TI	—	(k*)	FM	—	—	36132
1579	$CsTiBr_3$	$P6_3/mmc$ (194)	SM	—	(k*)	FM	—	—	41320 400053
1580	$Rb(TiCl_3)$	$P6_3/mmc$ (194)	SM	—	(k*)	FM	—	—	49747
1581	$Cs(TiCl_3)$	$P6_3/mmc$ (194)	SM	—	(k*,b,s)	FM	—	—	49748
1582	$CsNiCl_3$	$P6_3/mmc$ (194)	SM	—	(k*,b,s)	FM	—	—	59371 60262 423828
1583	$Rb(CuCl_3)$	$P6_3/mmc$ (194)	SM	—	(k*,b,s)	FM	—	—	84212
1584	$Rb(TiBr_3)$	$P6_3/mmc$ (194)	SM	—	(k*)	FM	—	HQ	154257
1585	$Cs(TiI_3)$	$P6_3/mmc$ (194)	SM	—	(k*)	FM	—	HQ	154258
1586	$LaCrGe_3$	$P6_3/mmc$ (194)	SM	—	—	FM	—	HQ	158976 290669 290670 290671 290672
1587	$CsFeBr_3$	$P6_3/mmc$ (194)	Triv.	—	(k*)	FM	—	—	174041
1588	$CsVBr_3$	$P6_3/mmc$ (194)	SM	—	(k*,b,s)	FM	—	—	201829 201833
1589	$RbVCl_3$	$P6_3/mmc$ (194)	SM	—	(k*)	FM	—	—	201830 201834
1590	$RbVBr_3$	$P6_3/mmc$ (194)	SM	—	(k*)	FM	—	—	201831
1591	$Cs(FeCl_3)$	$P6_3/mmc$ (194)	Triv.	—	(k*,b,s)	NM	—	—	300249
1592	$CsNiBr_3$	$P6_3/mmc$ (194)	SM	—	(k*,b,s)	FM	—	HQ	423829
1593	$CsNiI_3$	$P6_3/mmc$ (194)	SM	—	(k*,b,s)	—	—	HQ	423830
1594	$BaTaSe_3$	$P6_3/mmc$ (194)	SM	—	(k*)	NM	SC*	—	616129 659547
1595	$BaNbS_3$	$P6_3/mmc$ (194)	SM	—	(k*)	NM	SC	—	659538
1596	$Y(MnO_3)$	$P6_3/mmc$ (194)	TI	—	(b)	FM	—	—	73361 182284 422982 422990
1597	$Cs_3Ru_2Cl_9$	$P6_3/mmc$ (194)	Triv.	—	(k*)	NM	—	—	201057
1598	$Cs_3(Nb_2I_9)$	$P6_3/mmc$ (194)	Triv.	—	(k*)	FM	—	HQ	421295
1599	$CuAlO_2$	$P6_3/mmc$ (194)	Triv.	—	—	NM	—	—	31368 60845 95661
1600	$CuScO_2$	$P6_3/mmc$ (194)	Triv.	Fig. 49	—	NM	—	—	60847 95667 151929 670128
1601	$AgAlO_2$	$P6_3/mmc$ (194)	Triv.	—	—	NM	—	—	95662 300020
1602	$CuGaO_2$	$P6_3/mmc$ (194)	Triv.	—	—	NM	—	—	95664
1603	$AgGaO_2$	$P6_3/mmc$ (194)	Triv.	—	—	NM	—	—	95665

1604	$AgScO_2$	$P6_3/mmc$ (194)	Triv.	—	—	NM	—	—	95668 670073
1605	$CuInO_2$	$P6_3/mmc$ (194)	Triv.	—	—	NM	—	—	95670 186620
1606	$AuInO_2$	$P6_3/mmc$ (194)	Triv.	—	—	NM	—	—	95672
1607	$AgYO_2$	$P6_3/mmc$ (194)	Triv.	—	—	NM	—	—	95674 670075
1608	$AuYO_2$	$P6_3/mmc$ (194)	Triv.	—	—	NM	—	—	95675 670100
1609	Ni	$P6_3/mmc$ (194)	SM	—	—	FM	—	—	76668 671412
1610	NiMnGe	$P6_3/mmc$ (194)	SM	Fig. 49	—	FM	—	—	41921 637011 637019 637029
1611	AlAuTi	$P6_3/mmc$ (194)	SM	—	—	FM	—	—	57506
1612	$InNi_2$	$P6_3/mmc$ (194)	SM	—	—	NM	—	—	59436 59437 185624 640098 640107 670969
1613	CoNiSn	$P6_3/mmc$ (194)	SM	Fig. 49	—	FM	—	—	102582 196627
1614	Co_2Sn	$P6_3/mmc$ (194)	TI	—	—	FM	—	—	102673 625262
1615	CoFeGe	$P6_3/mmc$ (194)	SM	—	—	—	—	—	196628
1616	Co_2Ge	$P6_3/mmc$ (194)	TI	—	—	FM	—	—	623418 623430
1617	$GaNi_2$	$P6_3/mmc$ (194)	SM	—	—	NM	—	—	634869 670968
1618	$Ni_1Sb_1V_1$	$P6_3/mmc$ (194)	SM	—	—	—	—	—	671080 671081
1619	$K_5(AuAs_2)$	$P6_3/mmc$ (194)	Triv.	—	(b)	NM	—	—	40698
1620	$K_5(AuP_2)$	$P6_3/mmc$ (194)	Triv.	—	(b)	NM	—	—	40700
1621	Co_2Ge	$P6_3/mmc$ (194)	SM	—	—	FM	—	—	108289
1622	LaI	$P6_3/mmc$ (194)	TI	—	—	NM	—	—	83678 171451
1623	Co_3Nb_2Si	$P6_3/mmc$ (194)	SM	—	(k*)	NM	—	—	53018
1624	$ZrAl_2$	$P6_3/mmc$ (194)	TI	—	(k*)	NM	—	—	55594 191009 603593 609703 609713 609721 609743
1625	$ZrAl_2$	$P6_3/mmc$ (194)	TI	—	(k*)	NM	SC	—	150527
1626	Na_2Cs	$P6_3/mmc$ (194)	SM	—	(k*)	NM	—	—	246932 627052
1627	Ni_3Sc_2Si	$P6_3/mmc$ (194)	SM	—	(k*)	—	—	—	646484
1628	$TiNb_4S_8$	$P6_3/mmc$ (194)	SM	—	(b)	NM	—	—	645332
1629	VNb_4S_8	$P6_3/mmc$ (194)	SM	—	(b)	FM	—	—	645339
1630	K_3P	$P6_3/mmc$ (194)	Triv.	—	—	NM	—	—	25550
1631	K_3Bi	$P6_3/mmc$ (194)	SM	—	—	NM	—	—	26885
1632	K_3Sb	$P6_3/mmc$ (194)	Triv.	—	—	NM	—	—	26886 656327
1633	Rb_3Sb	$P6_3/mmc$ (194)	Triv.	—	—	NM	—	—	77991 650044
1634	Na_2MgPb	$P6_3/mmc$ (194)	SM	—	—	NM	—	HQ	238202
1635	Na_2MgSn	$P6_3/mmc$ (194)	SM	—	—	NM	—	HQ	262676
1636	$BiRb_3$	$P6_3/mmc$ (194)	SM	—	—	NM	—	—	616995 616997
1637	$Na_2O(Al_2O_3)_{11}$	$P6_3/mmc$ (194)	Triv.	—	(b)	NM	—	—	15970 16933 60635
1638	$AlTi_3$	$P6_3/mmc$ (194)	SM	—	(k*)	NM	—	—	58188 99779 181338 609523 609538
1639	Co_3Mo	$P6_3/mmc$ (194)	SM	Fig. 49	(k*)	FM	—	—	102542 624214 624216 671172
1640	Co_3W	$P6_3/mmc$ (194)	SM	Fig. 49	(k*)	FM	—	—	102722 187993 625553 671174
1641	$GaTi_3$	$P6_3/mmc$ (194)	SM	—	(k*)	NM	SC	—	103991 182429 635554
1642	Ni_3In	$P6_3/mmc$ (194)	SM	Fig. 49	(k*)	FM	—	—	151196 185623 185627 640100
1643	Co_3Ta	$P6_3/mmc$ (194)	SM	—	(k*)	NM	—	—	187991 671178
1644	La_3Al	$P6_3/mmc$ (194)	SM	—	(k*)	NM	—	—	603210 608280
1645	Ti_3In	$P6_3/mmc$ (194)	SM	—	(k*)	NM	—	—	640656
1646	Co_3Nb	$P6_3/mmc$ (194)	SM	—	(k*)	—	—	—	671176
1647	FeSe	$P6_3/mmc$ (194)	SM	—	—	FM	—	—	29308 53541 53542 166442 166443 166444 169252 169254 169256 169258 169260 169262 169264 169266 169268 169270 169272 169284 169286 169288 169290 169292 169294 169296 169298 169300 169302 169307 290407 290410 633482 633490
1648	FeSb	$P6_3/mmc$ (194)	SM	Fig. 49	—	FM	SC	—	53535 53971 633396
1649	MnSb	$P6_3/mmc$ (194)	TI	—	—	FM	SC	—	53970 54266 76212 76258 76620 163322 191176 191783 601839 603577 643511 643513 643514 643515 643517 643519 643522 643523 643527 643529 643530 643532 643533 643535
1650	BiMn	$P6_3/mmc$ (194)	SM	—	—	FM	SC	—	58805 192873 192874 192875 192876 192877 192878 192879 192880 192881 616808 616811 616812 672818
1651	CoSb	$P6_3/mmc$ (194)	TI	—	—	NM	SC	—	76118 169166 169167 169168 169169 189946 624893 624900 624901 624909 657491

1652	IrSn	$P6_3/mmc$ (194)	SM	—	—	NM	—	—	104561 641051
1653	$Sr_3P(BO_3)$	$P6_3/mmc$ (194)	Triv.	—	—	NM	—	—	401207
1654	AgBaBi	$P6_3/mmc$ (194)	SM	—	—	NM	—	—	56978
1655	BaBiCu	$P6_3/mmc$ (194)	SM	—	—	NM	—	—	106303
1656	LaPdSb	$P6_3/mmc$ (194)	SM	—	—	NM	—	—	641676
1657	InO(OH)	$P2_13$ (198)	Triv.	—	—	NM	—	—	166255 166256
1658	$Hg_3(AsO_4)Cl$	$P2_13$ (198)	Triv.	—	(b)	NM	—	—	89687 92963 411757
1659	$Na_3(AsS_3)$	$P2_13$ (198)	Triv.	—	—	NM	—	HQ	645 1036
1660	$K_3(SbO_3)$	$P2_13$ (198)	Triv.	—	(b)	NM	—	HQ	279579
1661	$Cs_3(SbO_3)$	$P2_13$ (198)	Triv.	—	(b)	NM	—	HQ	279580
1662	$Cs_3(BiO_3)$	$P2_13$ (198)	Triv.	—	—	NM	—	HQ	406563
1663	$Rb_3(BiO_3)$	$P2_13$ (198)	Triv.	—	(b)	NM	—	HQ	407294
1664	Cs_3SbS_3	$P2_13$ (198)	Triv.	—	—	NM	—	HQ	426551
1665	K_3SbS_3	$P2_13$ (198)	Triv.	—	—	NM	—	HQ	426552 641323
1666	Rb_3SbS_3	$P2_13$ (198)	Triv.	—	(b)	NM	—	HQ	426554
1667	$Na(ClO_3)$	$P2_13$ (198)	SM	—	—	NM	—	—	31056
1668	SiO_2	$P2_13$ (198)	Triv.	—	(b,s)	NM	—	—	24587 44269 162616 162617
1669	$Tl_2Pb(Cu(NO_2)_6)$	$Fm\bar{3}$ (202)	SM	—	—	NM	—	HQ	16
1670	$K_2Sr(Ni(NO_2)_6)$	$Fm\bar{3}$ (202)	SM	—	—	AFM	—	HQ	179
1671	$CaCu_3Ru_4O_{12}$	$Im\bar{3}$ (204)	SM	—	(k,b)	FM	—	HQ	51894 95715 183110
1672	$LaCu_3Ir_4O_{12}$	$Im\bar{3}$ (204)	SM	—	(k,b)	—	—	HQ	251657
1673	CoN_3	$Im\bar{3}$ (204)	TI	—	—	NM	—	—	162105
1674	CoN_3	$Im\bar{3}$ (204)	SM	—	—	NM	—	—	162106
1675	RhN_3	$Im\bar{3}$ (204)	Triv.	—	—	NM	—	—	162107
1676	RhN_3	$Im\bar{3}$ (204)	SM	—	—	NM	—	—	162108
1677	$Ge(SeO_3)_2$	$Pa\bar{3}$ (205)	Triv.	—	(b,s)	NM	—	—	422884
1678	$MgSe_2$	$Pa\bar{3}$ (205)	Triv.	—	—	NM	—	—	642815
1679	$Ca(NO_3)_2$	$Pa\bar{3}$ (205)	Triv.	—	—	NM	—	—	52351 56089
1680	$Sn(SeO_3)_2$	$Pa\bar{3}$ (205)	Triv.	—	(b)	NM	—	—	154716
1681	$Si(P_2O_7)$	$Pa\bar{3}$ (205)	Triv.	—	(b,s)	NM	—	—	19047
1682	SiO_2	$Ia\bar{3}$ (206)	Triv.	—	(b,s)	NM	—	—	170545
1683	SiO_2	$F4_132$ (210)	SM	—	(b,s)	NM	—	—	170504
1684	SiO_2	$I432$ (211)	SM	—	(b,s)	NM	—	—	170506
1685	$Na(BH_4)$	$P\bar{4}3m$ (215)	Triv.	—	—	NM	—	—	182734
1686	$Cs_4(CO_4)$	$P\bar{4}3m$ (215)	Triv.	—	—	NM	—	—	245445
1687	$Cd(CN)_2$	$P\bar{4}3m$ (215)	Triv.	—	—	NM	—	—	20748 66938
1688	$Zn(CN)_2$	$P\bar{4}3m$ (215)	Triv.	—	—	NM	—	—	22392 670038
1689	$Be_4O(TeO_6)$	$F\bar{4}3m$ (216)	Triv.	—	(k*,p*,b)	NM	—	HQ	1322
1690	$CsLi(MoO_4)$	$F\bar{4}3m$ (216)	Triv.	Fig. 50	(k*,p*,b,s)	NM	—	HQ	20805
1691	$IrIn_7GeO_8$	$F\bar{4}3m$ (216)	Triv.	—	(k*,b)	NM	—	—	417829
1692	Ni_5Zr	$F\bar{4}3m$ (216)	SM	Fig. 50	(k*)	FM	—	—	54985 150648 150939 189201 647156
1693	Ni_4ZnZr	$F\bar{4}3m$ (216)	SM	Fig. 50	(k*,p*)	NM	—	—	105477
1694	$MgYNi_4$	$F\bar{4}3m$ (216)	SM	Fig. 51	(k*,p*)	NM	—	—	107033 107424 183095 191556
1695	$CaMgNi_4$	$F\bar{4}3m$ (216)	TI	Fig. 50	(k*,p*)	FM	—	—	107419
1696	$LaMgNi_4$	$F\bar{4}3m$ (216)	SM	Fig. 51	(k*,p*)	FM	—	—	107420 162119 184164 242011 242012 242013 242014 242015 242021 242022 242023 242024 242025
1697	$ScNi_4Cd$	$F\bar{4}3m$ (216)	SM	Fig. 51	(k*,p*)	NM	—	—	185106
1698	YNi_4Cd	$F\bar{4}3m$ (216)	SM	Fig. 51	(k*,p*)	—	—	HQ	423939
1699	$ZrNi_5$	$F\bar{4}3m$ (216)	TI	Fig. 50	(k*)	FM	—	—	601018
1700	$ScAuNi_4$	$F\bar{4}3m$ (216)	TI	Fig. 50	(k*,p*)	NM	—	—	612227
1701	$YAuNi_4$	$F\bar{4}3m$ (216)	TI	Fig. 50	(k*,p*)	—	—	—	612233
1702	Be_5Fe	$F\bar{4}3m$ (216)	SM	—	(k*)	FM	—	—	616267
1703	YNi_4Mn	$F\bar{4}3m$ (216)	SM	—	(k*,p*)	FM	—	—	643173
1704	$HfNi_5$	$F\bar{4}3m$ (216)	SM	Fig. 50	(k*)	—	—	—	672665
1705	$CsMn(Cr(CN)_6)$	$F\bar{4}3m$ (216)	SM	—	—	FM	—	—	56602
1706	Li_2IrGa	$F\bar{4}3m$ (216)	TI	—	—	NM	—	—	107085
1707	Li_2IrIn	$F\bar{4}3m$ (216)	TI	—	—	NM	—	—	107089
1708	Mn_2CoIn	$F\bar{4}3m$ (216)	Triv.	—	—	FM	—	—	160705
1709	Mn_2CoSi	$F\bar{4}3m$ (216)	SM	—	—	FM	—	—	160706

1710	Mn_2CoGe	$F\bar{4}3m$ (216)	SM	—	—	FM	—	—	160707
1711	Mn_2CoSn	$F\bar{4}3m$ (216)	SM	—	—	FM	—	—	160708 183043
1712	Mn_2CoSb	$F\bar{4}3m$ (216)	Triv.	—	—	FM	—	—	160709
1713	$RuMn_2Sn$	$F\bar{4}3m$ (216)	TI	—	—	FM	—	—	182829
1714	$RuMn_2Si$	$F\bar{4}3m$ (216)	SM	—	—	FM	—	—	182830
1715	Ti_2CoIn	$F\bar{4}3m$ (216)	SM	—	—	FM	—	—	185664
1716	Ti_2ZnAl	$F\bar{4}3m$ (216)	SM	—	—	FM	—	—	185882
1717	CoFeMnGa	$F\bar{4}3m$ (216)	SM	—	—	FM	—	—	186830
1718	CoFeMnGe	$F\bar{4}3m$ (216)	Triv.	—	—	FM	—	—	186831
1719	Mn_2CoAs	$F\bar{4}3m$ (216)	SM	Fig. 51	—	FM	—	—	191648
1720	CoFeTiAl	$F\bar{4}3m$ (216)	Triv.	Fig. 52	—	NM	—	—	191657 673236
1721	CoFeTiGa	$F\bar{4}3m$ (216)	SM	Fig. 51	—	NM	—	—	191658
1722	CoFeTiSi	$F\bar{4}3m$ (216)	SM	Fig. 51	—	FM	—	—	191659
1723	CoFeTiGe	$F\bar{4}3m$ (216)	SM	Fig. 52	—	FM	—	—	191660
1724	CoFeTiAs	$F\bar{4}3m$ (216)	SM	Fig. 52	—	FM	—	—	191661
1725	CoFeTiSb	$F\bar{4}3m$ (216)	SM	Fig. 52	—	FM	—	—	191662
1726	CoFeVGa	$F\bar{4}3m$ (216)	SM	Fig. 52	—	FM	—	—	191664
1727	CoFeVAs	$F\bar{4}3m$ (216)	SM	—	—	FM	—	—	191667
1728	CoFeVSb	$F\bar{4}3m$ (216)	SM	—	—	FM	—	—	191668
1729	CoRhMnAl	$F\bar{4}3m$ (216)	TI	—	—	—	—	—	670591
1730	CoRhMnGa	$F\bar{4}3m$ (216)	TI	—	—	—	—	—	670592
1731	CoRhMnGe	$F\bar{4}3m$ (216)	SM	—	—	—	—	—	670593
1732	CoRhMnSi	$F\bar{4}3m$ (216)	SM	—	—	—	—	—	670594
1733	CoFeSiZr	$F\bar{4}3m$ (216)	SM	—	—	—	—	—	670706
1734	CoFeGeZr	$F\bar{4}3m$ (216)	SM	—	—	—	—	—	670707
1735	CrVScSi	$F\bar{4}3m$ (216)	Triv.	—	—	—	—	—	670792
1736	Zr_2CoAl	$F\bar{4}3m$ (216)	SM	—	—	—	—	—	671654
1737	Fe_2MnGe	$F\bar{4}3m$ (216)	SM	Fig. 52	—	—	—	—	671982
1738	Fe_2MnAl	$F\bar{4}3m$ (216)	TI	Fig. 51	—	—	—	—	672261
1739	CoRuFeSi	$F\bar{4}3m$ (216)	SM	—	—	—	—	—	672893 672894 672895
1740	CoRuFeGe	$F\bar{4}3m$ (216)	SM	—	—	—	—	—	672896 672897 672898
1741	CoRuFeSn	$F\bar{4}3m$ (216)	SM	—	—	—	—	—	672899 672900 672901
1742	Co_2MnSi	$F\bar{4}3m$ (216)	SM	—	—	—	—	—	672941 672942 675078
1743	VCoHfGa	$F\bar{4}3m$ (216)	SM	—	—	—	—	—	674822
1744	Co_2MnAl	$F\bar{4}3m$ (216)	Triv.	—	—	—	—	—	675066
1745	Co_2MnGa	$F\bar{4}3m$ (216)	Triv.	—	—	—	—	—	675070
1746	Co_2MnGe	$F\bar{4}3m$ (216)	SM	—	—	—	—	—	675074
1747	CoMnCrSb	$F\bar{4}3m$ (216)	SM	—	—	—	—	—	675083 675084 675085 675086 675087 675088
1748	$GaMo_4S_8$	$F\bar{4}3m$ (216)	SM	—	—	FM	—	HQ	33994$^{(b)}$ 41935$^{(b)}$ 49566$^{(b)}$ 158198$^{(b)}$ 634707
1749	GeV_4Se_8	$F\bar{4}3m$ (216)	Triv.	—	—	FM	—	HQ	50503$^{(b)}$ 195256
1750	GaV_4S_8	$F\bar{4}3m$ (216)	SM	—	(b)	FM	—	HQ	89980 158194 603133
1751	$Al(V_4S_8)$	$F\bar{4}3m$ (216)	SM	—	(b)	FM	—	HQ	195251
1752	PdMnTe	$F\bar{4}3m$ (216)	SM	—	—	FM	—	HQ	40908 44996
1753	CuMnSb	$F\bar{4}3m$ (216)	SM	—	—	FM	—	—	42978 53311 76251 628385 628386 628393
1754	LiZnP	$F\bar{4}3m$ (216)	Triv.	—	—	NM	—	—	44824 642242 670561
1755	AuMnSb	$F\bar{4}3m$ (216)	SM	—	—	FM	—	—	52673 612166 612167 612171
1756	CdLiP	$F\bar{4}3m$ (216)	Triv.	—	—	NM	—	—	52813 670566
1757	CoMnSb	$F\bar{4}3m$ (216)	SM	Fig. 52	—	FM	—	—	53001 624126 624133
1758	CoVSb	$F\bar{4}3m$ (216)	SM	—	—	FM	—	—	53071 107117 624925
1759	NiMnSb	$F\bar{4}3m$ (216)	SM	Fig. 52	—	FM	—	—	54255 76078 182485 643105 643108 643111 643121
1760	RhMnSb	$F\bar{4}3m$ (216)	SM	Fig. 53	—	FM	—	—	54343 76199 76201 643415
1761	AuMnSn	$F\bar{4}3m$ (216)	SM	—	—	FM	—	HQ	54465 240860
1762	CoNbSn	$F\bar{4}3m$ (216)	Triv.	Fig. 53	—	FM	—	—	102552 102553
1763	IrMnSn	$F\bar{4}3m$ (216)	SM	—	—	FM	—	—	104498
1764	MnPtSn	$F\bar{4}3m$ (216)	SM	Fig. 53	—	FM	—	—	104955 104956 643383 643387
1765	CoHfSb	$F\bar{4}3m$ (216)	Triv.	—	—	NM	—	—	108294
1766	GaMnPt	$F\bar{4}3m$ (216)	SM	—	—	FM	—	—	108482
1767	NiCrSb	$F\bar{4}3m$ (216)	SM	—	—	FM	—	—	182484
1768	RbCsN	$F\bar{4}3m$ (216)	SM	—	—	FM	—	—	191639

1769	RbCsP	$F\bar{4}3m$ (216)	SM	—	—	FM	—	—	191640
1770	RbCsAs	$F\bar{4}3m$ (216)	SM	—	—	FM	—	—	191641
1771	FeVTe	$F\bar{4}3m$ (216)	SM	—	—	FM	—	—	191683
1772	CoCrTe	$F\bar{4}3m$ (216)	SM	—	—	FM	—	—	191684
1773	LiMnAs	$F\bar{4}3m$ (216)	SM	—	—	FM	—	HQ	192816
1774	LiCdAs	$F\bar{4}3m$ (216)	SM	—	—	NM	—	—	609965 609966 670567
1775	MnNiSb	$F\bar{4}3m$ (216)	Triv.	—	—	FM	—	—	643109 643120
1776	MnPtSb	$F\bar{4}3m$ (216)	Triv.	—	—	FM	—	—	643377
1777	PtMnBi	$F\bar{4}3m$ (216)	SM	—	—	—	—	—	671364 671368 671372
1778	PtFeBi	$F\bar{4}3m$ (216)	SM	—	—	—	—	—	671365 671369 671373
1779	PtCoBi	$F\bar{4}3m$ (216)	Triv.	—	—	—	—	—	671366 671374
1780	PtCoBi	$F\bar{4}3m$ (216)	TI	—	—	—	—	—	671370
1781	MnTiTe	$F\bar{4}3m$ (216)	SM	—	—	—	—	—	671981
1782	LiCaC	$F\bar{4}3m$ (216)	SM	Fig. 53	—	—	—	—	672030
1783	NaCaC	$F\bar{4}3m$ (216)	SM	—	—	—	—	—	672032
1784	PtCoSb	$F\bar{4}3m$ (216)	Triv.	—	—	—	—	—	672160
1785	PtCrSb	$F\bar{4}3m$ (216)	SM	—	—	—	—	—	672161
1786	PtMnSb	$F\bar{4}3m$ (216)	TI	—	—	—	—	—	672162
1787	CrTiGe	$F\bar{4}3m$ (216)	Triv.	—	—	—	—	—	675079
1788	CrTiSi	$F\bar{4}3m$ (216)	Triv.	—	—	—	—	—	675081
1789	Mn_2Te	$F\bar{4}3m$ (216)	SM	—	—	—	—	—	675105
1790	Li_6PO_5Cl	$F\bar{4}3m$ (216)	Triv.	—	(k*,b)	NM	—	HQ	421479
1791	Li_6PO_5Br	$F\bar{4}3m$ (216)	Triv.	—	(k*,b)	NM	—	HQ	421480 421481
1792	MnSe	$F\bar{4}3m$ (216)	SM	—	—	FM	—	—	24252 41526 670505 671667
1793	FeN	$F\bar{4}3m$ (216)	SM	—	—	NM	—	—	41258 184376 236789 236790 670506
1794	MnS	$F\bar{4}3m$ (216)	SM	—	—	FM	—	—	76205 670482
1795	CoN	$F\bar{4}3m$ (216)	SM	—	—	NM	—	—	79936 161754 184378 236791 236792 670475
1796	YN	$F\bar{4}3m$ (216)	Triv.	—	—	NM	—	—	161077 183180 190624 670502
1797	CaSe	$F\bar{4}3m$ (216)	Triv.	—	—	NM	—	—	167834 670485
1798	ScC	$F\bar{4}3m$ (216)	SM	—	—	FM	—	—	169407 189086 670497
1799	CrTe	$F\bar{4}3m$ (216)	TI	—	—	FM	—	—	169766 181056 670501 671345
1800	MnTe	$F\bar{4}3m$ (216)	SM	—	—	FM	—	—	181324
1801	YC	$F\bar{4}3m$ (216)	SM	—	—	NM	—	—	183160
1802	ZrC	$F\bar{4}3m$ (216)	Triv.	—	—	NM	—	—	183162
1803	MnAs	$F\bar{4}3m$ (216)	Triv.	—	—	FM	—	—	184925 191787
1804	MnSn	$F\bar{4}3m$ (216)	SM	Fig. 53	—	FM	—	—	191171
1805	MnSb	$F\bar{4}3m$ (216)	Triv.	—	—	FM	—	—	191175 191786
1806	RbSb	$F\bar{4}3m$ (216)	SM	—	—	FM	—	—	191491
1807	RbTe	$F\bar{4}3m$ (216)	SM	—	—	FM	—	—	191493
1808	MnP	$F\bar{4}3m$ (216)	Triv.	—	—	FM	—	—	191788
1809	ScN	$F\bar{4}3m$ (216)	Triv.	—	—	NM	—	—	236779 236780
1810	CaO	$F\bar{4}3m$ (216)	Triv.	—	—	—	—	—	670280
1811	SrO	$F\bar{4}3m$ (216)	Triv.	—	—	—	—	—	670287
1812	CrSe	$F\bar{4}3m$ (216)	TI	—	—	—	—	—	671343
1813	CaN	$F\bar{4}3m$ (216)	SM	—	—	—	—	—	672205 672206
1814	TiBi	$F\bar{4}3m$ (216)	SM	—	—	—	—	—	674898
1815	KSe	$F\bar{4}3m$ (216)	SM	—	—	—	—	—	675036
1816	KTe	$F\bar{4}3m$ (216)	SM	—	—	—	—	—	675040
1817	$GaMo_4CS_8$	$F\bar{4}3m$ (216)	SM	Fig. 53	(b,s)	NM	—	—	76848
1818	MgV_2O_4	$F\bar{4}3m$ (216)	SM	Fig. 53	(k*,p*,b)	—	—	—	674693
1819	$Cu_2Al_4O_7$	$F\bar{4}3m$ (216)	SM	Fig. 53	(k*,p*,b)	FM	—	—	100355
1820	SiO_2	$I\bar{4}3m$ (217)	Triv.	Fig. 54	(b,s)	NM	—	HQ	183701
1821	$Ni_3Sb_4O_6F_6$	$I\bar{4}3m$ (217)	TI	—	(k,b)	FM	—	HQ	427047 427048
1822	$Ca_3Ir_4Ge_4$	$I\bar{4}3m$ (217)	SM	—	(k)	NM	SC	HQ	195500 429727
1823	$Sr_3Ir_4Sn_4$	$I\bar{4}3m$ (217)	SM	—	(k)	NM	—	HQ	410992
1824	$Sr_3Ir_4Ge_4$	$I\bar{4}3m$ (217)	SM	—	(k)	—	—	HQ	429725
1825	Na_3BiO_3	$I\bar{4}3m$ (217)	Triv.	—	(b)	NM	—	—	23347
1826	$Zn_4O(BO_2)_6$	$I\bar{4}3m$ (217)	Triv.	—	(b)	NM	—	—	15800$^{(\mathrm{s})}$ 16826 27357 34085$^{(\mathrm{s})}$ 100290$^{(\mathrm{s})}$ 261810$^{(\mathrm{s})}$
1827	$Mg_4P_6(SN_{12})$	$I\bar{4}3m$ (217)	Triv.	—	(b)	NM	—	HQ	65838$^{(\mathrm{s})}$ 642665

1828	$Cd_4P_6N_{12}S$	$I\bar{4}3m$ (217)	Triv.	—	(b,s)	NM	—	HQ	71019
1829	$Zn_8(P_{12}N_{24})O_2$	$I\bar{4}3m$ (217)	Triv.	—	(b)	NM	—	—	417324
1830	$Na_8(Al_6Si_6O_{24})Cl_2$	$P\bar{4}3n$ (218)	Triv.	—	(b,s)	NM	—	—	15336 29443 30263 40129 41188 41189 41190 68426 71432 83323 83324 83325 83326 98807 98808 98809 98810 98811 98812 98813 98814 98815 98816 98817 98818 98819 98820 162491 166827 402574 417689 673830
1831	$Na_8(Al_6Si_6O_{24})$	$P\bar{4}3n$ (218)	SM	—	(b,s)	NM	—	—	56710
1832	$Na_4Cl(Al_3Si_3O_{12})$	$P\bar{4}3n$ (218)	Triv.	—	(b,s)	NM	—	—	65004 74537
1833	$Cd_8(BeSiO_4)_6S_2$	$P\bar{4}3n$ (218)	Triv.	—	(b,s)	NM	—	—	81485
1834	$K_8(AlSiO_4)_6$	$P\bar{4}3n$ (218)	SM	—	(b,s)	NM	—	—	237001
1835	Si_3N_4	$I\bar{4}3d$ (220)	Triv.	—	(b)	NM	—	—	97567
1836	Ge_3N_4	$I\bar{4}3d$ (220)	Triv.	—	(b)	NM	—	—	97569
1837	$PbPd_3$	$Pm\bar{3}m$ (221)	SM	Fig. 54	(k)	NM	SC	—	42600 648357
1838	Ni_3Ge	$Pm\bar{3}m$ (221)	TI	Fig. 54	(k)	NM	—	—	53745 104162 600112 637356 637358 637362 637364
1839	$AlNi_3$	$Pm\bar{3}m$ (221)	SM	Fig. 54	(k)	FM	—	—	58038 58039 105529 151385 185893 187989 196567 196568 604410 608781 608782 608790 608797 608799 608811 608814 671563 671564 672104 672243 673108
1840	$InNi_3$	$Pm\bar{3}m$ (221)	SM	Fig. 54	(k)	FM	—	—	59438 59439
1841	Ni_3Si	$Pm\bar{3}m$ (221)	TI	Fig. 54	(k)	NM	—	—	76413 77960 105343 105344 163353 600224 646572 646573 646579 646584
1842	Co_3Ti	$Pm\bar{3}m$ (221)	SM	—	(k)	FM	—	—	97992 97993 102708 187964 187984 625462 625468 625481 625484
1843	Co_3Ta	$Pm\bar{3}m$ (221)	SM	—	(k)	FM	—	—	102689 187967 187985 671179
1844	$FePd_3$	$Pm\bar{3}m$ (221)	SM	—	(k)	FM	—	—	103582 103583 181720 633132 633134 633135 633140 633141 675019
1845	$GaNi_3$	$Pm\bar{3}m$ (221)	SM	Fig. 55	(k)	FM	—	—	103856 103857 634857 634864
1846	$MnNi_3$	$Pm\bar{3}m$ (221)	SM	—	(k)	FM	—	—	104920
1847	$MnZn_3$	$Pm\bar{3}m$ (221)	SM	Fig. 55	(k)	FM	—	—	105020
1848	Ni_3Sn	$Pm\bar{3}m$ (221)	TI	Fig. 54	(k)	NM	—	—	105353 671094
1849	Pd_3Sc	$Pm\bar{3}m$ (221)	SM	—	(k)	NM	—	—	105673 105674 648807 659956
1850	Pd_3Sn	$Pm\bar{3}m$ (221)	SM	Fig. 55	(k)	NM	—	—	105689 105690 648912 648916 648921 672133
1851	Pd_3Ti	$Pm\bar{3}m$ (221)	SM	—	(k)	NM	—	—	105724 167655 185637
1852	$GeNb_3$	$Pm\bar{3}m$ (221)	SM	—	(k)	NM	—	—	108521 672135
1853	Nb_3Si	$Pm\bar{3}m$ (221)	SM	—	(k)	NM	SC	—	108629 645435
1854	$MgPd_3$	$Pm\bar{3}m$ (221)	SM	—	(k)	NM	—	—	153055
1855	Co_3W	$Pm\bar{3}m$ (221)	SM	Fig. 55	(k)	FM	—	—	187963 187987 671175
1856	Co_3V	$Pm\bar{3}m$ (221)	TI	—	(k)	NM	—	—	187965 187988
1857	Co_3Nb	$Pm\bar{3}m$ (221)	TI	—	(k)	NM	—	—	187966 671177
1858	Co_3Mo	$Pm\bar{3}m$ (221)	SM	Fig. 55	(k)	FM	—	—	187969 671173
1859	$MgNi_3$	$Pm\bar{3}m$ (221)	SM	Fig. 54	(k)	FM	SC*	—	193569
1860	$InPd_3$	$Pm\bar{3}m$ (221)	SM	Fig. 55	(k)	NM	—	—	247193 247197
1861	Cu_3Ni	$Pm\bar{3}m$ (221)	SM	Fig. 55	(k)	—	—	—	670622
1862	$CuNi_3$	$Pm\bar{3}m$ (221)	SM	Fig. 55	(k)	—	—	—	670623
1863	Ni_3Pd	$Pm\bar{3}m$ (221)	SM	—	(k)	—	—	—	670625
1864	$CuPd_3$	$Pm\bar{3}m$ (221)	SM	Fig. 56	(k)	—	—	—	670626 675018
1865	Ni_3Zr_1	$Pm\bar{3}m$ (221)	SM	—	(k)	—	—	—	671414
1866	KCl	$Pm\bar{3}m$ (221)	Triv.	—	—	NM	—	—	31232 60402 61557 290513 290514 290515 290516 290517 290518 290519 290520 290521 290522 290523 290524 290525 290526 290527 290528 290529 290530 290531 290532 290533 290534 290535 290536 290537 290538 290539 290540 290541 290542 290543 290544 290545 290546 290547 290548 671476 674957
1867	RhSi	$Pm\bar{3}m$ (221)	SM	—	—	NM	—	—	44385 182507
1868	RbI	$Pm\bar{3}m$ (221)	Triv.	—	—	NM	—	—	44619 61523 61559 674967

1869	FeAl	$Pm\bar{3}m$ (221)	SM	—	—	FM	—	—	55601 57791 165164 165165 169548 169549 607481 607487 658488 671099
1870	CoFe	$Pm\bar{3}m$ (221)	SM	—	—	FM	—	—	56273 155839 187982 622884
1871	AlCo	$Pm\bar{3}m$ (221)	TI	—	—	NM	—	—	57596 187973 606532 606533 606535 657493
1872	BeCo	$Pm\bar{3}m$ (221)	SM	—	—	FM	—	—	58693 150619 616204 616206
1873	BeNi	$Pm\bar{3}m$ (221)	TI	—	—	FM	—	—	58726 616363 616367
1874	CaCd	$Pm\bar{3}m$ (221)	SM	—	—	NM	—	—	58874 619188
1875	InRh	$Pm\bar{3}m$ (221)	SM	—	—	NM	SC	—	59515 59516
1876	RbBr	$Pm\bar{3}m$ (221)	Triv.	—	—	NM	—	—	61522 61560 674964
1877	KBr	$Pm\bar{3}m$ (221)	Triv.	—	—	NM	—	—	61556 290554 290555 290556 290557 290558 290559 290560 290561 290562 290563 290564 290565 290566 290567 290568 290569 290570 290571 290572 290573 290574 290575 290576 290577 290578 290579 290580 290581 290582 674956
1878	PbS	$Pm\bar{3}m$ (221)	TI	—	—	NM	—	—	77865
1879	TiFe	$Pm\bar{3}m$ (221)	TI	—	—	NM	—	—	96139 150938 189111 189112
1880	FeTi	$Pm\bar{3}m$ (221)	TI	—	—	NM	SC	HQ	100533 103660 103661 190972 633925 633930 633937 633946 633950
1881	CdSc	$Pm\bar{3}m$ (221)	SM	—	—	NM	—	—	102061 620407 670253
1882	CoGa	$Pm\bar{3}m$ (221)	SM	—	—	FM	—	—	102423 603022 623049 623050 623053 623057 657494
1883	CoSc	$Pm\bar{3}m$ (221)	TI	—	—	FM	SC	—	102642 624932
1884	CoTi	$Pm\bar{3}m$ (221)	SM	—	—	FM	SC	—	102705 108322 150937 187975 189225 625473 625477 625488 670727
1885	CoZr	$Pm\bar{3}m$ (221)	SM	—	—	FM	SC	—	102737 102738 189944 625667 625675 625704 670613 670728
1886	CuY	$Pm\bar{3}m$ (221)	SM	—	—	NM	SC	—	103142 163697 185944 629426 629433 629435 672101
1887	FeV	$Pm\bar{3}m$ (221)	SM	—	—	FM	—	—	103681 103682 634034 670598 670599 670600 670601 670602
1888	GaRh	$Pm\bar{3}m$ (221)	SM	—	—	NM	—	—	103948 657338
1889	GaRu	$Pm\bar{3}m$ (221)	SM	—	—	NM	—	—	103950
1890	HgLa	$Pm\bar{3}m$ (221)	SM	—	—	NM	—	—	104305 639065 670252
1891	IrSc	$Pm\bar{3}m$ (221)	TI	—	—	NM	SC	—	104557 640974 657998 670271
1892	LiPd	$Pm\bar{3}m$ (221)	SM	—	—	NM	—	—	104769 642255 642257
1893	MgPd	$Pm\bar{3}m$ (221)	TI	—	—	NM	—	—	104847 104848 163195 642749
1894	MgRh	$Pm\bar{3}m$ (221)	SM	Fig. 56	—	NM	—	—	104859 656818
1895	MnRh	$Pm\bar{3}m$ (221)	TI	—	—	FM	—	—	104960 643391
1896	MnZn	$Pm\bar{3}m$ (221)	SM	—	—	FM	—	—	105017
1897	NiZn	$Pm\bar{3}m$ (221)	SM	—	—	NM	—	—	105470 647135
1898	RhY	$Pm\bar{3}m$ (221)	TI	—	—	NM	SC	—	105972 105973 650527 650530 650535 650536 650541
1899	RuTi	$Pm\bar{3}m$ (221)	TI	—	—	NM	SC	—	106004 106005 650737 650738
1900	RuZr	$Pm\bar{3}m$ (221)	TI	—	—	NM	SC	—	106022 650789
1901	TlY	$Pm\bar{3}m$ (221)	SM	—	—	NM	—	—	106195
1902	YZn	$Pm\bar{3}m$ (221)	SM	—	—	NM	SC	—	106225 106226 653454 653455 653460 653464 653468
1903	RhZn	$Pm\bar{3}m$ (221)	SM	—	—	NM	—	HQ	107574
1904	MgSc	$Pm\bar{3}m$ (221)	SM	—	—	NM	—	—	108583 161737
1905	AuMn	$Pm\bar{3}m$ (221)	SM	—	—	FM	—	—	109348
1906	TiRu	$Pm\bar{3}m$ (221)	TI	—	—	NM	—	—	150936
1907	CoSi	$Pm\bar{3}m$ (221)	SM	—	—	FM	—	—	155928 670610 672131
1908	ZnO	$Pm\bar{3}m$ (221)	Triv.	—	—	NM	—	—	163382 182360 670357
1909	PdN	$Pm\bar{3}m$ (221)	SM	—	—	NM	—	—	169396 191243
1910	ZrRu	$Pm\bar{3}m$ (221)	TI	—	—	NM	—	—	181289 672519
1911	PbS	$Pm\bar{3}m$ (221)	Triv.	—	—	NM	—	—	183242
1912	MgNi	$Pm\bar{3}m$ (221)	TI	—	—	NM	—	—	187256
1913	CoMn	$Pm\bar{3}m$ (221)	TI	—	—	FM	—	—	187981
1914	CoNi	$Pm\bar{3}m$ (221)	SM	—	—	FM	—	—	187983
1915	MnSn	$Pm\bar{3}m$ (221)	SM	Fig. 56	—	FM	—	—	191170
1916	FeN	$Pm\bar{3}m$ (221)	SM	—	—	FM	—	—	236829 236830

1917	CoN	$Pm\bar{3}m$ (221)	SM	—	—	FM	—	—	236831 236832
1918	CuN	$Pm\bar{3}m$ (221)	SM	—	—	NM	—	—	236835 236836
1919	ZnN	$Pm\bar{3}m$ (221)	SM	—	—	NM	—	—	236837 236838 670709
1920	RuTa	$Pm\bar{3}m$ (221)	SM	—	—	FM	—	—	650690
1921	CoAl	$Pm\bar{3}m$ (221)	TI	—	—	—	—	—	670160 671171
1922	PdCu	$Pm\bar{3}m$ (221)	SM	—	—	—	—	—	670618 670621
1923	KSe	$Pm\bar{3}m$ (221)	SM	—	—	—	—	—	675033
1924	Rb(HgF$_3$)	$Pm\bar{3}m$ (221)	Triv.	—	(k,b,s,l)	NM	—	—	15169
1925	K(CoF$_3$)	$Pm\bar{3}m$ (221)	SM	—	(k,b,s,l)	FM	—	HQ	15246 15425 44785 189368
1926	KMnF$_3$	$Pm\bar{3}m$ (221)	SM	Fig. 56	(k,b,s,l)	FM	—	—	15423 37254 43721 44783 75409 75410 75411 189367 201254 201255
1927	KFeF$_3$	$Pm\bar{3}m$ (221)	Triv.	Fig. 59	(k,b,s,l)	FM	—	—	15424 37262 44784 107514
1928	Sr(TiO$_3$)	$Pm\bar{3}m$ (221)	Triv.	—	(k,b,s,l)	NM	SC	HQ	23076 27045 56092 56717 65088 65089 65090 76186 80871 80872 80873 80874 91899 94573 184455 184921 186725 186895 187296 187480 187619 191828 192314 201256 248379 262269 290370 290617 671735 672571 673179 673390 673418 673419 673892 674457 675010
1929	Tl(MnCl$_3$)	$Pm\bar{3}m$ (221)	SM	—	(k,b,s,l)	FM	—	—	23167
1930	GaMn$_3$C	$Pm\bar{3}m$ (221)	SM	—	(k,b,s,l)	AFM	—	—	23586 76845 617912 617913 617914
1931	Cs(HgBr$_3$)	$Pm\bar{3}m$ (221)	SM	Fig. 56	(k,b,s,l)	NM	—	—	24479
1932	Cs(HgCl$_3$)	$Pm\bar{3}m$ (221)	Triv.	—	(k,b,s,l)	NM	—	—	24482
1933	Sr(ZrO$_3$)	$Pm\bar{3}m$ (221)	Triv.	—	(k,b,s,l)	NM	—	—	27046 29153 89365 89366 187481 188448 191829 290618 671952
1934	Sr(SnO$_3$)	$Pm\bar{3}m$ (221)	Triv.	—	(k,b,s,l)	NM	—	—	27047 181089 674084
1935	Ba(ZrO$_3$)	$Pm\bar{3}m$ (221)	Triv.	—	(k,b,s,l)	NM	—	—	27048 43136 90049 97459 97460 97461 97462 290002 671502 672709 672997 673866 674065 674771
1936	Ba(SnO$_3$)	$Pm\bar{3}m$ (221)	Triv.	—	(k,b,s,l)	NM	—	—	27049 43138 180138 181091 184338 185615 186899 188149 190601 239582 424820 670659 672199 674074 674772
1937	Ca(SnO$_3$)	$Pm\bar{3}m$ (221)	SM	—	(k,b,s,l)	FM	—	—	27777
1938	BaTiO$_3$	$Pm\bar{3}m$ (221)	Triv.	—	(k,b,s,l)	NM	—	—	27970 27971 27972 27973 27975 27976 27977 28848 28849 28850 28851 28852 28853 28854 29147 43125 56093 67518 95437 99736 154344 166225 185374 186437 187291 190924 252562 290019 670888 670895 670904 671088 671604 672744 673178 674385
1939	KVF$_3$	$Pm\bar{3}m$ (221)	SM	Fig. 56	(k,b,s,l)	FM	—	—	28145
1940	RbVF$_3$	$Pm\bar{3}m$ (221)	SM	Fig. 56	(k,b,s,l)	FM	—	—	28146
1941	Na(NbO$_3$)	$Pm\bar{3}m$ (221)	Triv.	—	(k,b,s,l)	NM	—	—	28588 28589 28590 31867 192407 192408 236890 252485
1942	Na(TaO$_3$)	$Pm\bar{3}m$ (221)	Triv.	—	(k,b,s,l)	NM	—	—	28617 28618 28619 88378 239693
1943	La(CrO$_3$)	$Pm\bar{3}m$ (221)	SM	Fig. 56	(k,b,s,l)	FM	—	—	28930 29120 41061 673194
1944	KMgF$_3$	$Pm\bar{3}m$ (221)	Triv.	—	(k,b,s,l)	NM	—	—	28949 40476 40477 56096 94089 192409 674545
1945	AgZnF$_3$	$Pm\bar{3}m$ (221)	Triv.	—	(k,b,s,l)	NM	—	—	28950 673278
1946	Ca(ZrO$_3$)	$Pm\bar{3}m$ (221)	Triv.	—	(k,b,s,l)	NM	—	—	29003 56094
1947	BaFeO$_3$	$Pm\bar{3}m$ (221)	SM	—	(k,b,s,l)	FM	—	—	29096 262131 262132 672484
1948	La(FeO$_3$)	$Pm\bar{3}m$ (221)	SM	—	(k,b,s,l)	FM	—	—	29118 673197 674500
1949	La(MnO$_3$)	$Pm\bar{3}m$ (221)	Triv.	Fig. 59	(k,b,s,l)	FM	—	—	29119 188401 673199 674501 674623 674779
1950	Sr(HfO$_3$)	$Pm\bar{3}m$ (221)	Triv.	—	(k,b,s,l)	NM	—	—	29154 89386 161593 164620 184791 673486
1951	Ca(TiO$_3$)	$Pm\bar{3}m$ (221)	Triv.	—	(k,b,s,l)	NM	SC	—	31865 77060 153174 162924 162925 162926 165076 187293
1952	Sr(ZrO$_3$)	$Pm\bar{3}m$ (221)	SM	—	(k,b,s,l)	NM	—	—	33666
1953	K$_3$OBr	$Pm\bar{3}m$ (221)	Triv.	—	(k,b,s,l)	NM	—	HQ	33920
1954	K$_3$OI	$Pm\bar{3}m$ (221)	Triv.	—	(k,b,s,l)	NM	—	HQ	36512
1955	K(TaO$_3$)	$Pm\bar{3}m$ (221)	Triv.	—	(k,b,s,l)	NM	SC*	HQ	39673 39905 56439 56440 184922 280424 674515

1956	$Rb(MnF_3)$	$Pm\bar{3}m$ (221)	SM	Fig. 57	(k,b,s,l)	FM	—	—	43722
1957	$AlCo_3C$	$Pm\bar{3}m$ (221)	SM	—	(k,b,s,l)	NM	—	—	43847
1958	$AlFe_3C$	$Pm\bar{3}m$ (221)	SM	—	(k,b,s,l)	FM	—	—	43853 656541 672402
1959	Mn_3GeC	$Pm\bar{3}m$ (221)	SM	—	(k,b,s,l)	FM	—	—	44351
1960	Rh_3YB	$Pm\bar{3}m$ (221)	SM	Fig. 57	(k,b,s,l)	NM	—	—	44568 615341
1961	$K(CdF_3)$	$Pm\bar{3}m$ (221)	Triv.	—	(k,b,s,l)	NM	—	—	44788
1962	$CsCdF_3$	$Pm\bar{3}m$ (221)	Triv.	—	(k,b,s,l)	NM	—	—	49582 290343 290344 290345 674681
1963	$CsFeF_3$	$Pm\bar{3}m$ (221)	Triv.	—	(k,b,s,l)	FM	—	—	49583
1964	$RbMgF_3$	$Pm\bar{3}m$ (221)	Triv.	—	(k,b,s,l)	NM	—	—	49585
1965	$RbFeF_3$	$Pm\bar{3}m$ (221)	Triv.	—	(k,b,s,l)	FM	—	—	49586 671396
1966	$RbCdF_3$	$Pm\bar{3}m$ (221)	Triv.	—	(k,b,s,l)	NM	—	—	49587
1967	$Ca(SnO_3)$	$Pm\bar{3}m$ (221)	Triv.	—	(k,b,s,l)	NM	—	—	56095 181086 181087
1968	$NaVF_3$	$Pm\bar{3}m$ (221)	SM	Fig. 57	(k,b,s,l)	FM	—	—	60611
1969	$Sr(RuO_3)$	$Pm\bar{3}m$ (221)	SM	Fig. 57	(k,b,s,l)	FM	—	HQ	69360 82981 82982 82983 82984 162777 187484
1970	Rb_3AuO	$Pm\bar{3}m$ (221)	Triv.	—	(k,b,s,l)	NM	—	HQ	75499 79087
1971	Mn_3NiN	$Pm\bar{3}m$ (221)	SM	—	(k,b,s,l)	FM	—	—	76056
1972	Mn_3ZnN	$Pm\bar{3}m$ (221)	SM	—	(k,b,s,l)	FM	—	—	76070 237710
1973	Fe_3ZnC	$Pm\bar{3}m$ (221)	SM	Fig. 57	(k,b,s,l)	FM	—	—	76763
1974	Co_3MgC	$Pm\bar{3}m$ (221)	SM	Fig. 57	(k,b,s,l)	FM	—	—	76790
1975	Co_3ScC	$Pm\bar{3}m$ (221)	SM	—	(k,b,s,l)	NM	—	—	76793
1976	Co_3ZnC	$Pm\bar{3}m$ (221)	SM	Fig. 57	(k,b,s,l)	FM	—	—	76797
1977	Fe_3SnC	$Pm\bar{3}m$ (221)	SM	—	(k,b,s,l)	NM	—	—	76842
1978	$Sr(CoO_3)$	$Pm\bar{3}m$ (221)	SM	—	(k,b,s,l)	FM	—	—	77142 184078
1979	Mn_3SnC	$Pm\bar{3}m$ (221)	SM	—	(k,b,s,l)	FM	—	—	77153 194052 618271 618272
1980	Mn_3ZnC	$Pm\bar{3}m$ (221)	SM	—	(k,b,s,l)	FM	—	—	77154 150829 618284
1981	Rb_3BrO	$Pm\bar{3}m$ (221)	Triv.	—	(k,b,s,l)	NM	—	—	77196
1982	$CsCaBr_3$	$Pm\bar{3}m$ (221)	Triv.	—	(k,b,s,l)	NM	—	—	77242
1983	YRh_3C	$Pm\bar{3}m$ (221)	SM	Fig. 57	(k,b,s,l)	NM	—	—	77389
1984	K_3AuO	$Pm\bar{3}m$ (221)	Triv.	—	(k,b,s,l)	NM	—	HQ	79086
1985	$Sr(VO_3)$	$Pm\bar{3}m$ (221)	SM	Fig. 58	(k,b,s,l)	FM	—	HQ	88982 96291 108826 672730 673312
1986	$La(AlO_3)$	$Pm\bar{3}m$ (221)	Triv.	—	(k,b,s,l)	NM	—	—	90550 90551 90552 90553 90554 90555 90556 92561 92562 153831 153832 153833 153834 153835 153836 170772 191414 191415 191416 191417 191424 191425 191426 191427 191428 191429 191464 672200 673133 673339 674095
1987	$SrFeO_3$	$Pm\bar{3}m$ (221)	SM	—	(k,b,s,l)	FM	—	HQ	91062 92335 163228
1988	$CaPd_3C$	$Pm\bar{3}m$ (221)	SM	—	(k,b,s,l)	NM	—	—	108128
1989	Co_3SnC	$Pm\bar{3}m$ (221)	SM	—	(k,b,s,l)	FM	—	—	108129
1990	$Sr(CrO_3)$	$Pm\bar{3}m$ (221)	SM	—	(k,b,s,l)	FM	—	—	108903 245834
1991	$Sr(TcO_3)$	$Pm\bar{3}m$ (221)	SM	Fig. 58	(k,b,s,l)	NM	—	—	109076 183453 671084 671085
1992	$Pb(TiO_3)$	$Pm\bar{3}m$ (221)	Triv.	—	(k,b,s,l)	NM	—	HQ	153406 162043 162047 187295 187505 262090 672655 673003
1993	$KCaF_3$	$Pm\bar{3}m$ (221)	Triv.	—	(k,b,s,l)	NM	—	—	154073 154074 670413
1994	$BiAlO_3$	$Pm\bar{3}m$ (221)	Triv.	—	(k,b,s,l)	NM	—	—	157549 158756
1995	$BiGaO_3$	$Pm\bar{3}m$ (221)	Triv.	—	(k,b,s,l)	NM	—	—	157550 158757
1996	$Bi(InO_3)$	$Pm\bar{3}m$ (221)	Triv.	—	(k,b,s,l)	NM	—	—	158758
1997	$Bi(ScO_3)$	$Pm\bar{3}m$ (221)	Triv.	—	(k,b,s,l)	NM	—	—	158759 181115 181116 181117 181118 181119 181120
1998	$Pb(CrO_3)$	$Pm\bar{3}m$ (221)	SM	—	(k,b,s,l)	FM	—	HQ	160196 194155
1999	$Pb(HfO_3)$	$Pm\bar{3}m$ (221)	Triv.	—	(k,b,s,l)	NM	—	HQ	161702
2000	$Ca(MnO_3)$	$Pm\bar{3}m$ (221)	SM	Fig. 58	(k,b,s,l)	FM	—	—	168902 168903 168905 181782 673449
2001	$NaMgF_3$	$Pm\bar{3}m$ (221)	Triv.	—	(k,b,s,l)	NM	—	HQ	171813 193089
2002	$Pb(GeO_3)$	$Pm\bar{3}m$ (221)	Triv.	—	(k,b,s,l)	NM	—	—	185693 185694 185695 185696 185697 185698 185699 185700 185701
2003	$Pb(VO_3)$	$Pm\bar{3}m$ (221)	SM	Fig. 58	(k,b,s,l)	FM	—	—	187637
2004	$Sr(MnO_3)$	$Pm\bar{3}m$ (221)	SM	Fig. 58	(k,b,s,l)	AFM	—	—	188415 236949
2005	$K(NbO_3)$	$Pm\bar{3}m$ (221)	Triv.	—	(k,b,s,l)	NM	—	HQ	190920 673080
2006	$Ba(VO_3)$	$Pm\bar{3}m$ (221)	SM	Fig. 58	(k,b,s,l)	FM	—	HQ	191203 673477
2007	$SrGeO_3$	$Pm\bar{3}m$ (221)	Triv.	—	(k,b,s,l)	NM	—	HQ	195084 672202 674088

2008	$RbCaF_3$	$Pm\bar{3}m$ (221)	Triv.	—	(k,b,s,l)	NM	—	—	201252 201253 670414
2009	$CaLiF_3$	$Pm\bar{3}m$ (221)	Triv.	—	(k,b,s,l)	NM	—	—	236756 236757
2010	$InNCo_3$	$Pm\bar{3}m$ (221)	SM	Fig. 58	(k,b,s,l)	FM	—	HQ	247066
2011	$TlPd_3H$	$Pm\bar{3}m$ (221)	TI	—	(k,b,s,l)	NM	—	HQ	247273
2012	$PbZrO_3$	$Pm\bar{3}m$ (221)	Triv.	—	(k,b,s,l)	NM	—	HQ	262104 262105 290872 290873 290874 290875 290876 290877 290878 290879 672047 673004
2013	$CdCo_3N$	$Pm\bar{3}m$ (221)	SM	Fig. 58	(k,b,s,l)	FM	—	HQ	422858
2014	YPd_3H	$Pm\bar{3}m$ (221)	SM	—	(k,b,s,l)	—	—	—	670902
2015	$CaTcO_3$	$Pm\bar{3}m$ (221)	SM	Fig. 59	(k,b,s,l)	—	—	—	671082 671083
2016	$BaTcO_3$	$Pm\bar{3}m$ (221)	SM	Fig. 59	(k,b,s,l)	—	—	—	671086 671087
2017	$YBiO_3$	$Pm\bar{3}m$ (221)	SM	—	(k,b,s,l)	—	—	—	672990
2018	$ZnSnO_3$	$Pm\bar{3}m$ (221)	SM	Fig. 59	(k,b,s,l)	—	—	—	673496
2019	$BaRuO_3$	$Pm\bar{3}m$ (221)	SM	—	(k,b,s,l)	—	—	—	673893
2020	$BaHfO_3$	$Pm\bar{3}m$ (221)	Triv.	—	(k,b,s,l)	—	—	—	674059
2021	$KSbO_3$	$Pm\bar{3}m$ (221)	Triv.	Fig. 59	(k,b,s,l)	—	—	—	674060
2022	$LiSrF_3$	$Pm\bar{3}m$ (221)	Triv.	—	(k,b,s,l)	—	—	—	674527
2023	ReO_3	$Pm\bar{3}m$ (221)	SM	—	(k,b,s,l)	NM	—	—	16810 77679 105546 647350 647352 671107
2024	NbF_3	$Pm\bar{3}m$ (221)	SM	—	(k,b,s,l)	FM	—	—	25596 60246
2025	MoF_3	$Pm\bar{3}m$ (221)	SM	Fig. 59	(k,b,s,l)	FM	—	—	30612
2026	ScF_3	$Pm\bar{3}m$ (221)	Triv.	Fig. 60	(k,b,s,l)	NM	—	—	77071 194248 194249 194250 194273 261067 261068 261069 261070 261071 261072 261073 261074 261075 261076 261077 261078 261079 261080 261081 261082 261083 261084 261085 261086 261087 261088 261089 261090 261091 261092 261093 261094 261095 671108 673424 673425 673426 673427 673428 673429 673430 673431 673432 673433 673434 673435 673436
2027	WO_3	$Pm\bar{3}m$ (221)	Triv.	Fig. 60	(k,b,s,l)	NM	SC*	—	108651 183408 674843
2028	AlF_3	$Pm\bar{3}m$ (221)	Triv.	—	(k,b,s,l)	NM	—	HQ	130021
2029	Na_3N	$Pm\bar{3}m$ (221)	SM	Fig. 59	(k,b,s,l)	NM	—	—	165988 249566 412313 421109 421110 421111 421112 421113 421115 421116 421117 421118
2030	MgO	$Pm\bar{3}n$ (223)	Triv.	Fig. 60	—	NM	—	—	181465
2031	$AuTa_3$	$Pm\bar{3}n$ (223)	SM	—	—	NM	—	—	58599
2032	AuV_3	$Pm\bar{3}n$ (223)	SM	—	—	FM	SC	—	58612 612451 612456 612459
2033	PdV_3	$Pm\bar{3}n$ (223)	SM	—	—	NM	SC	—	105739 649092
2034	Al_3Mo	$Pm\bar{3}n$ (223)	SM	—	—	—	—	—	672120
2035	SiC_2N_4	$Pn\bar{3}m$ (224)	Triv.	Fig. 60	(b)	NM	—	—	93543
2036	$MoZn_7$	$Fm\bar{3}m$ (225)	SM	—	(k)	NM	—	—	130003 644500
2037	$LiPd_7$	$Fm\bar{3}m$ (225)	SM	—	(k)	NM	—	—	642266
2038	Co_9S_8	$Fm\bar{3}m$ (225)	SM	—	(k*)	NM	—	HQ	23929 31753 40046 600664 624834 657415 660368
2039	$Cs_2Mn(Mn(CN)_6)$	$Fm\bar{3}m$ (225)	Triv.	—	—	FM	—	HQ	248046
2040	$Cs_2NaBiCl_6$	$Fm\bar{3}m$ (225)	Triv.	—	(k*,b,s)	NM	—	HQ	2738 59195
2041	$Ba_2Mn(ReO_6)$	$Fm\bar{3}m$ (225)	Triv.	Fig. 61	(k*,b,s)	FM	—	—	4169 109256
2042	$K_2Na(AlF_6)$	$Fm\bar{3}m$ (225)	Triv.	Fig. 61	—	NM	—	HQ	6027 22109$^{(b)}$ 40886$^{(b)}$
2043	KTl_2MoF_6	$Fm\bar{3}m$ (225)	SM	Fig. 60	(b)	FM	—	—	15775
2044	$NaTl_2MoF_6$	$Fm\bar{3}m$ (225)	SM	Fig. 60	(k*,b,s)	FM	—	—	15776
2045	K_2NaCuF_6	$Fm\bar{3}m$ (225)	SM	—	(b)	FM	—	—	22111
2046	K_2NaScF_6	$Fm\bar{3}m$ (225)	Triv.	—	(k*,b,s)	NM	—	—	22112 65730
2047	K_2NaInF_6	$Fm\bar{3}m$ (225)	Triv.	—	(k*,b,s)	NM	—	—	22113 23430
2048	K_2NaTlF_6	$Fm\bar{3}m$ (225)	Triv.	Fig. 61	(k*,b,s)	NM	—	—	22114
2049	Cs_2NaTlF_6	$Fm\bar{3}m$ (225)	Triv.	Fig. 62	(k*,b,s)	NM	—	—	22118
2050	Ba_2MgWO_6	$Fm\bar{3}m$ (225)	Triv.	—	(k*,b,s)	NM	—	—	24982 152572 152573 183771 262318 423033
2051	Ba_2ZnWO_6	$Fm\bar{3}m$ (225)	Triv.	—	(b)	NM	—	—	24983 185847 243794$^{(k,s)}$ 423034$^{(k,s)}$
2052	Ba_2NiWO_6	$Fm\bar{3}m$ (225)	SM	—	(k*,b,s)	AFM	—	—	24984 27426 28342 243798
2053	Ba_2CaWO_6	$Fm\bar{3}m$ (225)	Triv.	—	(b)	NM	—	—	24985 60499$^{(k,s)}$ 76436$^{(k,s)}$ 195954 245599$^{(k,s)}$ 246111$^{(k,s)}$
2054	Ba_2LaReO_6	$Fm\bar{3}m$ (225)	SM	—	(k*,b,s)	FM	—	—	25392
2055	Sr_2YReO_6	$Fm\bar{3}m$ (225)	SM	—	(k*,b,s)	FM	—	—	25404

2056	Ba_2CoWO_6	$Fm\bar{3}m$ (225)	SM	Fig. 60	(k*,b,s)	FM	—	—	27425 97029 195130 672551
2057	$Sr_2Ni(WO_6)$	$Fm\bar{3}m$ (225)	SM	—	—	AFM	—	—	28597$^{(k,b,s)}$ 109165
2058	$Sr_2Co(WO_6)$	$Fm\bar{3}m$ (225)	SM	Fig. 60	(k*,b,s)	FM	—	—	28598
2059	$Sr_2Ni(MoO_6)$	$Fm\bar{3}m$ (225)	SM	—	(k*,b,s)	FM	—	—	28600 155733 157027
2060	$Sr_2Co(MoO_6)$	$Fm\bar{3}m$ (225)	SM	Fig. 61	(k*,b,s)	AFM	—	—	28601 153543
2061	$Sr_2Ca(WO_6)$	$Fm\bar{3}m$ (225)	Triv.	—	(k*,b,s)	NM	—	—	36459
2062	$Rb_2K(CoF_6)$	$Fm\bar{3}m$ (225)	Triv.	—	(b)	NM	—	—	42147
2063	$Rb_2Na(CoF_6)$	$Fm\bar{3}m$ (225)	Triv.	—	(b)	NM	—	—	42148
2064	$Rb_2Na(NiF_6)$	$Fm\bar{3}m$ (225)	SM	—	(b)	FM	—	—	42150
2065	$K_2Na(NiF_6)$	$Fm\bar{3}m$ (225)	SM	—	(k*,b,s)	FM	—	—	42151
2066	K_3WF_6	$Fm\bar{3}m$ (225)	SM	—	—	FM	—	HQ	51264
2067	Ba_2MnWO_6	$Fm\bar{3}m$ (225)	SM	—	(k*,b,s)	AFM	—	HQ	51607 51608 51609 51610 51611 51612 51613
2068	Cs_2KScCl_6	$Fm\bar{3}m$ (225)	Triv.	—	(k*,b,s)	NM	—	HQ	59196
2069	Cs_2LiYCl_6	$Fm\bar{3}m$ (225)	Triv.	—	(k*,b,s)	NM	—	HQ	65731
2070	Cs_2NaYCl_6	$Fm\bar{3}m$ (225)	Triv.	—	(k*,b,s)	NM	—	HQ	65732 245353 245354
2071	$Pb_2Mg(WO_6)$	$Fm\bar{3}m$ (225)	Triv.	—	(k*,b,s)	NM	—	HQ	67880
2072	$Sr_2Ca(MoO_6)$	$Fm\bar{3}m$ (225)	Triv.	—	(k*,b,s)	NM	—	HQ	72815
2073	$Ba_2Ca(IrO_6)$	$Fm\bar{3}m$ (225)	SM	—	(k*,b,s)	FM	—	HQ	74029
2074	$Pb_2(ScTaO_6)$	$Fm\bar{3}m$ (225)	Triv.	—	(k*,b,s)	NM	—	—	77739
2075	$(NH_4)_2NaInF_6$	$Fm\bar{3}m$ (225)	Triv.	—	(k*,b,s)	NM	—	HQ	79099
2076	$Ca_2Fe(WO_6)$	$Fm\bar{3}m$ (225)	Triv.	—	(k*,b,s)	FM	—	—	81203
2077	Ca_2TiSiO_6	$Fm\bar{3}m$ (225)	Triv.	—	(k*,b,s)	NM	—	HQ	83455
2078	$Ba_2(YSbO_6)$	$Fm\bar{3}m$ (225)	Triv.	—	(k*,b,s)	NM	—	HQ	84650 155253 155346 163373
2079	$YBa_2(ReO_6)$	$Fm\bar{3}m$ (225)	SM	—	(b)	FM	—	HQ	94215$^{(k,s)}$ 94216$^{(k,s)}$ 168215$^{(k,s)}$ 168216
2080	Ba_2FeMoO_6	$Fm\bar{3}m$ (225)	Triv.	Fig. 62	(k*,b,s)	FM	—	—	96688 99063 184909 190613 190614 191681 246545 246546
2081	$Ba_2(CoMoO_6)$	$Fm\bar{3}m$ (225)	SM	Fig. 61	(k*,b,s)	AFM	—	HQ	97028 184910 672550
2082	Ba_2NiMoO_6	$Fm\bar{3}m$ (225)	SM	—	(k*,b,s)	AFM	—	HQ	98192
2083	$Ba_2(MnMoO_6)$	$Fm\bar{3}m$ (225)	SM	—	(k*,b,s)	AFM	—	HQ	98739 99090
2084	$Ba_2(FeWO_6)$	$Fm\bar{3}m$ (225)	Triv.	Fig. 62	(k*,b,s)	AFM	—	HQ	99061 672159
2085	$Ba_2(InNbO_6)$	$Fm\bar{3}m$ (225)	Triv.	—	(b)	NM	—	—	99698$^{(k,s)}$ 109162 172166$^{(k,s)}$
2086	$Ba_2Ni(ReO_6)$	$Fm\bar{3}m$ (225)	SM	—	(k*,b,s)	FM	—	—	109251
2087	$Ba_2Fe(ReO_6)$	$Fm\bar{3}m$ (225)	SM	Fig. 61	(k*,b,s)	FM	—	—	109252 155175
2088	$Ba_2Co(ReO_6)$	$Fm\bar{3}m$ (225)	SM	—	(k*,b,s)	FM	—	—	109254 672552 674903
2089	$Ba_2Zn(ReO_6)$	$Fm\bar{3}m$ (225)	SM	—	(k*,b,s)	FM	—	—	109255
2090	$Ba_2Li(ReO_6)$	$Fm\bar{3}m$ (225)	Triv.	—	(k*,b,s)	NM	—	—	109259 418994
2091	$Ba_2Na(ReO_6)$	$Fm\bar{3}m$ (225)	Triv.	—	(b)	NM	—	—	109260$^{(k,s)}$ 200876 418993
2092	$Sr_2Mg(WO_6)$	$Fm\bar{3}m$ (225)	Triv.	—	(k*,b,s)	NM	—	HQ	152575 152576
2093	Ba_2YIrO_6	$Fm\bar{3}m$ (225)	Triv.	—	(k*,b,s)	FM	—	HQ	152679 427064
2094	$Sr_2(GaSbO_6)$	$Fm\bar{3}m$ (225)	Triv.	Fig. 62	(k*,b,s)	NM	—	HQ	157016 157017 157018 157019
2095	$Sr_2(FeMoO_6)$	$Fm\bar{3}m$ (225)	Triv.	Fig. 62	(k*,b,s)	AFM	—	HQ	157603 181752 248459
2096	$Sr_2Y(SbO_6)$	$Fm\bar{3}m$ (225)	Triv.	Fig. 62	(k*,b,s)	NM	—	—	157886 157887
2097	Ba_2YTaO_6	$Fm\bar{3}m$ (225)	Triv.	—	(k*,b,s)	NM	—	HQ	160172 171172 171173 171174 171175 261453
2098	Ba_2CaOsO_6	$Fm\bar{3}m$ (225)	SM	—	(k*,b,s)	FM	—	HQ	171988 171989 192844 192845
2099	Ba_2BiIrO_6	$Fm\bar{3}m$ (225)	Triv.	—	(b)	FM	—	HQ	174289
2100	Sr_2CrZrO_6	$Fm\bar{3}m$ (225)	SM	—	(k*,b,s)	AFM	—	—	181750
2101	Sr_2MnNbO_6	$Fm\bar{3}m$ (225)	Triv.	—	(k*,b,s)	FM	—	—	181751
2102	Pb_2MnReO_6	$Fm\bar{3}m$ (225)	Triv.	—	(k*,b,s)	FM	—	HQ	182001
2103	Ba_2MgTeO_6	$Fm\bar{3}m$ (225)	Triv.	—	(k*,b,s)	—	—	HQ	191563
2104	Pb_2MnWO_6	$Fm\bar{3}m$ (225)	SM	—	(k*,b,s)	AFM	—	—	239438
2105	Ba_2CaTeO_6	$Fm\bar{3}m$ (225)	Triv.	Fig. 62	(k*,b,s)	NM	—	HQ	246112
2106	$Sr_2Li(ReO_6)$	$Fm\bar{3}m$ (225)	Triv.	—	(k*,b,s)	NM	—	—	246731 418992
2107	$(NH_4)_2Na(AlF_6)$	$Fm\bar{3}m$ (225)	Triv.	—	—	NM	—	HQ	249157
2108	Sr_2FeOsO_6	$Fm\bar{3}m$ (225)	SM	Fig. 61	(k*,b,s)	AFM	—	—	251068
2109	$Cs_2InAgCl_6$	$Fm\bar{3}m$ (225)	Triv.	Fig. 62	(k*,b,s)	—	—	—	257115
2110	K_3AlF_6	$Fm\bar{3}m$ (225)	Triv.	—	(b)	NM	—	HQ	262078
2111	$Rb_2Na(AlF_6)$	$Fm\bar{3}m$ (225)	Triv.	—	(b)	NM	—	HQ	290318
2112	$K_2Li(AlF_6)$	$Fm\bar{3}m$ (225)	Triv.	—	(k*,b,s)	NM	—	HQ	408553
2113	$Ba_2Li(OsO_6)$	$Fm\bar{3}m$ (225)	SM	—	(k*,b,s)	FM	—	HQ	412142

2114	$Ba_2Na(OsO_6)$	$Fm\bar{3}m$ (225)	SM	—	(b)	FM	—	HQ	412143
2115	$Rb_2K(GaF_6)$	$Fm\bar{3}m$ (225)	Triv.	—	(b)	NM	—	HQ	416605
2116	$(NH_4)_2Na(GaF_6)$	$Fm\bar{3}m$ (225)	Triv.	—	—	NM	—	HQ	418737
2117	Pb_2NaIO_6	$Fm\bar{3}m$ (225)	SM	Fig. 61	(k*,b,s)	NM	—	HQ	427115
2118	PbF_2	$Fm\bar{3}m$ (225)	Triv.	—	—	NM	—	—	5270 5271 20597 24523 53984 60013 60014 60372 76420 180950 180951 180952 180953 181557 201113 201114 201115
2119	K_2S	$Fm\bar{3}m$ (225)	Triv.	Fig. 63	—	NM	—	—	26735 60439 183837 641321
2120	Rb_2Te	$Fm\bar{3}m$ (225)	Triv.	—	—	NM	—	—	55115 55116 55117 55131 55132 55133 55134 55135 55136 182743
2121	Na_2O	$Fm\bar{3}m$ (225)	Triv.	—	—	NM	—	—	60435 180570 644917
2122	K_2Se	$Fm\bar{3}m$ (225)	Triv.	Fig. 63	—	NM	—	—	60440 168448 196758
2123	K_2Te	$Fm\bar{3}m$ (225)	Triv.	Fig. 63	—	NM	—	—	60441 96739 182742 631721 641376
2124	CrO_2	$Fm\bar{3}m$ (225)	SM	—	—	FM	—	—	186838
2125	Ca_2Pb	$Fm\bar{3}m$ (225)	Triv.	—	—	NM	—	—	191749
2126	$LiCo_2Ge$	$Fm\bar{3}m$ (225)	SM	Fig. 64	—	NM	—	—	25324
2127	$LiPd_2Ge$	$Fm\bar{3}m$ (225)	SM	—	—	NM	—	—	42130
2128	K_3Sb	$Fm\bar{3}m$ (225)	Triv.	—	—	NM	—	—	44677 246648
2129	$LiNi_2Si$	$Fm\bar{3}m$ (225)	SM	—	—	NM	—	—	44819
2130	$InMgNi_2$	$Fm\bar{3}m$ (225)	SM	—	—	NM	—	—	51982
2131	$InMnNi_2$	$Fm\bar{3}m$ (225)	SM	—	—	FM	—	—	51984 51985 639954 639955 639956 639958
2132	$InMnPd_2$	$Fm\bar{3}m$ (225)	SM	—	—	FM	—	—	51988
2133	$CoFe_2Ge$	$Fm\bar{3}m$ (225)	SM	Fig. 64	—	FM	—	—	52954
2134	Co_2FeSi	$Fm\bar{3}m$ (225)	SM	—	—	FM	—	—	52958 247649 622985 672918 675045
2135	Co_2MnGe	$Fm\bar{3}m$ (225)	SM	—	—	FM	—	—	52971 623489 623490 623496 672229 674762 675071 675072 675073
2136	Co_2ZnGe	$Fm\bar{3}m$ (225)	SM	Fig. 64	—	FM	—	—	52994
2137	Co_2MnSb	$Fm\bar{3}m$ (225)	SM	—	—	FM	—	—	53002 624129
2138	Co_2MnSi	$Fm\bar{3}m$ (225)	SM	—	—	FM	—	—	53007 624141 624143 624144 624157 659021 672228 672940 673044 675047 675075 675076 675077
2139	Co_2TiSi	$Fm\bar{3}m$ (225)	SM	Fig. 64	—	FM	—	—	53080 53081 185969 189222 625083
2140	Co_2VSi	$Fm\bar{3}m$ (225)	SM	Fig. 64	—	FM	—	—	53086 659022
2141	CsK_2Sb	$Fm\bar{3}m$ (225)	Triv.	—	—	NM	—	—	53237
2142	Fe_3Ge	$Fm\bar{3}m$ (225)	Triv.	—	—	FM	—	—	53462 672765
2143	$FeRu_2Si$	$Fm\bar{3}m$ (225)	Triv.	Fig. 67	—	FM	—	—	53525 633245 633246
2144	Fe_3Si	$Fm\bar{3}m$ (225)	SM	—	—	FM	—	—	53545 56281 157941 412838 600519 633528 633531 633534 633535 633537 633545 633552 658523 672766
2145	Fe_2VSi	$Fm\bar{3}m$ (225)	SM	Fig. 64	—	FM	—	—	53555 633623 659019
2146	$MnNi_2Ge$	$Fm\bar{3}m$ (225)	SM	—	—	FM	—	—	53687 192566
2147	$MnPd_2Ge$	$Fm\bar{3}m$ (225)	SM	—	—	FM	—	—	53705
2148	$MnRh_2Ge$	$Fm\bar{3}m$ (225)	SM	—	—	FM	—	—	53706 637070 637071
2149	$ZrNi_2In$	$Fm\bar{3}m$ (225)	SM	Fig. 64	—	NM	—	HQ	54546 59460
2150	$HfNi_2In$	$Fm\bar{3}m$ (225)	SM	Fig. 65	—	NM	—	—	54595
2151	$TiNi_2In$	$Fm\bar{3}m$ (225)	SM	—	—	NM	SC	—	54596 59451 59452
2152	$AlCo_2Cr$	$Fm\bar{3}m$ (225)	SM	—	—	FM	—	—	57600 291940 672915 675041
2153	Co_2HfAl	$Fm\bar{3}m$ (225)	SM	—	—	FM	—	—	57611 110809 606590
2154	$AlCo_2Mn$	$Fm\bar{3}m$ (225)	TI	—	—	FM	—	—	57618 606611 606614 672231 675063 675064 675065
2155	$AlCo_2Nb$	$Fm\bar{3}m$ (225)	SM	—	—	FM	—	—	57620 606622
2156	$AlCo_2Ta$	$Fm\bar{3}m$ (225)	SM	—	—	FM	—	—	57634 606667
2157	$AlCo_2V$	$Fm\bar{3}m$ (225)	SM	—	—	FM	—	—	57643 188397 606704 606705 674449
2158	$AlCo_2Zr$	$Fm\bar{3}m$ (225)	SM	—	—	FM	—	—	57648 606733 606737 606738
2159	$AlCrFe_2$	$Fm\bar{3}m$ (225)	SM	Fig. 65	—	FM	—	—	57654 184446
2160	$AlFe_3$	$Fm\bar{3}m$ (225)	SM	Fig. 65	—	FM	—	—	57793 607482 607484 607485 672764
2161	$AlFe_2Mo$	$Fm\bar{3}m$ (225)	SM	Fig. 65	—	FM	—	—	57807
2162	$AlFe_2V$	$Fm\bar{3}m$ (225)	Triv.	—	—	NM	—	—	57832 57833 107814
2163	$AlMnPt_2$	$Fm\bar{3}m$ (225)	SM	—	—	FM	—	—	57985
2164	$AlMnRh_2$	$Fm\bar{3}m$ (225)	TI	—	—	FM	—	—	57986

2165	$\mathrm{AlNi_2Sc}$	$Fm\bar{3}m$ (225)	SM	—	—	NM	—	—	58050
2166	$\mathrm{AlNi_2Ti}$	$Fm\bar{3}m$ (225)	SM	—	—	NM	SC	—	58063 165902
2167	$\mathrm{BiK_3}$	$Fm\bar{3}m$ (225)	SM	—	—	NM	SC	—	58793
2168	$\mathrm{BiRb_3}$	$Fm\bar{3}m$ (225)	SM	—	—	NM	—	—	58849
2169	$\mathrm{InNi_2Sc}$	$Fm\bar{3}m$ (225)	SM	—	—	NM	—	—	59446
2170	$\mathrm{MnNi_2Sb}$	$Fm\bar{3}m$ (225)	TI	—	—	FM	—	—	76080 643107 643114
2171	$\mathrm{Pd_2MnSb}$	$Fm\bar{3}m$ (225)	SM	—	—	FM	—	—	76100 643311 643312 643318
2172	$\mathrm{Mn_3Si}$	$Fm\bar{3}m$ (225)	SM	Fig. 65	—	FM	SC	—	76227 643616 643621 643647
2173	$\mathrm{Co_2CrGa}$	$Fm\bar{3}m$ (225)	SM	—	—	FM	—	—	102318 675042
2174	$\mathrm{CoFe_2Ga}$	$Fm\bar{3}m$ (225)	TI	Fig. 63	—	FM	—	—	102385
2175	$\mathrm{Co_2FeGa}$	$Fm\bar{3}m$ (225)	SM	—	—	FM	—	—	102386 247653
2176	$\mathrm{Co_2HfGa}$	$Fm\bar{3}m$ (225)	SM	Fig. 65	—	FM	—	—	102433 623080
2177	$\mathrm{Co_2MnGa}$	$Fm\bar{3}m$ (225)	TI	—	—	FM	—	—	102438 623116 623118 623121 672230 675067 675068 675069
2178	$\mathrm{Co_2GaNb}$	$Fm\bar{3}m$ (225)	TI	—	—	FM	—	—	102441 623126
2179	$\mathrm{Co_2GaTa}$	$Fm\bar{3}m$ (225)	TI	—	—	FM	—	—	102451
2180	$\mathrm{Co_2GaTi}$	$Fm\bar{3}m$ (225)	SM	—	—	FM	—	—	102453 102454 623206 623207 623209 623211
2181	$\mathrm{Co_2GaV}$	$Fm\bar{3}m$ (225)	TI	—	—	FM	—	—	102456 623228 623230 674450
2182	$\mathrm{Co_2HfSn}$	$Fm\bar{3}m$ (225)	TI	Fig. 63	—	FM	—	—	102483 108295 291934 623806 659656
2183	$\mathrm{Co_2MnSn}$	$Fm\bar{3}m$ (225)	SM	—	—	FM	—	—	102531 102532 624165 624166 624169 624171 624172 624173 624177 672407
2184	$\mathrm{Co_2NbSn}$	$Fm\bar{3}m$ (225)	SM	—	—	FM	—	—	102554 102555 190615 624326 624333
2185	$\mathrm{Co_2ScSn}$	$Fm\bar{3}m$ (225)	SM	—	—	FM	—	—	102646
2186	$\mathrm{Co_2SnTi}$	$Fm\bar{3}m$ (225)	TI	Fig. 63	—	FM	—	—	102682 102683 625282 625285 625286 625289 625291 625292 672408
2187	$\mathrm{Co_2SnV}$	$Fm\bar{3}m$ (225)	SM	—	—	FM	—	—	102684 102685 625303 625306
2188	$\mathrm{Co_2SnZr}$	$Fm\bar{3}m$ (225)	TI	Fig. 63	—	FM	—	—	102687 108321 190131 625312 625314 625318
2189	$\mathrm{CrFe_2Ga}$	$Fm\bar{3}m$ (225)	SM	Fig. 65	—	FM	—	—	102755 184448
2190	$\mathrm{Cu_2MnIn}$	$Fm\bar{3}m$ (225)	TI	Fig. 63	—	FM	—	—	102996 102997 628019
2191	$\mathrm{CuRh_2Sn}$	$Fm\bar{3}m$ (225)	SM	—	—	NM	—	—	103092
2192	$\mathrm{Fe_2GaV}$	$Fm\bar{3}m$ (225)	Triv.	Fig. 67	—	NM	—	—	103473 103474 631850
2193	$\mathrm{Fe_2SnTi}$	$Fm\bar{3}m$ (225)	SM	Fig. 65	—	NM	—	—	103641 103642 186058 633766
2194	$\mathrm{Fe_2SnV}$	$Fm\bar{3}m$ (225)	SM	Fig. 66	—	FM	—	—	103644 291933
2195	$\mathrm{GaHfNi_2}$	$Fm\bar{3}m$ (225)	SM	—	—	NM	SC	—	103734 634320
2196	$\mathrm{GaNi_2Sc}$	$Fm\bar{3}m$ (225)	SM	—	—	NM	—	—	103874
2197	$\mathrm{GaNi_2Ti}$	$Fm\bar{3}m$ (225)	SM	—	—	NM	—	—	103886
2198	$\mathrm{MnNi_2Sn}$	$Fm\bar{3}m$ (225)	SM	Fig. 66	—	FM	—	—	104926 104927 191631 291935 643152 643153 643156 643157 643158 643159 643161 674344
2199	$\mathrm{MnPbRh_2}$	$Fm\bar{3}m$ (225)	SM	—	—	FM	—	—	104936 104937 643290
2200	$\mathrm{MnPd_2Sn}$	$Fm\bar{3}m$ (225)	SM	—	—	FM	—	—	104945 104946 643324 643325 643327
2201	$\mathrm{MnRh_2Sn}$	$Fm\bar{3}m$ (225)	SM	—	—	FM	—	—	104964 104965 643424 643427 643428
2202	$\mathrm{Mn_2WSn}$	$Fm\bar{3}m$ (225)	TI	—	—	NM	—	—	104980
2203	$\mathrm{NiRh_2Sn}$	$Fm\bar{3}m$ (225)	TI	Fig. 64	—	FM	—	—	105327
2204	$\mathrm{Ni_2ScSn}$	$Fm\bar{3}m$ (225)	SM	Fig. 66	—	NM	—	HQ	105339 657254
2205	$\mathrm{Ni_3Sn}$	$Fm\bar{3}m$ (225)	SM	—	—	NM	—	—	105354 671093 671334
2206	$\mathrm{Ni_2SnV}$	$Fm\bar{3}m$ (225)	SM	—	—	FM	SC	—	105376 105377 646810
2207	$\mathrm{Rh_2SnV}$	$Fm\bar{3}m$ (225)	SM	—	—	FM	—	—	105933
2208	$\mathrm{AsMnPd_2}$	$Fm\bar{3}m$ (225)	SM	—	—	FM	—	—	107955
2209	$\mathrm{Fe_3Ga}$	$Fm\bar{3}m$ (225)	SM	Fig. 66	—	FM	—	—	108436 672763
2210	$\mathrm{Cu_2CoSn}$	$Fm\bar{3}m$ (225)	SM	—	—	FM	—	—	151207
2211	$\mathrm{Co_2TiGe}$	$Fm\bar{3}m$ (225)	SM	Fig. 66	—	FM	—	—	169468 169469 623633 623637
2212	$\mathrm{Co_2NiGa}$	$Fm\bar{3}m$ (225)	SM	—	—	FM	—	—	169731
2213	$\mathrm{Co_2FeGe}$	$Fm\bar{3}m$ (225)	SM	—	—	FM	—	—	185936 622905
2214	$\mathrm{Co_2TiAl}$	$Fm\bar{3}m$ (225)	SM	Fig. 66	—	FM	—	—	185966 606679 606680 606682 606685
2215	$\mathrm{Fe_2CrSn}$	$Fm\bar{3}m$ (225)	SM	Fig. 66	—	FM	—	—	185999
2216	$\mathrm{Fe_2TiIn}$	$Fm\bar{3}m$ (225)	SM	—	—	FM	—	—	186056
2217	$\mathrm{Fe_2TiGe}$	$Fm\bar{3}m$ (225)	Triv.	Fig. 67	—	NM	—	—	186057
2218	$\mathrm{Fe_2TiAs}$	$Fm\bar{3}m$ (225)	SM	Fig. 66	—	FM	—	—	186059
2219	$\mathrm{Fe_2TiSb}$	$Fm\bar{3}m$ (225)	SM	Fig. 67	—	FM	—	—	186060

2220	Ni_2FeGa	$Fm\bar{3}m$ (225)	SM	—	—	FM	—	—	187492 672424
2221	Sc_2MnSi	$Fm\bar{3}m$ (225)	SM	—	—	FM	—	—	190996
2222	Sc_2MnGe	$Fm\bar{3}m$ (225)	SM	—	—	FM	—	—	190998
2223	Pd_3N	$Fm\bar{3}m$ (225)	SM	—	—	NM	—	—	191232
2224	Co_2CrIn	$Fm\bar{3}m$ (225)	SM	—	—	FM	—	—	416260
2225	Ru_2VGe	$Fm\bar{3}m$ (225)	SM	Fig. 67	—	—	—	—	671340
2226	Co_2CrSi	$Fm\bar{3}m$ (225)	TI	—	—	—	—	—	672916 675044
2227	Ti_2CoAl	$Fm\bar{3}m$ (225)	SM	—	—	—	—	—	674767
2228	Ru_2ZrSb	$Fm\bar{3}m$ (225)	SM	—	—	—	—	—	675061
2229	Fe_2ZrP	$Fm\bar{3}m$ (225)	SM	Fig. 67	—	—	—	—	675102
2230	Co_2TiIn	$Fm\bar{3}m$ (225)	SM	—	—	—	—	—	675103
2231	Co_2VIn	$Fm\bar{3}m$ (225)	TI	—	—	—	—	—	675104
2232	$K_2(SnCl_6)$	$Fm\bar{3}m$ (225)	Triv.	Fig. 68	(k*)	NM	—	HQ	604 1668 6058 23991 26111
2233	$(NH_4)_2(SnCl_6)$	$Fm\bar{3}m$ (225)	Triv.	Fig. 68	(k*)	NM	—	HQ	605 9021 163660
2234	K_2PtCl_6	$Fm\bar{3}m$ (225)	Triv.	—	(k*)	NM	—	HQ	2582 2583 31114 36304 48137 52033 52034 52035 52036 52037 52038 52039 68765 68766 82375 82376 280458 280459 280460 280461 280462 280463 280464 280465 280466 280467 280468
2235	$(NH_4)_2ReCl_6$	$Fm\bar{3}m$ (225)	SM	—	(k*)	FM	—	HQ	8044
2236	Rb_2SnCl_6	$Fm\bar{3}m$ (225)	Triv.	Fig. 68	(k*)	NM	—	HQ	9022 26698 29026 65059 65060
2237	Cs_2SnCl_6	$Fm\bar{3}m$ (225)	Triv.	Fig. 68	(k*)	NM	—	HQ	9023 26699 29030
2238	Rb_2TeCl_6	$Fm\bar{3}m$ (225)	Triv.	—	(k*)	NM	—	—	9315 26703 29027
2239	Rb_2MnCl_6	$Fm\bar{3}m$ (225)	SM	Fig. 67	(k*)	FM	—	HQ	9347
2240	K_2MnCl_6	$Fm\bar{3}m$ (225)	SM	—	(k*)	FM	—	—	9679
2241	K_2TcCl_6	$Fm\bar{3}m$ (225)	SM	—	(k*)	FM	—	HQ	22096
2242	K_2ReCl_6	$Fm\bar{3}m$ (225)	SM	—	(k*)	FM	—	HQ	23769 26755 68763
2243	$K_2(ReBr_6)$	$Fm\bar{3}m$ (225)	SM	—	(k*)	FM	—	HQ	23770 26623
2244	$K_2(PtBr_6)$	$Fm\bar{3}m$ (225)	Triv.	—	(k*)	NM	—	HQ	23771
2245	Cs_2TeBr_6	$Fm\bar{3}m$ (225)	Triv.	—	(k*)	NM	—	HQ	24151 27695 65057 65058
2246	$K_2(MoCl_6)$	$Fm\bar{3}m$ (225)	SM	—	(k*)	FM	—	—	26643
2247	$Rb_2(TiCl_6)$	$Fm\bar{3}m$ (225)	Triv.	—	(k*)	NM	—	—	26689
2248	$Cs_2(TiCl_6)$	$Fm\bar{3}m$ (225)	Triv.	—	(k*)	NM	—	—	26690
2249	$Rb_2(SeCl_6)$	$Fm\bar{3}m$ (225)	Triv.	—	(k*)	NM	—	—	26692
2250	$Cs_2(SeCl_6)$	$Fm\bar{3}m$ (225)	Triv.	—	(k*)	NM	—	—	26693
2251	$Rb_2(ZrCl_6)$	$Fm\bar{3}m$ (225)	Triv.	—	(k*)	NM	—	—	26694
2252	$Cs_2(ZrCl_6)$	$Fm\bar{3}m$ (225)	Triv.	—	(k*)	NM	—	—	26695
2253	$Tl_2(SnCl_6)$	$Fm\bar{3}m$ (225)	Triv.	—	(k*)	NM	—	—	26700
2254	$Cs_2(TeCl_6)$	$Fm\bar{3}m$ (225)	Triv.	—	(k*)	NM	—	—	26704 29031
2255	$Tl_2(TeCl_6)$	$Fm\bar{3}m$ (225)	Triv.	—	(k*)	NM	—	—	26705
2256	$Rb_2(PtCl_6)$	$Fm\bar{3}m$ (225)	Triv.	—	(k*)	NM	—	—	26708 29028
2257	$Tl_2(PtCl_6)$	$Fm\bar{3}m$ (225)	Triv.	—	(k*)	NM	—	—	26710
2258	$Rb_2(PbCl_6)$	$Fm\bar{3}m$ (225)	Triv.	—	(k*)	NM	—	—	26712 29029
2259	$Cs_2(PbCl_6)$	$Fm\bar{3}m$ (225)	Triv.	—	(k*)	NM	—	—	26713 29033
2260	K_2TiCl_6	$Fm\bar{3}m$ (225)	Triv.	—	(k*)	NM	—	—	26934
2261	Cs_2PoBr_6	$Fm\bar{3}m$ (225)	Triv.	—	(k*)	—	—	—	27694
2262	$Cs_2(GeCl_6)$	$Fm\bar{3}m$ (225)	Triv.	—	(k*)	NM	—	—	28892
2263	K_2PdCl_6	$Fm\bar{3}m$ (225)	Triv.	—	(k*)	NM	—	—	33709 65037 65038 65039 73723
2264	$K_2(SeBr_6)$	$Fm\bar{3}m$ (225)	Triv.	—	(k*)	NM	—	—	36228 69441
2265	$PdBr_6Rb_2$	$Fm\bar{3}m$ (225)	Triv.	—	(k*)	NM	—	—	36305
2266	$K_2(TeBr_6)$	$Fm\bar{3}m$ (225)	Triv.	—	(k*)	NM	—	HQ	38346 65118
2267	$Tl_2(SiF_6)$	$Fm\bar{3}m$ (225)	Triv.	—	—	NM	—	—	38549 52292$^{(k)}$
2268	$K_2(HfF_6)$	$Fm\bar{3}m$ (225)	Triv.	—	(k*)	NM	—	—	47244
2269	$Rb_2(TeBr_6)$	$Fm\bar{3}m$ (225)	Triv.	—	(k*)	NM	—	HQ	49521 49522
2270	K_2TaCl_6	$Fm\bar{3}m$ (225)	SM	Fig. 68	(k*)	FM	—	HQ	59894
2271	Cs_2ReCl_6	$Fm\bar{3}m$ (225)	SM	—	(k*)	FM	—	HQ	64613
2272	$(NH_4)_2(PtCl_6)$	$Fm\bar{3}m$ (225)	Triv.	—	(k*)	NM	—	HQ	97927
2273	Mg_2FeH_6	$Fm\bar{3}m$ (225)	Triv.	—	(k*)	NM	—	—	107500 238723
2274	$K_2(SnBr_6)$	$Fm\bar{3}m$ (225)	Triv.	—	(k*)	NM	—	—	158955
2275	Cs_2PdBr_6	$Fm\bar{3}m$ (225)	Triv.	—	(k*)	—	—	—	243749

2276	$Rb_2(NbCl_6)$	$Fm\bar{3}m$ (225)	SM	Fig. 68	(k*)	FM	—	HQ	245747
2277	$Rb_2(WBr_6)$	$Fm\bar{3}m$ (225)	SM	—	(k*)	FM	—	HQ	402439
2278	$Cs_2(WBr_6)$	$Fm\bar{3}m$ (225)	SM	—	(k*)	FM	—	HQ	402441
2279	$Rb_2(WCl_6)$	$Fm\bar{3}m$ (225)	SM	—	(k*)	FM	—	HQ	409632
2280	$Cs_2(WCl_6)$	$Fm\bar{3}m$ (225)	SM	—	(k*)	FM	—	HQ	409674
2281	$Cs_2(MoCl_6)$	$Fm\bar{3}m$ (225)	SM	—	(k*)	FM	—	HQ	409808
2282	K_2WCl_6	$Fm\bar{3}m$ (225)	SM	—	(k*)	FM	—	HQ	409840
2283	$(NH_4)_2(ReBr_6)$	$Fm\bar{3}m$ (225)	SM	—	(k*)	FM	—	HQ	412159
2284	Sr_2FeH_6	$Fm\bar{3}m$ (225)	Triv.	—	(k*)	NM	—	—	632211
2285	Y_2Ni_6C	$Fm\bar{3}m$ (225)	SM	Fig. 67	(k*)	—	—	—	673582
2286	$K_2(B_6H_6)$	$Fm\bar{3}m$ (225)	Triv.	—	(k*)	NM	—	HQ	65507
2287	Mg_6MnO_8	$Fm\bar{3}m$ (225)	SM	—	(k,b)	AFM	—	HQ	24710 27874 76174 82182
2288	Mg_7VH_{16}	$Fm\bar{3}m$ (225)	SM	—	(k)	FM	—	—	169051
2289	Mg_7NbH_{16}	$Fm\bar{3}m$ (225)	SM	—	(k)	FM	—	—	169052
2290	$MoZn_6$	$Fm\bar{3}m$ (225)	SM	—	(k)	NM	—	—	260686
2291	$Na_6ClF(SO_4)_2$	$Fm\bar{3}m$ (225)	Triv.	—	—	NM	—	HQ	26914 29330 52291
2292	$(PtIn_6)(GaO_4)_2$	$Fm\bar{3}m$ (225)	Triv.	—	(k*)	NM	—	HQ	411505
2293	CoO	$Fm\bar{3}m$ (225)	SM	—	—	AFM	—	HQ	9865 28505 28506 29049 29081 29226 53057 53058 53929 61326 76638 191776 245319 245320 245321 245322 245323 245324 624575 624580 671734 673072 674028 675002
2294	NiO	$Fm\bar{3}m$ (225)	SM	—	—	AFM	—	HQ	9866 24014 24018 28834 28910 53930 53931 61318 61324 61544 76669 182948 184626 184918 241420 646096 646098 646099 671425 671943 674029 674434 674638 675004
2295	MnS	$Fm\bar{3}m$ (225)	SM	—	—	FM	—	—	18007 41331 76204 158647 158648 158649 158650 158651 158652 603118 643434 643435 643436 643437 643438 643439 643443 643444 643445 643450 643451 643453 643456
2296	FeO	$Fm\bar{3}m$ (225)	Triv.	—	—	FM	—	—	27856 31081 53519 60683 76639 82233 180972 180973 180974 633029 633036 633038 670891 674027
2297	ZnTe	$Fm\bar{3}m$ (225)	SM	—	—	NM	—	—	31840 52512 653197
2298	AgN	$Fm\bar{3}m$ (225)	SM	—	—	NM	—	—	167858 183195 185555
2299	CrTe	$Fm\bar{3}m$ (225)	SM	—	—	FM	—	—	169767
2300	NiC	$Fm\bar{3}m$ (225)	TI	—	—	NM	—	—	180457
2301	FeN	$Fm\bar{3}m$ (225)	SM	—	—	FM	—	—	184375 236810
2302	ZnTe	$Fm\bar{3}m$ (225)	Triv.	—	—	NM	—	—	184497 248454
2303	MnSb	$Fm\bar{3}m$ (225)	TI	—	—	FM	—	—	191173
2304	CuN	$Fm\bar{3}m$ (225)	SM	—	—	NM	—	—	236815 236816
2305	CsSe	$Fm\bar{3}m$ (225)	SM	—	—	—	—	—	670583
2306	Ba_2YSbO_6	$Fm\bar{3}m$ (225)	SM	—	(k,b,s,l)	NM	—	—	33624
2307	$Na(SbF_6)$	$Fm\bar{3}m$ (225)	Triv.	—	—	NM	—	HQ	16640 56251$^{(b)}$ 77919
2308	$Ca(PbF_6)$	$Fm\bar{3}m$ (225)	Triv.	—	(k*,b,s)	NM	—	—	25522
2309	$Ca(SnF_6)$	$Fm\bar{3}m$ (225)	Triv.	—	(k*,b,s)	NM	—	HQ	35713
2310	$Fe(ZrF_6)$	$Fm\bar{3}m$ (225)	Triv.	—	(k*,b,s)	FM	—	HQ	35716 100301
2311	$Cr(ZrF_6)$	$Fm\bar{3}m$ (225)	Triv.	—	(k*,b,s)	FM	—	HQ	35719
2312	$VZrF_6$	$Fm\bar{3}m$ (225)	SM	—	(k*,b,s)	FM	—	—	73354 94454
2313	$Co(ZrF_6)$	$Fm\bar{3}m$ (225)	SM	—	(k*,b,s)	FM	—	HQ	83724
2314	$V(HfF_6)$	$Fm\bar{3}m$ (225)	SM	—	(k*,b,s)	FM	—	HQ	94455
2315	$Ti(ZrF_6)$	$Fm\bar{3}m$ (225)	SM	—	(k*,b,s)	FM	—	HQ	94456
2316	$K(SbO_3)$	$Fd\bar{3}m$ (227)	Triv.	—	(k,p,b,s)	NM	—	—	77333
2317	As_2O_3	$Fd\bar{3}m$ (227)	Triv.	—	(b,s)	NM	—	—	2114 16850 24227 183098 409611
2318	As_4O_6	$Fd\bar{3}m$ (227)	Triv.	—	(b,s)	NM	—	—	36144 238612 238613 238614 238615 238616 238617 238618 238619 238620 238621 238622 238623 238624 238625 238626 238627 238628 238629 238630 238631 238632 238633 238634 238635 238636 238637
2319	Ca_2NH	$Fd\bar{3}m$ (227)	Triv.	Fig. 68	(k,p)	NM	—	—	292

2320	Hf_3Zn_3C	$Fd\bar{3}m$ (227)	SM	—	(k,p,b,s)	NM	—	—	42936 618069
2321	$CsAlO_2$	$Fd\bar{3}m$ (227)	Triv.	—	(k,p,b,s)	NM	—	—	28372
2322	$RbAlO_2$	$Fd\bar{3}m$ (227)	Triv.	—	(k,p,b,s)	NM	—	—	28373
2323	$CsNbN_2$	$Fd\bar{3}m$ (227)	Triv.	Fig. 68	(k,p,b,s)	NM	—	HQ	72546
2324	$KAlO_2$	$Fd\bar{3}m$ (227)	Triv.	—	(k,p,b,s)	NM	—	HQ	262975
2325	YS_2	$Fd\bar{3}m$ (227)	SM	Fig. 69	(k,p)	NM	—	—	52216
2326	Mn_2Y	$Fd\bar{3}m$ (227)	SM	—	(k,p)	FM	—	HQ	54375 105001 105002 150743 603250 643875 643894 643895 643896 643902 643910 643915
2327	YFe_2	$Fd\bar{3}m$ (227)	SM	—	(k,p)	FM	—	—	57792 103697 103698 106699 150744 601992 603459 634075 634079 634083 634084 634085 634088 634091 634096 634097 634099 634100 634102 634103 634105 634106 634107 634108 634117 634122 672932
2328	$BaPt_2$	$Fd\bar{3}m$ (227)	TI	Fig. 69	(k,p)	NM	SC	—	58675 616039 616040
2329	Be_2Nb	$Fd\bar{3}m$ (227)	SM	—	(k,p)	NM	SC	—	58721 616354
2330	$CaNi_2$	$Fd\bar{3}m$ (227)	SM	Fig. 69	(k,p)	NM	—	—	58915 619440 619441
2331	Fe_2Sc	$Fd\bar{3}m$ (227)	SM	—	(k,p)	FM	—	—	103618 103619 633420 633429 633433
2332	Ir_2Sc	$Fd\bar{3}m$ (227)	SM	—	(k,p)	NM	SC	—	104558 104559 640973 657997
2333	Ir_2Sr	$Fd\bar{3}m$ (227)	SM	—	(k,p)	NM	SC	—	104564 641065
2334	Ir_2Y	$Fd\bar{3}m$ (227)	SM	—	(k,p)	NM	SC	—	104601 104602 641175 641180 641183
2335	Ni_2Sc	$Fd\bar{3}m$ (227)	SM	Fig. 69	(k,p)	NM	—	—	105334 105335 646466
2336	Ni_2Y	$Fd\bar{3}m$ (227)	SM	Fig. 69	(k,p)	NM	SC	—	105458 105459 150746 183094 196784 647056 647057 647058 647072 647082 647083 647086 647087 647088 647090 647099 647108 657906 670873
2337	Zn_2Zr	$Fd\bar{3}m$ (227)	Triv.	Fig. 69	(k,p)	FM	SC	—	106236 106237 653507 653508 653510 653517 653523
2338	$CaIr_2$	$Fd\bar{3}m$ (227)	SM	—	(k,p)	NM	SC	—	108146
2339	Nb_2Fe	$Fd\bar{3}m$ (227)	TI	—	(k,p)	FM	—	—	188269
2340	Ni_2Cr	$Fd\bar{3}m$ (227)	TI	—	(k,p)	FM	—	—	188273
2341	$CaLi_2$	$Fd\bar{3}m$ (227)	SM	—	(k,p)	NM	—	HQ	413207
2342	$Sc_2(Si_2O_7)$	$Fd\bar{3}m$ (227)	Triv.	—	(k,p,b,s)	NM	—	HQ	1457
2343	$La_2(Zr_2O_7)$	$Fd\bar{3}m$ (227)	Triv.	—	(k,p,b,s)	NM	—	—	15165 51573 150206 153222 153814 154752 159321 248878 253061 253063 671158 671161 672848
2344	$Ca_2(Nb_2O_7)$	$Fd\bar{3}m$ (227)	Triv.	—	(k,p,b,s)	NM	—	—	22411 72206
2345	$Pb_2Sb_2O_7$	$Fd\bar{3}m$ (227)	SM	—	(k,p)	NM	—	—	24246
2346	$Sn_2(Ta_2O_7)$	$Fd\bar{3}m$ (227)	Triv.	Fig. 70	(k,p,b,s)	NM	—	—	27119 163818
2347	$Pb_2Sb_2O_7$	$Fd\bar{3}m$ (227)	SM	Fig. 69	(k,p,b,s)	NM	—	—	27120
2348	$Ca_2Ta_2O_7$	$Fd\bar{3}m$ (227)	Triv.	Fig. 70	(k,p,b,s)	NM	—	—	27121
2349	$Hg_2Cu_2F_6S$	$Fd\bar{3}m$ (227)	SM	—	(k,p,b,s)	FM	—	HQ	27327
2350	$Hg_2Zn_2F_6O$	$Fd\bar{3}m$ (227)	Triv.	Fig. 70	(k,p,b,s)	NM	—	HQ	27330
2351	$Cd_2Nb_2O_7$	$Fd\bar{3}m$ (227)	SM	Fig. 69	(k,p)	NM	—	—	33672
2352	$Bi_2(Ru_2O_7)$	$Fd\bar{3}m$ (227)	Triv.	—	(k,p,b,s)	NM	—	HQ	73787 78114 161102 163387 166566 166567
2353	$Hg_2Cu_2F_6S$	$Fd\bar{3}m$ (227)	SM	—	(k,p,b,s)	FM	—	HQ	156366 156367 156368
2354	$Bi_2(Rh_2O_7)$	$Fd\bar{3}m$ (227)	SM	—	(k,p,b,s)	NM	—	—	161099
2355	$Bi_2(Ti_2O_7)$	$Fd\bar{3}m$ (227)	Triv.	—	(k,p,b,s)	NM	—	—	161100 180394
2356	$Bi_2(Ir_2O_7)$	$Fd\bar{3}m$ (227)	SM	—	(k,p,b,s)	NM	—	—	161103 237820 252134 252135
2357	$Bi_2(Pt_2O_7)$	$Fd\bar{3}m$ (227)	Triv.	—	(k,p,b)	NM	—	—	161104$^{(s)}$ 202346
2358	$Sn_2(Nb_2O_7)$	$Fd\bar{3}m$ (227)	Triv.	Fig. 70	(k,p,b,s)	NM	—	—	163817
2359	$La_2(Zr_2O_7)$	$Fd\bar{3}m$ (227)	TI	—	(k,p,b,s)	NM	—	—	173795 184089 184090 184091 184092 184093 184094 184095 184096 184097 184098 184099 184100 184101 184102
2360	$Y_2(Ir_2O_7)$	$Fd\bar{3}m$ (227)	SM	Fig. 70	(k,p,b,s)	FM	—	HQ	187534
2361	$In_2Ge_2O_7$	$Fd\bar{3}m$ (227)	Triv.	—	(k,p,b,s)	NM	—	—	239593
2362	$La_2Ge_2O_7$	$Fd\bar{3}m$ (227)	Triv.	—	(k,p,b,s)	—	—	—	672851
2363	$Co_2(SiO_4)$	$Fd\bar{3}m$ (227)	TI	—	(k,p,b)	FM	—	HQ	859
2364	Ni_2SiO_4	$Fd\bar{3}m$ (227)	Triv.	—	(k,p,b)	FM	—	HQ	2136 40992 40993 40994 40995 100544 100545 100546 100547 100548 100549 100550 100551 200129 200130 200131

2365	$Mg_2(SiO_4)$	$Fd\bar{3}m$ (227)	Triv.	—	(k,p,b)	NM	—	—	27531 74535 83779 83780 83781 83782 83783 86504 161023 162347 162348 162406 191506 671941
2366	$LiMn_2O_4$	$Fd\bar{3}m$ (227)	SM	—	(k,p,b)	FM	—	—	40485 50415 50427 53603 85341 85345 88644 89459 89985 93599 94339 94340 151907 155282 155665 165871 165872 182717 192369 193444 195840 242138 261557
2367	$Fe_2(SiO_4)$	$Fd\bar{3}m$ (227)	Triv.	—	(k,p,b)	AFM	—	HQ	41002 41003 41004 41005 41006 87462 100552 185517 185518 185519 185520 185521 185522 185523 200133 200134 238745 238746 238747 238748 238749 238751 238752 238753 238754 238755 238756 238757
2368	$CuRh_2S_4$	$Fd\bar{3}m$ (227)	SM	—	(k,p,b)	NM	SC*	—	41900 291917 628767
2369	$CuRh_2Se_4$	$Fd\bar{3}m$ (227)	SM	—	(k,p,b)	NM	SC*	—	41903 602898 628775 628777
2370	$CuTi_2S_4$	$Fd\bar{3}m$ (227)	SM	—	(k,p,b)	FM	SC	—	44609 53336 170227 628916
2371	$FeAl_2O_4$	$Fd\bar{3}m$ (227)	SM	—	(k,p,b)	AFM	—	—	56117 185610 187920 252227
2372	Mg_2VO_4	$Fd\bar{3}m$ (227)	SM	Fig. 70	(k,p,b)	FM	—	—	76980
2373	Ge_3N_4	$Fd\bar{3}m$ (227)	Triv.	—	(k,b)	NM	SC	HQ	87767 97568 156338
2374	Sn_3N_4	$Fd\bar{3}m$ (227)	Triv.	—	(k,b)	NM	—	HQ	89525
2375	$SnZn_2O_4$	$Fd\bar{3}m$ (227)	Triv.	—	(k,p,b)	NM	—	—	187039
2376	$SnCd_2O_4$	$Fd\bar{3}m$ (227)	Triv.	—	(k,p,b)	NM	—	—	187040
2377	$CoAl_2O_4$	$Fd\bar{3}m$ (227)	SM	Fig. 70	(k,p,b)	AFM	—	HQ	290133
2378	Al_2NiO_4	$Fd\bar{3}m$ (227)	SM	Fig. 71	(k,p,b)	AFM	—	—	608815
2379	MoF_6	$Im\bar{3}m$ (229)	Triv.	—	—	NM	—	HQ	1879

2. List of curated materials with flat atomic bands

We have also searched for materials with flat atomic bands defined in Appendix B 1 and which are excluded in Appendix H 1. Since we cannot probe directly the absence of coupling between orbitals of neighboring atoms, we rely on a series of indicators that are easier to access using the database described in Appendix C. Our search criteria are:

- The bands should be extremely flat along all the directions in the BZ.
- The flat bands should be the first set of conduction bands or the last set of valence bands near the Fermi level.
- The DOS peak associated to the set of flat bands should have its center at a maximum distance of 1eV from the Fermi energy and its gaussian width lower than 1eV (see Appendix C 2 b).
- The BRs of the flat bands should be classified by the symmetry eigenvalues as topologically trivial and non-fragile (*i.e.*, LCEBR) [29,43–49,53,54].

For flat atomic bands, the electronic states are (exponentially) localized on one occupied Wyckoff position. In addition we could have *flat molecular bands* where the electronic states are (exponentially) localized on several occupied Wyckoff positions. In some cases, these flat molecular bands could be identified by properties such as bonding within molecular unit, such as poly-atomic ions, coordination-complexes and their ions, or neutral molecules. The rigorous distinction between flat atomic bands and flat molecular bands requires a systematic evaluation of the Wannier states which is beyond the scope of this article. For that reason, we include the compounds with flat molecular bands in the list of flat atomic band compounds.

Based on these criteria, we have obtained 1,102 unique materials (1,830 ICSD entries) exhibiting flat atomic bands near the Fermi level. These materials are listed in Table XIII.

Table XIII: Manually curated list of materials with atomic flat bands. We provide in this table the list of the 1,102 entries of atomic flat-band materials, indexed by the first column. The second column gives the chemical formula, the third column the space group symbol (and number in parentheses). The fourth column indicates the topological classification at the Fermi level: topological insulator (TI), topological semi-metal (SM) or trivial insulator (Triv.). The fifth column details the sublattices found for each material and common to every ICSD entries of this material. Here 'k' stands for Kagome, 'p' for pyrochlore, 'b' for bipartite, 's' for split lattice and 'l' for Lieb sublattice. A star superscript after 'k' ('l') indicates that only approximate Kagome (Lieb) sublattices were found (as defined in Appendix D). The sixth column gives the magnetic properties as obtained from Materials Project (NM for non-magnetic, FM for ferromagnetic, AFM for anti-ferromagnetic, FiM for ferrimagnetic, '—' when the information is not available). The seventh column indicates if the material is known to be superconductor according to the NIMS Materials Database. SC stands for superconductor while SC* means that alloys based on this material are superconductors. The eighth column tells which material are "high-quality" as defined in Appendix H 1. The last column gives all the ICSD entries related to each material. If a given ICSD has additional sublattices compared to those common to all ICSD entries, a superscript label provides the list of these additional sublattices.

Num.	chem. formula	space group	Topo. at E_f	sublat.	magn.	super-conduct.	high quality	ICSDs
1	$B_3H_7(CO)$	$P1$ (1)	Triv.	—	NM	—	HQ	10171
2	$Re_2Cl_5O_4$	$P1$ (1)	SM	—	FM	—	HQ	12111
3	$Bi_2Pb_2V_2O_{10}$	$P1$ (1)	Triv.	(b)	NM	—	HQ	60577
4	$NaBi_3V_2O_{10}$	$P1$ (1)	Triv.	—	NM	—	HQ	88455
5	SiO_2	$P1$ (1)	Triv.	—	NM	—	—	170536 39830$^{(b,s)}$ 56608$^{(b,s)}$ 75656$^{(b,s)}$ 75660$^{(b,s)}$ 75661$^{(b,s)}$ 75663 75666$^{(b,s)}$ 75667$^{(b,s)}$ 75670$^{(b,s)}$
6	$S_3N_2NH_2BF_4$	$P1$ (1)	Triv.	—	NM	—	HQ	201705
7	$NbCl_3OS_2(CH_3)_2(C_2H_4)$	$P1$ (1)	Triv.	—	—	—	—	241969
8	$Li_6Cu(B_4O_{10})$	$P1$ (1)	SM	—	FM	—	HQ	249215
9	CsB_3O_5	$P1$ (1)	Triv.	(b,s)	—	—	—	673574
10	$Ca(HPO_4)$	$P1$ (1)	Triv.	—	NM	—	HQ	918 10504 87196
11	$Ca((VO)(PO_4))_2(H_2O)_4$	$P1$ (1)	Triv.	—	FM	—	HQ	43608 67660
12	$LiH(C_2O_4)(H_2O)$	$P1$ (1)	Triv.	—	NM	—	HQ	246786
13	$(Cu(NH_3)_2)(Sn(OH)_6)$	$P\bar{1}$ (2)	SM	—	FM	—	—	103
14	$(F_2(ZrF_3(H_2O)_3)_2)$	$P\bar{1}$ (2)	Triv.	—	NM	—	—	1309
15	$Tl_2(Cu(SO_3)_2)$	$P\bar{1}$ (2)	SM	(b)	FM	—	—	2896
16	$K_3N(SO_3)_2H_2O$	$P\bar{1}$ (2)	Triv.	—	NM	—	—	8001 201190
17	$(S_4N_3)BiCl_4$	$P\bar{1}$ (2)	Triv.	—	NM	—	—	9460
18	$(Re_2O_3Cl_6)(ReO_3Cl)_2$	$P\bar{1}$ (2)	Triv.	—	NM	—	—	10302
19	$K_3(ReO_2(CN)_4)$	$P\bar{1}$ (2)	Triv.	—	NM	—	—	16121 26223 30430
20	$CsKNi(CN)_4$	$P\bar{1}$ (2)	Triv.	—	—	—	—	16399
21	$K_4((SO_3)_2(NO))_2$	$P\bar{1}$ (2)	Triv.	—	NM	—	—	16879
22	$Al_2(Si_4O_{10})O$	$P\bar{1}$ (2)	Triv.	(k*,b)	NM	—	—	30119
23	$Na_2(B_2(O_2)_2(OH)_4)(H_2O)_6$	$P\bar{1}$ (2)	Triv.	—	NM	—	—	30532
24	$S_3N_2AsF_6$	$P\bar{1}$ (2)	TI	—	FM	—	HQ	31787
25	$H_3OH_3F_4$	$P\bar{1}$ (2)	Triv.	—	NM	—	—	32569
26	$(I_3Cl_2)(SbCl_6)$	$P\bar{1}$ (2)	Triv.	—	NM	—	HQ	32662 26402
27	$((CO)_4MnPH_2)_2$	$P\bar{1}$ (2)	Triv.	—	—	—	HQ	33267
28	$Na_2Mg(SO_3)_2(H_2O)_2$	$P\bar{1}$ (2)	Triv.	—	NM	—	HQ	35767
29	$CsH_3P_2O_7(H_2O)$	$P\bar{1}$ (2)	Triv.	(b)	NM	—	—	38033
30	$(PtCl_2(NH_3)_4)(NO_3)_2$	$P\bar{1}$ (2)	Triv.	—	NM	—	HQ	38066
31	$(PdCl_2(SCl_2)_2)$	$P\bar{1}$ (2)	Triv.	—	NM	—	—	39434
32	$(ClF_2)(BiF_6)$	$P\bar{1}$ (2)	Triv.	—	NM	—	HQ	39555
33	MgF_2	$P\bar{1}$ (2)	Triv.	—	NM	—	—	51243
34	$MgCl_2$	$P\bar{1}$ (2)	Triv.	—	NM	—	—	51247
35	$SbF_4(PO_2F_2)$	$P\bar{1}$ (2)	Triv.	—	NM	—	HQ	51535
36	$PbCuAsO_4$	$P\bar{1}$ (2)	Triv.	(b)	NM	—	HQ	61677
37	$Na_4Cu(AsO_4)_2$	$P\bar{1}$ (2)	SM	(b,s)	FM	—	HQ	63058
38	$I_4(SbF_6)_2$	$P\bar{1}$ (2)	Triv.	—	NM	—	HQ	63301
39	$((SCl_2)_2Pt)Cl_2$	$P\bar{1}$ (2)	Triv.	—	NM	—	HQ	66013
40	$(CN_4H_8)(SO_4)$	$P\bar{1}$ (2)	Triv.	—	NM	—	—	74825
41	$Na_7AlH_2(CO_3)_4F_4$	$P\bar{1}$ (2)	Triv.	—	NM	—	HQ	77052
42	$K((CH_3)CO_3)$	$P\bar{1}$ (2)	Triv.	—	NM	—	HQ	77115
43	ReF_7	$P\bar{1}$ (2)	Triv.	—	NM	—	HQ	78311
44	$Ca((HSO_4)_2(H_2SO_4)_2)$	$P\bar{1}$ (2)	Triv.	—	NM	—	HQ	85073
45	$(Mg(H_2O)_6)(CoCl_4(H_2O)_2)$	$P\bar{1}$ (2)	SM	—	AFM	—	HQ	96559

46	$Na_2(HPO_4)(H_2O)$	$P\bar{1}$ (2)	Triv.	—	NM	—	HQ	108838
47	$(CH_3)_2NOSiH_2Cl$	$P\bar{1}$ (2)	Triv.	—	NM	—	—	110528
48	C_3F_6	$P\bar{1}$ (2)	Triv.	—	NM	—	HQ	151184
49	$AgSc(CrO_4)_2(H_2O)_2$	$P\bar{1}$ (2)	Triv.	—	NM	—	HQ	156676
50	$Cu(O_2N_2CN)_2(N_2C_4H_4)$	$P\bar{1}$ (2)	SM	—	—	—	HQ	168724
51	$Cu(NH_3)_4(ReO_4)_2$	$P\bar{1}$ (2)	SM	—	—	—	HQ	169583
52	$Ca_2CuTe_4O_{10}Cl_2$	$P\bar{1}$ (2)	SM	(b,s)	FM	—	HQ	171007
53	$(NH_4)(HSeO_3)$	$P\bar{1}$ (2)	Triv.	—	NM	—	HQ	171372
54	$Na_2S_2O_8$	$P\bar{1}$ (2)	Triv.	—	NM	—	HQ	171374
55	$Cu(SO_3CF_3)_2$	$P\bar{1}$ (2)	SM	(b)	FM	—	HQ	172335
56	$((C_2(NH_2)_2)(NH)_2N)_2(SiF_6)$	$P\bar{1}$ (2)	Triv.	—	NM	—	—	180801
57	$(Cd(NCS)_2(CS(NH_2)_2)_2)(H_2O)_2$	$P\bar{1}$ (2)	Triv.	—	—	—	HQ	187240
58	$Tl_4Cu(TeO_6)$	$P\bar{1}$ (2)	TI	(b)	FM	—	HQ	187561
59	$Y_2Cu(TeO_3)_2(SO_4)_2$	$P\bar{1}$ (2)	SM	(b,s)	FM	—	HQ	194348
60	$((CH_3)_2NH_2)(H(C_2O_4))(H_2C_2O_4)_{0.5}$	$P\bar{1}$ (2)	Triv.	—	NM	—	—	195083
61	$(XeF_3)(BiF_6)$	$P\bar{1}$ (2)	Triv.	—	NM	—	—	200043
62	$Al_4Si_8O_{22}$	$P\bar{1}$ (2)	Triv.	(k*,b)	NM	—	—	201706
63	$Ca_2Cu(OH)_4(B(OH)_4)_2$	$P\bar{1}$ (2)	SM	—	FM	—	HQ	202148
64	$Fe(H_2O)_2(C_4S_4)(H_2O)_4$	$P\bar{1}$ (2)	Triv.	—	—	—	HQ	203234
65	$Li_3CuB_3O_7$	$P\bar{1}$ (2)	Triv.	—	NM	—	HQ	237524
66	$K_3Zn_2Cl_7$	$P\bar{1}$ (2)	Triv.	—	NM	—	—	239665
67	$Sn(SO_4)$	$P\bar{1}$ (2)	Triv.	—	NM	—	—	245906 245907
68	$Tl_4(IO_3)_6$	$P\bar{1}$ (2)	Triv.	—	NM	—	HQ	247060
69	$(In_2(SeO_3)_2(C_2O_4)(H_2O)_2)(H_2O)_2$	$P\bar{1}$ (2)	Triv.	—	NM	—	HQ	249780
70	$Fe(NCS)_2(OC(CH_3)_2)_2$	$P\bar{1}$ (2)	Triv.	—	FM	—	HQ	250699
71	$Hg(CH_3SO_3)_2(H_2O)_2$	$P\bar{1}$ (2)	Triv.	—	NM	—	HQ	251311
72	$(C_2H_{10}N_2)Cu(H_2O)_2(V_2O_2F_8)$	$P\bar{1}$ (2)	SM	—	FM	—	—	251432
73	Na_4NiTeO_6	$P\bar{1}$ (2)	Triv.	(b)	—	—	—	253698
74	$K_3(TcO_2(CN)_4)$	$P\bar{1}$ (2)	Triv.	—	NM	—	HQ	260824
75	$(C_2H_8N)_2(Sn(CH_3)_2Cl_4)$	$P\bar{1}$ (2)	Triv.	—	NM	—	—	261582
76	$((Cu(H_2O)_2)Cl_2(CdCl_2))(H_2O)_2$	$P\bar{1}$ (2)	SM	—	FM	—	HQ	280299
77	$((N_2H_5)_2((N_4C)_2N_2))(N_2H_4)_2$	$P\bar{1}$ (2)	Triv.	—	NM	—	—	280661
78	$Te_4(HfCl_6)$	$P\bar{1}$ (2)	Triv.	—	NM	—	HQ	401589
79	$(CF_3)_2O_3$	$P\bar{1}$ (2)	Triv.	—	NM	—	HQ	401780
80	$(Li(NH_3)_4)_2Te_2$	$P\bar{1}$ (2)	Triv.	—	NM	—	—	409556
81	$(SeCl_3)(MoOCl_4)$	$P\bar{1}$ (2)	TI	(b)	FM	—	HQ	410101
82	$Ni((NH_2)SO_3)_2(H_2O)_4$	$P\bar{1}$ (2)	Triv.	—	AFM	—	—	410198
83	$(Cu(C_2N_2H_8)_2)(Ni(CN)_4)$	$P\bar{1}$ (2)	SM	—	FM	—	—	411632
84	$PbF(AsF_6)$	$P\bar{1}$ (2)	Triv.	—	NM	—	HQ	411788
85	$AuXe_2(SbF_6)_2$	$P\bar{1}$ (2)	SM	—	FM	—	HQ	412106
86	$Au_2Xe_2F(SbF_6)_3$	$P\bar{1}$ (2)	Triv.	—	NM	—	HQ	412107
87	$(Cu(NH_3)_4)(N(NO_2)_2)_2$	$P\bar{1}$ (2)	SM	—	FM	—	—	412606
88	$(Pd(NH_3)_4)(N(NO_2)_2)_2$	$P\bar{1}$ (2)	Triv.	—	NM	—	—	412607
89	$KNaS_2O_7$	$P\bar{1}$ (2)	Triv.	—	NM	—	HQ	413050
90	$(F_5S)(NCS)$	$P\bar{1}$ (2)	Triv.	—	NM	—	HQ	413754
91	$Li_4(PO_2NH)_4(H_2O)_4$	$P\bar{1}$ (2)	Triv.	—	NM	—	—	415548
92	$(ReO_3Cl)(ReOCl_4)$	$P\bar{1}$ (2)	Triv.	—	FM	—	HQ	416429
93	$(Cs_2(H_6Te_2O_{10}))(Te(OH)_6)$	$P\bar{1}$ (2)	Triv.	—	—	—	—	417437
94	$Ir(PO_3)_3$	$P\bar{1}$ (2)	Triv.	(b)	NM	—	HQ	419717
95	$Pd(NH_3)_2(NO_2)_2$	$P\bar{1}$ (2)	Triv.	—	NM	—	HQ	420291
96	$Pt(H_2O)_4(SbF_6)_2$	$P\bar{1}$ (2)	Triv.	—	NM	—	HQ	421861
97	$Rb_3In(IO_3)_6$	$P\bar{1}$ (2)	Triv.	(b)	NM	—	HQ	422058
98	$Ag_2BaCu(VO_4)_2$	$P\bar{1}$ (2)	TI	(b,s)	FM	—	HQ	422132
99	$H_6O_{12}P_4Rb_2$	$P\bar{1}$ (2)	Triv.	(b)	NM	—	HQ	423682
100	$H_6Cs_2O_{12}P_4$	$P\bar{1}$ (2)	Triv.	(b)	NM	—	HQ	423683
101	$Ba_2(Pd(HS_2O_7)_2(S_3O_{10})_2)$	$P\bar{1}$ (2)	Triv.	—	NM	—	—	425466
102	$NaClO_4(H_2O)_2$	$P\bar{1}$ (2)	Triv.	—	NM	—	HQ	425697
103	$CuSb_6O_8(SO_4)_2$	$P\bar{1}$ (2)	SM	(b)	FM	—	—	428356
104	$Cs(HS_2O_7)$	$P\bar{1}$ (2)	Triv.	—	NM	—	HQ	428724
105	$PbF(SbF_6)$	$P\bar{1}$ (2)	Triv.	—	NM	—	HQ	429016
106	$(PCl_4)_2(Re_2Cl_{10})$	$P\bar{1}$ (2)	Triv.	—	FM	—	HQ	410188

107	$Ag(TaF_6)_2$	$P\bar{1}$ (2)	SM	(b,s)	FM	—	HQ	62543
108	$Ag(BiF_6)_2$	$P\bar{1}$ (2)	SM	(b,s)	FM	—	HQ	79879
109	$Na(AgZr_2F_{11})$	$P\bar{1}$ (2)	SM	—	FM	—	HQ	65179
110	$NaCu(Zr_2F_{11})$	$P\bar{1}$ (2)	SM	—	FM	—	HQ	78869
111	$(InCl_2(NH_3)_4)(In(NH_3)_2Cl_4)$	$P\bar{1}$ (2)	Triv.	—	NM	—	—	281343
112	$(CH_3)NSOF_2$	$P\bar{1}$ (2)	Triv.	—	NM	—	HQ	237988
113	$Ba_6Mg_{11}F_{34}$	$P\bar{1}$ (2)	Triv.	(b)	NM	—	—	413125
114	$BaCoP_2O_7$	$P\bar{1}$ (2)	Triv.	(b)	FM	—	HQ	202853
115	$((C_2H_4(OH))NH_3)(CuBr_3)$	$P\bar{1}$ (2)	Triv.	—	FM	—	—	110471
116	$Ca(H_2PO_4)_2$	$P\bar{1}$ (2)	Triv.	—	NM	—	—	2632 2633$^{(b)}$
117	$Ca(C_2O_4)(H_2O)_3$	$P\bar{1}$ (2)	Triv.	—	NM	—	—	77096 159351
118	$(Co(H_2O)_6)(SnF_3)_2$	$P\bar{1}$ (2)	SM	—	AFM	—	—	27799
119	$(Ni(H_2O)_6)(SnF_3)_2$	$P\bar{1}$ (2)	Triv.	—	AFM	—	HQ	79718
120	$(Cd(H_2O)_6)(SnF_3)_2$	$P\bar{1}$ (2)	Triv.	—	—	—	HQ	166590
121	$Cu(ReO_4)_2(H_2O)_4$	$P\bar{1}$ (2)	SM	—	—	—	HQ	402669
122	$(Ni(H_2O)_4)(ReO_4)_2$	$P\bar{1}$ (2)	Triv.	—	FM	—	HQ	402773
123	$Co(H_2O)_4(ReO_4)_2$	$P\bar{1}$ (2)	SM	—	FM	—	HQ	402964
124	$Cs_4Cu(Si_2O_7)$	$P\bar{1}$ (2)	SM	(b)	FM	—	HQ	50444
125	$Rb_4(CuSi_2O_7)$	$P\bar{1}$ (2)	SM	(b,s)	FM	—	HQ	85405
126	$CuZn_2(AsO_4)_2$	$P\bar{1}$ (2)	SM	(b)	FM	—	—	18115 26839 100249
127	$Cd_2Cu(PO_4)_2$	$P\bar{1}$ (2)	SM	(b)	FM	—	HQ	249777
128	$CuH_{10}(AsO_4)_4$	$P\bar{1}$ (2)	SM	—	FM	—	—	59158
129	$Na_2Co(SeO_4)_2(H_2O)_2$	$P\bar{1}$ (2)	SM	—	—	—	HQ	98683
130	$Na_2Ni(SeO_4)_2(H_2O)_2$	$P\bar{1}$ (2)	Triv.	—	FM	—	HQ	98684
131	$(Co(O_2N_2CN)_2(H_2O)_2(N_2C_4H_4))(H_2O)_2$	$P\bar{1}$ (2)	SM	—	—	—	—	168723
132	$Fe(SC(NH_2)_2)_2(NCS)_2$	$P\bar{1}$ (2)	Triv.	—	FM	—	—	10452
133	H_3BO_3	$P\bar{1}$ (2)	Triv.	—	NM	—	—	24711 52290$^{(b)}$ 61354$^{(b)}$ 61365$^{(b)}$
134	H_3OBF_4	$P\bar{1}$ (2)	Triv.	—	NM	—	HQ	15591
135	$Hg(Mn(CO)_5)_2$	$P\bar{1}$ (2)	Triv.	—	NM	—	—	16124
136	$(Br_3)(AsF_6)$	$P\bar{1}$ (2)	Triv.	—	NM	—	HQ	33811
137	$K_2(O_2(SO_3)_2)$	$P\bar{1}$ (2)	Triv.	—	NM	—	—	16972 54024
138	$Cs_2Cu(Cr_2O_7)_2(H_2O)_2$	$P\bar{1}$ (2)	SM	—	FM	—	HQ	156678
139	$K_6(CuSi_2O_8)$	$P\bar{1}$ (2)	SM	(b,s)	FM	—	HQ	85404
140	$Cs_6(NiSi_2O_8)$	$P\bar{1}$ (2)	Triv.	(b,s)	NM	—	HQ	409506
141	$K(HCO_3)$	$P\bar{1}$ (2)	Triv.	—	NM	—	—	157166
142	$K(HSeO_3)$	$P\bar{1}$ (2)	Triv.	—	NM	—	HQ	20862
143	$KMgH(CO_3)_2(H_2O)_4$	$P\bar{1}$ (2)	Triv.	—	NM	—	HQ	63137 63138
144	$KNi(H(CO_3)_2)(H_2O)_4$	$P\bar{1}$ (2)	Triv.	—	AFM	—	HQ	68710
145	$NaLa(SO_4)_2$	$P\bar{1}$ (2)	Triv.	—	NM	—	—	20354
146	$Al_2O(SiO_4)$	$P\bar{1}$ (2)	Triv.	—	NM	—	—	16970$^{(b)}$ 16976$^{(b)}$ 27771$^{(b)}$ 27985 28272 77538$^{(b)}$ 77539$^{(b)}$ 77540$^{(b)}$ 77541$^{(b)}$ 77542$^{(b)}$ 83450$^{(b)}$ 83451$^{(b)}$ 83452$^{(b)}$ 83453$^{(b)}$ 83454$^{(b)}$ 85742$^{(b)}$ 86341$^{(b)}$ 100455$^{(b)}$ 100456$^{(b)}$ 100457$^{(b)}$ 167293$^{(b)}$ 167294$^{(b)}$ 167295$^{(b)}$
147	$Li_6Ga_2(BO_3)_4$	$P\bar{1}$ (2)	Triv.	—	NM	—	—	9987
148	$Li_4(P_2O_7)$	$P\bar{1}$ (2)	Triv.	—	NM	—	HQ	59243$^{(b)}$ 246859 248414$^{(b)}$
149	$LiAl(PO_4)(OH)$	$P\bar{1}$ (2)	Triv.	(b)	NM	—	HQ	68921
150	$(Mg(H_2O)_6)(S_2O_6)$	$P\bar{1}$ (2)	Triv.	—	FM	—	—	1834
151	$(Zn(H_2O)_6)(S_2O_6)$	$P\bar{1}$ (2)	Triv.	—	NM	—	—	1836
152	$(((Mn(CO)_5)_2In)_2Cl_2)$	$P\bar{1}$ (2)	Triv.	—	NM	—	—	889
153	$Li_6CuB_4O_{10}$	$P\bar{1}$ (2)	SM	(b)	FM	—	HQ	237526
154	$Na_2Ca(P_2O_7)$	$P\bar{1}$ (2)	Triv.	—	NM	—	HQ	89468
155	$Na_4(WO_2N_2)$	$P\bar{1}$ (2)	Triv.	(b)	NM	—	HQ	73101
156	$K(C(CN)_3)$	$P\bar{1}$ (2)	Triv.	—	NM	—	—	77046 428779
157	$Na(ClO_2)(H_2O)_3$	$P\bar{1}$ (2)	Triv.	—	NM	—	—	1858 1954
158	$Na(BrO_2)(H_2O)_3$	$P\bar{1}$ (2)	Triv.	—	NM	—	HQ	74654
159	$Os_3(CO)_9Se_2$	$P\bar{1}$ (2)	Triv.	(b)	NM	—	—	30552
160	$Ru_3Se_2(CO)_9$	$P\bar{1}$ (2)	Triv.	(b)	NM	—	—	72764
161	$Pb_4Cu(SO_4)_2(OH)_6$	$P\bar{1}$ (2)	SM	(b)	FM	—	HQ	380382
162	$PbBi_6O_4(PO_4)_4$	$P\bar{1}$ (2)	Triv.	—	NM	—	—	91258

163	$Mg(SO_4)(H_2O)_5$	$P\bar{1}$ (2)	Triv.	—	NM	—	—	2776
164	$((SCl_2)S(SCl))(AsF_6)$	$P\bar{1}$ (2)	Triv.	—	NM	—	HQ	75451 154804
165	$Ca_2Ba(Si_3O_9)$	$P\bar{1}$ (2)	Triv.	—	NM	—	—	24426
166	$K_2Co(H_2P_2O_7)_2(H_2O)_2$	$P\bar{1}$ (2)	SM	—	AFM	—	—	261585
167	$Tl_2Co(H_2P_2O_7)_2(H_2O)_2$	$P\bar{1}$ (2)	SM	(b)	AFM	—	—	416650
168	$Tl_2Ni(H_2P_2O_7)_2(H_2O)_2$	$P\bar{1}$ (2)	Triv.	(b)	FM	—	—	416651
169	$Rb_2Cu(H_2PO_4)_4$	$P\bar{1}$ (2)	SM	(b)	FM	—	—	421806
170	$Rb_2Co(H_2PO_4)_4$	$P\bar{1}$ (2)	SM	(b)	AFM	—	—	421807
171	$Rb_2Ni(H_2PO_4)_4$	$P\bar{1}$ (2)	Triv.	(b)	FM	—	—	421808
172	$Y_2(SiO_4)(CO_3)$	$P\bar{1}$ (2)	Triv.	—	NM	—	HQ	88878
173	Y_6OsI_{10}	$P\bar{1}$ (2)	Triv.	(b)	NM	—	HQ	74649
174	Y_6IrI_{10}	$P\bar{1}$ (2)	SM	(b)	NM	—	HQ	74650
175	$(PtY_6)I_{10}$	$P\bar{1}$ (2)	Triv.	(b)	NM	—	HQ	424468
176	$NH_4(POS(NH_2)_2)$	$P2_1$ (4)	Triv.	—	NM	—	HQ	25702
177	$Na_3Sr(PO_4)(CO_3)$	$P2_1$ (4)	Triv.	—	NM	—	HQ	39559
178	$(BrF_3)(AuF_3)$	$P2_1$ (4)	Triv.	—	NM	—	HQ	93481
179	$((CH_3)_3NH)(ClO_4)$	$P2_1$ (4)	Triv.	—	NM	—	—	110284
180	F_5TeNH_2	$P2_1$ (4)	Triv.	—	NM	—	HQ	171449
181	$(Li(BH_4))_3(NH_2NH_2)$	$P2_1$ (4)	Triv.	—	NM	—	—	189247
182	$KTeOF_3$	$P2_1$ (4)	Triv.	—	NM	—	HQ	201155
183	$Rb_4(CO_4)$	$P2_1$ (4)	Triv.	—	NM	—	—	245442
184	$Na(HCO_2)(H_2O)_2$	$P2_1$ (4)	Triv.	—	NM	—	HQ	250496
185	$(Zn(NH_3)_2Se_4)$	$P2_1$ (4)	Triv.	—	NM	—	HQ	425783
186	$Cs_2(S_5O_{16})$	$P2_1$ (4)	Triv.	—	—	—	—	428769
187	$Na_3(FeF_6)$	$P2_1$ (4)	SM	(b)	—	—	HQ	20157
188	$CaBa(CO_3)_2$	$P2_1$ (4)	Triv.	—	NM	—	—	24442 36201 157982
189	$Cs(AsF_4)$	$P2_1$ (4)	Triv.	—	NM	—	HQ	54852 413041
190	$Hg(C_2O_4)$	$P2_1$ (4)	Triv.	—	NM	—	HQ	56458 56459 151138 151139
191	$La(OH)_2NO_3$	$P2_1$ (4)	Triv.	—	—	—	—	243495
192	$Rb(SO_3(CF_3))$	$P2_1$ (4)	Triv.	—	NM	—	HQ	171662 415817
193	$Cs(SO_3(CF_3))$	$P2_1$ (4)	Triv.	—	NM	—	HQ	415056
194	$I_2Sb_2F_{11}$	$C2$ (5)	SM	—	FM	—	HQ	6031
195	$As(CN)_3$	$C2$ (5)	Triv.	—	NM	—	HQ	18199 35330
196	$Sr_3(Si_3O_9)$	$C2$ (5)	Triv.	—	—	—	HQ	32542
197	$Na_2(S_4O_6)(H_2O)_2$	$C2$ (5)	Triv.	—	NM	—	HQ	40833
198	K_2LiBO_3	$C2$ (5)	Triv.	—	NM	—	HQ	60949
199	$BaCu(B_2O_5)$	$C2$ (5)	SM	(b)	FM	—	HQ	84683
200	$Cs_4(CO_4)$	$C2$ (5)	Triv.	—	—	—	—	245453 245450 245452
201	$Ca(NH_2BH_3)_2$	$C2$ (5)	Triv.	—	NM	—	HQ	246139 246140
202	$(NO_2)(Ga(NO_3)_4)$	$C2$ (5)	Triv.	—	NM	—	HQ	280269 280270
203	$Ba_2(VO)(PO_4)_2$	$C2$ (5)	Triv.	(b)	—	—	HQ	405256
204	$Pt(NH_3)_2(NO_2)_2$	$C2$ (5)	Triv.	—	NM	—	HQ	420292
205	$CsMn(HP_3O_{10})$	$C2$ (5)	Triv.	(b)	FM	—	HQ	39871 51089
206	$CsGa(HP_3O_{10})$	$C2$ (5)	Triv.	(b)	NM	—	HQ	409692
207	$Li_4(CO_4)$	$C2$ (5)	Triv.	—	NM	—	—	245393$^{(b)}$ 245395 245397 245404 245405
208	$Ca_3ZnGeO_2(Ge_4O_{12})$	$C2$ (5)	Triv.	(b,s)	NM	—	—	252464
209	$F_6O_4Os_2$	Pc (7)	Triv.	—	NM	—	HQ	240330
210	$(NH_4)Na(PO_3F)(H_2O)$	Pc (7)	Triv.	—	NM	—	HQ	240974
211	$CuCO_3$	Cm (8)	SM	—	FM	—	—	6179
212	$K(NO_2)$	Cm (8)	Triv.	—	NM	—	—	26764 36202
213	$(C(NH_2)_3)_2(TiF_6)$	Cm (8)	Triv.	—	NM	—	HQ	36529
214	$K_3(VO(O_2)_2(CO_3))$	Cm (8)	Triv.	—	NM	—	HQ	60813
215	$(C(NH_2)_3)(NO_3)$	Cm (8)	Triv.	—	NM	—	HQ	75221
216	$LiCsSO_3(H_2O)_2$	Cm (8)	Triv.	—	NM	—	HQ	200780
217	$SrBO_2F$	Cm (8)	Triv.	—	—	—	—	674232
218	$Ca_4LaO(BO_3)_3$	Cm (8)	Triv.	—	NM	—	HQ	93152 180596
219	$In(PO_3)_3$	Cc (9)	Triv.	(b)	NM	—	HQ	39710 421261
220	$Ca(C_2O_4)$	$P2/m$ (10)	Triv.	—	NM	—	HQ	246004 246005
221	$AsSbF_8$	$P2_1/m$ (11)	Triv.	—	NM	—	HQ	9920
222	$S_4N_4AsF_5$	$P2_1/m$ (11)	Triv.	—	NM	—	HQ	14083

223	$Cs(HSO_4)$	$P2_1/m$ (11)	Triv.	—	NM	—	HQ	24377
224	$(C(NH_2)_3)_2(MoO_4)$	$P2_1/m$ (11)	Triv.	—	NM	—	—	49910
225	$Cu(NH_3)_4(MnO_4)_2$	$P2_1/m$ (11)	SM	—	FM	—	—	61243
226	$(Ag(H_2O)_2)(MnF_4(H_2O)_2)$	$P2_1/m$ (11)	Triv.	—	FM	—	—	74965
227	$Na_3OsO_4(OH)_2$	$P2_1/m$ (11)	SM	(b)	FM	—	HQ	172060
228	$K_2(HCO_3)F(H_2O)$	$P2_1/m$ (11)	Triv.	—	NM	—	HQ	188659
229	$Cs((CF_3)_2BF_2)$	$P2_1/m$ (11)	Triv.	—	NM	—	HQ	200869
230	$((CH_3)_3(CH_2Br)N)(BF_4)$	$P2_1/m$ (11)	Triv.	—	NM	—	—	249155
231	$((CO)_2(CF_2)(Fe(CO)_3)_2)$	$P2_1/m$ (11)	Triv.	—	NM	—	—	279643
232	$((ClCH_2)(CH_3)_3N)(BF_4)$	$P2_1/m$ (11)	Triv.	—	NM	—	—	320194
233	$(C_2H_6N)_3PO$	$P2_1/m$ (11)	Triv.	—	NM	—	—	409222
234	$(PBr_3H)(As_2F_{11})$	$P2_1/m$ (11)	Triv.	—	NM	—	—	412035
235	$((CH_3)_3NH)(ClO_4)$	$P2_1/m$ (11)	Triv.	—	NM	—	—	110285
236	$((CH_3)_3NH)(BF_4)$	$P2_1/m$ (11)	Triv.	—	NM	—	—	171202
237	$PbFeGe_3O_{10}H_4$	$P2_1/m$ (11)	Triv.	—	FM	—	—	5326 290250
238	$Co_2(CO)_8$	$P2_1/m$ (11)	Triv.	—	NM	—	—	16567 37252 37253
239	$Cs(H_2PO_4)$	$P2_1/m$ (11)	Triv.	(b)	NM	—	—	79608 79609 200895
240	$K_2(AlF_5)(H_2O)$	$P2_1/m$ (11)	Triv.	—	NM	—	HQ	81863
241	$K_2(S_2O_5)$	$P2_1/m$ (11)	Triv.	—	NM	—	HQ	16701 31817 60025
242	$KTi(SO_4)_2(H_2O)$	$P2_1/m$ (11)	SM	—	FM	—	HQ	159479
243	$KLi_2(OH)_3$	$P2_1/m$ (11)	Triv.	—	NM	—	HQ	65148
244	$Ag(Mo_3P_2O_{14})$	$P2_1/m$ (11)	SM	(b)	FM	—	—	74937
245	$K(Mo_3P_2O_{14})$	$P2_1/m$ (11)	SM	(b)	FM	—	—	78069
246	$K(Os(NO)F_5)$	$P2_1/m$ (11)	SM	—	FM	—	—	166586
247	$Cs(Os(NO)F_5)$	$P2_1/m$ (11)	SM	—	—	—	—	166587
248	$NaFe(SO_4)F(H_2O)_2$	$P2_1/m$ (11)	Triv.	—	AFM	—	—	169110
249	$NaNi(SO_4)F(H_2O)_2$	$P2_1/m$ (11)	Triv.	—	FM	—	—	169112
250	La_2Br_5	$P2_1/m$ (11)	SM	(b)	FM	—	HQ	65480
251	$NbCl_4$	$C2/m$ (12)	Triv.	(b,s)	NM	—	HQ	1010
252	$(Cu(NH_3)_4)(I_2)_2$	$C2/m$ (12)	SM	—	FM	—	HQ	4072
253	$AgCo(CO)_4$	$C2/m$ (12)	Triv.	—	NM	—	—	31388
254	$(I_4)(AsF_6)_2$	$C2/m$ (12)	Triv.	—	NM	—	HQ	37001
255	$K_2(Pd(NO_2)_2Cl_2)$	$C2/m$ (12)	Triv.	—	NM	—	HQ	39851
256	O_2	$C2/m$ (12)	Triv.	—	FM	—	—	43074 18311 173932 173933
257	$(I_2(IOs(CO)_3)_2)$	$C2/m$ (12)	Triv.	—	NM	—	HQ	68901
258	$Li_8Bi_2PdO_{10}$	$C2/m$ (12)	Triv.	(b)	NM	—	HQ	73000
259	$(NH_4)_2(Cu(H_2O)_2(PO_3F)_2)$	$C2/m$ (12)	SM	—	FM	—	HQ	74551
260	$(Ni(N(CN)_2)_2)(HCON(CH_3)_2)_2$	$C2/m$ (12)	Triv.	—	FM	—	—	109784
261	$(Co(C_2N_3)_2)(HCON(CH_3)_2)_2$	$C2/m$ (12)	SM	—	FM	—	—	109797
262	$Cs_2(Pt(C_2O_4)F_4)$	$C2/m$ (12)	Triv.	—	NM	—	—	109890
263	$((CH_3)_3NH)_2(SnF_6)(H_2O)_2$	$C2/m$ (12)	Triv.	—	NM	—	—	110229
264	$((CH_3)_2NH_2)I$	$C2/m$ (12)	Triv.	—	NM	—	HQ	110536 110537
265	$Rb_4(Cl_{12}C(ZrCl)_6)$	$C2/m$ (12)	Triv.	(b)	NM	—	HQ	165401
266	$(N(CH_3)_4)_2Cs(Co(CN)_6)$	$C2/m$ (12)	Triv.	—	NM	—	—	168575
267	$(NH_4)_2C_4O_4$	$C2/m$ (12)	Triv.	—	NM	—	HQ	172053 172054
268	$(NH_4)_2S_8$	$C2/m$ (12)	Triv.	—	NM	—	—	187244
269	$Mg(ClO_4)_2(H_2O)_2$	$C2/m$ (12)	Triv.	—	NM	—	HQ	261132
270	$C_{22}F_{14}$	$C2/m$ (12)	Triv.	—	NM	—	—	411879 411880
271	$NaBa(PO_2NH)_3$	$C2/m$ (12)	Triv.	—	NM	—	—	415259
272	$Na_2(CrF_6)(HF)_2$	$C2/m$ (12)	Triv.	—	FM	—	HQ	418677
273	$Rb_2(C_2)(NH_3)_2$	$C2/m$ (12)	Triv.	—	—	—	HQ	425117
274	$NaMn(Zr_2F_{11})$	$C2/m$ (12)	SM	—	FM	—	HQ	81219
275	$Na(VHf_2F_{11})$	$C2/m$ (12)	SM	—	FM	—	HQ	94460
276	$Li(SO_3F)$	$C2/m$ (12)	Triv.	(b)	NM	—	HQ	1384
277	$AlWO_4$	$C2/m$ (12)	Triv.	(b)	FM	—	HQ	4164
278	$Cs_4(IrO_4)$	$C2/m$ (12)	SM	—	FM	—	HQ	72287
279	$K_4(Nb_6Cl_{18})$	$C2/m$ (12)	Triv.	—	NM	—	—	41118
280	$K_4((NbBr)_6Br_{12})$	$C2/m$ (12)	Triv.	—	NM	—	HQ	49687
281	$K_4(Ta_6Cl_{12})Cl_6$	$C2/m$ (12)	Triv.	—	NM	—	HQ	59851
282	$Tl_4(Br_{12}(NbBr)_6)$	$C2/m$ (12)	Triv.	—	NM	—	HQ	402033

283	$Rb_4(Nb_6Cl_{18})$	$C2/m$ (12)	Triv.	—	NM	—	HQ	402272 404165
284	$KCr(C_2O_4)_2(H_2O)_2$	$C2/m$ (12)	SM	—	AFM	—	HQ	172524
285	$RbCr(C_2O_4)_2(H_2O)_2$	$C2/m$ (12)	SM	—	AFM	—	HQ	281565
286	$(Ni(NH_3)_4)(NCS)_2$	$C2/m$ (12)	Triv.	—	FM	—	HQ	72515
287	$Ni(NH_3)_4(NO_2)_2$	$C2/m$ (12)	Triv.	—	FM	—	HQ	201208 201209
288	$NiCl_2(H_2O)_6$	$C2/m$ (12)	Triv.	—	FM	—	—	22284 64878 64879
289	$CoCl_2(H_2O)_6$	$C2/m$ (12)	SM	—	AFM	—	—	34429 42744 69393
290	O_8	$C2/m$ (12)	Triv.	—	NM	—	—	156481 236855 236856 236857 236858
291	$(NO_2)(AsF_6)$	$C2/m$ (12)	TI	—	NM	—	HQ	68906
292	$In_2Ge_2O_7$	$C2/m$ (12)	Triv.	(b)	NM	—	HQ	20053 74896 239592 409548
293	$(V(H_2O)_6)(CF_3SO_3)_2$	$C2/m$ (12)	SM	—	FM	—	—	68779
294	$(Fe(H_2O)_6)((CF_3)SO_3)_2$	$C2/m$ (12)	Triv.	—	FM	—	—	109429 280328
295	$Zn_3(AsO_4)_2(H_2O)_8$	$C2/m$ (12)	Triv.	—	NM	—	—	100492
296	$TaCl_4$	$C2/m$ (12)	Triv.	(b,s)	NM	—	HQ	402406
297	WOF_4	$C2/m$ (12)	Triv.	—	NM	—	HQ	10393
298	$(Mn(N_2H_4)_2)Cl_2$	$C2/m$ (12)	SM	—	FM	—	HQ	25784
299	$Zr_2O(PO_4)_2$	$C2/m$ (12)	Triv.	(b)	NM	—	—	416014 424511 424513 424514 424515
300	$Cs_2(Sb_2F_{10}O)$	$P2/c$ (13)	Triv.	—	NM	—	HQ	21016
301	$Sr(Cu(OH)_4)(H_2O)$	$P2/c$ (13)	SM	—	FM	—	HQ	154808
302	$Li(BH_4)$	$P2/c$ (13)	Triv.	—	FM	—	—	168803
303	$LiC_2(CN)_4$	$P2/c$ (13)	SM	—	NM	—	HQ	251418 251419 251420 251421 251422 251423 251424 251425 251426
304	$Cs_2(CO_3)(H_2O)_3$	$P2/c$ (13)	Triv.	—	NM	—	HQ	411684 411685
305	$CuSr(HCOO)_4$	$P2/c$ (13)	SM	—	FM	—	HQ	150120
306	$CaCu(HCOO)_4$	$P2/c$ (13)	SM	—	FM	—	HQ	151315
307	$K((CF_3)BF_3)$	$P2_1/c$ (14)	Triv.	—	NM	—	—	1194
308	$Mg_2(Si_2O_6)$	$P2_1/c$ (14)	Triv.	(b)	NM	—	—	5218
309	$(K(H_2PO_3))(HF)$	$P2_1/c$ (14)	Triv.	—	NM	—	—	9151
310	$((POCl_3)OCl_2MoCl_2MoOCl_2(POCl_3))$	$P2_1/c$ (14)	Triv.	—	FM	—	—	15320
311	$K(Au(NO_3)_4)$	$P2_1/c$ (14)	Triv.	—	NM	—	—	16141
312	$K(PNH_3O_3)$	$P2_1/c$ (14)	Triv.	—	NM	—	—	23291
313	BF_3	$P2_1/c$ (14)	Triv.	—	NM	—	—	24783
314	$(PNF_2)_4$	$P2_1/c$ (14)	Triv.	—	NM	—	—	31038 31125
315	$S_6N_4(SO_3F)_2$	$P2_1/c$ (14)	Triv.	—	NM	—	—	31789
316	$CsHC_2O_4$	$P2_1/c$ (14)	Triv.	—	NM	—	—	39364
317	$Cs_2C_2O_4(H_2O)_2$	$P2_1/c$ (14)	Triv.	—	NM	—	HQ	39365
318	$K_2(SbF_5)$	$P2_1/c$ (14)	Triv.	—	NM	—	—	39634
319	$Rb(H_2PO_4)$	$P2_1/c$ (14)	Triv.	—	NM	—	—	47189
320	$(Ag(NCCl)_2)(SbF_6)$	$P2_1/c$ (14)	Triv.	—	NM	—	HQ	64638
321	$Bi_2Cu(SeO_3)_4$	$P2_1/c$ (14)	SM	(b,s)	FM	—	—	66826 66827
322	$Co(HSeO_3)_2(H_2O)_2$	$P2_1/c$ (14)	SM	—	FM	—	—	75134
323	$Cs(ReF_6O)$	$P2_1/c$ (14)	Triv.	—	NM	—	—	78392
324	$(Si(NH_3)_2)F_4$	$P2_1/c$ (14)	Triv.	—	NM	—	HQ	78902
325	$Cs(SO_3F)$	$P2_1/c$ (14)	Triv.	—	NM	—	HQ	82520
326	$(Pt(CO)_2Cl_2)$	$P2_1/c$ (14)	Triv.	—	NM	—	—	82803
327	$Na_2(Pd(NO_3)_4)$	$P2_1/c$ (14)	Triv.	—	NM	—	—	92625
328	$(NH_4)(Sn(C_2O_4)F)$	$P2_1/c$ (14)	Triv.	—	NM	—	—	109889
329	$((CH_3)_2NH)_2SnBr_4$	$P2_1/c$ (14)	Triv.	—	NM	—	—	110028
330	$Mo_2(HCOO)_4$	$P2_1/c$ (14)	Triv.	—	NM	—	—	151313
331	$Rb_2(Pd(NO_3)_4)$	$P2_1/c$ (14)	Triv.	—	NM	—	—	158878
332	$K_2(Pd(NO_3)_4)$	$P2_1/c$ (14)	Triv.	—	NM	—	—	166766
333	$SnCl_4(NH(CH_3)_2)_2$	$P2_1/c$ (14)	Triv.	—	NM	—	—	170799
334	$Cu(IO_3)_2(H_2O)_2$	$P2_1/c$ (14)	SM	—	FM	—	HQ	200326
335	$BaCu(SeO_3)_2$	$P2_1/c$ (14)	TI	(b)	FM	—	—	202387
336	$LiNH_2BH_3(NH_2NH_2)$	$P2_1/c$ (14)	Triv.	—	NM	—	—	238484
337	$Na_2Cu(C_2O_4)_2$	$P2_1/c$ (14)	SM	—	—	—	—	242098
338	$CuCl_2(C_2H_4N_4)_2$	$P2_1/c$ (14)	SM	—	—	—	—	250269
339	$Sr_2Pt(OH)_8$	$P2_1/c$ (14)	Triv.	—	NM	—	—	251043
340	$((NH_4)_2(Cu(C_2O_4)_2))$	$P2_1/c$ (14)	SM	—	—	—	—	253556
341	$Rb_2Cu(VO_2)_2(PO_4)_2$	$P2_1/c$ (14)	SM	(b)	FM	—	—	260010

342	$Cu(H_2PO_2)_2$	$P2_1/c$ (14)	SM	—	FM	—	HQ	280917 280918
343	$((CH_3)_2(H_3B)P_2(BH_3)(CH_3)_2)$	$P2_1/c$ (14)	Triv.	—	NM	—	—	281782
344	$Cu(C_2N_3)_2(NH_3)_2$	$P2_1/c$ (14)	SM	—	FM	—	—	290326
345	$CuMg_2(V_2O_8)$	$P2_1/c$ (14)	SM	(b)	FM	—	HQ	404851
346	$(F_3CSO_3SiH_2)_2$	$P2_1/c$ (14)	Triv.	—	NM	—	—	409803
347	$SnAl_2OCl_6$	$P2_1/c$ (14)	Triv.	—	NM	—	—	411777
348	$Na_2(Cu(NO_3)_4)$	$P2_1/c$ (14)	SM	—	FM	—	—	413267
349	$((Co(H_2O)_2)Cl_2)(H_2SeO_3)_2$	$P2_1/c$ (14)	SM	—	FM	—	—	415462
350	$K_2(C_2)(NH_3)_2$	$P2_1/c$ (14)	Triv.	—	NM	—	HQ	425116
351	Na_2AgF_4	$P2_1/c$ (14)	SM	(b)	FM	—	HQ	425149
352	$Pd(HS_2O_7)_2$	$P2_1/c$ (14)	Triv.	—	FM	—	—	426138
353	KNO_3	$P2_1/c$ (14)	Triv.	—	—	—	HQ	428909
354	$SrCrO_4$	$P2_1/c$ (14)	Triv.	—	—	—	—	670010 40922 159266 160793
355	Na_3MnF_6	$P2_1/c$ (14)	Triv.	(b)	—	—	—	673330 66315
356	$(COOH)_2(H_2O)_2$	$P2_1/c$ (14)	Triv.	—	NM	—	HQ	246777 246778
357	$Cu(AlCl_4)_2$	$P2_1/c$ (14)	SM	(b,s)	FM	—	HQ	14107 80107
358	$C_{14}H_8O_2$	$P2_1/c$ (14)	Triv.	—	NM	—	—	58089 58090
359	$Ba_2(TiO_4)$	$P2_1/c$ (14)	Triv.	—	NM	—	HQ	$2625^{(b)}$ 15450
360	$Sr_2(GeO_4)$	$P2_1/c$ (14)	Triv.	—	NM	—	HQ	56382
361	$Ni(PO_2(OH)_2)_2(H_2O)_2$	$P2_1/c$ (14)	Triv.	—	FM	—	—	417429 417430
362	$CsHSeO_4$	$P2_1/c$ (14)	Triv.	—	NM	—	HQ	290644 290645 411282
363	$Na_2Cu(CO_3)_2$	$P2_1/c$ (14)	SM	(b)	FM	—	HQ	10355 60858 426579
364	$Sr_2Cu(BO_3)_2$	$P2_1/c$ (14)	SM	(b)	FM	—	HQ	202934
365	$Cu(ZrF_6)(H_2O)_4$	$P2_1/c$ (14)	SM	—	FM	—	—	2618
366	$(Cu(H_2O)_4)(SiF_6)$	$P2_1/c$ (14)	SM	—	FM	—	—	165385
367	$FeY_2Be_2Si_2O_{10}$	$P2_1/c$ (14)	Triv.	(b,s)	FM	—	—	109310 109343
368	$(NH_2NH_3)(NO_3)$	$P2_1/c$ (14)	Triv.	—	NM	—	—	162750 170796
369	$Rb_2(CO_3)$	$P2_1/c$ (14)	Triv.	—	NM	—	—	14155 414123
370	$K_2(Pd(CN)_4)$	$P2_1/c$ (14)	Triv.	—	NM	—	—	413899
371	$K(HCO_3)$	$P2_1/c$ (14)	Triv.	—	NM	—	HQ	2074 2075 2076 43015
372	$Ni(IO_3)_2(H_2O)_4$	$P2_1/c$ (14)	Triv.	—	FM	—	—	10243
373	$Co(IO_3)_2(H_2O)_4$	$P2_1/c$ (14)	SM	—	FM	—	—	408060 411878
374	$Al_4Co(BO_4)_2O_2$	$P2_1/c$ (14)	SM	(b)	FM	—	—	1975
375	$Na_2(C_2O_4)$	$P2_1/c$ (14)	Triv.	—	NM	—	HQ	56906 171458 171459
376	$Na_2(Cu(H_2O)_2)(V_2O_4F_6)$	$P2_1/c$ (14)	SM	—	FM	—	—	424346
377	$Na_2(CuF_4)$	$P2_1/c$ (14)	SM	(b)	FM	—	—	34602
378	$K_2(AgF_4)$	$P2_1/c$ (14)	SM	(b)	FM	—	HQ	421461
379	Li_2PtF_6	$P2_1/c$ (14)	Triv.	(b,s)	NM	—	—	26168
380	$Cs(HCO_3)$	$P2_1/c$ (14)	Triv.	—	NM	—	HQ	300259
381	$Rb_2(Pt(CN)_4Br_2)$	$P2_1/c$ (14)	Triv.	—	NM	—	HQ	852
382	$K_2(Pt(CN)_4Br_2)$	$P2_1/c$ (14)	Triv.	—	NM	—	HQ	413705
383	$Na_2Cu(SO_4)_2(H_2O)_2$	$P2_1/c$ (14)	SM	—	FM	—	—	1915 422593
384	$(KrF)(AsF_6)$	$P2_1/c$ (14)	Triv.	—	NM	—	—	279624
385	$Sr_2Zn(OH)_6$	$P2_1/c$ (14)	Triv.	—	NM	—	HQ	66971
386	$Sr_2(Cu(OH)_6)$	$P2_1/c$ (14)	SM	(b)	FM	—	HQ	260446
387	$(XeF)(AsF_6)$	$P2_1/c$ (14)	Triv.	—	NM	—	—	1691 260951
388	$Au(AuF_4)_2$	$P2_1/c$ (14)	SM	(b,s)	FM	—	HQ	89620
389	$K_2(P_2O_5F_2)$	$C2/c$ (15)	Triv.	—	NM	—	HQ	1659
390	$Na_2Cu(PO_3)_4$	$C2/c$ (15)	SM	(b)	FM	—	—	2822
391	S_{10}	$C2/c$ (15)	Triv.	—	NM	—	HQ	38263
392	$Ni(NH_2NHCO_2)_2(H_2O)_2$	$C2/c$ (15)	Triv.	—	FM	—	—	48155
393	$K_2(SeO_4)(Te(OH)_6)$	$C2/c$ (15)	Triv.	(b)	NM	—	—	56856 154512 170043
394	$Cs_4(PbCl_6)$	$C2/c$ (15)	Triv.	(b,s)	NM	—	HQ	62351
395	$Be_2Rb(P_3O_{10})$	$C2/c$ (15)	Triv.	(b,s)	NM	—	—	72985
396	$Na_2O_2(H_2O)_8$	$C2/c$ (15)	Triv.	—	NM	—	—	79693
397	$Cd((H_3CO)CS_2)_2$	$C2/c$ (15)	Triv.	—	NM	—	—	110011
398	$Na_2(C_4O_4)(H_2O)_3$	$C2/c$ (15)	Triv.	—	NM	—	—	151153
399	$CrF(NC(CH_3))_2(BF_4)$	$C2/c$ (15)	Triv.	—	—	—	—	169664
400	$Li_2Pb_2(CuB_4O_{10})$	$C2/c$ (15)	SM	(b)	FM	—	—	180108
401	$Co(C_4O_4)(H_2O)_4$	$C2/c$ (15)	SM	—	FM	—	—	180990

402	$Bi_2(SO_4)_3$	$C2/c$ (15)	Triv.	—	NM	—	—	193352
403	$((CH_3)NH_3)_2SiF_6$	$C2/c$ (15)	Triv.	—	NM	—	—	240237
404	$Sn(CH_3)_2(Au(CN)_2)_2$	$C2/c$ (15)	Triv.	—	—	—	—	249795
405	$(C(NH_2)_3)(C(NO_2)_3)(H_2O)$	$C2/c$ (15)	Triv.	—	NM	—	—	417769
406	$Cu(C(CN)_3)_2(NH_3)_2$	$C2/c$ (15)	SM	—	—	—	—	428562
407	$Ca(CO_3)(H_2O)_6$	$C2/c$ (15)	Triv.	—	NM	—	—	16070 31305 151488 195903 195904 195905 195906 195907
408	$Ca(MnF_5)$	$C2/c$ (15)	Triv.	(b)	FM	—	HQ	69632
409	$Co(AlCl_4)_2$	$C2/c$ (15)	SM	(b,s)	FM	—	—	22143
410	$V(AlCl_4)_2$	$C2/c$ (15)	SM	(b,s)	FM	—	HQ	415951
411	$Ni(GaCl_4)_2$	$C2/c$ (15)	TI	(b,s)	FM	—	HQ	417870
412	$Ni(AlCl_4)_2$	$C2/c$ (15)	TI	(b,s)	FM	—	HQ	417872
413	$Mn(NO)(CO)_4$	$C2/c$ (15)	Triv.	—	NM	—	HQ	15221
414	$Zn(C_2O_4)(H_2O)_2$	$C2/c$ (15)	Triv.	—	NM	—	HQ	56466
415	$K_2(NH(SO_3)_2)$	$C2/c$ (15)	Triv.	—	NM	—	—	15880
416	$Co(HSeO_3)_2(H_2O)_4$	$C2/c$ (15)	SM	—	—	—	—	79091
417	$Ni(HSeO_3)_2(H_2O)_4$	$C2/c$ (15)	Triv.	—	FM	—	—	79092
418	$Pb_3(PO_4)_2$	$C2/c$ (15)	Triv.	—	NM	—	HQ	92582 4263 8092 8093 8094 14247 38007 38008 38009 38010 66379 93440 93441 93442 93443 93444 93445
419	$(Na_2(CO_3))(Na(HCO_3))(H_2O)_2$	$C2/c$ (15)	Triv.	—	NM	—	—	16641 34627 35191 44802
420	$Cs(SbO_2)$	$C2/c$ (15)	Triv.	(b,s)	NM	—	HQ	59329
421	$S(NSO)_2$	$C2/c$ (15)	Triv.	—	NM	—	HQ	14197 15795 41538
422	$NaCu(SO_4)F$	$C2/c$ (15)	SM	(b)	FM	—	HQ	262273
423	$S_{10}S_6$	$C2/c$ (15)	Triv.	—	NM	—	—	38264
424	$(VO)(H_2PO_2)_2(H_2O)$	$C2/c$ (15)	SM	—	FM	—	HQ	75435
425	$(NH_4)_2(C_2O_4)(H_2O)$	$P2_12_12$ (18)	Triv.	—	NM	—	—	64925 64927 64934 64935 64938
426	$(Sr_6N)(CoN_2)(CN_2)_2$	$P2_12_12$ (18)	Triv.	—	FM	—	—	162927
427	$(Sr_6N)(FeN_2)(CN_2)_2$	$P2_12_12$ (18)	SM	—	FM	—	—	409974
428	$K(Al(NH_2)_4)$	$C222_1$ (20)	Triv.	—	NM	—	HQ	2538
429	$Cs_3(VCl_2(H_2O)_4)Cl_4$	$I222$ (23)	Triv.	—	—	—	HQ	150082
430	$(Pd(NH_3)_4)(Ni(C_2O_4)_2(H_2O)_2)(H_2O)_2$	$I222$ (23)	Triv.	—	FM	—	—	417562
431	$(Pt(NH_3)_4)(Ni(C_2O_4)_2(H_2O)_2)(H_2O)_2$	$I222$ (23)	Triv.	—	FM	—	—	417564
432	$(Pt(NH_3)_4)(Co(C_2O_4)_2(H_2O)_2)(H_2O)_2$	$I222$ (23)	SM	—	FM	—	—	420437
433	$(Pt(NH_3)_4)(Zn(C_2O_4)_2(H_2O)_2)(H_2O)_2$	$I222$ (23)	Triv.	—	NM	—	—	417565
434	$NaRb_2(NO_3)_3$	$Pmc2_1$ (26)	Triv.	—	NM	—	HQ	195082
435	$KF(H_2O)_2$	$Pmc2_1$ (26)	Triv.	—	NM	—	HQ	165371 165372 165373
436	$Na_2(CO_3)(H_2O)$	$Pca2_1$ (29)	Triv.	—	NM	—	—	15959 1852 6293 34886
437	$(NH_4)F(NH_3)$	$Pca2_1$ (29)	Triv.	—	NM	—	—	419918
438	$Cl(CO)SNSO$	$Pca2_1$ (29)	Triv.	—	NM	—	HQ	91453 410061
439	HF_2N	$Pca2_1$ (29)	Triv.	—	NM	—	HQ	404200
440	$Na_2(HPO_3)(H_2O)_5$	$Pmn2_1$ (31)	Triv.	—	NM	—	—	1602 16138
441	$(VO)(SO_4)(H_2O)_5$	$Pmn2_1$ (31)	SM	—	FM	—	—	23308 92978
442	$MoO_2Cl_2(H_2O)$	$Pmn2_1$ (31)	Triv.	—	NM	—	HQ	25031
443	$Pb_2(NO_2)(NO_3)(SeO_3)$	$Pmn2_1$ (31)	Triv.	—	NM	—	HQ	60893
444	$K_3((SnCl_3)IrCl_5)$	$Pmn2_1$ (31)	Triv.	(b)	NM	—	HQ	69143
445	$(N(CH_3)_4)(OCN)$	$Pmn2_1$ (31)	Triv.	—	NM	—	—	150997
446	$(NH_3)(BH_3)$	$Pmn2_1$ (31)	Triv.	—	NM	—	—	180547 182301 159678 182300 187303
447	$BaCl(BF_4)$	$Pmn2_1$ (31)	Triv.	—	NM	—	HQ	188654
448	$Au_2(SeO_3)_2O$	$Pba2$ (32)	Triv.	(b)	NM	—	HQ	37009
449	$CuNa_2(OH)_4$	$Pna2_1$ (33)	SM	—	FM	—	—	65649
450	$Be(HPO_4)(H_2O)$	$Pna2_1$ (33)	Triv.	—	NM	—	—	83835
451	$Zn(OH)(NO_3)$	$Pna2_1$ (33)	Triv.	(b)	NM	—	HQ	415537
452	$(H_3O)(NO_3)$	$Pna2_1$ (33)	Triv.	—	NM	—	—	1900 1901
453	$KBePO_4$	$Pna2_1$ (33)	Triv.	(b)	NM	—	—	4255 202603$^{(s)}$
454	LiH_2PO_4	$Pna2_1$ (33)	Triv.	—	NM	—	—	100200 182308 182309
455	$(NH_4)Li(SeO_4)$	$Pna2_1$ (33)	Triv.	—	NM	—	—	300031
456	$OsOF_5$	$Pna2_1$ (33)	SM	—	FM	—	HQ	240332
457	$Na_3(ON(SO_3)_2)(H_2O)_3$	$Cmc2_1$ (36)	Triv.	—	NM	—	—	4288
458	$K_2(OsNCl_5)$	$Cmc2_1$ (36)	Triv.	—	—	—	—	43729

459	$(NH_4)_3Cr(O_2)_4$	$Cmc2_1$ (36)	SM	—	FM	—	—	237784 261390
460	$(Cl_3CCN)(NbCl_5)$	$Cmc2_1$ (36)	Triv.	—	NM	—	HQ	402856
461	H_2F_3P	$Cmc2_1$ (36)	Triv.	—	NM	—	HQ	406359 51680
462	ClN_3	$Cmc2_1$ (36)	Triv.	—	NM	—	HQ	424502
463	K_2S_3	$Cmc2_1$ (36)	Triv.	—	NM	—	HQ	1263
464	K_2Se_3	$Cmc2_1$ (36)	Triv.	—	NM	—	HQ	1264
465	Rb_2S_3	$Cmc2_1$ (36)	Triv.	—	NM	—	HQ	14092
466	Rb_2Se_3	$Cmc2_1$ (36)	Triv.	—	NM	—	HQ	14093 650051
467	Cs_2S_3	$Cmc2_1$ (36)	Triv.	—	NM	—	HQ	14094
468	$K_3(Pd((SO_3)_2H)Cl_2)$	$Cmc2_1$ (36)	Triv.	—	NM	—	HQ	49686
469	$Li_2(PO_2N)$	$Cmc2_1$ (36)	Triv.	—	NM	—	—	188493 188494
470	$Cs_2Li(MnO_4)$	$Cmc2_1$ (36)	Triv.	(b,s)	AFM	—	HQ	72361
471	$((CH_3)_4N)(OsFO_4)$	$Aem2$ (39)	Triv.	—	NM	—	—	110743
472	$Cs(B_3H_8)$	$Ama2$ (40)	Triv.	—	NM	—	HQ	65947
473	CrO_3	$Ama2$ (40)	Triv.	—	NM	—	HQ	16031 24043 38125 109366
474	$NaCa_4B_3O_9$	$Ama2$ (40)	Triv.	—	NM	—	—	239001
475	IF_7	$Aea2$ (41)	Triv.	—	NM	—	—	18191 31691
476	$(NH_4)_3(AlF_6)$	$Aea2$ (41)	Triv.	—	NM	—	—	96591
477	$(NH_4)_4(H_2(CO_3)_3)(H_2O)$	$Fmm2$ (42)	Triv.	—	NM	—	—	281534
478	$(CH_3)_2(SO_4)$	$Fdd2$ (43)	Triv.	—	NM	—	HQ	171689
479	$(C_2F_5)_2GeH_2$	$Fdd2$ (43)	Triv.	—	NM	—	—	196449
480	$NaAg(NO_2)_2$	$Fdd2$ (43)	Triv.	—	NM	—	HQ	200377
481	$(C_2F_5)_2SiH_2$	$Fdd2$ (43)	Triv.	—	—	—	—	241929
482	$K_2(B(CN)_3)$	$Fdd2$ (43)	Triv.	—	NM	—	HQ	262588
483	$(SeCl_3)_2(ReCl_6)$	$Fdd2$ (43)	SM	(b)	FM	—	HQ	68655 404534
484	$K_2(Cu(CO_3)_2)$	$Fdd2$ (43)	SM	(b)	FM	—	—	36447 200695 200779
485	$K(H_2PO_4)$	$Fdd2$ (43)	Triv.	(b)	NM	—	—	31151 68696 183037
486	$Rb(H_2PO_4)$	$Fdd2$ (43)	Triv.	—	NM	—	HQ	54873$^{(b)}$ 69318 200890$^{(b)}$
487	$(N_2H_5)Cl$	$Fdd2$ (43)	Triv.	—	NM	—	—	65334
488	$Cs_2(As_2Al_2O_7)$	$Imm2$ (44)	Triv.	(b,s)	NM	—	HQ	154363
489	$K_3Na_4(SiF_6)_3(BF_4)$	$Imm2$ (44)	Triv.	(b)	NM	—	—	160430
490	$NaAl(CO_3)(OH)_2$	$Ima2$ (46)	Triv.	(b)	NM	—	HQ	67435
491	$NaHCN_4H_2O$	$Pmma$ (51)	Triv.	—	NM	—	HQ	15874
492	$RbNb_4Br_{11}$	$Pmma$ (51)	Triv.	—	NM	—	—	380397
493	$Rb(Nb_4Cl_{11})$	$Pmma$ (51)	Triv.	—	NM	—	—	412126
494	$CsNb_4Cl_{11}$	$Pmma$ (51)	Triv.	—	NM	—	—	26076
495	Rb_3IO_5	$Pnna$ (52)	Triv.	—	NM	—	—	4326
496	$CuCl_2(H_2O)_2$	$Pmna$ (53)	SM	—	FM	—	HQ	15087 163013 34239 40290
497	$(BrF_2)(SbF_6)$	$Pcca$ (54)	Triv.	—	NM	—	—	9886
498	$CaBi(OF(CO_3))$	$Pcca$ (54)	Triv.	—	NM	—	—	157756
499	$F_2(OPOPO)F_2$	$Pcca$ (54)	Triv.	—	NM	—	—	248122
500	$(ClF_2)(NbF_6)$	$Pcca$ (54)	Triv.	—	NM	—	—	39501
501	$(ClF_2)(TaF_6)$	$Pcca$ (54)	Triv.	—	NM	—	—	39502
502	$NbBr_5$	$Pbam$ (55)	Triv.	—	—	—	—	35410
503	$(Mg(XeF_2)_2)(AsF_6)_2$	$Pbam$ (55)	Triv.	(b,s)	NM	—	—	281694
504	$K_5I_2(AuO_2)$	$Pbam$ (55)	Triv.	(b,s)	NM	—	HQ	40376
505	$Co(SO_4)(N_2H_4)$	$Pccn$ (56)	SM	—	FM	—	—	261204
506	$Na_2N_2O_3H_2O$	$Pbcm$ (57)	Triv.	—	NM	—	—	10182
507	$K(SCN)$	$Pbcm$ (57)	Triv.	—	NM	—	—	36203 28355 36073 65074 65075 67582
508	$K_2(HgS_2)$	$Pbcm$ (57)	Triv.	(b)	NM	—	HQ	74500
509	$(NF_4)(BF_4)$	$Pbcm$ (57)	Triv.	—	NM	—	—	165425
510	$((CH_3)_2Se)AlCl_3$	$Pbcm$ (57)	Triv.	—	NM	—	—	250558
511	$((CH_3)_2Te)AlCl_3$	$Pbcm$ (57)	Triv.	—	NM	—	—	250561
512	$((CH_3)_2Te)AlBr_3$	$Pbcm$ (57)	Triv.	—	NM	—	—	250562
513	$K(N(CN)_2)$	$Pbcm$ (57)	Triv.	—	NM	—	HQ	428975
514	$K_2Hg(BrO_3)_2(NO_3)_2$	$Pnnm$ (58)	Triv.	(b)	NM	—	—	24405
515	$(Ag(NCH)_2)(SbF_6)$	$Pnnm$ (58)	Triv.	—	NM	—	HQ	63287
516	$((CH_3)NH_3)_2(SiF_6)$	$Pnnm$ (58)	Triv.	—	NM	—	—	110673
517	$Ni(N(CN)_2)_2$	$Pnnm$ (58)	Triv.	(b)	FM	—	—	85617
518	$Co(N(CN)_2)_2$	$Pnnm$ (58)	SM	(b)	FM	—	—	85619

519	$(N(CH_3)_4)(NO_2)$	$Pmmn$ (59)	Triv.	—	NM	—	—	150985
520	NaB_3H_8	$Pmmn$ (59)	Triv.	—	NM	—	HQ	260964
521	$Tl((MoOCl_2)_2Cl_3)$	$Pmmn$ (59)	Triv.	(b,s)	FM	—	HQ	408775
522	$Rb(I(ICN)_2)$	$Pmmn$ (59)	Triv.	—	NM	—	HQ	35411
523	$CsNa_2(BO_3)$	$Pmmn$ (59)	Triv.	—	NM	—	HQ	67524
524	$(NH_4)(NO_3)$	$Pmmn$ (59)	Triv.	—	NM	—	—	2772 24013
525	$CsNO_3$	$Pmmn$ (59)	Triv.	—	NM	—	—	16339 16340
526	$Na_2(TeO_4)$	$Pbcn$ (60)	Triv.	(b,s)	NM	—	—	1108
527	S_4N_4	$Pbcn$ (60)	Triv.	—	NM	—	—	51516
528	$K_2(AlF_3(SO_4))$	$Pbcn$ (60)	Triv.	(b)	NM	—	—	161272
529	$Ba(PdCl_4)$	$Pbcn$ (60)	Triv.	(b)	NM	—	HQ	411837
530	$Na_2WO_2F_4$	$Pbcn$ (60)	Triv.	(b)	NM	—	—	201173 673329
531	$Ca_2F_2(CO_3)$	$Pbcn$ (60)	Triv.	—	NM	—	—	100607 158901
532	$Cs_2Re_2Br_8$	$Pbca$ (61)	Triv.	—	NM	—	—	26060
533	$S(CN)_2$	$Pbca$ (61)	Triv.	—	—	—	—	670398 14340 25520
534	$Se(CN)_2$	$Pbca$ (61)	Triv.	—	—	—	—	670399 27441
535	B_2Cl_4	$Pbca$ (61)	Triv.	—	NM	—	HQ	14213 31693
536	ClO_2	$Pbca$ (61)	Triv.	—	NM	—	HQ	67663 67664 67665 67666 180778
537	$Na_3(B_3O_5(OH)_2)$	$Pnma$ (62)	Triv.	—	NM	—	—	1939
538	$H_3B_3O_6$	$Pnma$ (62)	Triv.	—	NM	—	—	16545
539	$(HgCN)_2O$	$Pnma$ (62)	Triv.	—	NM	—	HQ	25708 28398 29037
540	$NH_4FH_2O_2$	$Pnma$ (62)	Triv.	—	NM	—	—	28552
541	$K_2(S_2CNCN)(H_2O)$	$Pnma$ (62)	Triv.	—	NM	—	—	36006
542	(HBO_2)	$Pnma$ (62)	Triv.	—	NM	—	—	39129
543	$RbLiO$	$Pnma$ (62)	Triv.	—	NM	—	HQ	65170
544	$Rb(SF_5)$	$Pnma$ (62)	Triv.	—	NM	—	HQ	65221
545	$K(NO_3)$	$Pnma$ (62)	Triv.	—	NM	—	HQ	85491 10289 10290 28077 52376 71397
546	$((CH_3)NH_3)(NO_3)$	$Pnma$ (62)	Triv.	—	NM	—	—	110635
547	$Na((CF_3)SO_3)(H_2O)$	$Pnma$ (62)	Triv.	—	NM	—	—	151032
548	$(CH_3)S(O)_2NCl_2$	$Pnma$ (62)	Triv.	—	NM	—	—	151036
549	CH_3FO_2	$Pnma$ (62)	Triv.	—	NM	—	HQ	170925
550	$Ba_3Cl_4(CO_3)$	$Pnma$ (62)	Triv.	—	NM	—	—	174065
551	$LiGaCl_3$	$Pnma$ (62)	Triv.	—	NM	—	—	202641
552	SrF_2	$Pnma$ (62)	Triv.	—	NM	—	—	248433 262349
553	$CaCO_3$	$Pnma$ (62)	Triv.	—	—	—	—	252923 252924 15194 15198 32100 34308 52152 56090 157992 157993 157994 157995 157996 157997 161817 166085 166086 166087 169890 169891 169892 169893 169894 169895 169896 169897 169898 169899 169900 169901 169902 169903 169904 169905 169906 169907 169909 169910 169911 169912 170225 190072 252901 252902 252903 252904 252905 252907 252908 252909 252910 252911 252912 252913 252914 252915 252916 252917 252918 252919 252920 252921 252922 27827 157301 157302
554	$K_2(SnCl_3)Cl(H_2O)$	$Pnma$ (62)	Triv.	—	NM	—	—	290298
555	$(TaCl_5)(SOCl_2)$	$Pnma$ (62)	Triv.	—	NM	—	—	411518
556	$Rb_2(CO_3)$	$Pnma$ (62)	Triv.	—	NM	—	HQ	414122
557	$Sr(CO_3)$	$Pnma$ (62)	Triv.	—	NM	—	HQ	15195 27293 56099 166088 202793
558	$Ba(CO_3)$	$Pnma$ (62)	Triv.	—	NM	—	HQ	15196$^{(k)}$ 26718$^{(k)}$ 56100$^{(k)}$ 91888$^{(k)}$ 91889$^{(k)}$ 91890 91891 91892 91893 91894 91895 91896 158378$^{(k)}$ 158379$^{(k)}$ 158380$^{(k)}$ 158381$^{(k)}$ 158382$^{(k)}$ 158383 158384 158385 158386 158387 158388 166090$^{(k)}$ 166091$^{(k)}$ 190075$^{(k)}$
559	$K(BF_4)$	$Pnma$ (62)	Triv.	—	NM	—	HQ	9875 21081 22260
560	NH_4SO_3F	$Pnma$ (62)	Triv.	—	—	—	—	16146

561	$Ba(SO_4)$	$Pnma$ (62)	Triv.	—	NM	—	HQ	16904 16917 31894 33730 33731 33732 33733 33734 33735 44414 68308 76926 100623 154286 167519 180337 180338 180339 186426 190065 200112
562	$Pb(SO_4)$	$Pnma$ (62)	Triv.	—	NM	—	HQ	16916 31896 44415 75955 75956 92609 109432 154273 190064
563	$Pb(BeF_4)$	$Pnma$ (62)	Triv.	—	NM	—	HQ	24568
564	$In(BF_4)$	$Pnma$ (62)	Triv.	—	NM	—	HQ	50218
565	$Tl(BF_4)$	$Pnma$ (62)	Triv.	—	NM	—	HQ	300222
566	$Cs(NH_2SO_3)$	$Pnma$ (62)	Triv.	—	NM	—	—	180845
567	Rb_2PO_3F	$Pnma$ (62)	Triv.	—	NM	—	HQ	172343 172344
568	Cs_2PO_3F	$Pnma$ (62)	Triv.	—	NM	—	HQ	172345 172346
569	K_2PO_3F	$Pnma$ (62)	Triv.	—	NM	—	HQ	200441 15691
570	$Rb(CN_3H_4)$	$Pnma$ (62)	Triv.	—	NM	—	—	422591 425942
571	$Cs(SCN)$	$Pnma$ (62)	Triv.	—	NM	—	—	19001 60523 60870 60871 60872 60873 60874 60875 60876 60877 60878 60879
572	$Cs(SO_2F)$	$Pnma$ (62)	Triv.	—	NM	—	HQ	93070 93072 93074 93076 93078
573	$(F_5S)(CN)$	$Pnma$ (62)	Triv.	—	NM	—	—	413755 413756 413757
574	$(H_3O)FSO_3$	$Pnma$ (62)	Triv.	—	NM	—	—	33866
575	K_2OsNCl_5	$Pnma$ (62)	Triv.	—	NM	—	—	27560 28208
576	$K_2(MoOCl_5)$	$Pnma$ (62)	SM	—	FM	—	—	28215
577	$K_2(ReCl_5O)$	$Pnma$ (62)	Triv.	—	NM	—	—	68907
578	$K_2(TcOCl_5)$	$Pnma$ (62)	Triv.	—	NM	—	—	188005
579	$K_2(Ru(NO)Cl_5)$	$Pnma$ (62)	Triv.	—	NM	—	—	20436 20713$^{(b)}$ 72617
580	$Li(ClO_4)$	$Pnma$ (62)	Triv.	(b)	NM	—	HQ	165579 413238
581	$Mg_2(BO_3)F$	$Pnma$ (62)	Triv.	(b)	NM	—	HQ	28096
582	K_2TaF_7	$Pnma$ (62)	Triv.	—	NM	—	—	260876 260877
583	$CsTeF_5$	$Pnma$ (62)	Triv.	—	NM	—	HQ	200252
584	$Na(TeF_5)$	$Pnma$ (62)	Triv.	—	NM	—	HQ	202879
585	$NaY(CO_3)F_2$	$Pnma$ (62)	Triv.	—	NM	—	—	89258
586	$LiFe(PO_4)$	$Pnma$ (62)	Triv.	—	AFM	—	—	38209$^{(b)}$ 56291$^{(b)}$ 72545$^{(b)}$ 92198$^{(b)}$ 97764$^{(b)}$ 99860$^{(b)}$ 153699$^{(b)}$ 154117$^{(b)}$ 155580$^{(b)}$ 155635$^{(b)}$ 159107 160776$^{(b)}$ 161479$^{(b)}$ 162282$^{(b)}$ 166815$^{(b)}$ 183874$^{(b)}$ 184652$^{(b)}$ 184862 184863$^{(b)}$ 185308$^{(b)}$ 189057$^{(b)}$ 190771$^{(b)}$ 190772$^{(b)}$ 193797$^{(b)}$ 193799$^{(b)}$ 193800$^{(b)}$ 194331$^{(b)}$ 200155$^{(b)}$ 241942$^{(b)}$ 246855$^{(b)}$ 246857$^{(b)}$ 260569$^{(b)}$ 260570$^{(b)}$ 260571$^{(b)}$ 260572$^{(b)}$ 290334$^{(b)}$ 290335$^{(b)}$ 290336 290339$^{(b)}$ 290718$^{(b)}$ 290719$^{(b)}$
587	$OsOF_5$	$Pnma$ (62)	SM	—	FM	—	HQ	16872
588	K_3OCl	$Pnma$ (62)	Triv.	(b,s)	NM	—	HQ	78891
589	$(NH_4)(PO_2F_2)$	$Pnma$ (62)	Triv.	—	NM	—	—	16152
590	KPO_2F_2	$Pnma$ (62)	Triv.	—	NM	—	HQ	26640
591	$Rb(H_2PO_2)$	$Pnma$ (62)	Triv.	—	NM	—	HQ	59834 250131
592	$S_3(CN)_2$	$Pnma$ (62)	Triv.	—	NM	—	—	1084 25505
593	$Se(SeCN)_2$	$Pnma$ (62)	Triv.	—	NM	—	HQ	10072 24054 171333 247099
594	$SC(NH_2)_2$	$Pnma$ (62)	Triv.	—	NM	—	—	14334 65783 69145 200408
595	$K_2(BiF_5)$	$Pnma$ (62)	Triv.	(b,s)	NM	—	—	418777
596	$Ca_3Cl_2C_3$	$Cmcm$ (63)	Triv.	—	NM	—	HQ	33818
597	$Ba_3WO_5Cl_2$	$Cmcm$ (63)	Triv.	—	NM	—	HQ	63518
598	$Rb_3(Re_3Cl_{12})$	$Cmcm$ (63)	Triv.	—	NM	—	—	63585
599	$LiBF_2(C_2O_4)$	$Cmcm$ (63)	Triv.	—	NM	—	HQ	185384
600	$Na(IO_2F_2)$	$Cmcm$ (63)	Triv.	(b)	NM	—	HQ	260003
601	$K_2(SbF_5)$	$Cmcm$ (63)	Triv.	—	NM	—	—	24742 39630
602	$K_2(TeOF_4)$	$Cmcm$ (63)	Triv.	—	NM	—	HQ	412955
603	$Na(B(C_2O_4)_2)$	$Cmcm$ (63)	Triv.	—	NM	—	HQ	281622
604	$Li(NO_3)(H_2O)_3$	$Cmcm$ (63)	Triv.	—	NM	—	—	1135 23109 23110 48039 48040
605	$RbCd(ZrF_7)$	$Cmcm$ (63)	Triv.	(b,s)	NM	—	HQ	245783
606	$(Re(CO)_5)I$	$Cmcm$ (63)	Triv.	—	NM	—	—	71219

607	$Mn(CO)_5I$	$Cmcm$ (63)	Triv.	—	NM	—	HQ	71878
608	$(Tc(CO)_5)I$	$Cmcm$ (63)	Triv.	—	NM	—	HQ	85335
609	$SrV(Si_2O_7)$	$Cmcm$ (63)	SM	(b)	FM	—	—	64766
610	$Sr_2(V_2Si_4O_{14})$	$Cmcm$ (63)	SM	(b)	FM	—	HQ	83361
611	Sr_2CuF_6	$Cmce$ (64)	SM	(b)	FM	—	—	9926
612	NbP_2S_8	$Cmce$ (64)	Triv.	—	NM	—	—	37326
613	$Na_2(W_2O_7)$	$Cmce$ (64)	Triv.	(b)	NM	—	—	1883 24041$^{(s)}$ 290459
614	$(Pt(NH_3)_4)(SnCl_6)$	$Cmce$ (64)	Triv.	—	NM	—	—	74556
615	Ta_6Br_{14}	$Cmce$ (64)	Triv.	—	NM	—	—	402031
616	$(Ni(H_2O)_4)(C_3H_2N_3O_3)_2$	$Fmmm$ (69)	Triv.	—	—	—	—	66806
617	$(Co(N_5)_2(H_2O)_4)(H_2O)_4$	$Fmmm$ (69)	SM	—	—	—	—	432489
618	TaI_2Cl_2	$Immm$ (71)	Triv.	—	NM	—	HQ	69688
619	$Cs(BrF_4)$	$Immm$ (71)	Triv.	—	NM	—	HQ	426292
620	$Na_3(AlF_6)$	$Immm$ (71)	Triv.	—	NM	—	HQ	74210 74211
621	$NaAl(OH)_2(CO_3)$	$Imma$ (74)	Triv.	(b)	NM	—	HQ	100140
622	$CrOF_3$	$P4_1$ (76)	SM	(b,s)	FM	—	—	59123
623	$C(HCO_2)_2$	$P4_1$ (76)	Triv.	—	—	—	—	109620
624	$(Ni(SC(NH_2)_2)_4Cl_2)$	$I4$ (79)	Triv.	—	FM	—	—	61122 61123
625	$Na_4(CO(PO_3)_2)(H_2O)_2$	$P\bar{4}$ (81)	Triv.	—	NM	—	—	19
626	$K_5(Nb(CN)_8)$	$I\bar{4}$ (82)	Triv.	—	NM	—	HQ	16458
627	$CsCo(CO)_4$	$I\bar{4}$ (82)	Triv.	—	NM	—	HQ	31359 31360
628	$LiNH_2$	$I\bar{4}$ (82)	Triv.	—	NM	—	HQ	173179 10354 51679 161017 165467 168792 168793 182470 182471 237203
629	$Cu(XeF_2)_4(SbF_6)_2$	$I\bar{4}$ (82)	SM	—	FM	—	HQ	249656
630	$Li_3Na(NH_2)_4$	$I\bar{4}$ (82)	Triv.	—	NM	—	HQ	201147 201148
631	$Re_4Te_4(TeBr_2)_4Br_8$	$I\bar{4}$ (82)	Triv.	—	NM	—	HQ	78924
632	$((S_4Re_4)Cl_8(TeCl_2)_4)$	$I\bar{4}$ (82)	Triv.	—	NM	—	HQ	165333
633	$((Te_4Re_4)Cl_8(TeCl_2)_4)$	$I\bar{4}$ (82)	Triv.	—	NM	—	HQ	165335
634	$(PCl_4)(SbF_6)$	$P4/n$ (85)	Triv.	—	NM	—	HQ	71876
635	$(Li(NH_3)_4)(C_2)H$	$P4/n$ (85)	Triv.	—	NM	—	—	425119
636	PCl_5	$P4/n$ (85)	Triv.	—	NM	—	—	26048 26661
637	$Cs(Al(NH_2)_4)$	$P4/n$ (85)	Triv.	—	NM	—	HQ	2537 40169
638	$(VO)(SO_4)$	$P4/n$ (85)	SM	(b)	AFM	—	HQ	18307
639	$MoO(PO_4)$	$P4/n$ (85)	SM	(b)	FM	—	HQ	24894 36095
640	$(PNCl_2)_4$	$P4_2/n$ (86)	Triv.	—	NM	—	—	23897 33711
641	KSb_4F_{13}	$I4/m$ (87)	Triv.	—	NM	—	—	24740
642	$Ba(VSi_2O_7)$	$I4/m$ (87)	Triv.	(b)	AFM	—	HQ	78029
643	$(N(CH_3)_4)_2(PtF_6)$	$I4/m$ (87)	Triv.	—	NM	—	—	151176
644	$Ba_2Zr_6Cl_{17}B$	$I4/m$ (87)	Triv.	(b)	NM	—	HQ	203141
645	$Cs_8(Ta_6O_{19})$	$I4/m$ (87)	Triv.	(b,s)	NM	—	—	411856
646	$((CH_3)_4N)_2K(Mn(CN)_6)$	$I4/m$ (87)	Triv.	—	FM	—	—	107665
647	$((CH_3)_4N)_2Rb(Co(CN)_6)$	$I4/m$ (87)	Triv.	—	NM	—	—	107666
648	$((CH_3)_4N)_2(KFe(CN)_6)$	$I4/m$ (87)	SM	—	FM	—	—	239245
649	$Na_4(IrO_4)$	$I4/m$ (87)	SM	(b)	FM	—	HQ	67826
650	$Na_2TiOSi_4O_{10}$	$I4/m$ (87)	Triv.	(b,s)	NM	—	—	16899
651	XeF_2IF_5	$I4/m$ (87)	Triv.	—	NM	—	HQ	26059
652	$(XeOF_4)(XeF_2)$	$I4/m$ (87)	Triv.	—	—	—	HQ	422962
653	$B_{10}F_{12}$	$I4_1/a$ (88)	Triv.	—	NM	—	—	412618
654	$TlB(CN)_4$	$I4_1/a$ (88)	Triv.	—	NM	—	HQ	414564
655	SO_2F_2	$P4_12_12$ (92)	Triv.	—	NM	—	HQ	62968
656	$Pb_2Cu(OH)_4Cl_2$	$P4mm$ (99)	SM	—	FM	—	HQ	81589
657	$Cs_2V_3O_8$	$P4bm$ (100)	SM	(b,s)	FM	—	HQ	251010 430710 430711 430708 430709
658	$(H_3O)_2V_3O_8$	$P4bm$ (100)	SM	—	FM	—	—	421914
659	$K_2(VO)(V_2O_7)$	$P4bm$ (100)	SM	(b,s)	FM	—	HQ	1925 245500
660	$Rb_2(VO)(V_2O_7)$	$P4bm$ (100)	SM	(b,s)	FM	—	HQ	72285 79378 150326
661	$(NH_4)_2V_3O_8$	$P4bm$ (100)	SM	—	FM	—	—	201900
662	$Cs_2V_5O_{13}$	$I4mm$ (107)	SM	(b)	FM	—	HQ	849
663	$KNa_2(CuO_2)$	$I4mm$ (107)	Triv.	(b)	NM	—	HQ	47105
664	$Ta_4S_9Br_8$	$I4mm$ (107)	Triv.	(b)	NM	—	HQ	171236
665	$Cu(Fe(CN)_5NO)$	$I4mm$ (107)	SM	—	FM	—	HQ	414021

666	$(Os(NO)(NH_3)_4Cl)Cl_2$	$I4mm$ (107)	Triv.	—	NM	—	—	39306
667	$K_3(NO_3)$	$I4cm$ (108)	Triv.	(b,s)	NM	—	—	37204
668	$(NO)(ClF_4)$	$I4cm$ (108)	Triv.	—	NM	—	HQ	50216
669	$Li_2VO(SO_4)_2$	$I4cm$ (108)	SM	(b)	—	—	—	241829
670	$(NH_4)(ClO_2)$	$P\bar{4}2_1m$ (113)	Triv.	—	NM	—	—	26511 59921
671	$(PCl_4)(ICl_2)$	$P\bar{4}2_1m$ (113)	Triv.	—	NM	—	—	26594
672	$(S_3N_3O_4)_2S$	$P\bar{4}2_1m$ (113)	Triv.	(b)	NM	—	—	49015
673	$(NF_4)(BF_4)$	$P\bar{4}2_1m$ (113)	Triv.	—	NM	—	—	63311 68017
674	$Li(ReO_2F_4)$	$P\bar{4}2_1m$ (113)	Triv.	(b)	NM	—	HQ	280011
675	$CO(NH_2)_2$	$P\bar{4}2_1m$ (113)	Triv.	—	NM	—	HQ	15432 15433 16692 29364 29365 29366 40049 43490 56901 100303 100304 100305 170090 280179
676	$C_{10}H_{16}$	$P\bar{4}2_1c$ (114)	Triv.	—	NM	—	—	5284
677	$(NSF)_4$	$P\bar{4}2_1c$ (114)	Triv.	—	NM	—	—	15422 18202 71039
678	$H_{10}O_8Se$	$P\bar{4}2_1c$ (114)	Triv.	—	—	—	—	404660
679	$CsLi_2I_3$	$P\bar{4}m2$ (115)	Triv.	(b)	NM	—	—	245988
680	$RbCuO$	$I\bar{4}m2$ (119)	Triv.	—	NM	—	HQ	49758 188523
681	$CsSbClF_3$	$I\bar{4}2m$ (121)	Triv.	—	NM	—	HQ	28222 200296
682	$(TcBr_2)(P(CH_3)_3)_4$	$I\bar{4}2m$ (121)	SM	—	FM	—	—	166912
683	$WCl_2(P(CH_3)_3)_4$	$I\bar{4}2m$ (121)	Triv.	—	FM	—	—	185488
684	$MoCl_2(P(CH_3)_3)_4$	$I\bar{4}2m$ (121)	Triv.	—	FM	—	—	185489
685	$Cs(NH_4)_2Cr(O_2)_4$	$I\bar{4}2m$ (121)	SM	—	FM	—	HQ	237787 261393
686	$Ba_4Na(CuO_4)(CO_3)_2$	$I\bar{4}2m$ (121)	Triv.	—	NM	—	HQ	66776 80606
687	$K_3(Cr(O_2)_4)$	$I\bar{4}2m$ (121)	SM	—	FM	—	HQ	9356 9676 23536 30404 280253
688	$K_3(VO_4)$	$I\bar{4}2m$ (121)	Triv.	—	NM	—	—	4138
689	$K_3(MnO_4)$	$I\bar{4}2m$ (121)	Triv.	—	AFM	—	—	108935
690	$K_4(CO_4)$	$I\bar{4}2m$ (121)	Triv.	—	NM	—	—	245419 245420
691	$Be(OH_2)_4(NO_3)_2$	$I\bar{4}2d$ (122)	Triv.	—	NM	—	—	15858
692	$K(HC(NO)_2)$	$I\bar{4}2d$ (122)	Triv.	—	NM	—	HQ	170586
693	$(NH_4)(H_2PO_4)$	$I\bar{4}2d$ (122)	Triv.	(b)	NM	—	HQ	28154 54776 63494 63634 84114 174048 174049 174050 246299$^{(s)}$
694	$(NH_4)(H_2AsO_4)$	$I\bar{4}2d$ (122)	Triv.	(b)	NM	—	HQ	28155 66203 66204$^{(s)}$ 66205$^{(s)}$ 66206$^{(s)}$ 174061$^{(s)}$ 200219
695	$Co(B(CN)_4)_2(H_2O)_2$	$I\bar{4}2d$ (122)	SM	—	—	—	—	260263
696	$Rb(H_2PO_4)$	$I\bar{4}2d$ (122)	Triv.	(b)	NM	—	HQ	69317
697	$Na_5(NiO_2)S$	$P4/mmm$ (123)	SM	(b,s)	FM	—	HQ	412972
698	$Na_5(CuO_2)S$	$P4/mmm$ (123)	Triv.	(b,s)	NM	—	HQ	412977
699	$(P(NH_2)_4)I$	$P4/nbm$ (125)	Triv.	—	NM	—	HQ	74814
700	$((NH_2)_4P)I$	$P4/nbm$ (125)	TI	—	—	—	HQ	400461
701	$(P(NH_2)_4)Br$	$P4/nbm$ (125)	Triv.	—	FM	—	HQ	410797
702	$Cs_3(SiF_6)F$	$P4/mbm$ (127)	Triv.	—	NM	—	—	9588
703	Rb_2CsSiF_7	$P4/mbm$ (127)	Triv.	—	NM	—	—	9592
704	Cs_3TiF_7	$P4/mbm$ (127)	Triv.	—	NM	—	—	9594
705	Cs_3CrF_7	$P4/mbm$ (127)	Triv.	—	FM	—	—	9596
706	Rb_3CrF_7	$P4/mbm$ (127)	Triv.	—	FM	—	—	9597
707	$Cs_3(MnF_6)F$	$P4/mbm$ (127)	SM	—	FM	—	—	9598
708	$Rb_3(MnF_6)F$	$P4/mbm$ (127)	SM	—	FM	—	—	9599
709	$K_3Cl(ReF_6)$	$P4/mbm$ (127)	SM	—	FM	—	—	80170
710	$Pb_2Cl_2(CO_3)$	$P4/mbm$ (127)	Triv.	—	NM	—	—	4240 29113 36241
711	$Pb_2Br_2(CO_3)$	$P4/mbm$ (127)	Triv.	—	NM	—	—	29114 250396
712	$Cs_2Li(Cr(CN)_6)$	$P4/mnc$ (128)	SM	—	FM	—	—	804
713	$Na_2Cl(B(OH)_4)$	$P4/nmm$ (129)	Triv.	—	NM	—	—	32518
714	$(N(CH_3)_4)I$	$P4/nmm$ (129)	Triv.	—	NM	—	—	55080
715	$Cs(ReF_8)$	$P4/nmm$ (129)	Triv.	—	NM	—	—	410829
716	$KNaWO_2F_4$	$P4/nmm$ (129)	Triv.	(b)	NM	—	—	422709
717	$KNaMoO_2F_4$	$P4/nmm$ (129)	Triv.	(b)	NM	—	—	422707
718	$BaFCl$	$P4/nmm$ (129)	Triv.	—	NM	—	—	2350 35487 35488 35489 35490 35491 35492 35493 85319 155004 183925 201514 201515 201516 201517 201518 201519
719	$(VO)(P_2SiO_8)$	$P4/ncc$ (130)	SM	(b,s)	FM	—	—	628

720	$Mo(AlP_2O_9)$	$P4/ncc$ (130)	SM	(b,s)	—	—	—	67221
721	$PtZn(CN)_4$	$P4_2/mcm$ (132)	Triv.	—	NM	—	HQ	169758
722	$PdZn(CN)_4$	$P4_2/mcm$ (132)	Triv.	—	—	—	HQ	169759
723	$NiZn(CN)_4$	$P4_2/mcm$ (132)	Triv.	—	—	—	HQ	169760
724	$Cs_4K_2Cu(SiO_4)_2$	$P4_2/mnm$ (136)	SM	(b,s)	FM	—	—	92493
725	Li_2PtF_6	$P4_2/mnm$ (136)	Triv.	(b)	NM	—	HQ	248725 165216
726	K_3NiO_2	$P4_2/mnm$ (136)	SM	(b)	FM	—	HQ	262579
727	Cs_3NiO_2	$P4_2/mnm$ (136)	SM	(b)	—	—	HQ	424578
728	Rb_3NiO_2	$P4_2/mnm$ (136)	SM	(b)	FM	—	HQ	424579
729	$K_2(CuCl_4)(H_2O)_2$	$P4_2/mnm$ (136)	SM	—	FM	—	—	15943 16052
730	$(NH_4)_2(CuCl_4)(H_2O)_2$	$P4_2/mnm$ (136)	SM	—	FM	—	—	23750 163014 420586
731	$Rb_2CuCl_4(H_2O)_2$	$P4_2/mnm$ (136)	SM	—	FM	—	HQ	71867
732	$(NH_4)_2(Cu(H_2O)_2Br_2)Br_2$	$P4_2/mnm$ (136)	SM	—	FM	—	—	88887 88888 88889
733	$Li_2(MoF_6)$	$P4_2/mnm$ (136)	Triv.	(b)	FM	—	HQ	74565
734	$Li_2(RhF_6)$	$P4_2/mnm$ (136)	SM	(b)	FM	—	HQ	95778 165211
735	$Li_2(PdF_6)$	$P4_2/mnm$ (136)	Triv.	(b)	NM	—	HQ	165212
736	$Li_2(CrF_6)$	$P4_2/mnm$ (136)	Triv.	(b)	FM	—	HQ	418676
737	$Mg(ClO_2)_2(H_2O)_6$	$P4_2/nmc$ (137)	Triv.	—	NM	—	—	69587
738	$(CsF)_2(Br_2)$	$I4/mmm$ (139)	Triv.	—	NM	—	HQ	84021 84022
739	$Rb_2Na(MnF_6)$	$I4/mmm$ (139)	Triv.	(b)	FM	—	—	9708
740	$Cs_2K(MnF_6)$	$I4/mmm$ (139)	Triv.	—	FM	—	—	22110 91036 91197$^{(b)}$
741	K_2NaMnF_6	$I4/mmm$ (139)	Triv.	(b,s)	FM	—	—	61117
742	$Cs_3(O(ReCl_5)_2)$	$I4/mmm$ (139)	SM	—	FM	—	HQ	31
743	$CsNi(CN)_2Br$	$I4/mmm$ (139)	TI	—	—	—	HQ	380468
744	$CsNi(CN)_2Cl$	$I4/mmm$ (139)	TI	—	—	—	HQ	380469
745	$RbNi(CN)_2Br$	$I4/mmm$ (139)	TI	—	FM	—	HQ	380470
746	$RbNi(CN)_2Cl$	$I4/mmm$ (139)	TI	—	FM	—	HQ	380471
747	$K_2(OsO_2Cl_4)$	$I4/mmm$ (139)	Triv.	—	NM	—	HQ	15454 36231
748	Cs_2NiO_2	$I4/mmm$ (139)	Triv.	(b)	AFM	—	HQ	423923
749	KrF_2	$I4/mmm$ (139)	Triv.	—	NM	—	HQ	279623
750	$Rb(BrF_4)$	$I4/mcm$ (140)	Triv.	—	NM	—	HQ	65713 670019
751	$Ba(C_4O_4)$	$I4/mcm$ (140)	Triv.	—	NM	—	HQ	412830
752	$Cs_3(MnCl_5)$	$I4/mcm$ (140)	SM	(b)	FM	—	HQ	24
753	Cs_3FeBr_5	$I4/mcm$ (140)	SM	(b)	FM	—	—	4065
754	$Cs_3(CoCl_4)Cl$	$I4/mcm$ (140)	SM	—	FM	—	HQ	14087$^{(b)}$ 15245$^{(b)}$ 16397$^{(b)}$ 16556 28533$^{(b)}$ 31032 280443$^{(b)}$
755	Cs_3NiCl_5	$I4/mcm$ (140)	Triv.	—	FM	—	HQ	59372
756	Cs_3CoBr_5	$I4/mcm$ (140)	SM	(b)	FM	—	HQ	201135
757	$SrCuF_4$	$I4/mcm$ (140)	SM	(b)	FM	—	—	9927
758	$CaCuF_4$	$I4/mcm$ (140)	SM	(b)	FM	—	—	9928
759	$SrPdF_4$	$I4/mcm$ (140)	Triv.	—	NM	—	—	108990
760	$NaBrF_4$	$I4/mcm$ (140)	Triv.	(b)	—	—	—	431176
761	$(Pd(NH_3)_4)(CrO_4)$	$I4_1/amd$ (141)	Triv.	—	NM	—	—	72997
762	$Cr(H_2O)_6F_3(H_2O)_3$	$R3$ (146)	SM	—	FM	—	—	2379
763	$Cl_3(Co(CO)_4)Sn$	$R3$ (146)	Triv.	—	NM	—	HQ	69685
764	$KNi(PO_3)_3$	$R3$ (146)	SM	(b)	AFM	—	HQ	91527
765	$(Cs_2(SO_4))(Te(OH)_6)$	$R3$ (146)	Triv.	—	—	—	HQ	93016
766	$Li_3VO_4(H_2O)_6$	$R3$ (146)	Triv.	—	NM	—	HQ	174238
767	$(Mg(H_2O)_6)(HPO_3)$	$R3$ (146)	Triv.	—	NM	—	HQ	74520 74521
768	$Cs_2Na(Bi(SCN)_6)$	$P\bar{3}$ (147)	Triv.	—	—	—	—	79593
769	$Li_2Pt(OH)_6$	$P\bar{3}$ (147)	Triv.	—	NM	—	HQ	251041
770	$Na_2Pt(OH)_6$	$P\bar{3}$ (147)	Triv.	—	NM	—	HQ	251042
771	$Cs_2Sn(OOH)_6$	$P\bar{3}$ (147)	Triv.	—	NM	—	HQ	260828
772	$Ca_{10}(PO_4)_6Se$	$P\bar{3}$ (147)	Triv.	—	NM	—	—	410781
773	$Ba_{10}(PO_4)_6S$	$P\bar{3}$ (147)	Triv.	—	NM	—	—	410785
774	$Cd_2(Os(CN)_6)$	$P\bar{3}$ (147)	Triv.	(b)	—	—	HQ	417821
775	$Cd_2(Ru(CN)_6)$	$P\bar{3}$ (147)	Triv.	(b)	—	—	HQ	417822
776	$Te(OTeF_5)_6$	$R\bar{3}$ (148)	Triv.	—	NM	—	—	2174
777	$C_2H_{30}MgO_{18}S_2$	$R\bar{3}$ (148)	Triv.	—	NM	—	—	5391 169171
778	$(Re(CO)_3I_3)_2Re$	$R\bar{3}$ (148)	SM	—	FM	—	HQ	15497

779	$(Co(NH_3)_6)(Os(SCN)_6)$	$R\bar{3}$ (148)	SM	—	—	—	—	92479
780	$(N(CH_3)_4)_2(OsF_6)$	$R\bar{3}$ (148)	Triv.	—	FM	—	—	151185
781	$(Cu(XeF_2)_6)(SbF_6)_2$	$R\bar{3}$ (148)	SM	—	—	—	—	416303
782	$Ba_2Co(B_3O_6)_2$	$R\bar{3}$ (148)	SM	(b)	AFM	—	HQ	391014
783	$Co(ClO_4)_2$	$R\bar{3}$ (148)	SM	(b)	FM	—	—	33288
784	$Ni(ClO_4)_2$	$R\bar{3}$ (148)	Triv.	(b)	FM	—	—	33289
785	$(Co(H_2O)_6)(SiF_6)$	$R\bar{3}$ (148)	SM	—	FM	—	HQ	2900
786	$Zn(TiF_6)(H_2O)_6$	$R\bar{3}$ (148)	Triv.	—	NM	—	HQ	62375 202787
787	$Co(SnF_6)(H_2O)_6$	$R\bar{3}$ (148)	SM	—	FM	—	HQ	75984
788	$Mn(TiF_6)(H_2O)_6$	$R\bar{3}$ (148)	SM	—	AFM	—	HQ	202786
789	$(Co(NH_3)_6)(Cr(CN)_6)$	$R\bar{3}$ (148)	SM	—	FM	—	—	805 806
790	$(Co(NH_3)_6)(Mn(CN)_6)$	$R\bar{3}$ (148)	Triv.	—	—	—	—	260055
791	$(Co(NH_3)_6)(Fe(CN)_6)$	$R\bar{3}$ (148)	SM	—	FM	—	—	411630 421507
792	$K_2SrNb_6Cl_{18}$	$R\bar{3}$ (148)	Triv.	—	—	—	HQ	280933
793	$Cs_2Pb(NbCl_3)_6$	$R\bar{3}$ (148)	Triv.	—	NM	—	HQ	409544
794	$(HSiO_{1.5})_8$	$R\bar{3}$ (148)	Triv.	(b,s)	NM	—	HQ	27154 75244
795	$K(Os(NH_3)_6)(ClO_4)_2Cl_2$	$R\bar{3}$ (148)	SM	—	FM	—	—	87619
796	$K(Cr(NH_3)_6)(ClO_4)_2Cl_2$	$R\bar{3}$ (148)	SM	—	FM	—	—	87621
797	$Rb(Ru(NH_3)_6)(ClO_4)_2Cl_2$	$R\bar{3}$ (148)	SM	—	FM	—	—	280492 280493
798	$Cs(Ru(NH_3)_6)(ClO_4)_2Cl_2$	$R\bar{3}$ (148)	SM	—	FM	—	—	280495
799	$Cs(Cr(NH_3)_6)(ClO_4)_2Cl_2$	$R\bar{3}$ (148)	SM	—	FM	—	—	280497
800	$Cs(Cr(NH_3)_6)(ClO_4)_2Br_2$	$R\bar{3}$ (148)	SM	—	FM	—	—	280499
801	$CsReF_6$	$R\bar{3}$ (148)	SM	—	FM	—	HQ	201511
802	$Ba(IrF_6)$	$R\bar{3}$ (148)	SM	—	—	—	HQ	240981
803	$Li_8(IrO_6)$	$R\bar{3}$ (148)	SM	—	FM	—	HQ	61217
804	$CdCrF_6$	$R\bar{3}$ (148)	Triv.	(b)	FM	—	—	10346
805	$NiSnF_6$	$R\bar{3}$ (148)	SM	(b,s)	FM	—	—	25015
806	$CuSnF_6$	$R\bar{3}$ (148)	SM	(b,s)	FM	—	—	25016
807	$CaPtF_6$	$R\bar{3}$ (148)	Triv.	(b,s)	NM	—	—	37443
808	$ZnPtF_6$	$R\bar{3}$ (148)	Triv.	(b,s)	NM	—	—	37444
809	$Cd(PtF_6)$	$R\bar{3}$ (148)	Triv.	(b,s)	NM	—	—	37445 78906
810	$NiPtF_6$	$R\bar{3}$ (148)	SM	(b,s)	FM	—	—	37448 78905
811	$PdPtF_6$	$R\bar{3}$ (148)	SM	(b,s)	FM	—	—	64661
812	$Li(IrF_6)$	$R\bar{3}$ (148)	Triv.	(b,s)	FM	—	HQ	95777 165207
813	$Li(OsF_6)$	$R\bar{3}$ (148)	SM	(b,s)	FM	—	HQ	165206 165213 165214
814	$Li(PtF_6)$	$R\bar{3}$ (148)	SM	(b,s)	FM	—	HQ	165208
815	$Ca(SiF_6)$	$R\bar{3}$ (148)	Triv.	—	—	—	HQ	183914
816	$Na(AsF_6)$	$R\bar{3}$ (148)	Triv.	—	NM	—	HQ	184562 184563
817	$Na_2Mg(CO_3)_2$	$R\bar{3}$ (148)	Triv.	(b)	NM	—	HQ	9518 100482
818	$AgGe_2(PO_4)_3$	$R\bar{3}$ (148)	Triv.	(b)	—	—	—	425869
819	$Na_2Pt(IO_3)_6$	$R\bar{3}$ (148)	Triv.	(b)	—	—	—	291621
820	$K_2Pt(IO_3)_6$	$R\bar{3}$ (148)	Triv.	(b)	—	—	—	291622
821	$Rb_2Pt(IO_3)_6$	$R\bar{3}$ (148)	Triv.	—	—	—	—	291623
822	$Cs_2Pt(IO_3)_6$	$R\bar{3}$ (148)	Triv.	—	—	—	—	291624
823	$KCo(Au(CN)_2)_3$	$P312$ (149)	SM	(k*,b)	FM	—	HQ	201056
824	$K(Ni(Au(CN)_2)_3)$	$P312$ (149)	SM	(k*,b)	FM	—	—	249724
825	$KMn(Ag(CN)_2)_3$	$P312$ (149)	SM	(k*,b)	FM	—	HQ	281280 262503 262504 262505 262506 262507
826	$BaCa(CO_3)_2$	$P321$ (150)	Triv.	—	NM	—	HQ	100477
827	$CaCl_2(H_2O)_6$	$P321$ (150)	Triv.	—	NM	—	—	1140 59142
828	$CaBr_2(H_2O)_6$	$P321$ (150)	Triv.	—	—	—	—	1141
829	$SrCl_2(H_2O)_6$	$P321$ (150)	Triv.	—	—	—	HQ	48110 59143
830	$K_2(S_2O_6)$	$P321$ (150)	Triv.	—	NM	—	HQ	16661 36154$^{(b)}$ 82843
831	$CaMg_3(CO_3)_4$	$R32$ (155)	Triv.	(b)	NM	—	HQ	201729
832	$Sr(Al_2B_2O_7)$	$R32$ (155)	Triv.	(b)	—	—	HQ	89423
833	$NaK(TeO_3)(H_2O)_3$	$P31c$ (159)	Triv.	—	NM	—	HQ	24781
834	$KLi(SO_4)$	$P31c$ (159)	Triv.	(b)	NM	—	—	62981 71365
835	$Ca_3(SiO_4)O$	$R3m$ (160)	Triv.	(k*,b)	NM	—	HQ	22501 24625
836	$(V(H_2O)_3F_3)$	$R3m$ (160)	SM	—	AFM	—	HQ	69571
837	$(N(CH_3)_3)(BH_3)$	$R3m$ (160)	Triv.	—	—	—	HQ	249799
838	$(Cl_2B)_3B(CO)$	$R3m$ (160)	Triv.	—	NM	—	HQ	280617

839	$Ba(CO_3)$	$R3m$ (160)	Triv.	—	NM	—	HQ	158389 158390
840	$Rb_4(CO_4)$	$R3m$ (160)	Triv.	—	NM	—	—	245430
841	$(NH_3OH)_3FeF_6$	$R3c$ (161)	SM	—	FM	—	—	424249
842	$(CH_2)_3O_3$	$R3c$ (161)	Triv.	—	NM	—	HQ	151224 151343
843	$Ca_3(C_6N_6O_6)$	$R3c$ (161)	Triv.	—	NM	—	—	428357
844	$LiCaNiF_6$	$P\bar{3}1c$ (163)	SM	(b,s)	FM	—	—	32732
845	$LiSrNiF_6$	$P\bar{3}1c$ (163)	SM	(b,s)	FM	—	—	32733
846	$LiCaCrF_6$	$P\bar{3}1c$ (163)	SM	(b)	FM	—	—	73985
847	$Na_3(CrCl_6)$	$P\bar{3}1c$ (163)	SM	(b)	FM	—	HQ	62035
848	$Hg(B(CN)_4)_2$	$P\bar{3}m1$ (164)	Triv.	(b)	—	—	HQ	412297
849	$Cs_2Na(TiF_6)$	$P\bar{3}m1$ (164)	SM	(b,s)	FM	—	HQ	67160
850	$(Hg(H_2O)_6)(ClO_4)_2$	$P\bar{3}m1$ (164)	Triv.	—	NM	—	HQ	1640
851	$(Co(H_2O)_6)(BrO_4)_2$	$P\bar{3}m1$ (164)	SM	—	AFM	—	HQ	73397
852	$K_2(ReF_6)$	$P\bar{3}m1$ (164)	SM	(k*)	FM	—	HQ	1528
853	K_2PtF_6	$P\bar{3}m1$ (164)	Triv.	—	NM	—	—	16892 87360$^{(k)}$
854	Cs_2PtF_6	$P\bar{3}m1$ (164)	Triv.	—	NM	—	HQ	35107
855	Rb_2PtF_6	$P\bar{3}m1$ (164)	Triv.	(k*)	NM	—	HQ	35108
856	$K_2(IrF_6)$	$P\bar{3}m1$ (164)	SM	(k*)	FM	—	HQ	95779
857	$Cs_2(TcF_6)$	$P\bar{3}m1$ (164)	SM	—	FM	—	HQ	425912
858	$K_2(TcF_6)$	$P\bar{3}m1$ (164)	SM	(k*)	FM	—	HQ	425914
859	$Na_2(TcF_6)$	$P\bar{3}m1$ (164)	SM	—	FM	—	HQ	425915
860	$Rb_2(TcF_6)$	$P\bar{3}m1$ (164)	SM	(k*)	—	—	HQ	425918
861	$K_2(SO_3)$	$P\bar{3}m1$ (164)	Triv.	—	NM	—	HQ	60762
862	$NaK_3(PO_3F)_2$	$P\bar{3}m1$ (164)	Triv.	—	—	—	HQ	1904
863	$BaNa_2Co(VO_4)_2$	$P\bar{3}m1$ (164)	SM	(k*,b)	—	—	—	429826
864	$Rb_2(IrF_6)$	$P\bar{3}m1$ (164)	SM	(k*)	FM	—	HQ	240955
865	$Cs_2(IrF_6)$	$P\bar{3}m1$ (164)	SM	—	FM	—	HQ	240956
866	$Os(S_2Cl_{12})$	$R\bar{3}m$ (166)	Triv.	—	FM	—	HQ	74680
867	$K_4Xe_3O_{12}$	$R\bar{3}m$ (166)	Triv.	(k*,b)	—	—	—	253443
868	$Cs_2Na(FeF_6)$	$R\bar{3}m$ (166)	TI	—	FM	—	—	9003$^{(b,s)}$ 16255
869	Cs_2NaMnF_6	$R\bar{3}m$ (166)	Triv.	(b,s)	FM	—	HQ	37006
870	$Cs_2Na(NiF_6)$	$R\bar{3}m$ (166)	TI	(b,s)	—	—	—	42152
871	$Cs_2Na(TiF_6)$	$R\bar{3}m$ (166)	Triv.	(b,s)	FM	—	—	42153
872	$Cs_4K(Li(FeF_6)_2)$	$R\bar{3}m$ (166)	TI	(b,s)	FM	—	HQ	78928
873	$PbPtF_6$	$R\bar{3}m$ (166)	Triv.	—	NM	—	—	4057
874	$Ba(RhF_6)$	$R\bar{3}m$ (166)	SM	—	FM	—	—	6038
875	$BaCrF_6$	$R\bar{3}m$ (166)	SM	—	FM	—	—	10341
876	$SrCrF_6$	$R\bar{3}m$ (166)	SM	—	FM	—	—	10342
877	$Sr(RhF_6)$	$R\bar{3}m$ (166)	SM	—	FM	—	—	42158
878	$K(AuF_6)$	$R\bar{3}m$ (166)	Triv.	—	—	—	HQ	415874
879	$K_2Mg(CO_3)_2$	$R\bar{3}m$ (166)	Triv.	(b)	NM	—	HQ	31295
880	$K(Cr(NH_3)_6)(ClO_4)_2Cl_2$	$R\bar{3}m$ (166)	SM	—	FM	—	—	87620
881	$K(Ru(NH_3)_6)(ClO_4)_2Cl_2$	$R\bar{3}m$ (166)	SM	—	FM	—	—	280489 280490
882	O_2	$R\bar{3}m$ (166)	Triv.	—	FM	SC*	HQ	15535 43430 173934 190368 190369
883	Re_3Cl_9	$R\bar{3}m$ (166)	Triv.	(k*)	NM	—	HQ	14209
884	$ReCl_3$	$R\bar{3}m$ (166)	Triv.	—	NM	—	HQ	62222
885	$Rb(C(CN)_3)$	$R\bar{3}c$ (167)	Triv.	—	—	—	HQ	428450
886	$Cs(C(CN)_3)$	$R\bar{3}c$ (167)	Triv.	—	—	—	HQ	428451
887	$((H_2O)_6Cr)Cl_3$	$R\bar{3}c$ (167)	SM	—	FM	—	—	66000
888	$(Bi_5)(GaCl_4)_3$	$R\bar{3}c$ (167)	Triv.	(b,s)	NM	—	—	81468
889	$Bi_5(AlCl_4)_3$	$R\bar{3}c$ (167)	Triv.	(b,s)	NM	—	—	201993 420082
890	$Sr_3(BO_3)_2$	$R\bar{3}c$ (167)	Triv.	—	NM	—	HQ	93395
891	$K_3(Cr(OH)_6)$	$R\bar{3}c$ (167)	SM	—	AFM	—	—	62653
892	$Rb_3(Cr(OH)_6)$	$R\bar{3}c$ (167)	SM	—	FM	—	—	72315
893	$InSr_3(NiO_6)$	$R\bar{3}c$ (167)	SM	(b,s)	AFM	—	HQ	81660
894	$K_3NaMnCl_6$	$R\bar{3}c$ (167)	SM	(b,s)	FM	—	HQ	290109
895	Rb_6Cl_4O	$R\bar{3}c$ (167)	Triv.	(b)	NM	—	HQ	405193
896	Cs_6Cl_4O	$R\bar{3}c$ (167)	Triv.	(b,s)	NM	—	HQ	411634
897	Rb_6Br_4O	$R\bar{3}c$ (167)	Triv.	—	NM	—	HQ	411955
898	$Rb_3B_3O_6$	$R\bar{3}c$ (167)	Triv.	—	NM	—	HQ	59826

899	$Cs(BO_2)$	$R\bar{3}c$ (167)	Triv.	—	NM	—	HQ	74888
900	$Rb_3(B_3S_6)$	$R\bar{3}c$ (167)	Triv.	—	NM	—	HQ	79615
901	$K_3F(CO_3)$	$R\bar{3}c$ (167)	Triv.	(b,s)	NM	—	HQ	66028
902	$Rb_3F(CO_3)$	$R\bar{3}c$ (167)	Triv.	(b,s)	NM	—	HQ	66029
903	$K_3(AuSe_2)$	$R\bar{3}c$ (167)	Triv.	—	NM	—	HQ	402000
904	$K_3SbS_3(Sb_2O_3)_3$	$P6_3$ (173)	Triv.	(b,s)	NM	—	—	4215
905	$NaPO_3NH_3$	$P6_3$ (173)	Triv.	—	NM	—	—	16608
906	$PS(N(CH_3)NH_2)_3$	$P6_3$ (173)	Triv.	—	NM	—	—	189680
907	$(Sn(H_2O)_3)(ClO_4)_2$	$P6_3$ (173)	Triv.	—	NM	—	—	237716 253553
908	$Sn(SnCl)(W_3Cl_{13})$	$P6_3$ (173)	Triv.	—	NM	—	—	421915
909	$Al(IO_3)_3$	$P6_3$ (173)	Triv.	(b,s)	NM	—	HQ	152758
910	$Li(IO_3)$	$P6_3$ (173)	Triv.	(b)	NM	—	—	9508$^{(s)}$ 14344 14377$^{(s)}$ 35472 35473 35474 35475$^{(s)}$ 35476 40358 40359 40360 40361 40362$^{(s)}$ 40363 40364 40365 46025 46026 46027$^{(s)}$ 80025$^{(s)}$ 80026$^{(s)}$
911	$KLi(SO_4)$	$P6_3$ (173)	Triv.	(b)	NM	—	HQ	20851 33251 36038 36471 48136 56106 71364 88827 88828 280391
912	$LiNa(CO_3)$	$P\bar{6}$ (174)	Triv.	(b)	NM	—	—	80459 89650 89651
913	$TcOF_4$	$P6_3/m$ (176)	SM	—	FM	—	—	16143
914	$B(OTeF_5)_3$	$P6_3/m$ (176)	Triv.	—	NM	—	—	27200
915	$TlCu(OH)(CO_3)$	$P6_3/m$ (176)	SM	(k,b)	FM	—	—	74875
916	$Na(W_6NCl_{18})$	$P6_3/m$ (176)	Triv.	(b)	—	—	—	414409
917	$Sr_5(PO_4)_3Cl$	$P6_3/m$ (176)	Triv.	—	NM	—	—	2089 80084 80085 253053
918	$Sr_{10}(PO_4)_6F_2$	$P6_3/m$ (176)	Triv.	(b)	NM	—	—	163792
919	$Ca_5(PO_4)_3Cl$	$P6_3/m$ (176)	Triv.	—	NM	—	—	184824 184825 670545
920	$B(OCH_3)_3$	$P6_3/m$ (176)	Triv.	—	NM	—	—	245045
921	$BaZn(CO_3)F_2$	$P6_3/m$ (176)	Triv.	(b)	NM	—	HQ	95739
922	$Fe_2(CO)_9$	$P6_3/m$ (176)	Triv.	(b)	NM	—	—	6010 31030
923	SiO_2	$P622$ (177)	Triv.	(b,s)	NM	—	—	170519 170520 170522
924	$CsLi(NH_2)_2$	$P6_222$ (180)	Triv.	—	NM	—	HQ	62654
925	$Ba_5(ReO_5)_3Cl$	$P6_3cm$ (185)	Triv.	—	NM	—	—	73928
926	Li_8CoO_6	$P6_3cm$ (185)	SM	(b,s)	FM	—	—	21026
927	$BiCo_3(CO)_9$	$P6_3mc$ (186)	Triv.	—	—	—	—	62542 66163
928	$(NH_4)(In(HPO_3)_2)$	$P6_3mc$ (186)	Triv.	(k*,b)	—	—	—	188660
929	$((CH_3)_4P)(FeCl_4)$	$P6_3mc$ (186)	SM	(k*)	FM	—	—	194586
930	$Cl_4H_{12}N_3O_3Re$	$P6_3mc$ (186)	Triv.	(k*)	—	—	—	419767
931	$(NH_4)_2(SiF_6)$	$P6_3mc$ (186)	Triv.	—	NM	—	—	280755
932	$(NH_4)_2(MnF_6)$	$P6_3mc$ (186)	SM	—	FM	—	—	406381
933	$Rb_2(MnF_6)$	$P6_3mc$ (186)	SM	—	—	—	—	25578
934	$K_2(MnF_6)$	$P6_3mc$ (186)	SM	—	FM	—	HQ	60417 61275 76273
935	$Li(ClO_4)(H_2O)_3$	$P6_3mc$ (186)	Triv.	—	NM	—	HQ	1321 1913 1914 27730 32534
936	$SrKF(CO_3)$	$P\bar{6}m2$ (187)	Triv.	—	NM	—	HQ	262231
937	$SrRbF(CO_3)$	$P\bar{6}m2$ (187)	Triv.	—	NM	—	HQ	262233
938	$KCo(PO_3)_3$	$P\bar{6}c2$ (188)	SM	(b)	AFM	—	HQ	193216
939	$KZn(BeF_3)_3$	$P\bar{6}c2$ (188)	Triv.	(b)	NM	—	HQ	18022
940	$RbMgCO_3F$	$P\bar{6}2m$ (189)	Triv.	(b)	NM	—	HQ	238611 670338$^{(s)}$
941	$CaRbF(CO_3)$	$P\bar{6}2m$ (189)	Triv.	—	NM	—	HQ	262232
942	$CaCsF(CO_3)$	$P\bar{6}2m$ (189)	Triv.	—	—	—	HQ	262234
943	$K_2(HfF_6)$	$P\bar{6}2m$ (189)	Triv.	—	NM	—	—	47246
944	N_2O_5	$P6_3/mmc$ (194)	Triv.	—	NM	—	—	30638
945	N_2O_5	$P6_3/mmc$ (194)	SM	—	NM	—	—	30639
946	$K_6(BiCl_6)Cl_2(H_3F_4)$	$P6_3/mmc$ (194)	Triv.	(k)	NM	—	—	68226
947	$K_4(O_3(IO_3)_2)$	$P6_3/mmc$ (194)	Triv.	(b,s)	NM	—	—	25694
948	$(K_2(SiF_6))(K(NO_3))$	$P6_3/mmc$ (194)	Triv.	—	NM	—	HQ	159390 417735
949	$Cs(NiF_3)$	$P6_3/mmc$ (194)	SM	(b,s)	FM	—	—	15092 61278
950	$Cs_2Ni_2F_6$	$P6_3/mmc$ (194)	SM	(b,s)	FM	—	—	410394
951	$Rb_3((OsBr_3)_2Br_3)$	$P6_3/mmc$ (194)	Triv.	(k*)	NM	—	—	56896
952	He	$P6_3/mmc$ (194)	Triv.	—	NM	—	—	43426 44394 44396 426943
953	$K_2(CO_3)$	$P6_3/mmc$ (194)	Triv.	—	NM	—	—	52535

954	$Na_2(CO_3)$	$P6_3/mmc$ (194)	Triv.	—	NM	—	—	81004 81005 81006 81007 81008 81009 81010 81011 81012 81013
955	$Cs_3(Mo_2O_7)Br$	$P6_3/mmc$ (194)	Triv.	—	—	—	HQ	260595
956	PF_5	$P6_3/mmc$ (194)	Triv.	(k*)	NM	—	—	62554
957	AsF_5	$P6_3/mmc$ (194)	Triv.	(k*)	NM	—	—	65477
958	$K_2Pb(Cu(NO_2)_6)$	$F23$ (196)	SM	—	FM	—	—	36135
959	$Bi_{12}MnO_{20}$	$I23$ (197)	SM	(b)	FM	—	—	75079
960	$Bi_{24}Mn_2O_{40}$	$I23$ (197)	SM	(b)	FM	—	—	75390
961	$Ba(NO_3)_2$	$P2_13$ (198)	Triv.	—	—	—	—	34902
962	$CsXeF_7$	$P2_13$ (198)	Triv.	—	NM	—	—	404986
963	NH_3	$P2_13$ (198)	Triv.	—	NM	—	—	638341 29321 84461 300149
964	$Na(ClO_3)$	$P2_13$ (198)	Triv.	—	NM	—	—	1117 1301 16714 22395 26684 28830 31121 31167 31168 80337 80338 80339 80340 80341
965	$Na(BrO_3)$	$P2_13$ (198)	Triv.	—	NM	—	HQ	1302$^{(b)}$ 22396 28831 30208$^{(b)}$ 31166 47174$^{(b)}$
966	$Tl(Co(CO)_4)$	$P2_13$ (198)	Triv.	—	NM	—	—	6011 31361 31362
967	$Tl(Fe(CO)_3(NO))$	$P2_13$ (198)	Triv.	—	NM	—	—	66317
968	$K_2Pb(Ni(NO_2)_6)$	$Fm\bar{3}$ (202)	SM	—	FM	—	HQ	1937
969	$Cs_2PbCu(NO_2)_6$	$Fm\bar{3}$ (202)	SM	—	FM	—	HQ	2381 56254
970	$K_2Pb(Cu(NO_2)_6)$	$Fm\bar{3}$ (202)	SM	—	FM	—	HQ	16127 26228 26749
971	$K_2Ca(Ni(NO_2)_6)$	$Fm\bar{3}$ (202)	SM	—	FM	—	—	26748
972	N_2O_4	$Im\bar{3}$ (204)	Triv.	—	NM	—	—	52347 29047 201140 201141 201142
973	$CaCu_3Ge_4O_{12}$	$Im\bar{3}$ (204)	SM	(k,b)	FM	—	—	1303 184279
974	$CaCu_3(Sn_4O_{12})$	$Im\bar{3}$ (204)	SM	(k,b)	FM	—	HQ	162100 184281
975	$SrCu_3(Sn_4O_{12})$	$Im\bar{3}$ (204)	SM	(k,b)	FM	—	HQ	162101
976	$PbCu_3(Sn_4O_{12})$	$Im\bar{3}$ (204)	SM	(k,b)	FM	—	HQ	162102
977	$Cs(NO_3)$	$Pa\bar{3}$ (205)	Triv.	—	NM	—	—	35555
978	$(IF_6)(AsF_6)$	$Pa\bar{3}$ (205)	Triv.	—	NM	—	—	249129
979	N	$Pa\bar{3}$ (205)	Triv.	—	NM	—	—	426956
980	N_2	$Pa\bar{3}$ (205)	Triv.	—	NM	—	—	15472 26482 28179
981	NaO_2	$Pa\bar{3}$ (205)	SM	—	FM	—	—	26582 87178
982	$Ba(NO_3)_2$	$Pa\bar{3}$ (205)	Triv.	—	NM	—	—	35495 52353 95594 95595 109281
983	$(O_2)(SbF_6)$	$Ia\bar{3}$ (206)	SM	—	FM	—	—	78849
984	$K(SbF_6)$	$Ia\bar{3}$ (206)	Triv.	—	NM	—	—	76422 76653
985	$Li_2NiGe_3O_8$	$P4_332$ (212)	SM	(k*,b)	FM	—	—	68339
986	$Cs_3(Mo_4O_4)(PO_4)_3$	$P\bar{4}3m$ (215)	Triv.	(k,b)	FM	—	HQ	62225
987	$K_4(CO_4)$	$P\bar{4}3m$ (215)	Triv.	—	NM	—	—	245417
988	$Rb_4(CO_4)$	$P\bar{4}3m$ (215)	Triv.	—	NM	—	—	245429
989	$LiCo(CO)_4$	$P\bar{4}3m$ (215)	Triv.	—	NM	—	HQ	30854
990	$Ag(B(CN)_4)$	$P\bar{4}3m$ (215)	Triv.	—	NM	—	HQ	411179
991	$Ba(SO_4)$	$F\bar{4}3m$ (216)	Triv.	(k*,p*)	NM	—	—	23743 62368
992	$SrSO_4$	$F\bar{4}3m$ (216)	Triv.	(k*,p*)	NM	—	—	23744
993	$K(ClO_4)$	$F\bar{4}3m$ (216)	Triv.	(k*,p*)	NM	—	—	33562
994	$Tl(ClO_4)$	$F\bar{4}3m$ (216)	Triv.	(k*,p*)	NM	—	—	33564
995	$Cs(ClO_4)$	$F\bar{4}3m$ (216)	Triv.	(k*,p*)	NM	—	—	33566
996	$Na(ClO_4)$	$F\bar{4}3m$ (216)	Triv.	(k*,p*)	NM	—	—	33567
997	$Ag(ClO_4)$	$F\bar{4}3m$ (216)	Triv.	(k*,p*)	NM	—	—	33568
998	$CsFe(H_2O)_6PO_4$	$F\bar{4}3m$ (216)	Triv.	—	FM	—	HQ	172377
999	$Cs(Mg(H_2O)_6)(AsO_4)$	$F\bar{4}3m$ (216)	Triv.	—	NM	—	HQ	260150
1000	$Cs(Mg(H_2O)_6)(PO_4)$	$F\bar{4}3m$ (216)	Triv.	—	NM	—	HQ	281563
1001	$CsNi(Cr(CN)_6)$	$F\bar{4}3m$ (216)	SM	—	—	—	—	56603
1002	KI	$F\bar{4}3m$ (216)	Triv.	—	—	—	—	674991
1003	NaF	$F\bar{4}3m$ (216)	Triv.	—	—	—	—	674994
1004	RbI	$F\bar{4}3m$ (216)	Triv.	—	—	—	—	674999
1005	$(Zn(NH_3)_4)(ClO_4)_2$	$F\bar{4}3m$ (216)	Triv.	—	NM	—	HQ	74790
1006	$(Zn(NH_3)_4)(MnO_4)_2$	$F\bar{4}3m$ (216)	Triv.	—	NM	—	—	162384
1007	$(Ru(CO)_3)_4Se_4$	$I\bar{4}3m$ (217)	Triv.	—	NM	—	—	92913
1008	$(Li(NH_3)_4)_3(AsSe_4)$	$I\bar{4}3m$ (217)	Triv.	(k)	NM	—	—	409539
1009	$K_3(BiO_3)$	$I\bar{4}3m$ (217)	Triv.	(b)	NM	—	HQ	407293
1010	$Ca_8(Al_{12}O_{24})S_2$	$I\bar{4}3m$ (217)	Triv.	(b,s)	NM	—	HQ	67589

1011	$Sr_8(Al_{12}O_{24})S_2$	$I\bar{4}3m$ (217)	Triv.	(b,s)	NM	—	HQ	67590
1012	$Sr_8(AlO_2)_{12}Te_2$	$I\bar{4}3m$ (217)	Triv.	(b,s)	NM	—	HQ	82609
1013	$Na_8(Al_6Ge_6O_{24})I_2$	$P\bar{4}3n$ (218)	Triv.	(b,s)	NM	—	—	65666 85349
1014	$Na_8(Al_6Si_6O_{24})I_2$	$P\bar{4}3n$ (218)	Triv.	(b,s)	NM	—	—	68960 71434
1015	$Li_8Br_2(Be_6P_6O_{24})$	$P\bar{4}3n$ (218)	Triv.	(b,s)	NM	—	—	80472
1016	$Li_8(GaSiO_4)_6Br_2$	$P\bar{4}3n$ (218)	Triv.	(b,s)	NM	—	—	87988
1017	$Li_8(GaSiO_4)_6I_2$	$P\bar{4}3n$ (218)	Triv.	(b,s)	NM	—	—	87989
1018	$Li_8(AlGeO_4)_6Br_2$	$P\bar{4}3n$ (218)	Triv.	(b)	NM	—	—	87991
1019	$Li_8(AlGeO_4)_6I_2$	$P\bar{4}3n$ (218)	Triv.	(b)	NM	—	—	87992
1020	$Mg_3(B_7O_{13}Cl)$	$F\bar{4}3c$ (219)	Triv.	(k,b)	NM	—	—	30351$^{(s)}$ 30615
1021	$(Si_5Cl_{12})(SiCl_4)$	$F\bar{4}3c$ (219)	Triv.	—	NM	—	—	2767
1022	YF_3	$Pm\bar{3}m$ (221)	Triv.	(k)	NM	—	—	15961
1023	LaF_3	$Fm\bar{3}m$ (225)	Triv.	—	NM	—	—	164054 167556
1024	$Cs_2Li(Fe(CN)_6)$	$Fm\bar{3}m$ (225)	SM	—	FM	—	HQ	1000 1001 10179 60540 60541 60542
1025	$Cs_2Li(Cr(CN)_6)$	$Fm\bar{3}m$ (225)	SM	—	FM	—	—	6085 68068
1026	$Cs_2MgFe(CN)_6$	$Fm\bar{3}m$ (225)	Triv.	—	NM	—	—	6086
1027	$Cs_2LiIr(CN)_6$	$Fm\bar{3}m$ (225)	Triv.	—	NM	—	—	9032
1028	$Cs_2LiMn(CN)_6$	$Fm\bar{3}m$ (225)	Triv.	—	FM	—	HQ	10180 68067
1029	$Cs_2Li(Co(CN)_6)$	$Fm\bar{3}m$ (225)	Triv.	—	NM	—	HQ	10181 23204 60538 60539
1030	$MnCs_2(Fe(CN)_6)$	$Fm\bar{3}m$ (225)	SM	—	FM	—	HQ	151695
1031	$CdCs_2(Fe(CN)_6)$	$Fm\bar{3}m$ (225)	Triv.	—	NM	—	HQ	151696
1032	$NiCs_2(Fe(CN)_6)$	$Fm\bar{3}m$ (225)	SM	—	FM	—	HQ	151706
1033	$Cs_2Co(Fe(CN)_6)$	$Fm\bar{3}m$ (225)	SM	—	—	—	HQ	416443
1034	Rb_2NaFeF_6	$Fm\bar{3}m$ (225)	SM	(b)	FM	—	—	4030$^{(k,s)}$ 40966$^{(k,s)}$ 42146
1035	Cs_2KMoF_6	$Fm\bar{3}m$ (225)	SM	(b)	FM	—	—	4053
1036	$Cs_2K(RhF_6)$	$Fm\bar{3}m$ (225)	Triv.	—	NM	—	—	4056
1037	K_3MoF_6	$Fm\bar{3}m$ (225)	SM	(b)	FM	—	HQ	4403
1038	$Cs_2K(TiF_6)$	$Fm\bar{3}m$ (225)	SM	—	FM	—	—	6035 67146
1039	$Cs_2Tl(FeF_6)$	$Fm\bar{3}m$ (225)	SM	—	FM	—	—	6036
1040	$Cs_2K(CoF_6)$	$Fm\bar{3}m$ (225)	Triv.	—	NM	—	—	6037
1041	$Cs_2K(NiF_6)$	$Fm\bar{3}m$ (225)	SM	—	FM	—	—	6039
1042	$Rb_2K(FeF_6)$	$Fm\bar{3}m$ (225)	SM	—	FM	—	—	9001 40967 42145
1043	Cs_2NaBiF_6	$Fm\bar{3}m$ (225)	Triv.	(k*,b,s)	NM	—	—	9382
1044	Rb_2NaBiF_6	$Fm\bar{3}m$ (225)	Triv.	(k*,b,s)	NM	—	—	9386
1045	Cs_2KCrF_6	$Fm\bar{3}m$ (225)	SM	—	FM	—	—	9705
1046	Rb_2NaCrF_6	$Fm\bar{3}m$ (225)	SM	(k*,b,s)	FM	—	—	9706
1047	$Rb_2K(CrF_6)$	$Fm\bar{3}m$ (225)	SM	(b)	FM	—	—	9707
1048	Cs_2TlMoF_6	$Fm\bar{3}m$ (225)	SM	(b)	FM	—	—	15772
1049	KRb_2MoF_6	$Fm\bar{3}m$ (225)	SM	(b)	FM	—	—	15773
1050	K_2NaMoF_6	$Fm\bar{3}m$ (225)	SM	(k*,b,s)	FM	—	—	15777
1051	$Cs_2K(AgF_6)$	$Fm\bar{3}m$ (225)	SM	(k*,b,s)	FM	—	—	16783
1052	K_2NaCrF_6	$Fm\bar{3}m$ (225)	SM	(k*,b,s)	FM	—	—	22199 40965
1053	$K_2Na(FeF_6)$	$Fm\bar{3}m$ (225)	SM	(k*,b,s)	FM	—	—	22200 61277
1054	Rb_2KRhF_6	$Fm\bar{3}m$ (225)	Triv.	(b)	NM	—	—	27339
1055	Rb_2NaRhF_6	$Fm\bar{3}m$ (225)	Triv.	(k*,b,s)	NM	—	—	27341
1056	K_2NaRhF_6	$Fm\bar{3}m$ (225)	Triv.	(k*,b,s)	NM	—	—	27342
1057	Cs_2TlVF_6	$Fm\bar{3}m$ (225)	SM	—	FM	—	—	27343
1058	Cs_2KVF_6	$Fm\bar{3}m$ (225)	SM	—	FM	—	—	27344
1059	Rb_2KVF_6	$Fm\bar{3}m$ (225)	SM	(b)	FM	—	—	27345
1060	Cs_2NaMnF_6	$Fm\bar{3}m$ (225)	Triv.	(b)	FM	—	—	37005
1061	$Rb_2K(TiF_6)$	$Fm\bar{3}m$ (225)	SM	(b)	FM	—	—	42142 67147
1062	$Rb_2Na(TiF_6)$	$Fm\bar{3}m$ (225)	SM	(k*,b,s)	FM	—	—	42143
1063	$Cs_2K(FeF_6)$	$Fm\bar{3}m$ (225)	SM	—	FM	—	—	42144
1064	$Rb_2K(NiF_6)$	$Fm\bar{3}m$ (225)	SM	(b)	FM	—	—	42149
1065	$Tl_3(TiF_6)$	$Fm\bar{3}m$ (225)	SM	(k*,b,s)	FM	—	—	42154
1066	$Cs_2K(CuF_6)$	$Fm\bar{3}m$ (225)	SM	—	FM	—	HQ	59102
1067	Cs_2NaFeF_6	$Fm\bar{3}m$ (225)	SM	(b)	FM	—	HQ	65503
1068	Cs_2KMnF_6	$Fm\bar{3}m$ (225)	Triv.	—	FM	—	HQ	91037
1069	K_2NaVF_6	$Fm\bar{3}m$ (225)	SM	(k*,b,s)	FM	—	—	186883
1070	$(NH_4)_2Na(CrF_6)$	$Fm\bar{3}m$ (225)	SM	(k*)	FM	—	—	418735

1071	$(NH_4)_2Na(FeF_6)$	$Fm\bar{3}m$ (225)	SM	(k*)	FM	—	HQ	418736
1072	Rb_2CoF_6	$Fm\bar{3}m$ (225)	SM	—	FM	—	—	9701
1073	Cs_2CoF_6	$Fm\bar{3}m$ (225)	SM	—	FM	—	—	9702
1074	$Rb_2(MnF_6)$	$Fm\bar{3}m$ (225)	SM	—	FM	—	—	25579 47207 202536
1075	Cs_2SiF_6	$Fm\bar{3}m$ (225)	Triv.	—	NM	—	—	26871 38548
1076	$Rb_2(PdF_6)$	$Fm\bar{3}m$ (225)	Triv.	—	NM	—	—	28675
1077	$Rb_2(CrF_6)$	$Fm\bar{3}m$ (225)	SM	—	FM	—	—	29006
1078	$Cs_2(CrF_6)$	$Fm\bar{3}m$ (225)	SM	—	FM	—	—	29007
1079	K_2SiF_6	$Fm\bar{3}m$ (225)	Triv.	—	NM	—	HQ	29407 38546 64763 73722
1080	$Cs_2(GeF_6)$	$Fm\bar{3}m$ (225)	Triv.	—	NM	—	—	35547
1081	$Rb_2(SiF_6)$	$Fm\bar{3}m$ (225)	Triv.	—	NM	—	—	38547
1082	$Cs_2(MnF_6)$	$Fm\bar{3}m$ (225)	SM	—	FM	—	—	47201 76272
1083	$K_2(MnF_6)$	$Fm\bar{3}m$ (225)	SM	(k*)	FM	—	—	47213
1084	$Rb_2(GeF_6)$	$Fm\bar{3}m$ (225)	Triv.	—	NM	—	HQ	68982
1085	$Cs_2(IrCl_6)$	$Fm\bar{3}m$ (225)	SM	(k*)	FM	—	HQ	69142
1086	$Cs_2(PtF_6)$	$Fm\bar{3}m$ (225)	Triv.	—	NM	—	HQ	78955
1087	Sr_2OsH_6	$Fm\bar{3}m$ (225)	Triv.	(k*)	NM	—	—	638409
1088	Na_6MnCl_8	$Fm\bar{3}m$ (225)	SM	(k,b)	FM	—	HQ	1845
1089	Li_6FeCl_8	$Fm\bar{3}m$ (225)	Triv.	(k,b)	FM	—	HQ	73217
1090	Li_6VCl_8	$Fm\bar{3}m$ (225)	SM	(k,b)	FM	—	—	100834
1091	$Na_6O(SO_4)_2$	$Fm\bar{3}m$ (225)	Triv.	(k*)	NM	—	HQ	411442
1092	KF	$Fm\bar{3}m$ (225)	Triv.	—	NM	—	—	52241 53824 64686 671925 673325 673985 674974
1093	CsCl	$Fm\bar{3}m$ (225)	Triv.	—	NM	—	—	52274 61515 674969
1094	RbF	$Fm\bar{3}m$ (225)	Triv.	—	NM	—	—	53828 673989 674982
1095	$Na(MoF_6)$	$Fm\bar{3}m$ (225)	SM	—	FM	—	—	27484 31033
1096	$Na(PF_6)$	$Fm\bar{3}m$ (225)	Triv.	—	NM	—	HQ	90615
1097	$Na(AsF_6)$	$Fm\bar{3}m$ (225)	Triv.	—	NM	—	HQ	184564 184565
1098	SiO_2	$Fd\bar{3}m$ (227)	Triv.	(b,s)	NM	—	—	170476 35536$^{(k,p)}$ 77458$^{(k,p)}$ 77459$^{(k,p)}$ 77460$^{(k,p)}$ 162620$^{(k,p)}$
1099	$K_2Cd(CN)_4$	$Fd\bar{3}m$ (227)	Triv.	(k,p,b)	NM	—	—	23994 168524
1100	$Mg_2Na_6(CO_3)_4Br_2$	$Fd\bar{3}m$ (227)	Triv.	(k,p)	NM	—	—	27791
1101	Nb_6F_{15}	$Im\bar{3}m$ (229)	SM	(b,s)	NM	—	—	25769 415950
1102	SF_6	$Im\bar{3}m$ (229)	Triv.	—	NM	—	HQ	63362 252619 252620

3. Best flat bands near or at the Fermi level

Among the 2,379 curated flat-band materials given in Table XII of non-atomic flat-band materials, we present in this subsection the 345 best candidates (corresponding to 949 ICSD entries). They have been selected with their experimental relevance in mind: we have targeted materials where flat bands are located at or close to the Fermi level, without any gating/doping. For that purpose, we have applied the following two criteria:

1. The highest occupied band or the lowest unoccupied band near the Fermi level is classified as a flat band according to the definition given in Appendix C 2 a.

2. The highest occupied or lowest unoccupied flat band is perfectly flat, *i.e.*, almost dispersionless, along at least one high-symmetry line of the BZ. Note that we did not apply here any bandwidth threshold.

The band structure and projected density of states of each of these 345 best candidates are given in Figs. 28, 29, 30, 31, 32, 33, 34, 35, 36, 37, 38, 39, 40, 41, 42, 43, 44, 45, 46, 47, 48, 49, 50, 51, 52, 53, 54, 55, 56, 57, 58, 59, 60, 61, 62, 63, 64, 65, 66, 67, 68, 69, 70 and 71. In Fig. 27, we detail the information provided for each material. Note that the materials $KAg[CN]_2$ [ICSD 30275, SG 163 ($P\bar{3}1c$)], $Pb_2Sb_2O_7$ [ICSD 27120, SG 227 ($Fd\bar{3}m$)], Rb_2CaH_4 [ICSD 65196, SG 139 ($I4/mmm$)], Ca_2NCl [ICSD 62555, SG 166 ($R\bar{3}m$)] and WO_3 [ICSD 108651, SG 221 ($Pm\bar{3}m$)] have been used as prototypical cases with line-graph or bipartite sublattice in the main text. The five materials and $CaNi_5$ [ICSD 54474, SG 191 ($P6/mmm$)] appearing in this list of best candidates are discussed in details in Appendix F, focusing on the origin of their flat bands. As pointed out in Appendix H 1, some candidates presented here have been reported theoretically or experimentally to host flat bands near the Fermi level: $Co_3Sn_2S_2$ [ICSD 624867, SG 166 ($R\bar{3}m$)][86,96,97], Sr_2FeMoO_6 [ICSD 181752, SG 225 ($Fm\bar{3}m$)][94] and Pd_3Pb [ICSD 42600, SG 221 ($Pm\bar{3}m$)][93].

Compounds with the same crystal structure and varying chemical composition can have remarkably similar band structures. In the following subsections, we briefly describe structural and composition requirements for the 8 most prominent groups of these 122 unique materials (including 323 ICSDs) among the list of best compounds.

a. *Heusler-$AlCu_2Mn$*

Heusler compounds are a class of intermetallic crystals with generic chemical formula X_2YZ, which crystallize in the cubic space group SG 225 ($Fm\bar{3}m$). X and Y are transition metals and Z is a main-group element. In some cases, Y can be an alkaline earth element. Atoms of X, Y, and Z elements occupy $8c$, $4a$, and $4b$ Wyckoff positions, respectively. They are known for easily-tunable band gaps, diverse magnetic properties, such as magneto-optical, magnetocaloric, and magneto-structural characteristics, half-metallic ferromagnetism, and flat bands[98,99]. Moreover, Heusler compounds with electron counts near 27 electrons are superconductive[98,100–103]. We refer the reader to the review Ref.[98] for a detailed discussion about Heusler compounds.

The list of best compounds contains 35 unique materials (corresponding to 100 ICSD entries) that are Heusler compounds. These materials are given in Table XIV.

Table XIV: List of best compounds belonging to the family of Heusler-$AlCu_2Mn$ compounds. The first column is the chemical formula, the second column is the representative ICSD used for the band structure and projected DOS plots. The third column is the space group, the fourth column is the link to figure showing the corresponding band structure and projected DOS. The last two columns provide the magnetic and superconducting properties, following the same notations than Table. XII.

chem. formula	ICSD	space group	figure	magn.	superconduct.
$LiCo_2Ge$	25324	SG 225 ($Fm\bar{3}m$))	Fig. 64	NM	—
$CoFe_2Ge$	52954	SG 225 ($Fm\bar{3}m$))	Fig. 64	FM	—
Co_2ZnGe	52994	SG 225 ($Fm\bar{3}m$))	Fig. 64	FM	—
Co_2TiSi	53080	SG 225 ($Fm\bar{3}m$))	Fig. 64	FM	—
Co_2VSi	53086	SG 225 ($Fm\bar{3}m$))	Fig. 64	FM	—
$FeRu_2Si$	53525	SG 225 ($Fm\bar{3}m$))	Fig. 67	FM	—
Fe_2VSi	53555	SG 225 ($Fm\bar{3}m$))	Fig. 64	FM	—
$ZrNi_2In$	54546	SG 225 ($Fm\bar{3}m$))	Fig. 64	NM	—
$HfNi_2In$	54595	SG 225 ($Fm\bar{3}m$))	Fig. 65	NM	—
$AlCrFe_2$	57654	SG 225 ($Fm\bar{3}m$))	Fig. 65	FM	—
$AlFe_3$	57793	SG 225 ($Fm\bar{3}m$))	Fig. 65	FM	—
$AlFe_2Mo$	57807	SG 225 ($Fm\bar{3}m$))	Fig. 65	FM	—
Mn_3Si	76227	SG 225 ($Fm\bar{3}m$))	Fig. 65	FM	SC
$CoFe_2Ga$	102385	SG 225 ($Fm\bar{3}m$))	Fig. 63	FM	—
Co_2HfGa	102433	SG 225 ($Fm\bar{3}m$))	Fig. 65	FM	—
Co_2HfSn	102483	SG 225 ($Fm\bar{3}m$))	Fig. 63	FM	—
Co_2SnTi	102682	SG 225 ($Fm\bar{3}m$))	Fig. 63	FM	—
Co_2SnZr	102687	SG 225 ($Fm\bar{3}m$))	Fig. 63	FM	—
$CrFe_2Ga$	102755	SG 225 ($Fm\bar{3}m$))	Fig. 65	FM	—
Cu_2MnIn	102996	SG 225 ($Fm\bar{3}m$))	Fig. 63	FM	—
Fe_2GaV	103473	SG 225 ($Fm\bar{3}m$))	Fig. 67	NM	—
Fe_2SnTi	103641	SG 225 ($Fm\bar{3}m$))	Fig. 65	NM	—
Fe_2SnV	103644	SG 225 ($Fm\bar{3}m$))	Fig. 66	FM	—
$MnNi_2Sn$	104926	SG 225 ($Fm\bar{3}m$))	Fig. 66	FM	—
$NiRh_2Sn$	105327	SG 225 ($Fm\bar{3}m$))	Fig. 64	FM	—
Ni_2ScSn	105339	SG 225 ($Fm\bar{3}m$))	Fig. 66	NM	—
Fe_3Ga	108436	SG 225 ($Fm\bar{3}m$))	Fig. 66	FM	—
Co_2TiGe	169468	SG 225 ($Fm\bar{3}m$))	Fig. 66	FM	—
Co_2TiAl	185966	SG 225 ($Fm\bar{3}m$))	Fig. 66	FM	—
Fe_2CrSn	185999	SG 225 ($Fm\bar{3}m$))	Fig. 66	FM	—
Fe_2TiGe	186057	SG 225 ($Fm\bar{3}m$))	Fig. 67	NM	—
Fe_2TiAs	186059	SG 225 ($Fm\bar{3}m$))	Fig. 66	FM	—
Fe_2TiSb	186060	SG 225 ($Fm\bar{3}m$))	Fig. 67	FM	—
Ru_2VGe	671340	SG 225 ($Fm\bar{3}m$))	Fig. 67	n.a.	—
Fe_2ZrP	675102	SG 225 ($Fm\bar{3}m$))	Fig. 67	n.a.	—

b. *Heusler-AlLiSi*

Heusler-AlLiSi compounds, a sub-class of half-Heusler compounds, have the XYZ general formula and non-centrosymmetric SG 216 ($F\bar{4}3m$). There is a wide range of choices for X, Y, and Z elements. The compounds can contain main-group elements, transition metals, and elements whose atoms form cations, which can be an alkaline, alkaline earth, or transition-metal, or rate-earth elements. The lattice can be viewed as zinc blende-type sub-lattice ($4a$ and $4c$ Wyckoff positions) with occupied $4b$ positions.[98]. Members of half-Heusler family are known for superconductivity[104–106] and theromelectric properties[107,108].

The list of best compounds contains 6 unique materials (corresponding to 21 ICSD entries) that are Heusler-AlLiSi compounds. These materials are given in Table XV.

Table XV: List of best compounds belonging to the family of Heusler-AlLiSi compounds. The first column is the chemical formula, the second column is the representative ICSD used for the band structure and projected DOS plots. The third column is the space group, the fourth column is the link to figure showing the corresponding band structure and projected DOS. The last two columns provide the magnetic and superconducting properties, following the same notations than Table. XII.

chem. formula	ICSD	space group	figure	magn.	super-conduct.
CoMnSb	53001	SG 216 ($F\bar{4}3m$))	Fig. 52	FM	—
NiMnSb	54255	SG 216 ($F\bar{4}3m$))	Fig. 52	FM	—
RhMnSb	54343	SG 216 ($F\bar{4}3m$))	Fig. 53	FM	—
CoNbSn	102552	SG 216 ($F\bar{4}3m$))	Fig. 53	FM	—
MnPtSn	104955	SG 216 ($F\bar{4}3m$))	Fig. 53	FM	—
LiCaC	672030	SG 216 ($F\bar{4}3m$))	Fig. 53	n.a.	—

c. *Heusler-$CuHg_2Ti$*

Intermetallic compounds in the $CuHg_2Ti$ structure type, known as inverse Heusler structure, have a X_2YZ generalized chemical formula. Similarly to the Heusler compounds discussed in Apppendix H 3 a, they are composed of transition metals X and Y, and a main-group element Z. They crystallize in the cubic space group SG 216 ($F\bar{4}3m$), like half-Heusler compounds (Apppendix H 3 b). However, the coordination around all sites is tetrahedral, unlike in the Heusler compounds. Two X atoms occupy non-equivalent $4a$ and $4d$ Wyckoff positions, while Y and Z atoms occupy $4b$ and $4c$ positions, respectively. This lattice type arises in cases when Y element is more electronegative than X element. Sometimes atoms at $4a$ and $4d$ positions belong to different element leading to XX'YZ structure[98].

The list of best compounds contains 10 unique materials (corresponding to 11 ICSD entries) that have $CuHg_2Ti$ structure type. These materials are given in Table XVI.

Table XVI: List of best compounds belonging to the family of $CuHg_2Ti$ compounds. The first column is the chemical formula, the second column is the representative ICSD used for the band structure and projected DOS plots. The third column is the space group, the fourth column is the link to figure showing the corresponding band structure and projected DOS. The last two columns provide the magnetic and superconducting properties, following the same notations than Table. XII.

chem. formula	ICSD	space group	figure	magn.	super-conduct.
Mn_2CoAs	191648	SG 216 ($F\bar{4}3m$))	Fig. 51	FM	—
CoFeTiAl	191657	SG 216 ($F\bar{4}3m$))	Fig. 52	NM	—
CoFeTiGa	191658	SG 216 ($F\bar{4}3m$))	Fig. 51	NM	—
CoFeTiSi	191659	SG 216 ($F\bar{4}3m$))	Fig. 51	FM	—
CoFeTiGe	191660	SG 216 ($F\bar{4}3m$))	Fig. 52	FM	—
CoFeTiAs	191661	SG 216 ($F\bar{4}3m$))	Fig. 52	FM	—
CoFeTiSb	191662	SG 216 ($F\bar{4}3m$))	Fig. 52	FM	—
CoFeVGa	191664	SG 216 ($F\bar{4}3m$))	Fig. 52	FM	—
Fe_2MnGe	671982	SG 216 ($F\bar{4}3m$))	Fig. 52	n.a.	—
Fe_2MnAl	672261	SG 216 ($F\bar{4}3m$))	Fig. 51	n.a.	—

d. *Perovskite-$CaTiO_3$*

Cubic perovskites which crystallize in SG 221 ($Pm\bar{3}m$) have a generalized chemical formula XYZ_3, where X and Y are cations, while Z is an anion. In traditional structures, smaller Y atoms are octahedrally coordinated by 6

Z atoms, while larger X atoms have XII-fold Z shell. X atoms are at $1a$, Y atoms are at $1b$, and Z atoms are at $3c$ Wyckoff positions[109]. The covalent framework of these compounds is formed by Y-Z bonds, while X-Z bonds are ionic in character, and X cations provide the charge balance. Perovskites are known for magnetism[110–115], and superconductivity[116–118].

The list of best compounds contains 27 unique materials (corresponding to 69 ICSD entries) that are Perovskite-$CaTiO_3$ compounds. These materials are given in Table XVII.

Table XVII: List of best compounds belonging to the family of Perovskite-$CaTiO_3$ compounds. The first column is the chemical formula, the second column is the representative ICSD used for the band structure and projected DOS plots. The third column is the space group, the fourth column is the link to figure showing the corresponding band structure and projected DOS. The last two columns provide the magnetic and superconducting properties, following the same notations than Table. XII.

chem. formula	ICSD	space group	figure	magn.	super-conduct.
$KMnF_3$	15423	SG 221 ($Pm\bar{3}m$))	Fig. 56	FM	—
$KFeF_3$	15424	SG 221 ($Pm\bar{3}m$))	Fig. 59	FM	—
$Cs(HgBr_3)$	24479	SG 221 ($Pm\bar{3}m$))	Fig. 56	NM	—
KVF_3	28145	SG 221 ($Pm\bar{3}m$))	Fig. 56	FM	—
$RbVF_3$	28146	SG 221 ($Pm\bar{3}m$))	Fig. 56	FM	—
$La(CrO_3)$	28930	SG 221 ($Pm\bar{3}m$))	Fig. 56	FM	—
$La(MnO_3)$	29119	SG 221 ($Pm\bar{3}m$))	Fig. 59	FM	—
$Rb(MnF_3)$	43722	SG 221 ($Pm\bar{3}m$))	Fig. 57	FM	—
Rh_3YB	44568	SG 221 ($Pm\bar{3}m$))	Fig. 57	NM	—
$NaVF_3$	60611	SG 221 ($Pm\bar{3}m$))	Fig. 57	FM	—
$Sr(RuO_3)$	69360	SG 221 ($Pm\bar{3}m$))	Fig. 57	FM	—
Fe_3ZnC	76763	SG 221 ($Pm\bar{3}m$))	Fig. 57	FM	—
Co_3MgC	76790	SG 221 ($Pm\bar{3}m$))	Fig. 57	FM	—
Co_3ZnC	76797	SG 221 ($Pm\bar{3}m$))	Fig. 57	FM	—
YRh_3C	77389	SG 221 ($Pm\bar{3}m$))	Fig. 57	NM	—
$Sr(VO_3)$	88982	SG 221 ($Pm\bar{3}m$))	Fig. 58	FM	—
$Sr(TcO_3)$	109076	SG 221 ($Pm\bar{3}m$))	Fig. 58	NM	—
$Ca(MnO_3)$	168902	SG 221 ($Pm\bar{3}m$))	Fig. 58	FM	—
$Pb(VO_3)$	187637	SG 221 ($Pm\bar{3}m$))	Fig. 58	FM	—
$Sr(MnO_3)$	188415	SG 221 ($Pm\bar{3}m$))	Fig. 58	AFM	—
$Ba(VO_3)$	191203	SG 221 ($Pm\bar{3}m$))	Fig. 58	FM	—
$InNCo_3$	247066	SG 221 ($Pm\bar{3}m$))	Fig. 58	FM	—
$CdCo_3N$	422858	SG 221 ($Pm\bar{3}m$))	Fig. 58	FM	—
$CaTcO_3$	671082	SG 221 ($Pm\bar{3}m$))	Fig. 59	n.a.	—
$BaTcO_3$	671086	SG 221 ($Pm\bar{3}m$))	Fig. 59	n.a.	—
$ZnSnO_3$	673496	SG 221 ($Pm\bar{3}m$))	Fig. 59	n.a.	—
$KSbO_3$	674060	SG 221 ($Pm\bar{3}m$))	Fig. 59	n.a.	—

e. *Double perovskite crystal structure: K_2PtCl_6, Elpasolite-K_2NaAlF_6, and Sr_2NiWO_6*

Unit cell of double perovskites is created by the doubling of perovskite unit cell, XYZ_3 along all three crystallographic axes and introducing a change every other Y site. In K_2PtCl_6 lattice type, with a generalized formula X_2YZ_6, a vacancy is introduced. In elpasolites, with a $X_2Y'YZ_6$ general formula, Y atom is substitute by Y' atom. The symmetry reduces from SG 221 ($Pm\bar{3}m$) to SG 225 ($Fm\bar{3}m$). Finally, in compounds of Sr_2NiWO_6 lattice type elpasolite lattice is tetragonally distorted as the size of X cations decreases with respect to sizes of Y and Y' cations. Space group reduces farther to SG 87 ($I4/m$)[119,120].

Usually, X is an alkaline, alkaline earth, or rare-earth elements, Y is a transition metal or a main-group element, and Z is a halide. In elpasolites, Y' can be an alkaline or alkaline earth metal, a transition metal, or a main-group element. Moreover, Y and Y' can be the same element, but in different oxidation states[121]. Additionally, Z element in elpasolites can be an oxide anion instead of a halide. Transition from elpasolite to the Sr_2NiWO_6 lattice is the most common when Y and Y' are transition metals[119,120,122,123].

The list of best compounds contains 8 unique materials (20 ICSD entries), 20 unique materials (44 ICSD entries) and 11 unique materials (41 ICSD entries) that are K_2PtCl_6, elpasolites, and Sr_2NiWO_6 compounds, respectively. These materials are given in Tables XIX, XVIII and XX.

Table XVIII: List of best compounds belonging to the family of Elpasolite-K_2NaAlF_6 compounds. The first column is the chemical formula, the second column is the representative ICSD used for the band structure and projected DOS plots. The third column is the space group, the fourth column is the link to figure showing the corresponding band structure and projected DOS. The last two columns provide the magnetic and superconducting properties, following the same notations than Table. XII.

chem. formula	ICSD	space group	figure	magn.	super-conduct.
$Ba_2Mn(ReO_6)$	4169	SG 225 ($Fm\bar{3}m$))	Fig. 61	FM	—
$K_2Na(AlF_6)$	6027	SG 225 ($Fm\bar{3}m$))	Fig. 61	NM	—
KTl_2MoF_6	15775	SG 225 ($Fm\bar{3}m$))	Fig. 60	FM	—
$NaTl_2MoF_6$	15776	SG 225 ($Fm\bar{3}m$))	Fig. 60	FM	—
K_2NaTlF_6	22114	SG 225 ($Fm\bar{3}m$))	Fig. 61	NM	—
Cs_2NaTlF_6	22118	SG 225 ($Fm\bar{3}m$))	Fig. 62	NM	—
Ba_2CoWO_6	27425	SG 225 ($Fm\bar{3}m$))	Fig. 60	FM	—
$Sr_2Co(WO_6)$	28598	SG 225 ($Fm\bar{3}m$))	Fig. 60	FM	—
$Sr_2Co(MoO_6)$	28601	SG 225 ($Fm\bar{3}m$))	Fig. 61	AFM	—
Ba_2FeMoO_6	96688	SG 225 ($Fm\bar{3}m$))	Fig. 62	FM	—
$Ba_2(CoMoO_6)$	97028	SG 225 ($Fm\bar{3}m$))	Fig. 61	AFM	—
$Ba_2(FeWO_6)$	99061	SG 225 ($Fm\bar{3}m$))	Fig. 62	AFM	—
$Ba_2Fe(ReO_6)$	109252	SG 225 ($Fm\bar{3}m$))	Fig. 61	FM	—
$Sr_2(GaSbO_6)$	157016	SG 225 ($Fm\bar{3}m$))	Fig. 62	NM	—
$Sr_2(FeMoO_6)$	157603	SG 225 ($Fm\bar{3}m$))	Fig. 62	AFM	—
$Sr_2Y(SbO_6)$	157886	SG 225 ($Fm\bar{3}m$))	Fig. 62	NM	—
Ba_2CaTeO_6	246112	SG 225 ($Fm\bar{3}m$))	Fig. 62	NM	—
Sr_2FeOsO_6	251068	SG 225 ($Fm\bar{3}m$))	Fig. 61	AFM	—
$Cs_2InAgCl_6$	257115	SG 225 ($Fm\bar{3}m$))	Fig. 62	n.a.	—
Pb_2NaIO_6	427115	SG 225 ($Fm\bar{3}m$))	Fig. 61	NM	—

Table XIX: List of best compounds belonging to the family of K_2PtCl_6 compounds. The first column is the chemical formula, the second column is the representative ICSD used for the band structure and projected DOS plots. The third column is the space group, the fourth column is the link to figure showing the corresponding band structure and projected DOS. The last two columns provide the magnetic and superconducting properties, following the same notations than Table. XII.

chem. formula	ICSD	space group	figure	magn.	super-conduct.
$K_2(SnCl_6)$	604	SG 225 ($Fm\bar{3}m$))	Fig. 68	NM	—
$(NH_4)_2(SnCl_6)$	605	SG 225 ($Fm\bar{3}m$))	Fig. 68	NM	—
Rb_2SnCl_6	9022	SG 225 ($Fm\bar{3}m$))	Fig. 68	NM	—
Cs_2SnCl_6	9023	SG 225 ($Fm\bar{3}m$))	Fig. 68	NM	—
Rb_2MnCl_6	9347	SG 225 ($Fm\bar{3}m$))	Fig. 67	FM	—
K_2TaCl_6	59894	SG 225 ($Fm\bar{3}m$))	Fig. 68	FM	—
$Rb_2(NbCl_6)$	245747	SG 225 ($Fm\bar{3}m$))	Fig. 68	FM	—
Y_2Ni_6C	673582	SG 225 ($Fm\bar{3}m$))	Fig. 67	n.a.	—

Table XX: List of best compounds belonging to the family of Sr_2NiWO_6 compounds. The first column is the chemical formula, the second column is the representative ICSD used for the band structure and projected DOS plots. The third column is the space group, the fourth column is the link to figure showing the corresponding band structure and projected DOS. The last two columns provide the magnetic and superconducting properties, following the same notations than Table. XII.

chem. formula	ICSD	space group	figure	magn.	super-conduct.
$Sr_2Ni(WO_6)$	91791	SG 87 ($I4/m$))	Fig. 34	AFM	—
$Ba_2(FeWO_6)$	95518	SG 87 ($I4/m$))	Fig. 34	AFM	—
$Sr_2(FeMoO_6)$	150701	SG 87 ($I4/m$))	Fig. 34	FM	—
$Sr_2(FeReO_6)$	150702	SG 87 ($I4/m$))	Fig. 33	FM	—
$Sr_2Mg(WO_6)$	151703	SG 87 ($I4/m$))	Fig. 34	NM	—
$Sr_2(CoMoO_6)$	153544	SG 87 ($I4/m$))	Fig. 33	FM	—
Sr_2CoReO_6	173488	SG 87 ($I4/m$))	Fig. 33	AFM	—
Sr_2MgMoO_6	187662	SG 87 ($I4/m$))	Fig. 34	NM	—
Sr_2MnMoO_6	187669	SG 87 ($I4/m$))	Fig. 33	FM	—
Sr_2CoWO_6	190593	SG 87 ($I4/m$))	Fig. 33	AFM	—
Sr_2CoNbO_6	192327	SG 87 ($I4/m$))	Fig. 34	n.a.	—

f. Shandite-$Ni_3Pb_2S_2$

Ni3Pb2S2 lattice type in SG 166 ($R\bar{3}m$), known as shandite, is a lattice with a $X_3Y_2Z_2$ general formula. But this lattice type also includes compounds with a $X_3YY'Z_2$ formula. X atoms belong to a transition metal element, while Y (Y') and Z atoms are main-group elements. X atoms occupy $3a$ Wyckoff positions, Y atoms are at $3b$ positions, and Z atoms are at $6c$ positions. The bonding in these compounds can be approximated by a Kagome Hamiltonian for d orbitals, though small contributions form Y's and Z's orbitals to the bands near the Fermi level are possible[124,125].

The list of best compounds contains 5 unique materials (corresponding to 17 ICSD entries) that are Shandite-$Ni_3Pb_2S_2$ compounds, and are listed in Table XXI. Note that all of them host a rigorous Kagome sublattice, as expected.

Table XXI: List of best compounds belonging to the family of $Ni_3Pb_2S_2$ compounds. The first column is the chemical formula, the second column is the representative ICSD used for the band structure and projected DOS plots. The third column is the space group, the fourth column is the link to figure showing the corresponding band structure and projected DOS. The last two columns provide the magnetic and superconducting properties, following the same notations than Table. XII.

chem. formula	ICSD	space group	figure	magn.	super-conduct.
$Co_3Sn_2S_2$	5435	SG 166 ($R\bar{3}m$))	Fig. 44	FM	—
Co_3InSnS_2	5437	SG 166 ($R\bar{3}m$))	Fig. 44	NM	—
Rh_3InPbS_2	5440	SG 166 ($R\bar{3}m$))	Fig. 44	NM	—
$Rh_3Sn_2S_2$	420728	SG 166 ($R\bar{3}m$))	Fig. 44	NM	—
$InSnCo_3S_2$	425137	SG 166 ($R\bar{3}m$))	Fig. 44	n.a.	—

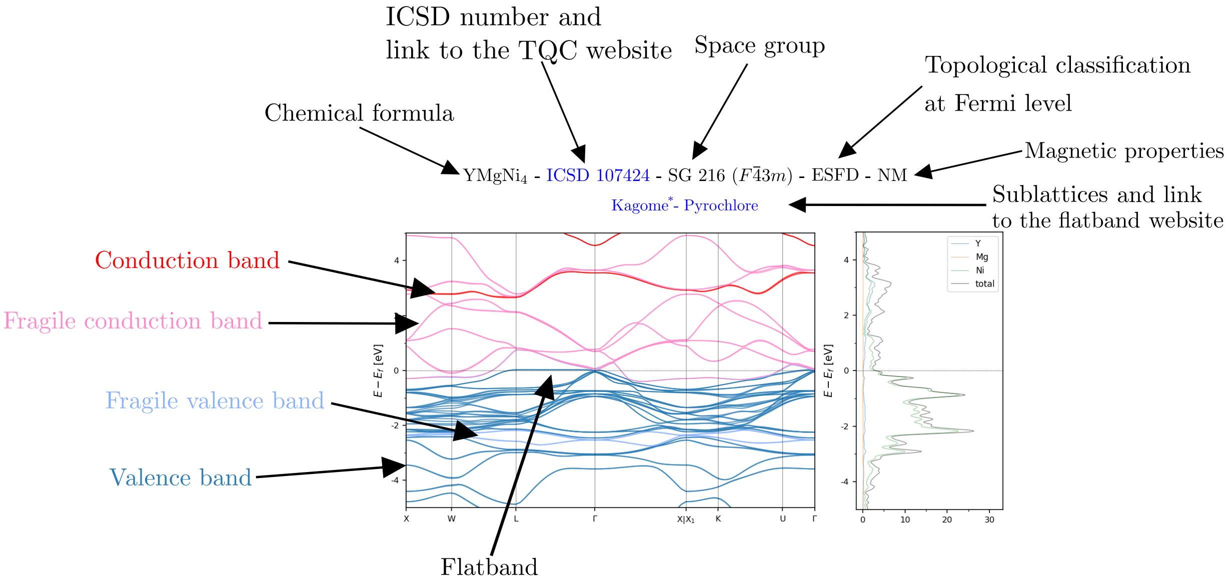

Figure 27. Example band structure and projected density of states plots. In this figure, we show the band structure and the projected density of states of $YMgNi_4$ [ICSD 107424, SG 216 $F\bar{4}3m$] as an example of the labeling scheme and information contained within each of the band structure plots shown in this section. First, at the top of each band structure plot, we provide the chemical formula, ICSD number with a hyperlink to `https://www.topologicalquantumchemistry.org/`, space group symbol and number, the topological classification at the Fermi level (LCEBR, NLC, SEBR, ES, or ESFD) and the magnetic properties as available from Materials Project (NM for non-magnetic, FM for ferromagnetic, AFM for anti-ferromagnetic, FiM for ferrimagnetic and n.a. when the information is not available). Then we further list the hosted sublattices: Kagome, pyrochlore, bipartite, split or Lieb. A superscript * for Kagome (Lieb) means that only approximate sublattices exist for Kagome (Lieb), as defined in Appendix D. In the band structure plot, trivial and stable topological conduction (valence) bands are labeled in red (blue), and fragile conduction (valence) bands are labeled in pink (light blue).

AgBrO$_2$ - ICSD 670051 - SG 1 ($P1$) - LCEBR - n.a.

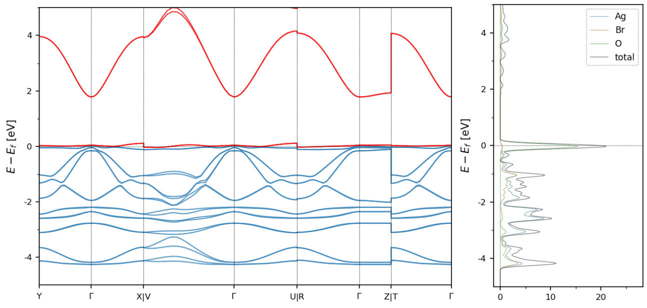

AgHO$_2$ - ICSD 670060 - SG 1 ($P1$) - LCEBR - n.a.

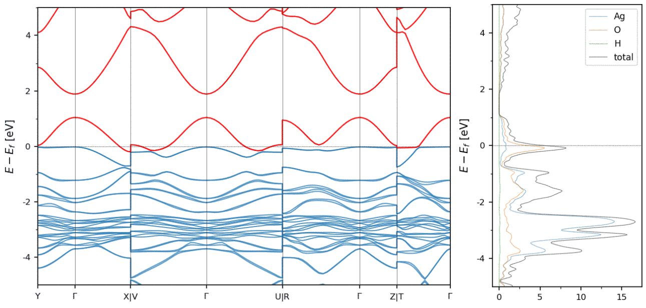

CaNi$_5$H - ICSD 189752 - SG 1 ($P1$) - ESFD - FM

Kagome*

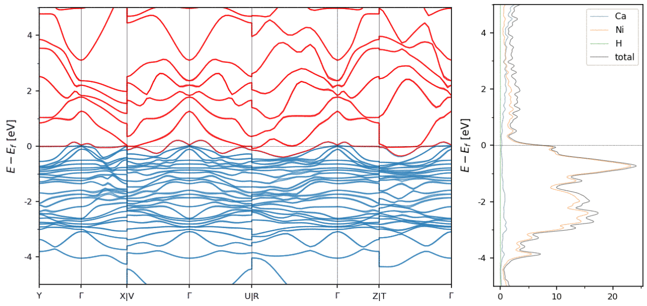

Cu(F(AuF$_4$)) - ICSD 62544 - SG 2 ($P\bar{1}$) - ESFD - FM

Bipartite - Split

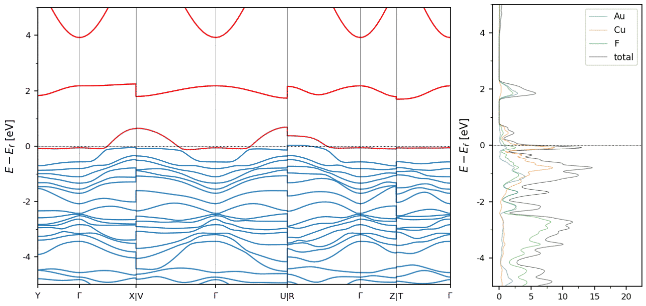

Cu$_3$Bi$_4$V$_2$O$_{14}$ - ICSD 75222 - SG 2 ($P\bar{1}$) - ESFD - FM

Bipartite - Split

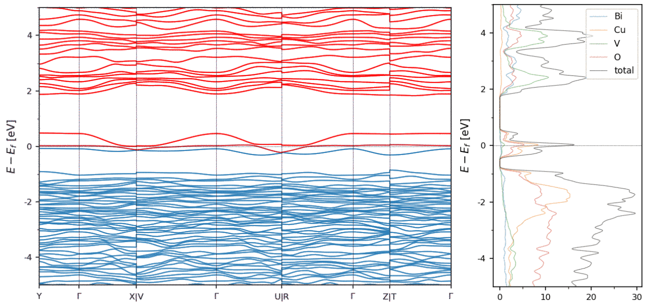

Na$_2$(Cu$_2$Si$_4$O$_{11}$)(H$_2$O)$_2$ - ICSD 154123 - SG 2 ($P\bar{1}$) - LCEBR - FM

Bipartite - Split

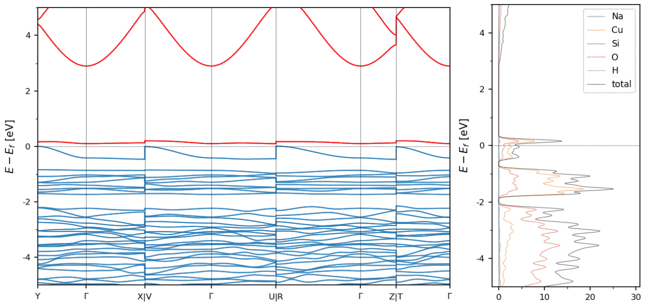

NbOI$_2$ - ICSD 36255 - SG 5 ($C2$) - LCEBR - NM

Bipartite - Split

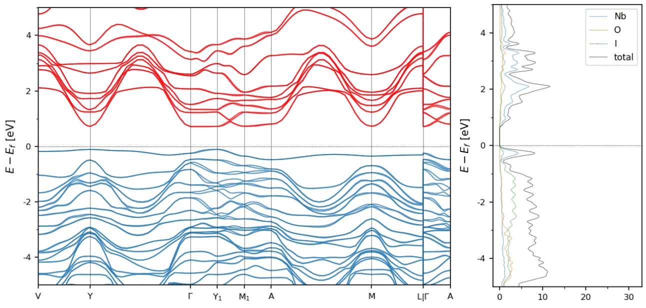

NbOBr$_2$ - ICSD 416669 - SG 5 ($C2$) - LCEBR - NM

Bipartite - Split

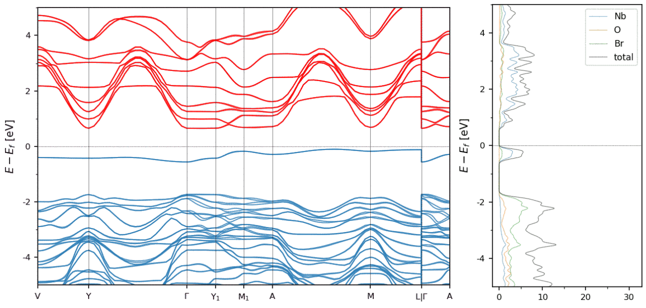

Figure 28. Band structure and density of states for materials with the most remarkable flat-band features near the Fermi energy. (part 1/44)

$\mathrm{CrAuTe_4}$ - ICSD 150279 - SG 10 ($P2/m$) - ESFD - FM

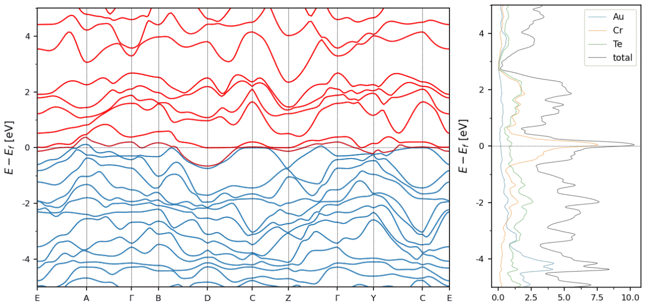

$\mathrm{Ba_2(Co_2F_7Cl)}$ - ICSD 79479 - SG 11 ($P2_1/m$) - LCEBR - FM

Bipartite - Split

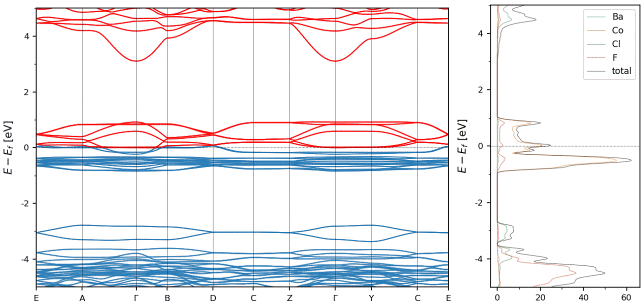

$\mathrm{Ba_2Ni_2F_7Cl}$ - ICSD 84782 - SG 11 ($P2_1/m$) - LCEBR - FM

Bipartite - Split

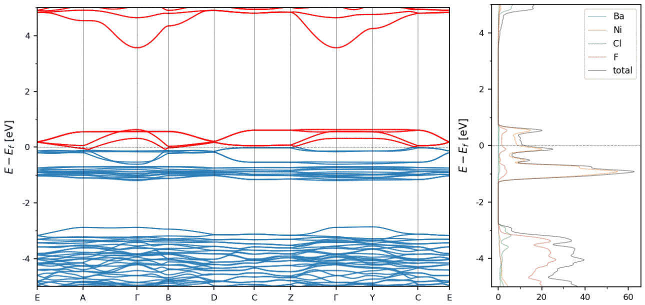

$\mathrm{MoV_2O_8}$ - ICSD 28471 - SG 12 ($C2/m$) - NLC - NM

Bipartite

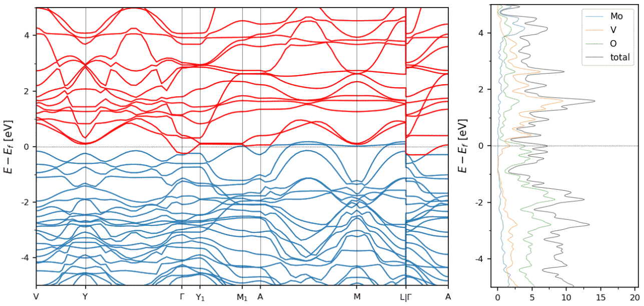

$\mathrm{Cr_3O_8}$ - ICSD 155847 - SG 12 ($C2/m$) - NLC - FM

Bipartite

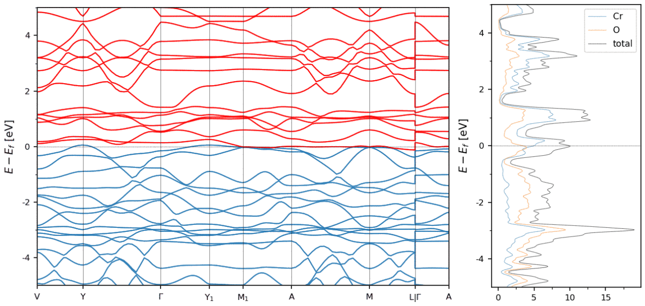

$\mathrm{(Sr_2CoO_3)}$ - ICSD 99894 - SG 12 ($C2/m$) - ESFD - FM

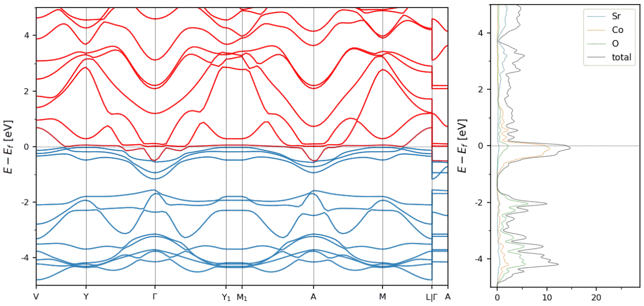

$\mathrm{K_2Na(Ag(CN)_2)_3}$ - ICSD 59723 - SG 12 ($C2/m$) - LCEBR - NM

Kagome* - Bipartite

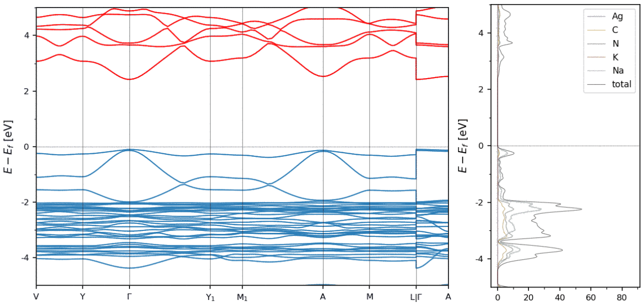

$\mathrm{Y_5Mo_2O_{12}}$ - ICSD 60957 - SG 12 ($C2/m$) - ESFD - FM

Bipartite

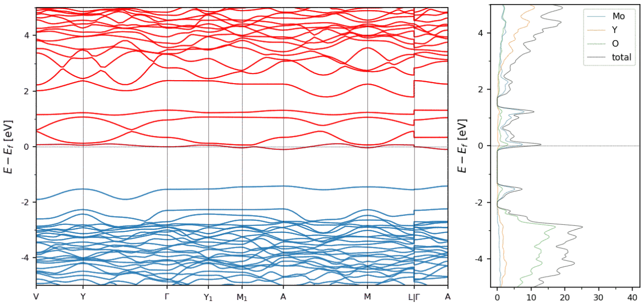

Figure 29. Band structure and density of states for materials with the most remarkable flat-band features near the Fermi energy. (part 2/44)

$\mathrm{K(H_2PO_4)}$ - ICSD 79341 - SG 13 ($P2/c$) - LCEBR - NM

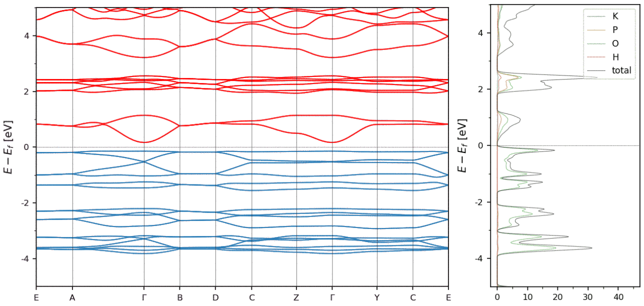

$\mathrm{KAgAsS_2}$ - ICSD 431760 - SG 14 ($P2_1/c$) - LCEBR - n.a.

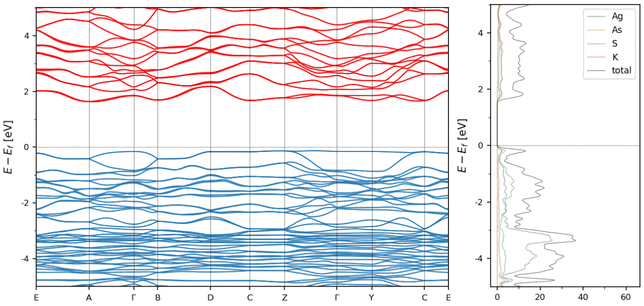

$\mathrm{PbPd_2O_4}$ - ICSD 263050 - SG 15 ($C2/c$) - LCEBR - NM

Bipartite

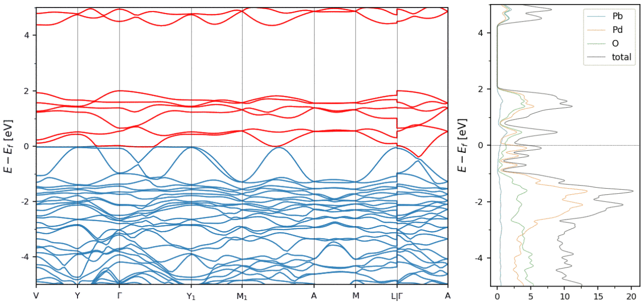

$\mathrm{YCu_2O_4}$ - ICSD 83493 - SG 15 ($C2/c$) - ESFD - n.a.

Bipartite - Split

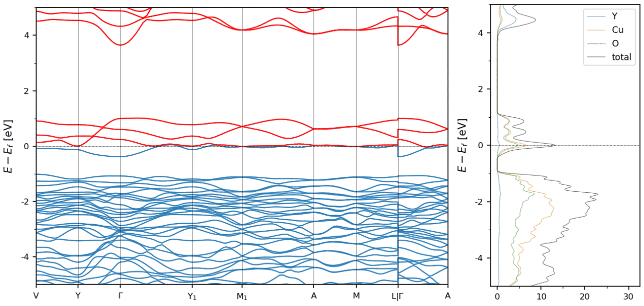

$\mathrm{BaZnF_4}$ - ICSD 672719 - SG 36 ($Cmc2_1$) - LCEBR - n.a.

Bipartite - Split

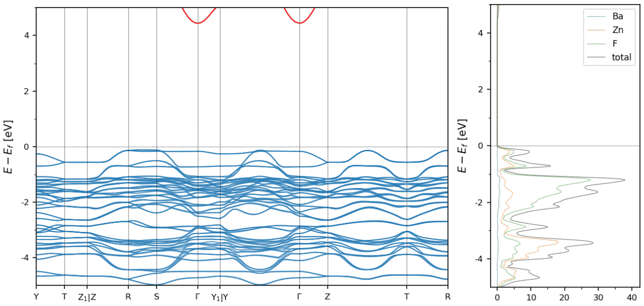

$\mathrm{Na_3(VOS_3)}$ - ICSD 281593 - SG 36 ($Cmc2_1$) - LCEBR - NM

Bipartite

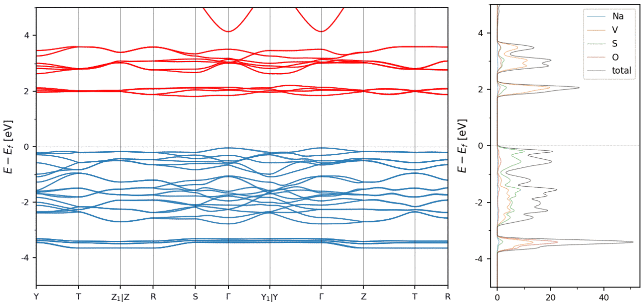

$\mathrm{Bi_2(CO_3)O_2}$ - ICSD 94740 - SG 44 ($Imm2$) - LCEBR - NM

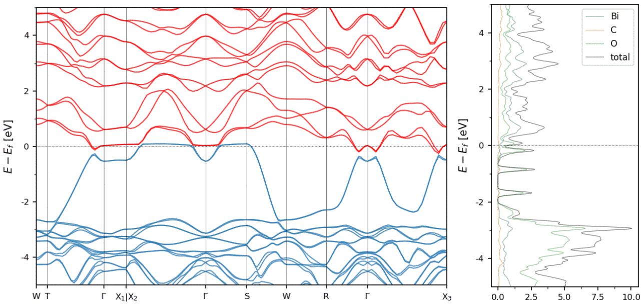

$\mathrm{Ba_4In_6O_{13}}$ - ICSD 72887 - SG 45 ($Iba2$) - LCEBR - NM

Bipartite

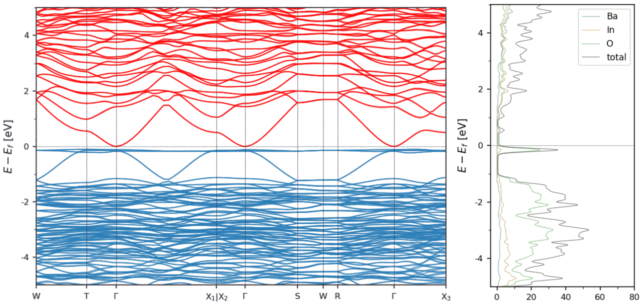

Figure 30. Band structure and density of states for materials with the most remarkable flat-band features near the Fermi energy. (part 3/44)

LaBa$_2$Cu$_3$O$_7$ - ICSD 81167 - SG 47 ($Pmmm$) - NLC - NM

Bipartite - Split

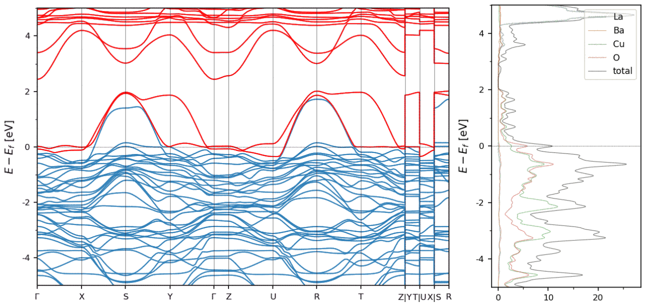

MnS$_2$ - ICSD 643441 - SG 58 ($Pnnm$) - ESFD - FM

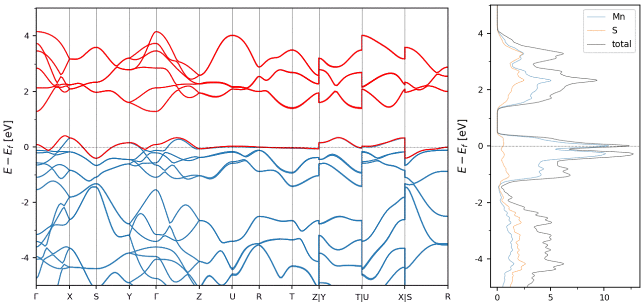

CoCu$_2$O$_3$ - ICSD 33996 - SG 59 ($Pmmn$) - ESFD - FM

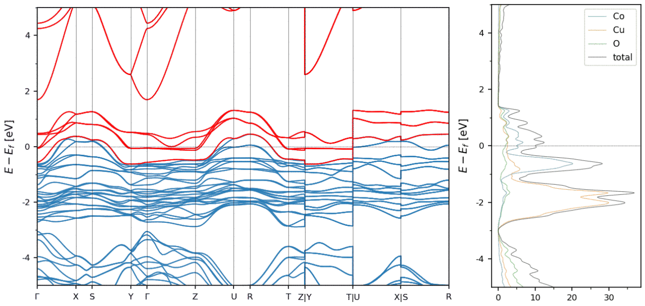

Li(VO)(AsO$_4$) - ICSD 90991 - SG 62 ($Pnma$) - ES - FM

Bipartite

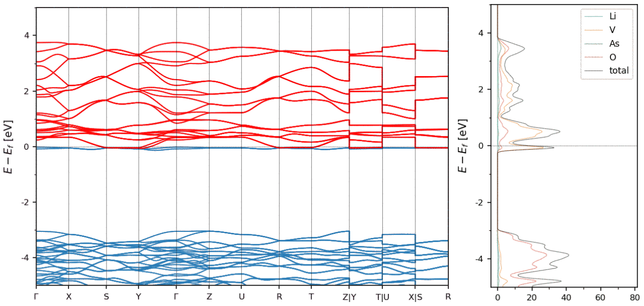

Na$_2$Ni(HPO$_3$)$_2$ - ICSD 247564 - SG 62 ($Pnma$) - LCEBR - FM

Bipartite

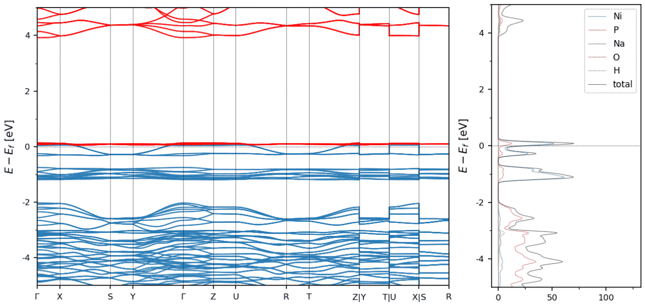

Na(NiF$_3$) - ICSD 9008 - SG 62 ($Pnma$) - LCEBR - FM

Bipartite

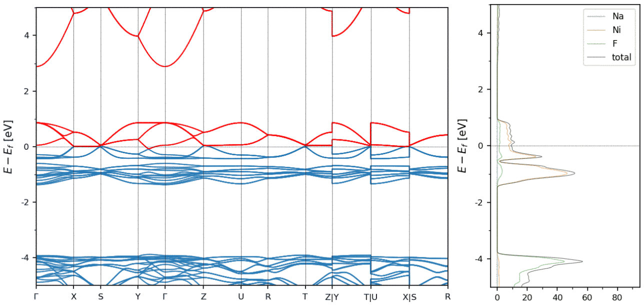

BaVS$_3$ - ICSD 63228 - SG 63 ($Cmcm$) - ESFD - n.a.

Kagome*

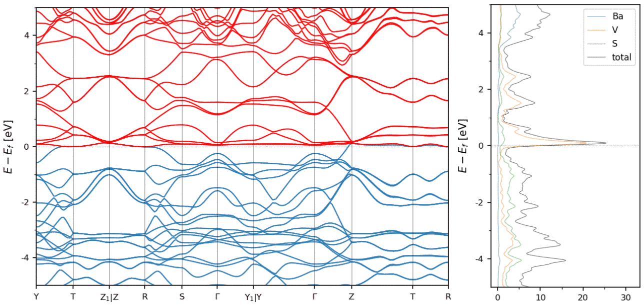

NiSO$_4$ - ICSD 16691 - SG 63 ($Cmcm$) - LCEBR - AFM

Bipartite

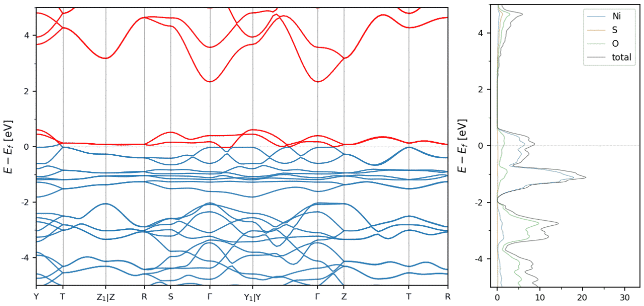

Figure 31. Band structure and density of states for materials with the most remarkable flat-band features near the Fermi energy. (part 4/44)

Ni(SeO$_4$) - ICSD 25700 - SG 63 ($Cmcm$) - LCEBR - FM

Bipartite

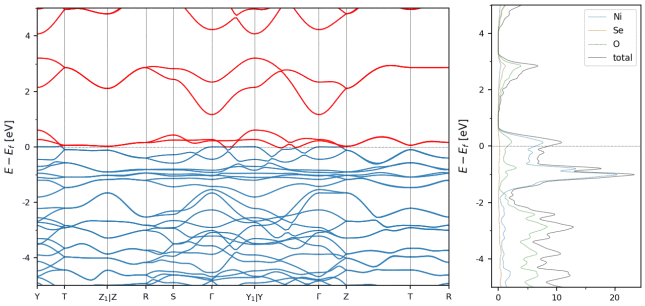

Na(NbO$_3$) - ICSD 22065 - SG 63 ($Cmcm$) - LCEBR - NM

Bipartite - Split - Lieb*

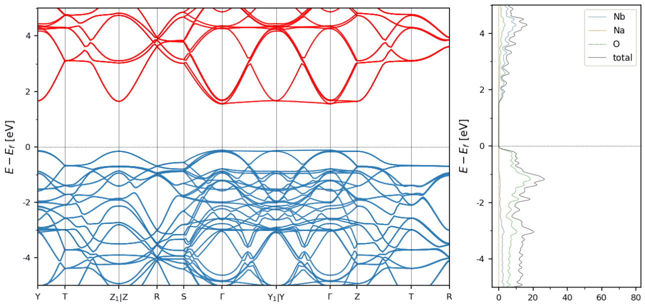

Na(IO$_3$) - ICSD 33664 - SG 65 ($Cmmm$) - SEBR - NM

Kagome* - Bipartite - Split - Lieb*

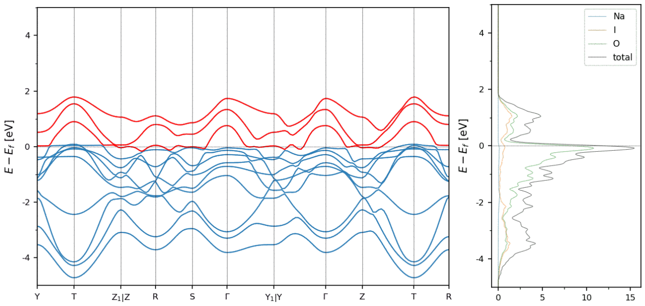

K$_2$(MnS$_2$) - ICSD 65453 - SG 72 ($Ibam$) - ESFD - FM

Bipartite - Split

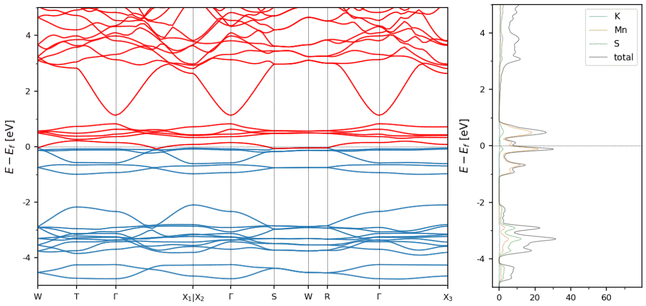

Rb$_2$(MnS$_2$) - ICSD 65454 - SG 72 ($Ibam$) - ESFD - AFM

Bipartite - Split

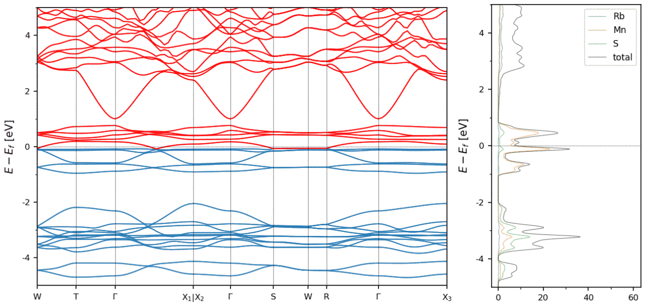

Cs$_2$(MnS$_2$) - ICSD 65455 - SG 72 ($Ibam$) - ESFD - FM

Bipartite - Split

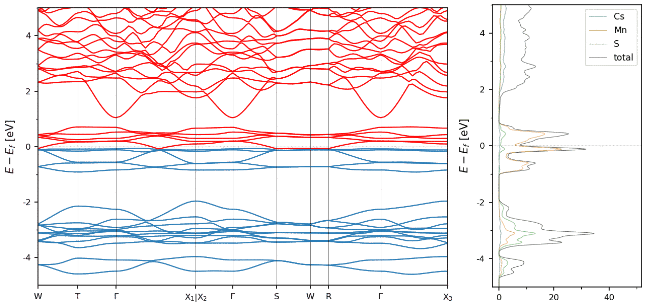

K$_2$(MnSe$_2$) - ICSD 65456 - SG 72 ($Ibam$) - ESFD - FM

Bipartite - Split

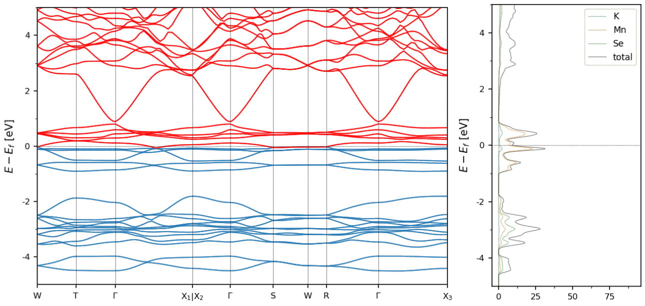

Rb$_2$(MnSe$_2$) - ICSD 65457 - SG 72 ($Ibam$) - ESFD - FM

Bipartite - Split

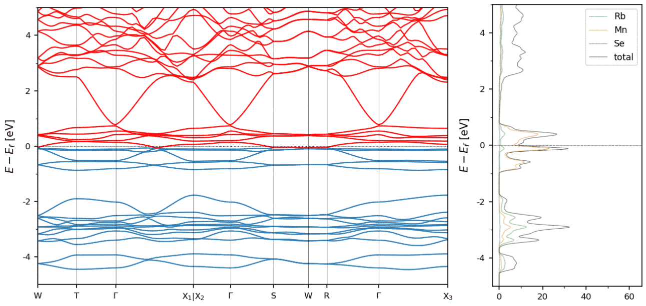

Figure 32. Band structure and density of states for materials with the most remarkable flat-band features near the Fermi energy. (part 5/44)

$\mathrm{Cs_2(MnSe_2)}$ - ICSD 65458 - SG 72 ($Ibam$) - ESFD - FM

Bipartite - Split

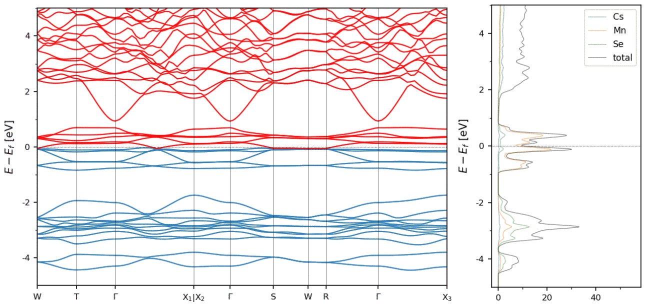

$\mathrm{Rb_2(MnTe_2)}$ - ICSD 65460 - SG 72 ($Ibam$) - ESFD - FM

Bipartite - Split

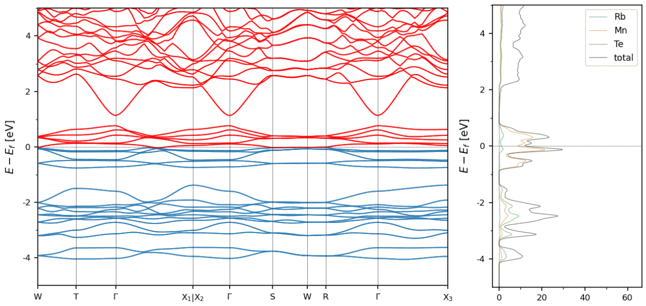

$\mathrm{Cs_2(MnTe_2)}$ - ICSD 65461 - SG 72 ($Ibam$) - ESFD - FM

Bipartite - Split

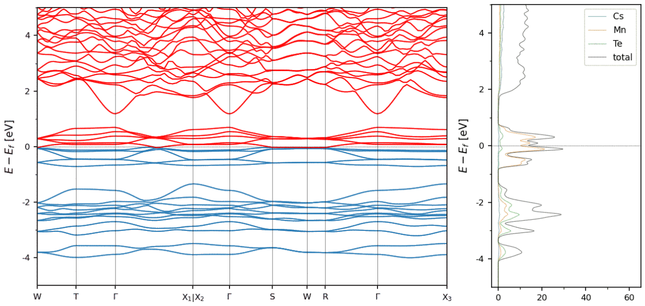

$\mathrm{Sr_2CoReO_6}$ - ICSD 173488 - SG 87 ($I4/m$) - SEBR - AFM

Bipartite - Split

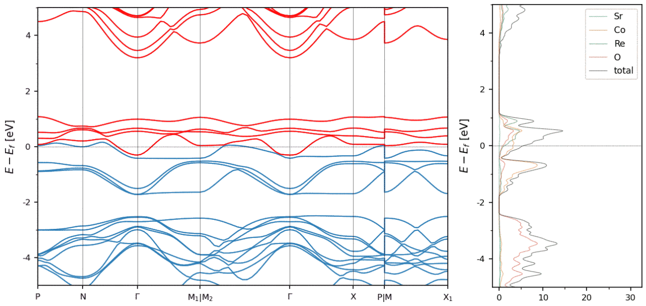

$\mathrm{Sr_2(FeReO_6)}$ - ICSD 150702 - SG 87 ($I4/m$) - ESFD - FM

Bipartite - Split

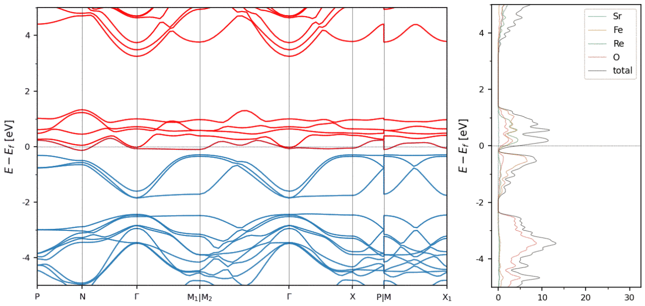

$\mathrm{Sr_2(CoMoO_6)}$ - ICSD 153544 - SG 87 ($I4/m$) - ESFD - FM

Bipartite - Split

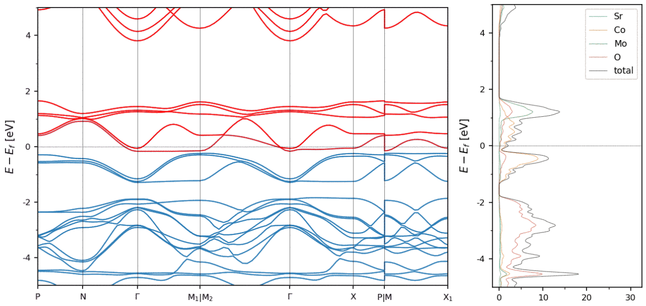

$\mathrm{Sr_2MnMoO_6}$ - ICSD 187669 - SG 87 ($I4/m$) - ESFD - FM

Bipartite - Split

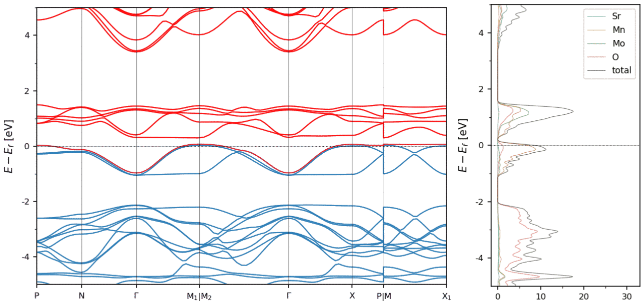

$\mathrm{Sr_2CoWO_6}$ - ICSD 190593 - SG 87 ($I4/m$) - ESFD - AFM

Bipartite - Split

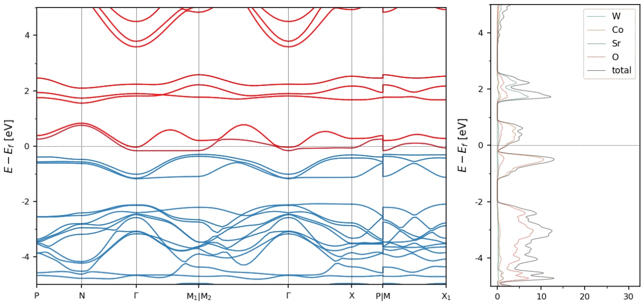

Figure 33. Band structure and density of states for materials with the most remarkable flat-band features near the Fermi energy. (part 6/44)

Sr$_2$Ni(WO$_6$) - ICSD 91791 - SG 87 ($I4/m$) - LCEBR - AFM

Bipartite - Split

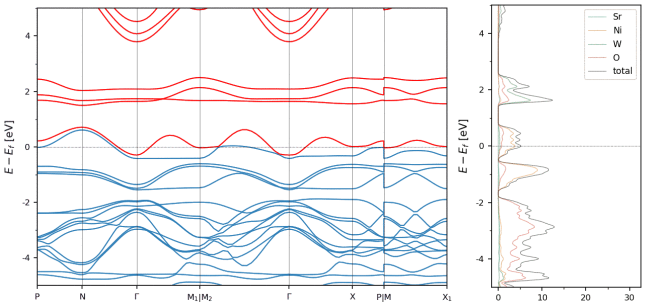

Ba$_2$(FeWO$_6$) - ICSD 95518 - SG 87 ($I4/m$) - LCEBR - AFM

Kagome* - Bipartite - Split

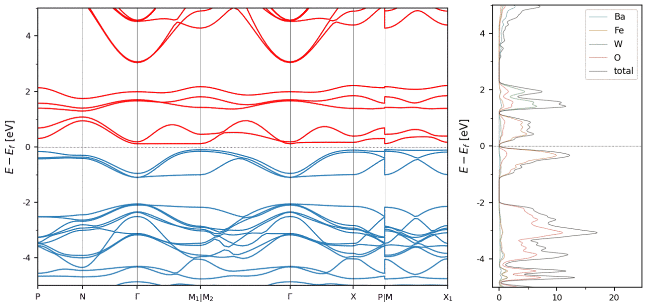

Sr$_2$(FeMoO$_6$) - ICSD 150701 - SG 87 ($I4/m$) - LCEBR - FM

Bipartite - Split

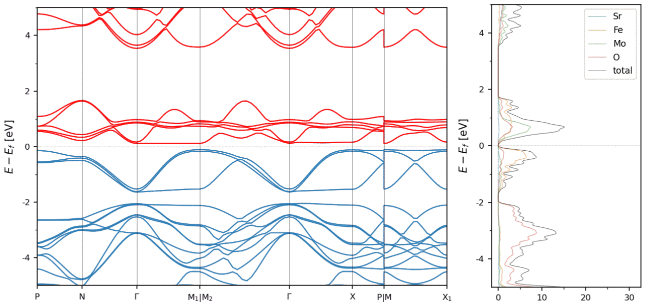

Sr$_2$Mg(WO$_6$) - ICSD 151703 - SG 87 ($I4/m$) - LCEBR - NM

Bipartite - Split

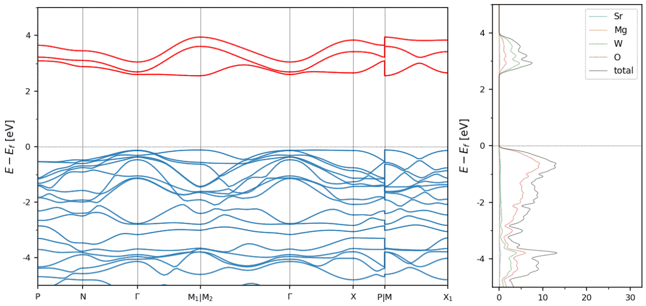

Sr$_2$MgMoO$_6$ - ICSD 187662 - SG 87 ($I4/m$) - LCEBR - NM

Bipartite - Split

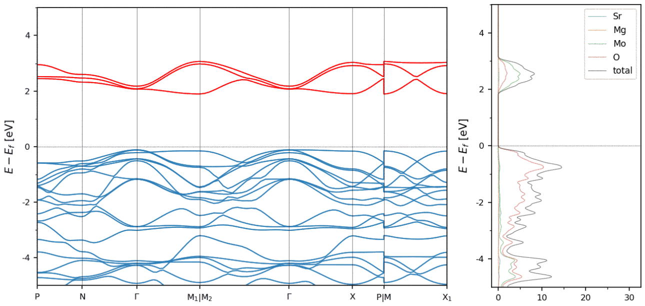

Sr$_2$CoNbO$_6$ - ICSD 192327 - SG 87 ($I4/m$) - LCEBR - n.a.

Bipartite - Split

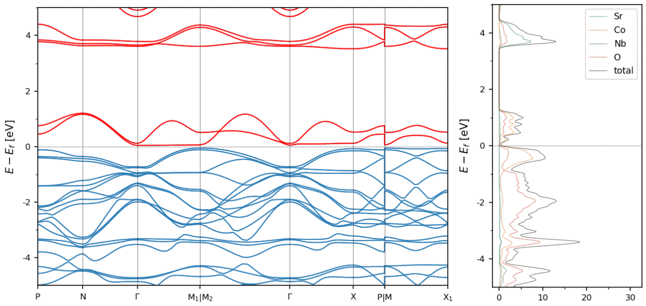

PbPd$_2$O$_4$ - ICSD 263049 - SG 88 ($I4_1/a$) - LCEBR - NM

Bipartite

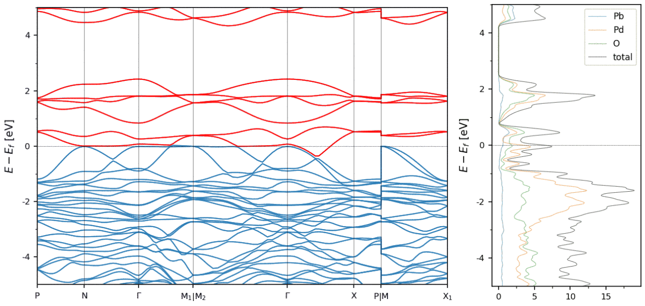

La$_1$Mn$_1$O$_3$ - ICSD 673198 - SG 99 ($P4mm$) - LCEBR - n.a.

Kagome* - Bipartite - Split - Lieb*

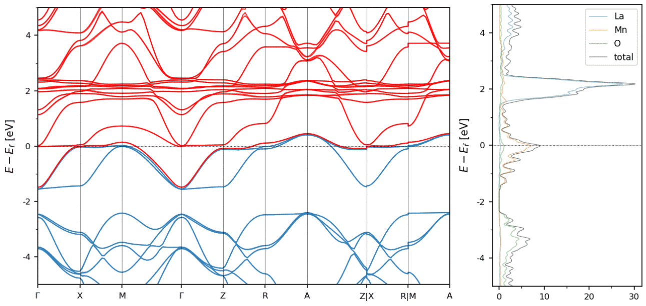

Figure 34. Band structure and density of states for materials with the most remarkable flat-band features near the Fermi energy. (part 7/44)

(VO)$_3$(AsO$_3$)$_2$ - ICSD 424067 - SG 100 ($P4bm$) - ESFD - FM

Bipartite

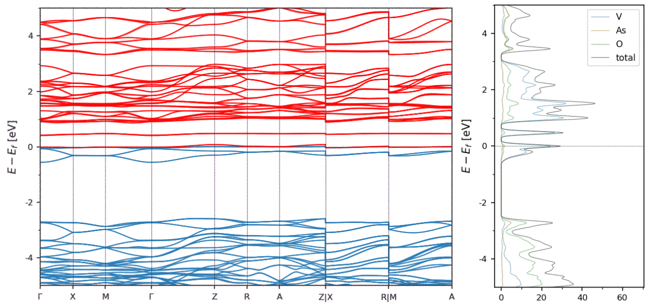

MnRh$_2$Sb - ICSD 76202 - SG 123 ($P4/mmm$) - ES - FM

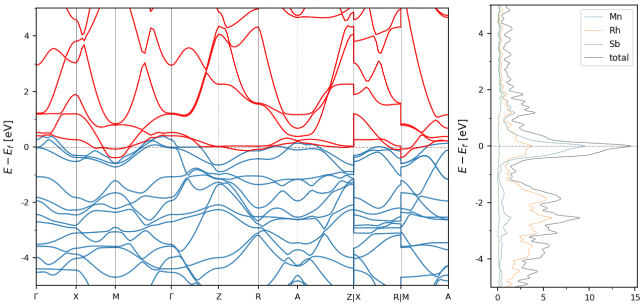

SiO$_2$ - ICSD 170538 - SG 125 ($P4/nbm$) - NLC - NM

Bipartite - Split

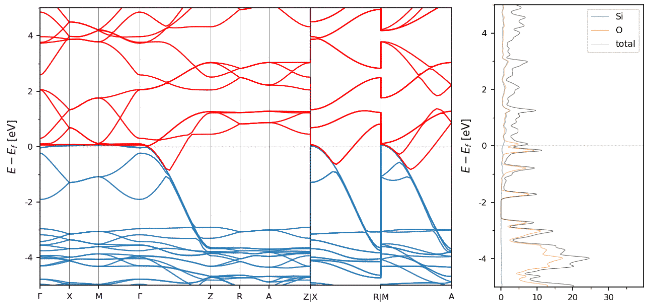

Cs$_3$(GeF$_7$) - ICSD 202917 - SG 127 ($P4/mbm$) - LCEBR - NM

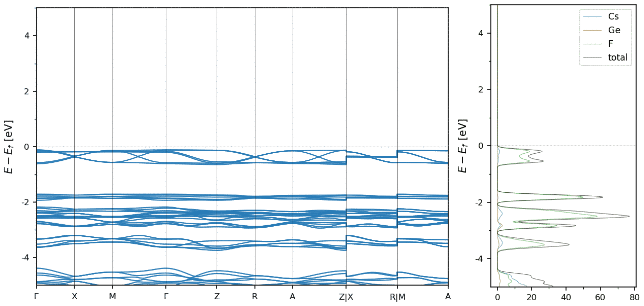

Na(NbO$_3$) - ICSD 23563 - SG 127 ($P4/mbm$) - LCEBR - NM

Bipartite - Split - Lieb*

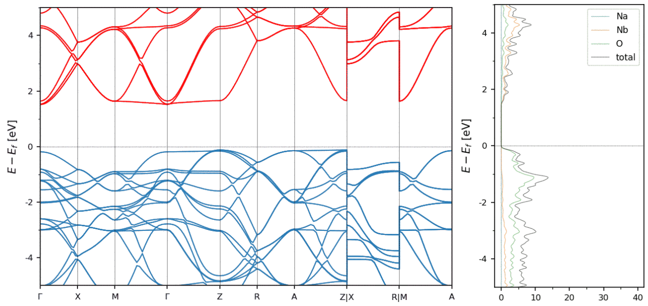

WO$_3$ - ICSD 89092 - SG 129 ($P4/nmm$) - LCEBR - NM

Bipartite - Split

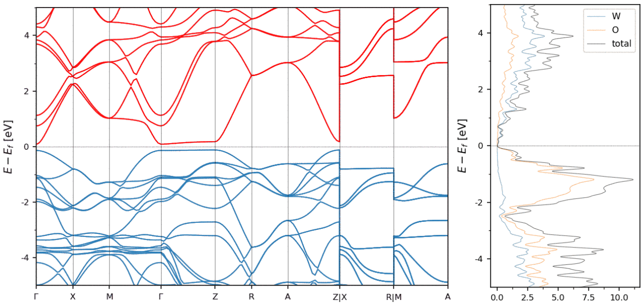

Cu(As$_2$O$_4$) - ICSD 4287 - SG 135 ($P4_2/mbc$) - ESFD - FM

Bipartite

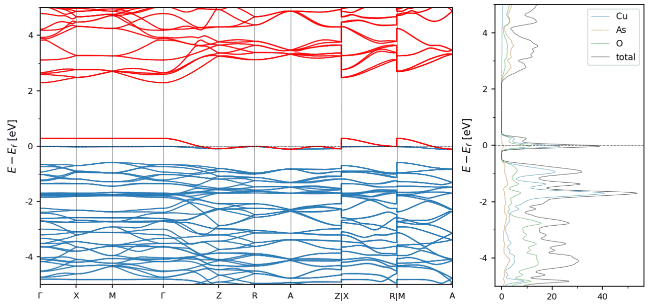

MnO$_2$ - ICSD 393 - SG 136 ($P4_2/mnm$) - ESFD - AFM

Bipartite

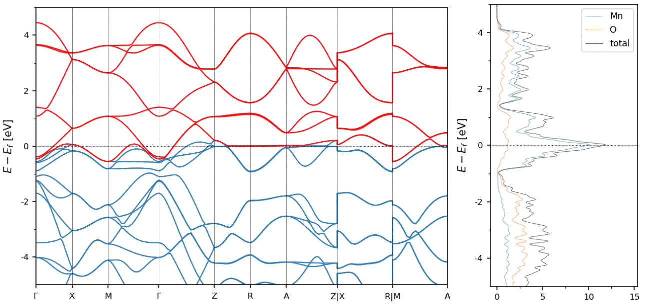

Figure 35. Band structure and density of states for materials with the most remarkable flat-band features near the Fermi energy. (part 8/44)

$\mathrm{Cu(Ta_2O_6)}$ - ICSD 83367 - SG 136 ($P4_2/mnm$) - ESFD - FM

Bipartite

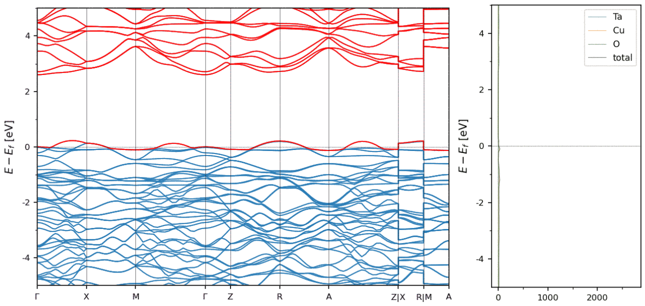

$\mathrm{Ni(Ta_2O_6)}$ - ICSD 61198 - SG 136 ($P4_2/mnm$) - LCEBR - FM

Bipartite

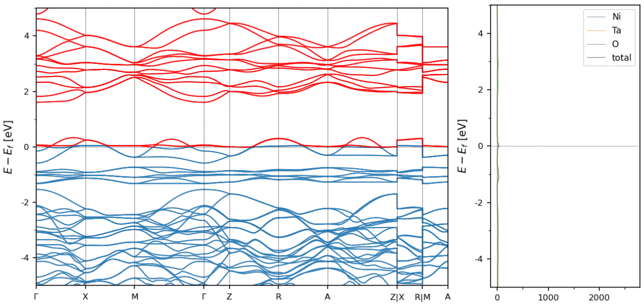

$\mathrm{Al_3V}$ - ICSD 58201 - SG 139 ($I4/mmm$) - ES - NM

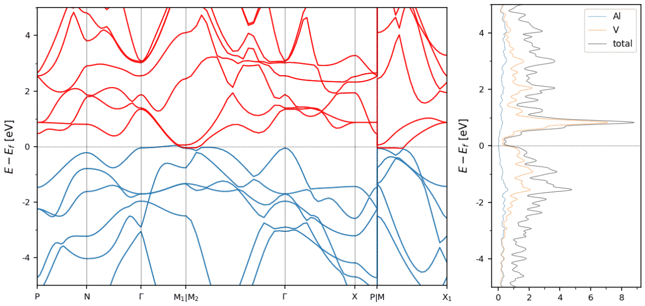

$\mathrm{Co_2KS_2}$ - ICSD 623956 - SG 139 ($I4/mmm$) - ESFD - FM

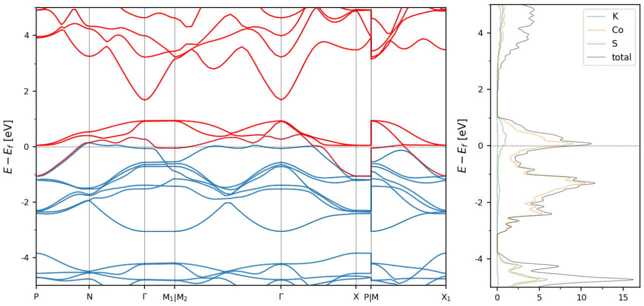

$\mathrm{Sr_3(Co_2O_5Cl_2)}$ - ICSD 90123 - SG 139 ($I4/mmm$) - SEBR - FM

Bipartite - Split

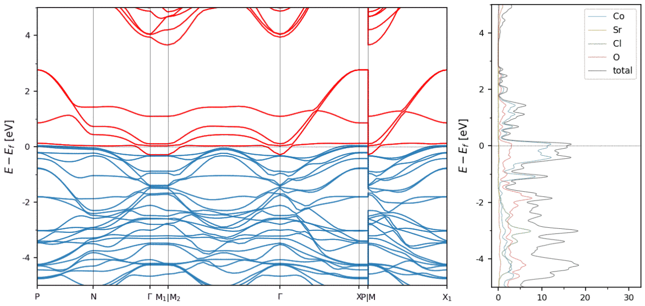

$\mathrm{Ba_2(FeReO_6)}$ - ICSD 155174 - SG 139 ($I4/mmm$) - ESFD - FM

Kagome* - Bipartite - Split

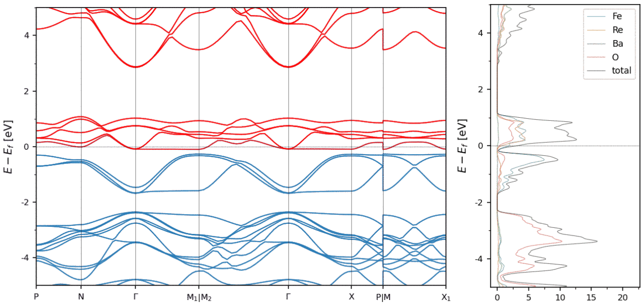

$\mathrm{Sr_2VZrO_6}$ - ICSD 191359 - SG 139 ($I4/mmm$) - ESFD - FM

Kagome* - Bipartite - Split

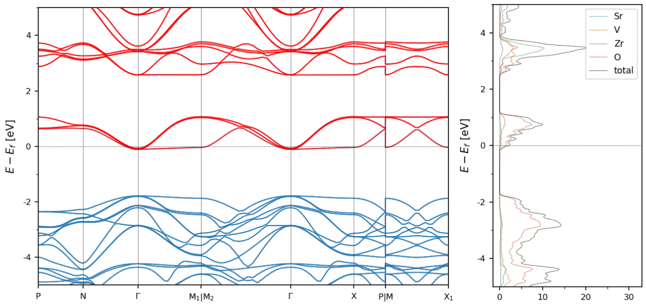

$\mathrm{Sr_2VHfO_6}$ - ICSD 191360 - SG 139 ($I4/mmm$) - ESFD - FM

Kagome* - Bipartite - Split

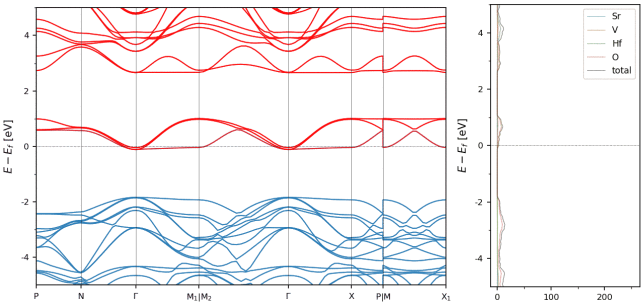

Figure 36. Band structure and density of states for materials with the most remarkable flat-band features near the Fermi energy. (part 9/44)

Sr$_2$FeMoO$_6$ - ICSD 94079 - SG 139 ($I4/mmm$) - LCEBR - n.a.

Bipartite - Split

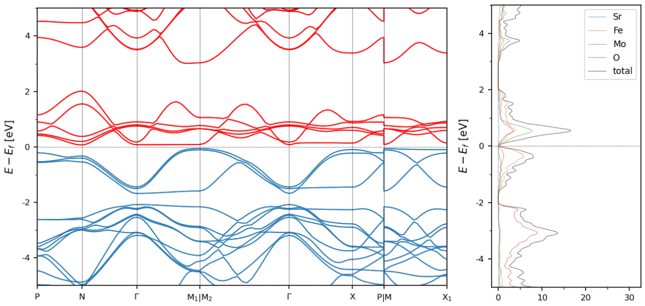

Ba$_2$Fe(MoO$_6$) - ICSD 246541 - SG 139 ($I4/mmm$) - LCEBR - FM

Kagome* - Bipartite - Split

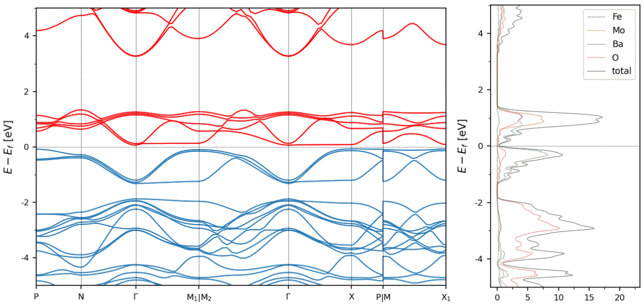

Cs$_2$AgF$_4$ - ICSD 16254 - SG 139 ($I4/mmm$) - ESFD - FM

Bipartite - Split - Lieb

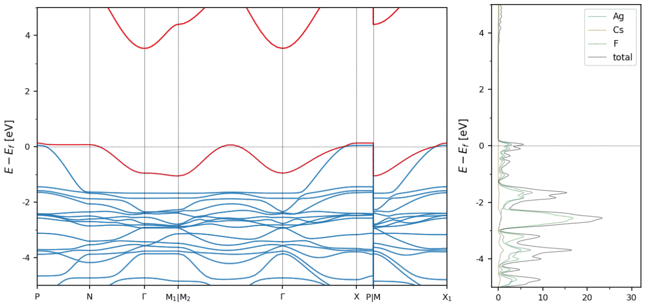

Rb$_2$CaH$_4$ - ICSD 65196 - SG 139 ($I4/mmm$) - LCEBR - NM

Bipartite - Split - Lieb

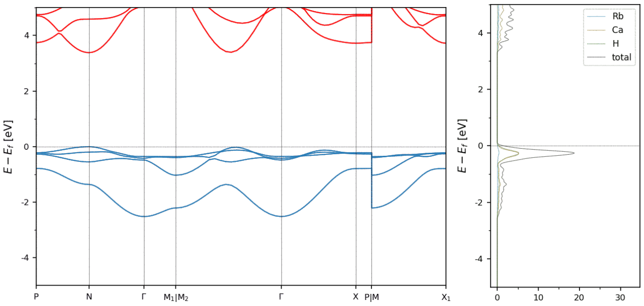

K$_2$MgH$_4$ - ICSD 68358 - SG 139 ($I4/mmm$) - LCEBR - NM

Bipartite - Split - Lieb

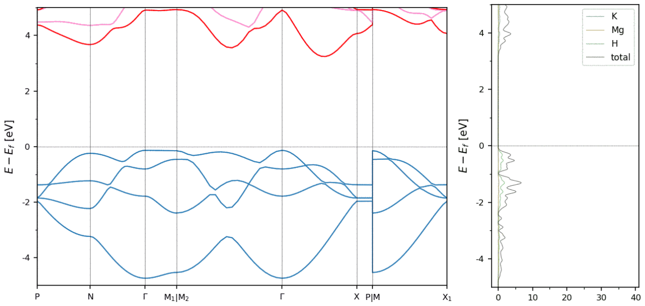

Cs$_2$MgH$_4$ - ICSD 162261 - SG 139 ($I4/mmm$) - LCEBR - NM

Bipartite - Split - Lieb

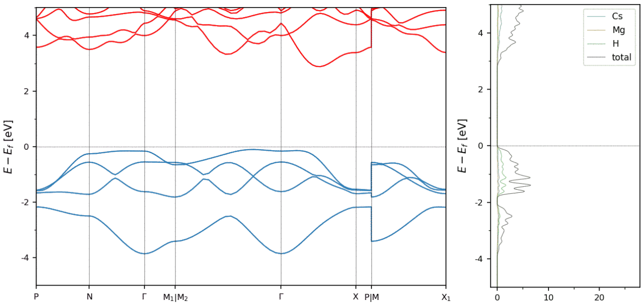

Pd$_3$Tl - ICSD 105729 - SG 139 ($I4/mmm$) - ESFD - NM

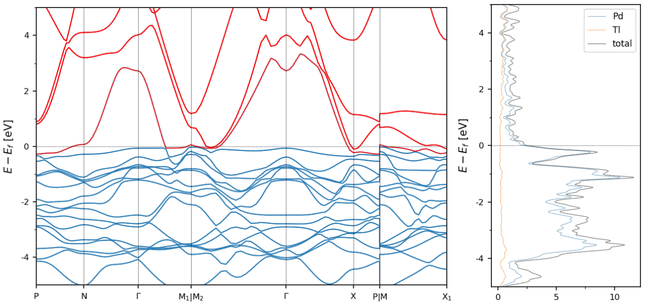

InPd$_3$ - ICSD 247194 - SG 139 ($I4/mmm$) - ESFD - NM

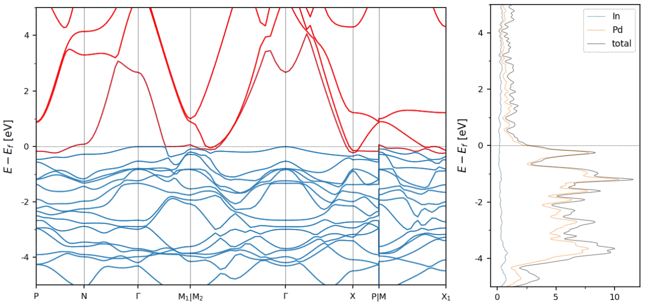

Figure 37. Band structure and density of states for materials with the most remarkable flat-band features near the Fermi energy. (part 10/44)

Rb_3YF_6 - ICSD 19077 - SG 139 ($I4/mmm$) - LCEBR - NM

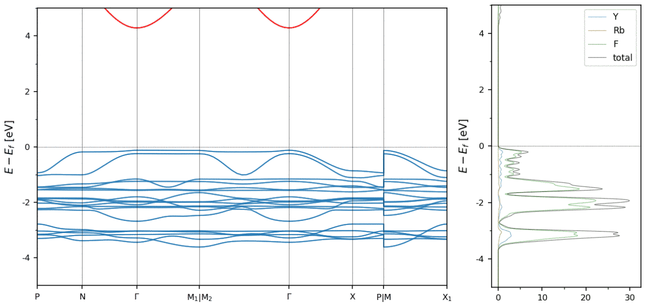

$(SrO)_3(TiO_2)_2$ - ICSD 20294 - SG 139 ($I4/mmm$) - LCEBR - NM

Bipartite - Split - Lieb*

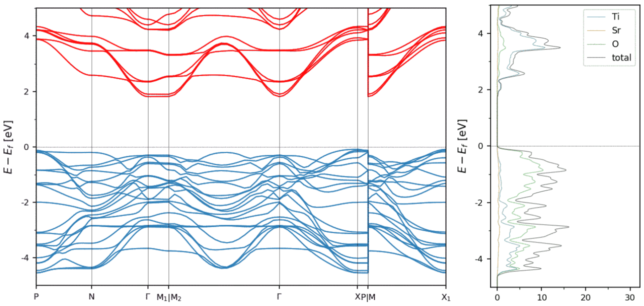

$CaRh_2P_2$ - ICSD 50185 - SG 139 ($I4/mmm$) - SEBR - NM

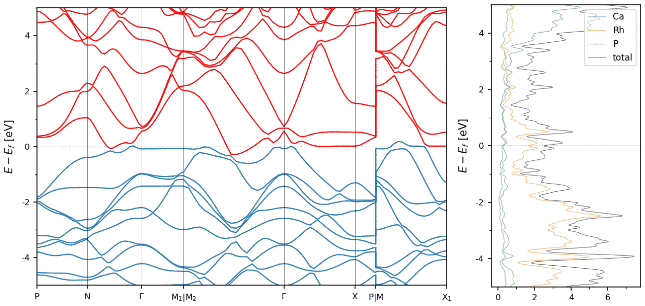

$LaCo_2B_2$ - ICSD 41787 - SG 139 ($I4/mmm$) - ESFD - NM

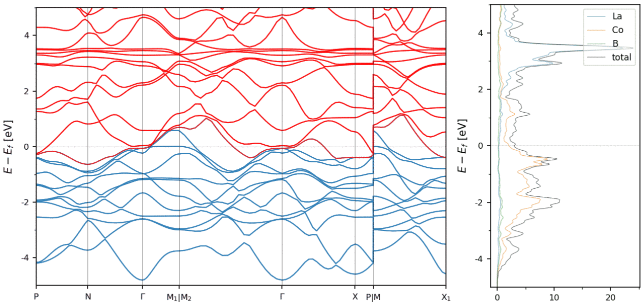

$LaCo_2Si_2$ - ICSD 52999 - SG 139 ($I4/mmm$) - ESFD - NM

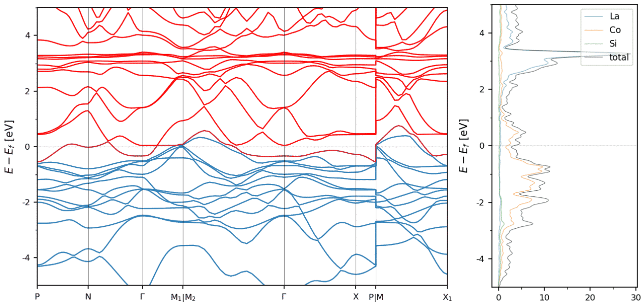

$LaRh_2Ge_2$ - ICSD 55926 - SG 139 ($I4/mmm$) - ESFD - NM

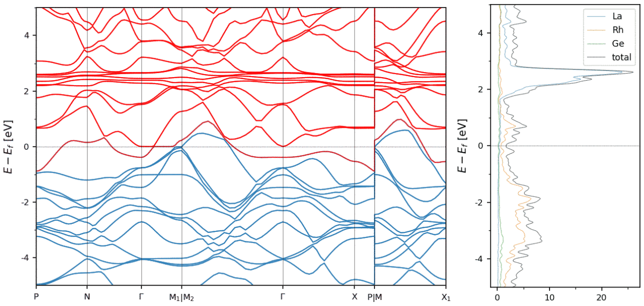

Al_8Fe_4Hf - ICSD 607535 - SG 139 ($I4/mmm$) - SEBR - FM

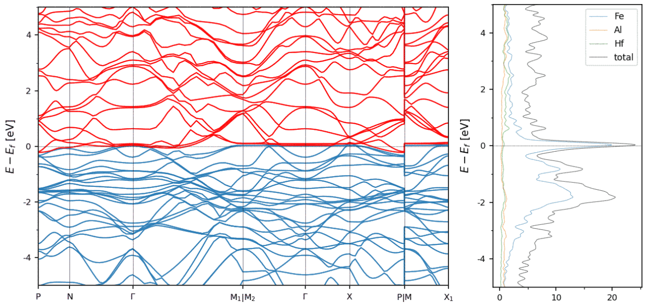

Al_8Fe_4Zr - ICSD 607756 - SG 139 ($I4/mmm$) - SEBR - FM

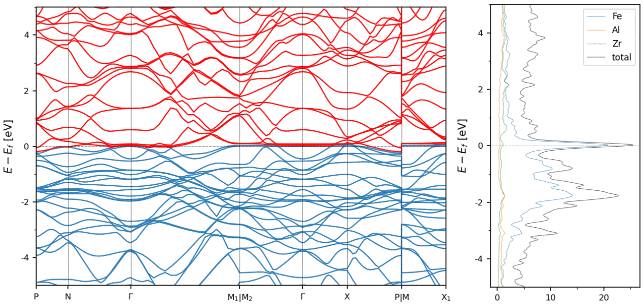

Figure 38. Band structure and density of states for materials with the most remarkable flat-band features near the Fermi energy. (part 11/44)

Al_8Fe_4Y - ICSD 57842 - SG 139 ($I4/mmm$) - ESFD - FM

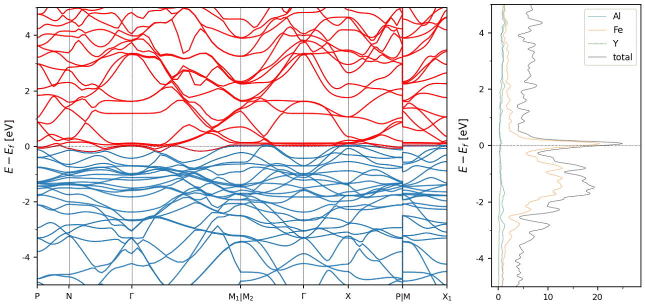

$FeSn_2$ - ICSD 24570 - SG 140 ($I4/mcm$) - ES - FM

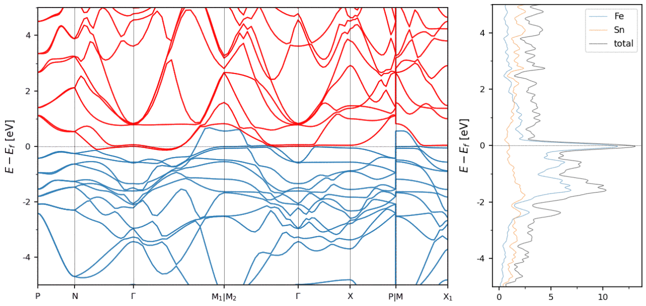

$FeGe_2$ - ICSD 42519 - SG 140 ($I4/mcm$) - ES - FM

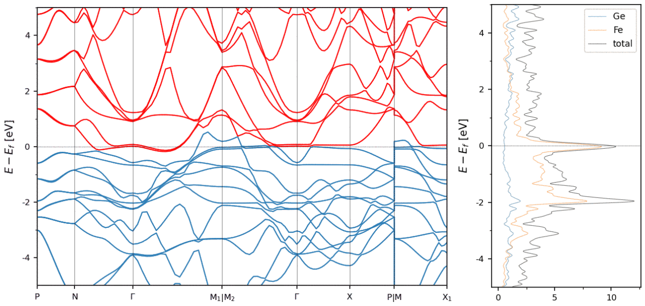

Ca_5Ge_3 - ICSD 42139 - SG 140 ($I4/mcm$) - ES - NM

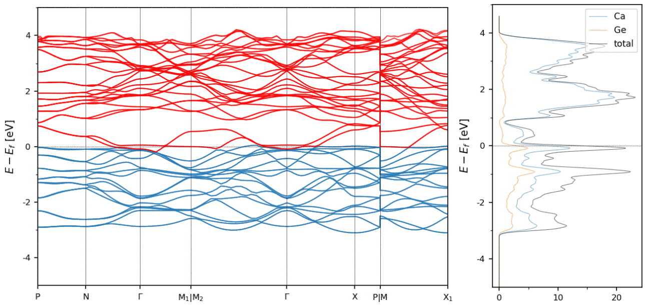

Ca_5Si_3 - ICSD 93699 - SG 140 ($I4/mcm$) - ES - NM

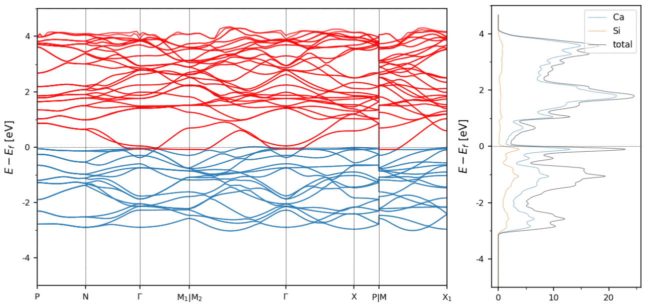

$Sr(ZrO_3)$ - ICSD 1522 - SG 140 ($I4/mcm$) - LCEBR - NM

Bipartite - Split

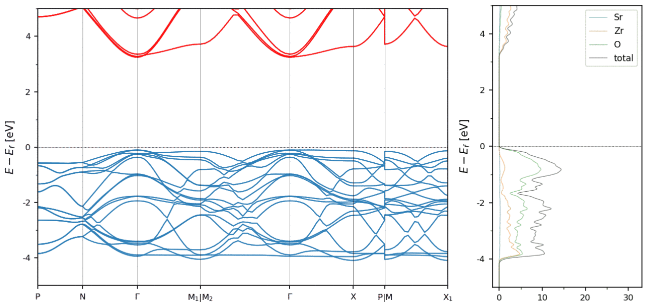

$Ca(TiO_3)$ - ICSD 153173 - SG 140 ($I4/mcm$) - LCEBR - NM

Bipartite - Split - Lieb*

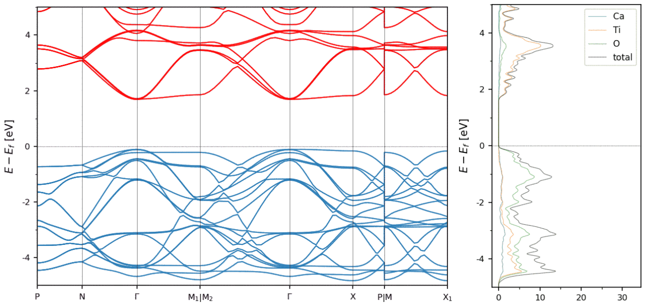

$Li_3(BN_2)$ - ICSD 155126 - SG 141 ($I4_1/amd$) - LCEBR - NM

Bipartite - Split

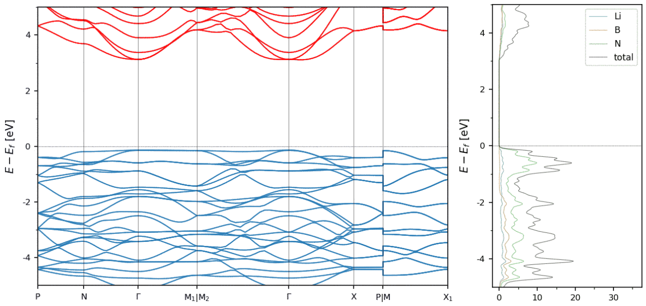

Figure 39. Band structure and density of states for materials with the most remarkable flat-band features near the Fermi energy. (part 12/44)

CsFe(MoO$_4$)$_2$ - ICSD 191592 - SG 147 ($P\bar{3}$) - ESFD - FM

Bipartite - Split

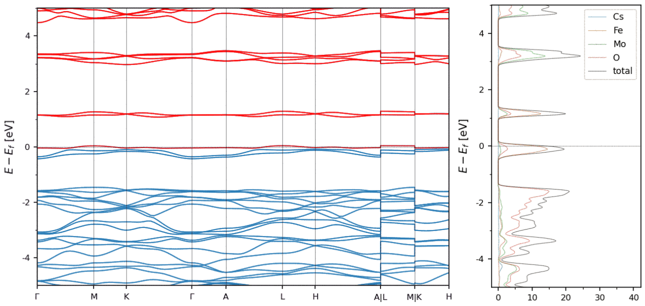

RbAg$_2$Fe(VO$_4$)$_2$ - ICSD 194588 - SG 147 ($P\bar{3}$) - ESFD - AFM

Bipartite - Split

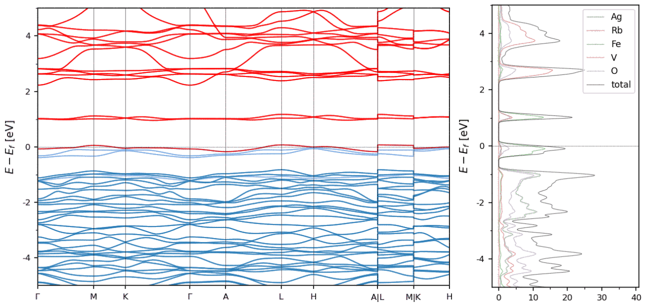

Zn(ReO$_4$)$_2$ - ICSD 51017 - SG 147 ($P\bar{3}$) - LCEBR - NM

Bipartite - Split

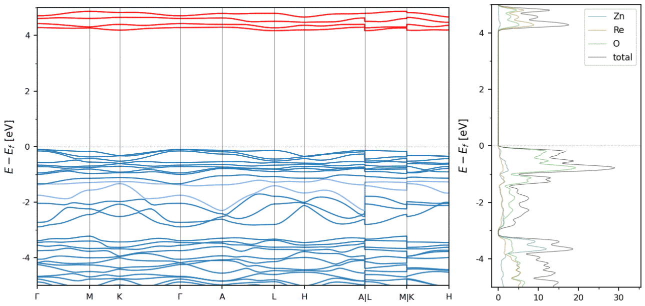

Mn(TiO$_3$) - ICSD 60006 - SG 148 ($R\bar{3}$) - SEBR - AFM

Bipartite

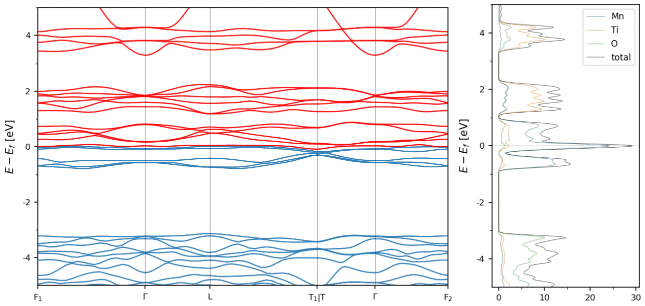

Pb$_3$Ga$_2$Ge$_4$O$_{14}$ - ICSD 250123 - SG 150 ($P321$) - LCEBR - NM

Bipartite - Split

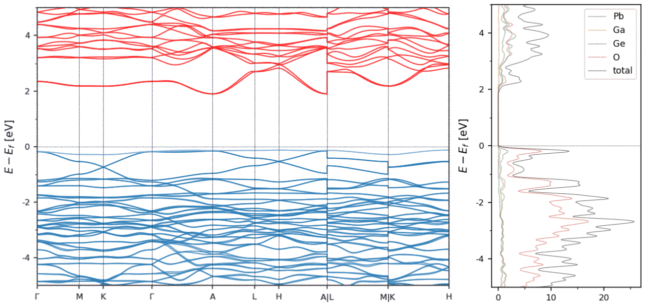

K$_2$Na(Ag(CN)$_2$)$_3$ - ICSD 65699 - SG 162 ($P\bar{3}1m$) - LCEBR - NM

Kagome - Bipartite

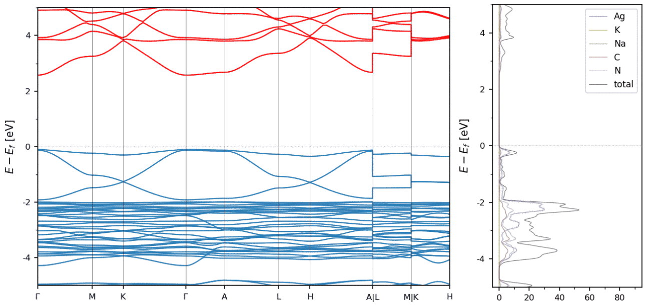

Cd(Sb$_2$O$_6$) - ICSD 71028 - SG 162 ($P\bar{3}1m$) - LCEBR - NM

Bipartite

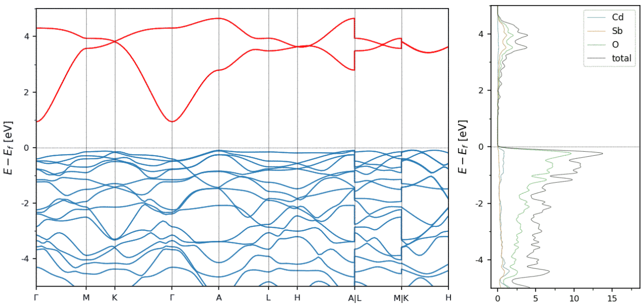

K(Ag(CN)$_2$) - ICSD 30275 - SG 163 ($P\bar{3}1c$) - LCEBR - NM

Kagome* - Bipartite

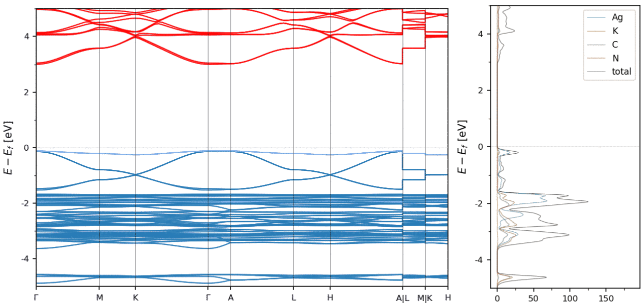

Figure 40. Band structure and density of states for materials with the most remarkable flat-band features near the Fermi energy. (part 13/44)

Ti_3O - ICSD 20041 - SG 163 ($P\bar{3}1c$) - ES - n.a.

Bipartite - Split

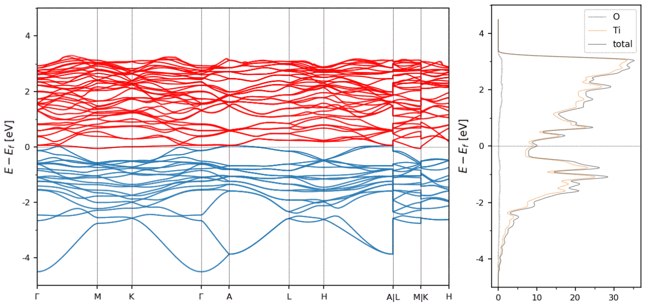

POF_3 - ICSD 250498 - SG 164 ($P\bar{3}m1$) - LCEBR - n.a.

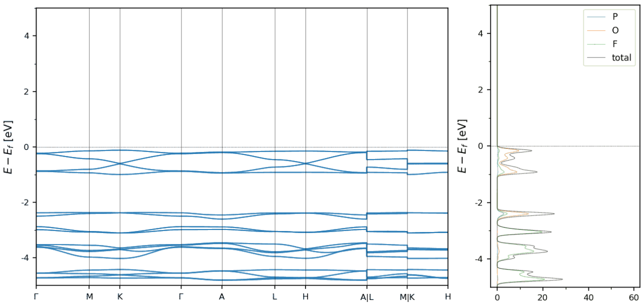

$Na_2(SO_4)$ - ICSD 27955 - SG 164 ($P\bar{3}m1$) - ES - FM

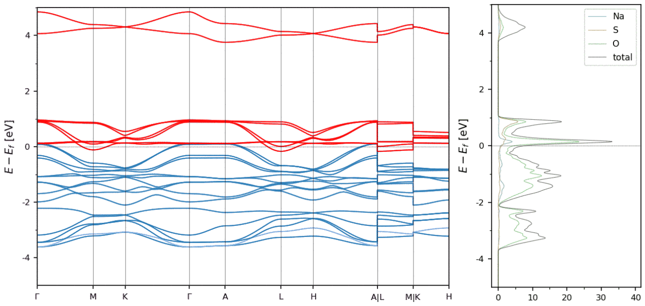

$Ca_2(GeO_4)$ - ICSD 182051 - SG 164 ($P\bar{3}m1$) - LCEBR - NM

Kagome* - Bipartite

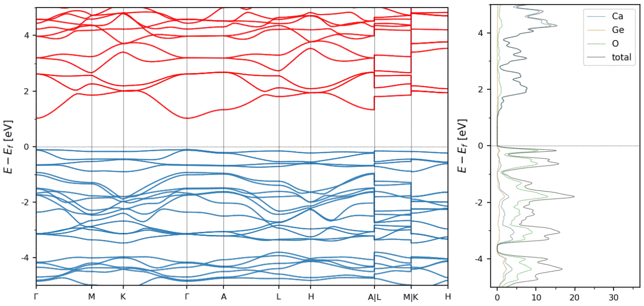

$Ca_2(SiO_4)$ - ICSD 182052 - SG 164 ($P\bar{3}m1$) - LCEBR - NM

Kagome* - Bipartite

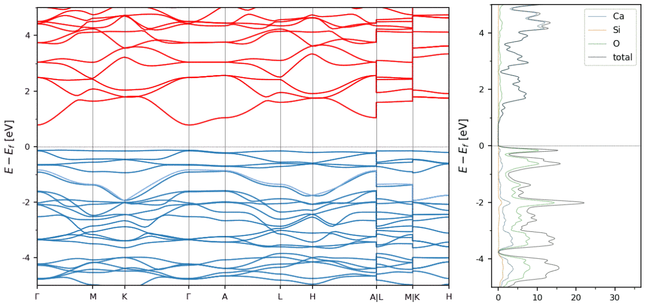

$KFe(MoO_4)_2$ - ICSD 153864 - SG 164 ($P\bar{3}m1$) - ESFD - AFM

Kagome* - Bipartite - Split

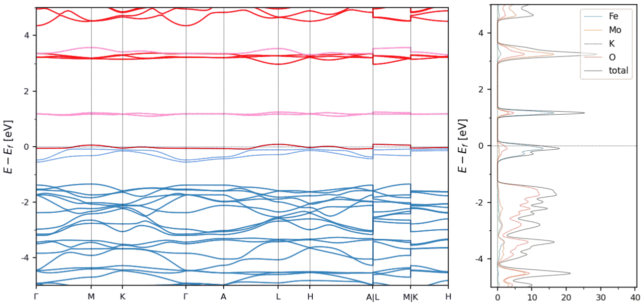

$RbFe(MoO_4)_2$ - ICSD 245665 - SG 164 ($P\bar{3}m1$) - ESFD - FM

Kagome* - Bipartite - Split

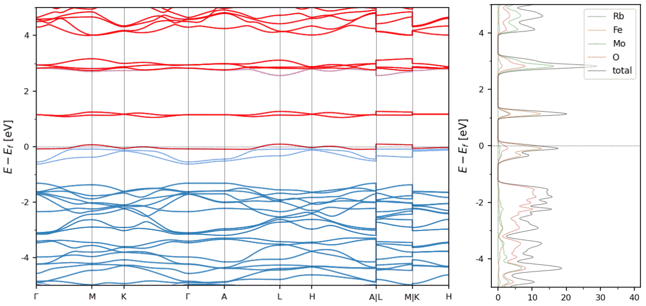

$CsFe(MoO_4)_2$ - ICSD 260887 - SG 164 ($P\bar{3}m1$) - ESFD - FM

Kagome* - Bipartite - Split

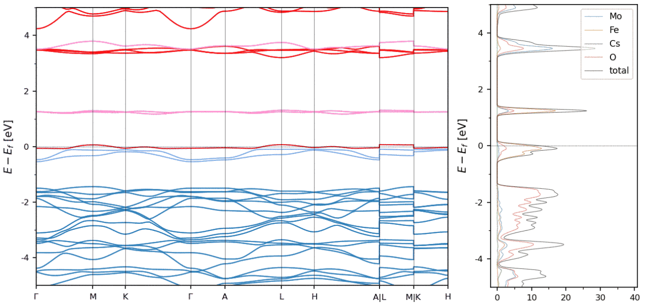

Figure 41. Band structure and density of states for materials with the most remarkable flat-band features near the Fermi energy. (part 14/44)

RbIn(WO$_4$)$_2$ - ICSD 24859 - SG 164 ($P\bar{3}m1$) - LCEBR - NM

Kagome* - Bipartite

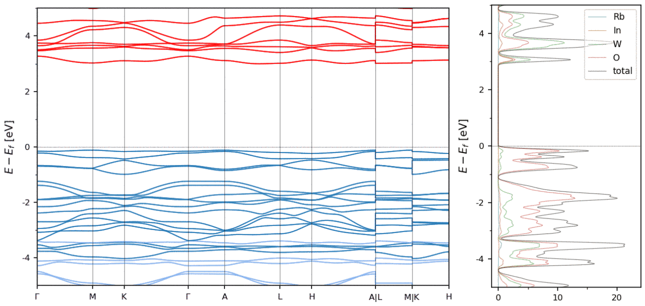

K$_2$Pt$_3$PtS$_6$ - ICSD 40062 - SG 166 ($R\bar{3}m$) - LCEBR - NM

Kagome* - Bipartite

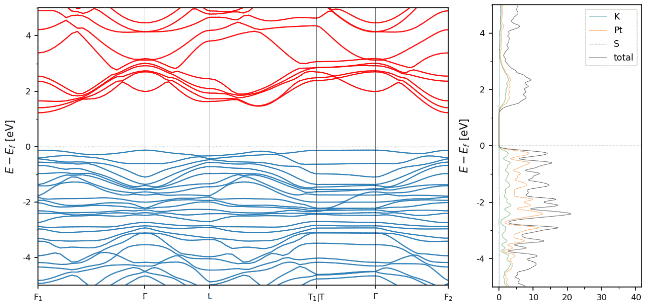

Ba$_2$NiTeO$_6$ - ICSD 25005 - SG 166 ($R\bar{3}m$) - SEBR - AFM

Kagome* - Bipartite - Split

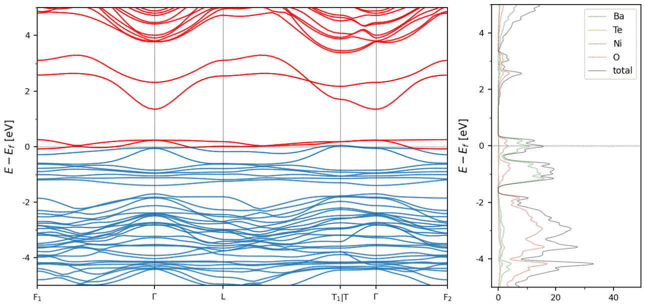

Cs$_9$Ni$_9$F$_{27}$ - ICSD 410393 - SG 166 ($R\bar{3}m$) - SEBR - FM

Kagome - Bipartite - Split

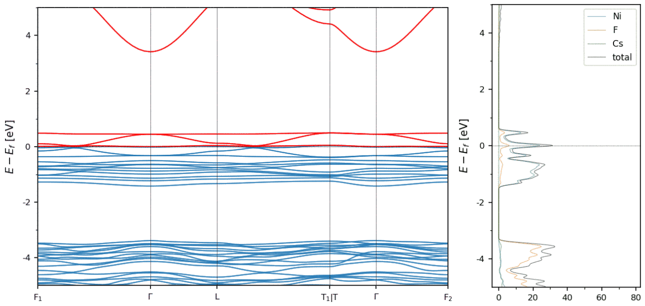

Cu$_3$Zn(OH)$_6$Cl$_2$ - ICSD 425834 - SG 166 ($R\bar{3}m$) - ESFD - FM

Kagome - Bipartite

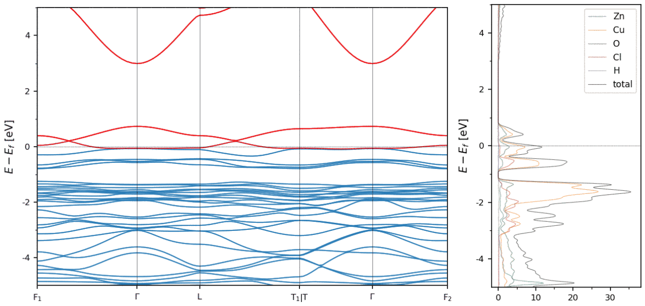

Ca$_2$NCl - ICSD 62555 - SG 166 ($R\bar{3}m$) - LCEBR - NM

Bipartite

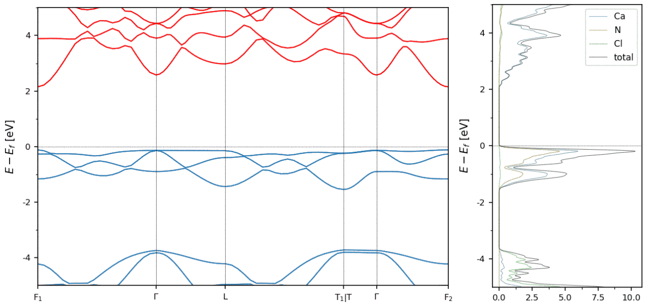

Ca$_2$NBr - ICSD 62556 - SG 166 ($R\bar{3}m$) - LCEBR - NM

Bipartite

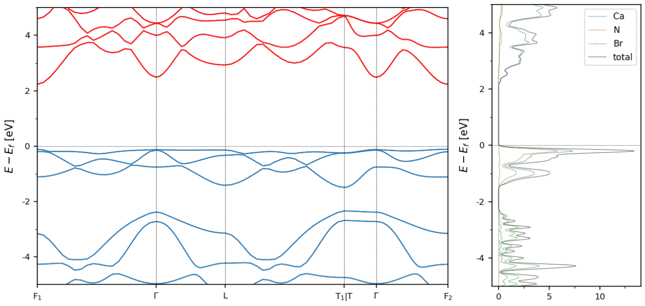

Mg$_2$Ni$_3$Si - ICSD 44926 - SG 166 ($R\bar{3}m$) - SEBR - NM

Kagome

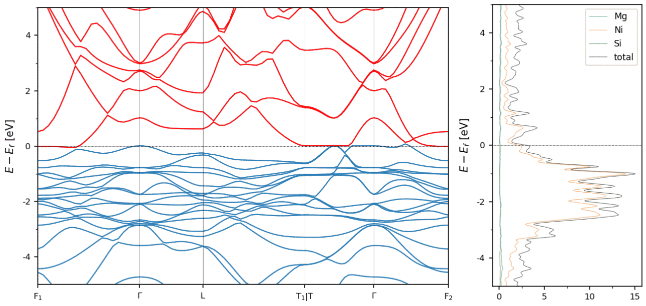

Figure 42. Band structure and density of states for materials with the most remarkable flat-band features near the Fermi energy. (part 15/44)

Mg$_2$Ni$_3$P - ICSD 72409 - SG 166 ($R\bar{3}m$) - ESFD - NM

Kagome

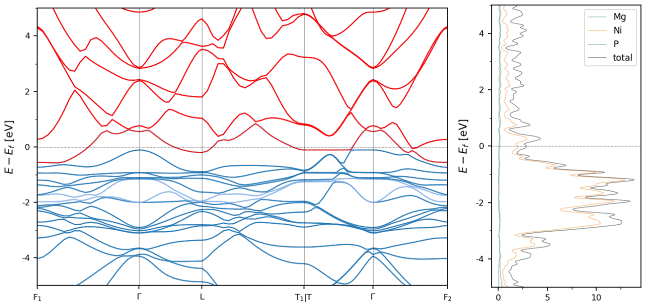

K$_4$ZnP$_2$ - ICSD 67261 - SG 166 ($R\bar{3}m$) - LCEBR - NM

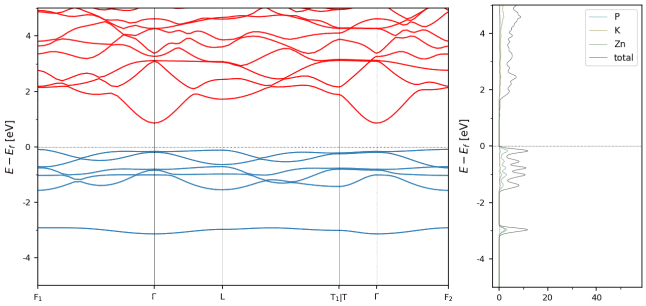

K$_4$HgP$_2$ - ICSD 67263 - SG 166 ($R\bar{3}m$) - LCEBR - NM

Bipartite

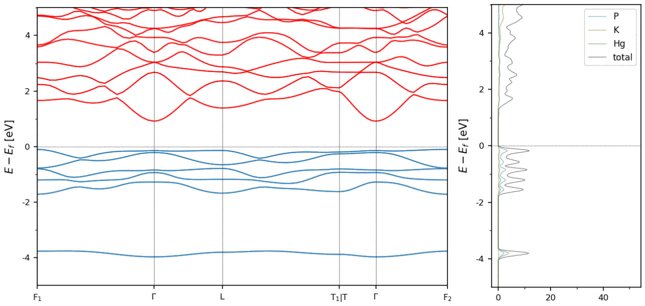

K$_4$(BeP$_2$) - ICSD 300110 - SG 166 ($R\bar{3}m$) - LCEBR - NM

Bipartite

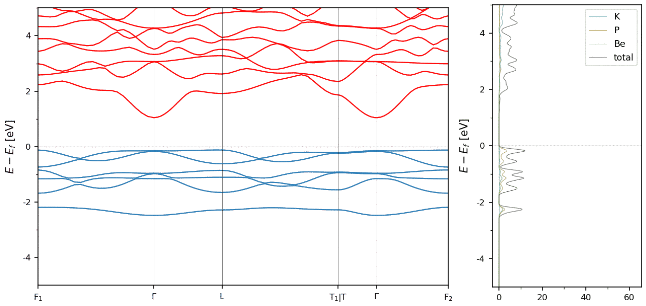

K$_4$(BeAs$_2$) - ICSD 300111 - SG 166 ($R\bar{3}m$) - LCEBR - NM

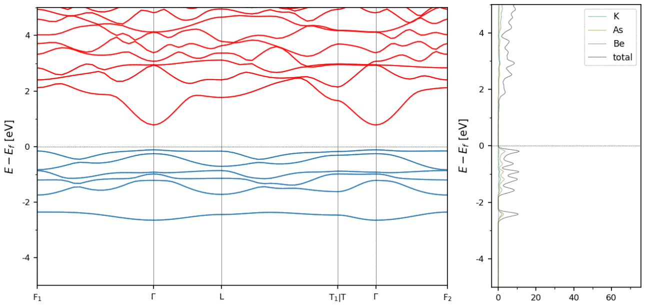

K$_4$(CdAs$_2$) - ICSD 300190 - SG 166 ($R\bar{3}m$) - LCEBR - NM

Bipartite

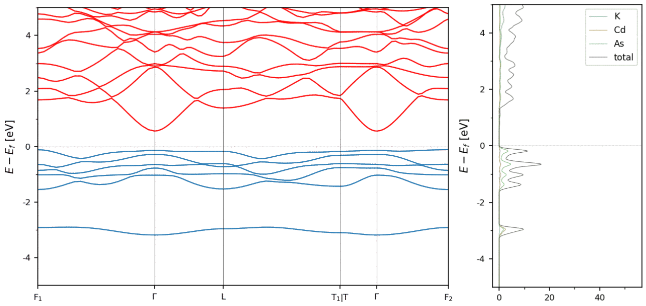

K$_4$(HgAs$_2$) - ICSD 402573 - SG 166 ($R\bar{3}m$) - LCEBR - NM

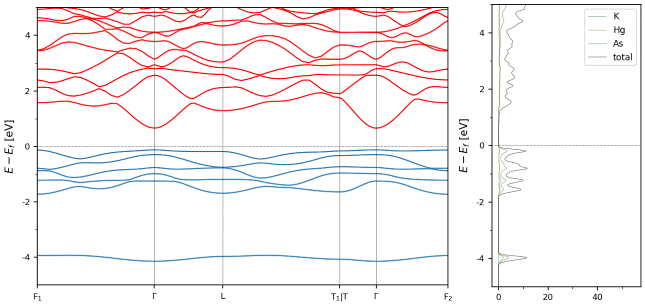

K$_4$ZnAs$_2$ - ICSD 409919 - SG 166 ($R\bar{3}m$) - LCEBR - NM

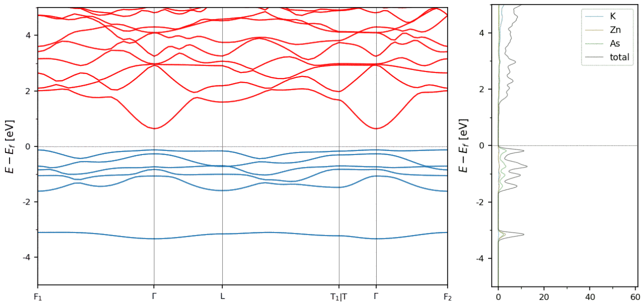

Figure 43. Band structure and density of states for materials with the most remarkable flat-band features near the Fermi energy. (part 16/44)

$Na_2(Ti_3Cl_8)$ - ICSD 401026 - SG 166 ($R\bar{3}m$) - SEBR - FM

Kagome - Bipartite

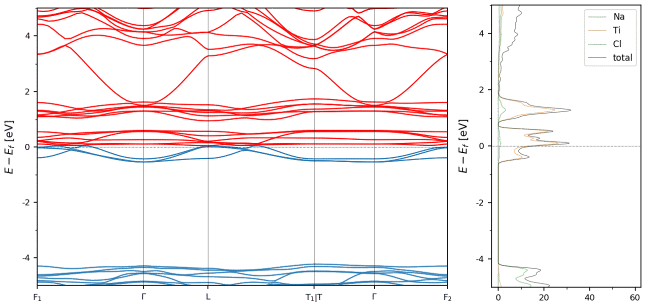

Nb_3Br_8 - ICSD 25766 - SG 166 ($R\bar{3}m$) - LCEBR - NM

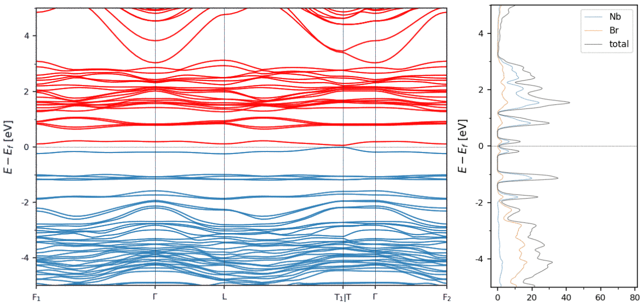

Nb_3I_8 - ICSD 25767 - SG 166 ($R\bar{3}m$) - LCEBR - NM

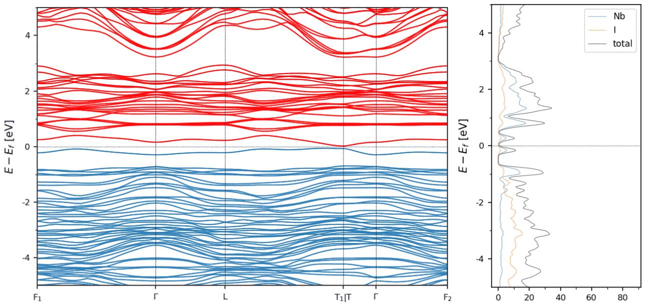

Rh_3InPbS_2 - ICSD 5440 - SG 166 ($R\bar{3}m$) - ES - NM

Kagome - Bipartite - Split

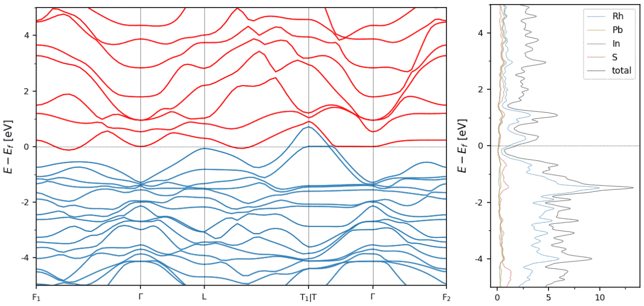

$InSnCo_3S_2$ - ICSD 425137 - SG 166 ($R\bar{3}m$) - ES - n.a.

Kagome - Bipartite - Split

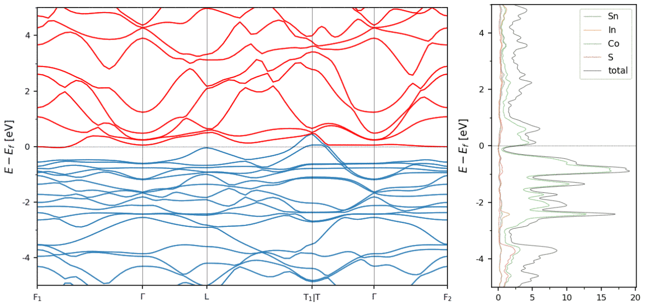

$Co_3Sn_2S_2$ - ICSD 5435 - SG 166 ($R\bar{3}m$) - ESFD - FM

Kagome - Bipartite - Split

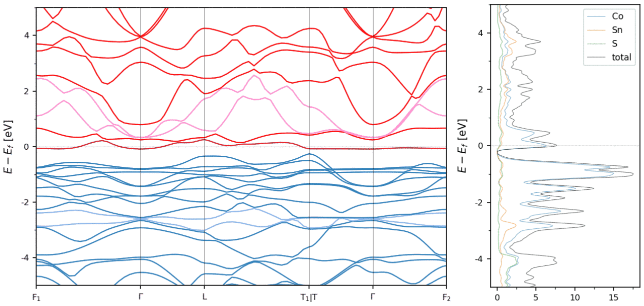

$Rh_3Sn_2S_2$ - ICSD 420728 - SG 166 ($R\bar{3}m$) - ESFD - NM

Kagome - Bipartite - Split

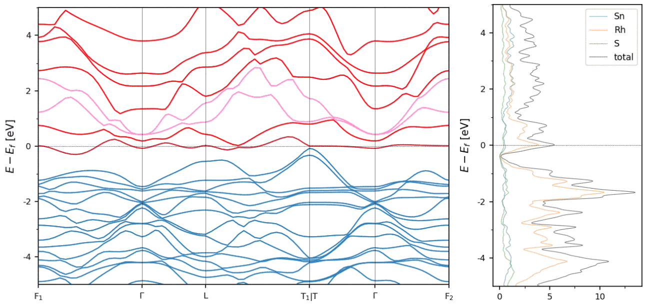

Co_3InSnS_2 - ICSD 5437 - SG 166 ($R\bar{3}m$) - LCEBR - NM

Kagome - Bipartite - Split

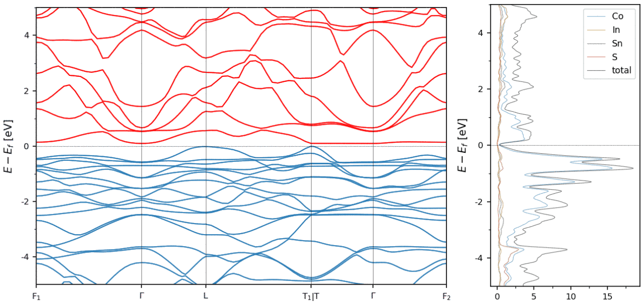

Figure 44. Band structure and density of states for materials with the most remarkable flat-band features near the Fermi energy. (part 17/44)

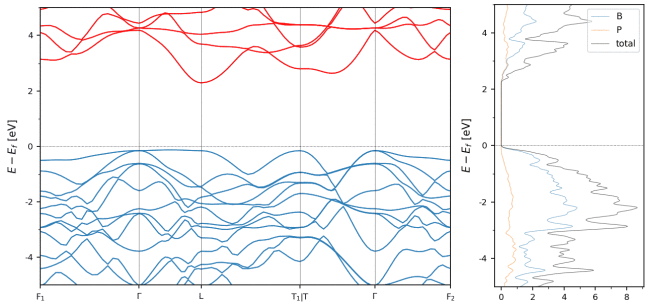
$B_{12}P_2$ - ICSD 62748 - SG 166 ($R\bar{3}m$) - LCEBR - NM

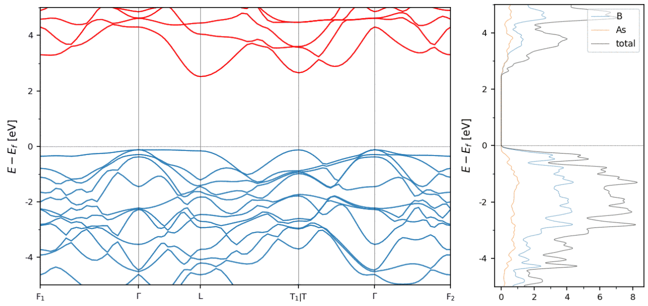
$B_{12}As_2$ - ICSD 62749 - SG 166 ($R\bar{3}m$) - LCEBR - NM

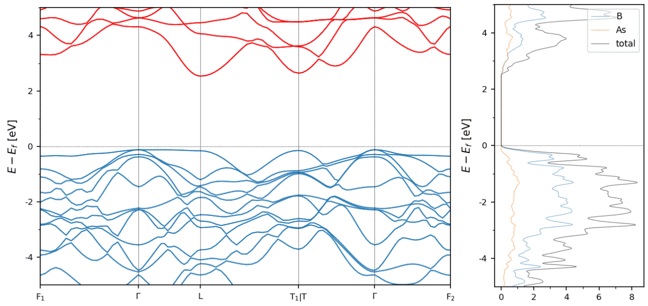
B_6As - ICSD 68151 - SG 166 ($R\bar{3}m$) - LCEBR - NM

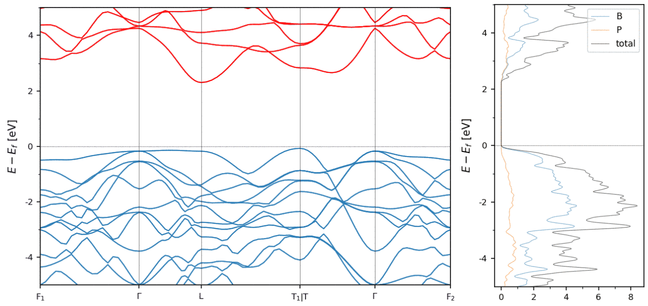
B_6P - ICSD 615156 - SG 166 ($R\bar{3}m$) - LCEBR - NM

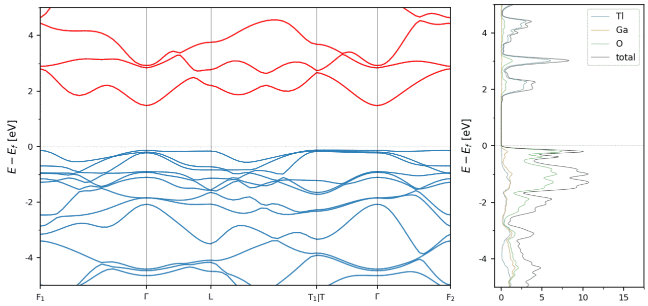
$TlGaO_2$ - ICSD 33579 - SG 166 ($R\bar{3}m$) - LCEBR - n.a.

Kagome - Bipartite - Split

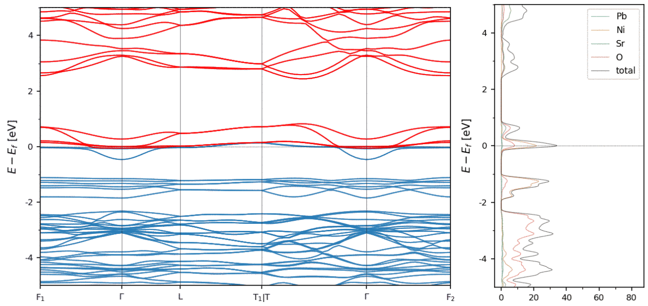
$Sr_3(PbNiO_6)$ - ICSD 152588 - SG 167 ($R\bar{3}c$) - LCEBR - AFM

Bipartite

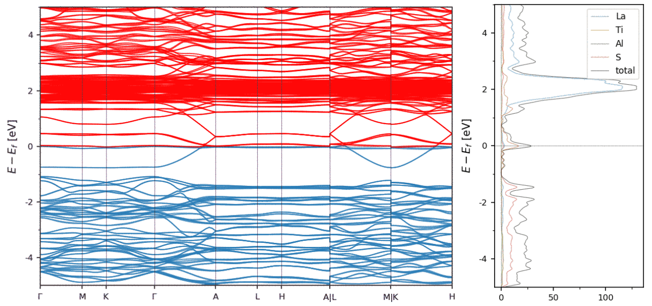
La_3AlTiS_7 - ICSD 608322 - SG 173 ($P6_3$) - ES - FM

Bipartite

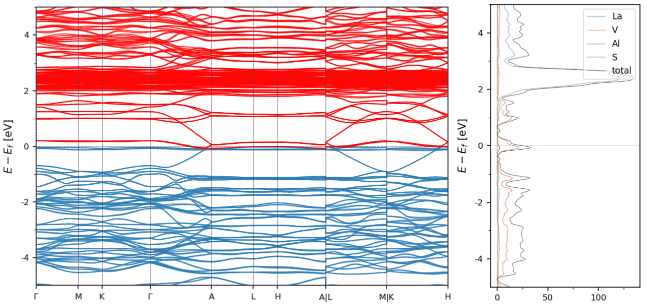
La_3AlVS_7 - ICSD 608323 - SG 173 ($P6_3$) - ES - FM

Bipartite

Figure 45. Band structure and density of states for materials with the most remarkable flat-band features near the Fermi energy. (part 18/44)

KAl(SiO$_4$) - ICSD 34350 - SG 173 ($P6_3$) - LCEBR - NM

Bipartite - Split

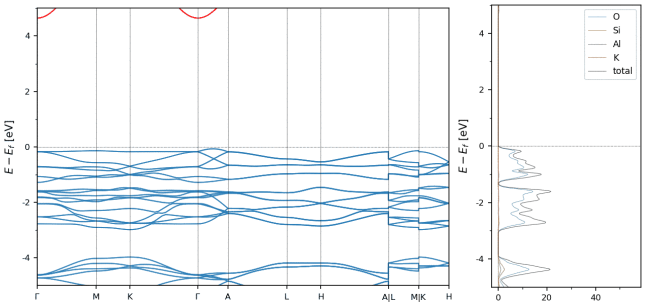

BaZn(BO$_3$)F - ICSD 248042 - SG 174 ($P\bar{6}$) - LCEBR - NM

Bipartite

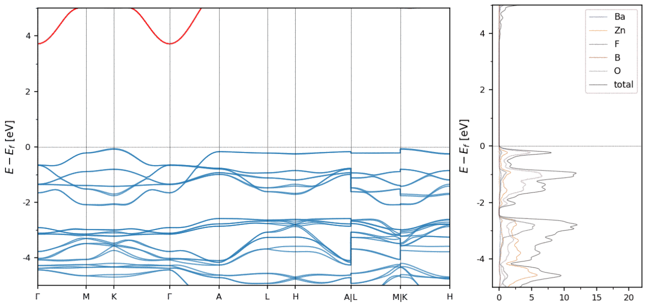

Mg$_3$F$_3$(BO$_3$) - ICSD 4226 - SG 176 ($P6_3/m$) - LCEBR - n.a.

Bipartite

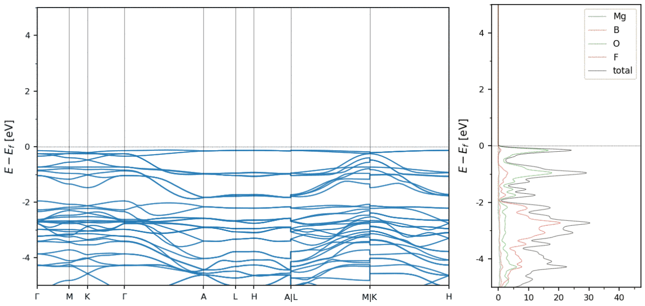

NaCs$_2$(C$_2$N$_3$)$_3$ - ICSD 407809 - SG 176 ($P6_3/m$) - LCEBR - NM

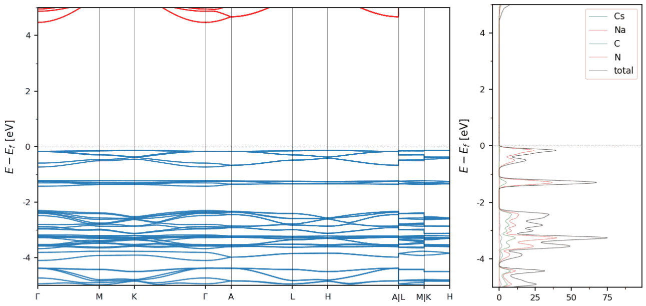

TlSbO$_3$ - ICSD 10142 - SG 182 ($P6_322$) - LCEBR - NM

Bipartite - Split

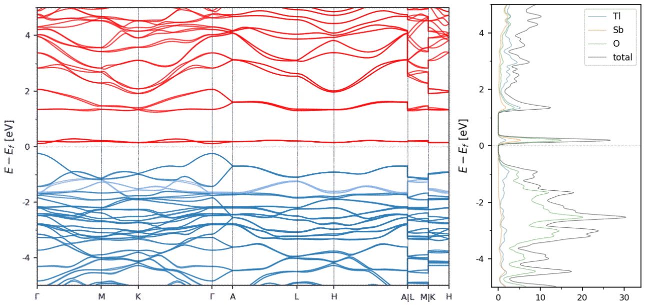

SiO$_2$ - ICSD 29343 - SG 182 ($P6_322$) - LCEBR - NM

Bipartite - Split

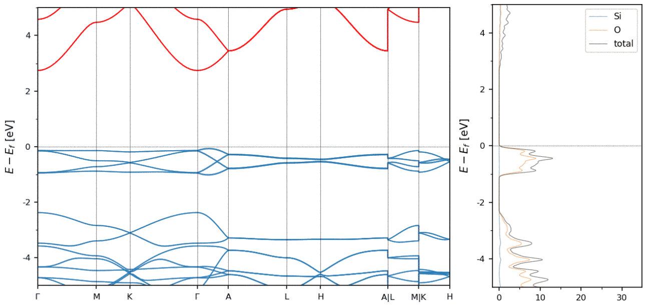

Ba$_3$Cu(Sb$_2$O$_9$) - ICSD 2279 - SG 186 ($P6_3mc$) - ESFD - FM

Kagome* - Bipartite - Split

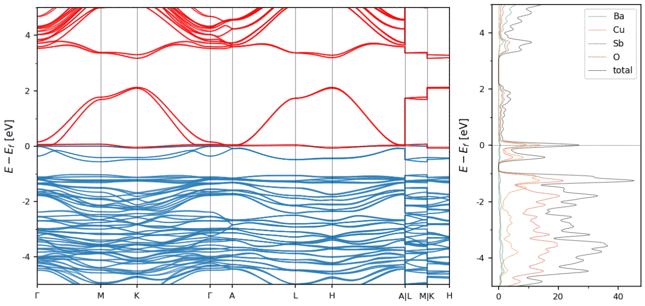

Na(Be$_4$SbO$_7$) - ICSD 27599 - SG 186 ($P6_3mc$) - LCEBR - NM

Kagome* - Bipartite

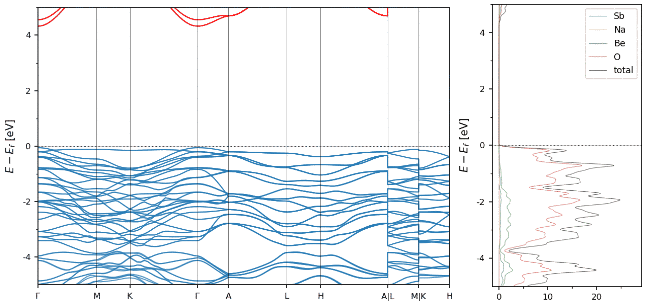

Figure 46. Band structure and density of states for materials with the most remarkable flat-band features near the Fermi energy. (part 19/44)

LaSiO$_2$N - ICSD 9752 - SG 188 ($P\bar{6}c2$) - ES - NM

Bipartite

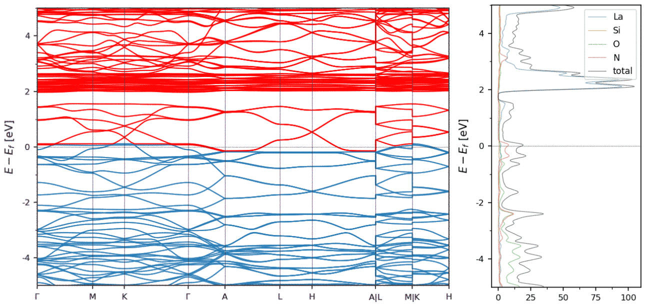

Sr(GeO$_3$) - ICSD 28603 - SG 189 ($P\bar{6}2m$) - LCEBR - NM

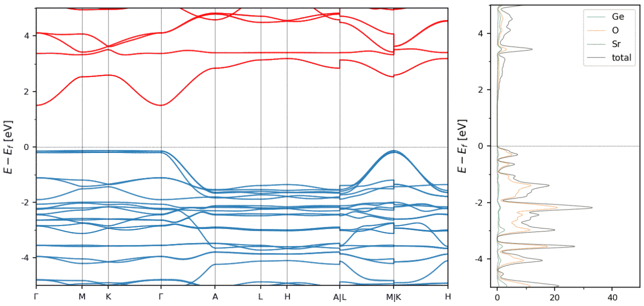

TiCoSi - ICSD 42735 - SG 189 ($P\bar{6}2m$) - ESFD - FM

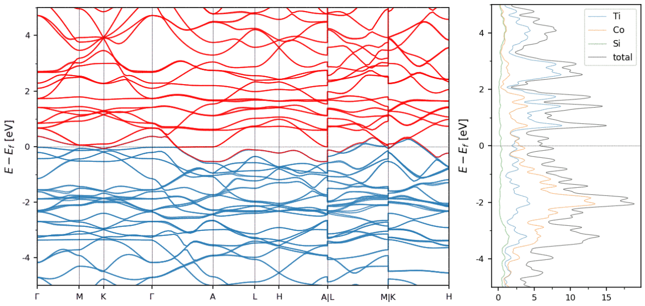

Pd$_5$Sr - ICSD 105707 - SG 191 ($P6/mmm$) - SEBR - NM

Kagome

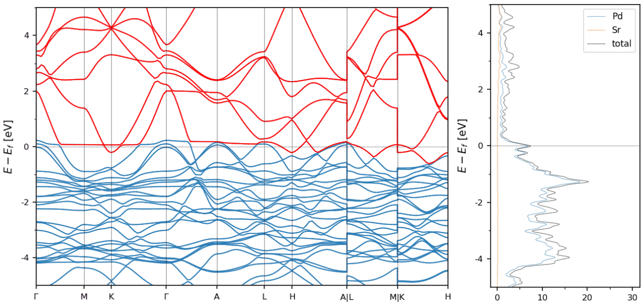

CaPd$_5$ - ICSD 106357 - SG 191 ($P6/mmm$) - SEBR - NM

Kagome

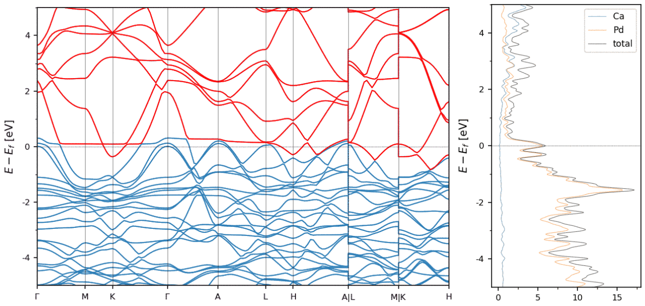

CaNi$_5$ - ICSD 54474 - SG 191 ($P6/mmm$) - ES - FM

Kagome

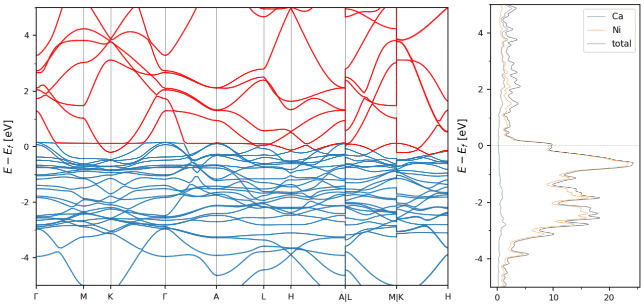

BaPd$_5$ - ICSD 58672 - SG 191 ($P6/mmm$) - ES - NM

Kagome

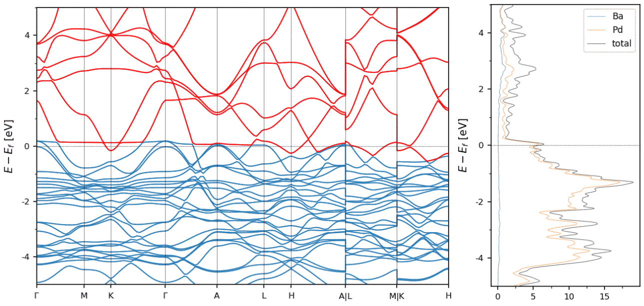

LaNi$_5$ - ICSD 54245 - SG 191 ($P6/mmm$) - ESFD - FM

Kagome

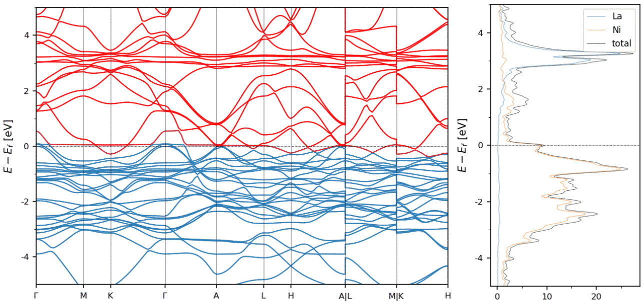

Figure 47. Band structure and density of states for materials with the most remarkable flat-band features near the Fermi energy. (part 20/44)

YNi$_5$ - ICSD 54422 - SG 191 ($P6/mmm$) - ESFD - FM

Kagome

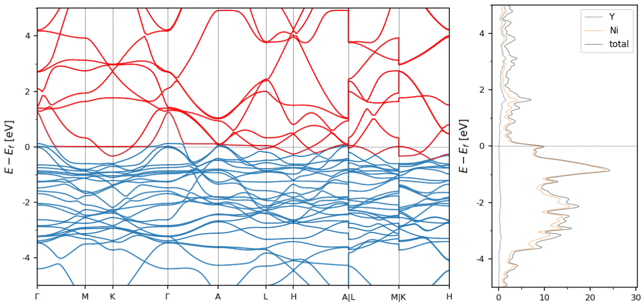

Ni$_5$Sc - ICSD 105336 - SG 191 ($P6/mmm$) - ESFD - FM

Kagome

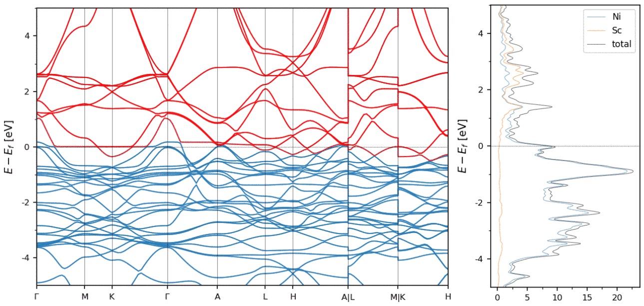

InNi - ICSD 59435 - SG 191 ($P6/mmm$) - ESFD - NM

Kagome

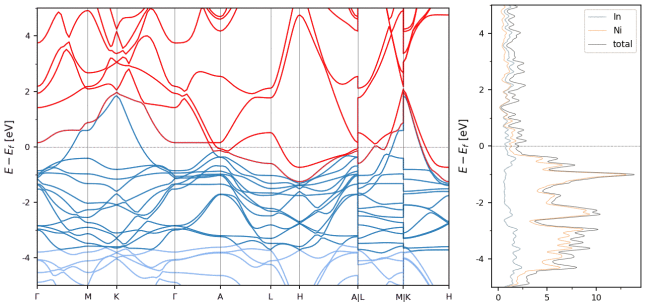

YCr$_6$Ge$_6$ - ICSD 658018 - SG 191 ($P6/mmm$) - ESFD - NM

Kagome

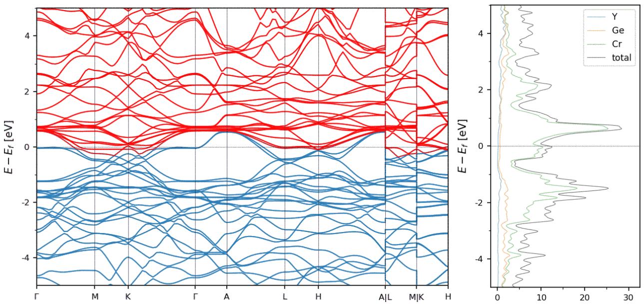

K$_3$N - ICSD 99999 - SG 193 ($P6_3/mcm$) - SEBR - NM

Bipartite - Split

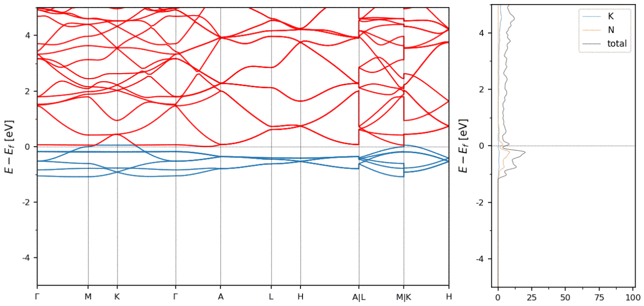

NbI$_3$ - ICSD 109145 - SG 193 ($P6_3/mcm$) - ES - FM

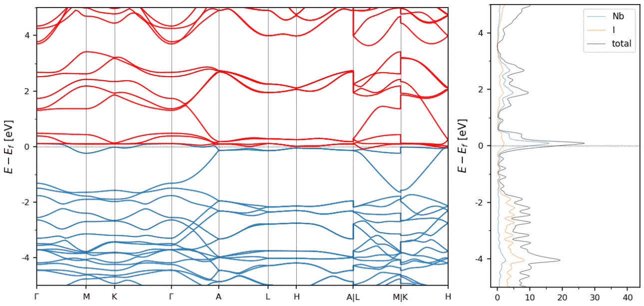

Rb$_6$Ni$_6$F$_{18}$ - ICSD 410390 - SG 194 ($P6_3/mmc$) - ES - FM

Kagome* - Bipartite - Split

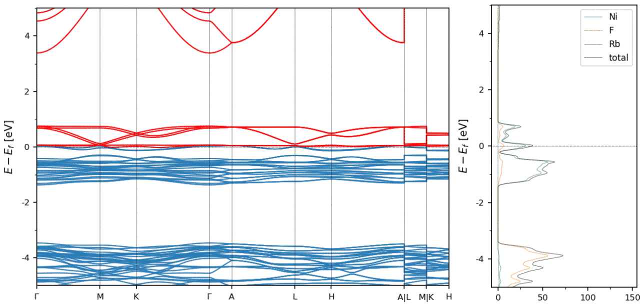

BaVS$_3$ - ICSD 8193 - SG 194 ($P6_3/mmc$) - ESFD - FM

Kagome*

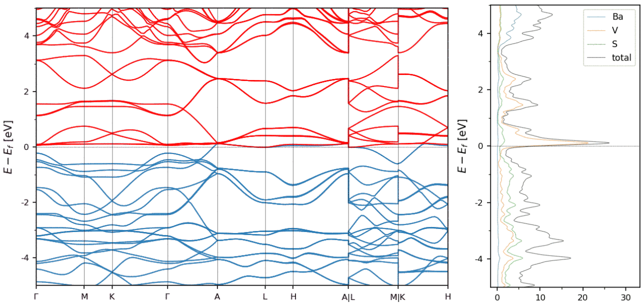

Figure 48. Band structure and density of states for materials with the most remarkable flat-band features near the Fermi energy. (part 21/44)

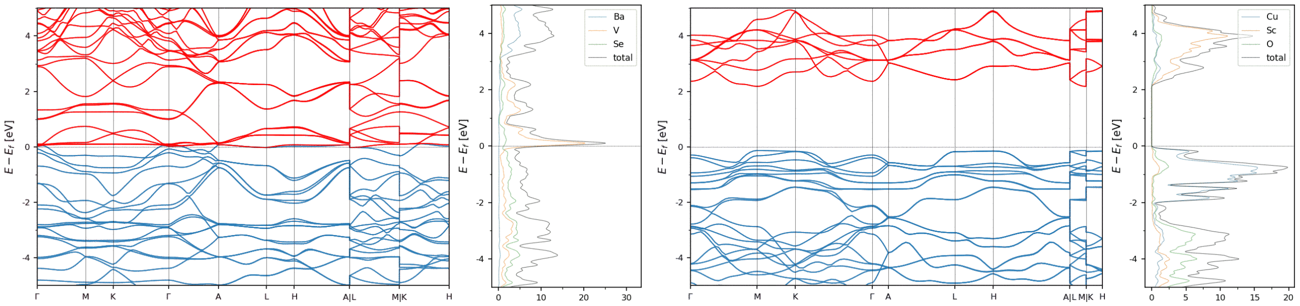

Ba(VSe$_3$) - ICSD 10486 - SG 194 ($P6_3/mmc$) - ESFD - FM

Kagome*

CuScO$_2$ - ICSD 60847 - SG 194 ($P6_3/mmc$) - LCEBR - NM

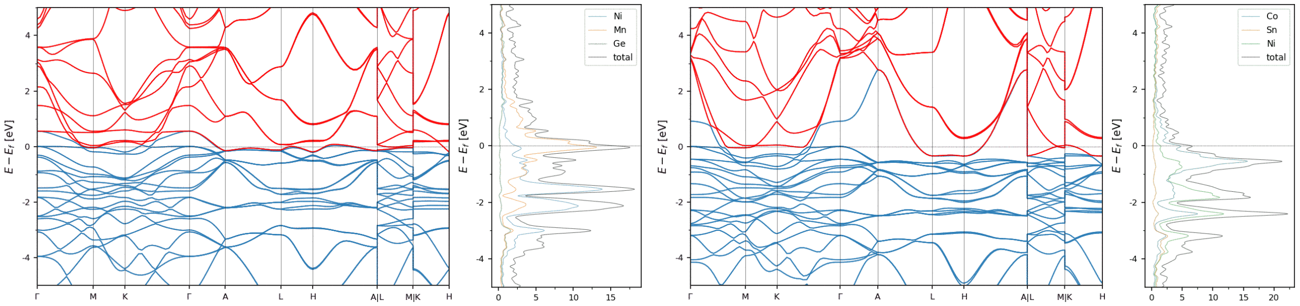

NiMnGe - ICSD 41921 - SG 194 ($P6_3/mmc$) - ESFD - FM

CoNiSn - ICSD 102582 - SG 194 ($P6_3/mmc$) - ESFD - FM

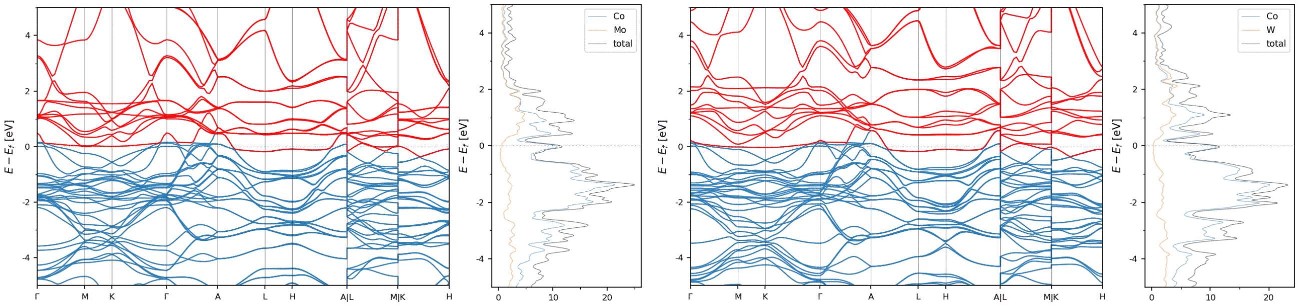

Co$_3$Mo - ICSD 102542 - SG 194 ($P6_3/mmc$) - ESFD - FM

Kagome*

Co$_3$W - ICSD 102722 - SG 194 ($P6_3/mmc$) - ESFD - FM

Kagome*

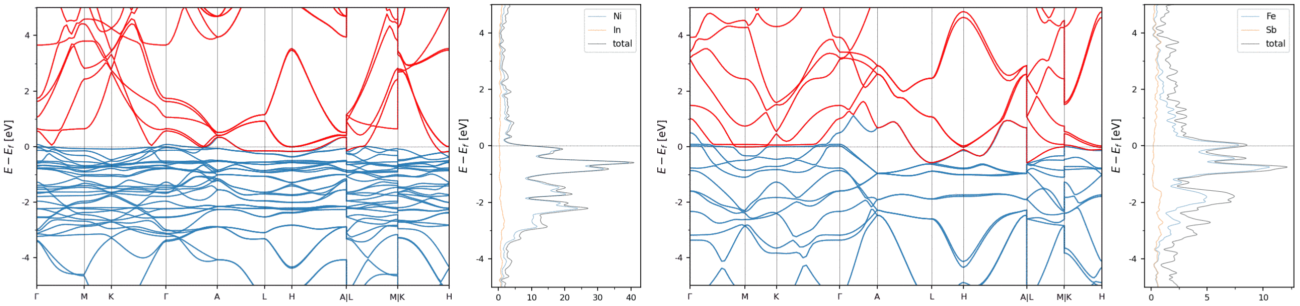

Ni$_3$In - ICSD 151196 - SG 194 ($P6_3/mmc$) - ESFD - FM

Kagome*

FeSb - ICSD 53535 - SG 194 ($P6_3/mmc$) - ESFD - FM

Figure 49. Band structure and density of states for materials with the most remarkable flat-band features near the Fermi energy. (part 22/44)

CsLi(MoO$_4$) - ICSD 20805 - SG 216 ($F\bar{4}3m$) - LCEBR - NM

Kagome* - Pyrochlore - Bipartite - Split

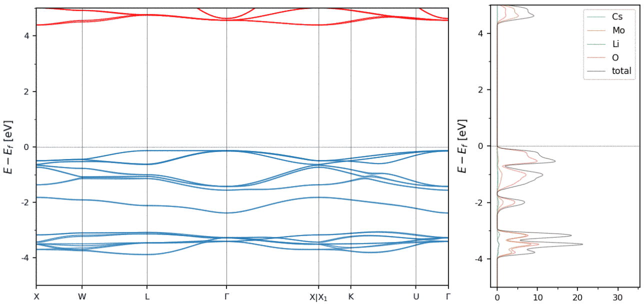

CaMgNi$_4$ - ICSD 107419 - SG 216 ($F\bar{4}3m$) - NLC - FM

Kagome* - Pyrochlore

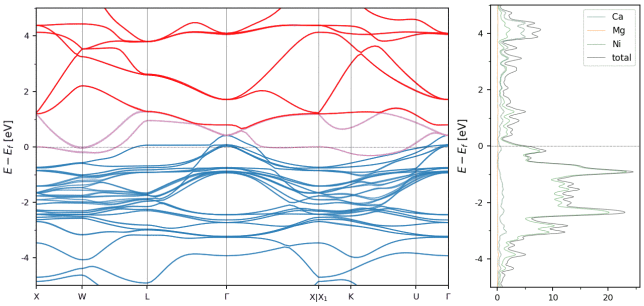

ZrNi$_5$ - ICSD 601018 - SG 216 ($F\bar{4}3m$) - NLC - FM

Kagome*

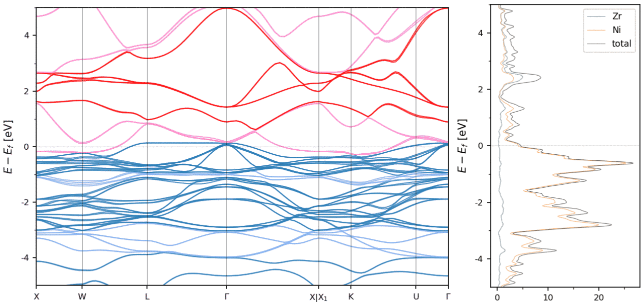

ScAuNi$_4$ - ICSD 612227 - SG 216 ($F\bar{4}3m$) - NLC - NM

Kagome* - Pyrochlore

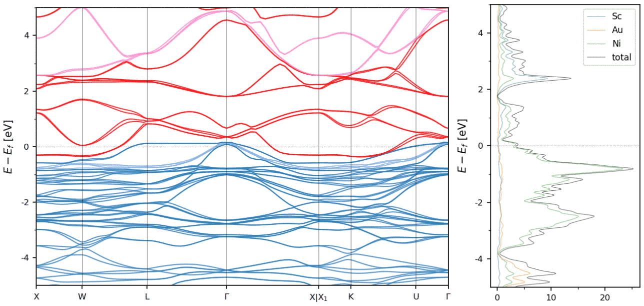

YAuNi$_4$ - ICSD 612233 - SG 216 ($F\bar{4}3m$) - NLC - n.a.

Kagome* - Pyrochlore

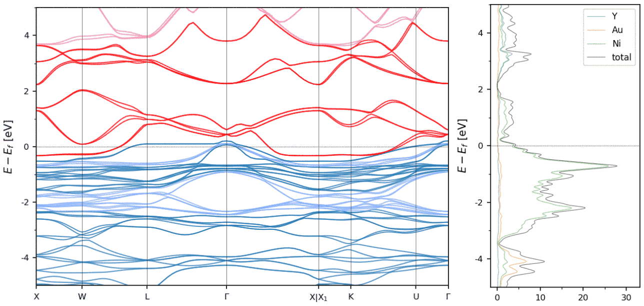

Ni$_5$Zr - ICSD 54985 - SG 216 ($F\bar{4}3m$) - ES - FM

Kagome*

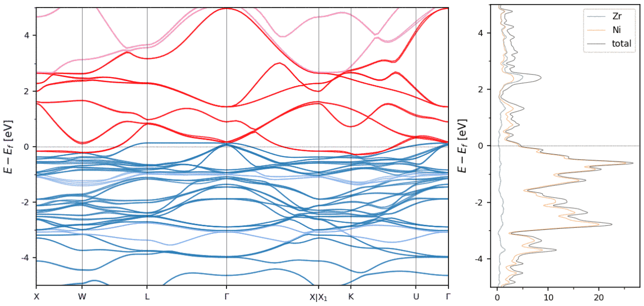

HfNi$_5$ - ICSD 672665 - SG 216 ($F\bar{4}3m$) - ES - n.a.

Kagome*

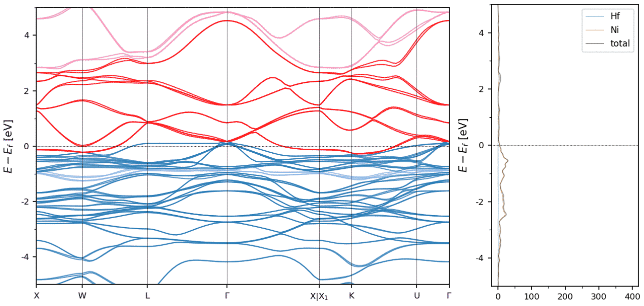

Ni$_4$ZnZr - ICSD 105477 - SG 216 ($F\bar{4}3m$) - ESFD - NM

Kagome* - Pyrochlore

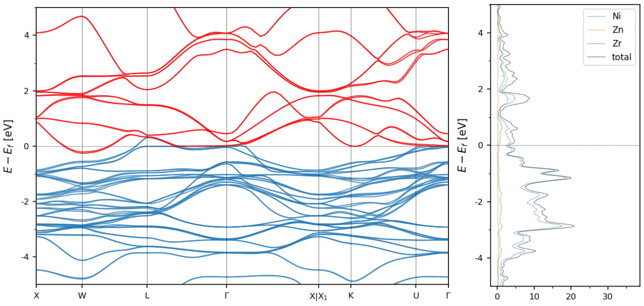

Figure 50. Band structure and density of states for materials with the most remarkable flat-band features near the Fermi energy. (part 23/44)

MgYNi$_4$ - ICSD 107033 - SG 216 ($F\bar{4}3m$) - ESFD - NM

Kagome* - Pyrochlore

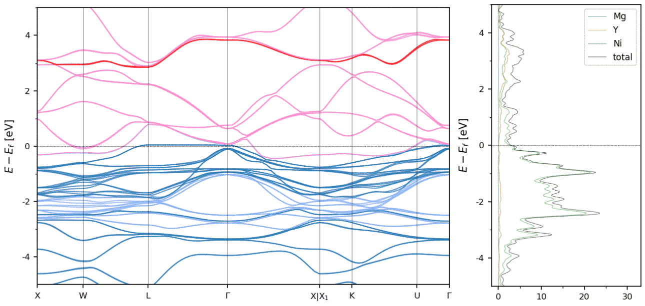

LaMgNi$_4$ - ICSD 107420 - SG 216 ($F\bar{4}3m$) - ESFD - FM

Kagome* - Pyrochlore

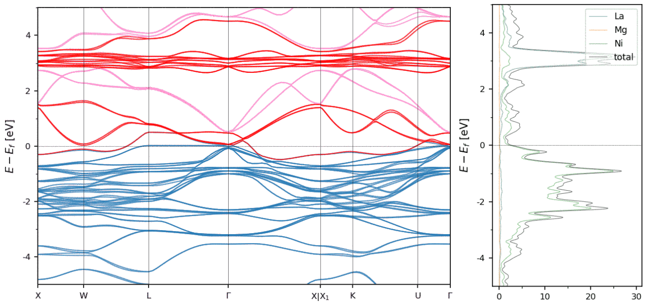

ScNi$_4$Cd - ICSD 185106 - SG 216 ($F\bar{4}3m$) - ESFD - NM

Kagome* - Pyrochlore

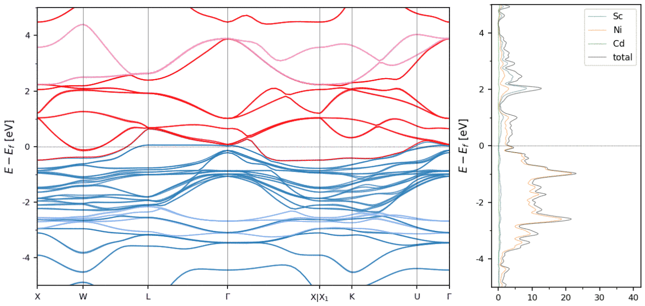

YNi$_4$Cd - ICSD 423939 - SG 216 ($F\bar{4}3m$) - ESFD - n.a.

Kagome* - Pyrochlore

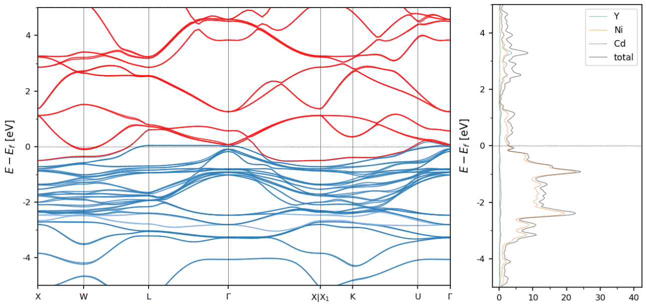

Fe$_2$MnAl - ICSD 672261 - SG 216 ($F\bar{4}3m$) - NLC - n.a.

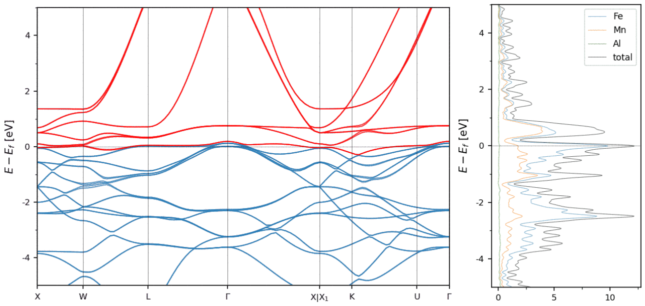

Mn$_2$CoAs - ICSD 191648 - SG 216 ($F\bar{4}3m$) - ES - FM

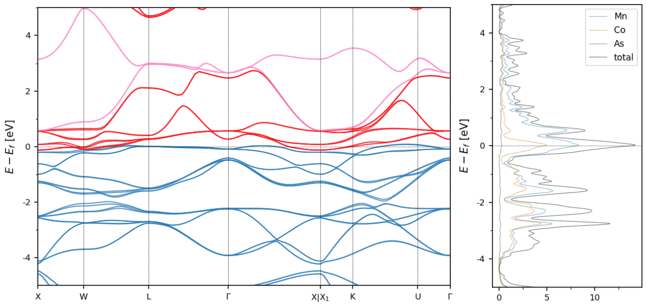

CoFeTiGa - ICSD 191658 - SG 216 ($F\bar{4}3m$) - ESFD - NM

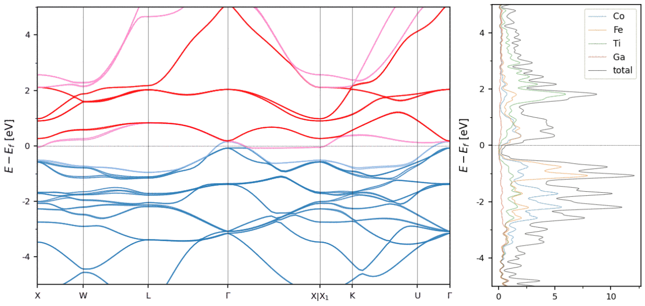

CoFeTiSi - ICSD 191659 - SG 216 ($F\bar{4}3m$) - ESFD - FM

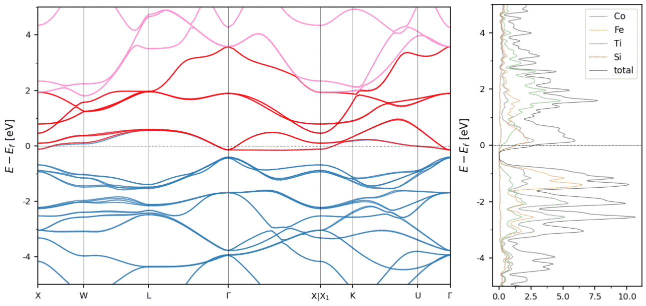

Figure 51. Band structure and density of states for materials with the most remarkable flat-band features near the Fermi energy. (part 24/44)

CoFeTiGe - ICSD 191660 - SG 216 ($F\bar{4}3m$) - ESFD - FM

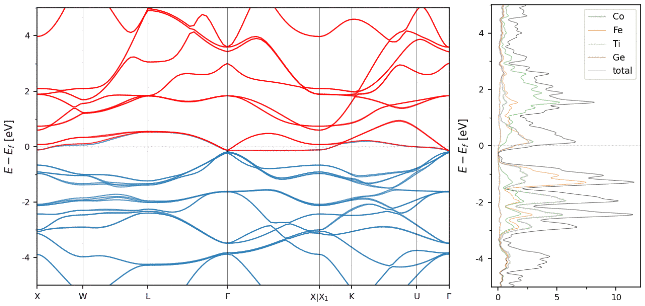

CoFeTiAs - ICSD 191661 - SG 216 ($F\bar{4}3m$) - ESFD - FM

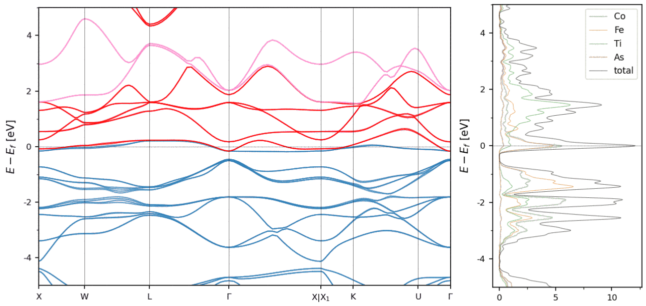

CoFeTiSb - ICSD 191662 - SG 216 ($F\bar{4}3m$) - ESFD - FM

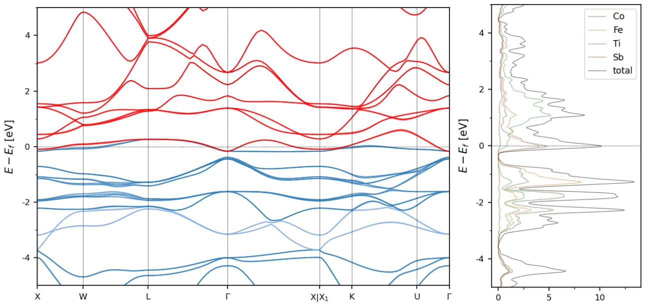

CoFeVGa - ICSD 191664 - SG 216 ($F\bar{4}3m$) - ESFD - FM

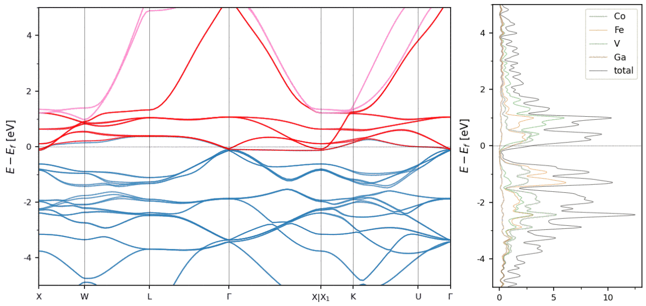

Fe$_2$MnGe - ICSD 671982 - SG 216 ($F\bar{4}3m$) - ESFD - n.a.

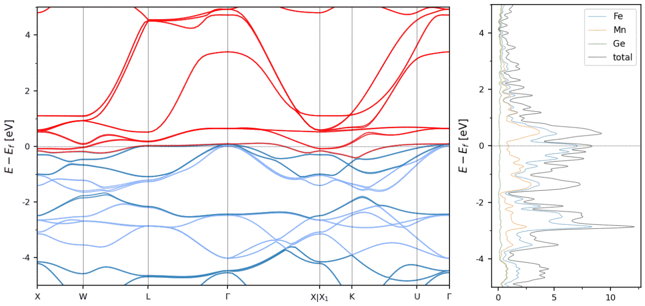

CoFeTiAl - ICSD 191657 - SG 216 ($F\bar{4}3m$) - LCEBR - NM

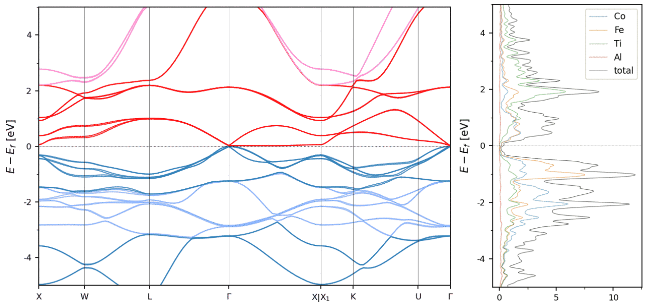

NiMnSb - ICSD 54255 - SG 216 ($F\bar{4}3m$) - ES - FM

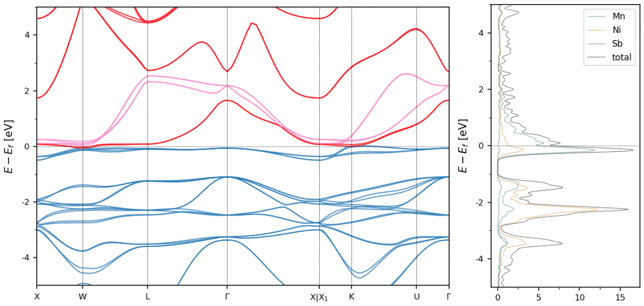

CoMnSb - ICSD 53001 - SG 216 ($F\bar{4}3m$) - ESFD - FM

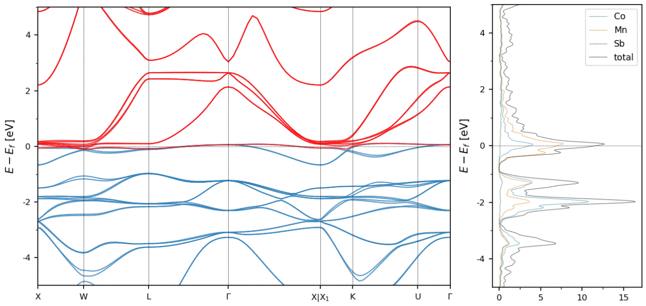

Figure 52. Band structure and density of states for materials with the most remarkable flat-band features near the Fermi energy. (part 25/44)

RhMnSb - ICSD 54343 - SG 216 ($F\bar{4}3m$) - ESFD - FM

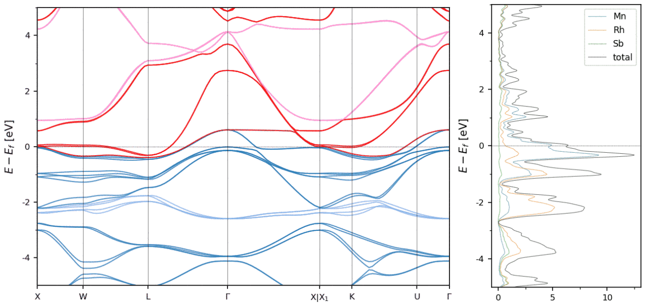

MnPtSn - ICSD 104955 - SG 216 ($F\bar{4}3m$) - ESFD - FM

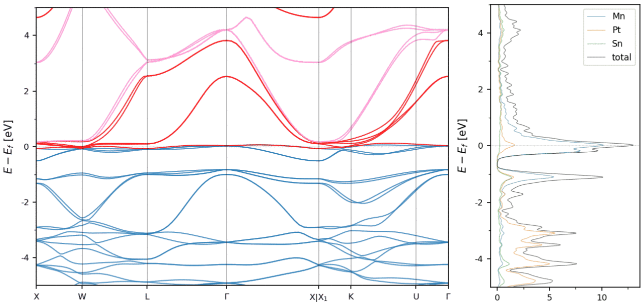

LiCaC - ICSD 672030 - SG 216 ($F\bar{4}3m$) - ESFD - n.a.

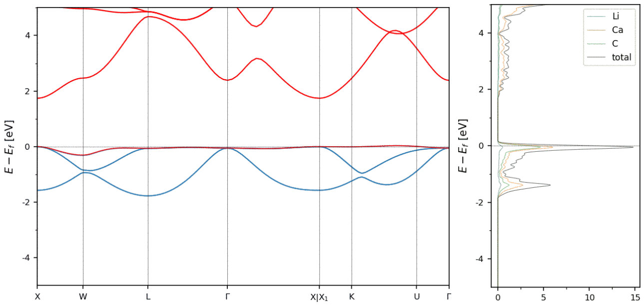

CoNbSn - ICSD 102552 - SG 216 ($F\bar{4}3m$) - LCEBR - FM

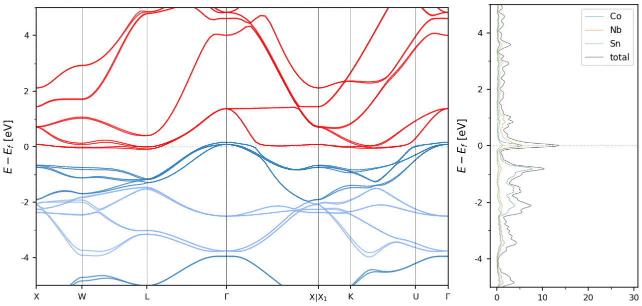

MnSn - ICSD 191171 - SG 216 ($F\bar{4}3m$) - ESFD - FM

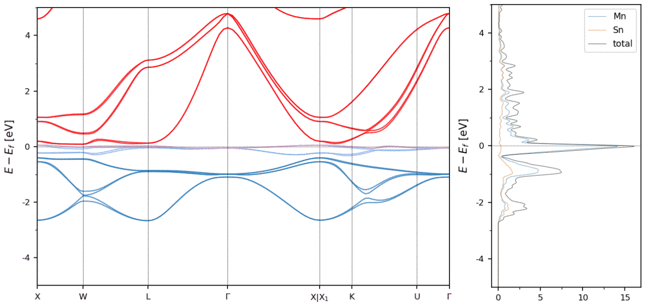

GaMo$_4$CS$_8$ - ICSD 76848 - SG 216 ($F\bar{4}3m$) - ESFD - NM

Bipartite - Split

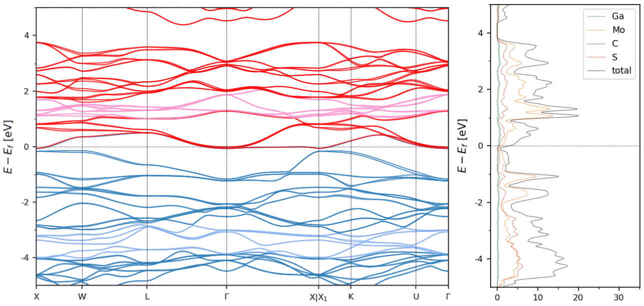

MgV$_2$O$_4$ - ICSD 674693 - SG 216 ($F\bar{4}3m$) - ESFD - n.a.

Kagome* - Pyrochlore - Bipartite

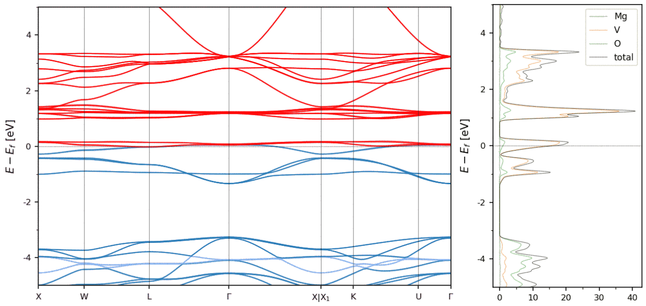

Cu$_2$Al$_4$O$_7$ - ICSD 100355 - SG 216 ($F\bar{4}3m$) - ES - FM

Kagome* - Pyrochlore - Bipartite

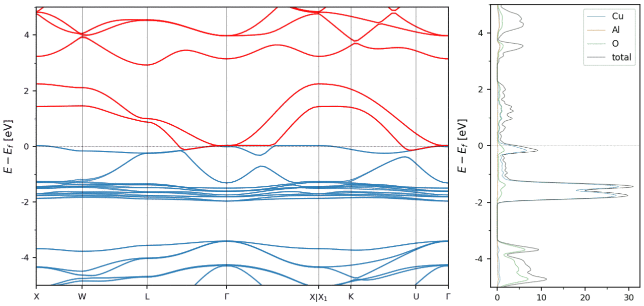

Figure 53. Band structure and density of states for materials with the most remarkable flat-band features near the Fermi energy. (part 26/44)

SiO_2 - ICSD 183701 - SG 217 ($I\bar{4}3m$) - LCEBR - NM

Bipartite - Split

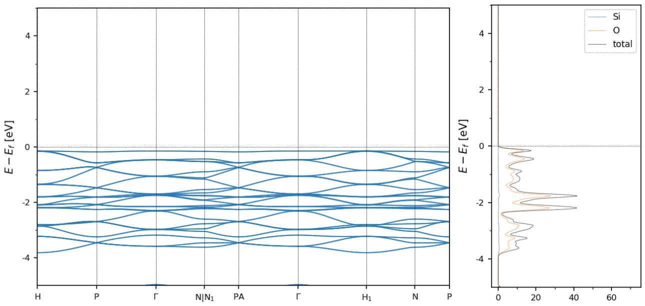

Ni_3Ge - ICSD 53745 - SG 221 ($Pm\bar{3}m$) - SEBR - NM

Kagome

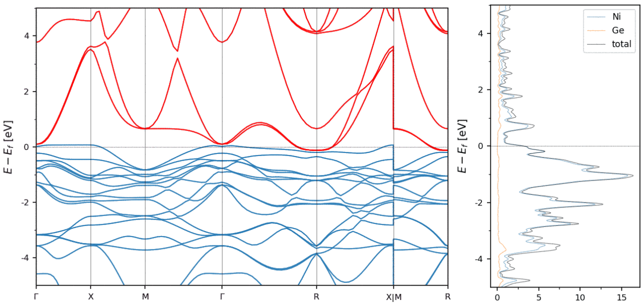

Ni_3Si - ICSD 76413 - SG 221 ($Pm\bar{3}m$) - SEBR - NM

Kagome

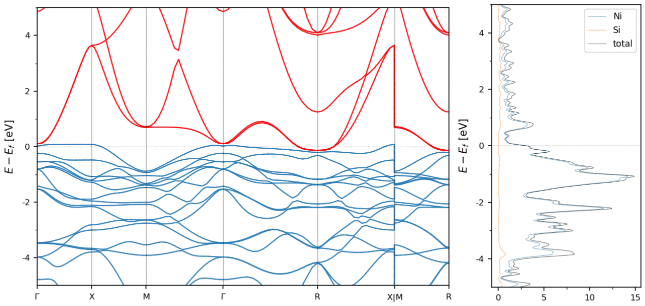

Ni_3Sn - ICSD 105353 - SG 221 ($Pm\bar{3}m$) - SEBR - NM

Kagome

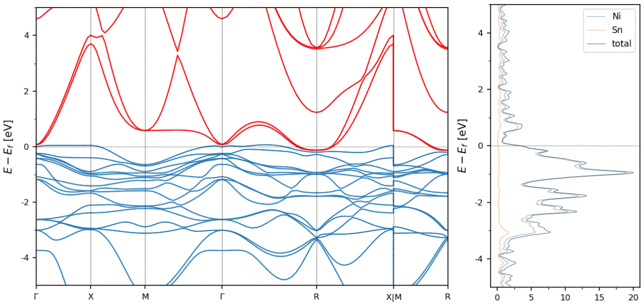

$MgNi_3$ - ICSD 193569 - SG 221 ($Pm\bar{3}m$) - ES - FM

Kagome

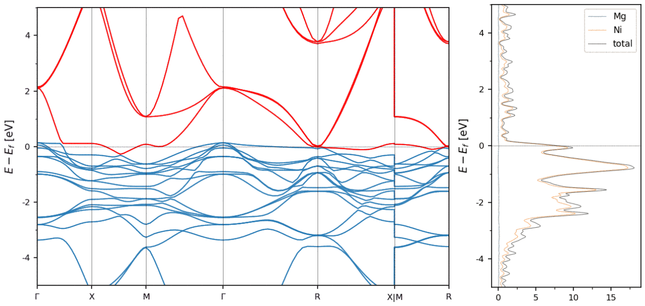

$PbPd_3$ - ICSD 42600 - SG 221 ($Pm\bar{3}m$) - ESFD - NM

Kagome

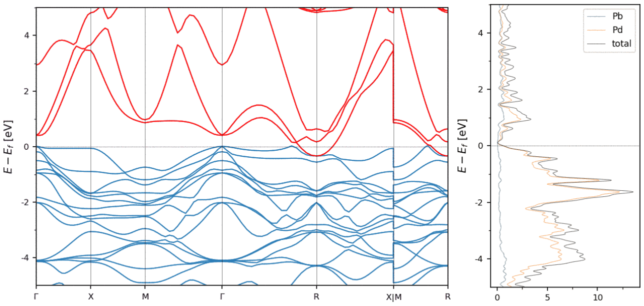

$AlNi_3$ - ICSD 58038 - SG 221 ($Pm\bar{3}m$) - ESFD - FM

Kagome

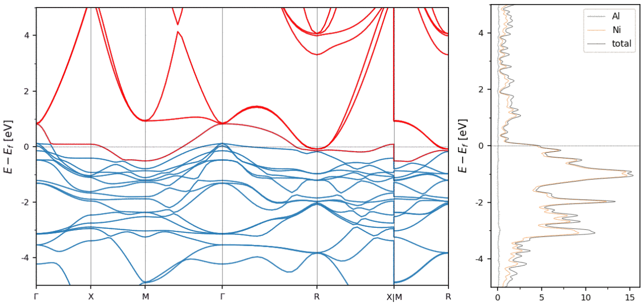

$InNi_3$ - ICSD 59438 - SG 221 ($Pm\bar{3}m$) - ESFD - FM

Kagome

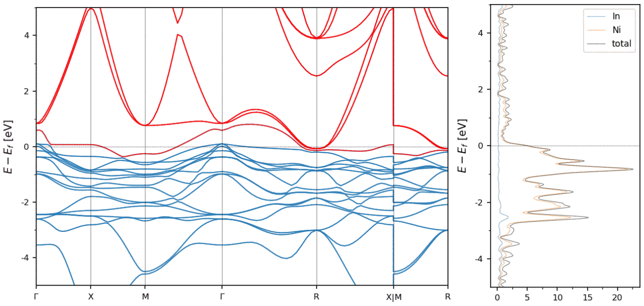

Figure 54. Band structure and density of states for materials with the most remarkable flat-band features near the Fermi energy. (part 27/44)

$GaNi_3$ - ICSD 103856 - SG 221 ($Pm\bar{3}m$) - ESFD - FM

Kagome

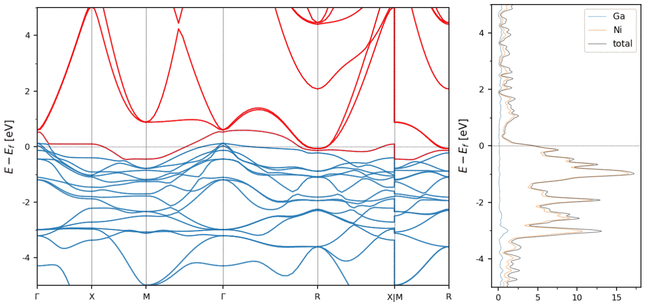

$MnZn_3$ - ICSD 105020 - SG 221 ($Pm\bar{3}m$) - ESFD - FM

Kagome

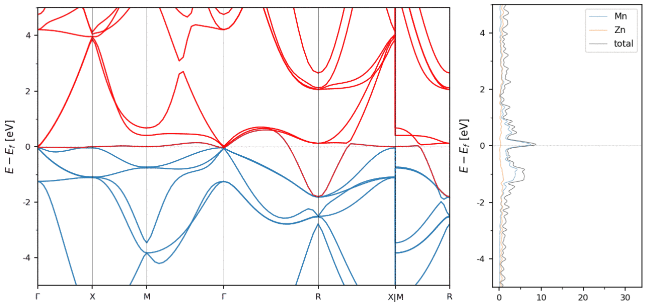

Pd_3Sn - ICSD 105689 - SG 221 ($Pm\bar{3}m$) - ESFD - NM

Kagome

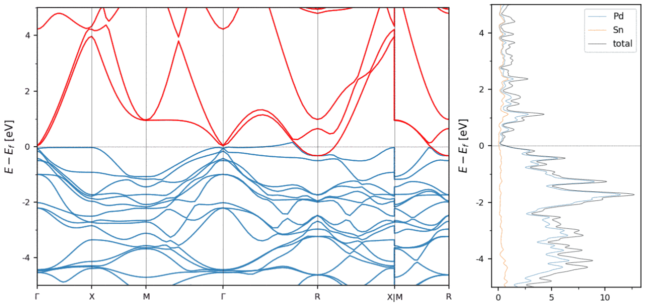

Co_3W - ICSD 187963 - SG 221 ($Pm\bar{3}m$) - ESFD - FM

Kagome

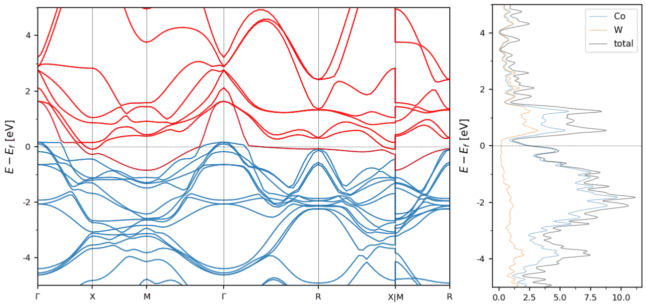

Co_3Mo - ICSD 187969 - SG 221 ($Pm\bar{3}m$) - ESFD - FM

Kagome

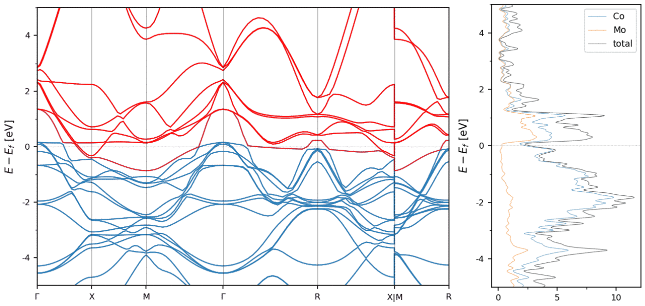

$InPd_3$ - ICSD 247193 - SG 221 ($Pm\bar{3}m$) - ESFD - NM

Kagome

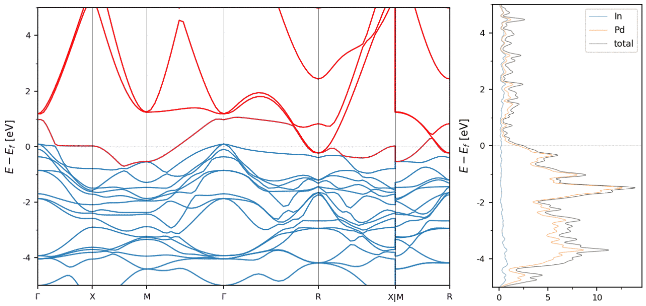

Cu_3Ni - ICSD 670622 - SG 221 ($Pm\bar{3}m$) - ESFD - n.a.

Kagome

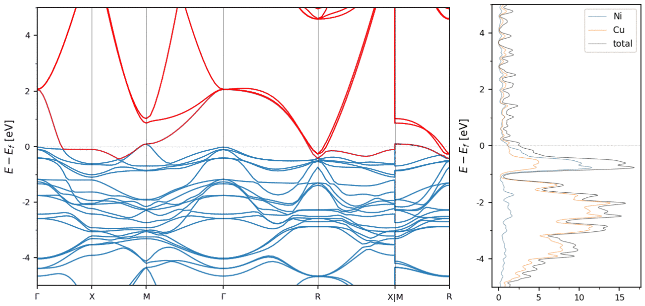

$CuNi_3$ - ICSD 670623 - SG 221 ($Pm\bar{3}m$) - ESFD - n.a.

Kagome

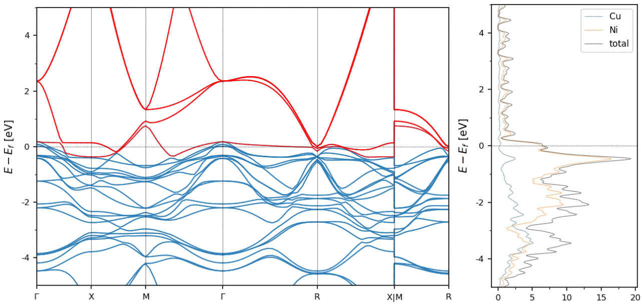

Figure 55. Band structure and density of states for materials with the most remarkable flat-band features near the Fermi energy. (part 28/44)

$CuPd_3$ - ICSD 670626 - SG 221 ($Pm\bar{3}m$) - ESFD - n.a.

Kagome

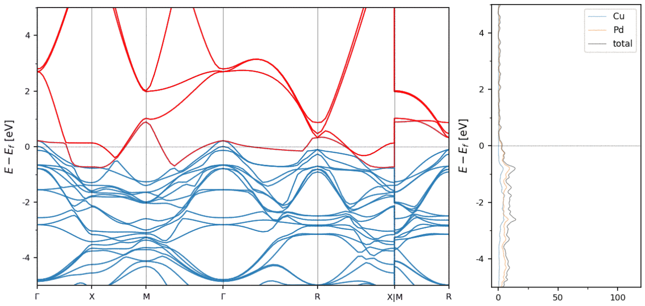

MgRh - ICSD 104859 - SG 221 ($Pm\bar{3}m$) - ESFD - NM

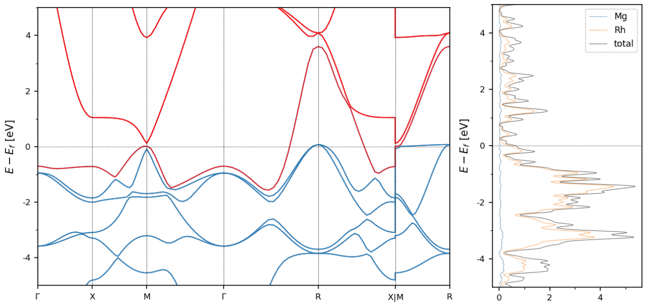

MnSn - ICSD 191170 - SG 221 ($Pm\bar{3}m$) - ESFD - FM

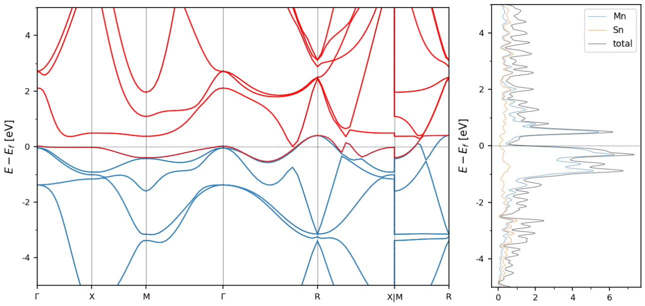

$KMnF_3$ - ICSD 15423 - SG 221 ($Pm\bar{3}m$) - ESFD - FM

Kagome - Bipartite - Split - Lieb

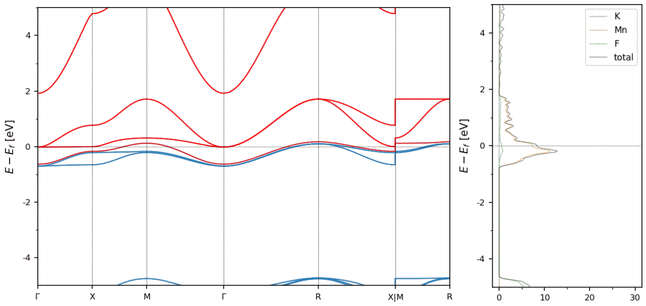

$Cs(HgBr_3)$ - ICSD 24479 - SG 221 ($Pm\bar{3}m$) - ESFD - NM

Kagome - Bipartite - Split - Lieb

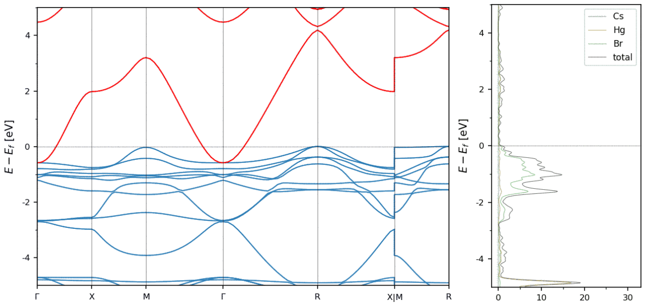

KVF_3 - ICSD 28145 - SG 221 ($Pm\bar{3}m$) - ESFD - FM

Kagome - Bipartite - Split - Lieb

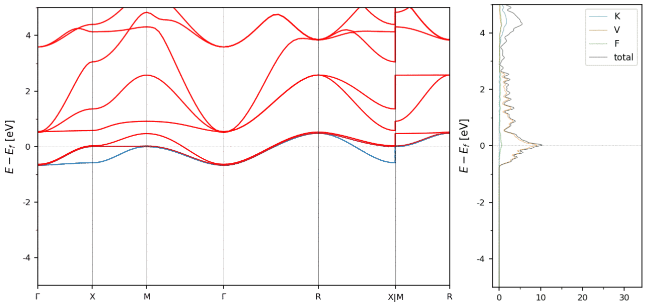

$RbVF_3$ - ICSD 28146 - SG 221 ($Pm\bar{3}m$) - ESFD - FM

Kagome - Bipartite - Split - Lieb

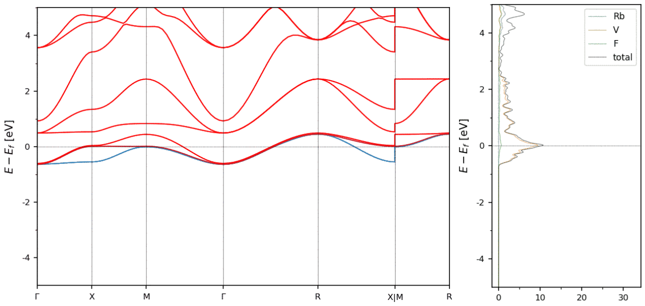

$La(CrO_3)$ - ICSD 28930 - SG 221 ($Pm\bar{3}m$) - ESFD - FM

Kagome - Bipartite - Split - Lieb

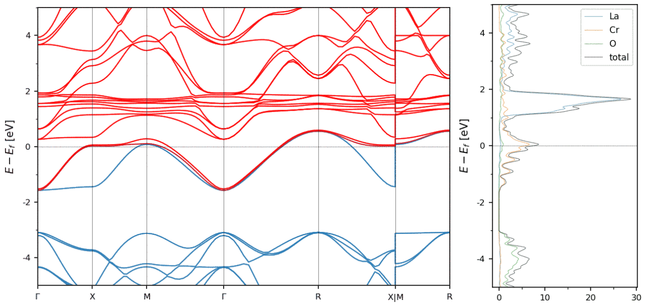

Figure 56. Band structure and density of states for materials with the most remarkable flat-band features near the Fermi energy. (part 29/44)

Rb(MnF$_3$) - ICSD 43722 - SG 221 ($Pm\bar{3}m$) - ESFD - FM

Kagome - Bipartite - Split - Lieb

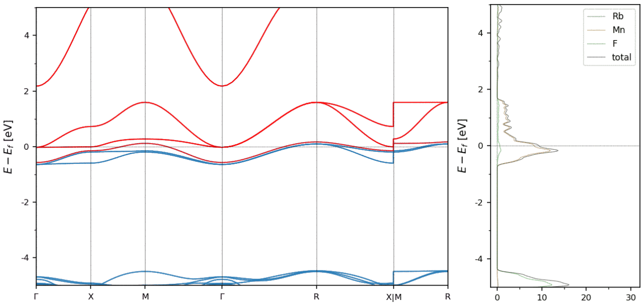

Rh$_3$YB - ICSD 44568 - SG 221 ($Pm\bar{3}m$) - ESFD - NM

Kagome - Bipartite - Split - Lieb

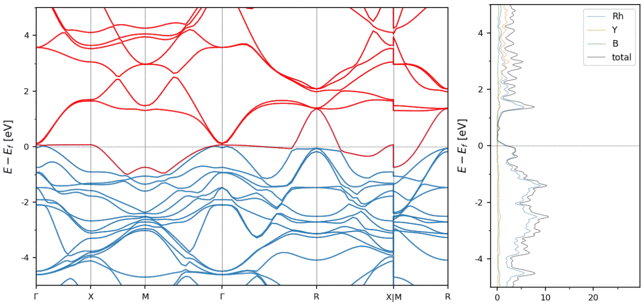

NaVF$_3$ - ICSD 60611 - SG 221 ($Pm\bar{3}m$) - ESFD - FM

Kagome - Bipartite - Split - Lieb

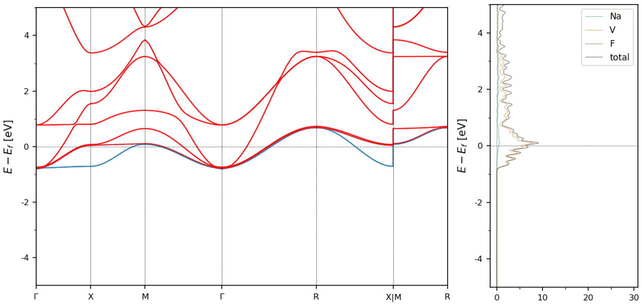

Sr(RuO$_3$) - ICSD 69360 - SG 221 ($Pm\bar{3}m$) - ESFD - FM

Kagome - Bipartite - Split - Lieb

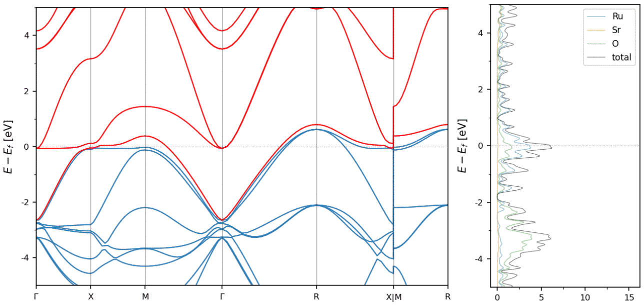

Fe$_3$ZnC - ICSD 76763 - SG 221 ($Pm\bar{3}m$) - ESFD - FM

Kagome - Bipartite - Split - Lieb

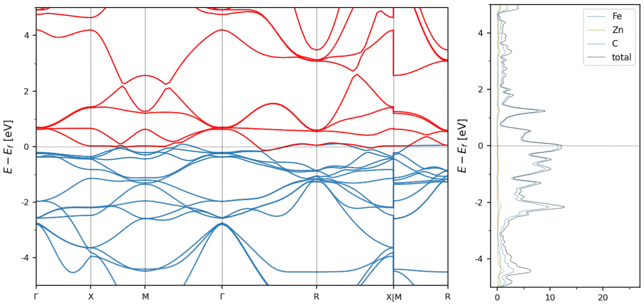

Co$_3$MgC - ICSD 76790 - SG 221 ($Pm\bar{3}m$) - ESFD - FM

Kagome - Bipartite - Split - Lieb

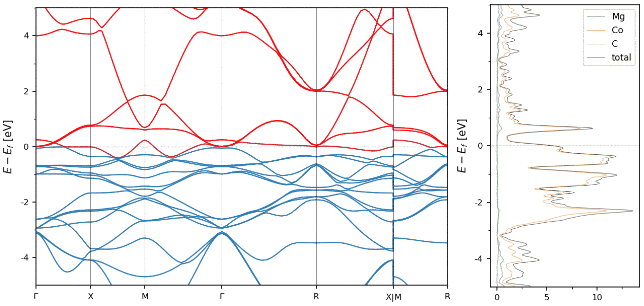

Co$_3$ZnC - ICSD 76797 - SG 221 ($Pm\bar{3}m$) - ESFD - FM

Kagome - Bipartite - Split - Lieb

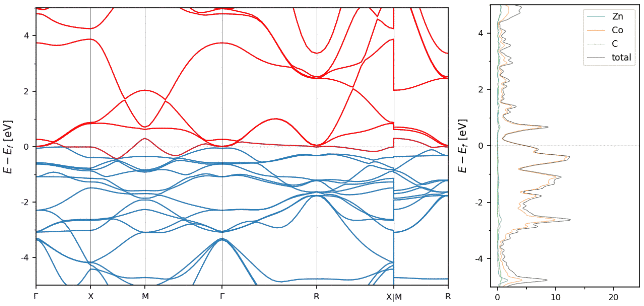

YRh$_3$C - ICSD 77389 - SG 221 ($Pm\bar{3}m$) - ESFD - NM

Kagome - Bipartite - Split - Lieb

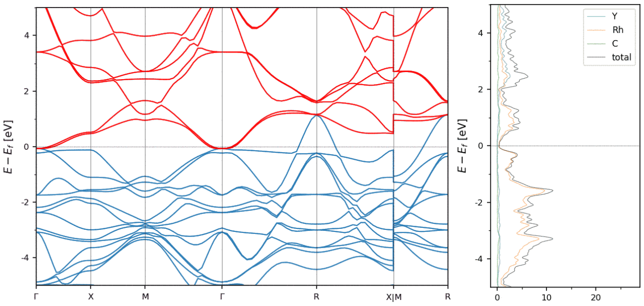

Figure 57. Band structure and density of states for materials with the most remarkable flat-band features near the Fermi energy. (part 30/44)

Sr(VO$_3$) - ICSD 88982 - SG 221 ($Pm\bar{3}m$) - ESFD - FM

Kagome - Bipartite - Split - Lieb

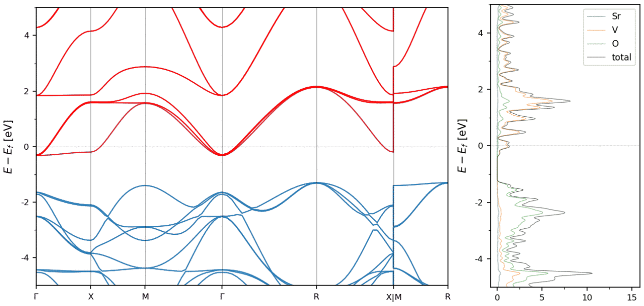

Sr(TcO$_3$) - ICSD 109076 - SG 221 ($Pm\bar{3}m$) - ESFD - NM

Kagome - Bipartite - Split - Lieb

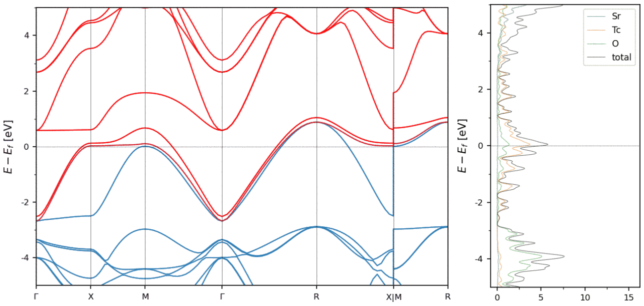

Ca(MnO$_3$) - ICSD 168902 - SG 221 ($Pm\bar{3}m$) - ESFD - FM

Kagome - Bipartite - Split - Lieb

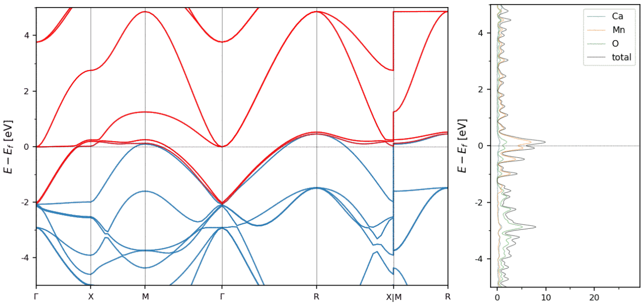

Pb(VO$_3$) - ICSD 187637 - SG 221 ($Pm\bar{3}m$) - ESFD - FM

Kagome - Bipartite - Split - Lieb

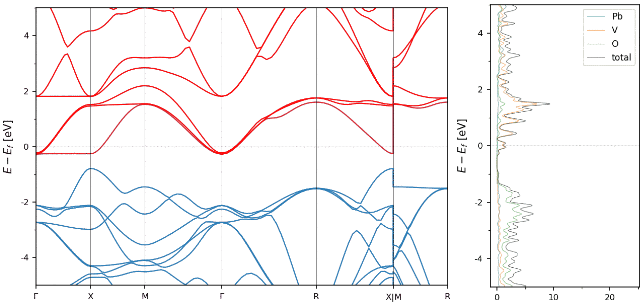

Sr(MnO$_3$) - ICSD 188415 - SG 221 ($Pm\bar{3}m$) - ESFD - AFM

Kagome - Bipartite - Split - Lieb

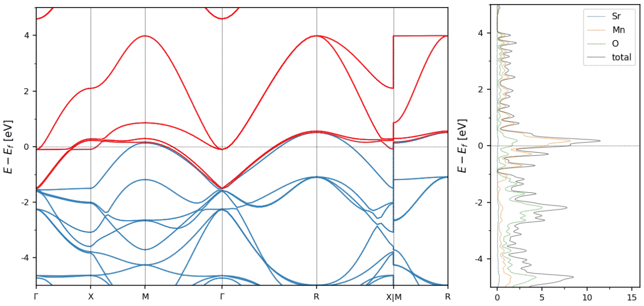

Ba(VO$_3$) - ICSD 191203 - SG 221 ($Pm\bar{3}m$) - ESFD - FM

Kagome - Bipartite - Split - Lieb

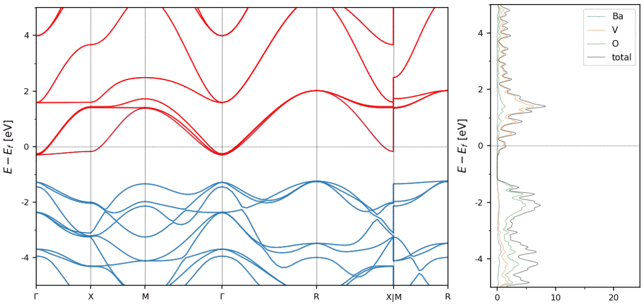

InNCo$_3$ - ICSD 247066 - SG 221 ($Pm\bar{3}m$) - ESFD - FM

Kagome - Bipartite - Split - Lieb

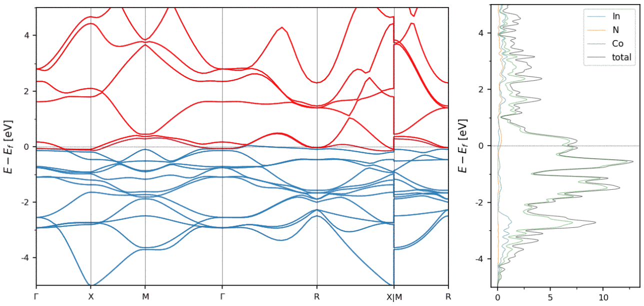

CdCo$_3$N - ICSD 422858 - SG 221 ($Pm\bar{3}m$) - ESFD - FM

Kagome - Bipartite - Split - Lieb

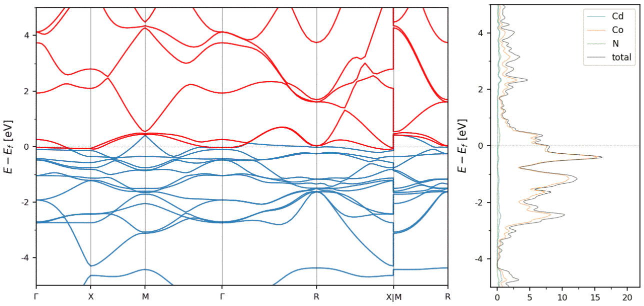

Figure 58. Band structure and density of states for materials with the most remarkable flat-band features near the Fermi energy. (part 31/44)

CaTcO$_3$ - ICSD 671082 - SG 221 ($Pm\bar{3}m$) - ESFD - n.a.

Kagome - Bipartite - Split - Lieb

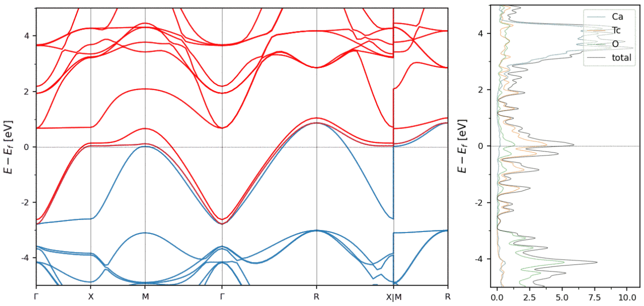

BaTcO$_3$ - ICSD 671086 - SG 221 ($Pm\bar{3}m$) - ESFD - n.a.

Kagome - Bipartite - Split - Lieb

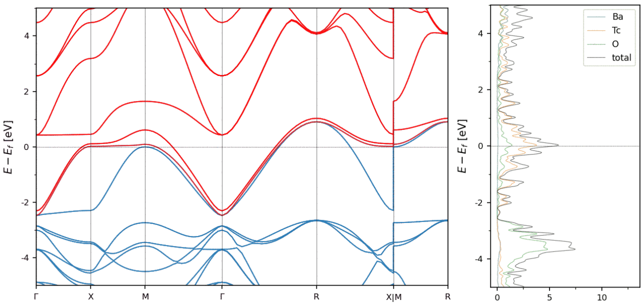

ZnSnO$_3$ - ICSD 673496 - SG 221 ($Pm\bar{3}m$) - ESFD - n.a.

Kagome - Bipartite - Split - Lieb

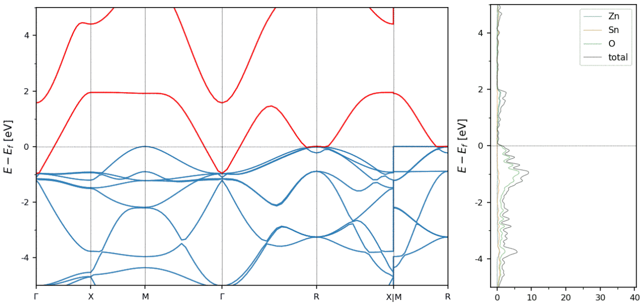

KFeF$_3$ - ICSD 15424 - SG 221 ($Pm\bar{3}m$) - LCEBR - FM

Kagome - Bipartite - Split - Lieb

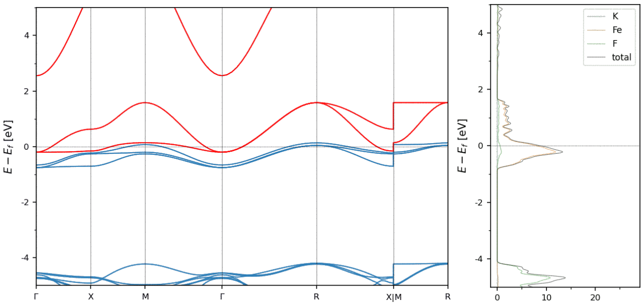

La(MnO$_3$) - ICSD 29119 - SG 221 ($Pm\bar{3}m$) - LCEBR - FM

Kagome - Bipartite - Split - Lieb

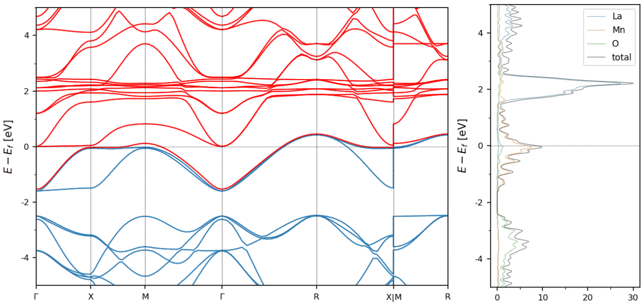

KSbO$_3$ - ICSD 674060 - SG 221 ($Pm\bar{3}m$) - LCEBR - n.a.

Kagome - Bipartite - Split - Lieb

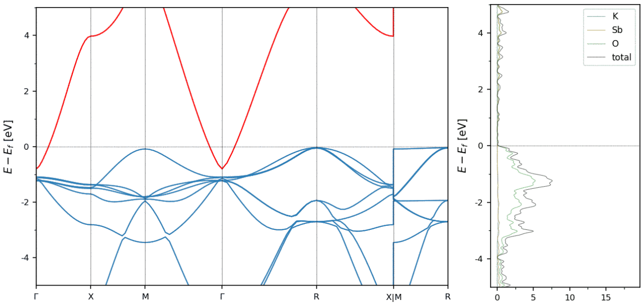

MoF$_3$ - ICSD 30612 - SG 221 ($Pm\bar{3}m$) - ESFD - FM

Kagome - Bipartite - Split - Lieb

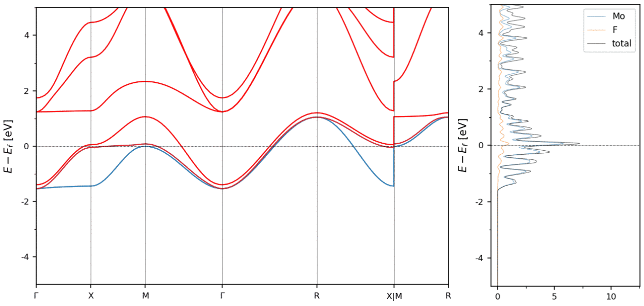

Na$_3$N - ICSD 165988 - SG 221 ($Pm\bar{3}m$) - ESFD - NM

Kagome - Bipartite - Split - Lieb

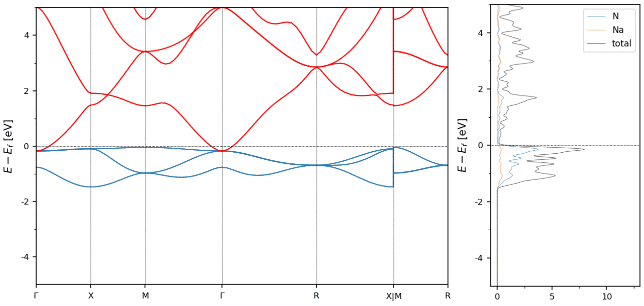

Figure 59. Band structure and density of states for materials with the most remarkable flat-band features near the Fermi energy. (part 32/44)

ScF$_3$ - ICSD 77071 - SG 221 ($Pm\bar{3}m$) - LCEBR - NM

Kagome - Bipartite - Split - Lieb

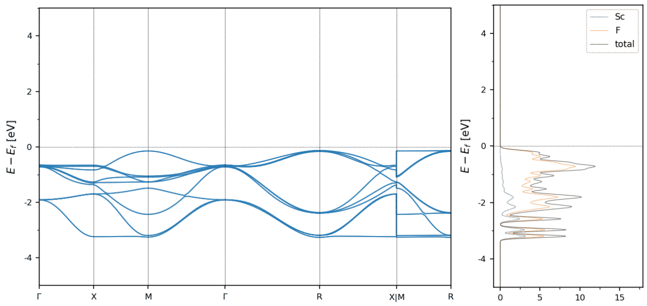

WO$_3$ - ICSD 108651 - SG 221 ($Pm\bar{3}m$) - LCEBR - NM

Kagome - Bipartite - Split - Lieb

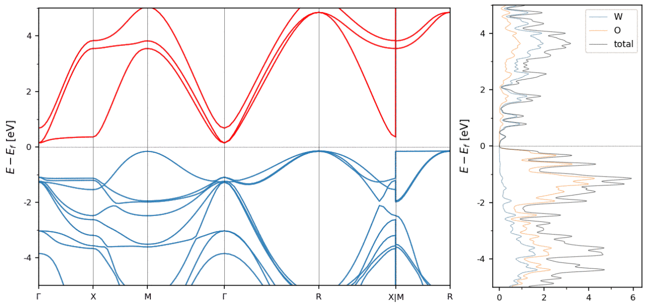

MgO - ICSD 181465 - SG 223 ($Pm\bar{3}n$) - LCEBR - NM

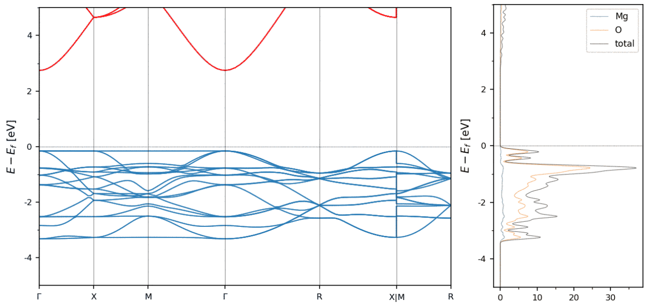

SiC$_2$N$_4$ - ICSD 93543 - SG 224 ($Pn\bar{3}m$) - LCEBR - NM

Bipartite

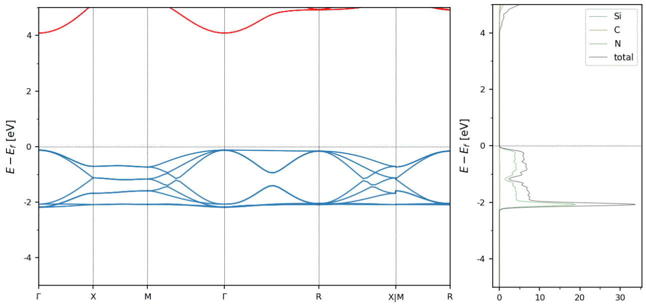

KTl$_2$MoF$_6$ - ICSD 15775 - SG 225 ($Fm\bar{3}m$) - ESFD - FM

Bipartite

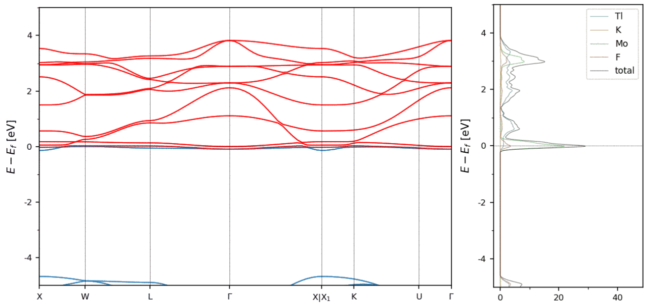

NaTl$_2$MoF$_6$ - ICSD 15776 - SG 225 ($Fm\bar{3}m$) - ESFD - FM

Kagome* - Bipartite - Split

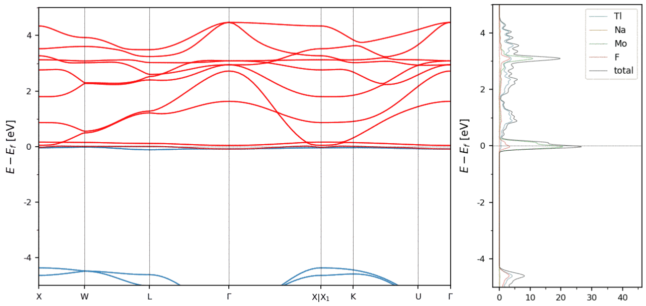

Ba$_2$CoWO$_6$ - ICSD 27425 - SG 225 ($Fm\bar{3}m$) - ESFD - FM

Kagome* - Bipartite - Split

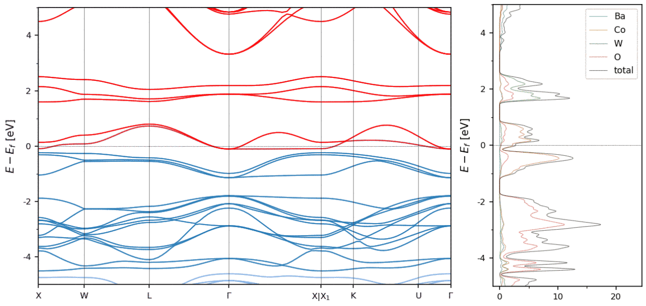

Sr$_2$Co(WO$_6$) - ICSD 28598 - SG 225 ($Fm\bar{3}m$) - ESFD - FM

Kagome* - Bipartite - Split

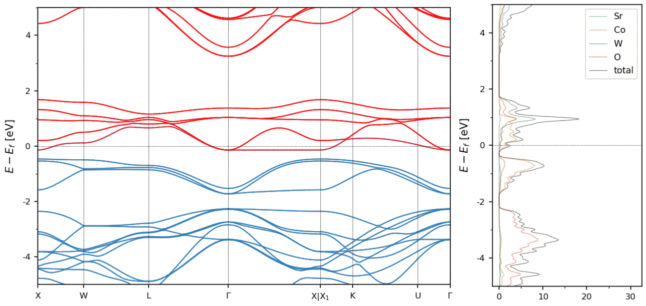

Figure 60. Band structure and density of states for materials with the most remarkable flat-band features near the Fermi energy. (part 33/44)

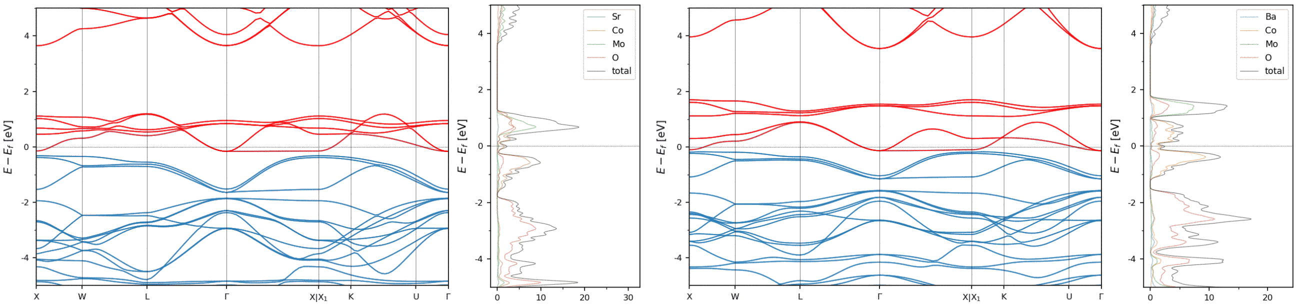

Sr$_2$Co(MoO$_6$) - ICSD 28601 - SG 225 ($Fm\bar{3}m$) - ESFD - AFM

Kagome* - Bipartite - Split

Ba$_2$(CoMoO$_6$) - ICSD 97028 - SG 225 ($Fm\bar{3}m$) - ESFD - AFM

Kagome* - Bipartite - Split

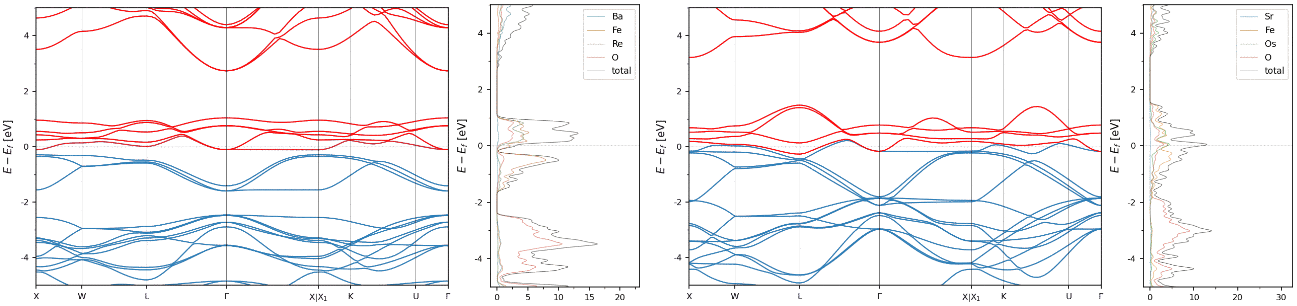

Ba$_2$Fe(ReO$_6$) - ICSD 109252 - SG 225 ($Fm\bar{3}m$) - ESFD - FM

Kagome* - Bipartite - Split

Sr$_2$FeOsO$_6$ - ICSD 251068 - SG 225 ($Fm\bar{3}m$) - ESFD - AFM

Kagome* - Bipartite - Split

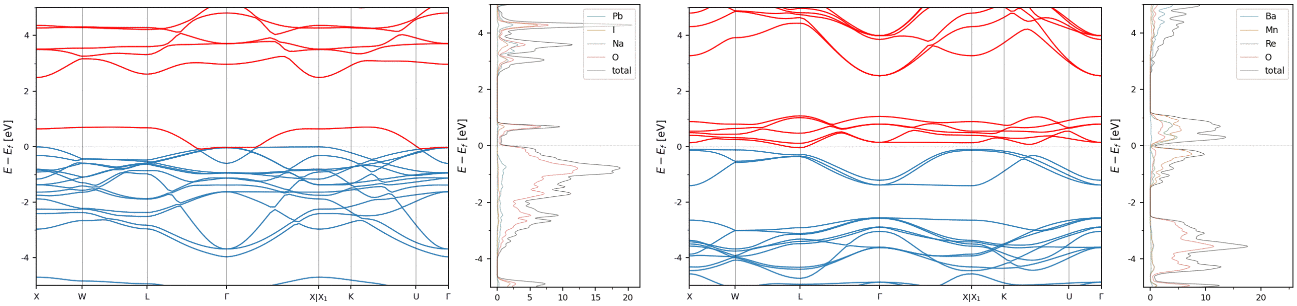

Pb$_2$NaIO$_6$ - ICSD 427115 - SG 225 ($Fm\bar{3}m$) - ESFD - NM

Kagome* - Bipartite - Split

Ba$_2$Mn(ReO$_6$) - ICSD 4169 - SG 225 ($Fm\bar{3}m$) - LCEBR - FM

Kagome* - Bipartite - Split

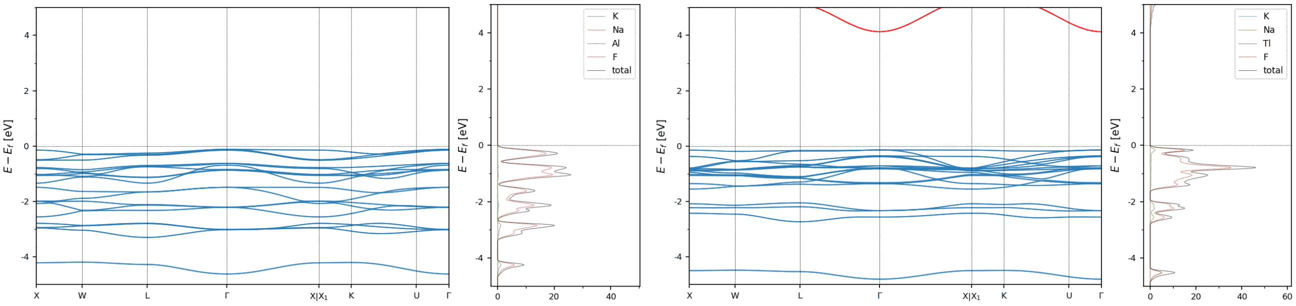

K$_2$Na(AlF$_6$) - ICSD 6027 - SG 225 ($Fm\bar{3}m$) - LCEBR - NM

K$_2$NaTlF$_6$ - ICSD 22114 - SG 225 ($Fm\bar{3}m$) - LCEBR - NM

Kagome* - Bipartite - Split

Figure 61. Band structure and density of states for materials with the most remarkable flat-band features near the Fermi energy. (part 34/44)

Cs$_2$NaTlF$_6$ - ICSD 22118 - SG 225 ($Fm\bar{3}m$) - LCEBR - NM

Kagome* - Bipartite - Split

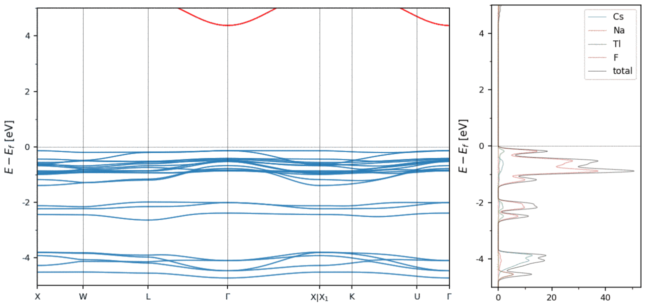

Ba$_2$FeMoO$_6$ - ICSD 96688 - SG 225 ($Fm\bar{3}m$) - LCEBR - FM

Kagome* - Bipartite - Split

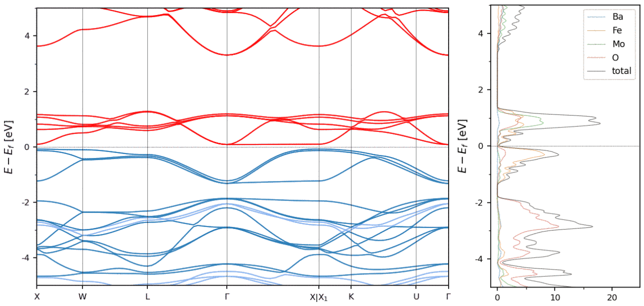

Ba$_2$(FeWO$_6$) - ICSD 99061 - SG 225 ($Fm\bar{3}m$) - LCEBR - AFM

Kagome* - Bipartite - Split

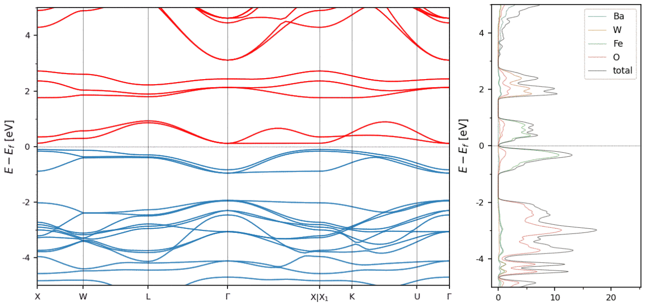

Sr$_2$(GaSbO$_6$) - ICSD 157016 - SG 225 ($Fm\bar{3}m$) - LCEBR - NM

Kagome* - Bipartite - Split

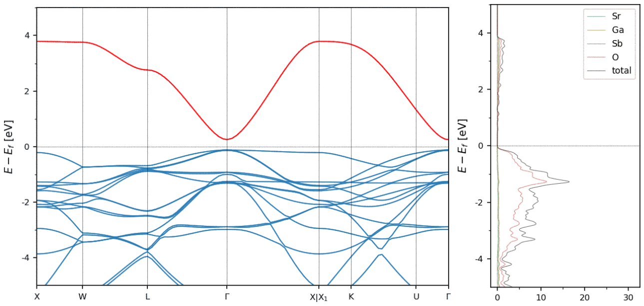

Sr$_2$(FeMoO$_6$) - ICSD 157603 - SG 225 ($Fm\bar{3}m$) - LCEBR - AFM

Kagome* - Bipartite - Split

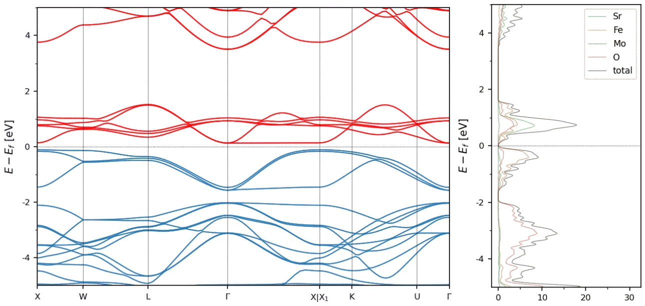

Sr$_2$Y(SbO$_6$) - ICSD 157886 - SG 225 ($Fm\bar{3}m$) - LCEBR - NM

Kagome* - Bipartite - Split

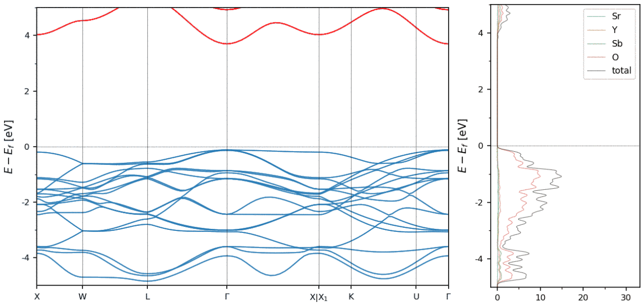

Ba$_2$CaTeO$_6$ - ICSD 246112 - SG 225 ($Fm\bar{3}m$) - LCEBR - NM

Kagome* - Bipartite - Split

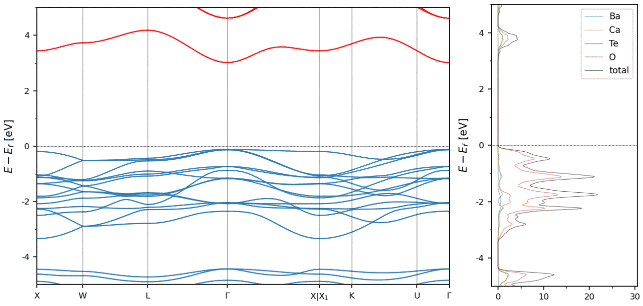

Cs$_2$InAgCl$_6$ - ICSD 257115 - SG 225 ($Fm\bar{3}m$) - LCEBR - n.a.

Kagome* - Bipartite - Split

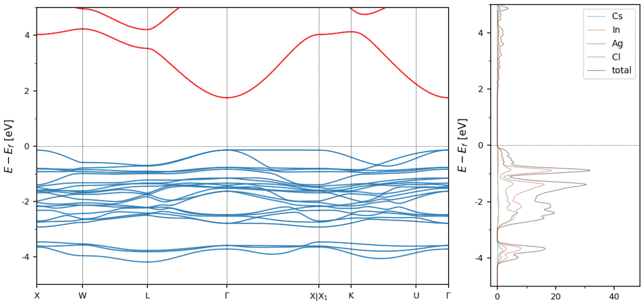

Figure 62. Band structure and density of states for materials with the most remarkable flat-band features near the Fermi energy. (part 35/44)

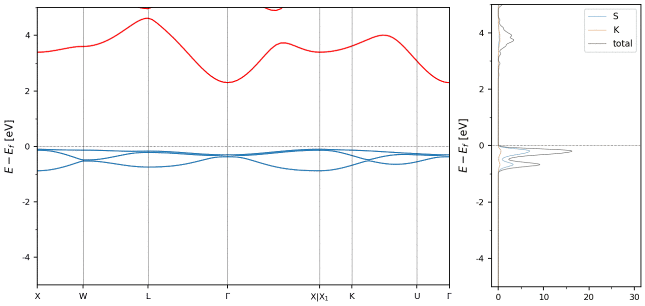
K$_2$S - ICSD 26735 - SG 225 ($Fm\bar{3}m$) - LCEBR - NM

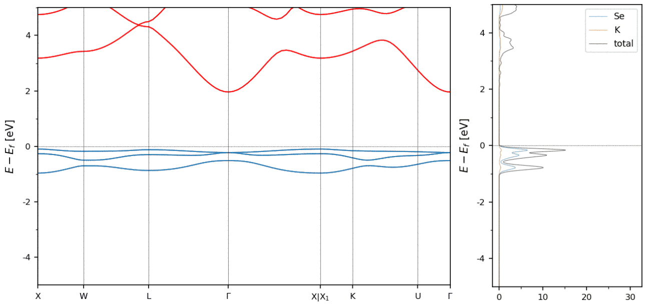
K$_2$Se - ICSD 60440 - SG 225 ($Fm\bar{3}m$) - LCEBR - NM

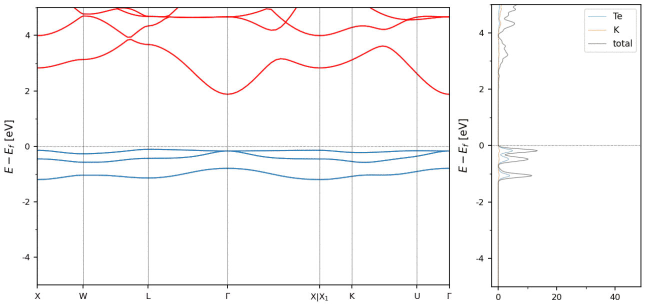
K$_2$Te - ICSD 60441 - SG 225 ($Fm\bar{3}m$) - LCEBR - NM

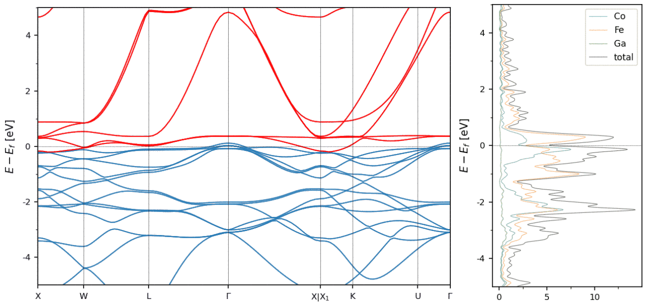
CoFe$_2$Ga - ICSD 102385 - SG 225 ($Fm\bar{3}m$) - SEBR - FM

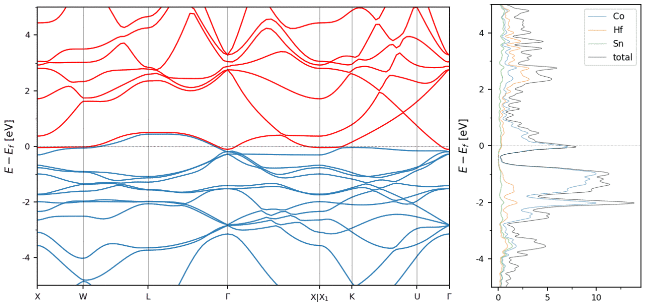
Co$_2$HfSn - ICSD 102483 - SG 225 ($Fm\bar{3}m$) - SEBR - FM

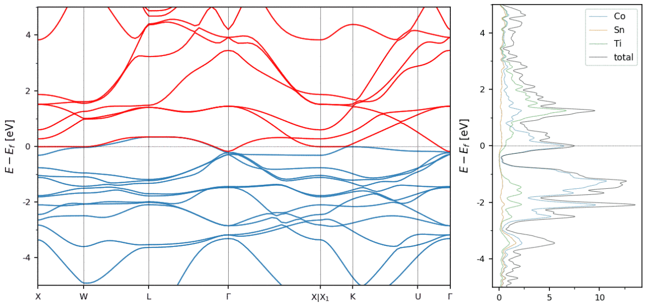
Co$_2$SnTi - ICSD 102682 - SG 225 ($Fm\bar{3}m$) - SEBR - FM

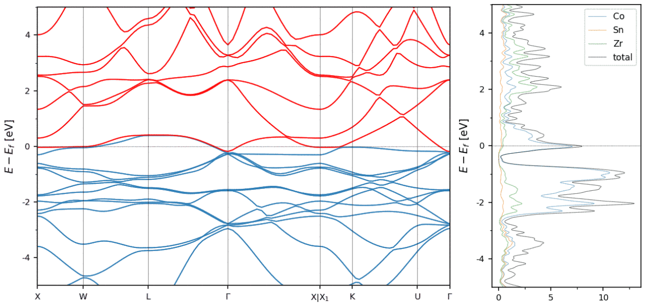
Co$_2$SnZr - ICSD 102687 - SG 225 ($Fm\bar{3}m$) - SEBR - FM

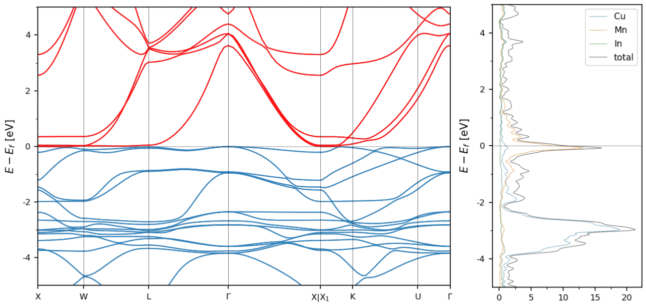
Cu$_2$MnIn - ICSD 102996 - SG 225 ($Fm\bar{3}m$) - SEBR - FM

Figure 63. Band structure and density of states for materials with the most remarkable flat-band features near the Fermi energy. (part 36/44)

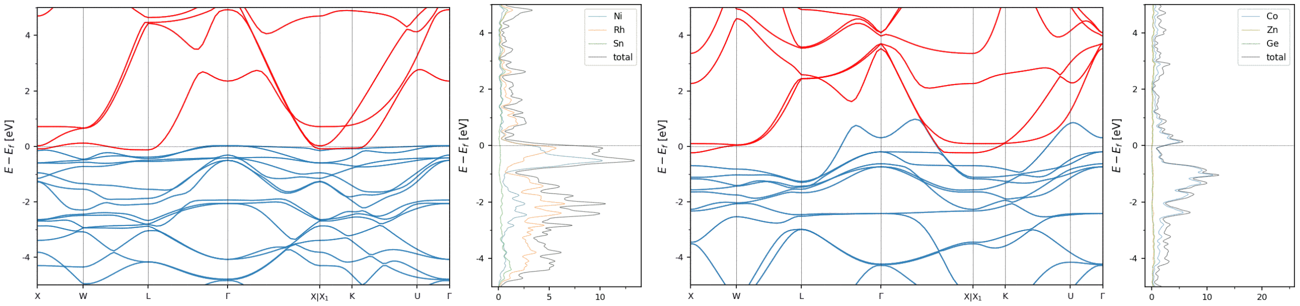

NiRh$_2$Sn - ICSD 105327 - SG 225 ($Fm\bar{3}m$) - SEBR - FM

Co$_2$ZnGe - ICSD 52994 - SG 225 ($Fm\bar{3}m$) - ES - FM

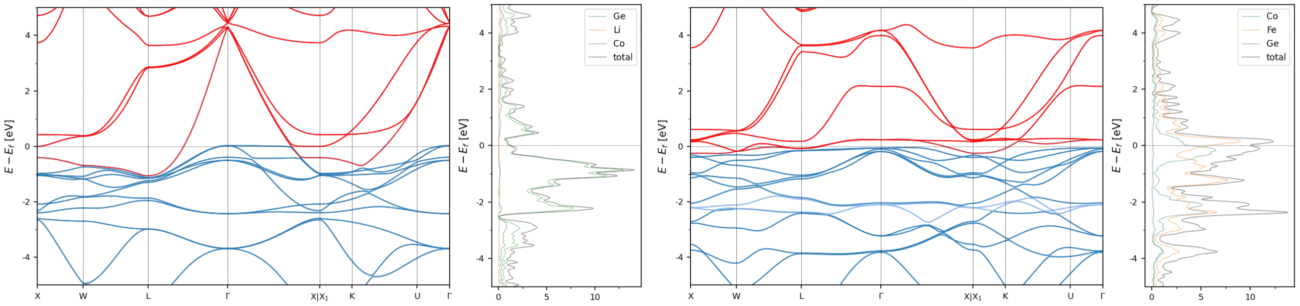

LiCo$_2$Ge - ICSD 25324 - SG 225 ($Fm\bar{3}m$) - ESFD - NM

CoFe$_2$Ge - ICSD 52954 - SG 225 ($Fm\bar{3}m$) - ESFD - FM

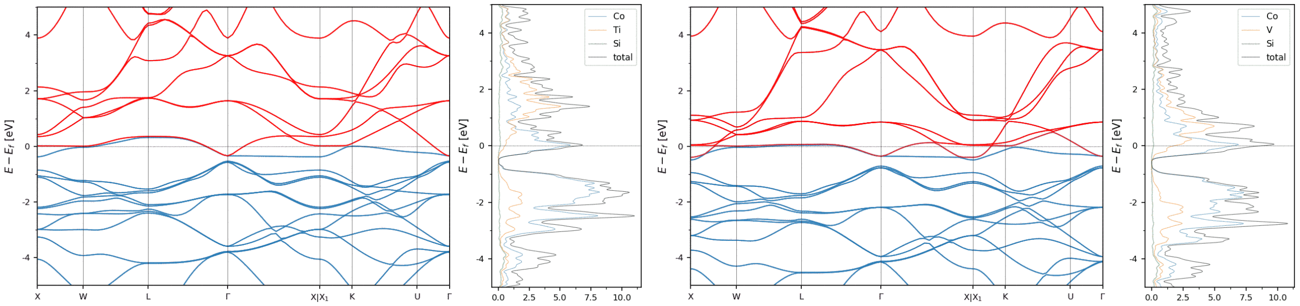

Co$_2$TiSi - ICSD 53080 - SG 225 ($Fm\bar{3}m$) - ESFD - FM

Co$_2$VSi - ICSD 53086 - SG 225 ($Fm\bar{3}m$) - ESFD - FM

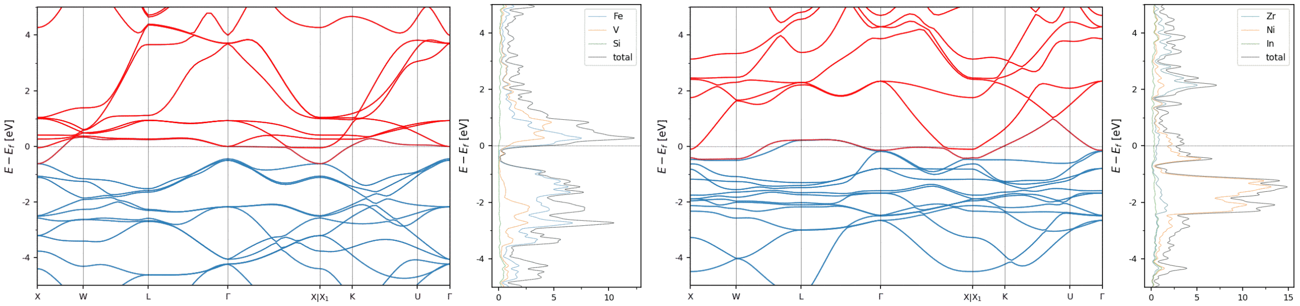

Fe$_2$VSi - ICSD 53555 - SG 225 ($Fm\bar{3}m$) - ESFD - FM

ZrNi$_2$In - ICSD 54546 - SG 225 ($Fm\bar{3}m$) - ESFD - NM

Figure 64. Band structure and density of states for materials with the most remarkable flat-band features near the Fermi energy. (part 37/44)

HfNi$_2$In - ICSD 54595 - SG 225 ($Fm\bar{3}m$) - ESFD - NM

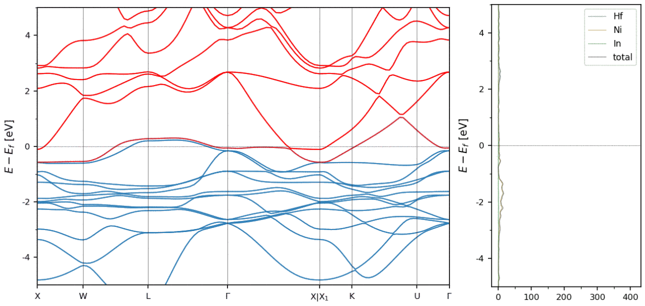

AlCrFe$_2$ - ICSD 57654 - SG 225 ($Fm\bar{3}m$) - ESFD - FM

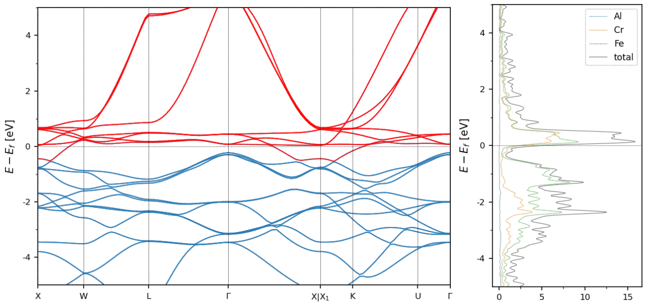

AlFe$_3$ - ICSD 57793 - SG 225 ($Fm\bar{3}m$) - ESFD - FM

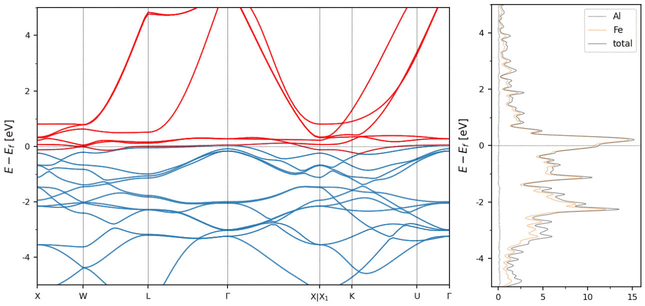

AlFe$_2$Mo - ICSD 57807 - SG 225 ($Fm\bar{3}m$) - ESFD - FM

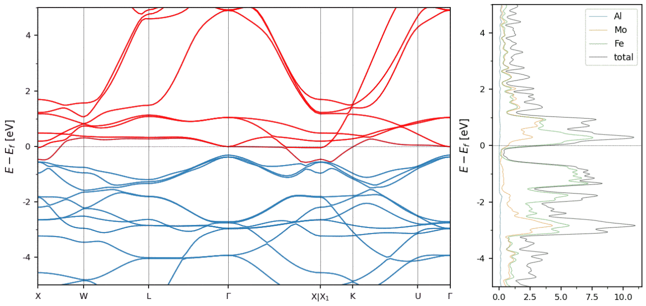

Mn$_3$Si - ICSD 76227 - SG 225 ($Fm\bar{3}m$) - ESFD - FM

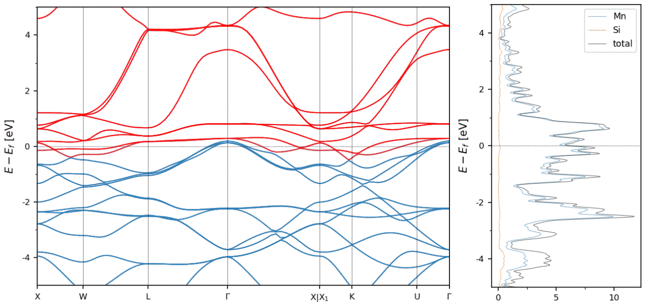

Co$_2$HfGa - ICSD 102433 - SG 225 ($Fm\bar{3}m$) - ESFD - FM

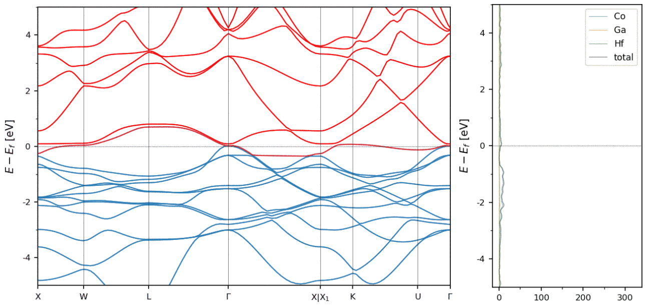

CrFe$_2$Ga - ICSD 102755 - SG 225 ($Fm\bar{3}m$) - ESFD - FM

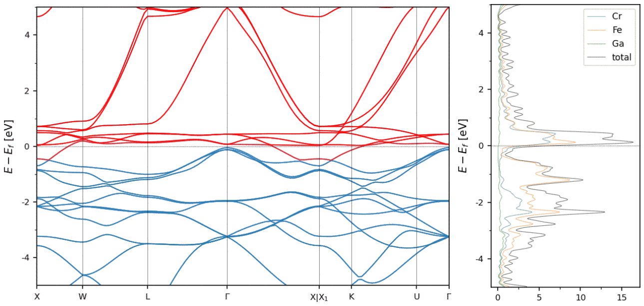

Fe$_2$SnTi - ICSD 103641 - SG 225 ($Fm\bar{3}m$) - ESFD - NM

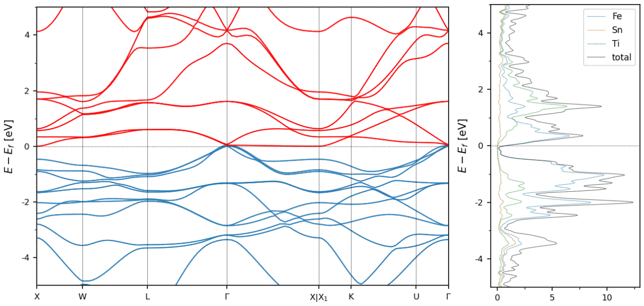

Figure 65. Band structure and density of states for materials with the most remarkable flat-band features near the Fermi energy. (part 38/44)

Fe_2SnV - ICSD 103644 - SG 225 ($Fm\bar{3}m$) - ESFD - FM

$MnNi_2Sn$ - ICSD 104926 - SG 225 ($Fm\bar{3}m$) - ESFD - FM

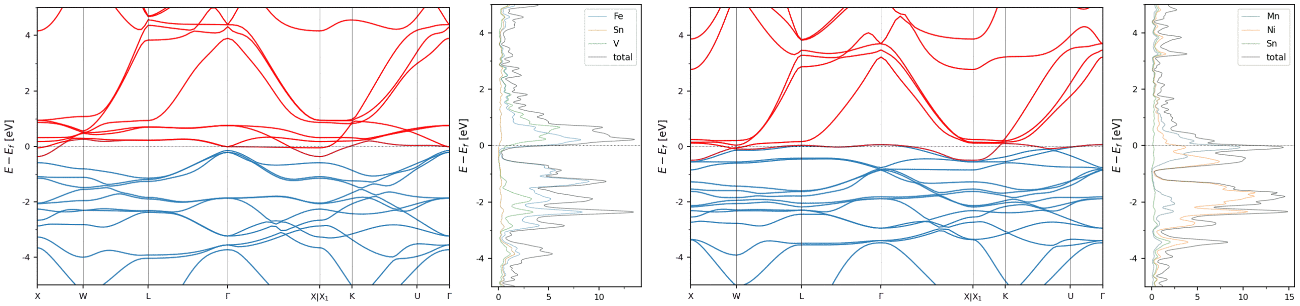

Ni_2ScSn - ICSD 105339 - SG 225 ($Fm\bar{3}m$) - ESFD - NM

Fe_3Ga - ICSD 108436 - SG 225 ($Fm\bar{3}m$) - ESFD - FM

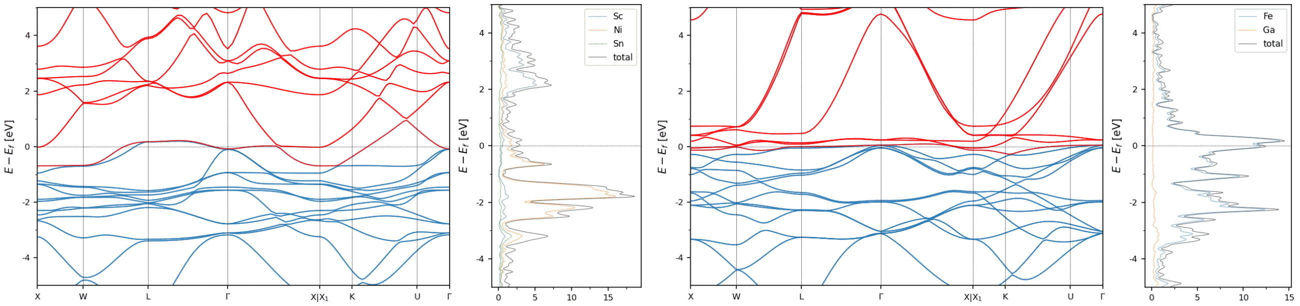

Co_2TiGe - ICSD 169468 - SG 225 ($Fm\bar{3}m$) - ESFD - FM

Co_2TiAl - ICSD 185966 - SG 225 ($Fm\bar{3}m$) - ESFD - FM

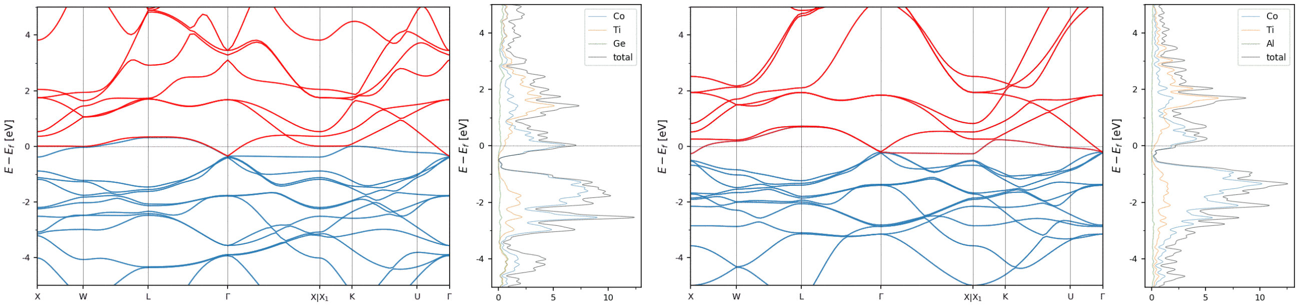

Fe_2CrSn - ICSD 185999 - SG 225 ($Fm\bar{3}m$) - ESFD - FM

Fe_2TiAs - ICSD 186059 - SG 225 ($Fm\bar{3}m$) - ESFD - FM

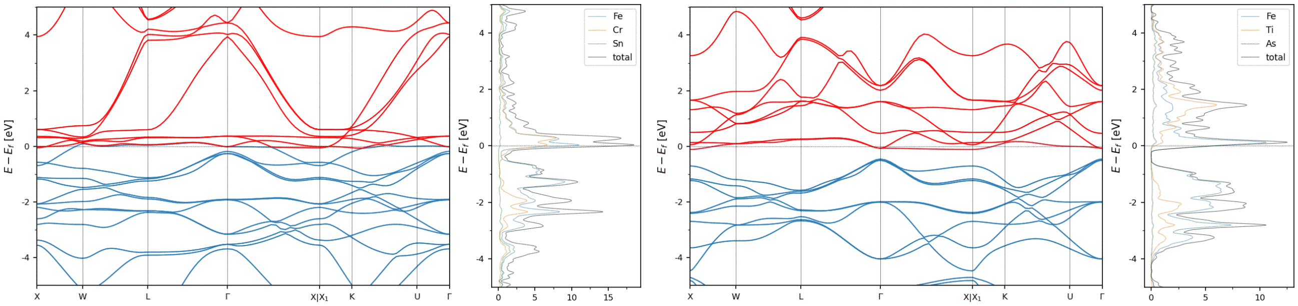

Figure 66. Band structure and density of states for materials with the most remarkable flat-band features near the Fermi energy. (part 39/44)

Fe_2TiSb - ICSD 186060 - SG 225 ($Fm\bar{3}m$) - ESFD - FM

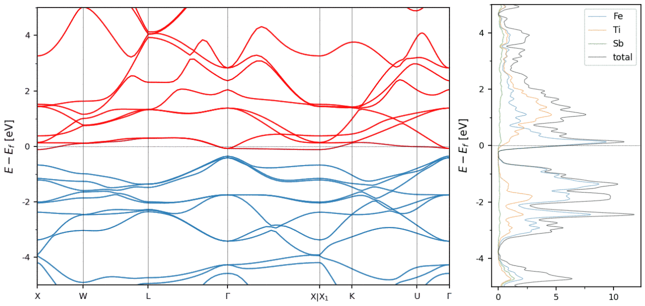

Ru_2VGe - ICSD 671340 - SG 225 ($Fm\bar{3}m$) - ESFD - n.a.

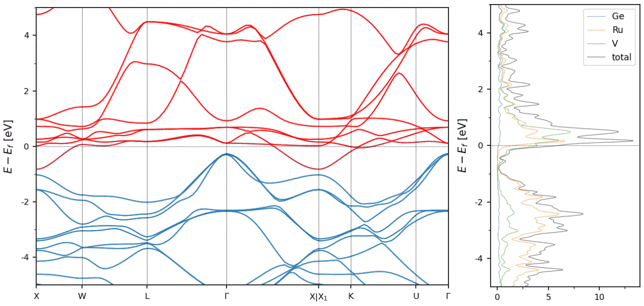

Fe_2ZrP - ICSD 675102 - SG 225 ($Fm\bar{3}m$) - ESFD - n.a.

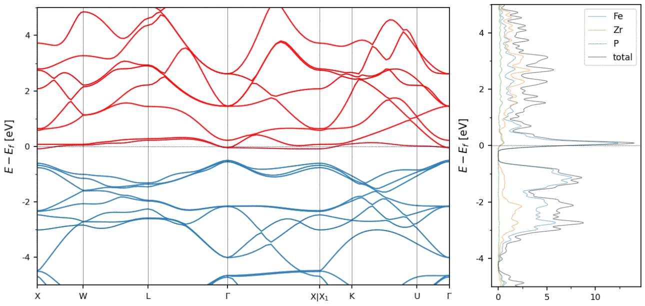

$FeRu_2Si$ - ICSD 53525 - SG 225 ($Fm\bar{3}m$) - LCEBR - FM

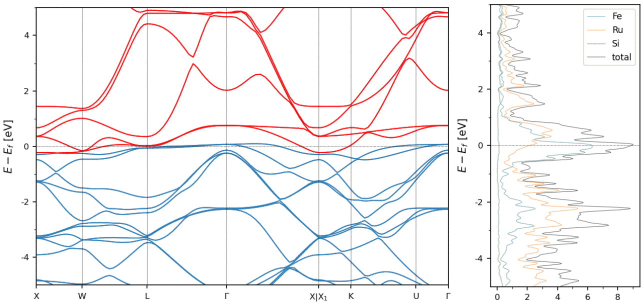

Fe_2GaV - ICSD 103473 - SG 225 ($Fm\bar{3}m$) - LCEBR - NM

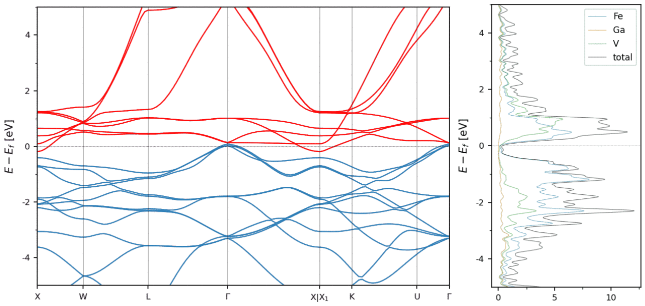

Fe_2TiGe - ICSD 186057 - SG 225 ($Fm\bar{3}m$) - LCEBR - NM

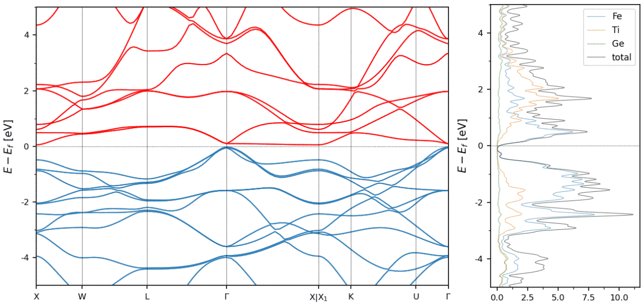

Y_2Ni_6C - ICSD 673582 - SG 225 ($Fm\bar{3}m$) - ES - n.a.

Kagome*

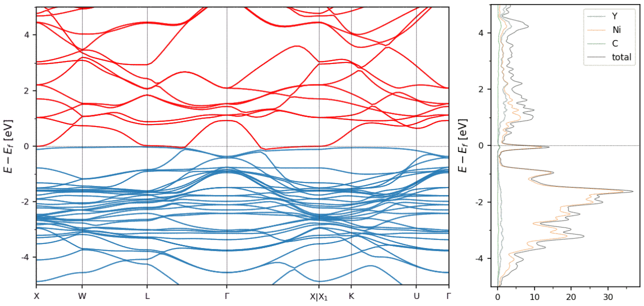

Rb_2MnCl_6 - ICSD 9347 - SG 225 ($Fm\bar{3}m$) - ESFD - FM

Kagome*

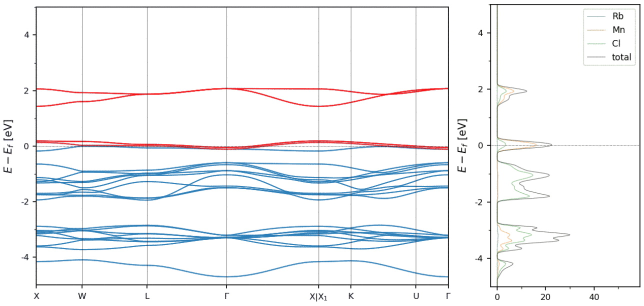

Figure 67. Band structure and density of states for materials with the most remarkable flat-band features near the Fermi energy. (part 40/44)

K_2TaCl_6 - ICSD 59894 - SG 225 ($Fm\bar{3}m$) - ESFD - FM

Kagome*

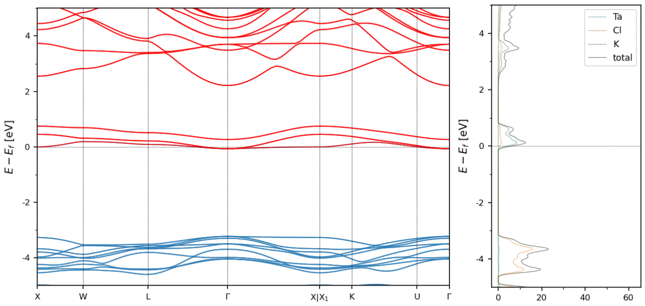

$Rb_2(NbCl_6)$ - ICSD 245747 - SG 225 ($Fm\bar{3}m$) - ESFD - FM

Kagome*

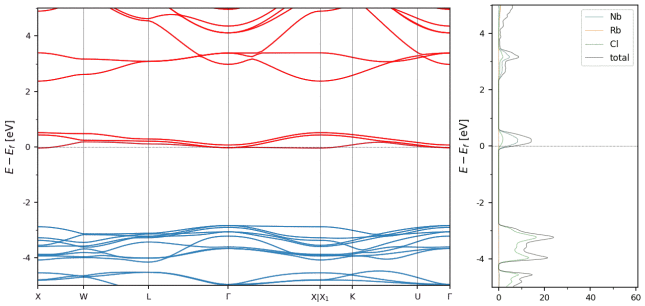

$K_2(SnCl_6)$ - ICSD 604 - SG 225 ($Fm\bar{3}m$) - LCEBR - NM

Kagome*

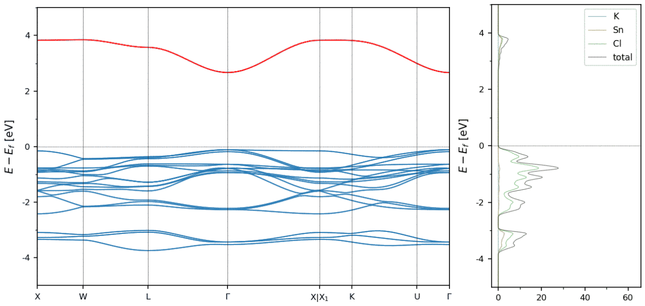

$(NH_4)_2(SnCl_6)$ - ICSD 605 - SG 225 ($Fm\bar{3}m$) - LCEBR - NM

Kagome*

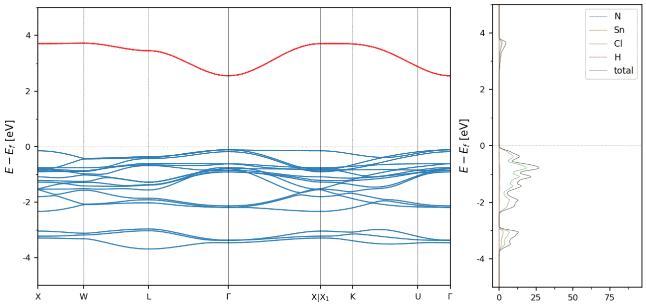

Rb_2SnCl_6 - ICSD 9022 - SG 225 ($Fm\bar{3}m$) - LCEBR - NM

Kagome*

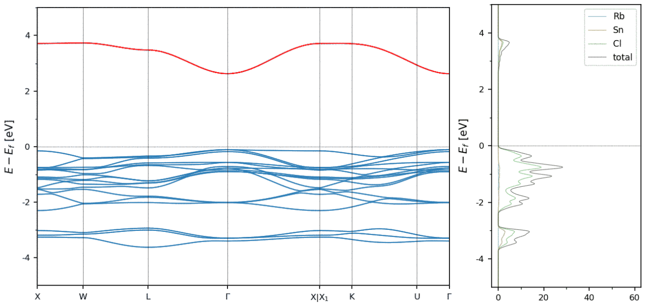

Cs_2SnCl_6 - ICSD 9023 - SG 225 ($Fm\bar{3}m$) - LCEBR - NM

Kagome*

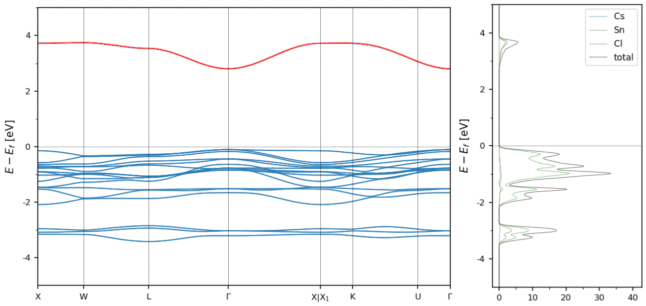

Ca_2NH - ICSD 292 - SG 227 ($Fd\bar{3}m$) - LCEBR - NM

Kagome - Pyrochlore

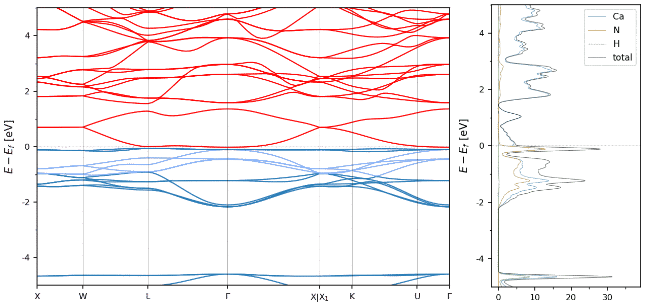

$CsNbN_2$ - ICSD 72546 - SG 227 ($Fd\bar{3}m$) - LCEBR - NM

Kagome - Pyrochlore - Bipartite - Split

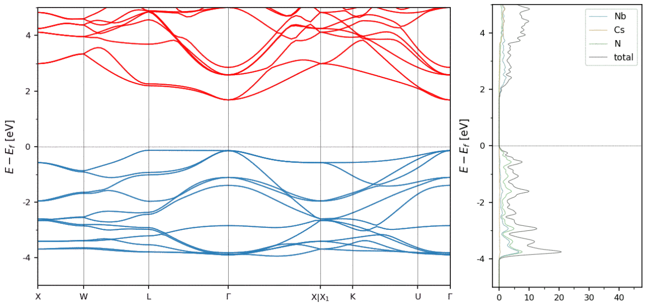

Figure 68. Band structure and density of states for materials with the most remarkable flat-band features near the Fermi energy. (part 41/44)

BaPt$_2$ - ICSD 58675 - SG 227 ($Fd\bar{3}m$) - SEBR - NM

Kagome - Pyrochlore

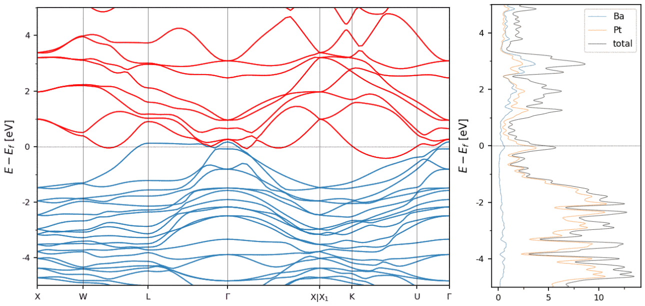

YS$_2$ - ICSD 52216 - SG 227 ($Fd\bar{3}m$) - ESFD - NM

Kagome - Pyrochlore

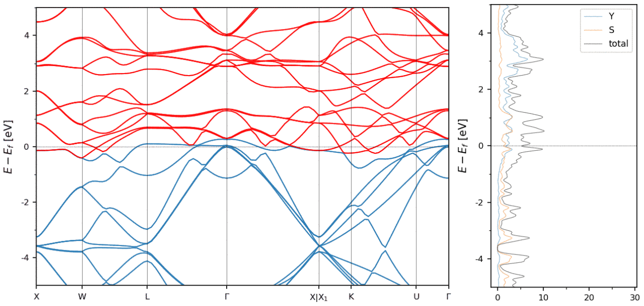

CaNi$_2$ - ICSD 58915 - SG 227 ($Fd\bar{3}m$) - ESFD - NM

Kagome - Pyrochlore

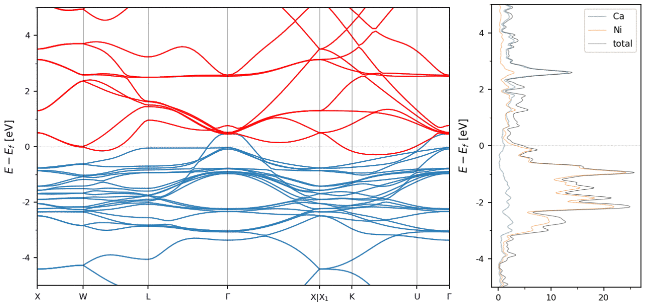

Ni$_2$Sc - ICSD 105334 - SG 227 ($Fd\bar{3}m$) - ESFD - NM

Kagome - Pyrochlore

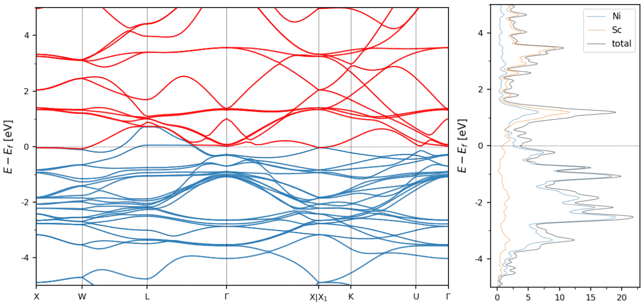

Ni$_2$Y - ICSD 105458 - SG 227 ($Fd\bar{3}m$) - ESFD - NM

Kagome - Pyrochlore

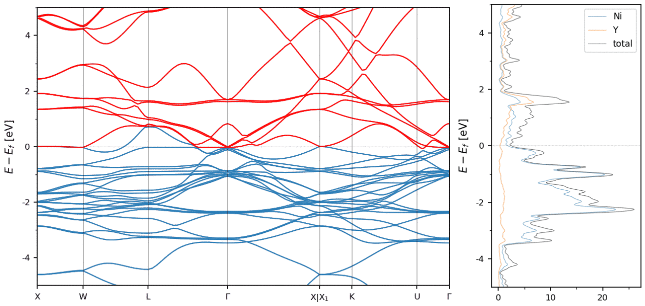

Zn$_2$Zr - ICSD 106236 - SG 227 ($Fd\bar{3}m$) - LCEBR - FM

Kagome - Pyrochlore

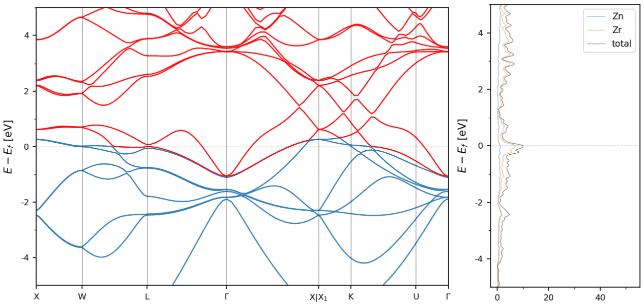

Pb$_2$Sb$_2$O$_7$ - ICSD 27120 - SG 227 ($Fd\bar{3}m$) - ES - NM

Kagome - Pyrochlore - Bipartite - Split

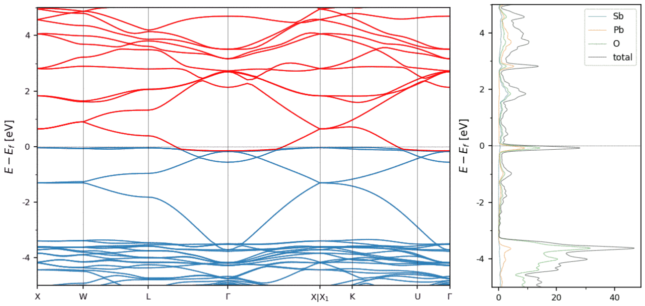

Cd$_2$Nb$_2$O$_7$ - ICSD 33672 - SG 227 ($Fd\bar{3}m$) - ESFD - NM

Kagome - Pyrochlore

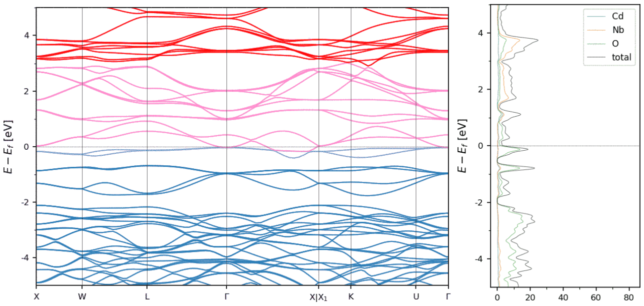

Figure 69. Band structure and density of states for materials with the most remarkable flat-band features near the Fermi energy. (part 42/44)

$Y_2(Ir_2O_7)$ - ICSD 187534 - SG 227 ($Fd\bar{3}m$) - ESFD - FM

Kagome - Pyrochlore - Bipartite - Split

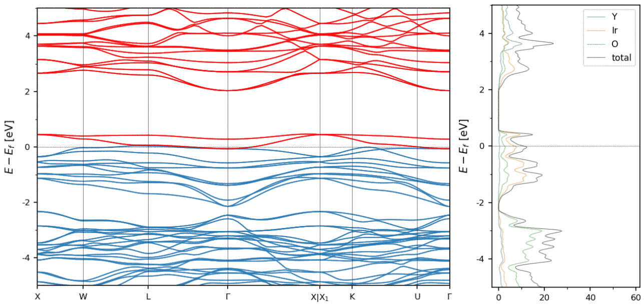

$Sn_2(Ta_2O_7)$ - ICSD 27119 - SG 227 ($Fd\bar{3}m$) - LCEBR - NM

Kagome - Pyrochlore - Bipartite - Split

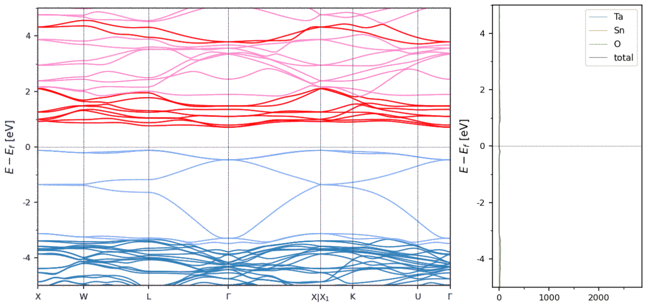

$Ca_2Ta_2O_7$ - ICSD 27121 - SG 227 ($Fd\bar{3}m$) - LCEBR - NM

Kagome - Pyrochlore - Bipartite - Split

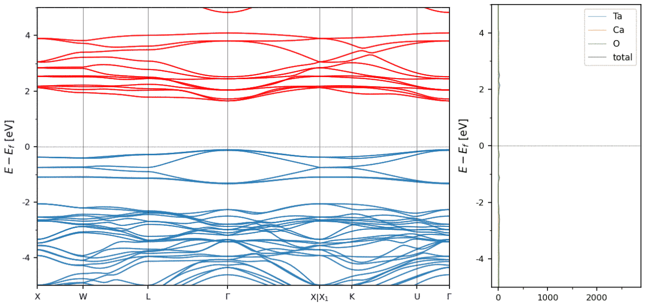

$Hg_2Zn_2F_6O$ - ICSD 27330 - SG 227 ($Fd\bar{3}m$) - LCEBR - NM

Kagome - Pyrochlore - Bipartite - Split

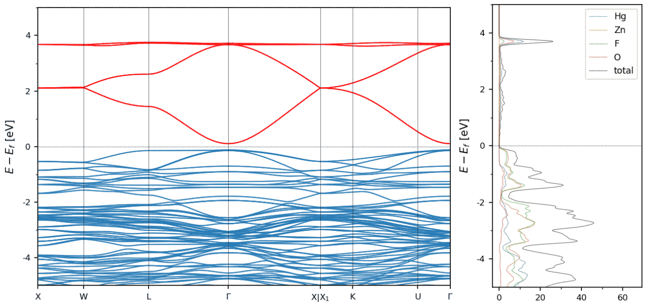

$Bi_2(Pt_2O_7)$ - ICSD 161104 - SG 227 ($Fd\bar{3}m$) - LCEBR - NM

Kagome - Pyrochlore - Bipartite - Split

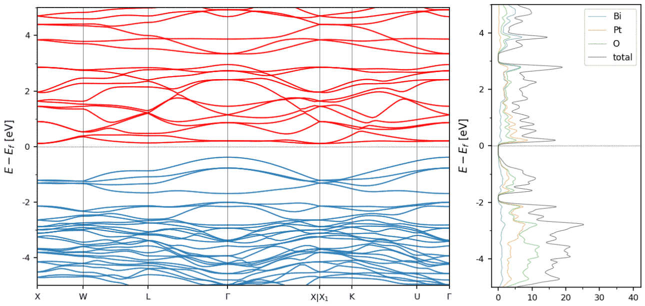

$Sn_2(Nb_2O_7)$ - ICSD 163817 - SG 227 ($Fd\bar{3}m$) - LCEBR - NM

Kagome - Pyrochlore - Bipartite - Split

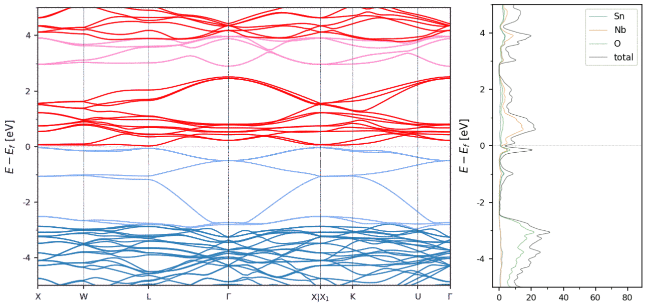

Mg_2VO_4 - ICSD 76980 - SG 227 ($Fd\bar{3}m$) - ESFD - FM

Kagome - Pyrochlore - Bipartite

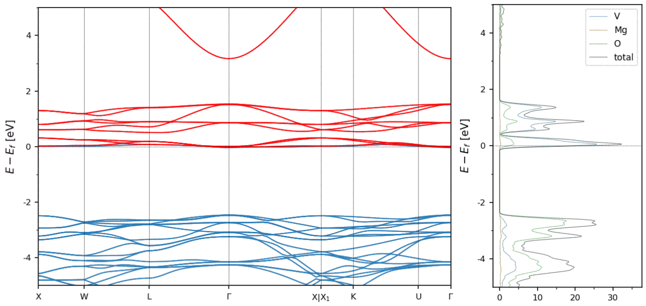

$CoAl_2O_4$ - ICSD 290133 - SG 227 ($Fd\bar{3}m$) - ESFD - AFM

Kagome - Pyrochlore - Bipartite

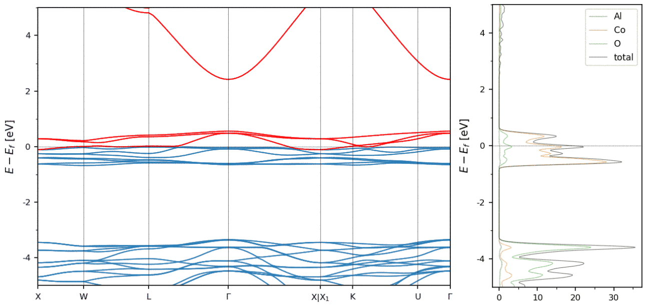

Figure 70. Band structure and density of states for materials with the most remarkable flat-band features near the Fermi energy. (part 43/44)

Al_2NiO_4 - ICSD 608815 - SG 227 ($Fd\bar{3}m$) - ESFD - AFM

Kagome - Pyrochlore - Bipartite

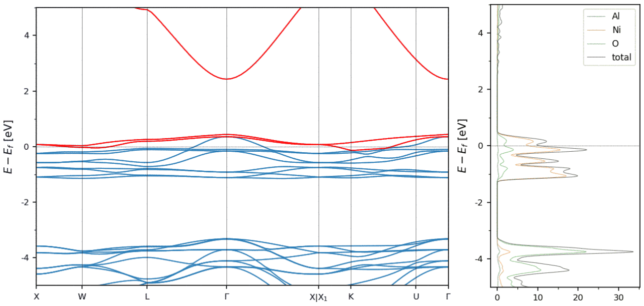

Figure 71. Band structure and density of states for materials with the most remarkable flat-band features near the Fermi energy. (part 44/44)